VOL.
1
1955

Journal of
Inorganic & Nuclear Chemistry

VOLUME I

EDITORS

JOSEPH J. KATZ, Chicago
H. C. LONGUET-HIGGINS, Cambridge
H. A. C. McKAY, Harwell

EDITORIAL ADVISORY BOARD

U.S.A.: JOHN C. BAILAR, JR., Univ. of Illinois · E. O. BRIMM, Linde Air Products · HERBERT C. BROWN, Purdue · ANTON B. BURG, Univ. South Cal. · CHARLES D. CORYELL, M.I.T. R. W. DODSON, Brookhaven · W. CONARD FERNELIUS, Penn. State Univ. · WARREN C. JOHNSON, Chicago · JACOB KLEINBERG, Univ. of Kansas · W. F. LIBBY, Washington, D.C. · W. M. MANNING, Argonne · THERALD MOELLER, Univ. of Illinois EUGENE G. ROCHOW, Harvard · H. I. SCHLESINGER, Chicago · WALTER C. SCHUMB, M.I.T. GLENN T. SEABORG, Univ. of California · P. W. SELWOOD, Evanston · F. H. SPEDDING, Ames W. H. ZACHARIASEN, Chicago

U.K. and Commonwealth: J. S. ANDERSON, F.R.S., Melbourne · F. M. BREWER, Oxford G. E. COATES, Durham · H. J. EMELEUS, F.R.S., Cambridge · F. FAIRBROTHER, Manchester H. M. N. H. IRVING, Oxford · A. G. MADDOCK, Cambridge · L. E. ORGEL, Cambridge A. R. POWELL, F.R.S., Wembley · P. L. ROBINSON, Newcastle-upon-Tyne · R. SPENCE, Harwell J. W. T. SPINKS, Saskatoon · H. G. THODE, F.R.S., Hamilton · L. YAFFE, Montreal

Austria: E. BRODA, BERTHA KARLIK, Vienna · *Denmark:* J. BJERRUM, Copenhagen

France: J. BÉNARD, Paris · J. CHÉDIN, Paris · J. GUÉRON, Paris · M. MAGAT, Paris

Germany: W. HIEBER, Munich · G. JANDER, Berlin · A. MUENSTER, Frankfurt

Netherlands: A. E. VAN ARKEL, Leiden · A. H. W. ATEN, JR., Amsterdam · J. H. DE BOER, Geleen · E. J. W. VERWEY, Eindhoven

Israel: M. BOBTELSKY, Jerusalem

Norway: H. HARALDSEN, Oslo · ODD HASSEL, Oslo

Sweden: G. HÄGG, Uppsala · L. G. SILLÉN, Stockholm

Switzerland: G. SCHWARZENBACH, Zurich

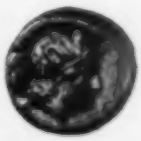

PERGAMON PRESS · LONDON · NEW YORK · 1955

JOURNAL OF INORGANIC AND NUCLEAR CHEMISTRY

Editors:

JOSEPH J. KATZ: *Argonne National Laboratory, Box 299, Lemont, Illinois, U.S.A.*

H. C. LONGUET-HIGGINS: *The University Chemical Laboratory, Cambridge, England.*

H. A. C. MCKAY: *Atomic Energy Research Establishment, Harwell, Didcot, Berks, England.*

NOTES FOR CONTRIBUTORS

I. General

1. Papers should, in general, be concerned with original work in the field of inorganic and nuclear chemistry. They should be submitted either to The Editors, c/o Pergamon Press Ltd., or to Dr. J. J. KATZ. Both addresses are given on this page.

2. Fifty free reprints of each paper are supplied. Additional copies can be supplied at a reasonable cost if ordered at the time when the first proofs are returned.

II. Manuscript Requirements

1. Manuscripts should be submitted in duplicate. They must be typewritten, and double-spaced. It will be appreciated if authors will make clear any Greek characters which may be confused with ordinary letters or with other characters. Authors will receive proofs for correction when their contribution is first set, but there is rarely time for page proofs also to be sent for checking. This will be done, however, where the amount of alteration makes it advisable.

2. Illustrations are to accompany the manuscript separately, and legends should also be typed on a separate sheet. It is requested that photographs should be kept to the minimum necessary. Line drawings that require to be re-drawn must include all relevant details. If these are already well drawn it may be possible to reproduce them direct from the original, but in this case it is essential that the original drawings or good photo-prints should be provided. It is not possible to reproduce from "die-line" prints, or from prints with weak lines. Illustrations for reproduction should normally be about twice the final size required.

3. References should be clearly indicated in the text with numbers. Full references should be given in numbered footnotes containing author's name, initials, title of paper (where desired), abbreviated title of journal, year, volume number and page number.

4. The text of articles submitted must be concise and in a readily understandable style. The technical description of the methods used should only be given in detail when such methods are new. The essential contents of each paper should be briefly recapitulated in an abstract. French and German papers should be submitted with English abstracts.

5. To conserve space authors are requested to mark less important portions of the paper (such as description of methods, record of experimental results, etc.) for printing in smaller type.

PERGAMON PRESS LTD., 4 & 5 FITZROY SQUARE, LONDON, W.1.
PERGAMON PRESS INC., 122 E. 55TH STREET, NEW YORK 22, N.Y.

LIST OF CONTENTS

NUMBERS 1/2

Foreword by WARREN C. JOHNSON and H. J. EMELÉUS 1
RICHARD A. GLASS, STANLEY G. THOMPSON and GLENN T. SEABORG: Nuclear thermo-dynamics of the heaviest elements 3
L. E. GLENDENIN and E. P. STEINBERG: Fission yields in spontaneous fission of Cf^{252} . . 45
D. J. M. BEVAN: Ordered intermediate phases in the system CeO_2-Ce_2O_3 49
H. C. LONGUET-HIGGINS and D. A. BROWN: The dynamics of binary hydrides 60
J. SUTTON: Hydrolyse de l'ion uranyle et formation d'uranates de sodium 68
HARO VON BUTTLAR and W. F. LIBBY: Natural distribution of cosmic-ray produced tritium. II 75
EUGENE G. ROCHOW and HUGH G. LECLAIR: On the molecular structure of methyl silicone . 92
F. G. A. STONE and DIETMAR SEYFERTH: The chemistry of silicon involving probable use of *d*-type orbitals 112
CHARLES D. CORYELL and RICHARD C. FIX: The Hammett acidity function $\mathbf{H_0}$ in H_2SO_4-SO mixtures; superacidity 119
G. JANDER und H. KLAUS: Über elektrometrische Titrationen in wasserfreier Essigsäure . 126
R. W. M. D'EYE and P. G. SELLMAN: The thermal decomposition of thorium oxalate . . 143
G. N. WALTON and I. F. CROALL: Chemical effects in fission product recoil 149
F. J. C. ROSSOTTI: The homogeneous exchange reaction between monovalent and trivalent thallium 159
Letter to the Editors:
J. G. CUNINGHAME, J. EAKINS, E. R. MERCER, M. L. SIZELAND and H. H. WILLIS: The rapid separation of rare earth fission products by cation exchange using lactic acid eluant 163

NUMBER 3

T. S. PIPER, F. A. COTTON, and G. WILKINSON: Cyclopentadienyl-carbon monoxide and related compounds of some transitional metals 165
F. A. COTTON, A. D. LIEHR, and G. WILKINSON: Infrared spectra and structures of cyclopentadienyl-carbon monoxide compounds of V, Mn, Fe, Co, Mo, and W 175
B. J. AYLETT, H. J. EMELÉUS, and A. G. MADDOCK: Phosphine and arsine derivatives of monosilane 187
H. J. EMELÉUS, A. G. MACDIARMID, and A. G. MADDOCK: Sulphur and selenium derivatives of monosilane 194
P. E. BROWN, J. M. CRABTREE, and J. F. DUNCAN: The kinetics of the reaction of elementary fluorine with copper metal 202
J. M. CRABTREE, C. S. LEES, and K. LITTLE: The copper fluorides. Part I—X-ray and electron microscope examination 213
E. SAITO et B. LAZARD: Sur l'absence d'effet isotopique dans la réaction d'échange entre l'ion carbonate et l'ion complexe cobalti-carbonato-tétrammine 218
G. JANDER und H. KLAUS: Über den Zustand gelöster Verbindungen in wasserfreier Essigsäure 228
GEORGETTE DELIBRIAS: Dosage de $^{14}CO_2$ dans un compteur C.M. 238

NUMBERS 4/5

F. BROWN, G. R. HALL, and A. J. WALTER: The half-life of Cs^{137} 241
F. BROWN: The yield of Cs^{137} in the pile neutron fission of natural uranium 248
GARMAN HARBOTTLE: The thermal neutron-capture cross-section of radium-223 253
C. I. BROWNE, D. C. HOFFMAN, W. T. CRANE, J. P. BALAGNA, G. H. HIGGINS, J. W. BARNES, R. W. HOFF, H. L. SMITH, J. P. MIZE, and M. E. BUNKER: The decay chain Pu^{245}-Am^{245}-Cm^{245} 254
P. R. FIELDS, M. H. STUDIER, A. M. FRIEDMAN, H. DIAMOND, R. SJOBLOM, and P. A. SELLERS: Production of Pu^{245} and Am^{245} by neutron irradiation of Pu^{244} 262
F. F. MOMYER, Jr., F. ASARO, and E. K. HYDE: Exact alpha particle energies for the isotopes Em^{211}, Em^{210}, EM^{209}, Em^{208} and Fr^{212} 267
F. F. MOMYER, Jr., and E. K. HYDE: The influence of the 126-neutron shell on the alpha-decay properties of the isotopes of emanation, francium and radium 274
R. D. SMITH and A. H. W. ATEN, Jr.: Chemical state of nitrogen-13 formed by the $(n, 2n)$ reaction in solid nitrogen compounds 296
CHR. KLIXBULL JØRGENSEN: Effective quantum numbers in *d*- and *f*-shells 301
E. WAIT: A cubic form of uranium trioxide 309
B. F. HALLAM, O. S. MILLS, and P. L. PAUSON: Dicyclopentadienyldiirontetracarbonyl . . 313
A. E. FINHOLT, GLEN D. BARBARAS, GERALDINE K. BARBARAS, GRANT URRY, THOMAS WARTIK, and H. I. SCHLESINGER: The preparation of sodium and calcium aluminum hydrides . . 317
R. W. M. D'EYE and G. W. BOOTH: The hydrates of thorium tetrafluoride 326

VOL.
1
1955

G. JANDER und H. KLAUS: Die Bestimmung des Ionenprodukts der wasserfreien Essigsäure aus Potentialmessungen 334
Letters to the Editors:
J. S. ANDERSON, I. F. FERGUSON and L. E. J. ROBERTS: Anionic vacancies in fluorite-type oxides 340
R. G. PEARSON, R. E. MEEKER and F. BASOLO: Mechanism of basic hydrolysis of cobalt (III) complexes 341
H. SCHMIED, R. W. FINK and B. L. ROBINSON: The half-life of emanation 220 . . 342

NUMBER 6

D. ENGELKEMEIR, P. R. FIELDS, S. FRIED, G. L. PYLE, C. M. STEVENS, L. B. ASPREY, C. I. BROWNE, H. LOUISE SMITH and R. W. SPENCE: The new isotopes Pu^{244} and Am^{244} 345
D. A. BROWN and H. C. LONGUET-HIGGINS: The vibrational frequencies of diborane . . 352
FREDRIK GRØNVOLD: High temperature X-ray study of uranium oxides in the UO_2—U_3O_8 region 357
J. S. ANDERSON and J. D. M. MCCONNELL: Ruthenium (IV) nitrates 371
J. M. FLETCHER, I. L. JENKINS, F. M. LEVER, F. S. MARTIN, A. R. POWELL and R. TODD: Nitrato and nitro compexes of nitrosylruthenium 378
ROBERT WONG and HERBERT C. BROWN: The catalytic halides—XIII. The interaction of gallium trichloride with ethyl, isopropyl, *n*-propyl and *t*-butyl chlorides 402
Letters to the Editors:
A. G. MACDIARMID and A. G. MADDOCK: The structure of silyl *iso*-thiocyanate . . 411
E. BRODA: Geiger counting of carbon dioxide 411

AUTHOR INDEX

ANDERSON, J. S. pp. 340, 371
ASARO, F. p. 267
ASPREY, L. B. p. 345
ATEN, A. H. W., Jr. p. 296
AYLETT, B. J. p. 187
BALAGNA, J. P. p. 254
BARBARAS, GLEN D. p. 317
BARBARAS, GERALDINE K. p. 317
BARNES, J. W. p. 254
BASOLO, F. p. 341
BEVAN, D. J. M. p. 49
BOOTH, G. W. p. 326
BRODA, E. p. 411
BROWN, D. A. pp. 60, 352
BROWN, F. pp. 241, 248
BROWN, HERBERT C. p. 402
BROWN, P. E. p. 202
BROWNE, C. I. pp. 254, 345
BUNKER, M. E. p. 254
BUTTLAR, HARO VON p. 75
CORYELL, CHARLES D. p. 119
COTTON, F. A. pp. 165, 175
CRABTREE, J. M. pp. 202, 213
CRANE, W. T. p. 254
CROALL, I. F. p. 149
CUNINGHAME, J. G. p. 163
DELIBRIAS, GEORGETTE p. 238
D'EYE, R. W. M. pp. 143, 326
DIAMOND, H. p. 262
DUNCAN, J. F. p. 202
EAKINS, J. p. 163
EMELÉUS, H. J. pp. 1, 187, 194
ENGELKEMEIR, D. p. 345
FERGUSON, I. F. p. 340
FIELDS, P. R. pp. 262, 345
FINHOLT, A. E. p. 317
FINK, R. W. p. 342
FIX, RICHARD C. p. 119
FLETCHER, J. M. p. 378
FRIED, S. p. 345
FRIEDMAN, A. M. p. 262
GLASS, RICHARD A. p. 3
GLENDENIN, L. E. p. 45
GRØNVOLD, FREDRIK p. 357
HALL, G. R. p. 241
HALLAM, B. F. p. 313
HARBOTTLE, GARMAN p. 253
HIGGINS, G. H. p. 254
HOFF, R. W. p. 254
HOFFMAN, D. C. p. 254
HYDE, E. K. pp. 267, 274
JANDER, G. pp. 126, 228, 334
JENKINS, I. L. p. 378
JOHNSON, WARREN, C. p. 1
JØRGENSEN, CHR. KLIXBULL p. 301
KLAUS, H. pp. 126, 228, 334
LAZARD, B. p. 218
LECLAIR, HUGH G. p. 92
LEES, C. S. p. 213
LEVER, F. M. p. 378
LIBBY, W. F. p. 75
LIEHR, A. D. p. 175
LITTLE, K. p. 213
LONGUET-HIGGINS, H. C. pp. 60, 352
MACDIARMID, A. G. pp. 194, 411
MADDOCK, A. G. pp. 187, 194, 411
MARTIN, F. S. p. 378
MCDONNELL, J. D. M. p. 371
MEEKER, R. E. p. 341
MERCER, E. R. p. 163
MILLS, O. S. p. 313
MIZE, J. P. p. 254
MOMYER, F. F., JR. pp. 267, 274
PAUSON, P. L. p. 313
PEARSON, R. G. p. 341
PIPER, T. S. p. 165
POWELL, A. R. p. 378
PYLE, G. L. p. 345
ROBERTS, L. E. J. p. 340
ROBINSON, B. L. p. 342
ROCHOW, EUGENE G. p. 92
ROSSOTTI, F. J. C. p. 159
SAITO, E. p. 218
SCHLESINGER, H. I. p. 317
SCHMIED, H. p. 342
SEABORG, GLENN T. p. 3
SELLERS, P. A. p. 262
SELLMAN, P. G. p. 143
SEYFERTH, DIETMAR p. 112
SIZELAND, M. L. p. 163
SJOBLOM, R. p. 262
SMITH, H. L. p. 254
SMITH, H. LOUISE p. 345
SMITH, R. D. p. 296
SPENCE, R. W. p. 345
STEINBERG, E. P. p. 45
STEVENS, C. M. p. 345
STONE, F. G. A. p. 112
STUDIER, M. H. p. 262
SUTTON, J. p. 68
THOMPSON, STANLEY G. p. 3
TODD, R. p. 378
URRY, GRANT p. 317
WAIT, E. p. 309
WALTER, A. J. p. 241
WALTON, G. N. p. 149
WARTIK, THOMAS p. 317
WILKINSON, G. pp. 165, 175
WILLIS, H. H. p. 163
WONG, ROBERT p. 402

Journal of
Inorganic & Nuclear Chemistry

VOL.
1
1955

In recent years, inorganic chemistry has accomplished a great deal. It seems to be at a stage of rather dramatic expansion into new fields, and the chemistry of a number of hitherto neglected elements has received an enormous stimulus. Inorganic chemistry has long since ceased to be primarily descriptive. Between the wars the subject branched off in at least two new directions as a result of the electronic theory of bonding and of the work on both stable and radioactive isotopes. Since about 1940 we have witnessed two other revolutions in the subject with the coming-of-age of theoretical inorganic chemistry on the one side, and the discovery of the fission process and of the transuranium elements on the other.

The editors and publishers of the new Journal of Inorganic and Nuclear Chemistry which we have pleasure in introducing have not gone light-heartedly into this new venture, but have assured themselves first of all of the support of a great many distinguished American and European chemists. The new journal will be international in character, and will be glad to publish research papers of the necessary scientific standard, wherever they may come from.

We wish the Editors—well known experts in their respective fields—and the Publishers, who have much experience in publishing international research journals, every success in this new venture.

Warren C. Johnson H. J. Emeléus

J. Inorganic and Nuclear Chemistry, 1955, Vol. 1, pp. 3–44. Pergamon Press Ltd., London

VOL.
1
1955

NUCLEAR THERMODYNAMICS OF THE HEAVIEST ELEMENTS[1]

By RICHARD A. GLASS,[2] STANLEY G. THOMPSON, and GLENN T. SEABORG
Radiation Laboratory and Department of Chemistry,
University of California, Berkeley, California

(*Received* 10 *November* 1954)

Abstract—An analysis of the radioactive decay data for the heavy alpha-particle emitting elements has been made in order to apply these data to the calculation of the isotopic masses of the transmercury nuclides. The study includes an interpretation of these results in terms of nuclear stability correlations and their use, together with a number of types of nuclear systematics, for the prediction of nuclear decay properties.

Decay-energy relationships leading to the calculation of masses are presented in the form of closed decay-energy cycles, alpha decay-energy systematics, and beta-decay-energy systematics. Relative masses are calculated from the decay energies and several measured neutron binding energies among the lead isotopes. These masses are determined absolutely when the mass of Pb^{208} is set equal to a measured mass spectrographic value. Once all the masses of the heaviest nuclides are known it is possible to construct the energy surfaces corresponding to this region and study the energetics as a whole. The latter is done in terms of neutron- and proton-binding energy systematics and parameters for the Bohr-Wheeler semi-empirical mass equation. Additional applications of mass data to the calculation of atomic weights and energy balances of induced nuclear reactions concludes the material on masses and their interpretation.

Systematics of alpha, beta, and spontaneous fission half-lives are added to the energy systematics for the purpose of predicting nuclear properties. Predictions of beta-stable isotopes from polonium through element 103 as well as energies and half-lives for selected unknown isotopes are made.

I. INTRODUCTION

THE increasing interest in and research on the chemical and nuclear properties of the heaviest elements and their isotopes has made available in recent years a considerable amount of data which can be used to study the energy relationships between the transmercury nuclides. Because of the phenomenon of alpha decay almost unique to this region of the isotope table, the various nuclides are related by networks of overlapping and branching decays which can be used to accurately define their relative energy content and mass differences. Further, many of the nuclides involved have long half-lives, so that for some isotopes absolute masses and neutron-binding energies have been directly determined. These measurements not only fix the absolute masses of all interrelated isotopes, but also serve to provide checks on the accuracy of the decay data.

Because of the usefulness of such mass data it seemed desirable to make an exhaustive and critical survey of the known transmercury decay data which are used in mass calculations. A number of correlations particularly useful for the present study have previously been discussed by PERLMAN *et al.*[3] in connection with the systematics of alpha decay. Preliminary studies of closed cycles and electron-capture systematics by THOMPSON[4] were used extensively. Further, correlations related to

[1] The literature from which data have been taken has been covered through September, 1954.

[2] This paper is based on part of a dissertation submitted by R. A. GLASS in partial fulfilment of the requirements for the Ph.D. degree in the University of California, June, 1954. For details consult this thesis or University of California Radiation Laboratory Unclassified Report UCRL-2560 (April 1954) (Ref. 2a).

[3] I. PERLMAN, A. GHIORSO, and G. T. SEABORG, *Phys. Rev.*, 77, 26 (1950).

[4] S. G. THOMPSON, *Phys. Rev.*, **76**, 319 (1949).

those of the present paper have been investigated by others for alpha decay,[5, 6] beta-decay energies,[7, 8] masses,[9–11] neutron- and proton-binding energies,[11–19] and Bohr-Wheeler parameters[20–24] in the light- as well as heavy-element region. Some preliminary values of heavy-element masses have been listed by SEABORG,[25] and recently NEWTON[26] has considered heavy-element nuclear properties on a broad basis.

The purpose of the present paper is to collect and tabulate a complete and self-consistent set of masses, neutron- and proton-binding energies, and associated energy correlations. Half-life relationships have also been included because of their predictive value for unknown isotopes as well as their value in testing the reliability of decay data and mass-number assignments. Although the data and correlations are constantly undergoing revision, this will not change significantly the values compiled for the great majority of the nuclides. It is also hoped, however, that one important value of such a compilation will lie in indicating just where more data should be obtained and/or improved.

The material has been arranged in the following manner. An initial discussion of the methods of closed cycles and their use in interrelating the decay energies among the various nuclear types is followed by the methods used to estimate certain decay-energy data not yet available. These latter methods of alpha- and beta-decay energy systematics greatly extend the usefulness and completeness of the actual experimental data themselves. After these sections there follows the calculations and listing of the masses and the nucleon-binding energies.

From these initial compilations certain features of the energy surfaces illuminated by neutron- and proton-binding energy systematics and more quantitative parameters of the Bohr-Wheeler semi-empirical mass equation are discussed. Additional applications of mass data to the calculation of atomic weights and Q values for certain induced reactions are also given. Finally the useful and interesting systematics of alpha, beta, and spontaneous fission half-lives are presented so that suitable predictions can be made for the decay properties of as yet unknown nuclides.

In a nuclear sense, mass data can be considered equivalent to energy data, and

[5] I. PERLMAN and FRANK ASARO, *Ann. Rev. Nuclear Sci.*, **4** (in press).
[6] M. L. CHAUDHURY, *Z. Physik.*, **133**, 561 (1952).
[7] K. WAY and M. WOOD, *Phys. Rev.*, **94**, 119 (1954).
[8] H. E. SUESS and J. H. D. JENSEN, *Arkiv. Fysik*, **3**, 577 (1951).
[9] B. C. HOGG and H. E. DUCKWORTH, *Phys. Rev.*, **91**, 1289 (1953); *Can. J. Phys.*, **32**, 65 (1954).
[10] M. O. STERN, *Revs. Modern Phys.*, **21**, 316 (1949).
[11] J. R. HUIZENGA and L. B. MAGNUSSON, Argonne National Laboratory Unclassified Report ANL-5158 (November 1953).
[12] J. A. HARVEY, *Phys. Rev.*, **81**, 353 (1951); *Can. J. Phys.*, **31**, 278 (1953).
[13] A. H. WAPSTRA, Ph.D. Thesis, University of Amsterdam (published by G. VAN SOEST, Amsterdam, 1953).
[14] A. H. WAPSTRA, *Physica*, **17**, 628 (1951).
[15] A. R. EDMONDS, *Proc. Phys. Soc.* (*London*), **66**, 796 (1953).
[16] B. KARLIK, *Nachr. Akad. Wiss. Wien.*, 217 (1953).
[17] N. FEATHER, *Phil. Mag. Supplement*, **2**, 141 (1953).
[18] S. SENGUPTA, *Phys. Rev.*, **87**, 1136 (1952).
[19] V. A. KRAVTSOV, *Doklady Academy Nauk SSR*, **78**, 43 (1951).
[20] N. BOHR and J. A. WHEELER, *Phys. Rev.*, **56**, 426 (1939).
[21] C. D. CORYELL, *Ann. Rev. Nuclear Sci.*, **2**, 305 (1953). (In this paper the difference $\pi - \nu$ is used to designate δ_{AO}).
[22] C. D. CORYELL, R. A. BRIGHTSEN and A. C. PAPPAS, *Phys. Rev.*, **85**, 732 (1952).
[23] T. P. KOHMAN, *Phys. Rev.*, **85**, 530 (1952).
[24] R. A. BRIGHTSEN, M.S. thesis, Massachusetts Institute of Technology, Cambridge, Massachusetts (1950).
[25] G. T. SEABORG, Third Annual Lecture Series of Phi Lambda Upsilon, Ohio State University (March 1952).
[26] J. O. NEWTON, *Progress in Nuclear Physics* (to be published).

with the further occurrence of closed decay-energy cycles or balances in this region it seems appropriate to consider this material as Nuclear Thermodynamics.[27]

2. DECAY-ENERGY RELATIONSHIPS[28]

A. *Closed Cycles*

The existence of simultaneous alpha and beta instability in the heavy-element nuclides has made it especially convenient to utilize energy balances in what are often termed *closed decay-energy cycles* to examine the internal consistency of the decay data and to predict properties which are unknown. These closed cycles merely reflect the fact that there are many possible energy paths through which various isotopes can be related energetically or masswise. The simplest type of closed cycle is made up of

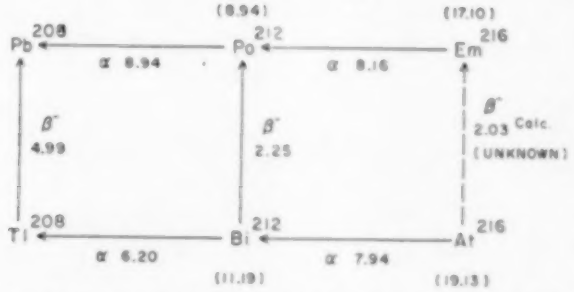

FIG. 1.—Closed decay-energy cycles involving a few nuclides decaying into Pb^{208}. Decay energies given in MeV.

four member nuclides, each one of which may be a member of as many as three other cycles. Such a cycle and its use in calculation of decay energies is illustrated in Fig. 1, which involves the decay of a number of nuclides into a terminal product Pb^{208}. Thus Bi^{212} has 11·9-MeV decay energy with respect to Pb^{208} in its successive beta and alpha decays through either Po^{212} or Tl^{208}. The mass of Bi^{212} is then fixed with respect to Pb^{208}, with checks from both branches of the decay cycle. Proceeding a step further, it can be seen that Em^{216} and At^{216} have 17·10- and 19·13-MeV decay energy, respectively, in relation to Pb^{208}. It follows that At^{216} must be a negative beta emitter (negatron emitter) of 19·13 minus 17·10, or 2·03, MeV, even though the beta decay of this nuclide has not yet been observed. This same process can be extended to include all nuclides of this $4n$ mass type.[30]

Such an energy summation has been made for all of the mass types and is given in Figs. 2 to 5. In some cases as indicated the energy values have been calculated with

[27] It is perhaps trivial to remark that this nomenclature should not be confused with theoretical considerations of level densities, nuclear temperatures, and entropy.

[28] References for energy and half-life data not specifically catalogued in the text will generally be found in the "Table of Isotopes," which is cited as reference 29. Recent data used in the present work but not included in this table are listed and given references in Appendixes I and II. Particle and gamma ray energies making up the total decay energies of closed cycle nuclides are also given in Appendix I for cases where these decay energies are not indicated in the "Table of Isotopes."

The terminology also used by PERLMAN and ASARO (ref. 5) has been adopted in referring to *decay energy* as the Q value for a particular decay process. In the case of alpha particles, the actual particle energy which is measured is of appreciably lower energy because of the kinetic energy imparted to the recoil atom. These measured particle energies will be referred to as *alpha* or *beta particle energies:* decay energy = particle energy × (4 + mass of recoiling nucleus)/(mass of recoiling nucleus).

[29] J. M. HOLLANDER, I. PERLMAN, and G. T. SEABORG, *Revs. Modern Phys.*, **25**, 469 (1953).

[30] As is customary we divide all of the possible alpha emitters into the four classes or mass types, $4n$, $4n + 1$, $4n + 2$, and $4n + 3$. For example, the type $4n + 2$ indicates that all members of the class have mass numbers divisible by four with remainder two.

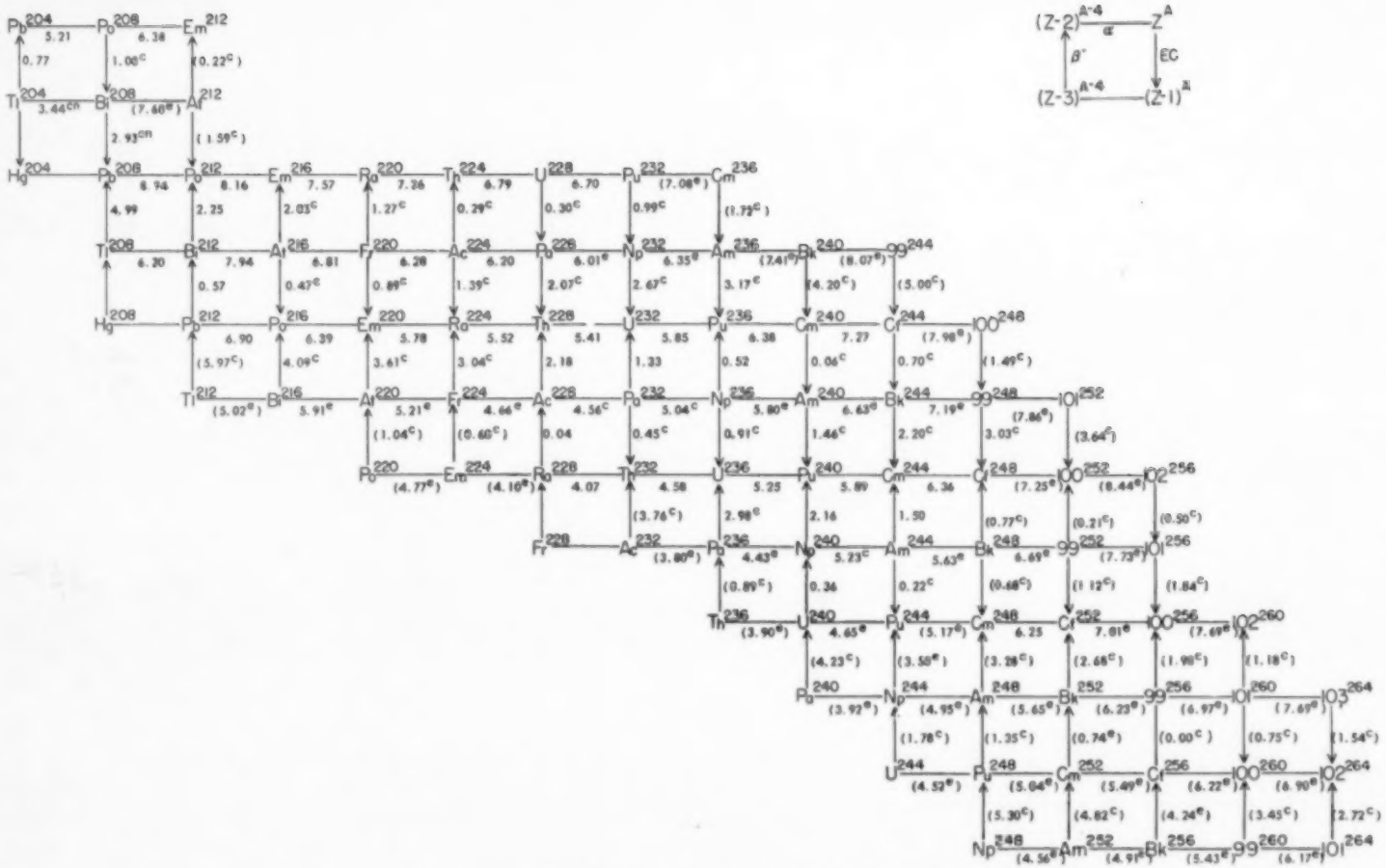

FIG. 2.—Closed decay-energy cycles for the $4n$ series: no superscript, measured energy; *c*, calculated; *cn*, calculated with neutron-binding energies; *e*, estimated; ( ), uncertain.

VOL. 1 1955

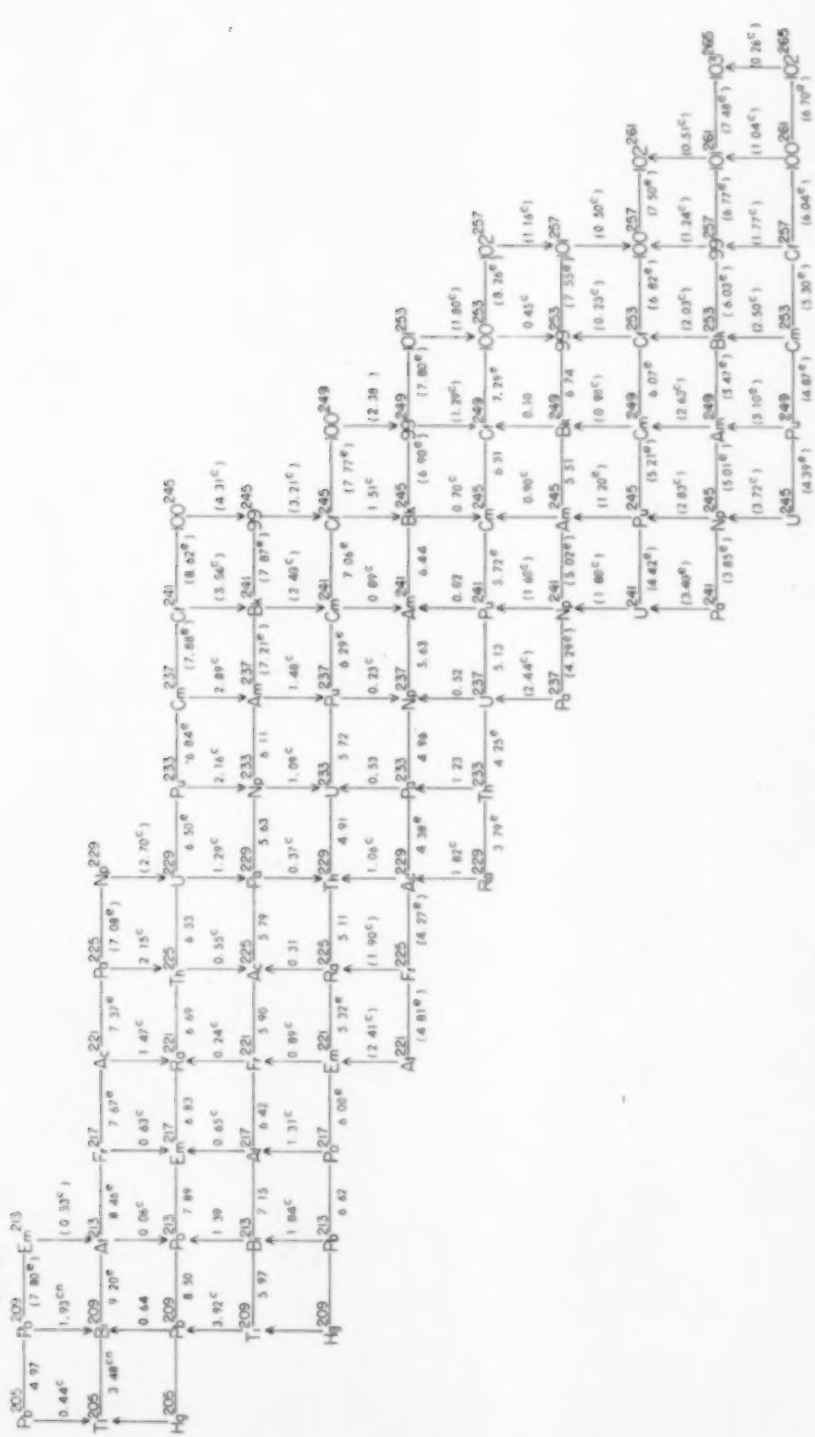

FIG. 3.—Closed decay-energy cycles for the $4n + 1$ series: no superscript, measured energy; *c*, calculated; *cn*, calculated with neutron-binding energies; *e*, estimated; ( ), uncertain.

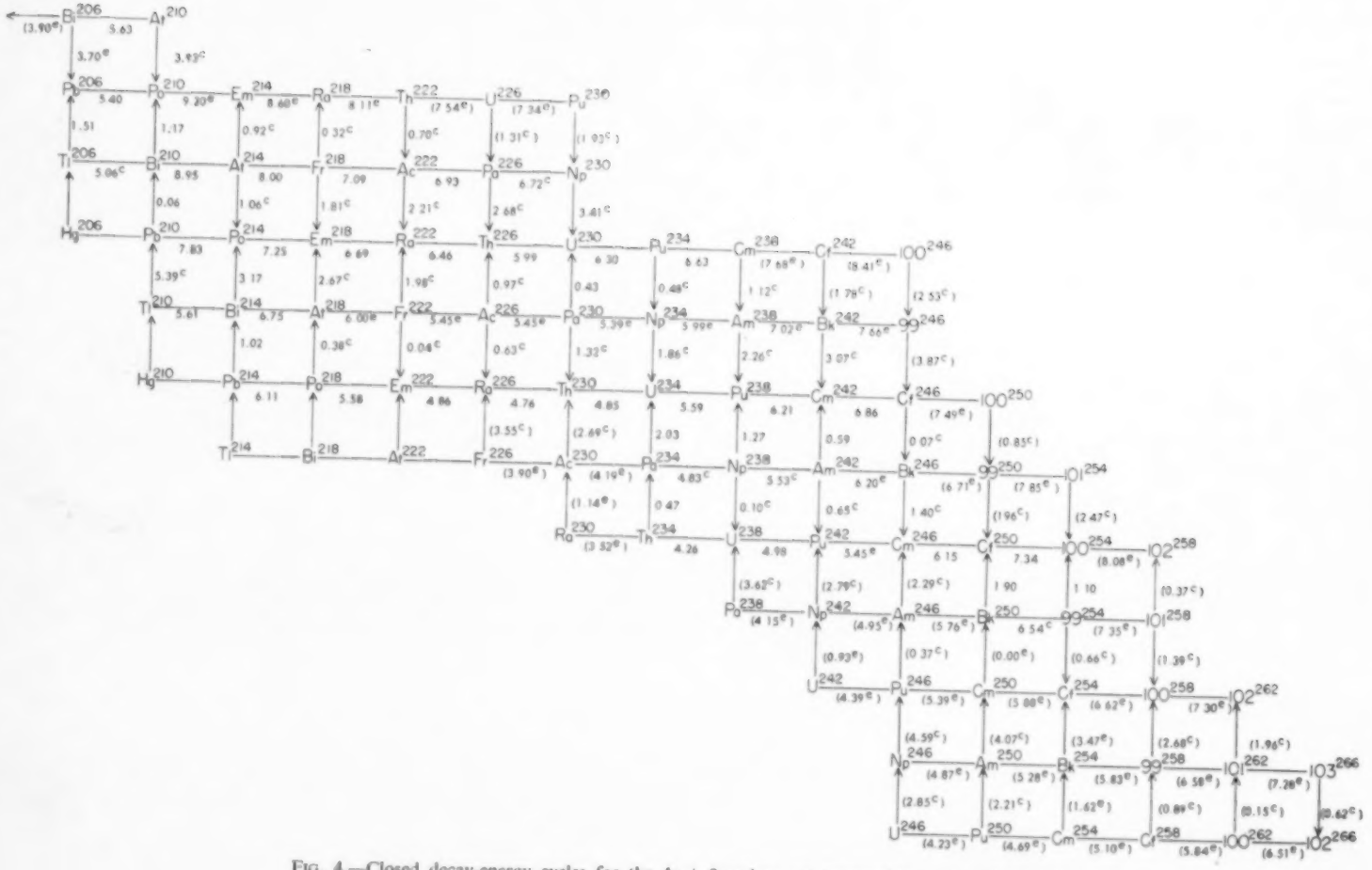

FIG. 4.—Closed decay-energy cycles for the $4n + 2$ series: no superscript, measured energy; *c*, calculated; *cn*, calculated with neutron-binding energies; *e*, estimated; ( ), uncertain.

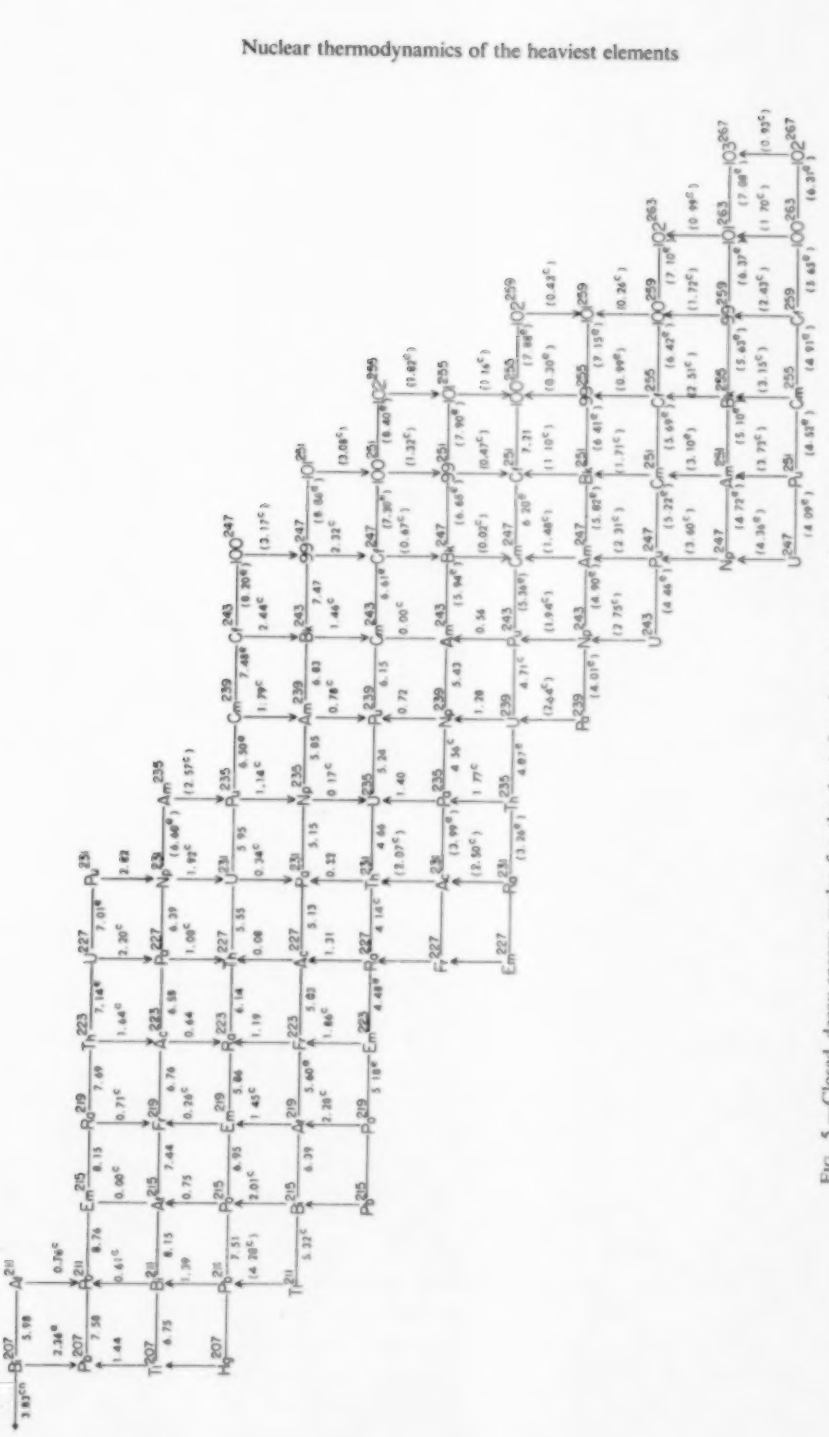

FIG. 5.—Closed decay-energy cycles for the $4n + 3$ series; no superscript, measured energy; c, calculated; e, estimated; ( ), uncertain.

VOL. 1 1955

the aid of neutron-binding energies available for lead and thallium isotopes. Neutron (and proton) binding energy cycles, as contrasted to decay-energy cycles, relate neighbouring isotopes (and isotones) through experimentally determined Q values for certain induced nuclear reactions and some others from calculations involving measured and estimated decay energies. These cycles, similar to those constructed by WAY and WOOD,[7] are given in Fig. 6 and are the mechanism by which the four nuclear mass types can be energetically interrelated.[31]

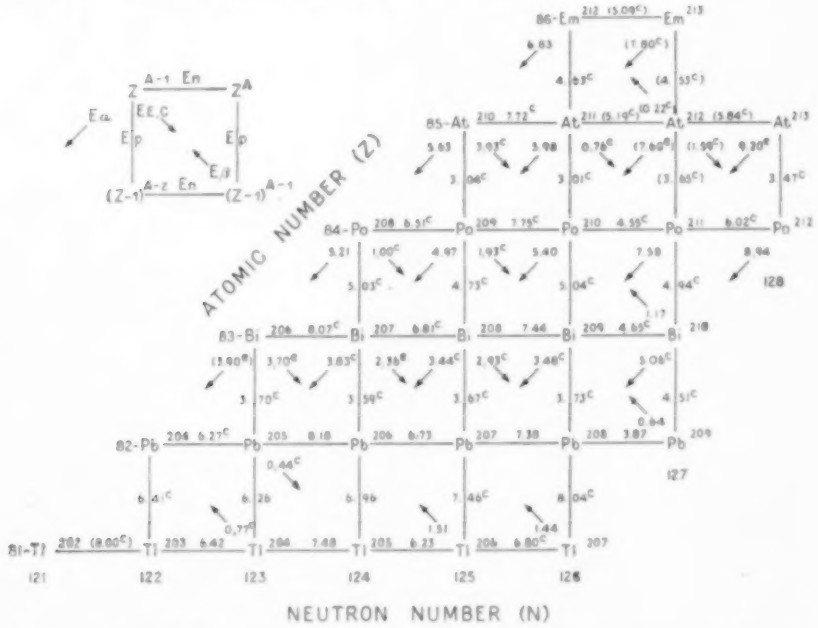

FIG. 6.—Neutron-binding energy cycles in the region of lead: no superscript, measured energy; *c*, calculated from decay and neutron-binding energies; *e*, estimated; ( ), uncertain.

The measured particle energies used are those chosen as the "best" values after a rather extensive and careful selection and with testing for internal consistency. In general the "calculated" energies result from the use of the other three energy values to "close" decay cycles. In some cases, an "estimated" value must be used in order to close a cycle if experimental or previously calculated values are available for only two branches of that cycle. This has been done whenever it was felt that the necessary estimations could be made with sufficient accuracy to be useful. For the alpha-decay process, the estimations were made with facility by extrapolation and interpolation from plots of the mass number against alpha energy (Fig. 7, section B). The beta energies were estimated with considerably less accuracy from similar plots (Fig. 8, section C) taking into account the mass type and properties of analogous nuclides. It

[31] A special type of energy balancing is useful for testing the accuracy of the mass data over the extreme ranges of the mass area being covered. Cycles are constructed between two (or more) isotopes of the same element (e.g. U^{236} and U^{239}) and two other isotopes far removed (e.g., Pb^{206} and Pb^{207}). Thus the two short sides of the cycle are related through neutron-binding energies and cut across different mass types. The two long sides are summations of alpha and beta energies, each of the same mass type. This type of cycle is useful between the Th-U region and Tl-Pb region where experimental neutron-binding energies are available.

VOL.
1
1955

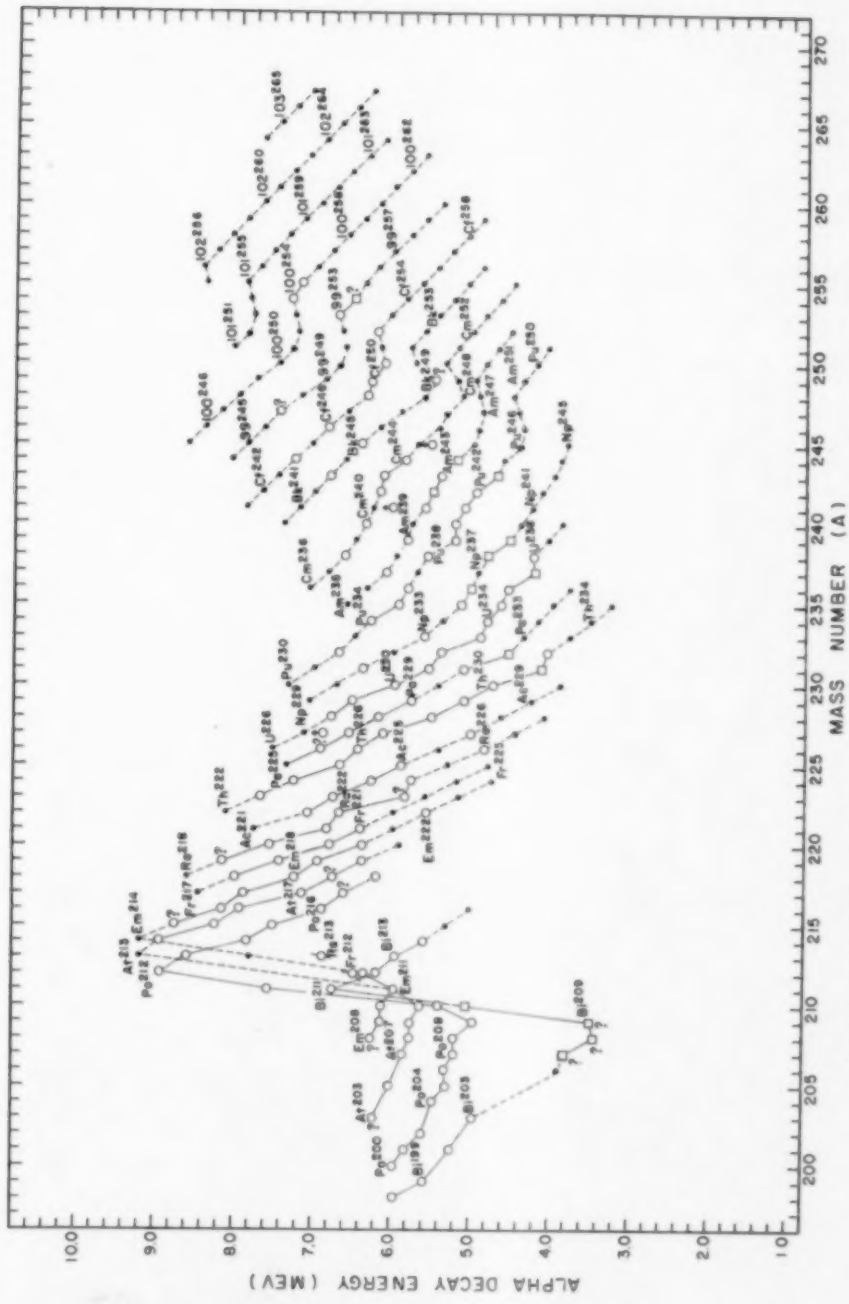

FIG. 7.—Alpha-decay energies for the isotopes of the elements above lead as a function of mass number: ○, experimental energy; □, calculated; •, estimated; ?, energy or mass assignment in question.

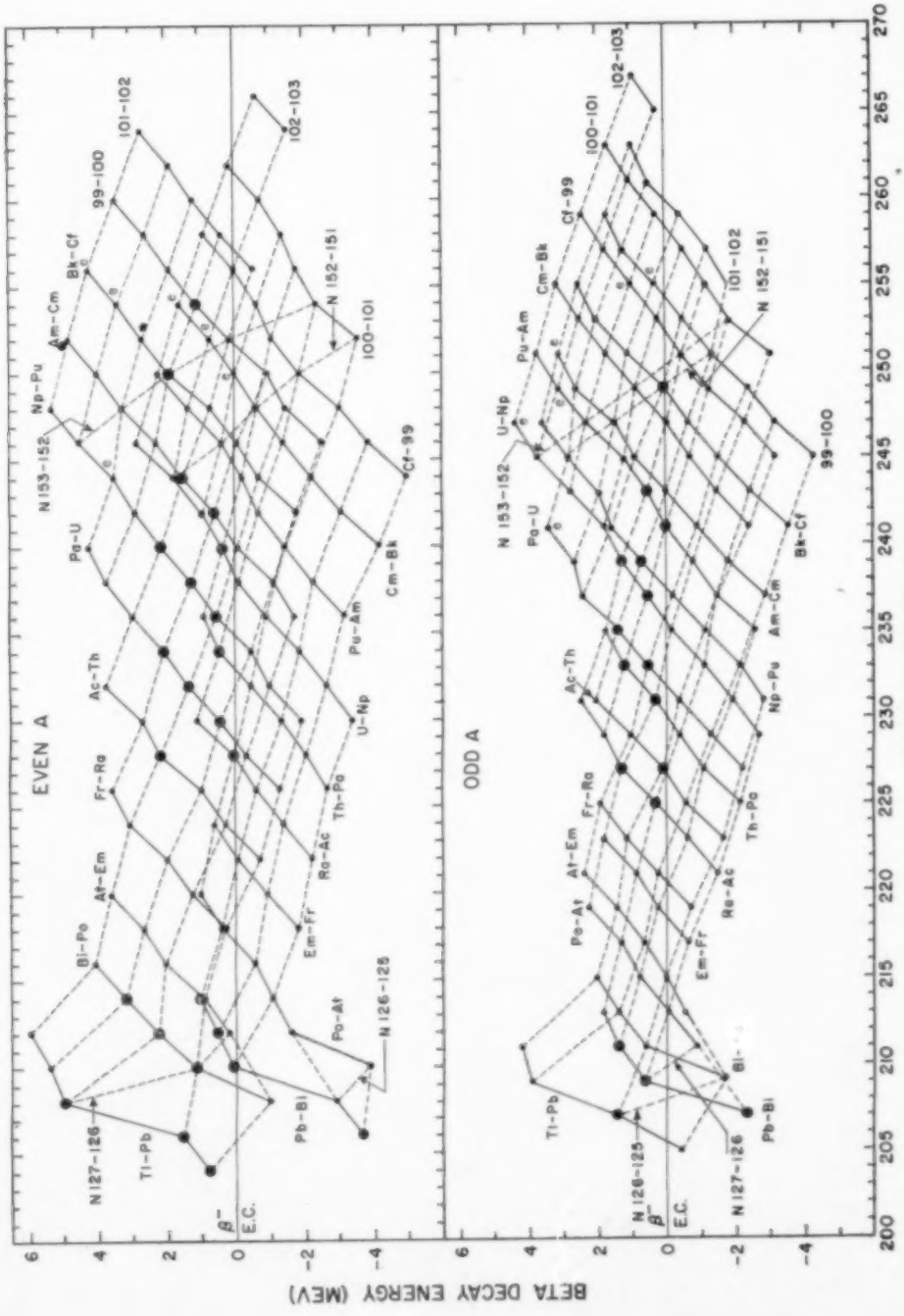

FIG. 8.—Beta-decay energies for the isotopes of the elements above mercury as a function of mass number: ●, experimental energy; •, calculated; ε, estimated.

is in this area of the precise determination of beta-decay energies that the greatest advances are to be made for the improvement of the energy relationships between nuclides. Individual errors arising from inaccurately measured beta-decay energies may sometimes lead to cumulative errors greater than 0·1 MeV.

The sources from which the decay energies were finally tabulated have been summarized in Table 1.

TABLE 1.—SOURCES OF ENERGY VALUES USED IN CLOSED CYCLES[32]

Type	Measured	Calculated	Estimated
Alpha	105	13	179
Negatron	41	108	13
Electron capture	0	116	2
Total	146	237	194
Total known nuclides:	181		
Total unknown nuclides:	163		

VOL. 1 1955

The cross checks provided at many points on the cycles help to minimize errors which might accumulate because of some particularly inaccurate measured values. Considerable care has been taken to minimize the error in the cycles by trial-and-error adjustment of all of the individual legs.[34] It should also be evident that the estimation of both beta- and alpha-decay energies in the manner described is based upon the assumption of a smooth and monatomic energy surface in the region concerned.[35]

[32] The most accurate measurements upon which the cycles are based are the spectrographically determined alpha- and beta-particle energies, accurate to about 0·005 MeV. Alpha energies from more abundant ionization chamber pulse analyzer measurements are usually precise to about 0·02 MeV. Because of the often observed similarity of decay schemes, the interpretation of alpha-decay data is frequently less complex and more certain than that of the beta-decay data. Errors in scintillation counter determinations for beta and gamma energies are comparable to the alpha pulse analyzer measurements, about 0·02 MeV. The greatest uncertainty in beta- and gamma-decay data frequently arises from the interpretation of the decay scheme.

Additional complications arise because of the existence of isomers. For example, it is not known whether the short-lived isomer of Bi^{210}(RaE) or the long-lived one represents the ground state of the nuclide; fortunately the error so introduced can amount to only about 0·03 MeV. The problem is more serious in the Th^{234}(UX − 1)—Pa^{234m}(UX − 2)—Pa^{234}(UZ)—U^{234}(UII) decay chain. In this case the values reported for the isomeric transition in UX −2 range from 0·23[33] to 0·39 MeV[29]. The exact negatron decay energies of Th^{234} and Pa^{234} may thus be in error by this amount. Such an error is, of course, carried into other neighbouring cycles.

[33] P. H. STOKER, M. HEERSHAP, and O. P. HOK, *Physica*, **19**, 433 (1953).

[34] The cycles were actually constructed, in general, in the following manner. (a) Experimentally determined alpha energies and certain estimated values from the alpha-energy systematics (Fig. 7, section B) were initially placed on the cycle diagram for each mass type. (Because of the reliability and uniformity of many of the alpha-emitter decay schemes such estimated values are almost as reliable as the experimental values.) Experimental beta energies were next entered. In principle one experimental beta energy can thus fix all of the other beta energies for one row of cycles, but in actual practice there are frequently others also available. Sometimes two or more beta energies are mutually exclusive and one must resort to further examination of where errors are most likely to have occurred in the reported values. In such cases the beta-energy systematics are extremely useful. It should also be noted that all of the beta energies for one row of cycles have the same neutron excess, designated as isotopic number ($I = A - 2Z$), and for this reason the beta-energy systematics (section *C*) contain lines of constant *I*.

[35] With the exception, of course, of the known effects at closed shells including that region of special stability in the neighbourhood of 152 neutrons which has recently been proposed. (Ref. 35a. A. GHIORSO, S. G. THOMPSON, G. H. HIGGINS, B. G. HARVEY, and G. T. SEABORG, *Phys. Rev.*, **95**, 293 (1954).)

Alpha- and beta-energy estimates and associated calculated energies considered to be uncertain by more than $\pm 0{\cdot}1$ MeV are so indicated in the figures through the use of parentheses.

B. *Alpha Energy Systematics*

The striking regularities in the alpha-decay energies have made it possible to extend the usefulness of the closed cycles by use of estimated decay energies with a high degree of confidence. Fig. 7 is a graph of the alpha-*decay energy* against the mass number for each element, and represents extensions of similar representations made previously.[3] It can be seen that for the elements francium through berkelium the alpha energies generally decrease in a regular fashion with increasing mass number, a consequence of the manner in which the alpha-decay process crosses the energy surfaces.[3] Although there appear to be many small irregularities in most of the lines connecting the isotopes of a given element, the estimates have been made, in general, from smooth lines extending between and beyond the measured values. This course has been followed, since there appears to be, as yet, no systematic reason for the slight deviations or irregularities. For example, although the alpha energies for many nuclides with an even number of protons and an odd number of neutrons are lower than average, those of Th^{227}, U^{229}, and Cm^{243} are somewhat higher. Further, in some cases this odd neutron effect may be due to the fact that the highest energy alpha particle has not yet been observed. In such nuclides the most abundant alpha group leads to an excited state.

The two most striking irregularities occur in the regions of mass numbers corresponding to 126 neutrons and 152 neutrons. The former, associated with the special stability of nuclei with 126 neutrons, is manifested in a discontinuity of approximately 3 to 4 MeV. The latter irregularity, of much smaller extent, can be associated with a "subshell" at 152 neutrons. The reasons for this postulated subshell have already been discussed,[35a] but essentially consist of the fact that the alpha energies for Cf^{250} and Cf^{252} are substantially higher than predicted by a linear extrapolation of the Cf^{244}, Cf^{246}, and Cf^{248} alpha energies. The irregularity is also manifested in Bk^{249}, and apparently in the isotopes of the new elements 99 and 100.

The greatest uncertainties lie in the region of extrapolation into the highest Z and A values. The lines for elements 101, 102, and 103 were placed on the graph by due consideration of the spacings and slopes of the admittedly poorly defined lines for elements 99 and 100. Should there occur some sudden change in the nature of the HEISENBERG[36] valley of the energy surfaces at these higher mass and Z values the values will be in somewhat more error. These lines should, however, provide very useful aids for predictive purposes.

It is perhaps of interest to note that other more limited correlations are frequently of use in many cases. For example, a nearly linear function is obtained when alpha energies for isotopes of the same neutron number are compared. Thus the line connecting the alpha energies of U^{238}, Np^{239}, Pu^{240}, Am^{241}, Cm^{242}, Bk^{243}, and Cf^{244} is useful in predicting energies for 99^{245} and 100^{246}.

C. *Beta Energy Systematics*

The beta-decay energies have been correlated with mass number and are given in Fig. 8 in a manner similar to the alpha energy graphs. In this case, however, two

[36] W. HEISENBERG, *Z. Physik*, **78**, 156 (1932).

different graphs are clearly indicated for the two different even and odd mass types. Further, it has been convenient to connect the same isotopic numbers ($I = A - 2Z$) for reasons discussed in reference 7. Similar graphs have been given by WAY and WOOD[7] and by SUESS and JENSEN.[8] Because of the nature of the shell effects, no estimations are given for any nuclides either at or decaying into the proposed 152-neutron subshell.

Aside from the predictions of absolute beta-decay energies, the beta systematics are also useful in defining the beta-stable species in which energy is not available for either negatron emission or electron capture.

3. MASSES AND BINDING ENERGIES[37]

Although the closed cycles fix the relative energies for each of the four mass types, it is obviously desirable to be able to further interrelate these types with each other, which can be done through the use of the proper neutron-binding energies. It would then, in principle, be necessary to know one absolute mass and thus fix the absolute masses of all the other nuclides. In practice, of course, more than one absolute mass is known, but it is still advantageous to use one mass as the absolute standard from which all others are calculated.

VOL. 1 1955

With regard to relating the four mass types, advantage is taken of data from certain nuclear reactions: (a) energy thresholds for reactions such as $Pb^{207}(\gamma, n)Pb^{206}$, (b) determination of the capture gamma-ray spectra in a reaction of the type $Pb^{207}(n, \gamma)Pb^{208}$, and (c) measurement of the deuteron and proton energies in a reaction like $Pb^{208}(d, p)Pb^{209}$. From the results of such determinations (see summary in Table 2 of Appendix II) the following averages of neutron-binding energies have been adopted for interrelating energetically the four mass types: $Pb^{206-207}$, 6·73 MeV; $Pb^{207-208}$, 7·38 MeV; and $Pb^{208-209}$, 3·87 MeV.

The absolute masses of the nuclides then have been calculated from their energies relative to the absolute mass of Pb^{208}, for which the values of $208{\cdot}0410 \pm 0{\cdot}0015$[38] and $208{\cdot}0409 \pm 0{\cdot}0013$[39] have been reported as a result of time-of-flight and magnetic-mass spectrographic measurements, respectively. The value adopted for this compilation is 208·04100 (physical scale).[40] This number of significant figures is carried throughout the calculations to be consistent with the *relative* accuracy of many of the energy values. Additional quantities used were the mass of the helium atom, 4·00387;[41] mass of the neutron, 1·00898;[41] and energy equivalent of mass, 931·2 MeV.[42] The atomic mass values are summarized in Table 2, where uncertain values are given in parentheses.

The proton-binding energies (not yet susceptible to direct measurement) and additional neutron-binding energies were calculated from the mass values given in Table 2, using the value 1·00814[41] for the mass of the proton. Measured neutron-binding energies and masses in addition to those selected as a basis for the mass

[37] Measured neutron-binding energies and masses are catalogued in Appendix II. The neutron-binding energy of a nuclide is the "separation" energy between the given nuclide and the isotope with one less neutron. Thus, the neutron-binding energy of Pb^{207} can be represented as $Pb^{206-207}$.

[38] P. I. RICHARDS, E. E. HAYS, and S. A. GOUDSMIT, *Phys. Rev.*, **85**, 630 (1952).

[39] G. S. STANFORD, H. E. DUCKWORTH, B. C. HOGG, and J. S. GEIGER, *Phys. Rev.*, **85**, 1039 (1952).

[40] After a careful study of measured masses and decay-energy data, HUIZENGA and MAGNUSSON (see Ref. 11) calculated an overall average mass for Pb^{208} of $208{\cdot}0411 \pm 0{\cdot}0012$. The mass of Pb^{208} determined by RICHARDS *et al.* (see Ref. 38) that was selected as the basis for the present calculated masses is very close to this value and well within the limits of error.

[41] F. AJZENBERG and T. LAURITSEN, *Revs. Modern Phys.*, **24**, 321 (1952).

[42] J. W. DUMOND and E. R. COHEN, *Revs. Modern Phys.*, **25**, 691 (1953).

TABLE 2.—MASSES AND NEUTRON- AND PROTON-BINDING ENERGIES OF THE TRANSMERCURY NUCLIDES

The bases for the following are:

1. Mass of $Pb^{208} = 208.04100$
   $He^4 = 4.00387$
   $_0n^1 = 1.00898$
   $H^1 = 1.00814$

2. Neutron binding energies
   $Pb^{206-207} = 6.73$ MeV
   $Pb^{207-208} = 7.38$ MeV
   $Pb^{208-209} = 3.87$ MeV

3. One atomic mass unit = 931.2 MeV

Element and Mass	Binding Energies (MeV)		Element and Mass	Binding Energies (MeV)	
	En	Ep		En	Ep
81—Thallium			84—Polonium		
(202.03411)			208.04522		5.03
203.03450	(8.00)		209.04721	6.51	4.73
204.03658	6.42 (meas)		210.04786	7.75	5.04
205.03753	7.48 (meas)		211.05196	4.55	4.94
206.03982	6.23 (meas)		212.05447	6.02	5.85
207.04149	6.80		213.05882	4.31	5.78
208.04636	3.83		214.06146	5.90	6.51
209.05003	4.94		215.06604	4.10	6.49
210.05497	3.76		216.06878	5.81	7.04
(211.05861)	(4.97)		217.07327	4.18	7.49
(212.06391)	(3.43)		218.07639	5.45	
			219.08138	3.72	
82—Lead			(220.08450)	(5.45)	
204.03576		6.41			
205.03800	6.27	6.26	85—Astatine		
206.03820	8.18 (meas)	6.96	210.05208		3.04
207.03995	6.73 (meas)	7.46	211.05292	7.72	3.01
208.04100	7.38 (meas)	8.04	(212.05618)	(5.19)	(3.65)
209.04582	3.87 (meas)	8.08	213.05889	(5.84)	3.47
210.04919	5.23	8.37	214.06260	4.90	4.06
211.05410	3.78	8.39	215.06523	5.91	4.07
212.05750	5.20	(8.62)	216.06928	4.59	4.56
213.06229	3.90	(9.09)	217.07186	5.96	4.71
214.06596	4.94		218.07599	4.52	5.05
			219.07893	5.62	5.22
83—Bismuth			220.08339	4.21	5.71
206.04217		3.70	(221.08617)	(5.77)	(6.03)
207.04248	8.07	3.59			
208.04415	6.81	3.67	86—Emanation		
209.04514	7.44 (meas)	3.73	212.05594		4.63
210.04912	4.65	4.51	(213.05945)	(5.09)	(4.53)
211.05261	5.11	4.39	214.06161	(6.35)	5.04
212.05689	4.38	4.99	215.06523	4.99	5.13
213.06031	5.17	4.96	216.06710	6.62	5.84
214.06487	4.12	5.18	217.07116	4.58	5.83
215.06820	5.26	5.50	218.07312	6.54	6.41
216.07317	3.73		219.07737	4.40	6.29

TABLE 2 (*continued*)

Element and Mass	Binding Energies (MeV)		Element and Mass	Binding Energies (MeV)	
	En	Ep		En	Ep
86—Emanation —*contd*			90—Thorium —*contd*		
220·07951	6·37	7·04	225·09342	5·89	5·40
221·08358	4·57	7·40	226·09498	6·91	5·58
222·08626	5·87	(7·50)	227·09800	5·55	5·74
223·09081	4·12		228·09939	7·07	6·37
(224·09350)	(5·86)		229·10252	5·44	6·84
			230·10433	6·68	6·96
87—Francium			231·10781	5·12	7·03
217·07184		3·17	232·11001	6·31	7·60
218·07506	5·36	3·95	233·11356	5·06	8·04
219·07709	6·47	3·88	234·11609	6·00	
220·08047	5·22	4·70	235·12009	4·64	
221·08263	6·35	4·68	(236·12296)	(5·69)	
222·08630	4·94	5·05			
223·08881	6·02	5·20	91—Protactinium		
224·09285	4·60	5·68	225·09573		2·96
(225·09521)	(6·17)	(5·99)	226·09786	6·38	3·45
(226·09916)	(4·68)		227·09916	7·15	3·69
			228·10161	6·08	4·22
88—Radium			229·10292	7·14	4·29
218·07472		4·90	230·10575	5·73	4·58
219·07786	5·44	4·98	231·10746	6·76	4·66
220·07910	7·20	5·71	232·11049	5·54	5·08
221·08237	5·32	5·81	233·11223	6·74	5·51
222·08417	6·68	6·14	234·11559	5·24	5·69
223·08754	5·23	6·43	235·11819	5·94	5·63
224·08959	6·45	6·86	236·12200	4·81	5·80
225·09317	5·03	7·29	(237·12461)	(5·93)	6·23
226·09535	6·33	(7·45)	(238·12842)	(4·81)	
227·09949	4·50	(7·27)	(239·13116)	(5·81)	
228·10177	6·24		(240·13556)	(4·27)	
229·10562	4·78		(241·13867)	(5·46)	
(230·10844)	(5·73)				
(231·11272)	(4·38)		92—Uranium		
			(226·09927)		(4·29)
89—Actinium			227·10152	(6·26)	4·17
221·08395		3·07	228·10193	7·98	5·00
222·08655	5·94	3·69	229·10431	6·15	5·07
223·08822	6·80	3·81	230·10528	7·45	5·38
224·09108	5·70	4·28	231·10783	5·99	5·64
225·09283	6·73	4·56	232·10907	7·21	6·09
226·09602	5·39	4·92	233·11167	5·94	6·49
227·09809	6·44	5·03	234·11341	6·74	6·49
228·10173	4·97	5·50	235·11668	5·31	6·56
229·10366	6·56	5·82	236·11880	6·39	7·01
(230·10722)	(5·05)	(6·09)	237·12199	5·39	7·59
(231·11003)	(5·74)	(6·10)	238·12454	5·99	(7·65)
(232·11405)	(4·62)	(6·34)	239·12833	4·83	(7·67)
			240·13101	5·86	(7·72)
90—Thorium			(241·13502)	(4·63)	(8·08)
222·08730		4·46	(242·13775)	(5·82)	(8·44)
223·08998	5·86	4·38	(243·14229)	(4·13)	
224·09077	7·63	5·21			

VOL. 1 1955

TABLE 2 (*continued*)

Element and Mass	Binding Energies (MeV)		Element and Mass	Binding Energies (MeV)	
	En	Ep		En	Ep
92—Uranium —*contd*			95—Americium (235·12085)		(2·99)
(244·14555)	(5·33)		236·12262	6·71	3·36
(245·15067)	(3·59)		237·12327	7·76	3·81
(246·15432)	(4·96)		238·12571	6·09	3·83
(247·15950)	(3·54)		239·12702	7·14	4·10
			240·12988	5·70	4·14
			241·13135	6·99	4·75
93—Neptunium (229·10720)		(2·67)	242·13445	5·47	4·71
230·10895	6·74	3·26	243·13665	6·31	4·88
231·10989	7·48	3·29	244·14011	5·14	4·92
232·11193	6·46	3·76	245·14235	6·28	5·28
233·11284	7·52	4·07	(246·14594)	(5·02)	(5·44)
234·11540	5·97	4·10	(247·14847)	(6·00)	(5·59)
235·11687	7·00	4·36	(248·15282)	(4·31)	(5·84)
236·11978	5·65	4·70	(249·15593)	(5·47)	(6·04)
237·12143	6·82	5·13	(250·16036)	(4·23)	(6·55)
238·12464	5·37	5·11	(251·16376)	(5·20)	(6·63)
239·12695	6·21	5·33	(252·16873)	(3·73)	(6·68)
240·13063	4·94	5·44			
(241·13309)	(6·07)	(5·65)	96—Curium (236·12447)		(4·21)
(242·13675)	(4·95)	(5·97)	237·12637	6·59	4·09
(243·13934)	(5·95)	(6·10)	238·12691	7·86	4·19
(244·14364)	(4·36)	(6·33)	239·12894	6·47	4·57
(245·14668)	(5·53)	(6·53)	240·12994	7·43	4·86
(246·15126)	(4·09)	(7·03)	241·13230	6·16	5·32
(247·15482)	(5·05)	(7·12)	242·13382	6·95	5·28
(248·15996)	(3·57)	(7·15)	243·13665	5·72	5·53
			244·13850	6·64	5·86
			245·14138	5·68	6·40
94—Plutonium (230·11102)		(4·03)	246·14348	6·41	6·53
231·11292	6·59	3·88	(247·14688)	(5·19)	(6·70)
232·11300	8·29	4·69	(248·14930)	(6·11)	(6·81)
233·11516	6·35	4·58	(249·15310)	(4·82)	(7·32)
234·11592	7·65	4·71	(250·15599)	(5·67)	(7·52)
235·11809	6·34	5·08	(251·16043)	(4·23)	(7·52)
236·11922	7·31	5·39	(252·16355)	(5·45)	(7·77)
237·12168	6·07	5·81	(253·16836)	(3·89)	(7·93)
238·12328	6·87	5·86	(254·17164)	(5·30)	
239·12618	5·66	6·15	(255·17649)	(3·85)	
240·12831	6·38	6·32			
241·13137	5·51	6·89	97—Berkelium (240·13445)		(2·45)
242·13375	6·14	(6·96)	(241·13488)	(7·96)	(2·98)
243·13726	5·10	(7·11)	242·13712	(6·28)	3·10
244·13988	5·92	(7·08)	243·13822	7·33	3·48
245·14364	(4·86)	(7·58)	244·14087	5·90	3·66
(246·14633)	(5·85)	(7·90)	245·14213	7·18	4·20
(247·15095)	(4·06)	(7·87)	246·14499	5·71	4·23
(248·15427)	(5·27)	(8·09)	(247·14690)	(6·57)	(4·39)
(249·15926)	(3·72)	(8·24)	248·15003	(5·45)	(4·65)
(250·16274)	(5·12)		249·15214	6·40	(4·94)
(251·16776)	(3·68)		250·15599	4·77	(4·89)

TABLE 2 (*continued*)

Element and Mass	Binding Energies (MeV)		Element and Mass	Binding Energies (MeV)	
	En	Ep		En	Ep
97—Berkelium —*contd*			100—*contd*		
(251·15859)	(5·94)	(5·16)	(249·15597)	(6·58)	(4·31)
(252·16276)	(4·48)	(5·41)	(250·15697)	(7·43)	(4·27)
(253·16567)	(5·65)	(5·61)	(251·15933)	(6·16)	(4·53)
(254·16990)	(4·42)	(6·14)	(252·16086)	(6·94)	(4·84)
(255·17310)	(5·38)	(6·22)	253·16373	(5·69)	5·12
(256·17787)	(3·92)	(6.29)	254·16570	6·52	5·29
			255·16902	5·27	5·59
98—Californium			(256·17128)	(6·26)	(5·78)
(241·13870)		(3·62)	(257·17468)	(5·19)	(6·31)
(242·13903)	(8·06)	(3·72)	(258·17716)	(6·06)	(6·52)
243·14084	(6·67)	4·11	(259·18117)	(4·62)	(6·52)
244·14162	7·64	4·42	(260·18387)	(5·85)	(6·79)
245·14375	6·37	4·89	(261·18827)	(4·26)	(6·93)
246·14506	7·15	4·86	(262·19113)	(5·72)	
247·14762	5·97	5·12	(263·19556)	(4·24)	
248·14920	6·89	(5·44)			
249·15203	5·73	5·72	101		
250·15395	6·57	5·89	(251·16264)		(2·30)
(251·15741)	(5·14)	(6·26)	(252·16477)	(6·38)	(2·52)
(252·15988)	(6·06)	(6·38)	(253·16566)	(7·53)	(3·11)
(253·16349)	(5·00)	(6·90)	(254·16836)	(5·85)	(3·27)
(254·16618)	(5·86)	(7·11)	(255·17027)	(6·58)	(3·33)
(255·17041)	(4·42)	(7·11)	(256·17225)	(5·58)	(3·64)
(256·17332)	(5·65)	(7·38)	(257·17522)	(6·53)	(3·91)
(257·17792)	(4·08)	(7·54)	(258·17865)	(5·17)	(3·89)
(258·18099)	(5·50)		(259·18089)	(6·27)	(4·10)
(259·18563)	(4·04)		(260·18467)	(4·84)	(4·32)
			(261·18716)	(6·05)	(4·52)
99			(262·19097)	(4·81)	(5·07)
(244·14699)		(1·86)	(263·19373)	(5·79)	(5·16)
(245·14720)	(8·16)	(2·38)	(264·19807)	(4·32)	(5·24)
(246·14921)	(6·49)	(2·50)			
(247·15011)	(7·52)	(2·87)	102		
(248·15246)	(6·18)	(3·08)	(255·17222)		(3·98)
(249·15341)	(7·47)	(3·66)	(256·17379)	(6·90)	(4·30)
(250·15606)	(5·90)	(3·83)	(257·17647)	(5·87)	(4·59)
(251·15791)	(6·63)	(3·89)	(258·17825)	(6·70)	(4·76)
252·16108	(5·41)	4·16	(259·18136)	(5·47)	(5·06)
253·16324	6·35	4·45	(260·18341)	(6·45)	(5·24)
254·16688	4·97	(4·42)	(261·18661)	(5·38)	(5·78)
(255·16934)	(6·07)	(4·63)	(262·18886)	(6·26)	(5·99)
(256·17332)	(4·66)	(4·87)	(263·19267)	(4·82)	(6·00)
(257·17602)	(5·85)	(5·07)	(264·19515)	(6·05)	(6·25)
(258·18003)	(4·61)	(5·61)	(265·19934)	(4·46)	(6·40)
(259·18302)	(5·58)	(5·69)	(266·20199)	(5·89)	
(260·18757)	(4·12)	(5·77)	(267·20620)	(4·45)	
			103		
100			(264·19680)		(3·73)
(245·15183)		(3·07)	(265·19906)	(6·26)	(3·94)
(246·15193)	(8·27)	(3·18)	(266·20266)	(5·01)	(4·49)
(247·15352)	(6·88)	(3·57)	(267·20520)	(5·99)	(4·59)
(248·15406)	(7·86)	(3·91)			

VOL. 1 1955

calculations are given in Table 1 of Appendix II, and a comparison afforded with calculated values. With Pb^{208} as the adopted absolute mass standard, it can be seen that the values have been adjusted so that only the mass of Pb^{207} appears to be just outside the quoted limits of error. Further, for the neutron-binding energies the measured values reported agree well with the calculated values except for Bi^{210} and possibly also U^{239}, whose calculated value is only slightly outside the quoted error for the measured value. The Bi^{210} neutron-binding energy has been discussed in detail previously by others,[11, 13] and the conclusion that the measured values are low and merely represent lower limits is further attested to in the present comparison.

4. DISCUSSION

A. *Energy Surfaces*

A very interesting use of the mass data is found in construction of energy surfaces for the heavy-nuclide region. There are four nearly parallel energy surfaces to be considered, which correspond to the four nuclear types.[43] A combined single surface has previously been constructed[3] with the object of relating alpha-decay-energy trends to the energy surface. The other energy systematics can also be related to the energy surfaces. Whereas individual alpha-decay energies are represented by lines on the energy surfaces in a direction forming a small angle with the line of maximum beta stability at the bottom of the Heisenberg valley, and thus are related to the slope along its length, beta-decay energies are represented by lines of constant A and outline the curvature of the valley.

Certain features on the energy surfaces can also be emphasized with the aid of the various calculated energy systematics. Thus, a sequence of beta disintegrations together with the assumption of a parabolic energy surface[44] is used to calculate parameters for the Bohr-Wheeler mass equation,[20, 21] which not only yield quantitative information about the curvature of the energy surfaces, but the separation energy between the surfaces as well. Nucleon-binding energies calculated from the masses likewise describe energy differences along different paths crossing the energy surfaces. In the following sections the nucleon-binding energies and Bohr-Wheeler parameters are discussed.

B. *Binding Energy Systematics*

As can be seen from Table 2, Appendix II, only a few neutron-binding energies in the lead and thorium regions have been measured directly. Others, as well as the proton-binding energies, have been calculated for all of the closed-cycle nuclides and are tabulated in Table 2, where uncertain values are given in parentheses. A number of previous studies of the systematics of these binding energies[11–19] have clearly pointed out the shell effect of the 126-neutron closed shell as well as other regularities.

The neutron- and proton-binding energies listed in Table 2 have been plotted against mass number for each element in Figs. 9 and 10, respectively. The neutron-binding energies for the even neutron and odd neutron isotopes of each element decrease regularly with increasing mass number. As expected, the neutron-binding

[43] Four types of nuclides can be distinguished according to whether all neutrons and protons in the nucleus can be paired (even-even nuclides); one neutron is left unpaired (even-odd); one proton is left unpaired (odd-even); or both one proton and one neutron are left unpaired (odd-odd). The order given is that of decreasing stability for the configuration.

[44] G. GAMOW, *Z. Physik*, **89**, 592 (1934).

VOL. 1 1955

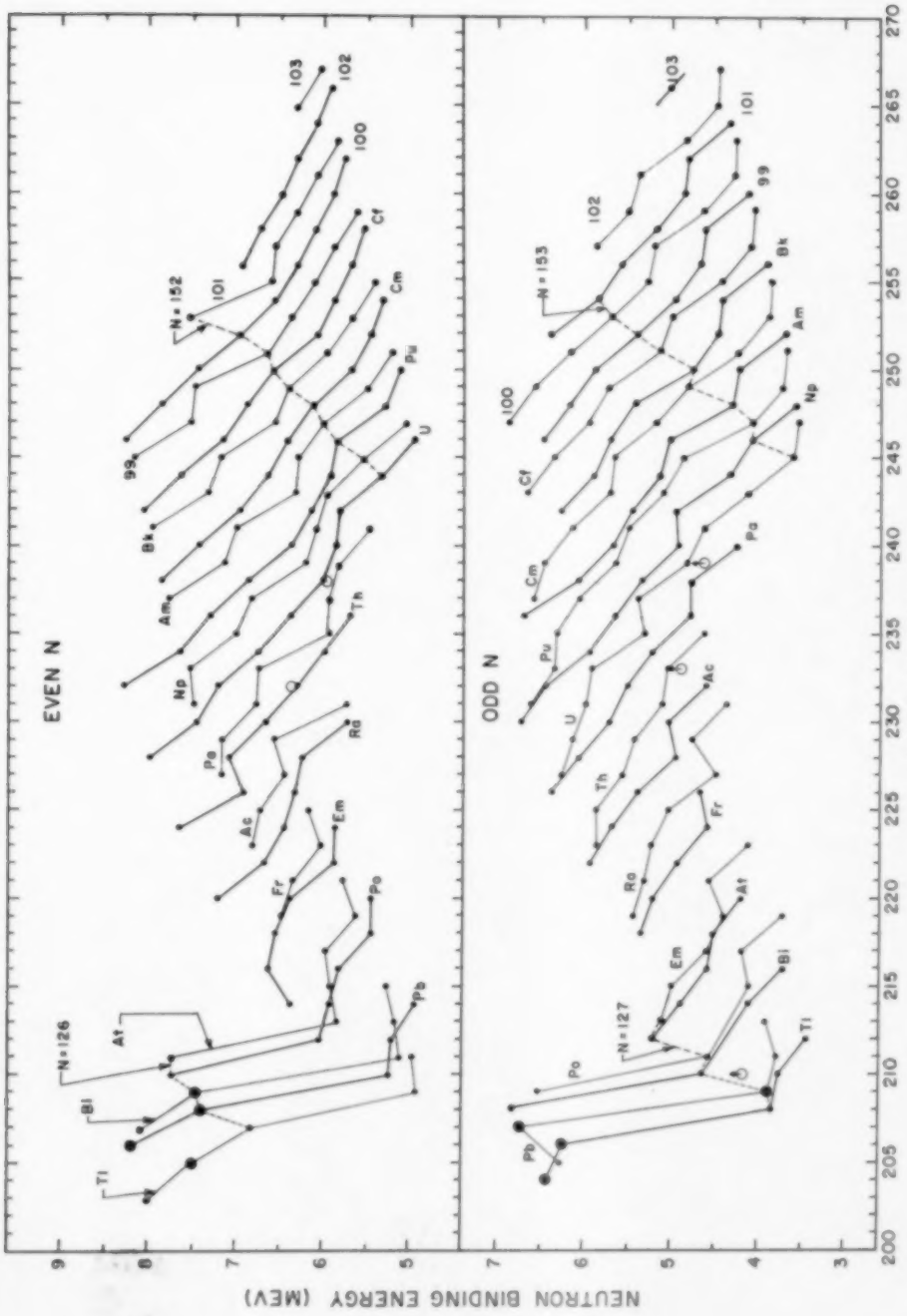

FIG. 9.—Neutron-binding energies for the isotopes of the elements above mercury as a function of mass number: ●, ○, experimental energy; •, calculated.

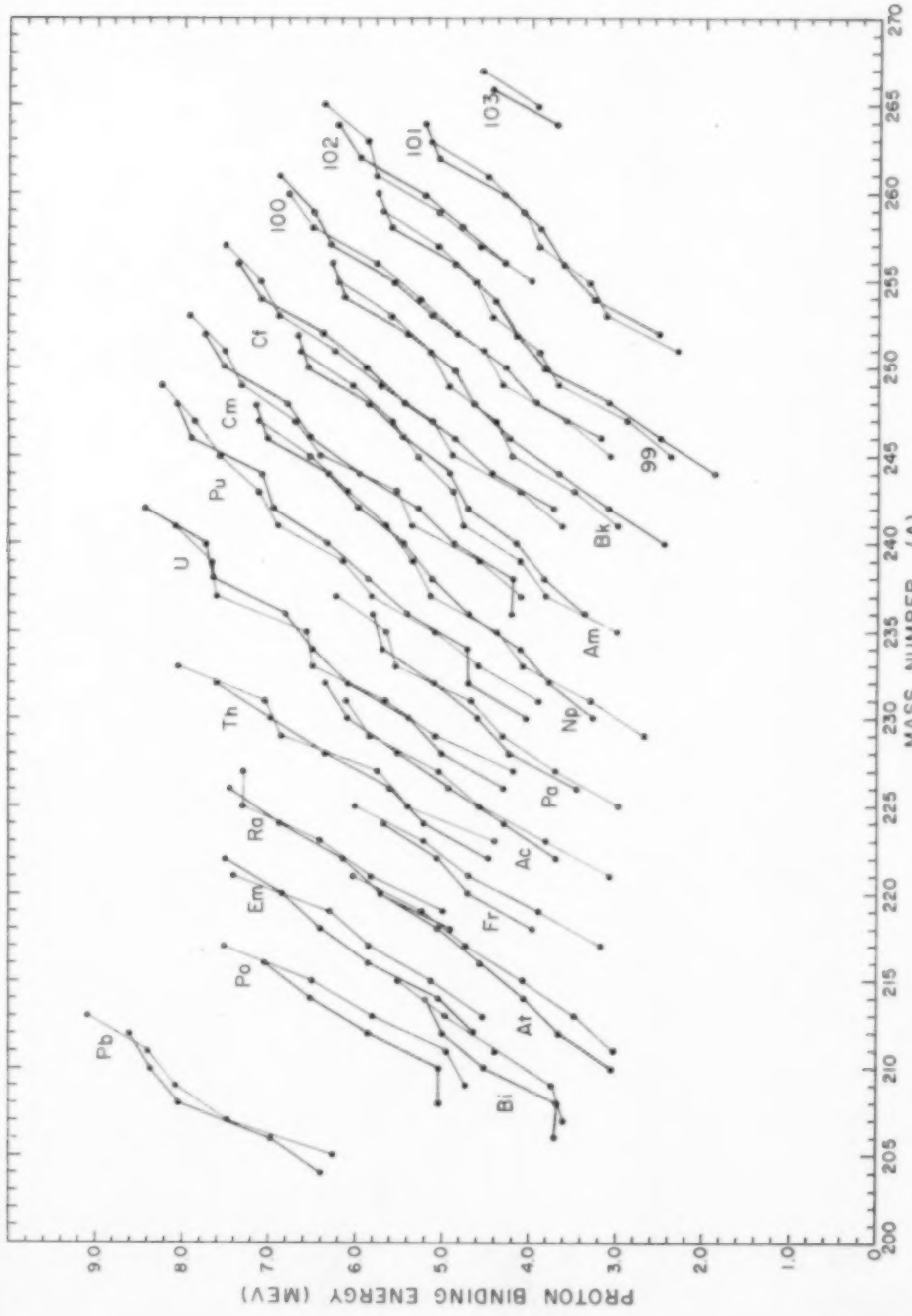

FIG. 10.—Proton-binding energies for the isotopes of the elements above thallium as a function of mass number: •, calculated energy.

energies for nuclides with an even number of neutrons are higher than those for nuclides with an odd number.

The proton-binding energies increase regularly with increasing mass number for each element as expected. For both the neutron- and proton-binding energies, as either type particles tend to become in relative excess, their binding energies decrease. The proton-binding energies for each element, unlike the neutron-binding energies, show only a small alternation in magnitude because of odd-even effects. The explanation probably lies in the different energy surfaces spanned by these separation energies. For both proton- and neutron-binding energies of the isotopes of an element, the Z relations between connected nuclides are constant. The situation with N relations, however, is quite different. Proton-binding energies always connect nuclides with the same neutron number, whereas neutron-binding energies alternately relate even and odd neutron numbers, which results in the fluctuations observed. The energy surfaces for the four nuclear types are further discussed in the next section.

VOL. 1 1955

The irregularities in the lines may be in part due to cumulative errors in decay energies. The sudden decrease of neutron-binding energies after the 126-neutron closed shell, however, is a real and striking effect. On the other hand, no noticeable effect can be observed in the 152-neutron region, as was apparent in the alpha-energy systematics. While the reason for this is not as yet apparent, it may be related to the fact that the nuclides are energetically far removed from the region of the lead-isotope neutron-binding energies which were used as a basis for the calculations.

The fact that the lines for the elements cross over at some points may also be related to cumulative errors. Although rather arbitrary adjustments on the alpha- and beta-energy plots could be made to obtain smoother binding energy curves, there is at present no clear justification for doing this.

C. *Bohr-Wheeler Parameters*

The alpha-energy, beta-energy, and nucleon-binding-energy systematics immediately reveal a great deal of qualitative information about the gross features of the energy surface. It is, however, also of interest to investigate the energy surface in quantitative detail. Due to the fact that a thoroughly satisfactory theory of mass-energy surfaces is as yet lacking, the best present description is made in terms of the semi-empirical mass equation and its parameters.

The Fermi-Weizsäcker[45, 46] and Bohr-Wheeler[20] expressions are equivalent forms of the mass equation. The latter form of the mass equation can be written to give the mass, $M(Z, A)$, of the nucleus with atomic number Z and mass number A as follows:

$$M(Z, A) = M(Z_A, A) + 1/2B_A(Z - Z_A)^2 + \begin{cases} 0 & A \text{ odd} \\ -1/2\delta_A & A \text{ even, } Z \text{ even} \\ +1/2\delta_A & A \text{ even, } Z \text{ odd.} \end{cases} \quad (1)$$

This equation has been formulated to indicate mass relations between isobars, and emphasizes the parabolic shape[44] of the energy surface along lines of constant A. In the equation, Z_A represents the most stable value of Z for a given A (bottom of the

[45] E. Fermi, "Nuclear Physics," notes by J. Orear, A. H. Rosenfeld, and R. A. Schluter (University of Chicago Press, Chicago, Illinois, 1949).
[46] C. F. von Weizsäcker, *Z. Physik*, **96**, 431 (1935).

parabola) and $M(Z_A, A)$ is its corresponding mass. An expression for beta energies readily follows from equation (1):

$$E_{\beta^-} = M(Z, A) - M(Z+1, A) \tag{2}$$

$$= B_A[\,|\,Z_A - Z\,|\,- 1/2] + \begin{cases} 0 & A \text{ odd} \\ -\delta_A & A \text{ even, } Z \text{ even} \\ +\delta_A & A \text{ even, } Z \text{ odd.} \end{cases}$$

It is the three parameters of this equation, Z_A, B_A, and δ_A, that have been evaluated from closed-cycle beta-decay energies listed in this paper.

The Fermi form of the mass equation can also be used to calculate theoretical values for the same parameters:

$$M(Z, A) = 0{\cdot}9939A - 0{\cdot}00081Z + 0{\cdot}14A^{2/3} + 0{\cdot}083\,\frac{(A/2 - Z)^2}{A} + 0{\cdot}000627\,\frac{Z^2}{A^{1/3}} \tag{3}$$

$$+ \begin{cases} 0 & A \text{ odd} \\ -0{\cdot}036/A^{3/4} & A \text{ even, } Z \text{ even} \\ +0{\cdot}036/A^{3/4} & A \text{ even, } Z \text{ odd.} \end{cases}$$

The parameter Z_A can be derived by differentiation of the equation holding A constant, obtaining:

$$Z_A = \frac{A}{1{\cdot}981 + 0{\cdot}015A^{2/3}}. \tag{4}$$

Similarly, the expression for B_A is:

$$B_A = 2\left(\frac{0{\cdot}083}{A} + \frac{0{\cdot}000627}{A^{1/3}}\right). \tag{5}$$

In addition, the δ_A term can be evaluated directly from the expression as:

$$\delta_A = 0 \qquad A \text{ odd} \tag{6a}$$

$$-0{\cdot}072/A^{3/4} \qquad A \text{ even, } Z \text{ even} \tag{6b}$$

$$+0{\cdot}072/A^{3/4} \qquad A \text{ even, } Z \text{ odd} \tag{6c}$$

The values of the parameters determined from the closed cycles and those calculated from the mass equation can then be compared if the values from the above equations are multiplied by 931·2 to convert from mass units to MeV.

The δ_A term is in reality not equal to zero for odd A nuclides; in fact, it soon becomes apparent that there are different energy surfaces composed of odd neutron and odd proton nuclides. The designation δ_{AO} will therefore be used to refer to the energy difference between these two surfaces. At the same time δ_{AE} will be used in place of the former δ_A. Thus there are two correction terms to the Bohr-Wheeler equation: δ_{AE} for use with nuclides with even mass numbers, and δ_{AO} for use with nuclides with odd mass numbers. The attempts to evaluate all the parameters of the equation have recently been reviewed by CORYELL.[21]

Since for any given A there are three parameters in the Bohr-Wheeler beta-energy equation: Z_A, B_A, and δ_{AE} or δ_{AO}, three beta-decay energies serve to define

their values. The parameters have been evaluated for each set of three successive beta-decay energies, both negatron and electron capture, in the cycles for the four radioactive series. Although there are a number of cases in which nonsuccessive beta-decay energies can be used to calculate further values for these parameters, the treatment has been restricted to successive beta chains.

The same approach has been used in these calculations that was used in the previously described systematics. Values for the parameters have been calculated for all possible cases, even those subject to considerable uncertainty, so that the values for parameters obtained from uncertain decay energies can be directly compared with the more certain values. Possible errors in the decay energies involved are thus clearly evident.

If β_1, β_2, and β_3 are three successive beta-decay energies connecting the isobars Z, $Z+1$, $Z+2$, and $Z+3$, it follows that the values for δ_{AE} and δ_{AO} can be calculated from the expression:

$$\delta_A(\text{MeV}) = \left| \frac{\beta_1 - 2\beta_2 + \beta_3}{4} \right|. \tag{7}$$

When β represents an electron-capture decay energy, it becomes negative. For B_A, equation (8) is obtained:

$$B_A(\text{MeV}) = \left| \frac{\beta_1 - \beta_3}{2} \right| \tag{8}$$

If β_1 is a negatron-decay energy and β_3 an electron-capture decay energy, the numerator is $\beta_1 + \beta_3$. In all other cases the signs are as given. For Z_A one obtains:

$$Z_A = Z_1 + 1/2 + \frac{\beta_1 \pm \delta_A}{B_A} \tag{9}$$

If Z_1 is an even number, δ_A is added to β_1. Further, if β_1 is an electron-capture decay energy it becomes negative.

The calculated values of the parameters are given in Figs. 11 (δ_A), 12 (B_A), and 13 (Z_A). The theoretical values from the Fermi mass equation are indicated by dashed lines in the figures. Average values of δ_{AE}, δ_{AO}, and B_A have also been calculated for the more certain beta energies (those not included in parentheses in Figs. 2 to 5). The average value of δ_{AE} obtained for mass numbers between 214 and 244 is $1{\cdot}44 \pm 0{\cdot}14$ MeV, indicating that the even-even energy surface is an average of 1·44 MeV lower in energy than the odd-odd surface. At the same time the average value of δ_{AO} is $0{\cdot}16 \pm 0{\cdot}07$ MeV for mass numbers between 213 and 245. In this case it appears that the even-odd energy surface is an average of 0·16 MeV lower in energy than the odd-even surface. The average value of B_A between mass numbers 213 and 245 for both even and odd mass numbers is $1{\cdot}14 \pm 0{\cdot}09$ MeV. The scatter among even the more reliable values of the parameter, as indicated in the figures, reveals the degree of inadequacy of the liquid drop considerations, so that conclusions about nuclear stability are limited.

The result that the energy surface made up of odd neutron nuclides is 0·16 MeV lower in energy than the surface for the odd proton nuclides can be interpreted as the proton-pairing energies being greater than the neutron-pairing energies among these heaviest elements. Thus in the negatron decay of an odd Z nuclide, two neutrons are

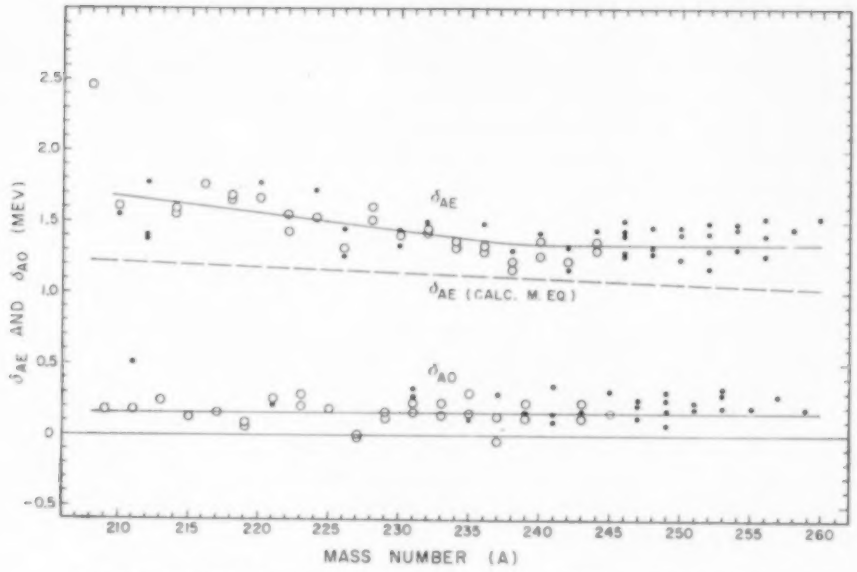

FIG. 11.—Bohr-Wheeler parameters, δ_{AE} and δ_{AO}, as a function of mass number: ○, reliable value; •, uncertain.

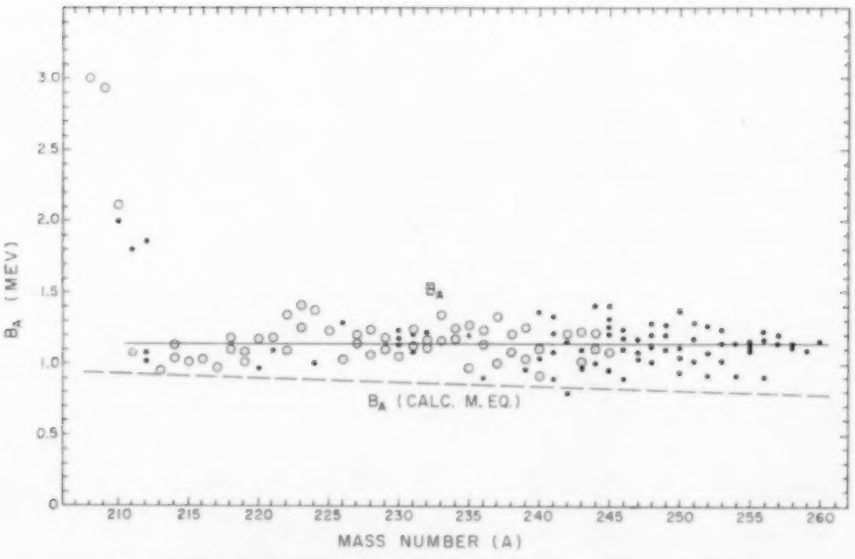

FIG. 12.—Bohr-Wheeler parameter, B_A, as a function of mass number: ○, reliable value; •, uncertain.

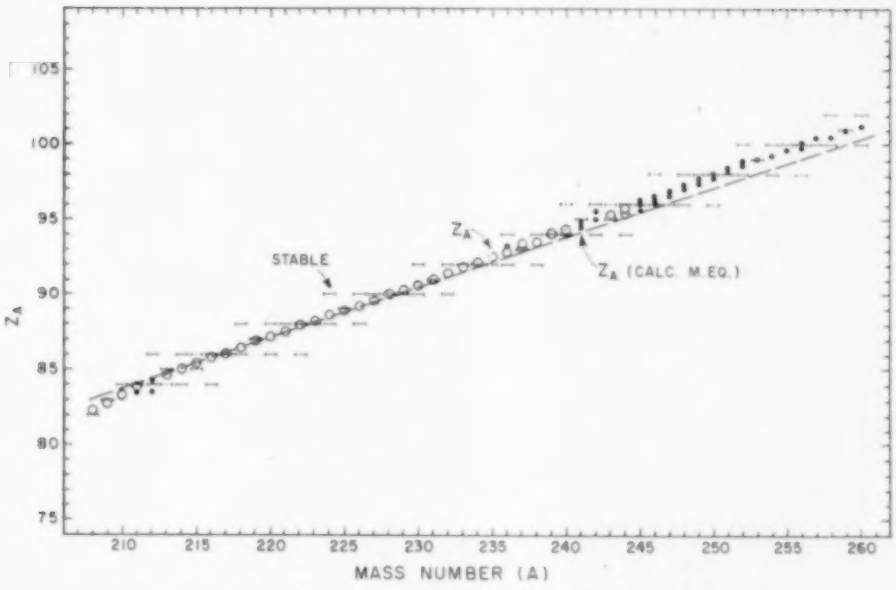

FIG. 13.—Bohr-Wheeler parameter, Z_A, as a function of mass number: ○, reliable value; •, uncertain.

unpaired and a pair of protons is formed, resulting in a relatively more stable configuration or lower-energy surface. Similar conclusions have also been reached previously.[47, 21]

The values of B_A (Fig. 12) are interpreted as the curvatures of the Bohr-Wheeler parabolas. The higher the value of B_A, the more steeply inclined are the sides of the energy valley for a given value of A. Although the high values of B_A around mass number 208 are of doubtful significance, due to the marked discontinuities in the energy surface at the 126-neutron and 82-proton closed shells, it is interesting to note that B_A has a very high value for mass number 208. This would indicate that the energy surface rises sharply along a line of constant A on both sides of Pb^{208}. As in the case of the δ_A graphs, the values of B_A calculated from the closed-cycle energies do not agree well with those calculated from the Fermi mass equation for this region of the isotope table.

Fig. 13, which shows the calculated values for Z_A, includes representations of stable nuclides. It will be noted that essentially all of the values of Z_A for odd mass numbers satisfy the reasonable requirement that they lie within 0·5 charge unit of the beta-stable element. In the cases of mass numbers 213 and 215, Z_A falls within 0·5 charge unit of astatine, which tends to indicate that At^{213} and At^{215} are both beta-stable; however, the results are not of a great enough certainty to make the conclusion definite. The average slope of the Z_A line ($\delta Z_A/\delta A$) is approximately 1/3. This indicates that the maximum beta-stability line above lead is maintained if two neutrons are added per proton. BRIGHTSEN[48] noticed that the slope of the Z_A versus A curve was of comparable value in the lower-element regions. He also concluded that the apparent bending over of the stability curve toward increased stability at larger A

[47] E. GLUECKAUF, *Proc. Phys. Soc.*, (London), **61**, 21 (1948).
[48] R. A. BRIGHTSEN, private communication (1954).

VOL. 1 1955

values with corresponding greater neutron excesses was caused by permanent shifts at shell discontinuities. If this is true, some doubt is cast on the validity of the terms in the semi-empirical equation which predicts a smooth curvature of the Z_A curve. This is not entirely unexpected because of the scatter of even the fairly reliable points on the δ_A and B_A graphs.

It is instructive to construct (Fig. 14) a segment of the parabolic energy surface

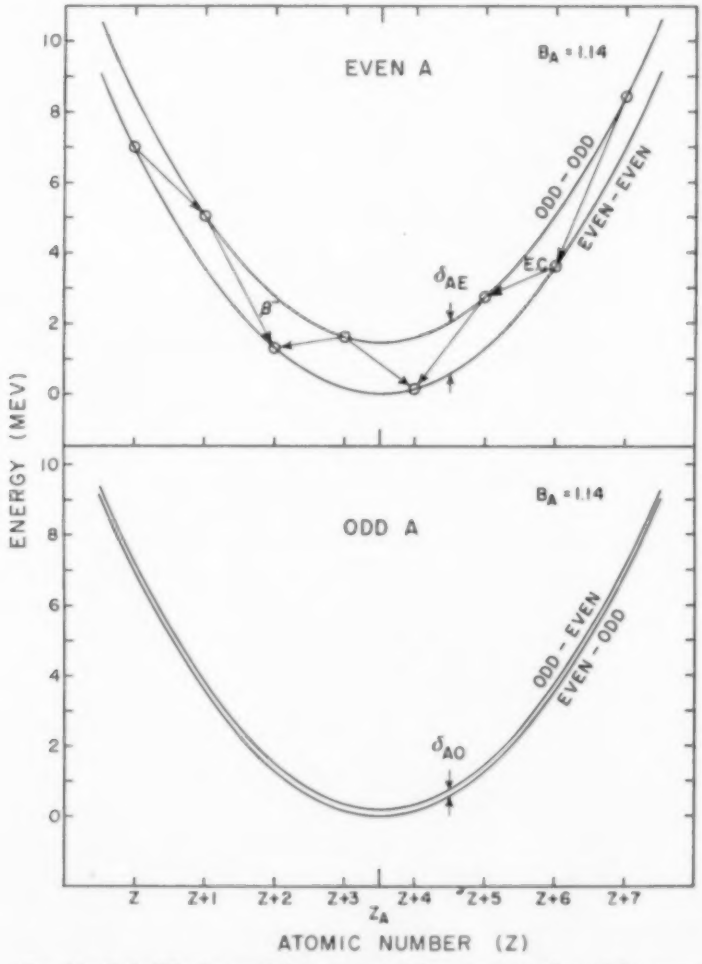

FIG. 14.—Bohr-Wheeler parabolas constructed from average values of the parameters.

from the average values of the parameters δ_{AE}, δ_{AO}, and B_A given above. For approximate "rule of thumb" estimates such figures can be used to predict beta-decay energies in a given isobaric sequence when the vertex is adjusted to the necessary Z_A value. Because of the individual deviations for each nuclide, such a procedure is of necessarily limited accuracy. Parabolas in the lower element region have also been constructed by BOUCHEZ *et al.*[49]

[49] R. BOUCHEZ, J. ROBERT, and J. TOBAILEM, Institute of Radium Curie Laboratory Report (January 1953).

5. ADDITIONAL APPLICATIONS

A. *Atomic Weights*

A valuable application of the mass data in Table 2 lies in the calculation of the atomic weights on the chemical scale. In Table 3 the values so calculated are compared with those of the International Commission on Atomic Weights adopted by the International Union of Chemistry.[50] The isotopic abundances were taken from the Table of Isotopes.[29]

TABLE 3.—CHEMICAL ATOMIC WEIGHT

Element	This paper	I.U.C. values (1953)
Thallium	204·39	204·39
Lead	207·18	207·21
Bismuth	208·99	209·00
Radium[a]	226·03	226·05
Thorium	232·05	232·05
Uranium	238·04	238·07

[a] Ra^{226} is in almost 100 per cent abundance.

VOL. 1 1955

In recent years it has often been the policy of the I.U.C. to adopt atomic weights based on mass spectrographic measurements rather than on the less accurate chemical determinations. Thus, the atomic weight of thorium was recently changed from the value 232·12 to the present value of 232·05.[50] Since the values in Table 1 should not be in error by more than 0·01 atomic weight unit, and probably are in error by less than this much, slight changes are recommended in the officially accepted values for bismuth and radium, which, like thorium, depend essentially on the mass of one isotope. The uncertainties in the isotopic abundances of the lead and uranium make it difficult to decide upon a "best" value for their atomic weights, although the value calculated here for uranium should be quite good.

B. *Q Values*

Another useful application of the mass data is in the calculation of energy balances (Q values) of induced nuclear reactions. The Q values of reactions (except those involving deuterons) can be calculated by summing the appropriate neutron, proton, and alpha-particle binding energies tabulated previously. Then, by simple conservation of momentum considerations, the energetic thresholds can be calculated.

As an example of threshold energy calculations, consider the alpha-particle bombardments of Pu^{239} to produce Cm^{240} by an $(\alpha, 3n)$ reaction.[2a] Neglecting the coulombic barrier, the energy requirement to put an alpha particle into Pu^{239} to form the compound nucleus Cm^{243*} is the alpha-decay energy of Cm^{243} (6·15 MeV). In order to "boil out" neutrons from various curium isotopes, the binding energies of these neutrons must be supplied. Thus the neutron binding energies from Table 2 of Cm^{243} (5·72 MeV), Cm^{242} (6·95 MeV), and Cm^{241} (6·16 MeV) are summed to yield a requirement of 18·83 to boil out three neutrons with zero kinetic energy from Cm^{243}. This figure is then added to 6·13 MeV to obtain the Q value of 24·96 MeV. The

[50] E. WICKERS, *J. Amer. Chem. Soc.*, **76**, 2033 (1954).

threshold for this reaction or absolute minimum energy required for the reaction to proceed is then $24{\cdot}96 \times 243/239 = 25{\cdot}38$ MeV. This value lies just above the coulombic barrier for plutonium.

This type of calculation frequently leads to some revealing information about the reactions responsible for certain products in situations such as the bombardment of U^{238} with nitrogen ions.[51] It was noted in these bombardments that there was a relatively high yield of Bk^{243}, which could have been produced by a number of reactions, but probably was formed by one of the following:

$$>100 \text{ MeV}$$
$$U^{238} + (N^{14}, 9n) \rightarrow 99^{243} \xrightarrow{EC} Cf^{243} \xrightarrow{EC} Bk^{243}$$
$$U^{238}(N^{14}, \alpha 5n)Bk^{243}.$$

Estimations reveal that the second path is energetically not only more favourable, but also indicate that when reasonable energies are assigned to the emitted neutrons the first path may be impossible.

Since the neutron-binding energies are the exothermic Q values of neutron-capture reactions and the first step of the neutron-fission reactions, correlations of neutron-binding energies of the compound nucleus have been made with neutron-capture cross-sections[52] and with the ratio of neutron-fission to -capture cross-sections.[53, 54]

6. HALF-LIFE RELATIONSHIPS[55]

A few empirical relationships are reviewed in this section for convenience so that interesting predictions can be made from them in the next section. Since the plotting of half-life data here is essentially only for use for predictive purposes, the selection of these data has been made to correlate a wide range of energies and half-lives rather than only precisely known energies and half-lives of "well behaved" nuclides such as even-even alpha emitters. In view of the present difficulty or almost impossibility of adequately doing so, no concerted effort has been made to interpret data in terms of forbiddenness or hindrance factors nor to predict half-lives from such considerations. Use is made solely of the empirical plots of the decrease in half-life with increasing particle energy for alpha and beta decay, and the severe limitations inherent in this necessarily over-simplified method are, of course, thoroughly recognized.

A. *Alpha Half-Life Systematics*

The alpha half-life energy relations and systematics have been thoroughly treated by PERLMAN, GHIORSO, and SEABORG[3] and PERLMAN and ASARO.[5] Although new data have been collected since the publication of these papers, the interpretation of the regularities observed is essentially the same. The partial alpha half-lives[55] for the highest energy alpha groups of even-even nuclei have been plotted against alpha-decay energies in Fig. 15. Although the lines for each element are in general continuous, the points for isotopes of polonium and emanation with less than 126

[51] A. GHIORSO, G. B. ROSSI, B. G. HARVEY, and S. G. THOMPSON, *Phys. Rev.*, **93**, 257 (1954).
[52] B. G. HARVEY, unpublished data (1954).
[53] G. T. SEABORG, *Phys. Rev.*, **88**, 1429 (1952).
[54] J. R. HUIZENGA and R. B. DUFFIELD, *Phys. Rev.*, **88**, 959 (1952).
[55] The partial half-lives used in graphing are obtained by dividing the total decay half-life for each nuclide by the fraction of the decay occurring by emission of a particular alpha, negatron, or neutrino particle. Thus if the total half-life of U^{230}, 20·8 days, is divided by 0·68, the fractional abundance of the 5·993 MeV alpha group, a partial alpha half-life of 31 days for this group is obtained.

VOL.
1
1955

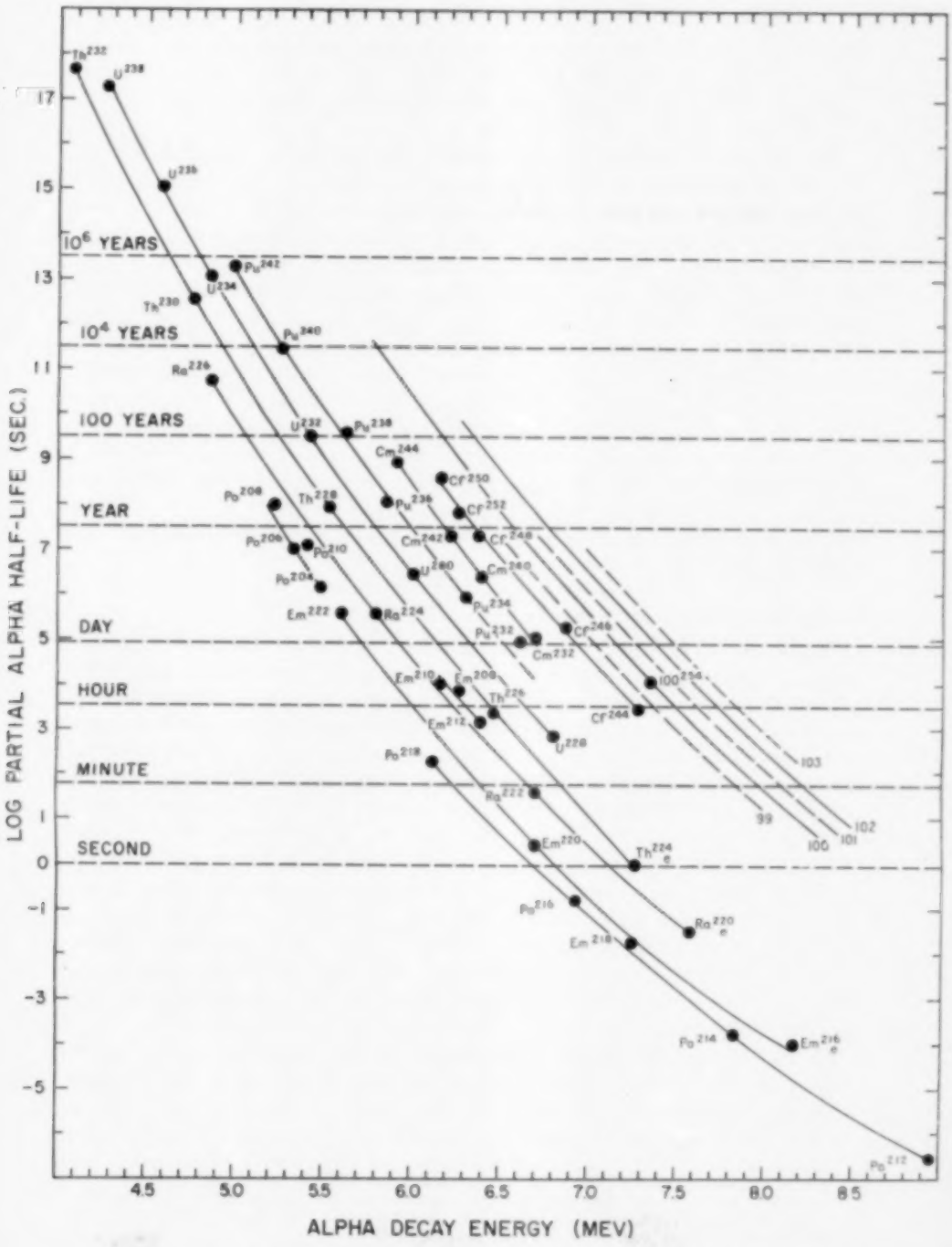

FIG. 15.—Partial alpha half-lives of even-even nuclides as a function of their alpha-decay energies. Subscript *e* denotes estimated value.

neutrons lie above the extensions of their respective lines for heavier isotopes, indicating that their decay is abnormally slow. This effect has been interpreted in terms of a radius shrinkage just below the closed shell.[3] Further, there are obvious experimental errors that may account for the few other irregularities in the alpha lines.[56]

In general, because of the regular trends on the alpha half-life *versus* energy plot, the partial alpha half-lives for the highest energy groups of even-even nuclides can be predicted with a fair degree of confidence from a knowledge of the estimated alpha energy and these are close to the total alpha half-lives because most of the decay is to the ground state. The half-life relationships for nuclides with one or two odd nucleons are much less regular than those for even-even nuclei, with the decay rate in general slower than (that is, "hindered" with respect to) that of even-even nuclides with the same alpha energy. "Departure" factors for the partial alpha-decay half-lives range from about 1 to 10^4 and the proportion of decay to the ground state exhibits irregular behaviour. Where predictions are made in Section VII B for the region beyond the measured values in the region of californium, lines parallel to the lower lines are drawn for even-even isotopes. Because of the lack of hindrance in the decay of the highest energy observed alpha particles of 99^{253} and 100^{255} the half-lives for isotopes of elements 99, 101, and 103 were estimated from the lines exactly half way between those for neighbouring even Z elements and therefore these half-lives really represent lower limits.

B. *Negatron Half-Life Systematics*

Negatron half-lives can also be correlated with particle energies. Graphs of $\log t_{1/2}$ (or $\log \lambda$) against $\log E$, first used by SARGENT,[57] have been used extensively to illustrate roughly the decrease in half-life with increase in negatron energy. Attempts to distinguish lines associated with various forbiddenness factors and selection rules have met with only limited success. A more quantitative method of classifying beta decay according to ft values is now more generally used to represent applicable selection rules.[58] The log of the partial negatron half-life for the negatron in greatest abundance has been plotted against the log of the negatron energy for the heavy elements in Fig. 16. Two solid lines have been included which correspond very roughly to the allowed and first forbidden transition lines. The former was constructed by assuming an average value of 5·1 for $\log ft$ for allowed transitions ($\Delta I = 0, 1$ no) and using MOSZKOWSKI's beta-decay graphs.[59] The upper line was constructed from data taken from the same graphs while assuming 6·8 as a reasonable average for $\log ft$ of the first forbidden transitions ($\Delta I = 0, 1$ yes). An atomic number of 90 was employed in both cases.

It is evident that the lines do not actually pass through those areas with greatest density of points although most of the points appear to lie between the very rough designations for allowed and first forbidden transitions. Also apparent is the fact

[56] The half-lives of Em^{216}, Ra^{220}, and Th^{224} listed in the Table of Isotopes[29] are estimated values and are used in Fig. 15 without change even though better estimates could probably now be made. The high partial alpha half-lives of Pu^{232} and Cm^{230} are probably due to the fact that the alpha/electron capture branching ratios of these isotopes are closer to 17 per cent and 5 per cent than the limits ≥ 2 per cent and > 10 per cent, respectively.

[57] B. W. SARGENT, *Proc. Roy. Soc.* (London), **139A**, 659 (1933).

[58] See, for example, M. G. MAYER, S. A. MOSZKOWSKI, and L. W. NORDHEIM, *Revs. Modern Phys.*, **23**, 316 (1951); *ibid.*, 322.

[59] S. A. MOSZKOWSKI, *Phys. Rev.*, **82**, 35 (1951).

that only points for odd-odd nuclei lie above the upper line with the exception of the one for U^{237}. The same exception occurs for electron capture (discussed in the next section). The negatron half-life estimations given in section VII B are made through the use of the dashed line as indicated, using the often erroneous assumption that the ground state transition is the most abundant, and are therefore subject to considerably more error than the corresponding estimated alpha half-lives.

Even though a large scatter of points in Fig. 16 is evident there are nevertheless certain features which are worth noting. First, the very high forbiddenness in the decay of Am^{242} makes its case similar to that of K^{40}. At the other extreme Ra^{228} and the 0·094-MeV beta group in Th^{231} may be superallowed; in these examples experimental errors are, of course, possible.

VOL. 1 1955

C. *Electron Capture Half-Life Systematics*

Fig. 17 summarizes the electron capture half-lives in a similar fashion to the treatment for negatron decay. The electron capture decay energies were obtained from the closed cycles and data on gamma ray energies to give partial decay schemes. The features of this type of plot have been rather thoroughly discussed by HOFF.[60] A number of points for nuclides with less than 126 neutrons have been included in Fig. 17, i.e., Bi^{207}, Po^{209} and At^{210}. In all three of these cases long half-lives are associated with high electron capture energies, which appears to be a characteristic of this region.

It can be seen that predictions of electron capture half-lives in this manner are exceedingly rough. In addition to the great uncertainties in most of the decay schemes, it is impossible to evaluate the relative effect of *K*, *L*, etc., electron capture. Lines with slopes of 2 and 4 have been included in Fig. 17 to correspond to allowed and first forbidden electron capture decay. For predictive purposes values given in section VII B are obtained through the use of the dashed line between the two solid lines.

In view of the limited number of complete decay schemes for electron capture nuclides that have been reported, it is evident that much more data are needed in this area. Such data as have been available have been treated by THOMPSON,[4] FEATHER,[61] HOFF,[60] and MAJOR and BIEDENHARM[62] in attempts to obtain some fundamental information about the nature of the electron decay process in the heaviest elements.

D. *Spontaneous-Fission Systematics*

Just as alpha decay becomes prominent in nuclides in the region of elements above lead, spontaneous fission appears to be rapidly becoming one of the predominant modes of decay in the region of californium and above. Two recently discovered nuclides, Cf^{252} and 100^{254}, were found to have spontaneous fission to alpha-decay branching ratios of almost 2 per cent, which results in a partial spontaneous fission half-life of only 200 days for the latter. Thus it is necessary to consider spontaneous fission competition with alpha and beta decay when predicting half-lives for nuclides in the heaviest element region. Fig. 18 is used for this purpose.

WHITEHOUSE and GALBRAITH[63] and SEABORG[64] made the interesting observation

[60] R. W. HOFF, Ph.D. thesis, University of California (September 1953); also published as University of California Radiation Laboratory Unclassified Document UCRL-2325 (September 1953).
[61] N. FEATHER, *Physica*, **18**, 1023 (1952).
[62] J. K. MAJOR and L. C. BIEDENHARM, *Revs. Modern Phys.*, **26**, 321 (1954).
[63] W. J. WHITEHOUSE and W. GALBRAITH, *Nature*, **169**, 494 (1952).
[64] G. T. SEABORG, *Phys. Rev.*, **85**, 157 (1952).

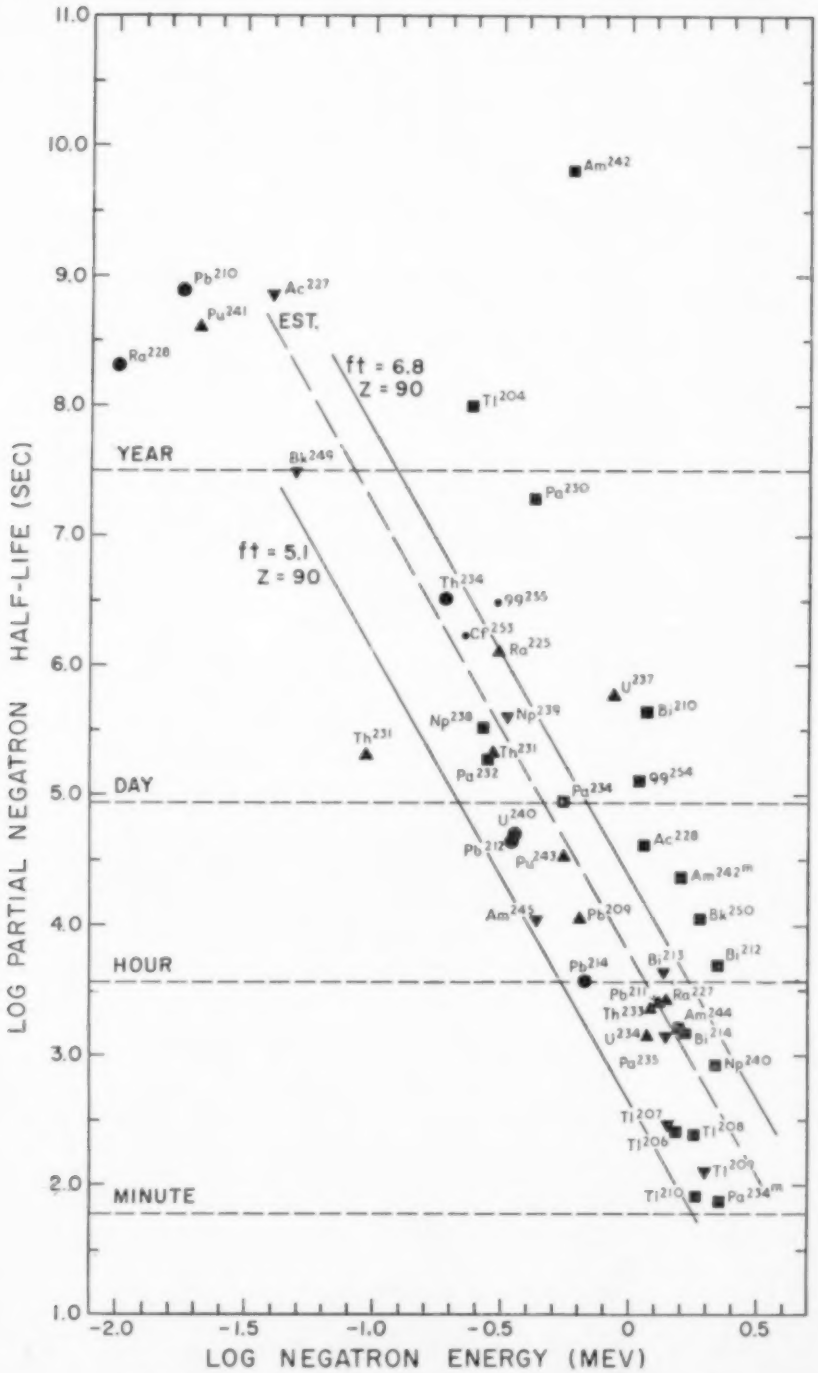

FIG. 16.—Partial negatron half-lives as a function of negatron energies: ●, even-even nuclide, ▲, even-odd; ▼, odd-even; ■, odd-odd; •, negatron energy estimated.

VOL. 1 1955

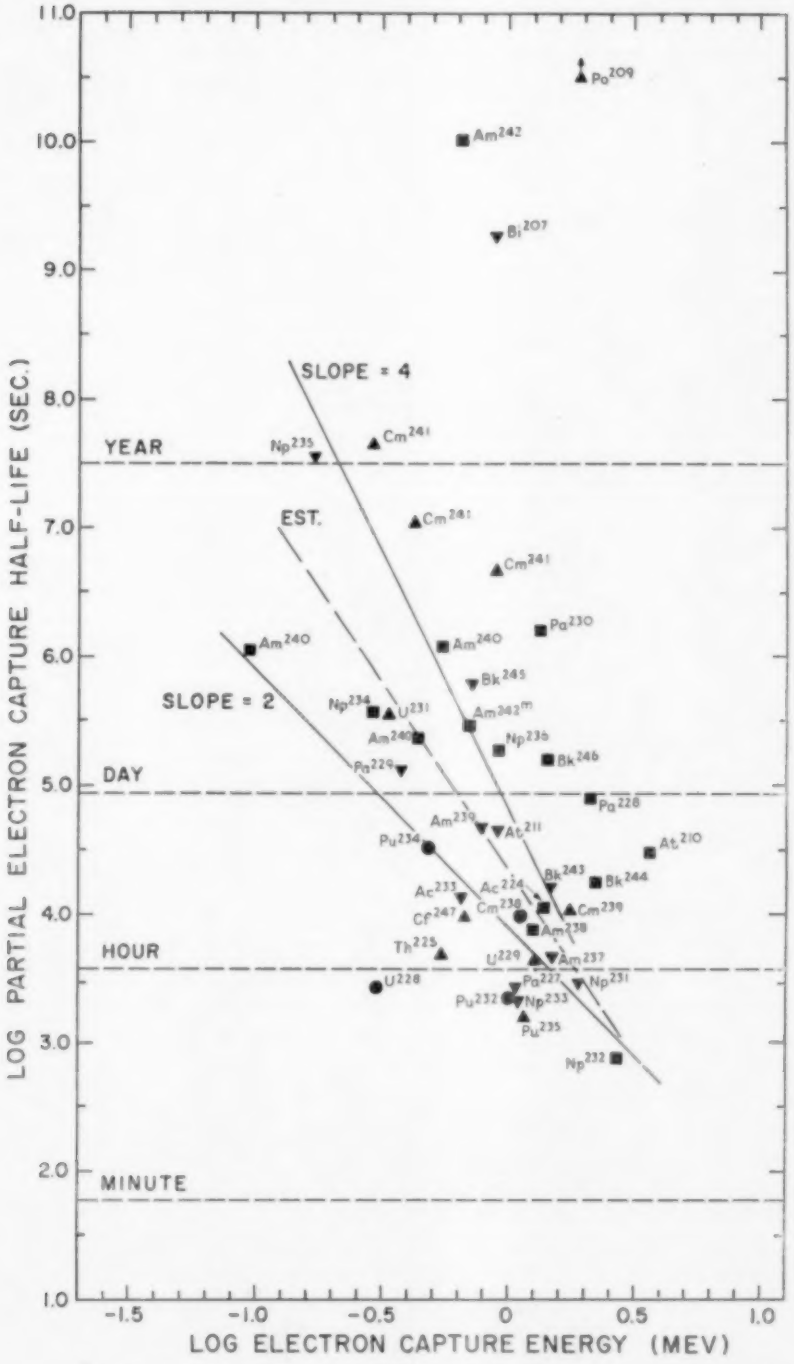

FIG. 17.—Partial electron-capture half-lives as a function of electron-capture energies: ●, even-even nuclide; ▲, even-odd; ▼, odd-even; ■, odd-odd.

that in the case of even-even nuclides the half-life for spontaneous fission seems to decrease with an exponential dependence on Z^2/A, while nuclides with an odd number of nucleons (neutrons or protons or both) decay by this process at a much slower rate.

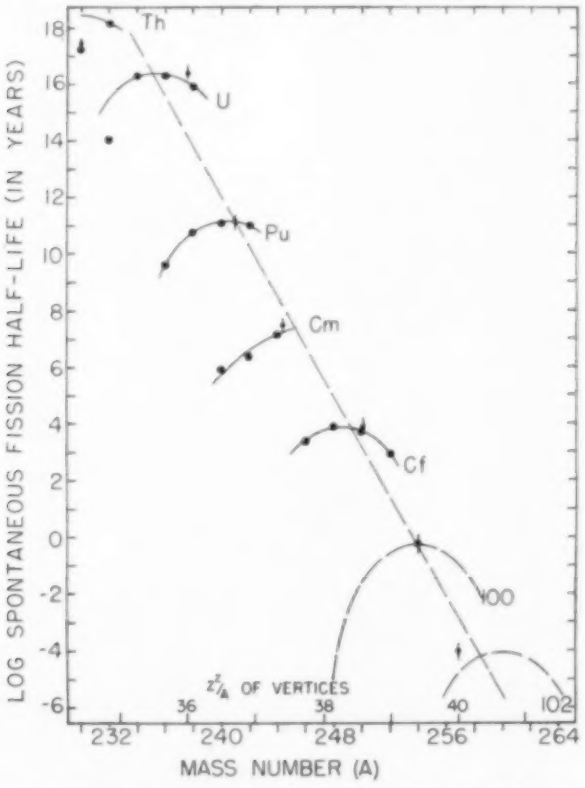

FIG. 18.—Partial spontaneous fission half-lives as a function of mass number.

Thus a plot of the logarithm of the partial spontaneous fission half-life against Z^2/A resulted in a fairly good straight line for the limited data available. With the accumulation of more data it became apparent that, although the parameter Z^2/A accounted in this manner broadly for the variation in half-life over a range of Z values, for a given value of Z this parameter did not account for the variation of half-life with A. Thus HUIZENGA[65] pointed out that for a given value of Z the half-life goes through a maximum as A varies. Other correlations involving the ratio of spontaneous fission to alpha half-lives[66] have also been useful for predictive purposes. Finally a recent Z^2/A plot[67] shows the fit of the newest data to this relation.

The averaged curves for the elements uranium through californium have been used to predict the shape for the element 100 and 102 lines. Also, the average spacing between the curves for the elements plutonium through element 100 is used to establish

[65] J. R. HUIZENGA, *Phys. Rev.*, **94**, 158 (1954).
[66] A. KRAMISH, *Phys. Rev.*, **88**, 1201 (1952); see also, M. H. STUDIER and J. R. HUIZENGA, *Phys. Rev.*, **96**, 545 (1954).
[67] P. R. FIELDS, M. H. STUDIER, L. B. MAGNUSSON, and J. R. HUIZENGA, *Nature*, **174**, 265 (1954).

the position of the element 102 curve.[68] For purposes of comparison a Z^2/A scale is also given in Fig. 18 in such a manner that the half-life points coincide with the vertices of the plutonium and element 100 curves; the dotted line is drawn through these two points and similar points are plotted for each of the other elements with the maximum value of the half-life as ordinate and the value of Z^2/A corresponding to the vertice as abscissa.

7. PREDICTIONS

A. *Beta-Stable Isotopes*

A valuable result from the cycles is the prediction of beta-stable nuclides. These nuclides are analogous to the stable isotopes in the lighter element region and, indeed, they would be stable themselves were it not for alpha and spontaneous fission instability. Beta stability results for a nuclide if both neighbouring isobars are beta unstable with respect to it. Thus, Np^{237} is beta stable due to the fact that U^{237} decays into it by negatron emission (0·52 MeV) and Pu^{237} decays into it by electron capture (0·23 MeV) as indicated in Fig. 3.

VOL. 1 1955

The beta-stable isotopes included in the cycles are summarized in a chart of the nuclides, Fig. 19. Beta-stable isotopes are indicated by shaded squares. In general, there are between five and seven beta-stable isotopes for each element with an *even* atomic number. There is usually only one beta-stable isotope for each *odd Z* element, although there are occasionally two.

For a number of mass numbers the beta-stable nuclide or nuclides are not clearly certain. These are indicated by cross-hatched squares representing possible beta-stable nuclides. It is possible that there are no beta-stable isotopes of astatine and probable that there are none of berkelium. These elements, then, would be analogous to technetium and promethium which are missing in nature. The fact that astatine may have no beta-stable isotopes may be a consequence of its position just beyond the 126-neutron closed shell. It is also interesting to note that Em^{212} may be beta stable, in spite of its relatively small mass number, because it has 126 neutrons. If Cm^{240}, Cm^{243}, and Cm^{250} are beta stable, curium has nine such isotopes, a number greater than that for any element with the exception of tin. This may be a consequence of a closed subshell at 96 protons as suggested by SEABORG.[69] (The absence of beta-stable isotopes of berkelium is possibly also related to the extra stability of curium.) The cases of Am^{243} and Cm^{243} are of particular interest inasmuch as both Am^{243} and Cm^{243} have been carefully examined for negatron[70] and electron capture decay,[71] respectively, with negative results. These isobars may, then, have essentially identical masses as is predicted by the closed cycles.

B. *Undiscovered Isotopes*

Predictions of the energies and partial half-lives for as yet undiscovered isotopes of elements 99–103 are tabulated in Table 4. Alpha energies have been estimated from Fig. 7 and beta energies from Fig. 8. All additional energies are calculated values from

[68] The predicted positions of the curves for elements 100 and 102 are, of course, quite uncertain; thus, for example, the curve for element 100 could equally well be drawn in such a position that partial spontaneous fission half-lives of 10 days and 1 day (rather than 100 days and 10 days as shown in Table 4) might be predicted for 100^{256} and 100^{255}.

[69] G. T. SEABORG, *Phys. Rev.*, **92**, 1074 (1954).

[70] G. H. HIGGINS, Ph.D. thesis, University of California (June, 1952); also published as University of California Radiation Laboratory Unclassified Report UCRL-1796 (June 1952).

[71] E. K. HULET, Ph.D. thesis, University of California (September 1953); also published as University of California Radiation Laboratory Unclassified Report UCRL-2283 (July 1953).

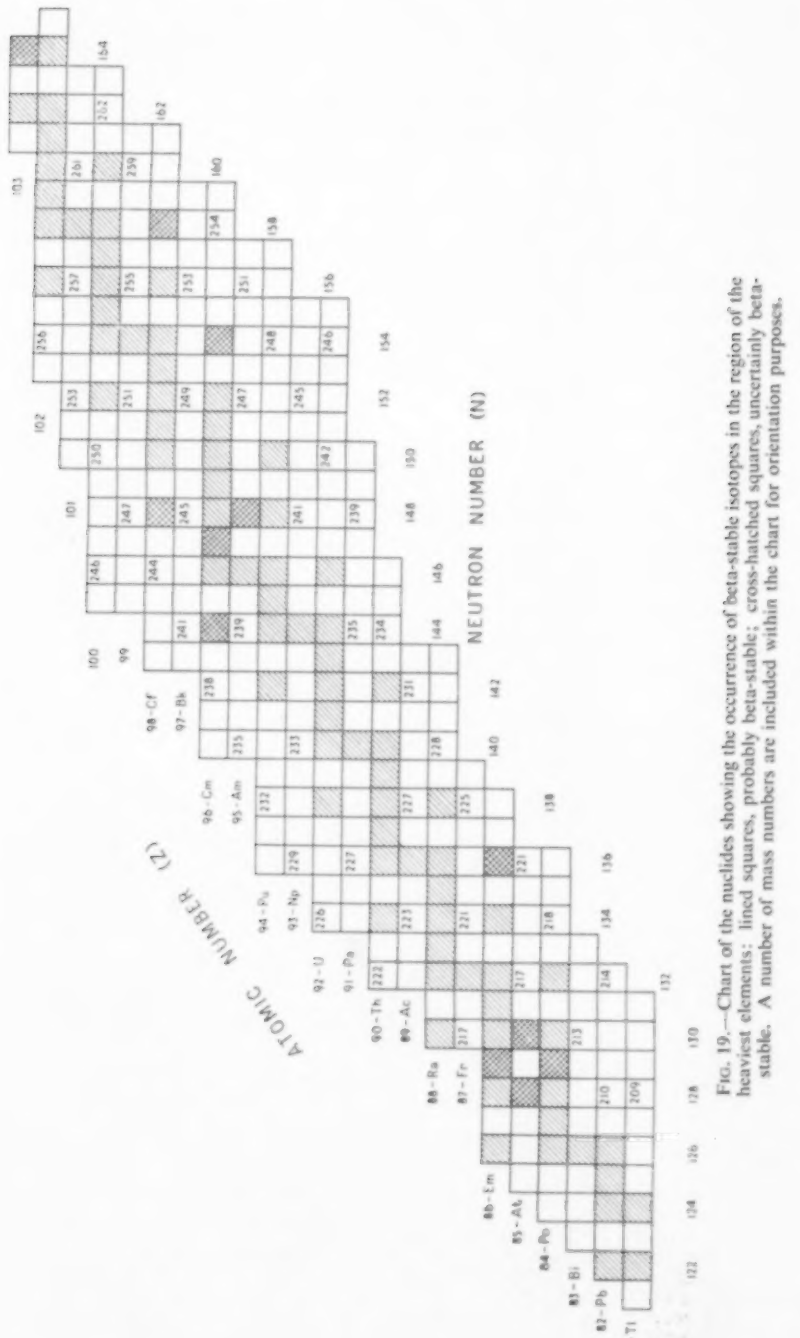

FIG. 19.—Chart of the nuclides showing the occurrence of beta-stable isotopes in the region of the heaviest elements: lined squares, probably beta-stable; cross-hatched squares, uncertainly beta-stable. A number of mass numbers are included within the chart for orientation purposes.

TABLE 4.—PREDICTED PROPERTIES FOR ISOTOPES OF ELEMENTS 99–103[a]

Nuclide	Alpha		Beta		Spont. fission half-life
	Energy (MeV)	Half-life	Energy (MeV)	Half-life	
99^{245}	7·87	1 m	3·21 *EC*	10 m	
99^{246}	7·66	5 m	3·87 *EC*	10 m	
99^{247}	7·19	5 h	3·03 *EC*	10 m	
99^{248}	6·90	5 d	1·50 *EC*	1 h	
99^{249}	6·61	50 d	1·86 *EC*	1 h	
99^{250}	6·65	50 d	0·62 *EC*	1 d	
99^{251}	6·69	50 d	1·07 *EC*	5 h	
99^{252}			1·90 β^-	10 m	
100^{247}	8·20	10 s	3·17 *EC*	10 m	
100^{248}	7·98	1 m	1·49 *EC*	1 h	10 m
100^{249}	7·77	5 m	2·38 *EC*	0·5 h	
100^{250}	7·49	1 h	0·95 *EC*	10 h	10 d
100^{251}	7·20	10 h	1·22 *EC*	5 h	
100^{252}	7·25	1 d			100 d
100^{253}	7·29	5 h	0·50 *EC*	1 d	
100^{254}	7·01	5 d			100 d
100^{255}	6·82	10 d			
100^{256}	6·62	100 d			10 d
100^{257}	6·42	5 y	0·26 β^-	10 d	
101^{251}	8·06	1 m	3·18 *EC*	10 m	
101^{252}	7·76	10 m	3·54 *EC*	10 m	
101^{253}	7·80	10 m	2·01 *EC*	1 h	
101^{254}	7·85	10 m	2·37 *EC*	0·5 h	
101^{255}	7·90	10 m	1·31 *EC*	5 h	
101^{256}	7·73	10 m	1·79 *EC*	1 h	
101^{257}	7·55	1 h	0·50 *EC*	1 d	
101^{258}	7·35	10 h	1·39 *EC*	1 h	
101^{259}	7·15	5 d			
101^{260}	6·97	10 d	1·18 β^-	1 h	
101^{261}	6·77	100 d	0·61 β^-	10 h	
102^{255}	8·40	10 s	1·72 *EC*	1 h	
102^{256}	8·44	10 s	0·55 *EC*	1 d	10 m
102^{257}	8·26	1 m	1·21 *EC*	5 h	
102^{258}	8·08	5 m			1 h
102^{259}	7·88	10 m	0·43 *EC*	1 d	
102^{260}	7·69	1 h			1 h
102^{261}	7·50	10 h			
102^{262}	7·30	5 d			10 m
102^{263}	7·10	10 d			
102^{264}	6·90	100 d			10 s
102^{265}	6·70	1 y	0·26 β^-	10 d	
102^{266}	6·51	10 y			<1 s
103^{264}	7·69	1 h	1·54 *EC*	1 h	
103^{265}	7·48	10 h			
103^{266}	7·28	5 d	0·62 *EC*	1 h	
103^{267}	7·08	1 mo			

[a] Only total decay energies and their consequent corresponding partial half-lives are listed due to the lack of suitable predictions concerning the decay schemes.

VOL. 1 1955

the closed cycles, Figs. 2–5. The half-lives were estimated from Figs. 15 (alpha), 16 (negatron), 17 (electron capture), and 18 (spontaneous fission). These three latter values are subject to considerable error for the reasons that have already been pointed out. The partial alpha half-lives for odd nucleon isotopes must be regarded as lower limits.

Nuclides are included which will eventually be produced by either or both heavy ion bombardments and neutron irradiations of heavy elements. Thus the isotope 101^{253}, which is expected to have both alpha and beta branching decay, might be produced by nitrogen ion bombardment of Pu^{242} or helium ion bombardment of 99^{253} through the reactions:

$$_{94}Pu^{242}(_{7}N^{14}, 3n)101^{253}$$

$$99^{253}(_{2}He^{4}, 4n)101^{253}.$$

The method which seems practical today for the eventual production of the beta-stable isotope of element 101, of mass number 259, on the other hand, seems to be through successive neutron capture reactions starting with 100^{255}:

$$100^{255} \xrightarrow{4(n,\gamma)\text{reactions}} 100^{259} \xrightarrow{\beta^-} 101^{259}.$$

8. ACKNOWLEDGMENTS

The authors wish to express their appreciation to RICHARD M. DIAMOND whose active participation in the early work contributed much to the development of the present paper. We regret that he was unable to remain with us until its completion. We also appreciate the generous help of JAMES W. COBBLE in preparing the final form of the paper. The assistance of MARGIE J. HOLLANDER in abstracting much of the literature in connection with the large number of data on radioactive properties which had to be evaluated, and the help of LORRAINE M. HANNA in typing several drafts and the final manuscript are gratefully acknowledged.

Many of the data incorporated in the paper were the results of work performed under the auspices of the U.S. Atomic Energy Commission.

VOL. 1 1955

APPENDIX I

RECENT DECAY DATA[73]

Nuclide	Decay type	Decay energy		Half-life
		Energies	Adopted	
Bi^{206}	*EC*	$0{\cdot}2EC^{(73)} + 3{\cdot}4\gamma^{(73)}$	3·70	
Bi^{207}	*EC*	$0{\cdot}01EC^{(74)} + 2{\cdot}35\gamma^{(74)}$	2·36	
Pb^{212}	β^-	$0{\cdot}569\beta^-$	0·57	
Pb^{214}	β^-	$0{\cdot}73\beta^{-(75)} + 0{\cdot}29\gamma^{(75)}$	1·02	
Po^{210}	α		5·40[76]	
Po^{211}	α		7·58[76]	
Po^{212}	α	8·945α	8·94[76, 77]	
Po^{215}	α		7·51[76]	
Em^{219}	α		6·95[76]	
Em^{220}	α	$6{\cdot}394\alpha^{(78)}$	6·39[76]	
Em^{222}	α	$5{\cdot}583\alpha^{(78)}$	5·58[76]	
Fr^{223}	β^-	$1{\cdot}14\beta^{-(79)} + 0{\cdot}05\gamma^{(79)}$	1·19	
Ra^{223}		$6{\cdot}687\alpha^{(80)}$	6·69	
Ra^{223}	α	$5{\cdot}855\alpha^{(81)}$	5·86[76]	
Ra^{227}	β^-	$1{\cdot}31\beta^{-(82)}$	1·31	
Ac^{226}			0·97[c (82)]	
Th^{226}	α	$6{\cdot}456\alpha^{(80)}$	6·46	
Th^{230}	α		4·76[76]	
	SF			$\geq 1{\cdot}5 \times 10^{17}$y[84]
Th^{232}	α	$4{\cdot}068\alpha^{(85)}$	4·07	
Th^{234}	β^-	$0{\cdot}19\beta^{-(86)} + 0{\cdot}28$ I.T.[87]	0·47	
Pa^{230}	β^-	$0{\cdot}43\beta^-$	0·43	
Pa^{233}	β^-	$0{\cdot}28\beta^- + 1{\cdot}05\gamma$	1·33[88]	
Pa^{234}	β^-	$1{\cdot}15\beta^{-(91)} + 0{\cdot}88\gamma^{(91)}$	2·03	
U^{230}	α	$5{\cdot}993\alpha\ (68\%)^{(89)}$	5·99	
U^{232}	α	$5{\cdot}411\alpha\ (69\%)^{(90)}$	5·41	
	SF			10^{14}y[93]
U^{236}	*SF*			2×10^{16}y[84]
U^{237}	β^-	$0{\cdot}25\beta^{-(94)} + 0{\cdot}27\gamma^{(94)}$	0·52	
U^{238}	α	$4{\cdot}259\alpha^{(85)}$	4·26	
U^{240}	β^-	$0{\cdot}356\beta^{-(86)}$	0·36	
Np^{236}	β^-	$0{\cdot}52\beta^{-(96)}$	0·52[97]	
Np^{237}		$4{\cdot}87\alpha + 0{\cdot}09\gamma^{(98)}$	4·96	
Np^{239}	β^-	$1{\cdot}272\beta^-$	1·27[99]	
Np^{240}	β^-	$2{\cdot}156\beta^{-(90)}$	2·16	
Pu^{236}	*SF*			$4{\cdot}9 \times 10^{10}$y[84]
Pu^{240}	*SF*			$1{\cdot}2 \times 10^{11}$y[84]
Pu^{241}	α	$4{\cdot}98\alpha^{(100)} + 0{\cdot}15\gamma$	5·13	
Pu^{242}	α	$4{\cdot}980\alpha\ (80\%)^{(100)}$	4·98	
	SF			$6{\cdot}7 \times 10^{10}$[84]
Pu^{243}	α	$0{\cdot}56\beta^-\ (53\%)^{(101)}$	0·56	
Am^{240}	*EC*	$0{\cdot}06EC\ (15\%)^{(2a)}$		
		$0{\cdot}44EC\ (70\%)^{(2a)}$		
		$0{\cdot}54EC\ (14\%)^{(2a)}$		
Am^{241}	α	$5{\cdot}63\alpha$	5·63	
Am^{242}	β^-	$0{\cdot}59\beta^-$	0·59	
Am^{244}	β^-	$1{\cdot}5\beta^{-(102)}$	1·50	26 min[102]
Cm^{240}	α	$6{\cdot}38\alpha^{(2a)}$	6·38	
Bk^{245}	*EC*			1·9 d[71]
Bk^{249}	β^-	$0{\cdot}10\beta^{-(103, 104)}$	0·10	~1 y[104]
Bk^{250}	β^-	$1{\cdot}9\beta^{-(102)}$	1·90	3·13 h[102]
Cf^{246}	α	$6{\cdot}86\alpha\ (78\%)^{(107)}$		

References are shown on page 42.

RECENT DECAY DATA (*continued*).

Nuclide	Decay type	Decay energy		Half-life
		Energies	Adopted	
Cf^{247}	*EC*			$\sim 2{\cdot}7$ h[71]
Cf^{248}	α	$6{\cdot}36\alpha$[71]	6·36	225 d[71]
	SF			$\sim 7 \times 10^5$y[88]
Cf^{249}	α	$6{\cdot}31\alpha$[106]	6·31	
Cf^{250}	α	$6{\cdot}15\alpha$[102]	6·15	12 y[102]
	SF			5×10^3y[102]
Cf^{252}	α	$6{\cdot}25\alpha$[88c]	6·25	2 y[102]
	SF			100 y[102]
Cf^{253}	β^-			20 d[109]
99^{247}		$7{\cdot}47\alpha$[51]	7·47	
99^{253}	α	$6{\cdot}74\alpha$[109]	6·74	20 d[109]
99^{254}	β^-	$1{\cdot}1\beta^-$[109]	1·10	36 h[109]
100^{249}	α		7·77[e][110]	
100^{254}	α	$7{\cdot}34\alpha$[109]	7·34	3·2 h[109]
	SF			200 d[109]
100^{255}	α	$7{\cdot}21$[109]	7·21	15 h[109]

[72] This table lists decay data used in the closed cycles and systematics plots which are supplementary to those given in the Table of Isotopes (Ref. 29). These are of two categories: (a) recent decay data; (b) previous data, reinterpreted. Superscript e denotes estimated value, c, calculated value.
[73] D. E. ALBURGER and M. H. L. PRYCE, *Phys. Rev.*, **95**, 1482 (1954).
[74] D. E. ALBURGER, private communication (1954).
[75] E. E. BERLOVICH, *Izvest. Akad. Nauk. Ser. Fiz. SSR*, **16**, 314 (1953).
[76] G. H. BRIGGS (*Revs. Modern Phys.*, **26**, 1 (1954) critically reviewed the energies of natural alpha particles and arrived at certain decay energy values different from those quoted here. These are as follows: Po^{210}, 5·406 MeV; Po^{211}, 7·586 MeV; Po^{212}, 8·949 MeV; Po^{215}, 7·526 MeV; Em^{219}, 6·934 MeV; Em^{220}, 6·399 MeV; Em^{222}, 5·587 MeV; Ra^{223}, 5·804 MeV; Th^{220}, 4·768 MeV.
[77] The alpha-decay energy for the 8·776 MeV alpha particle listed in the Table of Isotopes (Ref. 29) is in error by one keV.
[78] G. BASTIN-SCOFFIER and J. SANT'ANA-DIONISIO, *Compt. rend.*, **236**, 1016 (1953).
[79] E. K. HYDE, *Phys. Rev.*, **94**, 1221 (1954). The 1·14 MeV adopted negatron energy is actually listed as $1{\cdot}15 \pm 0{\cdot}05$ MeV by HYDE.
[80] F. ASARO, L. M. SLATER, F. STEPHENS, and I. PERLMAN, unpublished data (1953).
[81] Another value, 5·835 MeV, also in the Table of Isotopes (Ref. 29) is probably now to be preferred, but it is only 0·02 MeV lower than the value used, making recalculations unprofitable.
[82] J. P. BUTLER and J. S. ADAM, *Phys. Rev.*, **91**, 1219 (1953).
[83] Unpublished data of J. R. GROVER and G. T. SEABORG give evidence that a 0·232 MeV gamma ray may be in coincidence with the most abundant beta particle. If 0·232 MeV is added to 1·17 MeV the disintegration energy of 1·40 MeV is quite far from the calculated value of 0·97 MeV.
[84] References cited by J. R. HUIZENGA, W. M. MANNING, and G. T. SEABORG, "The Actinide Elements," edited by G. T. SEABORG and J. J. KATZ, (McGraw-Hill Book Company, Inc., New York, N.Y., 1954), National Nuclear Energy Series, Plutonium Project Record, Vol. 14A, chapt. 20.
[85] B. G. HARVEY, unpublished data (1953).
[86] E. F. DEHAAN, G. J. SIZOO, and P. KRAMER, *Physica*, **19**, 1205 (1953).
[87] The isomeric transition energy of Pa^{234m} was established as 0·28 MeV by subtraction of the 2·03 MeV Pa^{234} decay energy (Ref. 91) from the 2·31 MeV beta energy of Pa^{234m} (Ref. 86).
[88] Two more recent values of the disintegration energy 1·24 MeV and 1·27 MeV are reported in Ref. 89 and Ref. 90.
[89] O. P. HOK and G. J. SIZOO, *Physica*, **20**, 77 (1954).
[90] C. I. BROWNE, D. C. HOFFMAN, H. L. SMITH, M. E. BUNKER, J. P. MIZE, J. W. STARNER, R. L. MOORE, and J. P. BALAGNA, *Bull. Am. Phys. Soc.*, **29**, No. 5, Abstract H13 (1954).
[91] O. P. HOK and G. J. SIZOO, *Physica*, **19**, 1208 (1953).
[92] F. ASARO and I. PERLMAN, unpublished data (1953).
[93] This value represents a measurement by A. H. JAFFEY of the Argonne National Laboratory.
[94] F. WAGNER, Jr., M. S. FREEDMAN, D. W. ENGELKEMEIR, and J. R. HUIZENGA, *Phys. Rev.*, **89**, 502 (1953).
[95] J. D. KNIGHT, M. E. BUNKER, B. WARREN, and J. W. STARNER, *Phys. Rev.*, **91**, 889 (1953).
[96] T. O. PASSELL, Ph.D. thesis, University of California (June 1954); also published as University of California Radiation Laboratory Unclassified Document UCRL-2528 (March 1954).

[97] This value is subject to the uncertainty that the 22 hour activity with this energy may be an excited state of a long-lived isomer. Evidence that this may be the case was found by STUDIER, HOPKINS, GHIORSO, and BENTLEY (private communication).
[98] D. ENGELKEMEIR and L. B. MAGNUSSON, *Phys. Rev.*, **94**, 1395 (1954).
[99] Recent experiments by J. O. RASMUSSEN, Jr., F. S. STEPHENS, Jr., and D. STROMINGER (to be published), indicate that the 1·27 MeV negatron decays to a 0·04 MeV excited state of Pu^{238}, which would make the decay energy 1·31 MeV.
[100] F. ASARO, Ph.D. thesis, University of California (June 1953); also published as University of California Radiation Laboratory Unclassified Document UCRL-2180 (June 1953).
[101] D. W. ENGELKEMEIR, P. R. FIELDS, and J. R. HUIZENGA, *Phys. Rev.*, **90**, 6 (1953).
[102] A. GHIORSO, S. G. THOMPSON, G. R. CHOPPIN, and B. G. HARVEY, *Phys. Rev.*, **94**, 1081 (1954).
[103] Data on isotopes of Bk, Cf, 99, and 100 have been obtained by investigators at Argonne National Laboratory and are published in References 104–106 and Reference 68.
[104] H. DIAMOND, L. B. MAGNUSSON, J. F. MECH, C. M. STEVENS, A. M. FRIEDMAN, M. H. STUDIER, P. R. FIELDS, and J. R. HUIZENGA, *Phys. Rev.*, **94**, 1083 (1954).
[105] M. H. STUDIER, P. R. FIELDS, H. DIAMOND, J. F. MECH, A. M. FRIEDMAN, P. A. SELLERS, G. PYLE, C. M. STEVENS, L. B. MAGNUSSON, and J. R. HUIZENGA, *Phys. Rev.*, **93**, 1428 (1954).
[106] P. R. FIELDS, M. H. STUDIER, J. F. MECH, H. DIAMOND, A. M. FRIEDMAN, L. B. MAGNUSSON, and J. R. HUIZENGA, *Phys. Rev.*, **94**, 209 (1954).
[107] J. HUMMEL, A. CHETHAM-STRODE, F. ASARO, and I. PERLMAN, unpublished data (1954).
[108] A. GHIORSO, private communication (1954).
[109] G. R. CHOPPIN, S. G. THOMPSON, A. GHIORSO, and B. G. HARVEY, *Phys. Rev.*, **94**, 1080 (1954).
[110] An isotope of element 100 with an alpha disintegration energy of 7·8 MeV found by H. ATTERLING, W. FORSLING, L. W. HOLM, L. MELANDER, and B. ÅSTRÖM, *Phys. Rev.*, **95**, 585 (1954) is probably 100^{249} rather than 100^{250}.

VOL. 1 1955

APPENDIX II

TABLE 1.—MEASURED AND CALCULATED MASSES AND NEUTRON-BINDING ENERGIES

(Masses in atomic mass units)[111]

Nuclide	Measured	Calculated
$_0n^1$	1·008982 ± 0·000003[41]	
H^1	1·008142 ± 0·000003[41]	
He^4	4·003873 ± 0·000015[41]	
Pb^{207}	207·0429 ± 0·0016[20]	207·03995
Pb^{208}	208·0409 ± 0·0013[20]	208·04100
Pb^{208}	208·0410 ± 0·0015[20]	208·04100[a]
Bi^{209}	209·0471 ± 0·0015[20]	209·04514
Th^{232}	232·1092 ± 0·0010[20]	232·11001
U^{234}	234·1133 ± 0·0011[20]	234·11341
U^{238}	238·1234 ± 0·0010[20]	238·12454

[a] Measured value adopted.

[111] In all cases the unadjusted doublet values of the masses given by the authors quoted were used.

TABLE 2.—MEASURED AND CALCULATED NEUTRON-BINDING ENERGIES IN THE TRANSMERCURY REGION

Nuclide	Upper limit (γ, n)	Lower limit	Value adopted[a]
$Tl^{202-203}$	8·80 ± 0·20[112]		8·00[e]
$Tl^{203-204}$		6·42 ± 0·15[d] [113]	6·42[a]
$Tl^{204-205}$	7·3 ± 0·25[114]	7·7 ± 0·2[b] [115]	7·48[a]
	7·48 ± 0·15[116]		
	7·55 ± 0·20[112]		
$Tl^{205-206}$		6·23 ± 0·05[c] [117]	6·23[a]
		6·16 ± 0·15[d] [118]	
$Pb^{205-206}$	8·25 ± 0·10[113]	8·10 ± 0·10[b] [115]	8·18[a]
$Pb^{206-207}$	6·9 ± 0·1[114]	6·70 ± 0·05[b] [115]	6·73[a]
	6·95 ± 0·10[116]	6·734 ± 0·008[c] [117]	
	6·75 ± 0·20[112]	6·71 ± 0·03[d] [115]	
$Pb^{207-208}$	8·1 ± 0·3[119]	7·37 ± 0·03[b] [115]	7·38[a]
	7·44 ± 0·10[116]	7.380 ± 0·008[c] [117]	
	7·30 ± 0·20[112]	7·37 ± 0·03[d] [115]	
$Pb^{208-209}$		3·87 ± 0·05[d] [115]	3·87[a]
$Bi^{208-209}$	7·2 ± 0·1[114]	7·44 ± 0·05[b] [115]	7·44[a]
	7·45 ± 0·2[120]		
	7·40 ± 0·20[112]		
$Bi^{209-210}$		4·170 ± 0·015[c] [117]	4·65[e]
		4·14 ± 0·03[d] [118]	
$Th^{231-232}$	6·0 ± 0·15[114]		6·31[e]
	6·35 ± 0·1[121]		
$Th^{232-233}$		4·9 ± 0·2[d] [115]	5·06[e]
$U^{237-238}$	5·8 ± 0·15[114]	5·9 ± 0·2[b] [115]	5·99[e]
	5·97 ± 0·1[121]		
$U^{238-239}$		4·63 ± 0·15[d] [115]	4·83[e]

[a] Measured value adopted; [b] (d, t) reaction; [c] (n, γ) reaction; [d] (d, p) reaction; [e] Value calculated in present paper.

[112] R. SHER, J. HALPERN, and A. K. MANN, *Phys. Rev.*, **84**, 387 (1951).
[113] J. A. HARVEY, private communication to A. H. WAPSTRA, *Physica*, **17**, 628 (1951).
[114] R. W. PARSONS and C. H. COLLIE, *Proc. Phys. Soc.*, (London) **63**, 839 (1950).
[115] J. A. HARVEY, *Phys. Rev.*, **81**, 353 (1951).
[116] A. O. HANSON, R. B. DUFFIELD, B. C. DIVEN, and H. PALEVSKY, *Phys. Rev.*, **76**, 578 (1949).
[117] B. B. KINSEY, G. A. BARTHOLOMEW, and W. H. WALKER, *Phys. Rev.*, **82**, 380 (1951).
[118] H. PALEVSKY and A. O. HANSON, *Phys. Rev.*, **79**, 242 (1950).
[119] R. W. PARSONS, D. J. LEES, and C. H. COLLIE, *Proc. Phys. Soc.* (London), **63**, 915 (1950).
[120] J. MCELHINNEY, A. O. HANSON, R. A. BECKER, R. B. DUFFIELD, and B. C. DIVEN, *Phys. Rev.*, **75**, 542 (1949).
[121] J. R. HUIZENGA, L. B. MAGNUSSON, M. S. FREEDMAN, and F. WAGNER, *Phys. Rev.*, **84**, 1264 (1951).

J. Inorganic and Nuclear Chemistry, 1955, Vol. 1, pp. 45–48. Pergamon Press Ltd., London

FISSION YIELDS IN SPONTANEOUS FISSION OF Cf^{252}*

By L. E. GLENDENIN and E. P. STEINBERG
Chemistry Division, Argonne National Laboratory, Lemont, Illinois

(*Received November* 1954)

Abstract—Spontaneous fission of Cf^{252} has been investigated by radiochemical determination of the yields of fifteen fission products ranging in mass number from 99 to 143. Fission is observed to be asymmetric with some indication of fine structure in the mass distribution associated with the 82-neutron shell. Both light- and heavy-fission product groups are shifted to higher masses relative to spontaneous fission of Cm^{242}. The yield-mass curve indicates a value of 5 ± 1 for the average number of neutrons emitted per fission.

VOL.
1
1955

RECENT work in this laboratory[1, 2] on pile-irradiated plutonium has made available a source of californium of sufficient quantity (about 10^{-10} gram) to make feasible a preliminary study of the mass distribution in the spontaneous fission of Cf^{252} by radiochemical determination of fission yields. The californium source was of high purity and contained no detectable amount of residual fission-product activity from the pile-irradiation with the exception of a small amount of Y^{91}. The nuclear properties of the source are summarized in Table 1. The spontaneous fission rate of the source was several thousand per minute, with a ratio of alpha to fission activity of about forty. Although the present investigation was limited by the low fission rate to those spontaneous fission products with yields greater than about one per cent, it was possible to obtain information on some of the features of the mass distribution.

Fission yields were determined for fifteen fission products ranging in mass number from 99 to 143. Radiochemical techniques were similar to those already described in a previous paper[3] on the spontaneous fission of Cm^{242}. No special handling precautions were required, because of the low level of alpha activity in the californium source. Neutron-induced fission in the californium source may arise from the spontaneous fission neutrons inducing fission in Cf^{251}, which has a high fission cross-section.[4] This effect is expected to be negligible, however, by the arguments given previously[3] in the case of Cm^{242}.

TABLE 1.—NUCLEAR PROPERTIES OF CALIFORNIUM SOURCE

Isotope	Abundance (%)	Alpha half-life (years)	Spontaneous fission half-life (years)
Cf^{249}	5	550	$> 10^6$
Cf^{250}	48	9·4	$> 10^4$
Cf^{251}	10		
Cf^{252}	37	2·1	60

* Work performed under the auspices of the U.S. Atomic Energy Commission.

[1] M. H. STUDIER *et al.*, *Phys. Rev.*, **93**, 1428 (1954).
[2] H. DIAMOND *et al.*, *Phys. Rev.*, **94**, 1083 (1954).
[3] E. P. STEINBERG and L. E. GLENDENIN, *Phys. Rev.*, **95**, 431 (1954).
[4] L. B. MAGNUSSON *et al.*, *Phys. Rev.*, in press.

For each fission-yield determination, activities of the element of interest were removed by quantitative separations establishing a zero time for growth in the source. A known weight of carrier was added, and the fission rate of the solution determined by fission counting a small aliquot. After suitable periods of time, the growth was ended by separation of the carrier from the californium. The carrier was purified by using standard radiochemical procedures, and the chemical yield determined. Counting rates ranging from about five to one hundred counts per minute were observed with an end-window proportional counter over a background rate of eleven counts per minute. The fission-product activities were identified by analysis of decay curves and the technique of differential absorption when applicable. Suitable corrections were applied for chemical yield, decay, fractional saturation, absorption, scattering, and geometry to obtain the saturation disintegration rate. This rate divided by the known spontaneous fission rate of the source gives the fission yield.

The results of the fission-yield determinations are presented in Table 2, column 2. Estimates of the independent yields in the fission chains beyond the members taken for analysis (column 1) are given, where significant, in column 3. These estimates are

TABLE 2.—FISSION YIELDS IN SPONTANEOUS FISSION OF Cf^{252}

Fission product	Observed fission yield (%)	Estimated independent fission yield of daughter (%)	Total fission yield of chain (%)
67-hr Mo^{99}	2·2 ± 0·5	—	2·2 ± 0·5
4·5-hr Ru^{105}	9·2 ± 1·4	—	9·2 ± 1·4
13·1-hr Pd^{109}	6·8 ± 1·3	—	6·8 ± 1·3
7·5-day Ag^{111}	4·5 ± 0·9	—	4·5 ± 0·9
21-hr Pd^{112}	4·5 ± 0·9	0·3	4·8 ± 1·0
5·3-hr Ag^{113}	4·2 ± 0·8	—	4·2 ± 0·8
53-hr Cd^{115}	2·8 ± 0·5	—	2·8 ± 0·5
2-hr In^{117}	< 1·0	—	< 1·0
77-hr Te^{132}	2·8 ± 0·4	0·7	3·5 ± 0·5
21-hr I^{133}	4·8 ± 0·7	0·3	5·1 ± 0·8
52·5-min I^{134}	4·2 ± 0·6	0·6	4·8 ± 0·7
6·7-hr I^{135}	4·0 ± 0·6	1·1	5·1 ± 0·8
33-min Cs^{136}	6·3 ± 0·9	—	6·3 ± 0·9
85-min Ba^{139}	6·2 ± 0·9	—	6·2 ± 0·9
33-hr Ce^{143}	7·8 ± 1·5	—	7·8 ± 1·5

based on an empirical rule of charge distribution in the same manner as described in a previous paper.[3] The total chain yields (sum of columns 2 and 3) are given in column 4 and plotted against mass number in Figs. 1 and 2. The relatively large estimates of reliability (error) given in the table are based on the difficulties of analyzing decay data from samples of low counting rate and on the number of determinations made. The value for In^{117} is an upper limit based on an observed activity of about 1 c/m which could not be adequately characterized.

A comparison of the yield-mass curves for spontaneous fission of Cf^{252} and Cm^{242} is shown in Fig. 1. Although the Cf^{252} data are preliminary in nature and neither as extensive nor as accurate as will be possible with larger sources, it is evident that the heavy group has shifted toward higher masses relative to Cm^{242}. In

all previous comparisons among fissile nuclei an increase in mass has been associated with a shift of the light group toward higher mass numbers, with the heavy group remaining relatively stationary or, if anything, shifting slightly toward lower mass

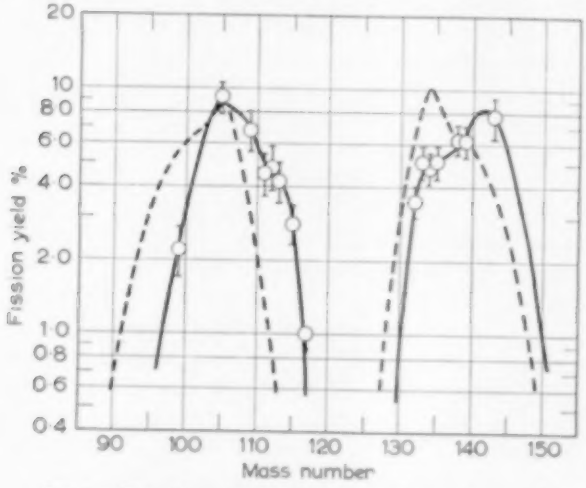

FIG. 1.—Comparison of yield-mass curves for spontaneous fission of Cf^{252} (solid line) and Cm^{242} (dashed line).

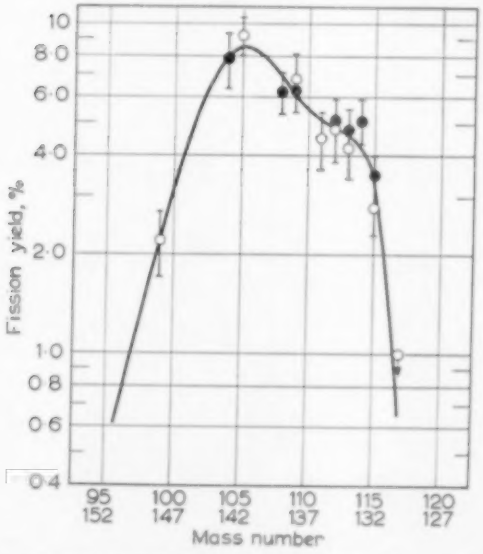

FIG. 2.—Yield-mass curve for spontaneous fission of Cf^{256}. Open and solid circles represent light- and heavy-group data, respectively.

numbers. It would be of considerable interest to study fissile nuclei of even higher mass number to see if the shift of the heavy group observed in the fission of Cf^{252} is indicative of a new trend.

If the data are plotted, as in Fig. 2, with the light and heavy groups superimposed

("folded curve"), it is possible to estimate the average number of neutrons associated with the fission process ($\bar{\nu}$) from the difference between the mass number of the fissioning nucleus and the sum of the product mass numbers having equal fission yield. The data indicate a value of about 5 for $\bar{\nu}$, with an uncertainty of perhaps ± 1 due to errors in the fission yields and the lack of data for the region above mass 143. This value is considerably larger than that for spontaneous fission of Cm^{242} ($\bar{\nu} = 3{\cdot}0$[3, 5]) and is indicative of higher internal excitation energies in the fission fragments.

It is interesting to note that the fission yield data presented in Figs. 1 and 2 indicate shoulders in the mass-yield curve in the mass regions 111-115 and 132-136. These regions are just those where fine structure may be expected[3] as a result of the influence of the 82-neutron shell at about mass 134 and its complement at about mass 113. The curve of Fig. 2 gives a yield summation of 102 per cent, in good agreement with the theoretically expected 100 per cent.

When larger sources of californium become available, it will be possible to extend the scope and accuracy of the present investigation, particularly with respect to the regions of fine structure, lower fission yields, and the rare-earth elements.

We wish to express our deep appreciation to H. DIAMOND, P. R. FIELDS, A. M. FRIEDMAN, J. R. HUIZENGA, L. B. MAGNUSSON, J. F. MECH, C. M. STEVENS, and M. H. STUDIER of the Chemistry Division of this laboratory, who prepared the californium source and kindly made it available to us for this work.

[5] F. R. BARCLAY and W. J. WHITEHOUSE, *Proc. Phys. Soc.* (*London*), **A 66**, 447 (1953).

J. Inorganic and Nuclear Chemistry, 1955, Vol. 1, pp. 49 to 59. Pergamon Press Ltd., London

ORDERED INTERMEDIATE PHASES IN THE SYSTEM CeO_2—Ce_2O_3

By D. J. M. Bevan
Atomic Energy Research Establishment, Harwell, Berks*

(*Received* 20 *September* 1954)

Abstract—The system CeO_2—Ce_2O_3 has been investigated over its entire range of composition. CeO_2 was reduced in hydrogen to varying degrees and the products examined by means of X-ray diffraction techniques to determine the phase relationships. The results indicate the formation of a number of ordered phases: $Ce_{22}O_{38}$, $Ce_{22}O_{37}$, $Ce_{11}O_{21}$ (?) having a rhombohedral structure, and a phase having the type-*C* rare-earth structure with a composition range extending between the approximate limits $Ce_{22}O_{33}$ and $Ce_{22}O_{34}$. The solid solution range of the $\alpha(CeO_2)$-phase is found to be very narrow. The type-*A* rare-earth (Ce_2O_3)-phase appears to have a solid solution range between $CeO_{1.50}$ and $CeO_{1.52}$.

VOL. 1 1955

INTRODUCTION

Much attention has been given in recent years to the formation of anomalous mixed crystals between compounds having the fluorite structure and substances of different formula type with the same anion but cations of differing valency from those of the fluorite-type compound. Zintl and Udgard (1939) have prepared mixed crystals of CaF_2 and YF_3 which have the CaF_2-structure and contain fluoride ions in excess of the formula MF_2 situated in interstitial positions in the lattice. Similar mixed crystal formation was observed in the systems SrF_2—LaF_3 and CaF_2—ThF_4. In oxide systems attention has been confined mainly to systems containing a fluorite-type oxide of formula MO_2 and an oxide of a tervalent rare-earth metal. Such mixed crystals, containing vacant anion sites in these cases, have been reported by Zintl and Croatto (1939) (CeO_2—La_2O_3), Hund and his co-workers (1951a, b; 1952) (ThO_2—La_2O_3, ThO_2—Y_2O_3, ZrO_2—Y_2O_3); Duwez, Bowen, and Odell (1951) (ZrO_2—Y_2O_3); McCullough and co-worker (1950, 1952) (CeO_2—Nd_2O_3, CeO_2—Pr_2O_3, PrO_2—Nd_2O_3, CeO_2—Sm_2O_3, CeO_2—Y_2O_3, PrO_2—Y_2O_3); and Brauer and Gradinger (1951) (CeO_2—Y_2O_3). The solubility of the rare-earth oxide in the fluorite-type oxide, i.e., the maximum permitted concentration of anion vacancies, varies from system to system, but in all cases is found to be large, ranging from 20 to 40 mol per cent. The cation lattice in both the interstitial and anion vacancy type of mixed crystal is found to be complete.

Variable valency exhibited by cerium in its oxides offers yet another such system for investigation. CeO_2 is a typical fluorite-type oxide, and the tervalent Ce_2O_3 has the rare-earth type-*A* structure, being isomorphous with La_2O_3. The CeO_2—Ce_2O_3 system might therefore be expected to have closely similar characteristics to the CeO_2—La_2O_3 and ThO_2—La_2O_3 systems and others described previously.

The formation of a blue-black substance on reducing CeO_2 in hydrogen was first observed nearly one hundred years ago by Rammelsberg (1859), and this result was confirmed by Sterba (1901), but the first investigation of a carefully purified ceria was carried out by Meyer (1903). He concludes from his experiment that hydrogen

* Present address: Nuffield Research Group, Imperial College of Science and Technology, London.

4—(20 pp.)

reduction leads to the formation of a blue-black substance having the formula Ce_4O_7. Subsequent work (e.g., that of CHASE, 1917; and FRIEDRICH and SITTIG, 1925) prior to the publication of a paper by SCHENCK and ROTERS (1933) tacitly assumes the existence of this compound. SCHENCK and ROTERS, in an investigation of the effect of admixed foreign oxides on the oxygen tension of certain mixed-oxide systems, reacted carbon monoxide with CeO_2 in a closed system and measured the equilibrium amount of carbon dioxide. Partial reduction of the CeO_2 occurred, giving the blue-black material, but their isotherms for 700°C and 900°C indicate a single phase of variable composition between $CeO_{1.90}$ and CeO_2. This result has been apparently confirmed by RIENÄCKER and BIRKENSTAEDT (1951), who determined the X-ray patterns of $CeO_{1.94}$ and the so-called "Ce_4O_7," and found them to be identical with that of CeO_2, although no measurements of the cubic cell-edge are given. However, previous to this, FOËX (1946) measured the volume change of a specimen of CeO_2 on reduction in hydrogen and found a 6 per cent increase between CeO_2 and Ce_4O_7. A similar volume increase was observed during the oxidation of Ce_2O_3. On the basis of these results, Ce_4O_7 is presumed to exist as a separate phase. Quite recently, but without publishing the experimental data, BRUNO (1950) has reported the results of experiments which show that CeO_2 can be appreciably reduced and yet retain the fluorite structure, the volume of the unit cell increasing in proportion to the concentration of Ce^{3+} ions in solution, results which are in complete accord with those previously described for similar systems. Density measurements confirmed the existence of anion vacancies. The electron diffraction experiments of COURTEL and LORIERS (1950; and LORIERS, 1950) on the constitution of oxide films on cerium metal show that type-*C* Ce_2O_3 ($a = 11{\cdot}26$ Å) is formed initially. On oxidizing further, CeO_2 lines appear which are considerably broadened. They conclude that there is a continuous solid solution range between cubic Ce_2O_3 and CeO_2. The kinetics of cerium oxidation are explained in terms of this model. In view of the uncertainty arising from this examination of the literature on this system, further investigation seemed desirable.

EXPERIMENTAL

CeO_2, prepared by the precipitation of cerous oxalate from a weakly acid solution of A.R. ceric ammonium nitrate and subsequent ignition to the oxide, was used as the starting material for all preparations of the lower oxides. Reduction was effected by dry oxygen-free hydrogen in the furnace described below.

The pyrophoric nature of the reduced oxide is well known. It is therefore essential that oxygen should be excluded from the system throughout the experiment, and with this object in view the following technique was devised. A sintered alumina tube 12-in. long and 1-in. in internal diameter was closely wound with 1·6 mm diameter molybdenum wire which was held in position and the turns insulated from each other by alumina cement. This tube was supported at each end in fused silica cups sealed inside a fused silica envelope 3 in. in diameter, and a cylindrical molybdenum radiation shield was inserted between the tube and the walls of the envelope. Heavy molybdenum leads were sealed through the envelope and connected to the ends of the winding. A diagrammatic representation of the completed arrangement is shown in Fig. 1. The CeO_2 to be reduced was contained in a platinum boat situated at the centre of the furnace. A quartz window at one end enabled the temperature of the boat to be measured by means of a calibrated optical pyrometer. Using a constant weight of CeO_2 and a constant rate of flow of hydrogen, the time of reduction was found to have little effect on the ultimate composition reached at a given temperature, the temperature being the deciding factor in determining the degree of reduction. Reduction time was therefore standardized at one hour. Experience enabled the temperature necessary to give any required composition to be estimated quite accurately.

After reduction was complete the hydrogen flow was cut off and the whole apparatus evacuated. The temperature was then adjusted to the required value for annealing, which was carried out for various times under a vacuum of better than 10^{-4} mm mercury. The sample was then quenched by withdrawing it from the hot zone of the furnace by means of a suitable magnetic device. When cold, the contents of the boat were transferred to the side arm to which was sealed the ball-mill A, any sintered lumps being broken up by the magnetically controlled crushing-rod B. When transfer of the sample to the ball-mill was complete, this was sealed off, still under vacuum, and the grinding of the sample finally completed by careful shaking of the mill. X-ray samples and a sample for analysis

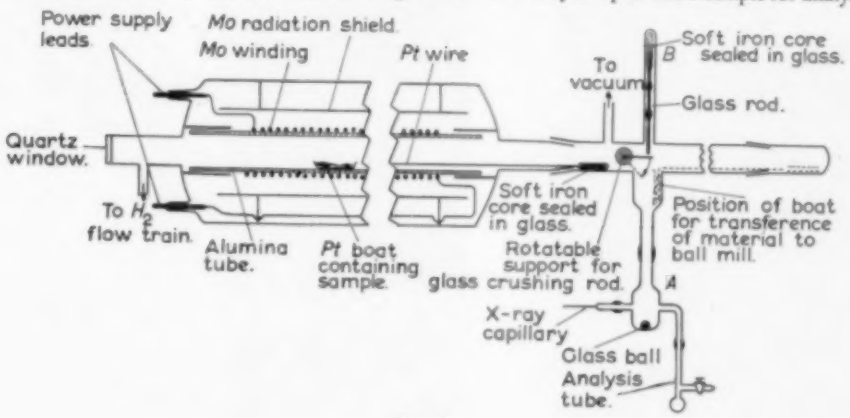

Fig. 1.

were then taken and the capillaries and analysis-bulb finally sealed off. Analysis was effected by measuring the volume of pure dry oxygen absorbed in oxidizing the sample to CeO_2, which was then tipped out and weighed. In some experiments a quartz tube with a septum at one end was sealed to the ball-mill, using a standard cone and socket joint, some of the sample being transferred to this. After sealing off, the quartz tube was wrapped in copper foil and sealed under vacuum inside another quartz tube. Annealing could then be conveniently carried out for much longer periods of time. When complete, the septum was broken under vacuum and X-ray samples and a sample for analysis taken as previously described.

X-ray patterns were obtained in a 19-cm Unicam camera using Cu ($K\alpha$) radiation.

RESULTS AND DISCUSSION

The results obtained are summarized in Table 1. The composition range of the α-phase on the oxygen-deficient side of the composition CeO_2 is clearly very small, appreciable reduction leading to a new β-phase, which although closely related to the face-centred cubic structure of CeO_2, has a rhombohedral structure arising from a distortion of the cube along its body diagonal. No density measurements were made here to confirm the existence of vacant anion sites, but other instances of defective fluorite structures, together with BRUNO'S work (1950), and the crystallization of the more strongly reduced oxides in the type-*C* rare-earth structure, support this assumption. The β-phase is therefore most probably an ordered phase containing anion vacancies. Since the β-phase is regarded as an ordered structure, derived from that of CeO_2 by the introduction of anion vacancies, it is probable that the ideal formula can be written as $Ce_{22}O_{38}$ ($CeO_{1\cdot812}$), derived from eight unit cells of the CeO_2 structure by the ordered omission of six O^{2-} ions. This β-phase appears to have a narrow composition range between $CeO_{1\cdot812}$ and $CeO_{1\cdot805}$. Another unique phase (γ-phase) appears at the composition $CeO_{1\cdot785}$, which also has a rhombohedral

TABLE 1

Composition	Colour	X-ray pattern	Annealing conditions	Phases present
$CeO_{2.000}$	Pale yellow	f.c.c. $a = 5{\cdot}409 \pm 0{\cdot}001$ Å	at 800°C in O_2 for 24 hr	α
$CeO_{1.947}$	Grey-blue (light)	*Two phases:* f.c.c. $a = 5{\cdot}411 \pm 0{\cdot}001$ Å rhombohedral—unmeasured	at 980°C in vac. for 1 hr (continuous pumping)	α β
$CeO_{1.902}$	Grey-blue (medium)	*Two phases:* f.c.c. $a = 5{\cdot}411 \pm 0{\cdot}001$ Å rhombohedral—unmeasured	at 1,200°C in vac. for 1½ hr	α β
$CeO_{1.883}$	Grey-blue (dark)	*Two phases:* f.c.c. $a = 5{\cdot}411 \pm 0{\cdot}001$ Å rhombohedral (pseudo-hexagonal) $a_H = 3{\cdot}888 \pm 0{\cdot}002$ Å; $c_H = 9{\cdot}537 \pm 0{\cdot}002$ Å	at 1,200°C in vac. for 21 hr (continuous pumping)	α β
$CeO_{1.863}$	Dark blue	*Two phases:* f.c.c. $a = 5{\cdot}411 \pm 0{\cdot}001$ Å rhombohedral (pseudo-hexagonal) $a_H = 3{\cdot}890 \pm 0{\cdot}002$ Å; $c_H = 9{\cdot}537 \pm 0{\cdot}002$ Å	at 960°C in vac. for 300 hr (sealed in quartz)	α β
$CeO_{1.850}$	Dark blue	*Two phases:* f.c.c.—unmeasured rhombohedral (pseudo-hexagonal) $a_H = 3{\cdot}888 \pm 0{\cdot}002$ Å; $c_H = 9{\cdot}537 \pm 0{\cdot}002$ Å	at 960°C in vac. for 150 hr (sealed in quartz)	α β
$CeO_{1.833}$	Dark blue	*Two phases:* f.c.c.—unmeasured rhombohedral (pseudo-hexagonal) $a_H = 3{\cdot}888 \pm 0{\cdot}002$ Å; $c_H = 9{\cdot}537 \pm 0{\cdot}002$ Å	at 960°C in vac. for 150 hr (sealed in quartz)	α β
$CeO_{1.821}$	Dark blue	*Two phases:* f.c.c.—just visible rhombohedral (pseudo-hexagonal) $a_H = 3{\cdot}890 \pm 0{\cdot}002$ Å; $c_H = 9{\cdot}536 \pm 0{\cdot}002$ Å	at 960°C in vac. for 150 hr (sealed in quartz)	α β
$CeO_{1.812}$	Dark blue	rhombohedral (pseudo-hexagonal) $a_H = 3{\cdot}890 \pm 0{\cdot}002$ Å; $c_H = 9{\cdot}538 \pm 0{\cdot}002$ Å	at 1,020°C in vac. for 2 hr (continuous pumping)	β

VOL. 1 1955

$CeO_{1.805}$	Dark blue	rhombohedral (pseudo-hexagonal) $a_H = 3.896 \pm 0.002$ Å; $c_H = 9.537 \pm 0.002$ Å	at 960°C in vac. for 150 hr (sealed in quartz)	β
$CeO_{1.804}$	Dark blue	rhombohedral (pseudo-hexagonal) $a_H = 3.900 \pm 0.002$ Å; $c_H = 9.538 \pm 0.002$ Å	at 960°C in vac. for 150 hr (sealed in quartz)	β
$CeO_{1.795}$	Dark blue	rhombohedral (pseudo-hexagonal) $a_H = 3.900 \pm 0.002$ Å; $c_H = 9.537 \pm 0.002$ Å	at 960°C in vac. for 150 hr (sealed in quartz)	β
$CeO_{1.785}$	Dark blue	rhombohedral (pseudo-hexagonal) $a_H = 3.910 \pm 0.002$ Å; $c_H = 9.502 \pm 0.002$ Å	at 960°C in vac. for 1,000 hr (sealed in quartz)	γ
$CeO_{1.775}$	Dark blue	rhombohedral (pseudo-hexagonal) $a_H = 3.910 \pm 0.002$ Å; $c_H = 9.502 \pm 0.002$ Å	at 1,020°C in vac. for 2 hr (continuous pumping)	γ
$CeO_{1.767}$	Dark blue	*Two phases:* rhombohedral (pseudo-hexagonal) $a_H = 3.910 \pm 0.002$ Å; $c_H = 9.502 \pm 0.002$ Å rhombohedral (pseudo-hexagonal)—unmeasured	at 1,020°C in vac. for 2 hr (continuous pumping)	γ δ
$CeO_{1.752}$	Dark blue	*Two phases:* rhombohedral (pseudo-hexagonal) $a_H = 3.910 \pm 0.002$ Å; $c_H = 9.502 \pm 0.002$ Å rhombohedral (pseudo-hexagonal) $a_H = 3.912 \pm 0.002$ Å; $c_H = 9.657 \pm 0.002$ Å	at 960°C in vac. for 150 hr (sealed in quartz)	γ δ
$CeO_{1.740}$	Blue-black	*Two phases:* rhombohedral (pseudo-hexagonal) $a_H = 3.910 \pm 0.002$ Å; $c_H = 9.502 \pm 0.002$ Å rhombohedral (pseudo-hexagonal) $a_H = 3.912 \pm 0.002$ Å; $c_H = 9.657 \pm 0.002$ Å and associated superstructure lines	at 960°C in vac. for 150 hr (sealed in quartz)	γ δ
$CeO_{1.722}$	Blue-black	rhombohedral (pseudo-hexagonal) and associated superstructure lines $a_H = 3.912 \pm 0.002$ Å; $c_H = 9.657 \pm 0.002$ Å	at 1,050°C in vac. for 2 hr (continuous pumping)	δ
$CeO_{1.717}$	Blue-black	rhombohedral (pseudo-hexagonal) and associated superstructure lines $a_H = 3.921 \pm 0.002$ Å; $c_H = 9.637 \pm 0.002$ Å	at 1,000°C in vac. for 2 hr (continuous pumping)	δ

TABLE 1 (*continued*)

Composition	Colour	X-ray pattern	Annealing conditions	Phases present
$CeO_{1.704}$	Blue-black	*Two phases:* b.c.c. $a = 11.109 \pm 0.002$ Å rhombohedral (pseudo-hexagonal) and associated superstructure lines	at 1,050°C in vac. for 3 hr (continuous pumping)	Type *C* δ
$CeO_{1.688}$	Black	b.c.c. $a = 11.107 \pm 0.001$ Å	at 1,050°C in vac. for 2 hr (continuous pumping)	Type *C*
$CeO_{1.686}$	Black	b.c.c. $a = 11.107 \pm 0.001$ Å	at 1,050°C in vac. for 1½ hr (continuous pumping)	Type *C*
$CeO_{1.684}$	Black	b.c.c. $a = 11.111 \pm 0.001$ Å	at 1,050°C in vac. for 1½ hr (continuous pumping)	Type *C*
$CeO_{1.682}$	Black	b.c.c. $a = 11.113 \pm 0.001$ Å	at 1,050°C in vac. for 2 hr (continuous pumping)	Type *C*
$CeO_{1.681}$	Black	b.c.c. $a = 11.114 \pm 0.001$ Å	at 1,050°C in vac. for 2 hr (continuous pumping)	Type *C*
$CeO_{1.668}$	Black	b.c.c. $a = 11.121 \pm 0.001$ Å	at 1,050°C in vac. for 1 hr (continuous pumping)	Type *C*
$CeO_{1.667}$	Black	b.c.c. $a = 11.124 \pm 0.001$ Å	at 1,050°C in vac. for 1 hr (continuous pumping)	Type *C*
$CeO_{1.651}$	Black	b.c.c. $a = 11.126 \pm 0.001$ Å	at 1,050°C in vac. for 2 hr (continuous pumping)	Type *C*
$CeO_{1.635}$	Black	*Two phases:* b.c.c. $a = 11.126 \pm 0.001$ Å hexagonal—unmeasured	at 1,050°C in vac. for 2 hr (continuous pumping)	Type *C* Type *A*
$CeO_{1.578}$	Olive green	*Two phases:* b.c.c.—unmeasured hexagonal $a = 3.894 \pm 0.002$ Å $c = 6.051 \pm 0.002$ Å	at 1,050°C in vac. for ½ hr (continuous pumping)	Type *C* Type *A*
$CeO_{1.569}$	Olive green	*Two phases:* b.c.c.—unmeasured hexagonal $a = 3.894 \pm 0.002$ Å $c = 6.051 \pm 0.002$ Å	at 1,050°C in vac. for ½ hr (continuous pumping)	Type *C* Type *A*
$CeO_{1.528}$	Mustard	hexagonal $a = 3.889 \pm 0.002$ Å $c = 6.054 \pm 0.002$ Å	at 1,050°C in vac. for ½ hr (continuous pumping)	Type *A*

VOL. 1 1955

TABLE 2

Face-centred cubic indices	Pseudo-hexagonal indices	$\sin^2\theta$-values								
		α-phase		β-phase			γ-phase	δ-phase		
		upper limit $CeO_{2\cdot000}$	lower limit CeO_{2-x}	upper limit $CeO_{1\cdot512}$	$CeO_{1\cdot505}$	lower limit $CeO_{1\cdot504}$	$CeO_{1\cdot785}$	upper limit $CeO_{1\cdot722}$	$CeO_{1\cdot717}$	lower limit $CeO_{1\cdot710}$
222	006	0·2437	0·2436	0·2318	0·2351	0·2369	0·2377	0·2300	0·2298	—
	022			0·2359	0·2346	0·2341	0·2335	0·2330	0·2326	—
331	017	0·3859	0·3857	0·3708	0·3730	0·3737	0·3749	0·3661	0·3658	—
	121;025			0·3735	0·3714	0·3707	0·3693	0·3692	0·3687	—
420	116	0·4062	0·4060	0·3907	0·3927	0·3927	0·3930	0·3847	0·3846	—
	212			0·3928	0·3915	0·3905	0·3887	0·3878	0·3871	—
422	108	0·4874	0·4872	0·4680	0·4711	0·4724	0·4742	0·4592	0·4595	—
	300;124			0·4717	0·4690	0·4681	0·4671	0·4655	0·4647	—

structure. On the basis of the reasoning already applied to the β-phase, its probable composition is $CeO_{1\cdot782}$, to which the formula $Ce_{32}O_{57}$ is ascribed. Further reduction leads to the formation of still another phase (δ-phase), the main diffraction lines of which are those of a rhombohedral structure like those of the β- and γ-phases, but the pattern is complicated by the presence of a number of superstructure lines. For the purpose of comparison, the parameters of the pseudo-rhombohedral cell have been calculated. This δ-phase also appears to have a narrow range of composition between $CeO_{1\cdot722}$ and $CeO_{1\cdot710}$.

Table 2 shows a selection of the X-ray data obtained for each phase. Values of $\sin^2\theta$ are given only for the components of those face-centred cubic lines which undergo measurable splitting when the cube is distorted to a rhombohedron. Various constants of these rhombohedral cells have been plotted as a function of composition in Fig. 2, and the result, looked at as a whole, constitutes strong evidence for the correctness of the phase-relationships described. Unfortunately, the lower limit of the δ-phase is uncertain. The X-ray pattern of a sample analyzing to $CeO_{1\cdot704}$ shows the presence of two phases, the lower limit of the δ solid solution and a type-*C* rare-earth phase. This is inferred from the appearance together on the film of fine structure lines which are unique to each of the separate phases. The main lines overlap to such a degree that measurement is meaningless. The estimated limit of this composition range has been obtained by making use of the qualitative observation that its pseudo-rhombohedral cell is very nearly cubic. Thus no 006 (hexagonal indices) line is visible when splitting of the face-centred cubic 222 line has been observed to a marked degree for $CeO_{1\cdot722}$ and $CeO_{1\cdot717}$, and no splitting of the 331, 420, and 422 lines of the cubic phase can be observed for $CeO_{1\cdot704}$. By extrapolating the plot of the rhombohedral angle (α) against composition to $\alpha = 60°$, the value of the limiting composition $CeO_{1\cdot710}$ is obtained, but this figure is approximate.

Determination of the true cell of the δ-phase has been attempted. Calculations on the measurements of a $CeO_{1\cdot722}$ film based on the assumption of a hexagonal cell for which $a = \sqrt{3}a'$ and $c = 2c'$ (where a' and c' are the hexagonal parameters of the pseudo-rhombohedral cell) give values of $\sin^2\theta$ in fair agreement with those observed, but the number of extinctions is rather large. Such a cell would contain eighteen cerium atoms, and on this basis an ideal formula $Ce_{18}O_{31}$ ($CeO_{1\cdot722}$) might be ascribed in good accord with the chemical evidence. There is, however, no obvious reason for the change from ideal formulae based on multiples of four cerium atoms to a formula not derivable from a whole number of CeO_2 cells. The formula $Ce_{32}O_{55}$ ($CeO_{1\cdot719}$) is therefore also a possibility, the observed composition range extending on either side of the ideal formula. In this connection it must be emphasized that the rational formulae assigned above to the β- and γ-phases are hypothetical and based entirely on the chemical evidence. No superstructure lines are observed which would indicate that the true cell is based on doubling the dimensions of the CeO_2 basic structure.

Samples having compositions ranging between $CeO_{1\cdot688}$ and $CeO_{1\cdot651}$ crystallize with the body-centred cubic type-*C* rare-earth oxide structure. Fig. 3 shows a plot of the cubic cell-edge as a function of composition and indicates the existence of a continuous range of solid solution intermediate between the two approximate limits $Ce_{32}O_{54}$ and $Ce_{32}O_{53}$, although too much significance should not be attached to the fact that these limits can be expressed as rational formulae. On reducing below

$CeO_{1.651}$, the type-*A* rare-earth oxide phase appears. Using ZACHARIASEN's (1926) data for Ce_2O_3 and those obtained here for three samples which show this structure (two of which give X-ray patterns showing type-*C* lines as well and must therefore represent the limiting type-*A* solid solution), the most probable composition of this limit has been determined. The value obtained ($CeO_{1.53}$) agrees well with that estimated by MARTIN (1950) for the Pr—O system on the basis of tensiometric and X-ray measurements.

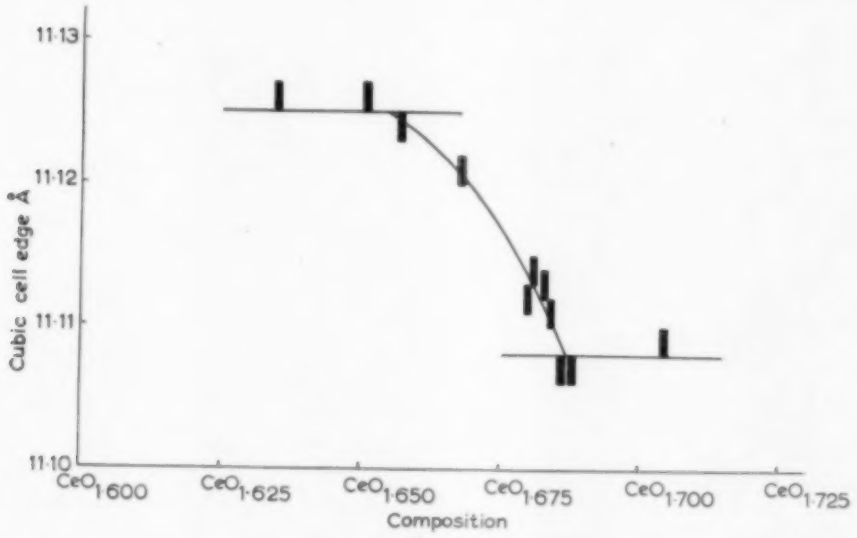

Fig. 3.

That the CeO_2—Ce_2O_3 system should exhibit such widely different characteristics from the closely analogous CeO_2—La_2O_3 and ThO_2—La_2O_3 systems requires some explanation. Some experiments carried out on the ThO_2—La_2O_3 system have confirmed the results reported by HUND and DURRWÄCHTER (1951b). In these, solutions of thorium nitrate and lanthanum nitrate of known concentration were mixed in different proportions to give the required Th/La ratios, and precipitated with ammonia solution. The washed and dried precipitate was then fired to 1,500°C in air and examined by X-ray diffraction. This method of preparation, or the alternative by which the mixed nitrate solutions are evaporated to dryness and fired to high temperatures, is common to most of the systems investigated. The two cations are initially mutually interspersed on an atomic scale, and if this atomic dispersion persists through the stage of conversion to oxide, the result is a mixed crystal. The choice of crystal habit is governed by the relative capacities of the separate oxide structures to nucleate with a sufficient degree of distortion, and the experimental results show that it is the fluorite structure which is preferred. The existence of a solid-solution limit at high concentrations of the rare-earth oxide is then simply an indication of the inability of the distorted fluorite phase to nucleate beyond a certain degree of distortion. Mixed crystals formed in this way are likely to be metastable with respect to the separate oxide phases, or some intermediate ordered phase if the sizes of the two cations concerned are greatly different. If, on the other hand, these

60·5
60·3
60·1
59·9
α′ – rhombohedral angle
42·8
42·6
42·4
42·2
42·0
41·8
Volume of hexagonal pseudo cell Å³

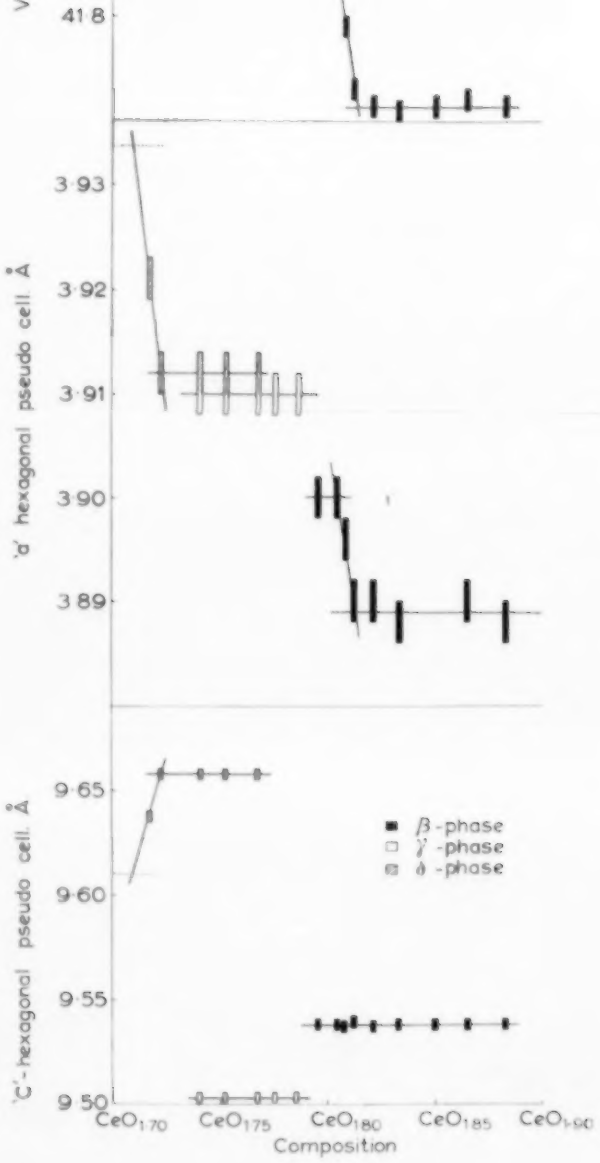
41·8
3·93
3·92
3·91
3·90
3·89
'a' hexagonal pseudo cell Å
9·65
9·60
9·55
9·50
'C' - hexagonal pseudo cell Å
β - phase
γ - phase
δ - phase
CeO1·70
CeO1·75
CeO1·80
CeO1·85
CeO1·90
Composition

Fig. 2

are nearly identical, the solid solutions may well be stable. Moreover, in the case of a metastable mixed crystal, the attainment of equilibrium is conditional upon the ability of the cation lattice to rearrange, and it is well known that cation mobility in fluorite-type compounds is extremely low. It is in respect of the ability of the cation lattice to rearrange that the CeO_2—Ce_2O_3 system differs significantly from the ThO_2—La_2O_3 system. In the latter system rearrangement necessitates a cation diffusion process, but in the former case exchange of positions between Ce^{4+} ions and Ce^{3+} ions may take place through electron switching, and since all the cations occupy crystallographically equivalent positions, this can occur relatively easily: no movement of the cation lattice is necessary. Anion vacancies are readily mobile in the defective fluorite structures, as shown by the ease of oxidation to CeO_2. True equilibrium may therefore be easily obtained. The only certain way of reaching equilibrium in mixed crystal systems containing cations of different species is to prepare them from the separate oxide phases. However, if the cation mobility is low, so that rearrangement within a metastable solid solution is an extremely slow process, attainment of equilibrium from the separate oxide phases will also be slow. In some systems (e.g., CeO_2—Y_2O_3 [MARTIN, R. L., private communication]) it has been established that equilibrium exists by the preparation of the same solid solution from both the separate oxides and from a co-precipitated hydroxide mixture, but the cation radii are nearly identical and the stability of the solid solutions might be expected.

ACKNOWLEDGMENTS

The author wishes to express his indebtedness to Prof. J. S. ANDERSON, F.R.S., for much helpful discussion, and to Mr. H. J. MORRIS and Mr. G. A. JUGGINS for assistance in the construction of the furnace used. This work was carried out during the tenure of a Junior Research Fellowship at the Atomic Energy Research Establishment, Harwell.

Note added in proof

Since the completion of this work BRAUER and GRADINGER (1954) have published their results on this system, and some comment on these is desirable. Their samples were prepared by admixing the appropriate weights of CeO_2 and Ce_2O_3 and firing under pure nitrogen at 1,400°C. Their experimental technique and the temperature at which equilibrium was established thus differ from the conditions employed in this investigation.

Comparison of the two sets of data shows a fair measure of agreement in the compositions regions CeO_2–$CeO_{1.81}$ and $CeO_{1.70}$–$CeO_{1.50}$. Thus BRAUER and GRADINGER find no evidence of any composition range for the CeO_2 (α) phase, a two-phase region existing between CeO_2 and $CeO_{1.81}$. Between $CeO_{1.70}$ and $CeO_{1.67}$ a single type-*C* rare earth phase is found with a continuously variable lattice parameter. Between $CeO_{1.67}$ and $CeO_{1.50}$ the type-*A* rare earth structure is found. However, for the region $CeO_{1.81}$–$CeO_{1.70}$, which in the present work constitutes the region of greatest interest, they quote no data. They assume the existence of a single homogeneous phase between $CeO_{1.81}$ and $CeO_{1.67}$ having the fluorite structure in the lower reduction state and the type-*C* structure in the higher reduction state. There is no mention of any deviation from cubic symmetry in their so-called intermediate phase, but since their X-ray patterns were obtained with a camera only 57·3 mm in

diameter, slight deviations might not be detected. However, it is by no means certain that rhombohedral phases which are stable at 1,050°C are also stable at 1,400°C. On the other hand, if their assumption of a homogeneous composition range is correct, the phase boundaries should, as they point out, vary with the annealing temperature. The constancy of the $CeO_{1.81}$ boundary over a temperature range of 350°C is thus additional evidence for the existence of a compound $Ce_{32}O_{58}$. The type-*C*/type-*A* boundary at 1,400°C occurs at the composition $CeO_{1.67}$; at 1,050°C this composition is $CeO_{1.65}$ and is clearly temperature dependent.

REFERENCES

Brauer, G., and Gradinger, H. (1951) *Naturwiss.*, **24,** 559.
Brauer, G., and Gradinger, H. (1954) *Z. anorg. Chem.* **277,** 89.
Bruno, M. (1950) *Ric. Sci.*, **20** (5), 645.
Chase, W. (1917) *J. Amer. Chem. Soc.*, **39,** 1576.
Courtel, R., and Loriers, J. (1950) *C.R. Acad. Sci.* (*Paris*), **230,** 735.
Duwez, P., Bowen, F. H., and Odell, F. (1951) *J. Electrochem. Soc.*, **98,** 356.
Foëx, M. (1946) *C.R. Acad. Sci.* (*Paris*), **222,** 660.
Friedrich, E., and Sittig, L. (1925) *Z. Anorg. Chem.*, **143,** 293.
Hund, F. (1951a) *Z. Elektrochem.*, **55,** 363.
Hund, F., and Durrwächter, W. (1951b) *Z. Anorg. Chem.*, **265,** 67.
Hund, F., and Mezger, R. (1952) *Z. Phys. Chem.*, **201,** 268.
Loriers, J. (1950) *C.R. Acad. Sci.* (*Paris*), **231,** 522.
Martin, R. L. (1950) *Nature*, **165,** 202.
McCullough, J. D. (1950) *J. Amer. Chem. Soc.*, **72,** 1386.
McCullough, J. D., and Britton, J. D. (1952) *J. Amer. Chem. Soc.*, **74,** 5225.
Meyer, R. (1903) *Z. Anorg. Chem.*, **37,** 378.
Rammelsberg, C. (1859) *Pogg. Ann.*, **108,** 63.
Rienäcker, G., and Birckenstaedt, M. (1951) *Z. Anorg. Chem.*, **265,** 99.
Schenck, R., and Roters, H. (1933) *Z. Anorg. Chem.*, **211,** 65.
Šterba, J. (1901) *C.R. Acad. Sci.* (*Paris*), **133,** 223.
Zachariasen, W. H. (1926) *Z. Phys. Chem.*, **23,** 134.
Zintl, E., and Croatto, U. (1939) *Z. Anorg. Chem.* **242,** 79.
Zintl, E., and Udgard, A. (1939) *Z. Anorg. Chem.*, **240,** 150.

VOL. 1 1955

J. Inorganic and Nuclear Chemistry, 1955, Vol. 1, pp. 60–67. Pergamon Press Ltd., London

THE DYNAMICS OF BINARY HYDRIDES

By H. C. LONGUET-HIGGINS* and D. A. BROWN
Wheatstone Physics Laboratory, University of London, King's College

(*Received November* 1954)

Abstract—The vibrational frequencies of the hydrides XH_2, XH_3, and XH_4 have been calculated on the assumption that the electron distribution in each molecule is spherical and rigid. The twisting frequencies ν_2 of the XH_4 molecules are shown to be determined by the formula

$$4\pi^2\nu_2^2 = \frac{9\sqrt{6}e^2}{32mr_0^3}$$

where e and m are the charge and mass of the proton and r_0 the equilibrium XH distance. This equation predicts the twisting frequencies of CH_4, SiH_4, GeH_4, and NH_4^+ within 5 per cent.

The other frequencies in these molecules involve the electron density ρ_H at a proton. Using one frequency to determine this parameter, the others are found to be in moderate agreement with experiment.

1. INTRODUCTION

THE purpose of this work has been to calculate theoretically the vibrational frequencies of some binary hydride molecules. It is a commonplace that *a priori* energy calculations on complex molecules are either worthless or impracticable; but equally it is true that "semi-empirical" theories lose all their value if they involve too many adjustable parameters. We have therefore attempted to base our calculations on the absolute minimum of theoretical assumptions, appealing to no experimental data except the known geometry of the molecules, and invoking not more than one unknown parameter for each molecule.

2. FIRST PRINCIPLES

Our method of approach is founded on a little-known but very important theorem due originally to HELLMANN (1937) and FEYNMAN (1939), and recently discussed by BERLIN (1951). This theorem is derived directly from the Schrödinger wave equation and the Born-Oppenheimer approximation, and is as follows:—

Let us envisage a molecule in a particular nuclear configuration, and imagine that the electronic wave equation has been solved for this configuration to give the total electron density ρ at every point in the molecule. Then the theorem asserts that the net force F acting on any particular nucleus is equal to the electrostatic repulsion of all the other nuclei together with electrostatic attraction of the electron cloud regarded as a classical charge distribution. In mathematical terms, if Z_μ is the atomic number of nucleus μ, then the force on the nucleus ν (taken at the origin) is given by

$$\boldsymbol{F}_\nu = Z_\nu e^2\left\{\sum_{\mu}^{\neq\nu}\left(-\frac{Z_\mu \boldsymbol{r}_\mu}{r_\mu^3}\right) + \int\frac{\rho(\boldsymbol{r})\boldsymbol{r}}{r^3}\,d\tau\right\}.$$

This equation shows that equilibrium, when $\boldsymbol{F}_\nu = 0$, the electrostatic force due to all the other nuclei is exactly balanced by the force due to the electron cloud.

The importance of this theorem is that it is independent of any assumptions about the electronic wave function, and is therefore to all intents and purposes exact.

* Present address: University Chemical Laboratory, Cambridge.

VOL. 1 1955

3. THE BINARY HYDRIDES

PLATT (1950) calculated the internuclear distances and force constants of some diatomic hydrides XH from the assumption that the electrons in XH were spherically distributed about the nucleus X in the same manner as in the "united atom" (X + 1). Using Hartree orbitals to estimate the electron densities, he obtained remarkable agreement with experiment; and where the Hartree orbitals were not available, Slater orbitals gave a moderate fit with the observed bond-lengths and force-constants. Platt's discussion of his model, which is superficially a classical model, can be justified immediately by an appeal to the Hellmann-Feynman theorem; and its success strongly suggests that the electron distribution in XH is not very different from that in X + 1 and is insensitive to changes in the XH distance.

The success of Platt's work, and the simplicity of his model, stimulated us to undertake a similar investigation of the polyatomic hydrides of Groups IV, V, and VI. In these hydrides the central atoms differ by 4, 3, and 2 in atomic number from the united atoms; so the electron distributions will obviously depart more from those of the united atoms than in the diatomic hydrides. However, it seems reasonable to retain the assumption of a spherical electron distribution, and to suppose that the structure of this distribution is unaffected by small movements of the hydrogen nuclei. These assumptions alone, as will appear, enable us to draw some quantitative conclusions about the molecular vibrations. We shall now discuss in turn the hydrides of Groups IV, VI, and V.

4. THE GROUP IV HYDRIDES XH_4

The known Group IV hydrides include CH_4, SiH_4, and GeH_4, and are tetrahedral in equilibrium. The observed values of r_0, the XH distance, are given in Table 1. We are assuming the electron distribution to be spherically symmetrical about X; hence, by the H.-F. theorem the outward force on each of the H nuclei due to the other 4 nuclei is balanced by a force Qe^2/r_0^2, where Q is the total number of electrons within a sphere of radius r_0 centred on X. When the molecule XH_4 vibrates, there is

TABLE 1.—THE VIBRATIONAL FREQUENCIES OF THE GROUP IV HYDRIDES

	r_0(Å) obs.	ν_1 obs.	ρ_H calc.	ν_2		ν_3		ν_4	
				obs.	calc.	obs.	calc.	obs.	calc.
CH_4	1·094[a]	2914[a]	2.189	1499[a]	1429	3018[a]	2084	1306[a]	1932
SiH_4	1·456[b]	2187[b]	1·233	978[b]	931	2191[b]	1730	914[b]	1202
GeH_4	1·478[b]	2089[d]	1·125	981[b]	910	2114[b]	1612	819[b]	1137
NH_4+	1·014[c]			1685	1601				

[a] D. F. HEATH, J. W. LINNETT, and P. J. WHEATLEY, *Trans. Faraday Soc.* **46**, 137 (1950).
[b] H. H. NIELSEN, *Phys. Rev.* **62**, 151 (1942).
[c] T. SIMANOUTI, *J. Chem. Phys.* **17**, 245 (1949).
[d] K. SCHÄFER, and J. M. GONZALEZ BARREDO, *Z. Physik. Chem.* **193**, 334 (1944).

the possibility that the centre of the electron distribution (assumed rigid) may become detached from the nucleus X. The following argument, however, shows that this effect may be ignored. By Poisson's equation

$$\frac{\partial^2\psi}{\partial x^2} + \frac{\partial^2\psi}{\partial y^2} + \frac{\partial^2\psi}{\partial z^2} = 4\pi\rho_X e,$$

where $\psi(x, y, z)$ is the electrical potential near the X atom and ρ_X is the electron density there. Hence the effective force constant for displacing X from the centre of the electron cloud is $\frac{4}{3}\pi\rho_X Ze^2$; and since Z and ρ_X are both large, there will be a strong tendency for the electron centre to remain in coincidence with the nucleus X.

The effective intramolecular potential is therefore of the form

$$V = e^2 \sum_{i<j} \frac{1}{r_{ij}} + \sum_i \phi(r_i),$$

where r_{ij} is the distance between protons i and j, and r_i is the distance of i from X. The first derivative of $\phi(r)$ is

$$\phi'(r) = \left\{\frac{Q(r) - Z}{r^2}\right\} e^2,$$

this being the net force exerted on i by X and the electron cloud. Setting $r_i = r$, $r_{ij} = \frac{2\sqrt{6}}{3} r$, and differentiating with respect to r we obtain

$$\frac{\partial V}{\partial r} = -\frac{3\sqrt{6}e^2}{2r^2} + 4\left\{\frac{Q(r) - Z}{r^2}\right\} e^2.$$

In equilibrium, therefore, $Q = Z + \frac{3\sqrt{6}}{8}$, which means that the protons come to rest on a sphere which excludes $4 - \frac{3\sqrt{6}}{8}$ of the electrons.

To calculate the vibrational frequencies we expand V to the second order in the increments δr_{ij}, δr_i. The result is

$$V = \text{const.} - \frac{3e^2}{8{r_0}^2} \sum_{i<j} \delta r_{ij} + \frac{3\sqrt{6}e^2}{8{r_0}^2} \sum_i \delta r_i + \frac{3\sqrt{6}e^2}{32{r_0}^3} \sum_{i<j} \delta r_{ij}^2 + \left(2\pi\rho_{II} - \frac{3\sqrt{6}}{8{r_0}^3}\right) e^2 \sum_i \delta r_i^2,$$

where ρ_{II} is the density of electrons at a distance r_0 from X.

DENNISON (1925) has solved the vibrational problem for XY_4, using a central-force potential of this kind. Substitution of our constants into his potential function yields the following equations for the frequencies ν_i (λ_i denotes $4\pi^2\nu_i^2$, m is the mass of H, and M that of X):—

(i) For the non-degenerate "breathing" mode (A):

$$\lambda_1 = 4\pi\rho_{II}e^2/m$$

(ii) For the doubly-degenerate "twisting" mode (E):

$$\lambda_2 = 9\sqrt{6}e^2/32m{r_0}^3$$

(iii) For the two triply degenerate modes (F):

$$\lambda_3 + \lambda_4 = \lambda_1\left(1 + \frac{4m}{3M}\right) - \frac{2\lambda_2}{3}$$

$$\lambda_3\lambda_4 = \frac{2\lambda_2}{9}(7\lambda_1 - 16\lambda_2)\left(1 + \frac{4m}{M}\right).$$

The most obvious point of interest is that the doubly-degenerate frequency ν_2 does not depend on ρ_H but *only on* r_0. (This is because in the twisting mode the X–H distance does not change to the first order.) We can therefore calculate ν_2 from the observed bond-length alone.

Secondly, ν_1 is determined by ρ_H alone, and may be used to determine this parameter. ν_3 and ν_4, which are related to ν_1 and ν_2, may then be evaluated as the roots of a quadratic equation. Table 1 compares the values of ν_2, ν_3, ν_4 calculated in this way with the experimental values. In the third column are given the values of ρ_H, as determined from ν_1 (obs.)

5. THE GROUP VI HYDRIDES XH_2

When we come to the hydrides of Groups V and VI it is no longer possible to suppose that the centre of the electron cloud coincides with the nucleus X. The reason for this is that the repulsive forces exerted on one hydrogen nucleus by the other and

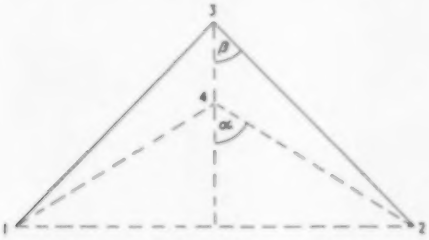

FIG. 1.

by nucleus X act in different directions, and can only be balanced by an attractive force in an intermediate direction. In Fig. 1, the numbers 1, 2, 3, and 4 represent the two hydrogen atoms, the X atom, and the centre of the electron cloud respectively.

The position of the electron centre is most directly found by elementary statics. Denoting the magnitudes of the electrostatic forces by F_{12}, etc., we have the equations

$$F_{12} + F_{13}\sin\beta = F_{14}\sin\alpha$$

$$F_{13}\cos\beta \qquad = F_{14}\cos\alpha$$

whence

$$\tan\alpha = \frac{F_{12} + F_{13}\sin\beta}{F_{13}\cos\beta}.$$

But

$$F_{13} = \frac{Ze^2}{r_{13}^2}, \quad F_{12} = \frac{e^2}{r_{12}^2} = \frac{e^2}{4r_{13}^2\sin^2\beta};$$

therefore

$$\tan\alpha = \frac{1 + 4Z\sin^3\beta}{4Z\sin^2\beta\cos\beta}.$$

This equation gives α in terms of the measured valence angle 2β, and locates the electron centre within the triangle 123. Using the further relations

$$F_{14} = F_{24} = \frac{Q_H e^2}{r_{14}^2}, \quad F_{34} = \frac{Q_X e^2}{r_{34}^2} = 2F_{13}\cos\beta,$$

we may finally determine Q_H and Q_X, which denote the numbers of electrons within spheres of radii r_{14} and r_{34}, centred at 4. The observed values of r_{13} and β, and the calculated values of α, Q_H, and Q_X, are given in Table 2.

The vibrational frequencies are then determined by the potential function

$$V = e^2\left(\frac{1}{r_{12}} + \frac{Z}{r_{13}} + \frac{Z}{r_{23}}\right) + \phi_H(r_{14}) + \phi_H(r_{24}) + \phi_X(r_{34}),$$

where

$$\frac{\partial\phi_H}{\partial r} = \frac{Q_H e^2}{r_{14}^2}, \quad \frac{\partial^2\phi_H}{\partial r^2} = \left(4\pi\rho_H - \frac{2Q_H}{r_{14}^3}\right)e^2,$$

$$\frac{\partial\phi_X}{\partial r} = \frac{Q_X Z e^2}{r_{34}^2}, \quad \frac{\partial^2\phi_X}{\partial r^2} = \left(4\pi\rho_X - \frac{2Q_X}{r_{34}^3}\right)e^2,$$

and ρ_H, ρ_X are the electron densities at the hydrogen and X-nuclei respectively.

TABLE 2.—MOLECULAR CONSTANTS OF THE GROUP VI HYDRIDES

	r_{13}(Å)	β	α	Q_H	Q_X	μ (Debyes)	
						calc.	obs.
H_2O	0·9584[e]	52° 15′[e]	53° 56′	7·961	·001627	3·96	1·84[h]
H_2S	1·334[f]	46° 08′[f]	47° 18′	15·743	·001069	5·70	0·93[h]
H_2Se	1·53[g]	45°[g]	45° 35′	33·676	·0002937	6·58	0·60[i]

[e] G. HERZBERG, *Infrared and Raman Spectra*, p. 439, Van Nostrand Co., New York (1945).
[f] P. C. CROSS, *J. Chem. Phys.* **5**, 370 (1937).
[g] W. GORDY, *J. Chem. Phys.* **14**, 305.
[h] Y. K. SYRKIN, and N. E. DYATKINA, *Structure of Molecules*, Butterworths Scientific Publications, London (1950).
[i] C. P. SMYTH, and S. A. MCNEIGHT, *J. Amer. Chem. Soc.* **58**, 1723 (1936).

This may be regarded as a central-force potential function with the electron centre as an extra interacting particle. Since the kinetic energy of vibration involves only the velocities of the three nuclei, this extra particle is to be assigned zero mass, and the corresponding infinite frequency discarded.

TABLE 3.—THE VIBRATIONAL FREQUENCIES OF THE GROUP VI HYDRIDES

	ν_1		ν_3		ν_2 (obs.)	ρ_H(Å^{-3}) (calc.)
	(obs.)	(calc.)	(obs.)	(calc.)		
H_2O	3652[k]	4467	1595[k]	1432	3756[k]	5·582
H_2S	2611[k]	3080	1290[k]	1137	2684[k]	2·893
H_2Se	2260[l]	2640	1074[l]	969·2	2350[l]	2·221

[k] W. G. PENNEY and G. B. B. M. SUTHERLAND, *Proc. Roy. Soc.* **A156**, 654 (1936).
[l] W. C. SEARS and H. H. NIELSEN, *J. Chem. Phys.* **7**, 994 (1939).

The vibrational frequencies of XH_2 are three in number, two symmetric and one antisymmetric. In the last the distance r_{34} does not change, so that ν_3 is determined by ρ_H alone and may be used to estimate this parameter. The symmetric frequencies ν_1, ν_2, however, depend also on ρ_X; and for our calculations to retain any value we

must estimate this parameter independently. What we have done is to assume the electron density to be constant within the sphere r_{34}; and this gives the result $Q_X = \frac{4}{3}\pi\rho_X r_{34}^3$ or $4\pi\rho_X = \frac{3Q_X}{r_{34}^3}$.

To calculate ρ_H from ν_3, and then ν_1, ν_2 from ρ_H is then a matter of routine. Due attention must be paid to the fact that the system is "pre-stressed," as is usual in a central-force problem. We have solved the vibrational problem by two independent methods: one a straightforward treatment based on cartesian displacement co-ordinates, and the other a method in which the secular equations involve the internal displacement co-ordinates δr_{ij} (LONGUET-HIGGINS, 1955). The fact that the two sets of calculations agree gives us added confidence in their correctness.

Table 3 gives the values of ν_3(obs.) which were used to calculate ρ_H, and compares the observed values of ν_1, ν_2 with those calculated from ρ_H and the molecular geometry.

VOL. 1 1955

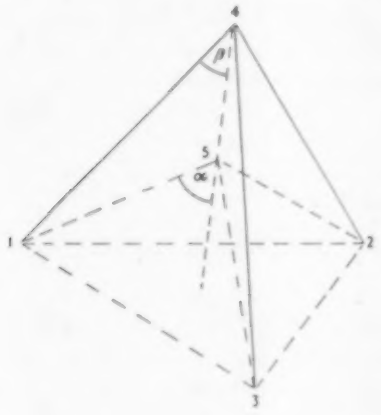

FIG. 2.

6. THE GROUP V HYDRIDES XH_3

The Group V hydrides XH_3 may be treated in a manner completely analogous to those of Group VI. The conditions of equilibrium determine the position of the electron centre and the quantities Q_H and Q_X, which denote the numbers of electrons within spheres of radii r_{15} and r_{45}, centred at 5 (see Fig. 2). The observed values of r_{14} and $\beta(= 1\hat{4}5)$ and the calculated values of $\alpha(= \pi - 1\hat{5}4)$, Q_H and Q_X are given in Table 4.

TABLE 4.—MOLECULAR CONSTANTS OF THE GROUP V HYDRIDES

	r_{14}(Å)	β	α	Q_H	Q_X	μ (Debyes)	
						calc.	obs.
NH_3	1·014[m]	67° 58′[m]	69° 52′	7·434	·001395	3·77	1·46[n]
PH_3	1·424[n]	57° 30′[n]	59° 6′	15·153	·001693	7·03	0·55[n]
AsH_3	1·523[n]	55° 51′[n]	56° 39′	33·099	·0004765	7·90	0·16[n]

[m] G. HERZBERG, *Ibid*, p. 439.
[n] H. H. NIELSEN, *J. Chem. Phys.* **20**, 758 (1952).

The vibrational frequencies are now determined by the potential function

$$V = e^2\left(\frac{1}{r_{12}}+\frac{1}{r_{23}}+\frac{1}{r_{31}}\right)+Ze^2\left(\frac{1}{r_{14}}+\frac{1}{r_{24}}+\frac{1}{r_{34}}\right)$$
$$+\phi_{\mathrm{H}}(r_{15})+\phi_{\mathrm{H}}(r_{25})+\phi_{\mathrm{H}}(r_{35})+\phi_{\mathrm{X}}(r_{45}),$$

where

$$\frac{\partial\phi_{\mathrm{H}}}{\partial r}=\frac{Q_{\mathrm{H}}e^2}{r_{15}^{\,2}},\quad \frac{\partial^2\phi_{\mathrm{H}}}{\partial r^2}=\left(4\pi\rho_{\mathrm{H}}-\frac{2Q_{\mathrm{H}}}{r_{15}^{\,3}}\right)e^2,$$

$$\frac{\partial\phi_{\mathrm{X}}}{\partial r}=\frac{Q_{\mathrm{X}}Ze^2}{r_{45}^{\,2}},\quad \frac{\partial^2\phi_{\mathrm{X}}}{\partial r^2}=\left(4\pi\rho_{\mathrm{X}}-\frac{2Q_{\mathrm{X}}}{r_{54}^{\,3}}\right)e^2,$$

and ρ_{H}, ρ_{X} are the electron densities at the protons and the X nucleus respectively.

As in the hydrides XH_2, we have here a central-force potential function with the electron centre as a "particle" of zero-mass. We know therefore that there will be four finite frequencies, of which two, ν_1 and ν_2, will be symmetric, and the other two, ν_3 and ν_4, doubly degenerate. The two degenerate frequencies involve no change in the distance r_{45} and are therefore independent of ρ_{X}. They do depend, however, on ρ_{H}, which is not determined by the observed geometry. We have accordingly determined ρ_{H} from the observed value of $\nu_3^2+\nu_4^2$, and used the resulting value of ρ_{H} to calculate ν_3 and ν_4 separately. In Table 5 the columns labelled ν_3(calc.) and ν_4(calc.) represent the values obtained in this way.

The symmetric frequencies ν_1, ν_2 depend on ρ_{X} as well as ρ_{H}. Setting $4\pi\rho_{\mathrm{X}}=\dfrac{3Q_{\mathrm{X}}}{r_{45}^{\,3}}$, as in Group VI hydrides, and using the value of ρ_{H} obtained already, we arrive at the theoretical estimates ν_1(calc.) and ν_2(calc.) given in Table 5. The calculations were again carried out by two independent methods, the cartesian method and the internal displacement method, with complete agreement.

TABLE 5.—THE VIBRATIONAL FREQUENCIES OF THE GROUP V HYDRIDES

	ν_1		ν_2		ν_3		ν_4		ρ_{H} (A^{-3})
	(obs.)	(calc.)	(obs.)	(calc.)	(obs.)	(calc.)	(obs.)	(calc.)	
NH_3	3337[p]	4255	950[p]	911·5	3414[p]	3511	1628[p]	1407	4·744
PH_3	2327[q]	2947	991[q]	871·5	2421[q]	2456	1121[q]	1042	2·474
AsH_3	2209[q]	2663	973[q]	838·1	2226[q]	2229	1012[q]	1005	2·178

[p] C. M. LEWIS and W. V. HOUSTON, *Phys. Rev.* **44**, 903 (1933).
[q] V. M. MCCONAGHIE and H. H. NIELSEN, *Phys. Rev.* **75**, 633 (1949).

7. DISCUSSION

In all these calculations we have proceeded on the assumption that the electron distribution is spherical (though not necessarily centred on the heavy atom X), and that it is "rigid," in the sense that its structure is unaffected by molecular vibrations. This hypothesis does not obviously guarantee the stability of the observed nuclear configurations in XH_2 and XH_3; it is therefore reassuring to find that our calculated frequencies are real, as this is a necessary and sufficient condition for stability.

It may appear that the comparison between theoretical and experimental frequencies in Tables 1, 3, and 5 is no better than might have been anticipated, since we have allowed ourselves one adjustable parameter (ρ_H) with which to correlate the separate frequencies of each molecule. But, as mentioned earlier, there is one type of frequency which is independent of ρ_H, namely the doubly degenerate frequency ν_2 of a Group IV hydride XH_4. This frequency is given by the expression

$$4\pi^2\nu_2^2 = 9\sqrt{6}e^2/32mr_0^3$$

where e, m are the charge and mass of the proton and r_0 is the equilibrium XH distance. The remarkable success of this equation, as indicated in Table 1, may be understood in the following terms. If the electron distribution in XH_4 is expanded in spherical harmonics, then the effect on this distribution of a molecular distortion will be to alter the contributions of the various harmonics. Now it is quite easily seen that the totally symmetric vibration ν_1 can alter the contributions of the s harmonics, and that the triply degenerate vibrations ν_3, ν_4 can alter the contributions of the p harmonics; but the doubly degenerate twisting vibration can only introduce d or higher harmonics. Therefore one might expect the electron distribution to be more rigid in the twisting mode than in the others: changes of hybridization at the central atom involving s and p orbitals only cannot assist a distortion of this symmetry. As for the other frequencies, it appears from the tables that the agreement between theory and experiment improves as one goes down the Periodic Table. Against this, however, must be set the fact that the dipole moments of the Group V and VI hydrides decrease with increasing atomic number, whereas according to our calculations they should increase sharply. (The dipole moment is easily calculated once the centre of the electron distribution has been located.) It is not difficult to think of possible reasons for this discrepancy; but the failure of the model to predict dipole moments is a warning against taking it too literally in detail.

We intend to extend these ideas in a forthcoming paper to diborane, of whose potential function no quantitative theory appears to exist at present.

VOL. 1 1955

ACKNOWLEDGMENT

One of us (D. A. B.) wishes to thank the Department of Scientific and Industrial Research for a Senior Award, during the tenure of which this work was carried out.

REFERENCES

BERLIN, T., (1951) *J. Chem. Phys.* **19**, 208.
DENNISON, D. M., (1925) *Astrophys J.* **62**, 84.
FEYNMAN, R. P., (1939) *Phys. Rev.* **56**, 340.
HELLMANN, H., (1937) *Einführung in die Quantenchemie*, Leipzig.
LONGUET-HIGGINS, H. C., (1955) *Phil. Mag.* (in press).
PLATT, J. R., (1950) *J. Chem. Phys.* **18**, 932.

J. Inorganic and Nuclear Chemistry, 1955, Vol. 1, pp. 68–74. Pergamon Press Ltd., London

HYDROLYSE DE L'ION URANYLE ET FORMATION D'URANATES DE SODIUM

J. SUTTON
Commissariat à l'Energie Atomique, Service de Chimie Physique, Paris

(*Received October* 1954)

Abstract—The compositions of the uranates precipitated by mixing solutions of sodium hydroxide and uranyl chloride have been investigated by the method of residues. The results indicate that two uranates are formed, $Na_2U_{16}O_{49}$ (yellow) and $Na_2U_2O_7$ (orange). The former yields yellow $Na_2U_7O_{22}$ on washing with water. Reasons for the disagreement between these and previous results are discussed.

LES phases initiales de l'hydrolyse de l'ion uranyle ont été interprétées en supposant la formation des ions complexes $U_2O_5^{++}$, $U_3O_8^{++}$, $U_3O_8(OH)^+$, etc. (SUTTON, 1949). Les changements de pH et d'absorption dans l'ultraviolet provoqués par l'addition d'une solution d'hydroxyde de sodium à une solution de sel d'uranyle (par exemple, le perchlorate) peuvent être expliqués par cette théorie. A un certain stade, déterminé par la composition de la solution, on trouve une forme anionique de l'ion uranyle, et pour une concentration supérieure à 0·01M environ, un précipité se produit immédiatement. Ce précipité qui est un uranate de sodium, passe graduellement du jaune à l'orange quand le rapport moléculaire NaOH : $UO_2(ClO_4)_2$ croît de 1·5 à 2·5 environ dans le mélange.

De tels uranates alcalins ont été étudiés par beaucoup de chercheurs, mais avec des résultats qui ne concordent pas toujours. Diverses formules ont été proposées pour ces uranates en se basant sur des données analytiques, des mesures de pH, de conductibilité etc. BRITTON (1925, 1932) a considéré que le précipité jaune est $UO_2(OH)_2$ hydraté, GUITER (1946, 1947) lui a attribué la formule $Na_2U_8O_{25}$ et TRIDOT (1950) a suggéré que pendant l'addition d'hydroxyde de sodium au nitrate d'uranyle, il se formait $Na_2U_5O_{16}$, $Na_2U_2O_7$, et $NaUO_4$. Ce dernier auteur prétend aussi qu'il y a formation de $Na_2U_4O_{13}$ par réaction entre la soude caustique et l'acétate d'uranyle.

Dans le système KOH—$UO_2(NO_3)_2$—H_2O, FLATT et HESS (1938) ont trouvé deux uranates, $K_2U_7O_{22}$ (jaune) et $K_4U_5O_{17}$ (orange), et ils ont montré que tous les précipités de couleurs intermédiaires peuvent être considérés comme des mélanges de ces deux uranates. WAMSER et ses collaborateurs (1952) ont étudié les uranates précipités par addition d'hydroxyde de sodium au nitrate d'uranyle. Ils ont séparé les précipités formés dans divers mélanges après cinq jours de repos pour laisser à l'équilibre le temps de s'établir. Après un lavage à l'eau poussé jusqu'à l'élimination de presque toute trace alcaline ils ont dosé l'uranium et le sodium dans ces précipités et ils ont observél eurs spectres de rayons X. Leurs résultats indiquent l'existence de deux uranates seulement, $Na_2U_7O_{22}$ (jaune) et $Na_6U_7O_{24}$ (orange), en assez bon accord avec les conclusions de FLATT et HESS.

Tandis que cette étude se poursuivait, nous nous attaquions au même problème,

* Ce travail a été commencé à A.E.R.E. Harwell; il est publier, pour cette part, avec la permission du Directeur.

mais nous avons obtenu des résultats différents. Nous avons établi que le premier précipité formé lors de l'addition d'hydroxyde de sodium à un excès de chlorure d'uranyle n'était pas de l'hydroxyde d'uranyle mais un uranate de sodium, et qu'il ne se formait probablement que deux uranates dans ce système. Les expériences préliminaires avaient aussi montré que le lavage de précipités avec de l'eau ou solvants organiques modifiait l'équilibre et par conséquent changeait la composition des précipités. Pour essayer de tourner cette difficulté on a lavé chaque précipité avec une solution de chlorure de sodium de même concentration que la solution en équilibre avec ce précipité, et amenée au même pH (par addition d'acide chlorhydrique ou d'hydroxyde de sodium). Les précipités étaient séchés d'abord sous vide, puis à l'étuve et on y dosait le sodium, l'uranium, et le chlore. En supposant qu'il n'y ait pas de chlorure combiné dans les précipités, on peut calculer (par le simple dosage de chlorure) la quantité de sodium provenant de la solution qui imprègne le précipité. On a calculé ainsi le rapport U : Na dans le précipité proprement dit. On a trouvé respectivement 6 : 1 environ pour les précipités jaunes et 1 : 1 pour les précipités oranges.

VOL. 1 1955

La divergence de nos résultats et de ceux des auteurs précédents nous a poussé à reprendre le travail en utilisant la méthode des restes. Nous avons d'abord montré que l'ion chlorure n'était pas absorbé sur les précipités d'uranate au cours de leur formation. Ceci a été démontré en précipitant des uranates dans une solution contenant du $^{38}Cl^-$. On a alors préparé plusieurs mélanges de solutions d'hydroxyde de sodium et de chlorure d'uranyle; une fois l'équilibre atteint, on a séparé par centrifugation les solutions claires des précipités. Les précipités humides étaient dissous dans l'acide nitrique dilué. On dosait, dans ces deux séries de solutions, le sodium, l'uranium et le chlore. Le dosage de l'ion Cl^- a permis dans chaque cas de calculer la quantité de solution mère imprégnant le précipité, et donc de faire les corrections nécessaires aux dosages de sodium et d'uranium dans le précipité et d'en déterminer la composition réelle. Voici le détail des expériences.

MÉTHODES EXPÉRIMENTALES

Un échantillon (0·2 g) de chlorure d'ammonium était irradié dans la pile de Châtillon et le produit actif était chauffé avec 60 ml d'une solution 0·9N d'hydroxyde de sodium jusqu'à élimination complète de l'ammoniac. On ajoutait deux parties aliquotes de 7 ml de cette solution marquée respectivement à 25 ml d'une solution de perchlorate d'uranyle, 0·23M, et à 25 ml d'eau. On répétait l'opération en utilisant 18 ml de solution active au lieu de 7 ml. De cette façon, un échantillon de chaque précipité était formé en présence d'ions $^{38}Cl^-$. Au bout de 2 heures on prélevait 10 ml de chaque solution mère, auxquels on ajoutait 1 ml d'acide chlorhydrique 0·2N et un excès d'une solution de nitrate d'argent. Les quatre précipités de chlorure d'argent étaient séparés et dissous dans de l'ammoniaque chaude et les solutions ainsi obtenues amenées au volume de 25 ml. Puis chacune d'elles étaitpassée dans un compteur pour liquides. Si N_0 est le nombre de coups par minute pour la première solution, et N le nombre donné par le témoin, mesuré t minutes plus tard, on a:

$$\log \frac{N_0}{N} = \frac{0{\cdot}693t}{37 \times 2{\cdot}303}$$

(37 minutes est la période de ^{38}Cl). Le temps t étant 16 minutes, $N_0/N = 1{\cdot}35$ s'il n'y a pas eu d'adsorption de Cl^- sur le précipité. S'il y avait eu adsorption on trouverait une valeur inférieure a 1·35. Pour le précipité jaune on a trouvé $N_0/N = 1{\cdot}35$ et pour l'orange 1·40. Puisque cette différence est inférieure à l'erreur expérimentale on peut dire qu'il n'y a pas absorption.

Avant de préparer les divers mélanges des solutions d'hydroxyde de sodium et de chlorure d'uranyle on a fait des titrages potentiométriques (mesures de pH) sur des dilutions convenables de

ces solutions. Ces résultats, ainsi que ceux de WAMSER sont rassemblés dans la Fig. 1. A l'aide de ces courbes, on a fait une série de mélanges destinés à donner en quantités variables les précipités des deux sortes. Ces mélanges étaient contenus dans des flacons de verre fermés avec des bouchons de chlorure de polyvinyle. Ils ont tous été amenés au même volume par addition d'eau exempte de gaz carbonique. Tous les mélanges étaient agités pendant deux jours puis laissés au repos quelques semaines à la température ambiante pour permettre à l'équilibre de s'établir. Dans chaque échantillon, la solution mère était alors séparée du précipité par centrifugation.

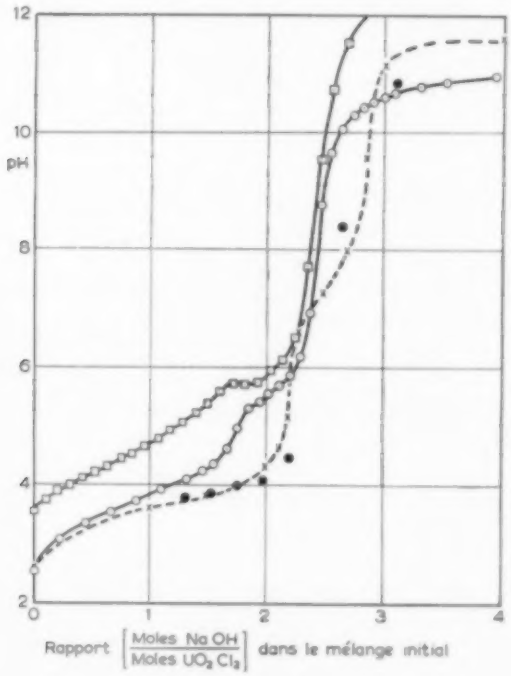

FIG. 1.—Titrages.
○ Série 1. Solutions diluées 5×
● Série 2. Valeurs à l'équilibre
⊡ Série 3. Sans dilution
× Résultats de WAMSER (à l'équilibre)

Le précipité humide était dissous dans l'acide nitrique, le flacon rincé à l'acide nitrique et le liquide de rinçage ajouté à la solution du précipité. On dosait alors le sodium, l'uranium et le chlore dans toutes ces solutions.

Le dosage du sodium se faisait à l'uranyle acétate de zinc (VOGEL, 1951), celui de l'uranium par colorimétrie du peroxy-uranate en solution alcaline (RODDEN, 1950), et celui du chlorure par titrage au nitrate d'argent dans les solutions mères et au nitrate mercureux dans les solutions de précipités. Le point d'équivalence était déterminé par potentiométrie avec le montage suivant

$$Hg \mid Hg_2Cl_2 \mid KNO_3 \text{ saturée} \mid KNO_3 \text{ agar} \mid \text{inconnue} \mid AgCl \mid Ag$$

pour les titrages avec le nitrate d'argent.

Dans le cas des titrages avec le nitrate mercureux une électrode à goutte de mercure remplaçait l'électrode de chlorure d'argent. Pour les faibles concentrations en ion chlorure qu'on trouve dans certaines des solutions de précipité, le titrage au nitrate mercureux n'a pas donné de résultats

assez précis. C'est ainsi que, pour la troisième série de solutions du tableau, on a dosé le chlorure par titrage du nitrate mercurique (CLARKE, 1950). En utilisant la diphénylcarbazone comme indicateur, on a obtenu de bons résultats avec des concentrations d'environ N/500.

Voici les résultats obtenus pour trois séries de solutions. Les deux premières n'ont pas donné de résultats assez précis pour la compositition du précipité jaune. Pour ce produit, la troisième série est la plus exacte; c'est pour cette raison que nous en présentons les résultats analytiques en plein détail.

RÉSULTATS

Série 1. Solution A 0·821M UO_2Cl_2
B 0·901M NaOH

Les mélanges étaient composés de 5 ml de solution A et 6, 7, 8, 9, 10, 11, 12, 14, et 20 ml de solution B. La température ambiante était 26°C, et on a séparé les mélanges après quatre mois de repos.

No. de la solution	Rapport initial $\frac{NaOH}{UO_2Cl_2}$	Rapport U/Na dans le précipité
1	1·32	7·6
2	1·54	6·8
3	1·76	7·3
4	1·98	7·5
5	2·20	6·1
6	2·44	3·1
7	2·64	1·9
8	3·05	1·01
9	4·37	0·94

Série 2. Solution A 0·830M UO_2Cl_2
B 1·001M NaOH

Les mélanges étaient composés de 5 ml de solution A, 25 ml d'eau et 5, 6, 7, 8, 9, 10, 11, 12, 14, 16, 18, 20, et 22 ml de solution B. La température ambiante était 25°C et les mélanges étaient agités pendant un mois avant la séparation.

No. de la solution	Rapport initial $\frac{NaOH}{UO_2Cl_2}$	Rapport U/Na dans le précipité
1	1·21	6·8
2	1·45	7·5
3	1·69	7·7
4	1·93	7·3
5	2·16	6·75
6	2·41	3·6
7	2·65	2·1
8	2·91	1·34
9	3·38	1·05
10	3·85	1·05
11	4·32	1·01
12	4·82	1·04
13	5·30	1·03

VOL. 1 1955

Série 3. Solution A 0·622M UO_2Cl_2
B 0·659M NaOH

Les mélanges étaient composés de 5 ml de solution A, 6, 6·5, 7, 7·5, 8, 8·5, 9, et 9·5 ml de solution B, et d'eau pour amener le volume à 30 ml. Ces mélanges étaient agités à la température ambiante pendant trois semaines avant la séparation et le dosage.

No. de la solution	Rapport initial $\frac{NaOH}{UO_2Cl_2}$	Résultats d'analyses (en millimoles)						Quantités totales et différences* (%)					
		Solution mère			Solution du précipité			Cl		U		Na	
		Cl	U	Na	Cl	U	Na						
1	1·26	6·045	1·919	3·700	0·286	1·231	0·332	6·331	+0·1	3·150	0·0	4·032	+2·0
2	1·37	5·925	1·659	3·910	0·358	1·475	0·416	6·283	−0·6	3·134	−0·5	4·326$_4$	+1·0
3	1·48	5·535	1·302	3·878	0·827	1·845	0·772	6·326	+0·6	3·147	−0·1	4·650	+0·6
4	1·59	5·500	1·085	4·153	0·793	2·060	0·838	6·292	−0·5	3·145	−0·2	4·991	+1·0
5	1·68	4·575	0·766	3·615	1·750	2·393	1·647	6·325	0·0	3·159	+0·3	5·262	−0·2
6	1·78	4·685	0·620	3·956	1·643	2·555	1·680	6·328	+0·05	3·175	+0·8	5·636	+0·5
7	1·88	4·560	0·451	4·055	1·775	2·706	1·883	6·334	+0·15	3·157	+0·2	5·937	+0·1
8	1·99	4·747	0·302	4·429	1·599	2·835	1·849	6·346	+0·3	3·137	−0·4	6·278	+0·3

*moins-trouvé

No. de la solution	Quantités de Na et U (en millimoles) dans				Rapport U/Na dans le précipité
	la solution adhérente		le précipité (par différence)		
	Na	U	Na	U	
1	0·175	0·091	0·158	1·140	7·22
2	0·236	0·100	0·179	1·137	7·66
3	0·579	0·195	0·193	1·650	8·55
4	0·599	0·156	0·239	1·904	7·96
5	1·383	0·293	0·264	2·100	7·96
6	1·389	0·218	0·291	2·337	8·00
7	1·580	0·176	0·303	2·530	8·35
8	1·491	0·102	0·358	2·733	7·64

DISCUSSION DES RÉSULTATS

Nos résultats et ceux de WAMSER et de ses collaborateurs sont présentés dans la Fig. 2. En abscisse sont portés le nombre des moles NaOH ajoutée à 1 mole du sel d'uranyle dans le mélange primitif. Les ordonnées donnent le rapport atomes U/atomes Na dans le précipité correspondant. Les résultats les plus dignes de foi donnent les formules $Na_2U_{16}O_{49}$ pour l'uranate jaune et $Na_2U_2O_7$ pour l'uranate orange. Ces formules sont très différentes de celles des auteurs américains et nous pensons que la divergence provient de la différence des méthodes de lavage. Le lavage abondant à l'eau d'un précipité jaune qui se trouverait en équilibre avec une solution mère de pH inférieur à 7 doit provoquer la décomposition du précipité:

$$Na_2U_{16}O_{19} \xrightarrow{H_2O} Na_2U_xO_{3x+1} + \text{tous produits d'hydrolyse solubles de l'ion } UO_2^{++}.$$

$Na_2U_xO_{3x+1}$ est la formule du précipité en équilibre avec une solution mère de pH = 7. Nos expériences ont montré qu'une telle décomposition se produit trés facilement et que le précipité final a la composition $Na_2U_7O_{22}$. On verra sur les figures 1 (courbe 3) et 2 que cette formule correspond à la valeur d'abscisse 2·4 et à pH 7. Donc le lavage prolongé donnera toujours un précipité de cette composition.

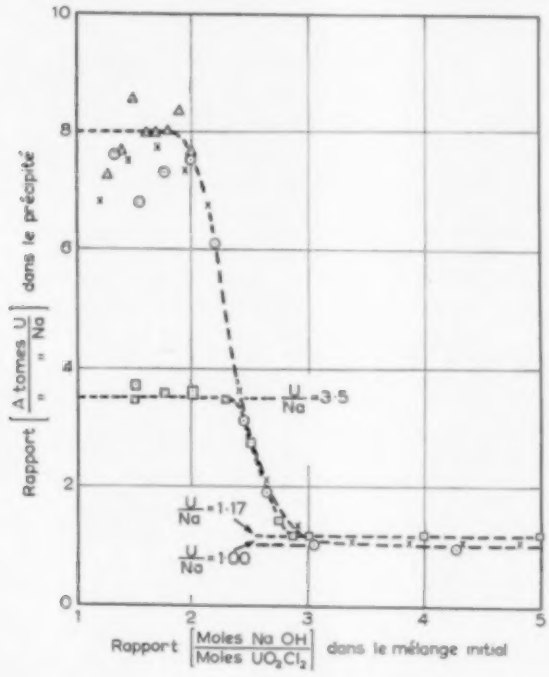

FIG. 2.—Composition des précipités.
○ Série 1
× Série 2
△ Série 3. La plus exacte pour l'uranate jaune
⊡ Résultats de WAMSER.

Pour les précipités oranges produits à pH élevé le raisonnement est le même. Pourtant, lorsqu'on lave ces précipités avec excès ils deviennent colloïdaux et on ne peut plus les séparer. Il est à remarquer que le pH du mélange est alors supérieur à 10. Donc, même si les précipités sont lavés jusqu'à ce qu'ils restent juste maniables leur rapport U/Na ne tombe jamais au-dessous de la valeur correspondant au précipité en équilibre avec une solution de pH 10. Même en l'absence d'état colloïdal l'élimination de petites quantités de Na^+ conserverait longtemps la valeur élevée du pH. On peut montrer que pour amener 5 g d'un précipité orange jusqu'à l'équilibre avec une solution de pH 7 il faudrait le laver avec environ 10^6 litres d'eau. On a tourné cette difficulté en agitant le précipité orange dans une solution tampon de phosphate de pH 7. On a alors obtenu le précipité jaune.

L'analyse d'un échantillon cristallin d'uranate de sodium a donné la formule $Na_2U_2O_7$. Cet échantillon avait été préparé par fusion d'un mélange de U_3O_8 et de chlorure de sodium. Le produit était refroidi et les cristaux étaient séparés par

lavage à l'eau de la masse fondue. Ils sont de couleur orange foncé et le spectre de rayons-X a montré quelques-unes des raies intenses remarquées par WAMSER dans le spectre de son produit B, l'uranate orange. Les précipités produits à partir de solutions étaient trop amorphes pour donner des spectres.

Il semble donc qu'il existe deux uranates de sodium formés en précipitant une solution d'un sel d'uranyle par l'hydroxyde de sodium. Leurs formules sont $Na_2U_{16}O_{49}$ et $Na_2U_2O_7$, en négligeant l'eau de constitution. Ce deuxième uranate peut aussi être obtenu par fusion à l'air de l'oxyde U_3O_8 avec du chlorure de sodium.

Je voudrais remercier Mlle M. VASSAL d'avoir fait une partie des analyses, et le Professeur J. S. ANDERSON qui m'a procuré l'échantillon d'uranate de sodium cristallin.

REFERENCES

BRITTON, H. T. S. (1949) *J. Chem. Soc.*, **127**, 2148.
BRITTON, H. T. S., and YOUNG (1932) *J. Chem. Soc.*, **134**, 2467.
CLARKE, F. E. (1950) *Analyt. Chem.*, **22**, 553 and 1458.
FLATT, R., and HESS, W. (1938) *Helv. Chim. Acta*, **21**, 1506.
GUITER, H. (1946) *Bull. Soc. Chim.*, 403.
GUITER, H. (1947) *Bull. Soc. Chim.*, 275.
RODDEN, J. (1950) *Analytical Chemistry of the Manhattan Project*, Vol. 1, p. 82 (McGraw-Hill).
SUTTON, J (1949) *J. Chem. Soc.*, S275.
TRIDOT, G. (1950) *Ann. Chim.*, **5**, 369.
VOGEL, A. I. (1951) *A Textbook of Quantitative Inorganic Analysis*, p. 482 (Longmans Green & Co.).
WAMSER, C. A., BELLE, J., BERNSOHN, E., and WILLIAMSON, B. (1952) *J. Amer. Chem. Soc.*, **74**, 1020.

J. Inorganic and Nuclear Chemistry, 1955, Vol. 1, pp. 75–91. Pergamon Press Ltd. ,London

VOL.
1
1955

NATURAL DISTRIBUTION OF COSMIC-RAY PRODUCED TRITIUM. II*

HARO VON BUTTLAR† and W. F. LIBBY‡
Institute for Nuclear Studies, University of Chicago

(*Received November* 1954)

Abstract—The measurement of the abundance of tritium in natural waters has been continued during the last eighteen months. The method used consists of the electrolytic concentration of the water samples, the measurement of the deuterium concentration in the final product from which the enrichment factor for any tritium present in the original sample can be calculated, followed by the determination of the tritium content of the concentrate by placing it as gaseous hydrogen in a Geiger counter.

It is shown that the data are in agreement with an average cosmic-ray production rate of about 0·14 tritium atoms per cm² per second of the earth's surface, on the assumption that essentially all of this tritium passes into water without decaying into helium and the tritiated water is precipitated out and goes into the sea.

The average tritium content of oceanic rain appears to be about 1 tritium atom per 10^{18} hydrogen atoms, whereas the continental rains have higher assays. The great Mississippi Valley shows about 6. The western coast of Europe runs about 2·5.

The ocean surface waters have about one-fifth the tritium content of ocean rain. This means that the ocean mixes to only an average depth of 100 metres in 18 years—the average life of tritium.

Several hot springs have been tested and most found to be rain water. Tests on wells agreed with expectations. As yet there is no significant meteorological understanding of the erratic fluctuations in the tritium assays for rain in a given location. It probably is due to variation in air-mass trajectories, origins, and water contents.

I. MEASUREMENT

THE method described earlier[1–4] continues in use. No essential changes have been made. Further study has indicated that the basic assumptions were even more completely justified than we had dared hope.

We calculate the enrichment factor for tritium in the following simple manner: If τ and τ_0 be the final and original concentrations of tritium, respectively, we can write

$$\frac{\tau}{\tau_0} = \sqrt{\frac{N(V_0)}{N_0(V)}} \tag{1}$$

in which N is the final concentration of deuterium, N_0 is the initial concentration of deuterium, which is 0·015 per cent for sea water, 0·0142 per cent for rain, and 0·0128

* This research was supported by the Office of Scientific Research of the Air Research and Development Command; Contract No. AF 18(600)–564.

† Now at New Mexico Institute of Mining and Technology, Socorro, New Mexico.

‡ Now at U.S. Atomic Energy Commission, Washington, D.C.

[1] Sensitive Radiation Detection Techniques for Tritium, Natural Radioactivity, and Gamma Radiation. W. F. LIBBY, Final Report, Air Force Contract No. AF33(038)–18013, December 1, 1951.

[2] Natural Tritium Assay, Routine Method for Absolute Assay of Beta Radioactivity, and The Reactions of Negative pi Mesons with Elementary Bromine. W. F. LIBBY, Final Report, Air Force Contract No. AF33(038)–18013, Supplemental Agreement No. 2(52–385), December 1, 1952.

[3] The Natural Distribution of Tritium. SHELDON KAUFMAN and W. F. LIBBY, *Phys. Rev.* **93**, 1337 (1954).

[4] The Natural Distribution of Tritium. SHELDON KAUFMAN, Ph.D. Thesis submitted to the Faculty of the Division of Physical Sciences, University of Chicago, December 1953.

per cent for snow.[5] V_0 is the original volume of water (10–20 litres in the case of rains and rivers, 100 litres for ocean water), and V is the final volume of water (0·3–0·5 ml). The square-root sign results from the fact that β/α (the ratio of the separation factors for tritium and deuterium) can be taken as 2·0 within the experimental error of the data.[3]

The counting technique outlined in the earlier reports[1–4] continues to operate well. The only change has been to substitute the shorter anticoincidence shield counters by longer ones. The tritium counters are 18 in. in length and 2 in. in diameter, and the shorter anticoincidence shield counters which were only 18 in. in length gave backgrounds of about eight counts per minute. Changing to 24-in. anticoincidence counters has dropped the background to about four counts per minute. This appreciable gain has increased the accuracy of our measurements considerably. Furthermore, practice and experience has shown that the reproducibility of the gas fillings is so good that we probably could measure a small fraction of the background with sufficient accuracy. It is our normal practice to measure the tritium concentration at two points during the enrichment, in order to increase the reliability of the result.[3]

2. NATURAL TRITIUM ASSAYS

The results obtained between December 1953 and October 1, 1954, are given in Table 1. It is obvious that the data for samples collected later than March 15, 1954, are not germane to our principal point—the cosmic-ray tritium. These high numbers were the consequences of the thermo-nuclear tests in the Pacific last spring. Most of our considerations in this paper will ignore them, except in connection with the samples from the hot springs. In this case the principal question—whether the springs run rain water or not—can be answered nearly as well with the contaminated rain as with the normal rain. In fact the appearance of unusually radioactive water in the effluent water in several springs must indicate turnover times of a few days or weeks at most since the test series began on about March 1. It is interesting to note in this connection that the one rain from Chile, collected on April 4, 1954, showed no contamination, while all northern hemisphere rain and river waters tested showed it from March 15 onward. Apparently the mixing of water vapour across the equator is much slower than is the east-west mixing.

3. CALCULATION OF THE TRITIUM PRODUCTION RATE, $\bar{Q}$

It would seem to be reasonable that whatever the mechanism by which the cosmic rays produce tritium by bombarding the air—whether by the (n,t) reaction of fast secondary neutrons on nitrogen[6, 7] or by direct production in cosmic-ray "stars"[7, 8] —the production rate should vary with latitude in a manner not too dissimilar from that in which the secondary neutrons vary. SIMPSON[9] has published data for the variation in neutron intensity with latitude at 30,000 feet altitude (22·5 cm Hg pressure). Using these data, we can calculate the expected ratio of the worldwide average production rate of tritium, $\bar{Q}$ (T atoms per cm² per second) to the local

[5] These numbers for the original abundance of deuterium are due to Dr. HARMON CRAIG of Professor UREY's laboratory. Dr. CRAIG advises that we use these numbers for the calculation of the enrichment.
[6] W. F. LIBBY, *Phys. Rev.* **69**, 671 (1946).
[7] E. L. FIREMAN, *Phys. Rev.* **91**, 922 (1953).
[8] P. MORRISON and D. B. BEARD, *Phys. Rev.* **75**, 1332 (1949).
[9] J. A. SIMPSON, Jr., *Phys. Rev.* **83**, 1175 (1951); **84**, 335 (1951).

production rate, Q, for various localities. For example, at Lake Mösvan, Norway, the local Q should be multiplied by 0·58 to obtain $\bar{Q}$. At the approximate centre of the Mississippi Valley the factor would be 0·64, and at Chicago it would again be 0·58. In this way the data given in Table 1 can be treated and corrected for the expected variation in latitude, though this variation has not yet been proven for natural tritium.

The most striking new development in the nature of the results of the assay of natural tritium is included in Section K of Table 1, the data on surface sea-water samples. Whereas we had originally supposed that the waves would certainly mix the sea to such an extent that the tritium would be undetectable in surface sea water, we find that indeed this is not so and that surface sea water does contain tritium. Four results given in Table 1, the beach water at Santa Monica (sample 75), the continental shelf Atlantic water (sample 117), the Gulf Stream sample (sample 115), and the Sargasso Sea (sample 116), all strongly indicate that there is definitely measurable tritium in the surface waters. In order to understand this we should know that uniform mixing to a depth of 113 metres would give an average T-value just equal to $\bar{Q}$. This result is obtained if one assumes that all tritium finds its way into the sea eventually before decaying into helium 3—in other words, that the storage in ground water and in the atmosphere is negligible relative to the run-off and direct rain into the oceans. Since, as we will show later, there is little doubt that $\bar{Q}$ is between 0·1 and 0·2 T atoms per cm² per second, one observes that the results in Section K of Table 1 would correspond to a mixing depth of about 100 metres. This comment assumes that the two coastal water samples are high because of rains from the neighbouring continents, which are richer, and takes the samples from the Gulf Stream and the Sargasso Sea as being more typical of the open ocean. It seems likely that $\bar{Q}$ is probably less than 0·24, the average of the Gulf Stream and Sargasso Sea samples, so we may expect that future measurements will show that the sea mixes to a depth of about 50 metres in the life-time of tritium. This result is in agreement with the notion that some stratification exists in the sea below the surface at a depth of fifty to one hundred metres. Measurements of the isotopic oxygen in air dissolved in Pacific Ocean water as a function of depth showed a point of inflection in the isotope ratio at a depth of about one hundred metres,[10] and the Baltic is known to behave as almost completely stratified with the bottom of the surface layer at about forty metres[11].

Though further measurements will be required to establish the tritium content of the surface of the ocean, it is clear that this tritium content is very low and water vapour evaporated from the sea is essentially tritium-free. It probably would be well to calculate $\bar{Q}$ assuming sea-water vapour on the average to have about 0·25 T atoms per 10^{18} H atoms. Using this we can set up an equation which expresses the balance between the production and decay processes. This equation is:

$$\bar{r}_s(\bar{T}_s - 0{\cdot}25) = 4{\cdot}7\bar{Q} \tag{2}$$

where $\bar{r}_s$ is the average annual precipitation over the seas in metres, $\bar{T}_s$ is the average tritium content of sea rain in T atoms per 10^{18} H atoms, $\bar{Q}$ is the cosmic-ray tritium

[10] N. M. Rakestraw, E. P. Rudd, and M. Dole, *J. Amer. Chem. Soc.* **73**, 2976 (1951).
[11] T. Gustafson and B. Kullenberg, *Svenska Hydrografisk-Biologiska Kommissionens Skrifter Ny Serie: Hydrografi XIII.*

TABLE 1.

Sample No.	Description of sample	Tritium abundance (T atoms per 10^{18} H atoms)
	A. *Chicago rains and snows.*	
51	Chicago rain. 3 April, 1953. Collected from 1,000 to 1,200. 0·07 in. rain	9·1 ± 0·3
56	Chicago rain. 15 April, 1953. Collected from heavy rain 1,130. 0·60 in. rain.	10·0 ± 0·3
61	Chicago rain. 30 April, 1953. Rained heavily from 1830 to 1915 with thunder and lightning. 0·87 in. rain.	6·6 ± 0·4
67	Chicago rain. 22 May, 1953. Collected at 0945. Heavy thunderstorm. 0·82 in. rain.	6·7 ± 0·3
74	Chicago rain. 5 June, 1953. Collected from 1530 to 1610. Thunderstorm. 0·43 in. rain.	6·2 ± 0·2
76	Chicago rain. 25 June, 1953. Collected from intermittent rain between 2130 and 2400. 0·02 in. rain.	7·9 ± 0·1
77	Chicago rain. 1, 2 July, 1953. Collected between 2300 on July 1 and 0300 on July 2. Trace rain on July 1, 0·06 in. on July 2.	4·3 ± 0·3
79	Chicago rain. 5 July, 1953. Collected from July 3 to July 6. Storm occurred about 2200 on July 5. 0·39 in. rain.	7·6 ± 1·5
86	Chicago rain. 17–20 July, 1953. Collected from 0930 July 17 to 1600 July 20. Rainstorms on morning of July 17, afternoon of July 17, night of July 18, and morning of July 20. Rainfalls were: 0·57 in. July 17; trace July 18; 0·10 in. July 20.	7·1 ± 0·4
91	Chicago rain. 3 August, 1953. Collected 1930 to 1945. Trace rain.	3·60 ± 0·4
92	Chicago rain. 4 August, 1953. Collected 1445 to 1455. 0·06 in. rain.	17·0 ± 0·4
96	Chicago rain. 4 September, 1953. Collected 0400 to 1100. 0·50 in. rain. This was the first rain after 3 weeks drought.	7·3 ± 0·6
97	Chicago rain. 18 September, 1953. Rained very hard—thunderstorm. Collected at 2145. 0·63 in. rain.	12·0 ± 0·4
101	Chicago rain. 18 October, 1953. Trace rain.	9·8 ± 0·9
102	Chicago rain. 26 October, 1953. First drops collected. Total rainfall was 0·31 in., but this sample consisted of the first drops. Collected at 1530.	19·9 ± 1·0
103	Chicago rain. 26 October, 1953. Same storm as sample No. 102 except water collected after three hours of continuous rain. Collected at 1800. 0·31 in. rain.	20·0 ± 1·0
106	Chicago rain. 20 November, 1953. Collected 9000 to 1100 from the first part of the rainstorm. 0·56 in. rain.	7·3 ± 0·9

TABLE 1.—(*continued*).

Sample No.	Description of sample	Tritium abundance (T atoms per 10^{18} H atoms)
107	Chicago rain. 20 November, 1953. Collected 1600 at end of rainstorm.	13·5 ± 1
109	Chicago snow. 27 November, 1953. Collected in the morning after an overnight snow.	34·5 ± 0·6
142	Chicago rain. 2 December, 1953. Collected at 1500.	7·85 ± 0·25
134	Chicago rain. 2 December, 1953. Collected at 1700.	8·3 ± 0·3
135	Chicago rain. 3 December, 1953. Collected from 0925 to 0930.	5·8 ± 0·4
142	Chicago rain. 12 December, 1953.	7·8 ± 0·3
136	Chicago rain. 20 January, 1954. Collected from 0845 to 0855.	10·5 ± 0·3
137	Chicago snow. 21 January, 1954. Collected at 1700.	18·7 ± 0·4
138	Chicago rain. 26 January, 1954. Collected from 1000 to 1400.	19·4 ± 0·5
139	Chicago rain and snow. 5 February, 1954. Collected after 1700.	23·0 ± 1·5
140	Chicago rain. 15 February, 1954. Heavy rain with thunder and lightning. Collected from 1900 to 2200.	9·5 ± 0·4
141	Chicago rain. 16 February, 1954. Snowy rain. Collected from 1500 to 1600.	15·6 ± 0·7
151	Chicago rain. 20 February, 1954. Collected from 1230 to 1315.	4·2 ± 0·2
147	Chicago snow. 2 March, 1954. Snow fell 1500 to 2400. Shovelled from the ground on March 3, 1954 at 1430.	20·8 ± 0·5
166	Chicago rain. 19 March, 1954. Collected from 1430 to 1540.	385 ± 5
167	Chicago rain. 24–25 March, 1954.	283 ± 3
169	Chicago snow. 29 March, 1954. Collected March 31, 1954, after most of the snow had melted.	145 ± 5
168	Chicago snow. 29 March, 1954. (Fresh snow).	196 ± 3
170	Chicago rain. 7 April, 1954. Heavy shower. Collected 1530.	248 ± 5
171	Chicago rain. 15 April, 1954. Short, heavy storm. Collected 1130–1145	360 ± 6
174	Chicago rain. 19 April, 1954. Collected at 1745. It had been raining since about noon.	425 ± 20
175	Chicago rain. 20 April, 1954. Collected at 0900 on 21 April, 1954.	260 ± 4
181	Chicago rain. 26–27 May, 1954. Collected during night.	450 ± 10

VOL. 1 1955

TABLE 1.—(*continued*).

Sample No.	Description of sample	Tritium abundance (T atoms per 10^{18} H atoms)
182	Chicago rain. 27 May, 1954. Collected at 1105–1110. Different rainstorm from sample No. 181.	416 ± 15
183	Chicago rain. 1 June, 1954. Collected 0930–0935. Rained previous night and all day.	390 ± 5
	Average tritium content for December 1, 1952 to December 1, 1953 weighted according to the total rainfall for storm samples for 27 samples amounting to 12 inches out of the total rainfall of 26 inches. (Some data from reference 3 used.)	8·2
	Unweighted average for the samples between December 1, 1952 and December 1, 1953. (Some data from reference 3 used.)	7·8
	Calculated average for rainfall over the last 18 years (Lake Michigan).	7·4
	B. *Other rains.*	
43	Wilson Springs, Arkansas rain. Collected on February 10, 1953 in a heavy thunderstorm.	2·25 ± 0·8
98	Manila, Philippine Islands rain. Collected 5 June, 1953 at the Bureau of Quarantine by Dr. R. Abriol.	0·90 ± 0·07
49	Honolulu, Hawaii rain. Collected on morning of March 26, 1953 at Honolulu, 5329 Keikilani Circle by Mrs. Terry Yoshida.	0·61 ± 0·10
95	Hickam Field, Oahu, Hawaii rain. Collected at Hickham Field, 17 July, 1953.	0·59 ± 0·08
110	Tantalus, Koolau Range, Oahu, Hawaii rain. Collected 13 November, 1953. The rain was collected by residents of Tantalus.	0·73 ± 0·11
120	Oahu, Hawaii rain. Collected by pooling the catches of several rain cages located at: Lower Laukaka, Nuuahu Reservoir No. 4, Wil. Rise No. 4, Manoa Valley, Palolo Valley, Nuuahu Pali, Kalihi, U.S.G.S. Station, Kaliha, Tunnel No. 2, Kaliha Reservoir Site, Tantalus Peak, Bureau of Water Supply, City and County of Honolulu.	0·67 ± 0·14
121	Manoa Valley, Hawaii rain. December 1953. Single rain.	1·53 ± 0·11
125	Wellington, New Zealand rain. Collected October 1, 1953 on the roof of the American Embassy at Wellington, New Zealand. The roof had recently been painted and consisted of galvanized iron. The meteorology: a vigorous depression was located at the Tasman Sea west of Cook's Strait. It moved ESE and came over Wellington in the early hours of October 2, 1953. Rainfall from the forward side of the depression began when the cloud base was at 3 kilometres. After it began to rain the cloud base moved down to one to two kilometres and the freezing level was at two kilometres. The clouds were alto stratus and nimbo stratus.	1·7 ± 0·2

TABLE 1.—(*continued*).

Sample No.	Description of sample	Tritium abundance (T atoms per 10^{18} H atoms)
126	Harwell, England rain. Two gallons collected after a windless week on October 24–25, 1953. Artificial tritium from Harwell may have been present in this sample. Sample sent by J. M. FLETCHER.	22·5 ± 0·6
127	Harwell, England rain. Collected October 26, to 28, 1953. Artificial tritium from Harwell may have been present in this sample.	25·5 ± 0·4
128	Santa Barbara, California, rain. Rain fell on 23 January and 24 January, 1954. Collected by Dr. V. L. VANDERHOOF on January 24, 1954 from Mission Creek, Santa Barbara. Total rainfall was 3 inches.	4·0 ± 0·1
164	Kobe, Japan rains. November, 1953 (4 or 5 storms). Sent by Prof. SEISHI KIKUCHI, Osaka University.	6·5 ± 0·4
179	Valparaiso, Chile, rain. 4 or 5 April, 1954. After 3 months' drought. Rained very heavily for about 36 hours.	4·3 ± 0·2
165	Puerto Rico rain. 26 March, 1954. Drained off a tin roof at Ramez Air Force Base. Total rainfall 0·42 inches.	65·6 ± 1·2
	Water from Lake Mösvan used to supply the Norsk-Hydro. The Lake Mösvan water probably was melted snow from the winter of 1946 and 1947. The water was taken from the lake at the end of January, 1948[13,17]	2·4
	C. *Mississippi River.*	
44	Mississippi River water from Rock Island. Collected March 16, 1953.	3·2 ± 0·2
47	Mississippi River water from St. Louis. Collected 0900 on March 17, 1953.	5·4 ± 2·4
57	Mississippi River water from Rock Island. Collected 1315 on April 17, 1953.	5·3 ± 0·3
58	Mississippi River water from St. Louis. Collected 1300 on April 17, 1953.	6·0 ± 0·4
80	Mississippi River water from Rock Island. Collected on June 30, 1953.	7·2 ± 0·7
88	Mississippi River water from St. Louis. Collected 1320 on July, 22, 1953.	7·3 ± 0·4
	Average for Rock Island (including data from reference 3):	4·7
	Average for St. Louis (including data from reference 3):	6·0
	D. *Other rivers.*	
10	Columbia University distilled water. Collected August 5, 1944.	2·4 ± 0·1 (4·5 ± 0·2 as of 1953)

[17] Professor P. HARTECK suggests we should recalculate the Lake Mösvan value using a lower separation factor. The old value[13] was 0·8, due to the different choice of separation factor. We now get 2·4.

VOL. 1 1955

TABLE 1.—(*continued*).

Sample No.	Description of sample	Tritium abundance (T atoms per 10^{18} H atoms)
143	Shasta Dam, California. January 30, 1954.	2·7 ± 0·1
111	River Main near Würzburg, Germany. September 13, 1953. Collected by Dr. H. v. BUTTLAR, who collected all the European samples.	1·76 ± 0·19
122	River Donau. Collected near Ulm, Germany, on September 12, 1953.	2·13 ± 0·38
112	River Loire. Collected at Digoin, France, on September 9, 1953.	2·11 ± 0·14
124	River Seine. Collected near Nogent, France, on September 8, 1953.	1·80 ± 0·3
108	River Rhone. Collected near Lyon, France, on September 10, 1953.	2·64 ± 0·16
123	River Mosel. Collected near Metz on September 7, 1953.	2·15 ± 0·12
104	River Elbe. Collected at Hamburg, Germany, on August 31, 1953.	2·57 ± 0·12
132	River Rhine. Collected between Geisenheim and Rüdesheim on September 7, 1953.	3·0 ± 0·3
105	River Weser. Collected at Bremen on September 1, 1953.	1·76 ± 0·10
131	River Fulda. Collected near Kassel on September 24, 1953.	2·35 ± 0·1
114	English stream near river Cam. Water taken about one mile from the source (a spring). Collected near Cambridge, England.	1·25 ± 0·10
	Average for the western European rivers (excluding the English River Cam).	2·17
133	River Marne at Joinville, collected September 8, 1953.	2·1 ± 0·2
172	River Slaney at Tuckmill near Baltinglass, Co. Wicklow, Ireland; collected about February 1, 1954, by Dr. G. F. MITCHELL, Trinity College, Dublin.	2·9 ± 0·2
173	Lower Glore River at Gelbertstown, near Castle Pollard, Co. Westmeath, Ireland, collected about February 1, 1954, by Dr. MITCHELL.	3·1 ± 0·15
144	El Rito de los Frijoles, Jemez Mountains, New Mexico. Collected February 7, 1954, at Bandelier Nat. Monument. Sample probably represents average over the winter snowfall in the Jemez Mountains. Sent by E. C. ANDERSON.	27·2 ± 0·4
145	Rio Grande, north-west of Santa Fe, February 7, 1954. The spring thaw was beginning to raise the river level, but it had not yet reached peak volume by any means. Sent by E. C. ANDERSON.	6·6 ± 0·2
146	Winsor Creek, taken February 22, 1954, at Cowles, New Mexico, just above junction with Pecos River. Sent by E. C. ANDERSON.	9·9 ± 0·2
152	Rio Guajataca, Puerto Rico, at Lares, collected March 2, 1954.	0·7 ± 0·2

TABLE 1.—(*continued*).

Sample No.	Description of sample	Tritium abundance (T atoms per 10^{18} H atoms)
153	Rio Arecibo, Puerto Rico, at Utuado, collected March 2, 1954.	1·1 ± 0·2
155	River Tomokoa, Florida, on Route 92 near Daytona Beach, collected March 19, 1954.	45·4 ± 0·6
156	Alafia River, Florida, on Route 60 about 20 miles east of Tampa, March 22, 1954.	60 ± 3
	E. *Lake Michigan and other lakes.*	
7	Distilled water from the Jones Chemical Laboratory at the University of Chicago. The intake for the water supply for the southern part of the city is two miles off the shore in southern Lake Michigan. Collected on May 12, 1952.	2·0 ± 0·1
25	Jones Chemical Laboratory distilled water. Collected on February 6, 1953.	2·4 ± 0·4
100	Jones Chemical Laboratory tap water. Collected on October 26, 1953.	1·59 ± 0·10
	Average for Lake Michigan (including data from reference 3).	1·64 ± 0·04
	Calculated average rain from the depth and area of the lake and the mean assay for tritium in the lake:	7·4 ± 0·07
143	Lake behind Shasta Dam, California. Collected by Dr. L. R. LIBBY probably January 30 or 31, 1954, certainly not later than February 15, 1954.	2·7 ± 0·15
148	Roundout Reservoir, south shore, collected February 6, 1954 by SETH HARRIS, Lamont Observatory, 500 yd in front of gate off New York 55. Ice cap over whole reservoir.	7·2 ± 0·3
149	Shandakan Tunnel effluent from Schoharie Reservoir at Allaben, New York, right off route N.Y. 28. Collected February 6, 1954, by SETH HARRIS.	8·4 ± 0·3
	F. *Hot springs.*	
53	Water from the main reservoir at Hot Springs, Arkansas. Collected on March 18, 1953.	2·5 ± 1·4
93	Water from the Lardarello, Italy, hot springs, near Pisa. These hot springs furnish about ½ of the electric power in the whole of Italy. The water actually was steam from the volcanic fumaroles.	−0·56 ± 0·538
158	South Steamboat Well, Steamboat Springs, Nevada. Collected March 11, 1954.	6·2 ± 0·4
159	Spring No. 24, Steamboat Springs, Nevada, collected March 11, 1954.	7·1 ± 0·4

VOL. 1 1955

TABLE 1.—(*continued*).

Sample No.	Description of sample	Tritium abundance (T atoms per 10^{18} H atoms)
160	Spring No. 50, Steamboat Springs, Nevada, collected March 11, 1954.	47 ± 3
157	Bowers Hot Springs, Bowers Mansion, Nevada, collected on March 11, 1954.	$10{\cdot}8 \pm 11$
161	Wilbur Springs, Colusa Co., California, collected probably on March 23, 1954, by DONALD E. WHITE, $T = 127{\cdot}2$°F. This water is exceptionally high in alkali chlorides, bicarbonates, boron, sulphide, iodine, and other compounds.	$1{\cdot}0 \pm 0{\cdot}1$
162	Devil's Kitchen and Range Spring, The Geysers, collected March 23, 1954, by D. E. WHITE. $T = 202$°F. No surface discharge, but probably slight sub-surface. Vigorous boiling, evaporation from pool about 15 feet in area. Acid reaction.	$10{\cdot}8 \pm 0{\cdot}4$
163	Magnesia Spring, The Geysers, California, collected March 23, 1954, by D. E. WHITE. $T = 122$°F. Discharge estimated 2 gpm.	$11{\cdot}8 \pm 0{\cdot}6$
176	Hot Springs, Arkansas, main reservoir. Collected at Government free Bath House, April 29, 1954.	$2{\cdot}92 \pm 0{\cdot}2$
177	Wilson Springs, Arkansas, drill hole No. 1, collected April 29, 1954.	$2{\cdot}06 \pm 0{\cdot}15$
185	Morgan Spring, Lassen Park. Growler Spring. This is a near neutral alkali chloride-boron-bicarbonate-sulphate spring opposite in type from sample 186. $T = 205{\cdot}4$°F; discharge about 8 gpm. Water believed to be in part volcanic but dominantly of surface origin, circulating deeply and mixing. Collected June 8, 1954.	$0{\cdot}57 \pm 0{\cdot}88$
186	Sulfur Works, Lassen Park. Big boiling spring. This is an acid spring typical of most of the Lassen hot springs. $T = 190$°F, no discharge. These springs appear to result from partial condensation of steam that is probably meteoric in origin. Some direct contribution of recently fallen snow. Collected June 5, 1954.	$54{\cdot}2 \pm 1{\cdot}2$
	G. *Well water.*	
41	Drill core water from the Wilson uranium prospecting area in Wilson Springs, Arkansas. Taken from the drill core on March 6, 1953.	$0{\cdot}17 \pm 0{\cdot}11$
99	Water from the 900 ft deep well at the MacDonald Observatory at Fort Davis, Texas. Sample given by Dr. GERARD KUIPER of Yerkes was pumped in June of 1953.	$-0{\cdot}48 \pm 0{\cdot}37$ (age greater than 50 years)
89 and 119	Champaign-Urbana city well water. Water taken in July 1953 from well No. 51, located west of Champaign. This well is 296 feet deep and is producing at a rate of 2,225 gallons per minute. The first hundred feet of formation is Wisconsin glacial drift and the next 200 feet are Illinoisan and Kansan drift. The very bottom of the well at 300 feet is at the top of the Pennsylvanian system. Nowhere in the entire log of the well is any clay formation which would prevent the down-seepage of rain. It was therefore thought that perhaps the well could contain some rainwater. It is generally thought that the well water which supplies the area is ancient and possibly of melted glacier origin. Sample furnished by T. E. LARSON, Head, Chemistry Subdivision of State Water Survey.	$0{\cdot}13 \pm 0{\cdot}05$ (age greater than 50 years)

TABLE 1.—(*continued*).

Sample No.	Description of sample	Tritium abundance (T atoms per 10^{18} H atoms)
	H. *Wines.*	
	Sherry, Jerez de la Frontera, Spain:	
85	1951 Vintage	$2{\cdot}73 \pm 1{\cdot}0$ $(3{\cdot}0 \pm 1{\cdot}0)$
84	1947 Vintage	$1{\cdot}99 \pm 0{\cdot}55$ $(2{\cdot}67 \pm 0{\cdot}75)$
83	1942 Vintage	$1{\cdot}93 \pm 0{\cdot}27$ $(3{\cdot}55 \pm 0{\cdot}5)$
	Average initial	$(3{\cdot}1 \pm 0{\cdot}4)$
	K. *Sea water samples.*	
75	Sea water collected from the beach at Santa Monica, California, on June 8, 1953.	$0{\cdot}54 \pm 0{\cdot}02$
115	Sea water collected from the surface of the Gulf Stream on September 11, 1953, at 38° 5′ N, 69° 30′ W. The water temperature was 82°F. This was collected by the ship, Vena, by Mr. BRUCE HEEZEN, Chief Scientist from the Geophysics Section of the Geology Department, Columbia University, the Lamont Laboratory. This is Lamont Sample No. T-32.	$0{\cdot}19 \pm 0{\cdot}05$
117	Atlantic sea water taken from 300 miles from New York on the continental slope at 30° 20′ N and 71° 30′ W. The water temperature was 75°F. Lamont Sample No. T-34.	$0{\cdot}55 \pm 0{\cdot}04$
116	Atlantic sea water taken in the Sargasso Sea at 34° 00′ N, 62° 50′ W. Temperature of the water was 81·5°F. Collected following a light drizzle. Lamont Sample No. T-28.	$0{\cdot}29 \pm 0{\cdot}02$
154	Atlantic sea water from the Sargasso Sea at 34° 00′ N, 52° 35′ W. Temperature of the water was 81·5°F. Collected September 7, 1953, immediately following a light drizzle of 1 hour. Lamont Sample No. T-25.	$1{\cdot}6 \pm 0{\cdot}1$

production rate in T atoms per cm^2 per second. The factor 4·7 is a numerical constant arising from the units. Equation (2) simply assumes that no appreciable storage of tritium in the atmosphere for times comparable to the lifetime of tritium—eighteen years, average life—occurs, and that essentially all of the tritium forms water. The latter assumption is well justified by the measurements of the tritium contents of atmospheric hydrogen which have been made,[12, 13] which indicate well less than one per cent of the tritium is found in this form. The value of $\bar{r}_s$ used is 0·77 metres per year.[14] Using the data in Table 1 and the latitudinal variation factor described

[12] V. FALTINGS and P. HARTECK, *Z. Naturforsch.* **5A**, 432 (1950).
[13] A. V. GROSSE, W. H. JOHNSTON, R. L. WOLFGANG, and W. F. LIBBY, *Science* **113**, 1 (1951).
[14] K. RANKAMA and TH. G. SAHAMA, *Geochemistry*, The University of Chicago Press, Chicago (1950).

VOL. 1 1955

above, it seems that $\bar{T}_s$ should lie between 0·9 and 1·0. This gives $\bar{Q}$ values of 0·11 and 0·12, respectively.

This calculation involves the implicit assumption that the tritium made over the oceans is precipitated into the oceans. We know, however, that on the western coasts of the continents considerable tritium from the skies over the seas precipitates on land. Also, our measurements show that rains on the east coast of continents are high in tritium. Thus the sea rain just east of the eastern continental coasts must be much richer in tritium than $\bar{T}_s$ as though land-born tritium were precipitating into the sea. In view of the prevailing westerly directions of the winds in the regions measured, these results suggest that $\bar{Q}$ may be somewhat higher than indicated by the ocean data.

TABLE 2.—CALCULATED LOCAL TRITIUM PRODUCTION RATES, Q, AND EXPECTED OCEAN RAIN AND SURFACE WATER TRITIUM CONTENTS

Locality	$\bar{Q}/Q$	Q (T atoms/cm²/sec)	$T_{\text{ocean rain}}$ (0·77 metre/year)	$T_{\text{ocean surface}}$ (50 metres mixing)
Chicago	0·58	0·24	2·0	0·55
Norway and the North Atlantic Ocean	0·55	0·26	2·2[17]	0·58
Mississippi Valley	0·60	0·23	1·9	0·53
Honolulu and the Hawaiian Islands	1·90	0·073	0·65	0·17
New Orleans, San Francisco, Southern Italy, Southern Spain	1·00	0·14	1·2	0·32
Puerto Rico	1·25	0·17	0·96	0·26
Marshall Islands	2·40	0·058	0·48	0·13

We can make similar calculation for the land areas by using the Mississippi Valley average of 6 multiplied by the latitudinal factor 0·6 as a worldwide average for land rain.

It seems that the continental rains must be richer than sea and coastal rains, for two reasons. First, the length of time that the moisture is exposed to contamination by cosmic-ray tritium after leaving the ocean is greater, and secondly, there is less moisture in the air over the continents than over the oceans and coastal regions. This raises the specific activity, that is, the number of tritium atoms per hydrogen atom.

We thus obtain

$$\bar{\rho}_l(6 \times 0{\cdot}6 - \bar{T}_s) = 4{\cdot}7\bar{Q} \qquad (3)$$

where $\bar{\rho}_l$ is the worldwide average run-off from the land, and the average composition of ocean rain is subtracted to correct for the tritium content of the sea-water vapour coming in over the western coasts and the Gulf of Mexico. The value of $\bar{\rho}_l$ used is 0·28.[14] The run-off must be used in equation (3) because re-evaporation allows a given tritium atom to be precipitated more than once over land. Only transport into the sea where wave action dilutes the tritium accomplishes the fixation on the surface,

and even in this case as we have seen previously the fixation is not complete. The value of $\bar{Q}$ so derived is 0·16. Therefore we conclude $\bar{Q}$ is likely to be close to 0·14, probably to within twenty per cent.

Using this result, we calculate the expected tritium contents for average ocean-rain and surface-ocean waters on the assumption of uniform mixing to fifty metres. These results are given in Table 2. It is pleasant to observe the agreement with the data given in Table 1.

4. METEOROLOGY

The large fluctuations in the tritium contents of successive rains in the Chicago area, excluding the large rise in March 1954 due to the test activities in the Pacific, require special consideration in a meteorological sense. Our basic equations (2) and (3) for the relations between the tritium content, T, and the cosmic-ray production rate, Q, are based on the assumption that tritium cannot stay in the air for years even if it is formed well above the tropopause—the stagnant layer at 30,000 to 50,000 feet between the stratosphere and the troposphere in which the normal weather phenomena occur. Half of the tritium probably is produced on the average above the tropopause. We assume that it cannot stay up there for times comparable to eighteen years—the average life of tritium. This assumption does not mean, however, that it may not mix horizontally in an east and west and in a north and south direction rather well due to stratospheric winds. Whatever evidence for latitudinal variation of Q is to be found in Tables 1 and 2 should be taken as indicating that the stratospheric storage time is less than the north and south horizontal mixing time.

Assuming perfect vertical mixing, we can speak of the atmospheric moisture content, w, in metres of water per cm², and the storage time, τ, in years, for the moisture in the air, counting total time elapsed in the air after the moisture leaves the ocean and until it returns eventually to the sea as rain or snow or run-off river water. These quantities then will be related to the tritium content of rain, T_r, and the production rate, Q, for the open sea by

$$T_r - T_0 = \frac{4{\cdot}7Q\tau}{w} \tag{4}$$

where T_0 is the tritium content of ocean-water vapour. For the continental areas this simple equation may not hold, because re-evaporation of precipitated moisture without dilution is an important phenomen.

The values of w are not well known, but it seems likely from available studies[15, 16] that the range of values will be 0·01 to 0·03, with corresponding average τ values of 0·013 and 0·039 or 4·7 days and 14 days, respectively. At an average wind velocity of ten miles per hour these numbers correspond to transport distances of 1,100 and 3,300 miles respectively.

It is clear that in general land rain should be richer in tritium because the atmospheric residence time should be longer and because the moisture content, w, should in general be lower. However, it remains to apply the equation to air masses of known

[15] W. C. Jacobs "The Energy Exchange Between Sea and Atmosphere" *Bulletin of the Scripps Institution of Oceanography*, Vol. 6, No. 2, pp 22–122 (1951).

[16] G. S. Benton, M. A. Estoque, and J. Dominitz, The Johns Hopkins University, Department of Civil Engineering. Scientific Report No. 1, Contract AF19(122)–365 of the Geophysics Research Division of Air Force Cambridge Research Center (1953).

VOL. 1 1955

w and with known trajectories so that the variation of Q with latitude can be introduced. It is to be hoped that careful co-ordination of meteorological data with tritium assays will yield results of importance to meteorology in general.

An attempt has been made to understand the variations of the tritium activity in single rainstorms. Forty samples of individual storms were collected on the campus of the University of Chicago over a period of more than a year. These samples correspond to 16·23 inches of rain, or 46 per cent of the total rainfall during this period. The T average of these rains, weighted by the amount of rainfall, gives 8·8 units, which compares reasonably well with the Lake Michigan assay of 7·4.

Approximate values for w were computed from radio sounding data for the period of December 2, 1952, to November 20, 1953; monthly means from the Weather Bureau Technical Paper No.10 had to be employed for the period from November 20, 1953, to March 2, 1954. Values for $w(T - T_0)$ are given in Table 3.

While the measured values for T show a minimum in winter, it can be seen that this effect is over-compensated by multiplication with the amount of precipitable water in the air, thus yielding the total tritium accumulated in the air mass. One then obtains a maximum in summer. This is probably due to the following causes: (1) In summer the wind velocities are lower, therefore the air mass is exposed longer to the tritium production. (2) It is known that the continent is a water donor during the summer-time. This means that the air mass picks up tritiated water from the continent. In winter the large water source for the atmosphere is the ocean, which is almost dead in tritium.

The argument that the vertical mixing may not be complete would yield a high value in summer also, since thunderstorms in summer are known to reach higher up than snowstorms in winter. But our measurements do not support this thesis, since thunderstorms do not average higher than rains while snow in general seems to be quite active.

5. THE AGE OF WATERS AND AGRICULTURAL PRODUCTS AND APPLICATIONS OF NATURAL TRITIUM TO HYDROLOGY

The data given in Table 1, Section G, and in reference 3 on the tritium contents of vintage wines, together with the comparison of the Lake Michigan average as shown in Section E and in reference 3 with the general average for the rainfall, show that without doubt the tritium content of rain up to March 15, 1954, was essentially the same as it had been for the last eighteen years. It is clear, of course, that if the calculation can be made for Lake Michigan in which the hydrology is known, and if the checks are satisfactory, that in the case of an unknown lake the measurement of the tritium and a comparison with the rainfall for the general region should give the hydrology, or at least some data on it. For example, the average depth might be calculated, or the average storage time for water in the lake.

The application of natural tritium to the determination of the storage or hold-up time for ground waters may be of considerable importance. Some applications have been made and are given in Sections F and G of Table 1. In Section F data are given for natural hot springs. It seems likely that all of the hot springs utilize surface water except the Lardarello (sample 93) near Pisa, which actually was steam from volcanic fumaroles, the Wilbur Springs at Colusa, California (sample 161), and the Morgan Spring at Lassen Park, California (sample 185).

VOL. 1 1955

TABLE 3.—RAINFALL DATA AT THE UNIVERSITY OF CHICAGO CAMPUS

Date	T	$T - T_0$	w in g/cm²	Monthly mean at Joliet, Ill., for w in g/cm²	$w(T - T_0)$
12-2-52	13·2	12·95	1·2	1·0	15·5
1-6-53	7·1	6·85	0·5	0·8	3·4
1-23	9·0	8·75	1·8		15·7
2-11	5·0	4·75	2·0		9·5
2-16	10·8	10·55	0·7	0·85	7·4
2-20	3·3	3·05	2·1		6·4
3-3	9·4	9·15	1·0		9·2
3-7	9·6	9·35	0·8		7·5
3-12	4·75	4·5	2·2	0·98	9·9
3-18	7·9	7·65	2·1		16·1
3-21/22	3·1	2·85	—		—
3-31	9·5	9·25	2·5		23·1
4-3	9·1	8·85	1·8		15·9
4-15	10·0	9·75	1·5	1·48	14·6
4-24	9·0	8·75	4·2		36·7
4-30	6·6	6·35	2·6		16·5
5-22	6·7	6·45	4·8	2·15	30·9
6-5	6·18	5·9	3·25	3·2	19·2
6-25	7·9	7·65	4·1		31·4
7-2	4·3	4·05	4·5		18·2
7-5	7·6	7·35	3·9	3·44	28·6
7-17/20	7·1	6·85	—		—
8-3	3·6	3·35	4·9	3·3	16·4
8-4	17·0	16·75	4·1		68·8
9-4	7·3	7·05	4·3		30·3
				2·5	
9-18	12·0	11·75	3·3		38·8
10-18	9·8	9·55	1·9	1·8	18·2
10-26	19·9	19·65	2·6		51·1
11-20	7·3	7·05	2·8		20·4
11-20	13·5	13·25		1·2	15·9
11-27	34·5	34·25			41·2
12-2/3	7·3	7·05		1·0	7·1
1-20-54	10·5	10·25			8·2
1-21	18·7	18·45		0·8	14·7
1-26	19·4	19·15			15·3
2-5	23·0	22·75			19·3
2-15	9·5	9·25		0·85	7·9
2-16	15·6	15·35			13·0
2-20	4·2	3·95			3·4
3-2	20·8	20·55		0·98	20·1

The wells tested gave old water in agreement with expectations. The lower limit of the age of these waters is fifty years. Thus we cannot distinguish water older than fifty years from very old or juvenile water.

It is clear from an examination of the data in Section H of Table 1 and reference 3 that tritium allows one to determine the age of wine. It is also clear that the water in the wines has essentially the same tritium content as the rain of the general area. For example, the Widmer Winery near Rochester, New York, shows a general tritium assay of $5{\cdot}8 \pm 0{\cdot}3$, in good agreement with what one might expect in view of the results of the Mississippi Valley as a whole. The French wines in the Rhone Valley near Bordeaux run around $3\frac{1}{2}$ or 4 of our units; Spanish wines about 3, which within the experimental error agrees with the general rainfall average, which is shown by the river-water assay. Therefore it is relatively certain that agricultural products can be dated and also that the presence of rain water in the agricultural products can be determined. It would be interesting of course to test for pumped irrigation water which might possibly be ancient in character, just how effectively the water was incorporated into the crop.

6. THE ESCAPE TIME FOR HELIUM 3 FROM THE EARTH

To balance the cosmic-ray production of tritium, there must be some mechanism for the product of the radioactive disintegration of tritium, helium 3, to escape from the earth. Being helium, no chemical compounds can be formed, and being non-radioactive, no nuclear transformations. Therefore, every second for each square centimetre of the earth's surface, 0·14 helium 3 atoms must escape on the average if the cosmic rays have been constant in intensity. A direct analysis of the air shows that there are $1{\cdot}5 \times 10^{14}$ helium 3 atoms per cm^2 of the earth's surface. Therefore we calculate that on the average a helium 3 atom must stay on the earth thirty-four million years. This escape time may well be about half this, since it is probable that the cosmic rays can also produce helium 3 directly as well as through the tritium, but it seems unlikely that this would more than double the total rate of production of helium 3. Therefore we rather definitely can say that if the cosmic rays have remained constant for the last fifty or one hundred million years, the amount of helium 3 on earth is such as to indicate an escape time of between twenty and forty million years. This is a rather reasonable magnitude considering the probable escape time for helium 4, as judged from other evidence. One finds in the acceptability of this result some evidence that the cosmic rays indeed have remained constant for this great period of time.

It is by no means obvious that on a time-scale of eighteen years the cosmic rays should remain completely constant, if any appreciable portion of them are connected with the solar sunspot cycle of eleven years' duration. The data given in this report so far, however, indicate that there is no real evidence that the present rate of cosmic-ray generation of helium 3 is any different from what it has been over the last eighteen years.

7. ACKNOWLEDGMENTS

The authors are extremely indebted to the Office of Scientific Research of the Air Research and Development Command of the U.S. Air Force for the support of this research. We wish to thank also the many individuals who offered samples of old water in response to a public appeal. Our special thanks are due to Mr. B. O.

CAPLENER, Port Captain of the Federal Barge Lines, St. Louis, and to the U.S. Army Engineers who kindly furnished our Mississippi Water samples. The vintage wines were selected by Professor MAYNARD AMERINE of the University of California at Davis, and were furnished by the co-operation of vintners, wholesalers, and tax authorities. We are indebted particularly to Dr. LAURENCE KULP of the Lamont Laboratory, Columbia University, and Mr. BRUCE HEEZEN of the Geophysics Section of the Lamont Laboratory, for the Atlantic Ocean water samples. The hot-springs samples were kindly furnished by Dr. D. E. WHITE and Dr. R. G. REEVES of the Department of the Interior.

We are grateful to Mr. WILLIAM TIMMONS for extremely able and devoted operation of the electrolytic plant for concentrating the water samples.

VOL.
1
1955

J. Inorganic and Nuclear Chemistry, 1955, Vol. 1, pp. 92–111. Pergamon Press Ltd., London

ON THE MOLECULAR STRUCTURE OF METHYL SILICONE

By Eugene G. Rochow and Hugh G. LeClair[1, 2]
Mallinckrodt Laboratory of Harvard University

(*Received November* 1954)

Abstract—Several cyclic and linear methylpolysiloxanes, together with the methylchlorosilanes used as their intermediates, have been investigated by the method of nuclear magnetic resonance absorption. Apparatus was constructed for the automatic recording of derivative curves of the proton absorption lines, and such curves were obtained for each substance over a variety of temperatures. Methods also were developed for the calculation of second moments and the prediction of line shapes due to various forms of molecular motion which might be expected. Comparison of the observed and predicted line shapes and second moments leads to the conclusion that methyl groups rotate about the carbon-silicon bond with unusual freedom, and that to a lesser extent the molecule as whole may rotate at low frequency if it is nearly spherical. The rotation of the methyl groups persists at low temperatures and is still extensive at −196°, whereas analogous organic compounds present a rigid lattice long before so low a temperature is reached.The possible interpretation of the unique physical properties of methyl silicones in the light of these results is considered.

INTRODUCTION

If we define silicones generally as polyorganosiloxanes, we see at once that the term embraces a large variety of compositions, each having one or more particular kinds of organic group attached to the silicon atoms of a siloxane framework. While this framework of alternate silicon and oxygen atoms always exerts its influence, it will be recognised that the size, shape, and chemical behaviour of the organic groups will have a marked or perhaps major effect on the properties of the polymer. It also is to be expected that as portions of the siloxane structure flex or rotate under thermal excitation, such intramolecular motion will be strongly dependent upon the size and structure of the organic groups.

If we were to begin a systematic study of the internal motion of organosiloxane molecules, which is the purpose of the present investigation, prudence would dictate starting with an examination of the methyl siloxanes as representatives of the simplest series. However, there are more cogent reasons for studying methyl silicones. Of the many possible organosiloxanes that fall within our definition, only a score or so have been prepared and studied in detail, but of these, methyl silicone has become the most interesting and commercially the most important. It not only exhibits the general properties of the whole class of silicone materials, but also has some unique properties of its own. For our purpose the most important properties to consider are (1) high thermal stability, (2) resistance to oxidation at elevated temperatures, (3) relative inertness to ionic reagents except very strong bases and hydrofluoric acid, (4) extreme insolubility in water and a high contact angle with liquid water, (5) poor solubility of the higher polymers in organic solvents, (6) small temperature coefficient of viscosity in the liquid linear polymers, (7) low boiling points (in relation

[1] Present address: E. I. duPont de Nemours and Co., Film Department, Buffalo, N.Y.
[2] Atomic Energy Commission Fellow at Harvard University, 1951–1953.

to the analogous organic compounds of equal molecular weight) of the lower polymers, (8) poor tensile strength of the unreinforced elastomeric polymer despite its high molecular weight, (9) moderate adhesion and strength of the purely methyl silicone resinous polymers, (10) small dielectric power absorption over a very wide range of frequencies, together with small change of loss factor and dielectric constant with change of temperature, and (11) comparatively large molar volumes and high compressibilities of the liquid polymers.

The chemical characteristics of methyl silicone, as summarized in items (1) to (5) above, are readily explained in terms of its chemical composition: the stable oxidized framework of silicon and oxygen atoms, the minimum of carbon and hydrogen, and the fortunate distribution of electronegative and electropositive elements lead to a qualitative expectation of just such properties.[3] At the same time, the physical properties of methyl silicone polymers as summarized in items (6) through (11) above seem to demand some explanation based upon molecular structure rather than upon composition. Two explanations have been offered: the first considers the molecule of methyl silicone to be tightly coiled at low temperatures and to uncoil to a more relaxed and entangled state at higher temperatures,[4] and the second considers the dimethylsilyl groups to be capable of unusually free motion about the silicon-oxygen bond as though the latter were a ball-and-socket joint.[5] There has been no direct evidence to support either hypothesis. The coiling-uncoiling theory is useful in explaining the behaviour of thin films of methyl silicone on water[6] and may be supported by such behaviour; it also will explain the low-temperature coefficient of viscosity if the entanglement at higher temperatures properly compensates for part of the normal fall in viscosity. The free-motion hypothesis arose from a consideration of the X-ray diffraction pattern of octamethylspiropentasiloxane, and is attractive as an explanation of the low intermolecular forces and high intermolecular distances that seem to be indicated by the physical properties (ref. 3, pp. 110—116).

However, difficulties are encountered in the detailed application of either hypothesis. Under the coiling-uncoiling view, the properties of silicone elastomers would require a helix of so many siloxane units per turn[7] as to make the distinction between coil and chain difficult. Moreover, the viscosities of liquid methyl siloxanes vary not only with temperature but also with the length of the chain (ref. 3, p. 81), so that the thermal coefficient of uncoiling would have to vary regularly with the length of the chain. Furthermore, the molar volumes of dimethylsiloxy units in the small cyclic polymers are much the same as those of dimethylsiloxy units in a chain, and the viscosity-temperature behaviour of the small rings is closer to that of the chains than to that of ordinary liquids. It is difficult to see how an uncoiling hypothesis could be applied to these small cyclic structures. On the other hand, despite the greater applicability of the free-motion theory its foundation becomes insecure if other interpretations of the observed diffraction pattern are made.[8] Similar objections may also be raised concerning the application of this theory to the small

[3] E. G. Rochow, *An Introduction to the Chemistry of the Silicones*, 2nd Edition, Chapters 2 and 6 (John Wiley & Sons, Inc., New York, 1951).
[4] L. Pauling, *General Chemistry*, 1st Edition, p. 5 (Freeman and Co., San Francisco, 1947).
[5] W. L. Roth, *J. Amer. Chem. Soc.*, **69**, 474 (1947);
W. L. Roth and D. Harker, *Acta. Cryst.*, **1**, 34 (1948).
[6] H. W. Fox, P. W. Taylor, and W. A. Zisman, *Ind. Eng. Chem.*, **39**, 1401 (1947).
[7] H. L. Frisch, I. Martin, and H. F. Mark, *Monatsh. Chem.*, **84**, 250 (1953).
[8] L. Pauling, private communication, 1951.

VOL. 1 1955

cyclic dimethylsiloxanes, for the flexing of silicon-oxygen bonds should be more difficult in cyclic trisiloxanes and tetrasiloxanes than in linear ones.

It should be possible to assess both hypotheses further if direct evidence for or against intramolecular motion could be obtained. We believed that the techniques of nuclear magnetic resonance absorption should be capable of providing such evidence, for the proton resonance of the methyl groups in methyl siloxanes should be very sensitive to the proximity and relative motion of neighbouring hydrogen atoms.[9] The attractiveness of the NMRA method is increased by the fortunate condition that the principal isotopes of carbon, oxygen, and silicon are even-even isotopes of zero nuclear magnetic moment,[10] so that only the hydrogen nuclei are magnetically significant and therefore only the relative positions and motions of hydrogen atoms will be observed. This is the opposite situation to that largely encountered in X-ray and electron diffraction studies of the same materials.

To submit these ideas to test, we have constructed a permanent magnet and a radiofrequency spectrometer designed especially for observing the width and shape of the proton absorption line. With these the proton resonance lines of hexamethylcyclotrisiloxane, octamethylcylcotetrasiloxane, decamethylcyclopentasiloxane, hexamethyldisiloxane, methyltrichlorosilane, dimethyldichlorosilane, trimethylchlorosilane, methoxytrichlorosilane, methyl chloroform, and silicone rubber were recorded automatically in the form of the first derivative or slope, as illustrated below. Each substance was examined at several temperatures, and in some instances the change of line width with temperature was studied intensively. The second moments, line widths, and line shapes for each substance were then compared with the corresponding calculated data based upon assumed forms of motion until a reasonable fit was obtained. Conclusions could then be drawn concerning the types of motion and their temperature dependence, as will be discussed later.

THEORY

Let us consider a nucleus having a spin of 1/2. In a magnetic field this nucleus may align itself in one of two energy levels, for which the magnetic quantum number $m = \pm 1/2$. The energy separation of these levels is given by $\Delta E = g\mu_0 H_0$, where μ_0 is the nuclear magneton, g is the gyromagnetic ratio, and H_0 is the magnitude of the external field. In a sample containing many such nuclei the populations of these two levels will differ according to the Boltzmann factor $\exp(\Delta E/kT)$, so that at equilibrium in the field there will be a slight excess in the lower state. The application of a radiation field at the resonance frequency r ($= \Delta E/h$) will induce transitions between the energy states which will result in energy being absorbed from the radiation field as the populations of the two levels tend to become equal. As can be seen from a consideration of the Boltzmann factors, any tendency to equalize the populations of the energy levels implies an increase in the temperature of the nuclear-spin system. This will result in the transfer of energy from the spin system to the surrounding lattice in the form of heat, and the efficiency of such transfer is measured by the

[9] See, for example, the distinctions between the proton absorption lines for ice and liquid water in E. M. PURCELL, *Science*, **107**, 433 (1948).

[10] The isotopes ^{13}C (1·1%), ^{17}O (0·04%), and ^{29}Si (4·7%) are considered to be in too low concentration to exert an influence of primary importance on the proton resonance. Moreover, the one present in largest proportion, ^{29}Si, has a nuclear magnetic moment much less than that of the proton (magnetic moments 0·55 vs. 2·79).

spin-lattice relaxation time T_1, which is a characteristic of the material. The net energy absorption by the sample will depend on the energy input, determined by the intensity of the radiation field, and the energy lost, determined by T_1.

The exchange of energy between the spin system and the lattice is caused by thermal motion of the atoms which cause fluctuations in the magnetic fields at the location of the nuclear spins.[11] Such motions may be due to lattice vibrations, rotation, or torsional oscillations in crystals, or to Brownian motion in fluids. The spin-lattice relaxation time gives a measure of these interactions. We will not consider it further here except to point out that materials having long relaxation times frequently present difficulties experimentally because the amplitude of absorption is severely reduced by the inefficiency of the energy transfer from spins to lattice.

In addition to the amplitude of absorption we must also consider the shape of the absorption line, for the shape depends markedly on the relative positions of the absorbing nuclei. This is the result of two factors: (1) two similar nuclei may simultaneously induce transitions in each other due to the interaction of their own magnetic fields, (2) the magnetic moment of one nucleus will produce a static magnetic field at other nuclei in its vicinity. The first factor limits the lifetime of a nuclear spin state and causes a dispersion of the energy level according to the uncertainty principle. The second factor causes the magnetic field at any nucleus to be the sum of the permanent field H_0 and all the local fields from all nuclei in the vicinity.

VOL. 1 1955

In certain molecules two or three nuclei may be relatively isolated from all other like nuclei (such as the protons in $CH_2Cl—CH_2Cl$, or in CH_3CCl_3), in which case the absorption line will exhibit fine structure. The actual line shape will then yield considerable information about the internuclear distances and orientation.[12, 13, 14] More commonly, the number of near neighbours is sufficiently great that the line shape exhibits no fine structure. In this case recourse may be had to the second moment of the line shape, which is expressed as:

$$\langle \Delta H_2 \rangle^2 = \frac{\int_{-\infty}^{\infty} (H - H_0)^2 f(H)\, dH}{\int_{-\infty}^{\infty} (fH)\, dH} \tag{1}$$

where H_0 is the magnetic field strength at the centre of the absorption line and $f(H)$ describes the line shape. The second moment has been related by VAN VLECK[15] to the molecular configuration of the sample, and for a sample containing only one magnetically active species the expression can be written as:

$$\langle \Delta H_2 \rangle^2_{\text{theor.}} = 3/2I(I+1)N^{-1}g^2\mu_0^2 \sum_{i>j} (3\cos^2\theta_{ij} - 1)^2 r_{ij}^{-6} \tag{2}$$

where r_{ij} and θ_{ij} are the internuclear distance and the angle between this internuclear direction and the external magnetic field. N is the number of nuclei at resonance in the molecule or subgroup to which the spin-spin interactions are considered to

[11] N. BLOEMBERGEN, E. M. PURCELL, and R. V. POUND, *Phys. Rev.*, **73**, 679 (1948).
G. E. PAKE, *Amer. J. Physics*, **18**, 438–452, and 473–486 (1950).
F. BLOCH, *Phys. Rev.*, **70**, 460 (1946).
[12] G. E. PAKE, *J. Chem. Phys.*, **16**, 327 (1948).
[13] H. S. GUTOWSKY, G. B. KISTIAKOWSKY, G. E. PAKE and E. M. PURCELL, *J. Chem. Phys.*, **17**, 972 (1949).
[14] E. R. ANDREW and R. BERSOHN, *J. Chem. Phys.*, **18**, 159 (1950).
[15] J. H. VAN VLECK, *Phys. Rev.*, **74**, 1168 (1948).

be confined. Thus a value of the second moment may be computed for any assumed model of the molecule being investigated. This value may then be compared with values obtained by graphical integration from the experimental curves. In practice, as we shall see, the experimental technique determines the first derivative of the absorption curve. However, equation (1) can be modified to use the derivative curve directly in the following relation:

$$\langle \Delta H_2 \rangle^2_{\text{exp.}} = \frac{\iint (H - H_0)^2 f'(H)\, dH dH}{\iint f'(H)\, dH dH} = \frac{1}{3} \frac{\int_{-\infty}^{\infty} (H - H_0)^3 f'(H)\, dH}{\int_{-\infty}^{\infty} (H - H_0) f'(H)\, dH} \tag{3}$$

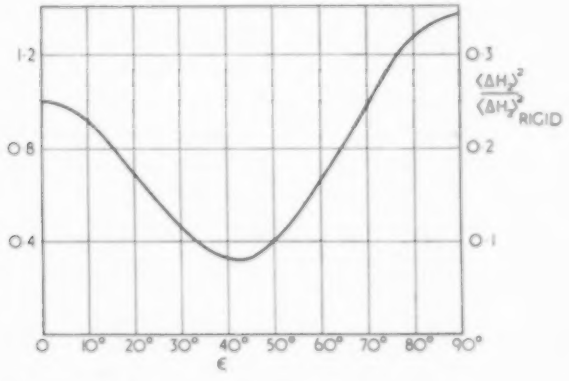

FIG. 1.—$\langle \Delta H_2 \rangle^2 = 5{\cdot}4 \left[\frac{27}{8} \sin^4 \varepsilon - 3 \sin^2 \varepsilon + 1\right]$ gauss² (rotation about ε only).

Before the values of the second moments obtained from equations (2) and (3) can be compared, some estimate of intermolecular broadening must be made. Such broadening (which is due to all other nuclei not included in the computation of the second moment) may be estimated from the shape of the curve.[16] Assuming that the broadening has a Gaussian character, the broadening parameter, β, is given by

$$\beta \cong \sqrt{2}\, \delta H_1 \tag{4}$$

where δH_1 is the spacing in gauss between the centre of the line and the peak of the derivative curve, and then

$$\langle \Delta H_2 \rangle^2_{\text{exp.}} = \langle \Delta H_2 \rangle^2_{\text{theor.}} + 1/2\beta^2 \tag{5}$$

We have thus far been assuming that the nuclei are fixed in space. However there may be rotation either of whole molecules or of groups. In such cases the time-average local field at any nucleus will be reduced, and the second moment will be decreased. The effect on the second moment may be determined by averaging the angles O_{ij} over time in equation (2).

We will be concerned herein only with the protons on methyl groups. If we assume a normal configuration for such groups, the inter-proton distances will be

[16] J. C. STERNBERG, private communication.

1·79 Å, and the theoretical rigid lattice second moment $\langle \Delta H_2 \rangle^2_{\text{theor.}} = 21{\cdot}7$ gauss^2. For rotation of the methyl groups about the C-X bond, the theoretical second moment is reduced by a factor of 4, or $\langle \Delta H_2 \rangle^2 = 5{\cdot}4$ gauss^2. We may also consider two other types of rotation, that of rotation of the molecule about an arbitrary axis at an angle ε from the C-X axis, and a combination of methyl group and molecular rotation. The second moments for these cases are given as a function of ε in Figs. 1 and 2 respectively.[17]

Line shapes for these cases may also be computed by extending the theory of ANDREW and BERSOHN.[14] However, the form of the equations is not amenable to general treatment similar to that used by POWLES and GUTOWSKY.[18] The overall unbroadened line shape must be obtained by addition of seven lines each of which has

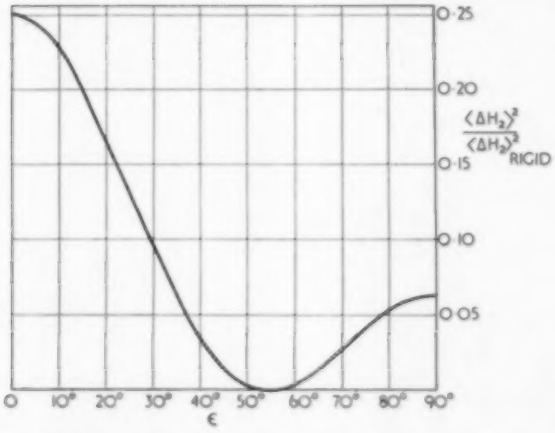

FIG. 2.—$\langle \Delta H_2 \rangle^2 = 5{\cdot}4\ [3/2 \cos^2 \varepsilon - 1/2]^2$ gauss^2 (double rotation).

a different dependence on the angle ε and must therefore be recalculated for each value of the angle. The equations for these line components are given below for reference, the nomenclature being based on ANDREW and BERSOHN'S paper.[14]

Case I: Rotation about an axis at angle ε from the C-X axis.

(a) central component is unchanged from rigid lattice value. Normalized

$$\text{probability} = 1/8 \left(1 + 3 \frac{E_1^2}{E_2^2}\right)$$

(b) component at $+y/\mu$

$$F_i(\Delta H) = \frac{\sqrt{3}}{16 E_2 \alpha} \left[1 - \left(\frac{E_1}{E_2}\right)^2\right] \left[1 - \frac{2}{E_2}\left(\frac{\Delta H}{\alpha}\right)\right]^{-1/2}$$

$$\text{limits: } -E_2\alpha < \Delta H < \frac{E_2}{2}\alpha$$

[17] Further details concerning the method for evaluating the intermolecular broadening and the effect of molecular rotation will be available in a forthcoming paper by J. C. STERNBERG and H. G. LECLAIR.
[18] J. G. POWLES and H. S. GUTOWSKY, *J. Chem. Phys.*, **21**, 1695 (1953).

(c) component at $\dfrac{(3x+y)}{2\mu}$

$$E_2(\Delta H) = \frac{1}{4\sqrt{3}(3E_1+E_2)}\left[1+\frac{E_1}{E_2}\right]\left[1-\frac{4}{(3E_1+E_2)}\left(\frac{\Delta H}{\alpha}\right)\right]^{-1/2}$$

limits:

$$-\frac{(3E_1+E_2)}{2}\alpha < \Delta H < \frac{(3E_1+E_2)}{4}\alpha$$

(d) component at $\dfrac{3x-y}{2\mu}$

$$F_3(\Delta H) = \frac{1}{4\sqrt{3}(3E_1-E_2)}\left[1-\frac{E_1}{E_2}\right]\left[1-\frac{4}{3E_1}-E_2\left(\frac{\Delta H}{\alpha}\right)\right]^{-1/2}$$

limits:

$$-\frac{(3E_1-E_2)}{2}\alpha < \Delta H < \frac{(3E_1-E_2)}{4}\alpha$$

(e) components at $-y/\mu$, $-(3x+y)/2\mu$, $-(3x-y)/2\mu$ are obtained by replacing ΔH by $-\Delta H$ in the above equations.

$$E_1 = (3/2\cos^2\varepsilon - 1/2)$$

$$E_2 = [27/4\sin^4\varepsilon - 3\sin^2\varepsilon + 1]^{1/2}$$

Case II: double rotation, about arbitrary axis as in Case I, plus simultaneous rotation of the methyl group about C-X bond.

(a) component at 0 is unchanged, probability = 1/2

(b) component at $\dfrac{3x+y}{2\mu}$

$$F(\Delta H) = \frac{1}{8\sqrt{3}\alpha E_3}\left[1-1/E_3\left(\frac{\Delta H}{\alpha}\right)\right]^{-1/2}$$

limits: $-2\alpha E_3 < \Delta H < \alpha E_3$

$$E_3 = (3/2\cos^2\varepsilon - 1/2)$$

Broadened curves are obtained by including broadening function $S = e^{-(H-H_0)^2/b^2}$ so that broadened line components are determined by:[12]

$$f_i(H) = \int_{H_0}^{e^{-(H-H_0)^2/b^2}} F_i^{(H_0-\overset{*}{H})} dH_0$$

where $\overset{*}{H}$ is the resonance frequency at the centre of the line (that at which isolated nuclei would absorb), H_0 is defined by $\Delta H = H_0 - \overset{*}{H}$, and H is an arbitrary field parameter.

These functions were computed numerically with the aid of a table compiled by the Whirlwind I computer at the Massachusetts Institute of Technology,[19] giving

[19] The authors are deeply indebted to Mr. JACK PORTER for carrying out these computations during the late hours when the Whirlwind was not in programmed use.

generalized $f_1(\Delta H)$ functions for several values of β. Details of the method and table of values will be published elsewhere.[17]

As mentioned previously, if the methyl groups are relatively isolated the line shape may exhibit fine structure, in which case the structure can yield considerable information. POWLES and GUTOWSKY[18] have illustrated the effect of the broadening parameter on the theoretical line shapes for the case of a rigid methyl group and for rotation of the methyl group about the C-X bond. With the aid of these line shapes a more unequivocal determination of the type of motion a material will undergo becomes possible.[20]

EXPERIMENTAL

Apparatus. As pointed out previously, if a sample is placed in an appropriate magnetic field, application of a radiation field of the proper frequency will cause the sample to absorb energy. The resonant frequency for nuclear spin transitions is of the order of 1–40 Mcps in fields of $< 10{,}000$ gauss. This is in the range of radio frequencies and the techniques used therefore are similar to those employed

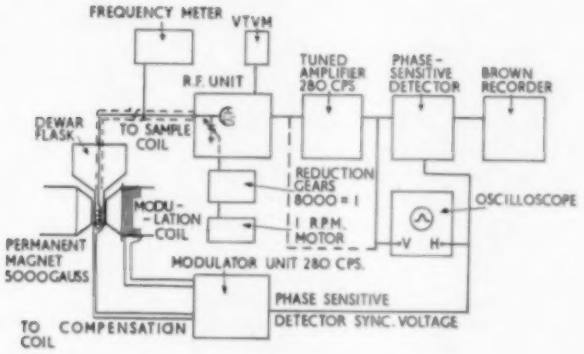

FIG. 3.—Block diagram of apparatus.

in commercial radio work. The particular technique used in this work involves placing the sample in a coil which is used as the inductive component of the tuning network of an oscillator. Sample and coil are then placed in the magnet gap, and as an oscillator frequency is varied through the resonant frequency of the nuclei, energy is absorbed, the oscillation level drops, and the change in level is detected and amplified. Amplification and detection are greatly simplified through use of a modulation system which entails superposition of a low audio frequency component on the fixed external magnetic field. This modulation causes the nuclear resonant frequency to vary at an audio frequency rate. Thus the sample goes in and out of resonance at this same rate, and the signal may then be amplified by standard radio and audio frequency techniques rather than by d.c. amplification which is difficult and unstable in operation.

The block diagram of the apparatus is shown in Fig. 3. The R-F unit contains the oscillator with its motor-driven tuning capacitor, and several stages of amplification. The audio output is fed to the tuned amplifier which eliminates all frequencies except those directly caused by the sample, which of course varies at the modulation frequency. In all the experiments of this work, the modulation amplitude was set to a fraction of the line width so the amplitude of the signal is determined by the slope of the line at the frequency determined by the oscillator. The signal is fed to the phase-sensitive detector which, when synchronized by a signal from the modulator unit, sends a d.c. signal to the recorder which is proportional to the first derivative of the absorption line intensity.

[20] A much more detailed treatment of the theory upon which our experimental technique is based is given in the thesis entitled *Molecular Motion in Organosilicon Compounds*, by H. G. LECLAIR (1953) in the Harvard University Library.

VOL. 1 1955

The actual circuits of all the units in Fig. 3 are based on circuits supplied by WATKINS and POUND.[21,22,23] Several adaptations to our purposes were made at the time the oscillator, modulator, and phase-sensitive detector were constructed, and several improvements suggested themselves during the course of the work.[24]

The design of the magnet was influenced in part by the materials on hand. A yoke was constructed of two soft iron bars $4 \times 7 \times 27$ inches and two $4 \times 7 \times 20$ inches ground flat at the bolted joints. Seven discs of Alnico V, each one inch thick and six inches in diameter,[25] were assembled to form either pole, and these were secured by a stainless steel bolt to the yoke and to the soft iron pole pieces four inches in diameter. The Alnico was magnetized by a current of 100 amperes through a pair of specially-wound coils which later were used as the modulation coils. A permanent field of 5,050 gauss was obtained within the gap of 1·4 inches, with an inhomogeneity of 0·3 gauss over a sample one inch long.[26]

A cryostat was necessary for the observations at low temperature, and this was built in the form of a Dewar vessel 8 inches in diameter at the top and tapering to a tubular section 1·25 inches in diameter at the lower end. The tubular section extended into the magnet gap, and the sample within its sample coil extended down into the magnetic field within a closed-end glass tube within the Dewar vessel. Temperatures were measured by means of a thermocouple extending through the cork of the sample vial and into the sample. The cryostat was filled directly with liquid nitrogen or with a mixture of acetone and dry ice, since the cooling liquid did not come into contact with the sample coil or vial. Measurements at temperatures other than 77°K and 193°K were attained by cooling the cryostat below the desired temperature and allowing it to warm slowly; the heat capacity was sufficient to allow scanning the absorption line in this manner.

The general procedure in examining a sample was to adjust the oscillator frequency until the absorption line could be observed on the oscilloscope, adjust the modulation level, compensation, and phasing controls, and then sweep through the line by means of the motor-driven oscillator tuning capacitor shown on the block diagram. The signal was then recorded as unbalance in the output push-pull stage of the phase-sensitive detector on the specially adapted recording potentiometer. A typical trace of a derivative line (that for methyl trichlorosilane) is shown in Fig. 4, in which the frequency-check marker caused by introducing a signal from the frequency meter is clearly shown. The recorded curves were smoothed by drawing a line through the mean points of the fluctuations, and the horizontal scale converted from cycles per second at fixed magnetic field to variation of gauss at fixed frequency in order to conform with the conventions of published work. Second moments were derived from the smoothed curves and were compared with the calculated second moments obtained as described under *Theory*. Those lines that exhibited fine structure were compared with a variety of theoretical line shapes predicted by the means described under *Theory*. In this manner two methods of interpretation could be brought to bear on at least some of the observations.

RESULTS AND ANALYSIS

1. Methyltrichlorosilane, CH_3SiCl_3

A typical recorded derivative line obtained at the temperature of liquid nitrogen is given in Fig. 4, and an average smoothed line appears in Fig. 5. Both should be compared with the derivative line for 1,1,1-trichloroethane (the analogous compound of carbon) in Fig. 6. The trichloroethane line indicates a rigid lattice, for if the C-H distance is assumed to be 1·094 A, the inter-proton distance in the methyl group is

[21] R. V. POUND, *Rev. Sci. Instr.*, **21**, 219 (1950).
[22] G. D. WATKINS, Thesis, An RF Spectrometer with Application to Studies of Nuclear Magnetic Resonance Absorption in Solids, Harvard, 1952.
[23] G. D. WATKINS, private communications.
[24] Full details of the circuits and their operation are given in the Harvard thesis, ref. 19, and in ONR report N5-ori-07661.
[25] The authors are indebted to the Carboloy Department of the General Electric Company for the loan of the Alnico at a time when it was not available without priorities and long delays.
[26] It should be emphasized that the objective of the present investigation was the determination of line widths ranging from five to twenty-five gauss or more, and so high resolution was neither necessary nor desirable. The same magnet would probably not do for chemical shift work, and a new one of greater field homogeneity is being constructed for such work.

VOL.
1
1955

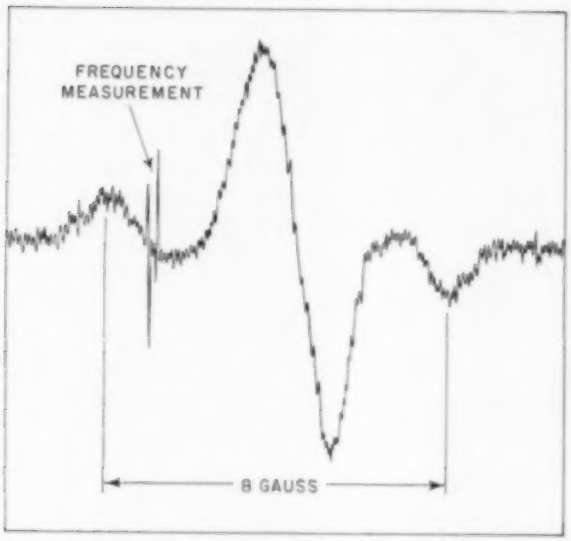

CH_3SiCl_3 at 77° K, Mod. 2·0 v., Osc. 0·20 v.

FIG. 4.—CH_3SiCl_3 at 77°K, Mod. 2·0 v, Osc. 0·20 v.

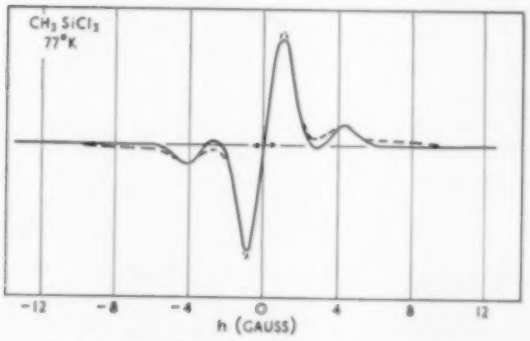

FIG. 5.—Line shape derivative curve for methyltrichlorosilane.

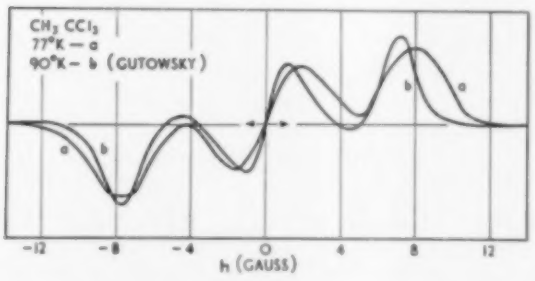

FIG. 6.—Line shape derivative curve for 1,1,1-trichloroethane.

1·79 A, the calculated intramolecular moment is 21·8 gauss^2 and the intermolecular contribution is 2·1 gauss^2,[14] or a total of 23·9 gauss^2 compared with our observed value of 21·7 gauss^2 from Fig. 6. On the other hand, the line for trichlorosilane is much more like that of a liquid; the line is only half as broad as that for 1,1,1-trichloroethane, and the subsidiary peaks (due to the influence of neighbouring methyl groups) are greatly suppressed. It must be concluded from even this qualitative comparison that there is a great deal of residual motion in the molecules of trichlorosilane at 77°K, or 118° below the melting point of the compound.

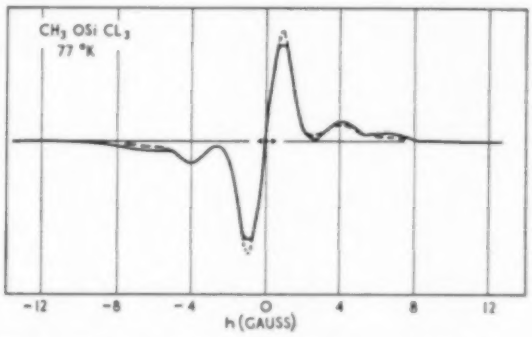

FIG. 7.—Line shape derivative curve for methoxytrichlorosilane.

The experimental second moment is 3·55 gauss^2, and the broadening factor β (from the line shape) is approximately 1·2 gauss, leaving a corrected second moment of 2·8 gauss^2. Since this is less than that predicted for rotation of the methyl group ($\langle \Delta H^2 \rangle_{\text{theor.}} = 5{\cdot}4$ gauss^2), other types of motion must be considered. The small value of the observed second moment predicts rotation about an axis at an angle $\varepsilon \cong 25°$ or 55°, or double rotation with $\varepsilon \cong 25°$. Curves were drawn from the equations given under *Theory*, but no close fit was obtained. Yet the spacings of the peaks fit well with those calculated for pure rotation of the methyl group (the dotted line of Fig. 5), and the shape of the observed line would seem to be explained by such motion. The discrepancy in values of the second moment is seen from Fig. 5 to be due to the missing tails of the experimental curve, perhaps due to low-frequency motion of the molecule. The near-spherical symmetry of the trichlorosilane molecule would readily permit such motion.

2. Methoxytrichlorosilane, CH_3OSiCl_3

In order to determine what influence a silicon-oxygen bond might have on the kind or extent of the molecular motion noticed in methyltrichlorosilane, methoxytrichlorosilane was prepared and examined. The smoothed derivative line is shown as the solid curve in Fig. 7, and the theoretical curve for rotation of the methyl group about the carbon-oxygen bond (with a broadening factor β of 1·3 gauss) is shown as the dashed line. The theoretical curve is exactly the same as that in Fig. 5, and it is seen that an even better fit is obtained here than with methyltrichlorosilane. The experimental second moment is 7·3 gauss^2 to which the intermolecular broadening contributes 1·0 gauss^2, leaving 6·3 gauss^2 for the principal motion. The theoretical second moment for rotation about the carbon-oxygen bond is 5·5 gauss^2. The

agreement is not remarkable, but again it is the long low-amplitude tails of the curves, sensitive to experimental error, which influence the second moment most. The agreement in line *shapes* is more striking but no more precise.

3. Dimethyldichlorosilane, $(CH_3)_2SiCl_2$

The replacement of one of the chlorine atoms of methyltrichlorosilane with a second methyl group produces a marked change in the line shape, as shown in Fig. 8. The line is broadened, and the side peaks are increased in amplitude. Both effects

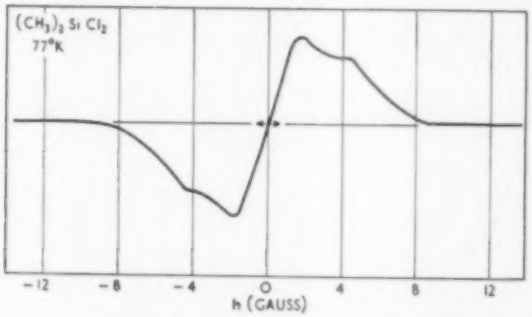

FIG. 8.—Line shape derivative curve for dimethyldichlorosilane.

might be expected from the interaction of the two methyl groups and the reduced intermolecular shielding of the methyl groups by chlorine atoms.

A more exact analysis shows that the experimental second moment is 6·9 gauss², which is reduced to 4·0 gauss² after removing the broadening contribution. The theoretical second moment computed for the spacings determined by electron diffraction[27] is 5·7 gauss² if the methyl groups are staggered with respect to each other, or 5·8 gauss² if eclipsed. A similar ambiguity remains when some fit is sought with the curves calculated for double rotation or rotation of the entire molecule about one of the carbon-silicon bonds, for in the former case the theoretical curve is devoid of fine structure and in the latter the peaks fall at different places. It can only be concluded that both methyl groups are tunnelling* about the carbon-silicon bond, with some residual motion of the entire molecule at low frequency which reduces the second moment and accentuates the fine structure without affecting the spacings of the maxima.

4. Trimethylchlorosilane, $(CH_3)_3SiCl$

The experimental curve given in Fig. 9 shows continuation of the trend shown in the monomethyl and dimethylchlorosilanes. When three methyl groups are present, their interaction masks all the fine structure and leaves only the broadened line. The experimental second moment is 10·3 gauss² before and 5·2 gauss² after correction for intermolecular broadening, the latter being only slightly less than that expected for tunnelling of the methyl groups. The spacing of the peaks (+ and − 2·6 gauss) falls

[27] R. L. LIVINGSTON and L. O. BROCKWAY, *J. Amer. Chem. Soc.*, **66**, 94 (1944).

* By tunnelling is meant exchanging of places by the hydrogen atoms through partial, irregular, or reciprocal rotation as distinguished from continuous spinning of the methyl group. Our method is incapable of differentiating between rotation and tunnelling of the methyl groups, since both produce the same result if they are rapid with respect to the time of one cycle.

VOL. 1 1955

between the calculated spacings for $\beta = 3{\cdot}0$ and $3{\cdot}7$ gauss. Once again the tail of the experimental curve cuts off more abruptly than theory would indicate, pointing to some low-frequency motion of the molecule as a whole which also reduces the second moment.

5. Hexamethyldisiloxane, $(CH_3)_3SiOSi(CH_3)_3$

The derivative curve shown in Fig. 10 is slightly narrower than that for trimethylchlorosilane, but is of the same general shape. The experimental second moment is

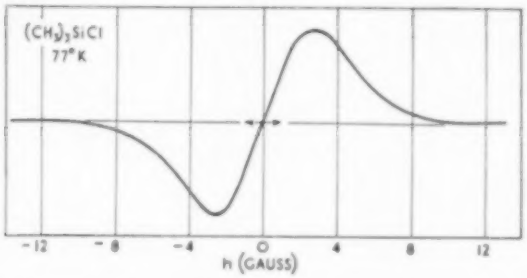

FIG. 9.—Line shape derivative curve for trimethylchlorosilane.

$9{\cdot}2$ gauss^2, and with β about $3{\cdot}5$ gauss the second moment is reduced to $3{\cdot}0$ gauss^2, about the same as that for methyltrichlorosilane. Thus there must be considerable motion in addition to the tunnelling of the methyl groups. As before, a theoretical line shape based only on methyl rotation gives a curve with wider tails than are observed. On the other hand, assumption that there is also molecular rotation about the silicon-oxygen bond gives a theoretical curve with *less* tail than is observed.

There is still the possibility that there is rotational oscillation of the methyl groups in addition to tunnelling about the carbon-silicon bond, as is indicated by the dispersion of values (from 140° to 180°) for the Si—O—Si bond angle by electron diffraction and dipole moment studies.[28] Since the angle is large compared with that for organic ethers, it may be concluded that the Si—O—Si bond is more flexible and may permit rotational oscillation about the Si—O axis. Such a conclusion is highly speculative, however, for second moments can be calculated for such a situation and these indicate that the angle of oscillation would have to be about 80° peak-to-peak, and this seems extraordinarily large. The result, therefore, could not be considered firm evidence for the free-motion theory, although that theory explains it.

6. Hexamethylcyclotrisiloxane, $[(CH_3)_2SiO]_3$, octamethylcyclotetrasiloxane, $[(CH_3)_2SiO]_4$, and decamethylcyclopentasiloxane, $[(CH_3)_2SiO]_5$:

Three cyclic siloxanes were examined in this study, and all had closely similar absorption lines at 77°K. That for the cyclic trimer is shown in Fig. 11. Fig. 12 shows the line at room temperature, 300°K, which is *broader* than that at 77°K. The strange appearance of a line broadening (becoming more solid-like) as the sample is warmed led us to examine the dependence of the line width (peak-to-peak distance) on temperature, and the result for the trimer is given in Fig. 13. Corresponding curves for the cyclic tetramer are given in Figs. 14 and 15, and for the cyclic pentamer in Figs. 16 and 17. All will be considered together.

[28] Ref. 3, pp. 109–110.

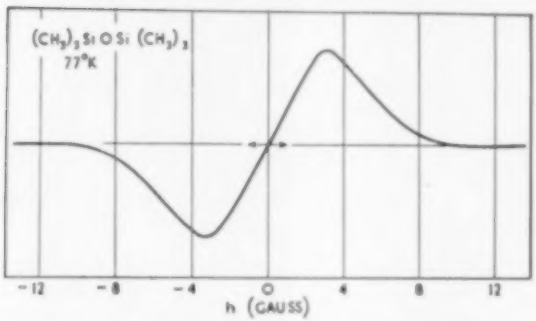

FIG. 10.—Line shape derivative curve for hexamethyldisiloxane.

VOL.
1
1955

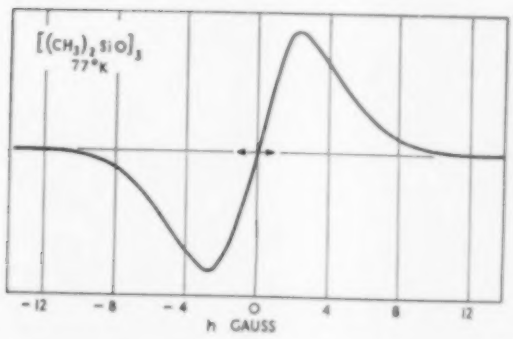

FIG. 11.—Line shape derivative curve for hexamethylcyclotrisiloxane

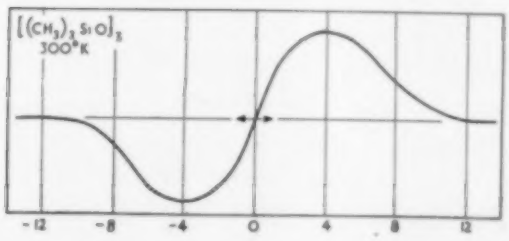

FIG. 12.—Line shape derivative curve for hexamethylcyclotrisiloxane

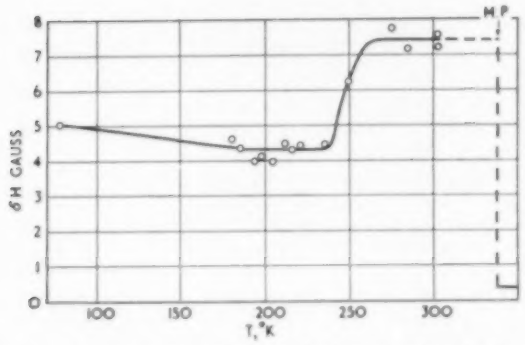

FIG. 13.—Line width vs. temperature for hexamethylcyclotrisiloxane.

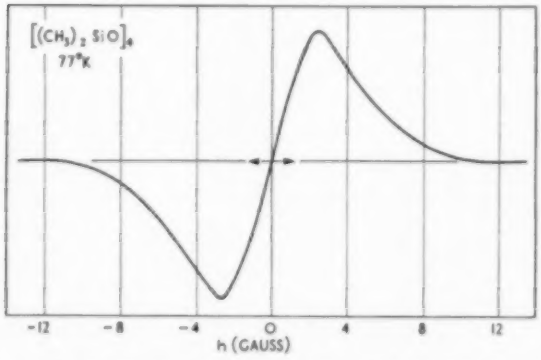

FIG. 14.—Line shape derivative curve for octamethylcyclotetrasiloxane.

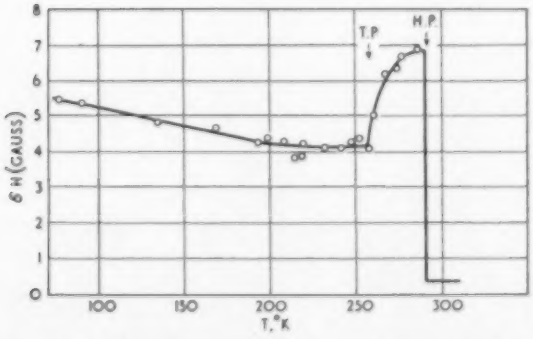

FIG. 15.—Line width vs. temperature for octamethylcyclotetrasiloxane.

The structure of the cyclic trimer has been investigated by electron diffraction[29] and X-ray diffraction,[30] and indirectly in the X-ray study of octamethylspiropentasiloxane. The average distances and angles are: Si—O 1·64Å, Si—C 1·92Å, O—Si—O 114° (individual values 115°, 104° and 110°), Si—O—Si 130° (125°, 136°, and 130°), and

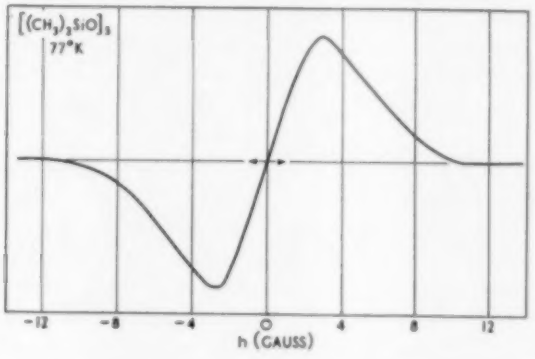

FIG. 16.—Line shape derivative curve for decamethylcyclopentasiloxane.

C—Si—C 110° (112°, 107°, and 110°). All the investigators agree that the trimer ring is planar, with the carbon atoms arranged above and below the ring, and all conclude that the thermal motion of the methyl groups is larger than normal (AGGARWALL and BAUER[29] find 0·09Å, compared with the normal motion of 0·03Å). No phase transitions were found down to 88°K.

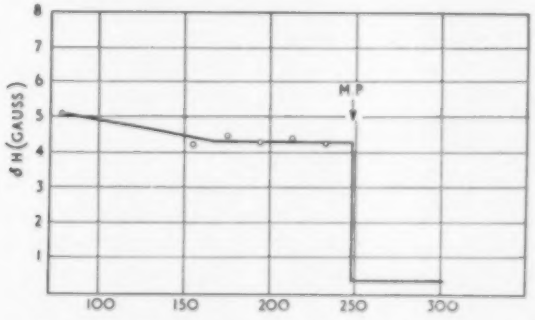

FIG. 17.—Line width vs. temperature for decamethylcyclopentasiloxane.

The cyclic tetramer has a nearly-planar ring in which the silicon atoms are coplanar and the oxygen atoms are slightly above and below the plane. The Si—O—Si bond angle is 160°. A transition occurs at −16·30°C,[31] above which there is either precession of the methyl groups or rotation of the molecule as a whole. The structure of the cyclic pentamer has not yet been determined, but the ring would be expected to be more puckered.

The line shape derivative curves for all these cyclic polymers at 77° are so similar

[29] E. W. AGGARWALL and S. H. BAUER, *J. Chem. Phys.*, **18**, 42 (1950).
[30] G. PEYRONEL, "Crystal Structure of Hexamethylcyclotrisiloxane," ONR report, Brooklyn Polytechnic Institute.
[31] J. D. HOFFMAN, *J. Amer. Chem. Soc.*, **75**, 6313 (1953).

that they may be superimposed within experimental error. The observed second moments, after deducting the broadening contributions, are 5·2 gauss^2 for the trimer, 5·4 gauss^2 for the tetramer, and 5·5 gauss^2 for the pentamer. The theoretical second moment for an isolated methyl group tunnelling about the carbon-silicon bond is 5·45 gauss^2, in good agreement. Furthermore, the line shape computed on the basis of such motion and using the broadening factor $\beta = 3{\cdot}0$ gauss agrees equally well with the experimental curves, the deviations being too minute to be visible when the line shape is plotted to the scale of the figure. Thus we may confidently say that the only motion within these three cyclic siloxanes at 77°K is rotation or tunnelling of the methyl groups about the carbon-silicon bonds.

The line widths as a function of temperature show a regular progression of behaviour. The width of the pentamer line decreases from 5·1 to 4·3 gauss between 77°K and 170°K, due to the normal thermal increase in low-frequency motion of the molecule or possibly to rotational oscillation with an amplitude of five to ten degrees, and then remains constant up to the melting point at 247°K. Above the melting point the width drops sharply to a value limited only by the field inhomogeneity, a thoroughly normal behaviour. The trimer and tetramer show similar normal behaviour below 240°K, with gradual increase of the width from 77°K to 200°K and then a fairly constant value. A sudden increase in the width of the tetramer line above 240°K occurs in the region of the transition point (−16°C), and so must involve either a restriction of the motion already present at lower temperatures or else a marked increase in the intermolecular broadening. The increase in volume observed at the transition point[31] seems to rule out the possibility that the interaction between methyl groups of different tetramer molecules is increasing, so we must conclude that the cause is intramolecular. It could be a flexing of the silicon oxygen bonds according to the free-motion theory, bringing about decreased separation of the methyl groups at least part of the time. This would increase the interactions between methyl groups, and at the same time might well increase the barrier to tunnelling of the groups about the carbon-silicon bonds, restricting this motion in favour of the swinging of the groups.

The same explanation may be applied to the cyclic trimer, which shows an even greater broadening because of the greater temperature range between increase in the line width and the melting point. The marked change at 238°K (−35°C) seems to indicate a transition which was missed during the diffraction studies but shows up in our more sensitive method.

The cyclic pentamer apparently melts before it reaches the interesting temperature of line broadening, or so it seems from extension of the behaviour of trimer and tetramer. The behaviour of the latter polymers is considered representative of the materials, for these were highly purified and contained no chloride impurities. Two samples of trimer, from different sources, showed exactly the same behaviour. Re-examination with a new oscillator system more stable at low R–F levels has confirmed the same abrupt points of increase in line width, although the extent of broadening was not as great and levelled off at just above 5 gauss.[32] The greater change in width depicted here is apparently due to saturation of the sample at an R–F level which was appropriate at the lower temperatures, but such saturation is itself as much an indication of decreased motion as is the increased line width.

[32] R. F. RILEY, private communication.

7. Silicone rubber $[(CH_3)_2SiO]_x$:

The line shape derivative curve and temperature dependence of line width for General Electric SE450 silicon rubber are depicted in Figs. 18 and 19. The line shape at 77°K is very similar to that obtained for the cyclic compounds and could be fit

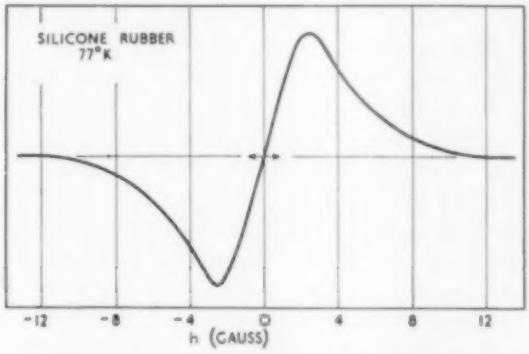

FIG. 18.—Line shape derivative curve for silicone rubber.

very well by assuming rotation of the methyl groups and using a broadening parameter $\beta = 2{\cdot}9$ gauss. The experimental second moment is 10·0 gauss^2, which falls to 5·8 gauss^2 after the broadening correction and agrees with the assumption of rotation. The temperature dependence differs but slightly from that of the cyclic compounds

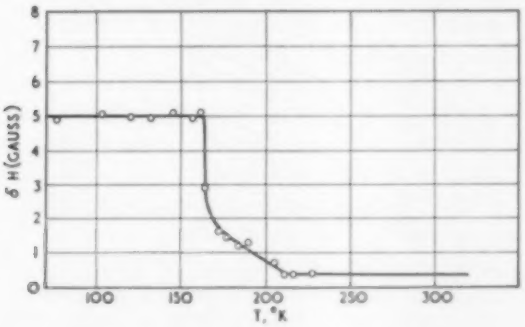

FIG. 19.—Line width vs. temperature for silicone rubber.

at low temperatures, and then there is an abrupt drop in width from 5·0 gauss to about 2·5 gauss at 164°K (−109°C). The line width then tapers off more gradually to the liquid line at 210°K. The rapid change at −109°C corresponds to the transition point of −110°C where crystallinity to X-rays becomes marked. Natural rubber shows a behaviour somewhat similar but shifted in temperature scale[33]; the break for natural rubber occurs at 220°K, or about 60° higher than that for silicone rubber. This difference explains the difference in low-temperature utility of the two elastomers.

Detailed analysis of the curves obtained between 77° and 164°K as the sample warmed showed that there was always a slight increase in second moment with each

[33] L. MEYER, Thesis, University of Illinois, 1952.

increase in temperature, although the line width (as measured by the separation between inverse peaks) did not change. This behaviour is consistent with a gradual increase in rotational oscillation of the methyl groups which, if the polymer molecules are closely packed, would increase the interactions between methyl groups on different chains. Above 164°K there is a more gradual sharpening of the line while the tails of the curves decrease. These line shapes may be explained qualitatively on the basis that they are combinations of two curves, one a narrow liquid-like curve and the other a broad curve similar to that obtained below 164°K. This would indicate that the molecules do not commence rotating simultaneously, probably because the polymer molecules vary widely in molecular weight.[34] A similar situation explained by a combination of curves due to crystalline and amorphous phases has been described by PAKE and WILSON.[35]

Silicone rubber and all the pure compounds studied in this series show the same behaviour at —77°K, a marked residual intramolecular motion here ascribed principally to rotation of the methyl groups. If it were possible to freeze out this motion completely at some lower temperature, the line shape would then be determined only the fixed proton-proton distance. Determination of this distance then would serve as a check on the assumption (carried throughout the present work) that the bond distances and angles of the methyl groups in methyl-silicon compounds are the same as those in methane. Measurements at the temperature of liquid helium therefore are being carried out in this laboratory, and preliminary results indicate that there is still some residual motion at 4°K in some of the compounds but not in all.[32]

DISCUSSION

The results of this investigation indicate that there is an unusual degree of motion of the hydrogen atoms in methylsilicon compounds. This motion is not confined to the siloxanes alone but is equally apparent in the methylsilicon chlorides and in methoxytrichlorosilane, showing that the presence of an Si—O bond is not essential to the motion. At 77°K the motion takes the principal form of rotation or tunnelling of the methyl groups about the carbon-silicon bonds, together with other contributory forms of motion. In the methylchlorosilanes and in hexamethyldisiloxane there appears to be additional rotation of the molecules themselves at low frequency about some other axis through the centre of mass, due probably to the near-spherical symmetry of these molecules. The cyclic dimethylsiloxanes show the same marked rotation of methyl groups, but differ in that they undergo what appears to be flexing of the silicon-oxygen bonds of the ring. Further differentiation is shown by silicone rubber, the very narrow line of which (above 164°K) indicates much motion not restricted to a particular axis or plane. Such random motion is usually considered characteristic of the liquid state, so in this sense silicone rubber is quite liquid. It is impossible to say how much of this random motion, if any, is due to flexing of the silicon-oxygen bonds.

No direct or unequivocal evidence has been obtained here for rotational oscillation about the silicon-oxygen bonds, although such oscillation may be adduced to lend qualitative support for some of our observations. On the other hand, there seems to be no necessity to assume a coiling-uncoiling mechanism, although our evidence

[34] D. W. SCOTT, *J. Amer. Chem. Soc.*, **68**, 1877 (1946).
[35] G. E. PAKE and C. W. WILSON, *J. Poly. Sci.*, **10**, 503 (1953).

does not exclude the possibility. Our position can be summarized by saying that it is quite possible that the coiling-uncoiling hypothesis applies to the siloxanes, but that this hypothesis alone is not sufficient to explain the major part of our observations. Neither theory mentioned in the introduction seems to apply wholly to the actual situation, and either theory may be modified to fit the observations.

The dominant fact that emerges from this work is that of free and persistent rotation of the methyl groups attached to silicon, even down to very low temperatures. This unusually free rotation may be due to the larger radius of the silicon atom[36] or to some combination of this factor with others. If it is agreed that a group in motion occupies more space than one at rest, then it must follow that the type of motion observed in this study contributes to a larger molar volume than would otherwise be observed. A necessary concomitant would be a decreased intermolecular attraction due to increased spacing, and low intermolecular attraction would explain the unusual physical properties of the methyl silicone polymers. It remains to be seen how the internal motion of silicones is influenced by the substitution of organic groups other than methyl, what changes occur when polar groups are introduced, and what effect is noticed when methylene groups are substituted for the oxygen of a siloxane structure. These matters are now under investigation.

VOL. 1 1955

ACKNOWLEDGMENT

The authors wish to express their appreciation to the Office of Naval Research for financial aid in obtaining the materials and components for our equipment.

[36] The radii are given as 0·771Å for carbon and 1·173Å for silicon by T. MOELLER in *Inorganic Chemistry*, p. 135 (John Wiley and Sons, Inc., New York, 1952).

J. Inorganic and Nuclear Chemistry, 1955, Vol. 1, pp. 112–118. Pergamon Press Ltd., London

THE CHEMISTRY OF SILICON INVOLVING PROBABLE USE OF *d*-TYPE ORBITALS

F. G. A. STONE and DIETMAR SEYFERTH
Department of Chemistry, Harvard University, Cambridge, Massachusetts

(*Received October* 1954)

Abstract—Certain aspects of silicon chemistry are discussed in which silicon may well utilize its 3*d*-orbitals. The discussion is treated from the standpoint of silicon compounds in which the ligancy of silicon is greater than four; tetravalent silicon compounds in which bonding is not of the pure sp^3-type; and silicon compounds in which chemical reactivities are unusual in terms of analogous carbon compounds.

ELEMENTS of the first short period can form only four covalent bonds since they have available for *chemical bonding* only four orbitals of the *L* shell. Thus, as is well known, carbon utilizes four sp^3 orbitals directed towards the corners of a tetrahedron in its usual 4-covalent state. The carbon atom is electronically saturated and cannot co-ordinate either as an electron acceptor or donor. Although the second-row element silicon has nine orbitals of the *M* shell available for bonding, tetravalence still plays a major part in the chemistry of silicon. This is because the 3*s*- and 3*p*-orbitals are energetically more stable than the 3*d*, and $3sp^3$ hybridization leads to the same result as $2sp^3$. However, it is now fairly well recognized that silicon and other elements of the second short period utilize some of their five 3*d*-orbitals in some of their compounds and reaction intermediates. The possibility of valency shell expansion is one reason for the often marked differences in chemical behaviour between first- and second-row elements, and it is the object of this article to summarize and discuss this property in the case of silicon.

The co-ordination number of silicon rises above four only when it is bonded to highly electronegative elements like fluorine, chlorine, oxygen, or nitrogen. Consequently the bonds between silicon and these elements have a considerable ionic character. Furthermore, although silicon possesses five 3*d*-orbitals, its covalency, like that of other elements in the second short period, does not seem to rise above six, presumably owing to steric limitations. It should perhaps be mentioned that a few materials in which silicon apparently exerts a co-ordination number greater than six, like $SiCl_4 \cdot 4NEt_3$ (TROST, 1952) have been reported, but they have not been well characterized.

A well-known example of the excitation of the silicon valency shell from $3sp^3$ hybridization to $3sp^3d^2$ hybridization is found in the fluosilicate ion. X-ray diffraction analysis shows that the $SiF_6^{=}$ ion has an octrahedral arrangement of fluorine around silicon (KETELAAR, 1935). There are no carbon analogues of the silicofluorides, nor corresponding complex halides formed by the other silicon tetrahalides.

Oxygen complexes in which silicon forms bonds beyond the electron-octet have been known for a long time. DILTHEY (1903) found that treatment of silicon tetrachloride, in chloroform, with several β-diketones, like acetylacetone, gave solid salts

of composition $[A_3Si]Cl \cdot HCl$ (A = acetylacetone). The latter may be converted into the less soluble salt

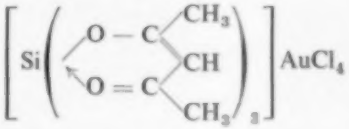

and other salts of complex anions.

It has been claimed (HAMILTON *et al.*, 1953) that silicon tetrachloride is sterically incapable of accepting electron pairs from oxygen bases, but the work of SISLER and co-workers (1948), who have conducted studies on Group IV tetrachloride-ether systems, would seem to indicate some molecular attraction between silicon tetrachloride and certain ethers. This work, however, is not well authenticated.

VOL. 1 1955

The nitrogen atom in tertiary amines is a better electron-donor than the oxygen atom in ethers; it is not too surprising, therefore, that BURG (1954) has been able to demonstrate a trimethylamine complex of silicon tetrachloride, $SiCl_4 \cdot NMe_3$ (dissociation pressure 0·7 mm at −68·8°). The adducts $SiHCl_3 \cdot NMe_3$ (begins to dissociate at −30°) and $SiH_2Cl_2 \cdot NMe_3$ (dissociation pressure 1·36 mm at −9·5°) were also prepared. The compound $SiH_3Cl \cdot NMe_3$ has also been described (EMELÉUS and MILLER, 1939), and its stability is comparable with the dichlorosilane-trimethylamine adduct. The order of stability is thus

$$SiCl_4 \cdot NMe_3 < SiHCl_3 \cdot NMe_3 < SiH_2Cl_2 \cdot NMe_3 = SiH_3Cl \cdot NMe_3.$$

From the standpoint of electronegativity, this is unusual, since substitution of a less electronegative group for a part of a molecule should decrease the acceptor power. However, as BURG (1954) has pointed out, the steric effect of chlorine would tend to counteract the electronegativity effect, and in this series of complexes steric effects are apparently predominant. There is yet another factor which may make the chlorosilanes better acceptors than silicon tetrachloride. The *d*-orbitals of silicon may already be involved in bond formation in silicon tetrachloride itself (see below) thus weakening the acceptor power. In the chlorosilanes with substitution of hydrogen for chlorine π-bonding might well be less marked. Silane, however, forms no trimethylamine derivatives, so some enhancement of the acceptor-power of silicon by replacement of hydrogen by a more electronegative group is apparently necessary for bond formation with amines. In connection with the complex $SiH_3Cl \cdot NMe_3$ it should perhaps be mentioned that this has also been formulated as a salt $[(Me)_3(SiH_3)N]^+Cl^-$ (EMELÉUS and MILLER, 1939), but in view of its instability and our increased knowledge of donor-acceptor bonding it seems more likely to be a pentacovalent silicon compound. Trimethylamine adducts of some fluorosilanes have also been described (SIMONS, 1950; A. B. BURG, unpublished). The solid molecular addition compound $SiF_4 \cdot NMe_3$ has a dissociation pressure of 6·0 mm at 0°, while $SiHF_3 \cdot NMe_3$ has a dissociation pressure of 24 mm at 0°. Both complexes are thus more stable than their chlorine analogues, as would be expected from electronegativity and steric factors. Silicon tetrafluoride should be a better "Lewis" acid than silicon tetrachloride, just as boron trifluoride is usually a better electron acceptor than boron trichloride. It is interesting also to note that $SiF_4 \cdot NMe_3$ is more stable than $SiHF_3 \cdot NMe_3$, yet as described above, $SiCl_4 \cdot NMe_3$ is less stable than $SiHCl_3 \cdot NMe_3$. Thus in

trimethylamine adducts of the fluorosilanes stability decreases with substitution of hydrogen for fluorine, the electronegativity factor apparently overcoming any opposing effects. The adduct $SiF_4 \cdot NMe_3$ has been used both to prepare very pure silicon tetrafluoride, by treatment with a suitable acid, and to remove silicon tetrafluoride from other gases which do not react with the amine. An adduct $SiF_4 \cdot 2NMe_3$ has also been described (WILKINS and GRANT, 1953), and a complex between silicon tetrafluoride and dimethylformamide of composition $SiF_4 \cdot 2HCONMe_2$ has been prepared (PIPER and ROCHOW, 1954). It will be noted that many of the trimethylamine complex compounds described above are rather unusual in exhibiting a co-ordination number of *five*.

The silicon analogue of trimethylamine, $(SiH_3)_3N$, first prepared by STOCK (1921), has been shown to have very weak electron-donor power, since it is unable to bond diborane or trimethylboron at temperatures down to −78° (BURG and KULJIAN, 1950). Furthermore, the adduct $(SiH_3)_3N \cdot BF_3$, formed at −78°, shows appreciable decomposition at −55°, yielding SiH_4, SiH_2F_2, and $SiHF_3$. It has been suggested (BURG and KULJIAN, 1950) that the far weaker electron-donor power of tris-silylamine compared with trimethylamine arises through wandering of the lone-pair on nitrogen into the *d*-orbitals of silicon. Such π-bonding between nitrogen and silicon would result in the molecular geometry of $(SiH_3)_3N$ changing from the expected tetrahedral shape to something approaching planarity. It is, therefore, very interesting that electron diffraction-studies indicate that tris-silylamine is planar (HEDBERG and STOSICK, 1951).* Similar behaviour should be found in the chemistry of $(SiH_3)_2O$ (STOCK and SOMIESKI, 1923), $(SiH_3)_2S$ (AYLETT *et al.*, 1953), and $(SiH_3)_3P$ (AYLETT *et al.*, 1953). Donor-power is in the order $N > O > S$, so disiloxane and disilyl sulphide should have no Lewis-base properties, and the Si—O—Si and Si—S—Si bond angles might approach 180°. Silyl groups attached to a ligand drastically reduce donor-power by providing weak orbitals into which electrons can enter. Further evidence for the electron-withdrawing tendency of silyl groups is found in the ability of trialkylsilanols to form sodium salts with aqueous sodium hydroxide at 0° (SOMMER *et al.*, 1946). Since carbinols do not do this, the hydrogen in the hydroxyl group of the silanol is more protonic, perhaps as a result of removal of electron density on oxygen by silicon, leading to easier rupture of the oxygen-hydrogen bond. However, an explanation in terms of steric factors is possible.

There are a number of other tetracovalent silicon compounds in which bonding appears not to be of pure sp^3-type and in which it is perhaps better to employ 3*d*-orbitals as well, weak though they are. Bond distances between silicon atoms and the chlorine or carbon atoms in the silicon tetrahalides, chlorosilanes, methylchlorosilanes, and methylsilanes are abnormally short. This may be illustrated by considering some very precise electron-diffraction results of BROCKWAY (BOND and BROCKWAY, 1954). The silicon-carbon distances in the methylsilanes were found to be: $MeSiH_3$, 1·857 ± 0·007 Å; Me_2SiH_2, 1·860 ± 0·004 Å; Me_3SiH, 1·873 ± 0·006 Å. In Me_4Si the silicon-carbon bond distance is reported as 1·888 ± 0·02 Å (SHEEHAN and SCHOMAKER, 1952). In disilane the silicon-silicon distance is 2·32 Å (BROCKWAY and BEACH, 1938), which would imply that the normal silicon-carbon distance should be 1·93 Å. In silicon carbide it is 1·90 Å. Perhaps in the methylsilanes the *d*-orbitals of silicon are

* Since our paper was accepted for publication in this journal, S. SUJISHI and S. WITZ, *J. Amer. Chem. Soc.* **76**, 4631 (1954), have also discussed the silicon-nitrogen partial double bond.

partially filled as a consequence of the well-established ability of methyl groups to supply electron-density by use of C–H bonding electrons. The problem of abnormally short bond distances in some silicon compounds was first taken up by PAULING (1940) in discussing the silicon tetrahalides. He ascribed the bond shortening to resonance among structures like

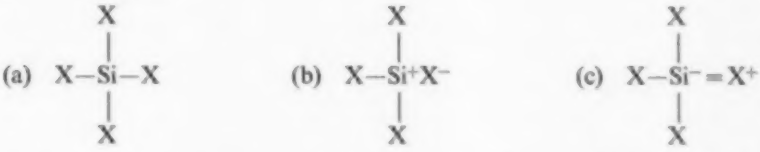

It will be observed that structures of the latter type involve 3*d*-orbitals of silicon. This idea, however, has been disputed. SCHOMAKER and STEVENSON (1941) believe that the bond shortening can be attributed to ionic structures $X_3Si^+X^-$, with the exception of SiF_4. PITZER (1948) also is against the idea of employment of the silicon 3*d*-orbitals, suggesting that closer approach than the covalent-radii sum can occur before repulsions between completed inner shells become large enough to establish bond distance. However, on the basis of microwave studies, DAILEY, MAYS, and TOWNES (1949), and GORDY and his collaborators (GILLIAM *et al.*, 1949), (SHERIDAN and GORDY, 1951), (MOCKLER *et al.*, 1953), (GORDY *et al.*, 1953), continue to support the idea of silicon-halogen double bonding. GORDY *et al.* have found that silicon-halogen bond distances in a large number of halosilanes are less than those predicted by use of the additivity rule, even allowing for corrections for ionic character of the bonds made by using the Schomaker-Stevenson equation (SCHOMAKER and STEVENSON, 1941). Dipole moment studies have led to similar conclusions. Purely electronegativity effects would imply a greater dipole moment for SiH_3Cl than for CH_3Cl, yet for the latter $\mu = 1{\cdot}87$ D and for SiH_3Cl $\mu = 1{\cdot}28$ D (BROCKWAY and COOP, 1938). Contributions from structures of the type $H_3Si^- = Cl^+$ would account for this result. Dipole moment studies on many organohalosilanes have also been used to support the idea of *d*-orbital bonding (CURRAN *et al.*, 1950), (REILLY *et al.*, 1954).

Back co-ordination leading to π-bonding could also explain bond shortening in the tetrahedral SiO_4^{-4} ion, and in the polysiloxanes. The silicon-oxygen distance in the latter has been discussed by CRAIG, MACCOLL, NYHOLM, ORGEL, and SUTTON (1954) in an article devoted to a consideration of bonds involving *d*-orbitals. The silicon-oxygen distance in a polysiloxane molecule is 1·64 Å as compared with an expected 1·76 Å calculated from radii obtained by SCHOMAKER and STEVENSON (1941).

Furthermore, considerable work (YAMASAKI *et al.*, 1950), (FLORY *et al.*, 1952), (FREISER *et al.*, 1953), has been done on the Si—O—Si bond angle in linear siloxanes, and it appears that this angle is larger (*ca.* 130°) than expected in terms of simple oxygen 2*p* or 2*sp*³ bonding. It is interesting that in silicon chemistry the familiar double and triple bonding of carbon compounds is replaced by polymerization as in $(SiH_2)_n$, $(SiCl_2)_n$, $(R_2SiO)_n$, $(SiO_2)_n$, and $(SiS_2)_n$. These effects may also relate to the possible use of 3*d*-electron orbitals of silicon.

The concept that unshared electrons on electronegative elements bonded to silicon can enter vacant silicon orbitals, possibly hybridized, is all the more likely, since the polarity of the silicon-other element single bond is such that silicon has a considerable positive charge.

There are a number of differences between the reactivity of some silicon compounds and their carbon analogues. Some of these differences will now be discussed, since they have either already been attributed or may be attributed to the ability of silicon to acquire electrons beyond the octette.

SIDGWICK (1927) first drew attention to the stability of the carbon tetrahalides compared with the silicon halides, towards hydrolysis and ammonolysis; suggesting that the reactivity of the silicon compounds resulted from co-ordination of the electron-donor molecules, water or ammonia, as a prelude to reaction. Such behaviour is not possible with carbon tetrahalides, since carbon has a completed *L* shell. A co-ordination mechanism also accounts for the ease of hydrolysis of silicon-hydrogen and silicon-silicon bonds. This aspect has been discussed in detail by ROCHOW (1951).

There is evidence that the base-catalyzed rearrangement of siloxanes in the relatively non-ionizing siloxane solvent medium involves an octette expansion of silicon. Thus, HURD, OSTHOFF, and CORRIN (1954) have found that polymerization of the siloxane system occurs more readily with increasing electropositivity of the alkali-metal component of the base. This is in accordance with enhancement of the donor power of the oxygen atom by attachment of a more electropositive group. Thus, whereas LiOH and NaOH were ineffective, efficiency of rearrangement increased in the order $KOH < RbOH < CsOH$. Furthermore, other substances with basic oxygen or nitrogen atoms like $KOCH_3$, K_2O, or KNH_2 also caused polymerization. Kinetic studies (GRUBB, 1954) on silanol condensations can also be interpreted in terms of the "pentacovalent intermediate" theory, but further experimental work is required.

Treatment of silicon tetrachloride and other halosilanes with diazomethane gives halomethylsilanes (YAKUBOVICH and GINSBURG, 1952), (SEYFERTH, 1954). This reaction possibly involves co-ordination of the polarized form of the diazomethane molecule, $:\overset{-}{C}H_2-\overset{+}{N}\equiv N$, to the silicon halide as a primary step, but kinetic evidence is lacking (SEYFERTH, 1954).

It is interesting that addition of hydrogen halides to triorganoallylsilanes, $R_3SiCH_2CH=CH_2$, follows Markownikoff's rule, but similar additions to vinlysilanes, $R_3SiCH=CH_2$, do not (LARSSON, 1953), (SOMMER *et al.*, 1954). Thus on the basis of purely inductive effects one would expect the halogen to enter the α-position to the silicon atom in the vinyl side-chain, but instead a product is obtained in which the halogen is in the β-position. This observed, and rather unexpected, anti-Markownikoff addition has been tentatively attributed (SOMMER *et al.*, 1954) to a non-inductive effect on the part of the trimethylsilyl group, resulting from the limited tendency of this group to partake in a conjugated system. In addition it is pointed out that the apparent non-inductive effect of trimethylsilyl is weak, since an α-methyl substituent at the vinyl group is sufficient to reverse the effect and give a Markownikoff addition. Perhaps when a vinyl group has its π-electron cloud *directly adjacent* to a silicon atom, electrons may enter the available *d*-orbitals of the silicon atom. The net effect would be to reverse the polarity of the carbon atoms of the vinyl group, and thus anti-Markownikoff addition would be observed. The $+I$ inductive effect of a single α-methyl substituent is apparently all that is required to overcome this π-bonding and give the result expected at first sight. Furthermore, in connection with these additions to vinylsilanes it is interesting to note that organo-lithium compounds add to triphenylvinylsilane in an anti-Markownikoff manner

(CASON and BROOKS, 1952). Usually organolithium compounds add to carbon-carbon double bonds only if they are part of a highly conjugated system.

In certain circumstances it seems likely that the electrons associated with a benzene ring can partially fill silicon *d*-orbitals in the π-bond manner. This is especially likely if electron-donating groups are in ortho or para positions with respect to the silicon atom attached to the aromatic system. This $-$T effect is, of course, opposed by the $+$I inductive effect of the trialkylsilyl group, consequently the electron density around silicon would not be increased much beyond neutrality. The concept of π-bonding between silicon and a benzene ring has been used to explain dipole moments of substituted phenyl trimethylsilanes (SOFFER and DE VRIES, 1951), (FREISER *et al.*, 1953), ionization constants of trimethylsilyl substituted phenols, anilines, and dimethylanilines (BENKESER and KRYSIAK, 1953), and the isomer distribution obtained by nitrating trimethylphenyl silane (SPEIER, 1953).

VOL. 1 1955

Finally, it should be remembered that there are two schools of thought as to the correct explanation of some of the observations described above, particularly those observations concerned with bond-angle and bond-length. One school attributes the effects mainly to bond polarities arising out of simple electronegativity differences, and the other invokes π-bonding. The subject is, therefore, still debatable, but it is perhaps important to point out that the π-bonding postulated is *not* of the ethylenic-type, p_π–p_π overlap in a homonuclear bond system, but invokes an ultimate *d*-orbital on one atom with a p_π-orbital of an atom of a different element. CRAIG *et al.* (1954) have discussed this question in detail, with results that lead them to conclude that d_π–p_π bonding is likely to be common, can give strong bonds, and that polar character in the σ-bond would confer extra stability by improving the d_π–p_π overlap.

ACKNOWLEDGMENT

The authors express their thanks to Professor E. G. ROCHOW for helpful discussions.

REFERENCES

AYLETT, B. J., EMELÉUS, H. J., and MADDOCK, A. G. (1953) *Research* (London) **6**, 30 S–1S.
BENKESER, R. A., and KRYSIAK, H. R. (1953) *J. Amer. Chem. Soc.*, **75**, 2421.
BOND, A. C., and BROCKWAY, L. O. (1954) *J. Amer. Chem. Soc.*, **76**, 3312.
BROCKWAY, L. O., and BEACH, J. Y. (1938) *J. Amer. Chem. Soc.*, **60**, 1836.
BROCKWAY, L. O., and COOP, I. E. (1938) *Trans. Faraday Soc.*, **34**, 1429.
BURG, A. B. (1954) *J. Amer. Chem. Soc.*, **76**, 2674.
BURG, A. B., and KULJIAN, E. S. (1950) *J. Amer. Chem. Soc.*, **72**, 3103.
CASON, L. F., and BROOKS, H. G. (1952) *J. Amer. Chem. Soc.*, **74**, 4582.
CRAIG, D. P., MACCOLL, A., NYHOLM, R. S., ORGEL, L. E., and SUTTON, L. E. (1954) *J. Chem. Soc.*, 332.
CURRAN, C., WITUCKI, R. M., and MCCUSKER, P. A. (1950) *J. Amer. Chem. Soc.*, **72**, 4471.
DAILEY, B. P., MAYS, J. M., and TOWNES, C. H. (1949) *Phys. Rev.*, **76**, 136.
DILTHEY, W. (1903) *Ber.* **36**, 932, 1595.
EMELÉUS, H. J., and MILLER, N. (1939) *J. Chem. Soc.*, 819.
FLORY, P. J., MANDELKERN, L., KINSINGER, J. B., and SCHULTZ, W. B. (1952) *J. Amer. Chem. Soc.*, **74**, 3364.
FREISER, H., EAGLE, M. V., and SPEIER, J. L. (1953) *J. Amer. Chem. Soc.*, **75**, 2824.
GILLIAM, O. R., EDWARDS, H. D., and GORDY, W. (1949) *Phys. Rev.*, **75**, 1014.
GORDY, W., SMITH, W. V., and TRAMBARULO, R. F. (1953) *Microwave Spectroscopy* (John Wiley & Sons, New York), Chapter 8.
GRUBB, W. T. (1954) *J. Amer. Chem. Soc.*, **76**, 3408.
HAMILTON, P. M., MCBETH, R., BEKEBREDE, W., SISLER, H. H. (1953) *J. Amer. Chem. Soc.*, **75**, 2881.

HEDBERG, K., and STOSICK, A. J. (1951) Abstracts of the XII International Congress of Pure and Applied Chemistry, New York, Sept. 10–13, p. 543.
HURD, D. T., OSTHOFF, R. C., and CORRIN, M. L. (1954) *J. Amer. Chem. Soc.*, **76,** 249.
KETELAAR, J. A. A. (1935) *Z. Krist.*, **92,** 155.
LARSSON, E. (1951) *Trans. Chalmers Univ. Technol.* No. 115, 25; (1953) C.A. **47,** 10470.
MOCKLER, R. C., BAILEY, J. H., and GORDY, W. (1953) *J. Chem. Phys.*, **21,** 1710.
PAULING, L. (1940) *Nature of the Chemical Bond* (Cornell Univ. Press, Ithaca, N.Y.), p. 228.
PIPER, T. S., and ROCHOW, E. G. (1954) *J. Am. Chem. Soc.* **76,** 4318.
PITZER, K. S. (1948) *J. Amer. Chem. Soc.*, **70,** 2140.
REILLY, E. L., CURRAN, C., and MCCUSKER, P. A. (1954) *J. Amer. Chem. Soc.*, **76,** 3311.
ROCHOW, E. G. (1951) *An Introduction to the Chemistry of the Silicones*, 2nd Ed. (John Wiley & Sons, New York), Chapter 2, p. 22–23.
SCHOMAKER, V., and STEVENSON, D. P. (1941) *J. Amer. Chem. Soc.*, **63,** 37.
SEYFERTH, D. (1954) Ph.D. Thesis, Harvard University.
SHEEHAN, W. F., and SCHOMAKER, V. (1952) *J. Amer. Chem. Soc.*, **74,** 3956.
SHERIDAN, J., and GORDY, W. (1951) *J. Chem. Phys.*, **19,** 965.
SIDGWICK, N. V. (1927) *The Electronic Theory of Valency* (Oxford University Press, London), p. 153.
SIMONS, J. H. (Editor), (1950) *Fluorine Chemistry* (Academic Press, Inc., New York) Vol. 1, pp. 77–123.
SISLER, H. H., WILSON, W. J., GIBBINS, B. J., BATEY, H. H., PFAHLER, B., and MATTAIR, R. (1948) *J. Amer. Chem. Soc.*, **70,** 3818, 3821, 3825, 3826.
SOFFER, H., and VRIES, T. DE (1951) *J. Amer. Chem. Soc.*, **73,** 5817.
SOMMER, L. H., BAILEY, D. L., GOLDBERG, G. M., BUCK, C. E., BYE, T. S., EVANS, J. F., and WHITMORE, F. C. (1954) *J. Amer. Chem. Soc.*, **76,** 1613.
SOMMER, L. H., PIETRUSZA, E. W., and WHITMORE, F. C. (1946) *J. Amer. Chem. Soc.*, **68,** 2282.
SPEIER, J. L. (1953) *J. Amer. Chem. Soc.*, **75,** 2930.
STOCK, A., and SOMIESKI, C. (1921) *Ber.*, **54B,** 740.
STOCK, A., and SOMIESKI (1923) *Ber.*, **56B,** 247.
TROST, W. R. (1952) *Canad. J. Chem.*, **30,** 835.
WILKINS, C. J., and GRANT, D. K. (1953) *J. Chem. Soc.*, **927**.
YAKUBOVICH, A. YA., GINSBURG, V. A. (1952) *J. Gen. Chem.* (U.S.S.R.), **22,** 1783.
YAMASAKI, K., KOTERA, A., YOKOI, M., and UEDA, Y. (1950) *J. Chem. Phys.*, **18,** 1414.

J. Inorganic and Nuclear Chemistry, 1955, Vol. 1, pp. 119–125. Pergamon Press Ltd., London

VOL.
1
1955

THE HAMMETT ACIDITY FUNCTION $\mathbf{H}_0$ IN H_2SO_4—SO_3 MIXTURES; SUPERACIDITY

By CHARLES D. CORYELL and RICHARD C. FIX

Department of Chemistry and Laboratory for Nuclear Science,[1]
Massachusetts Institute of Technology, Cambridge, Massachusetts, U.S.A.

(*Received November* 1954)

Abstract—The comparative quantitative acidities of mineral acids $H^+(ClO_4^-)$ and $H^+(HSO_4^-)$, the two superacids, then HI, HBr, HCl, HNO_3, Cl_3CCOOH, and HF are reviewed in the light of the Hammett and Michaelis acidity functions $\mathbf{H}_0$ and **G**. The great power of the Hammett quantitative acidity function $\mathbf{H}_0$ is emphasized, with evidence being provided for the independence of charge in Hammett general acidity function $\mathbf{H}_x$ with charge type of the indicator in concentrated water-type solutions. The Lewis-Bigeleisen extension of the Hammett function $\mathbf{H}_0$ to H_2SO_4—SO_3 mixtures, using vapour pressure of SO_3 as a measure of $\mathbf{H}_0$, is reviewed, and an error separating $\mathbf{H}_0$ from $-\log a_{H^+}$ is removed. The Lewis-Bigeleisen data provide by this interpretation new information on the polyacids $H_2O(SO_3)_n$, and the superacid anhydrous SO_3. The effective proton activity of anhydrous SO_3 is given as $10^{10.1}$ referred to that in $1M$ H_3O^+ as unity.

SOME twenty years ago HAMMETT [H1–4] introduced a family of experimentally established functions describing acidity in terms of proton activity. These are useful for concentrated aqueous solutions of strong (mineral) acids. The function, called $\mathbf{H}_0$, for a unipositive indicator acid HB^+ with an uncharged conjugate base B, is congruent with pH in very dilute aqueous solutions, but differs from it by an activity term (which becomes appreciable) as the molarity M of the strong acid exceeds unity. The function is defined as:

$$\mathbf{H}_0 = -\log_{10} a_{H^+} - \log_{10}(f_B/f_{BH^+}) \qquad (1)$$

where a_{H^+} is the activity of acid (normally considered as the hydronium ion H_3O^+) and f_{BH^+} and f_B are the activity coefficients of the reference acids and bases. HAMMETT [H3] has shown that the activity term becomes essentially independent of the solute concentration in strong acid media.[2]

The function $\mathbf{H}_0$ is conveniently established from indicator studies, but may also be determined from rate studies [H2, D1, K1], and is determinable for a given mineral acid with an error of less than 0·2 in logarithmic units, with suitable objective selection among indicators. The function is known [H2] for H_2SO_4 up to $18M$, for $HClO_4$ up to $7M$, for HCl up to $6M$, for HNO_3 up to $8M$, and for CCl_3COOH up to $5M$.[3] There is little information available about the other

[1] This work was supported in part by the U.S. Atomic Energy Commission.

[2] Other families, e.g., $\mathbf{H}_{+2}$, $\mathbf{H}_{+}$, $\mathbf{H}_{-}$, $\mathbf{H}_{-2}$, are possible for references based on the bases B^{++}, HB^+, BOH^-, $BO^{=}$. An experimentally defined Michaelis acidity function **G** for the indicators based on the acid dependence of semiquinone formation of the various acid-base forms of thionine, H_2Thi^{+++}, has been established by MICHAELIS and GRANICK [M1]. A plot of **G** versus the (volume) molarity of H_2SO_4 M gives a curve which is parallel to the plot of HAMMETT's $\mathbf{H}_0$ vs. M. The parallelism demonstrates the lack of dependence of the activity term on molarity of H_2SO_4, already anticipated by HAMMETT [H3].

[3] There is no reason why the **H**-type functions cannot be evaluated for mixed mineral acids, such as HNO_3—H_2SO_4, and indeed some of the perspicacious work of INGOLD's school [I1] implies this for nitrating mixtures.

functions[4] except in alcohol-water media of low dielectric constant studied by GRUNWALD [G4, G6], SWAIN [S5], and others, where the activity function causes trouble. SCHWARZENBACH [S2] has discussed indicators on the extended $\mathbf{H}_0$ (pH) scale.

It can be shown that the $\mathbf{H}_0$ function for H_2SO_4 follows the empirical rule:

$$-\mathbf{H}_0 \simeq 0{\cdot}5M - 0{\cdot}3 \qquad (2)$$

over the range $1 \leq M \leq 17{\cdot}8$ (10–95 per cent H_2SO_4), with an average deviation of 0·08. The values for 90, 95, and 100 per cent H_2SO_4 (by weight) are −8·17, −8·74, and −10·60[5] [H2]. These numbers show that in pure H_2SO_4 the proton activity exceeds that in $1M$ H_2SO_4 by the factor $10^{10{\cdot}6}$. Similar results have been obtained with $HClO_4$. Concentrated solutions of H_2SO_4 and $HClO_4$ are thus identified as spectacular superacids of roughly identical acidity behaviour [H2] at the same molarity. The hydrohalogen acids other than HF are medium superacids, decreasing in the order HI, HBr, and HCl; and HNO_3 is a weak-strong acid,[6] not much stronger than Cl_3CCOOH. BELL [B1] gives pK values (negative logarithm of ionization constant K) for the hydrohalides as HF 4, HCl −7, HBr −9, HI −11. SCHWARZENBACH [S1] has estimated the pK values H_2F^+ −9·0, HF +5·0, H_2Cl^+ −10, HCl −3, $H_3SO_4^+$ −8·3, H_2SO_4 −3·1, $H_2ClO_4^+$ −14, $HClO_4$ −8·6. These values are based on computations, for water as solvent, for isoelectronic species together with semi-theoretical estimate of the dependence of effective dielectric constant of water on structure.

HAMMETT [H1, H2] showed the general utility of the indicator method, by which $\mathbf{H}_0$ is measured within ± 2 **H** units (log units) from that of the acidity constant pK_{BH^+} of an indicator by:

$$\mathbf{H}_0 = \log\{(B)/(BH^+)\} + pK_{BH^+} \qquad (3)$$

where the concentrations of the neutral and protonated forms of the indicator B are indicated by parentheses. He lists pK_{BH^+} for numerous indicators, the strongest acid being the 2,4,6-trinitroanilinium ion of pK value −9·29.

In one of the latter research programmes of an extraordinarily creative career, G. N. LEWIS with J. BIGELEISEN [L1] found an indicator 2,2′-dinitro-4,4′-dibromofluorescein that resisted oxidation or sulfonation in fuming sulfuric-acid solutions up to 0·534 mole-fraction SO_3 in the H_2O—SO_3 system, at which acidity it is 80 per cent in the proton saturated form.[7] Thus the Lewis-Bigeleisen indicator is probably H_4B^{+4} (or H_6B^{+6} if the nitro groups have added protons):

[4] An isolated study of CORYELL and SHEPHERD [C2, S4] on $\mathbf{H}_-$ in H_2SO_4—H_2O up to $6M$, using picric acid as an indicator, shows that $\mathbf{H}_-$ and $\mathbf{H}_0$ become parallel above about $4M$, separated by about 0·8 log units.

[5] There is some ambiguity about the reference value −10·60 for 100 per cent H_2SO_4. BRAND [B3] proposes −10·89 or perhaps −11·05.

[6] The classical (thermodynamic) ionization constant of HNO_3 was measured by REDLICH and BIGELEISEN [R1] as 21 ± 4 by Raman spectrometry; more recent measurements by GOLDRING [G2, G5], using precision absorption spectrometry [G3], gives the value 7 ± 1 for the ionization constant at zero ionic strength, with a ΔH^0 of ionization of 1·1 ± 1·1 Kcal/mole. YOUNG [Y1, G5] has developed Raman spectrometry further for studies of the thermodynamic and concentration ionization constants of HNO_3, H_2SO_4, and HSO_4^-. DOSTROVSKY and co-workers [A1, D3] have developed an O^{18} isotope tracer method for the semiquantitative estimation of the acidity of acids HOX, which supports the evaluation.

[7] It is likely that the neutral molecule $R(NO_2)_2(COOH)(OH)(=O)(—O—)$ has in the proton-saturated form added protons to the carboxyl group ($-pK_{BH^+} \sim 8$), splitting out water, to the phenolic group (estimated $-pK_{BH^+} \sim 7$), to the oxo group =O of the 2,10-anthraquinoid (pyronine) dyestuff (estimated $-pK_{BH^+} \sim 8$), and to the oxo bridge —O— of the middle ring of the anthraquinoid structure $-pK_{BH^+} = \sim 10{\cdot}3$ (as established from the Lewis-Bigeleisen data). It is possible that the nitro-groups also add protons in the region of acidity under study, without, however, seriously perturbing the general interpretation, or affecting the absorption spectrum. The basicity of nitro groups is discussed by BRAND [B3].

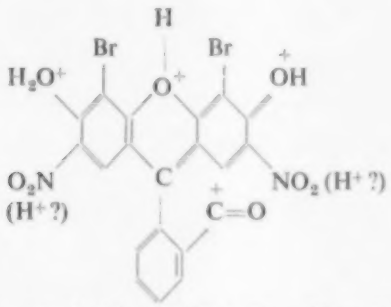

(4)

and the Hammett function studied is probably $\mathbf{H}_{+3}$. However, as indicated in footnotes 2 and 4, all of Hammett functions $\mathbf{H}_z$ are parallel functions of composition, and, as LEWIS and BIGELEISEN imply, $\mathbf{H}_{+3}$ can be tied to the rigorously defined $\mathbf{H}_0$ for extrapolation to H_2SO_4—SO_3 mixtures.

The important contribution of their paper [L1] is to permit a carry-over of acidity function to use the logarithm of the vapour pressure of SO_3 as a measure of generalized acidity (Hammett style) up to pure SO_3 (vapour pressure 0·33 atm at 25°C). Indeed, by fitting the dinitrodibromofluorescein data for three superacid mixtures to the end of HAMMETT's data (based on trinitroaniline), LEWIS and BIGELEISEN [L1] calibrated the $\mathbf{H}_0$ of pure SO_3 as −14·1 with a probable uncertainty of less than 0·3 **H** units. The Lewis-Bigeleisen calibration (their Fig. 5) is presented here[8] as Fig. 1. The solid circles give approximately log a_{SO_3}, plus 14·56 (standard state, SO_3 gas, 1 atm) as calculated by them.

There is an accessory piece of interpretation in Fig. 5 of the Lewis-Bigeleisen paper that is probably illusory, namely the proposal that log a_{H^+} goes through a maximum just before 50 mole-% SO_3 (100 per cent H_2SO_4). This illusion is apparently related to an ambiguity in LEWIS and RANDALL's famous textbook [L2], which says that the escaping tendency (fugacity) of a component of a solution might fail to increase with mole fraction in a solution of highly viscous or glassy character.

It is the purpose of the present paper to display the power of the Hammett treatment of inorganic acids, as fortified by the brilliant Lewis-Bigeleisen extension, and to show that it is proper to retain equation (1) of this paper even for pure SO_3, as one limit of an acid system based on production of free protons. LUDER and ZUFFANTI [L3] report on the work of HANTZSCH, LEWIS, USANOVICH, and others treating acidity in systems like BF_3, Al_2Cl_6, and $SnCl_4$, where the proton activity cannot be defined, but acidity can still be interpreted quantitatively.

Let us now return to the system H_2O—SO_3, or better H_2SO_4—SO_3. It is known that the following acids exist in concentrated H_2SO_4 and fuming sulfuric acid (H_2SO_4—SO_3 mixtures): H_2SO_4, pyrosulfuric acid $H_2S_2O_7$, and trisulfuric acid $H_2S_3O_{10}$. Indeed GOODARD, HUGHES, and INGOLD [G1] prepared nitronium salts of these (NO_2^+) ($HS_2O_7^-$), (NO_2^+)$_2$($S_2O_7^=$), and (NO_2^+)$_2$($S_3O_{10}^=$). It is probable [G1] that there exist higher polymeric sulfuric acids $H_2S_4O_{13}$, etc., typified by $H_2S_nO_{3n+1}$. The existence of polymerization reactions and of metastable liquid phases in pure SO_3 suggests that n may become a very large number in SO_3 nearly free of H_2SO_4. Let us call the typical acid in such a medium $H_2O(SO_3)_n$.

[8] This figure is presented here by courtesy of the *Journal of the American Chemical Society* and of Dr. BIGELEISEN.

The principal ionization reactions in such superacid systems should be:[9]

$$H_2SO_4 + H_2O = H_3O^+ + HSO_4^- \quad (5)$$

$$2H_2SO_4 = H_3SO_4^+ + HSO_4^- \quad (6)$$

$$H_2S_2O_7 + H_2SO_4 = H_3SO_4^+ + HS_2O_7^- \quad (7)$$

$$H_2S_3O_{10} + H_2S_2O_7 = H_3S_2O_7^+ + HS_3O_{10}^- \quad (8)$$

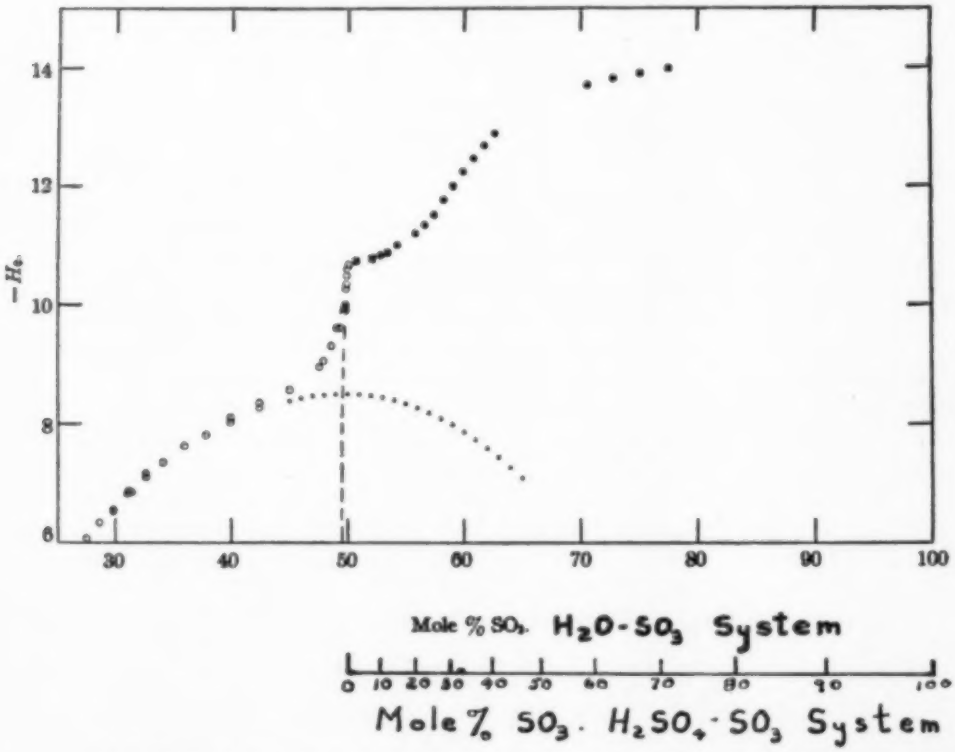

FIG. 1.—[Taken from LEWIS, G. N., and BIGELEISEN, J., *J. Amer. Chem. Soc.*, **65**, 1149 (1943).]—The acidity function, $-H_0$, measured by Hammett and Deyrup plotted against mole-% SO_3 in the H_2O—SO_3 system, open circles. The Lewis-Bigeleisen experimental extension, squares, and their extension based on the vapour pressure of SO_3, solid circles, plotted against mole-% SO_3 in the H_2O—SO_3 system, and against mole-% SO_3 in the H_2SO_4—SO_3 system. The dotted curve is the questionable Lewis-Bigeleisen interpretation of log a_{H^+}.

The Lewis-Bigeleisen Fig. 5, shown herewith as Fig. 1 with their questionable log a_{H^+} branch shown as a dotted curve of downward trend, indicates that removal of the base H_2O as the mole-fraction SO_3 increases, leads to a sharp rise in $-H_0$ just before 50 per cent SO_3 (as first shown by HAMMETT) because of the obvious reaction:

$$SO_3 + H_2O = H_2SO_4 \quad (9)$$

The build-up of polyacids in the region just beyond 50 mole-% SO_3 in the H_2O—SO_3 system leads to a further increase in acidity to a $-H_0$ value of 14 at about 75 per cent

[9] The relative strengths of these acids have been evaluated by GILLESPIE [G1]. Including the molarity of H_2SO_4 (18·7, or 10·2 moles per kg), the concentration equilibrium constants are $1{\cdot}5 \times 10^{-6}$ for equation (6) and $2{\cdot}8 \times 10^{-8}$ for equation (7). The higher acids are still stronger [G1].

SO_3. After this, n becomes fairly large, and successive polyacids are of about the same strength.[10]

The production of acidity by the polyacid $H_2O(SO_3)_n$, taken as a pure individual, would follow the equation:

$$2H_2O(SO_3)_n = H_3O(SO_3)_n^+ + HO(SO_3)_n^- \tag{10}$$

Since the co-existent acids of neighbouring different values of n are of closely similar strength when n is a fair-sized number, this equation is adequate, although a sharper treatment would show

$$H_2O(SO_3)_{n+1} + H_2O(SO_3)_n = H_3O(SO_3)_n^+ + HO(SO_3)_{n+1}^- \tag{11}$$

It is convenient to express the proton-producing reaction in H_2SO_4—SO_3 mixtures as

$$H_3O(SO_3)_n^+ = H^+ + H_2O(SO_3)_n \tag{12}$$

formally parallel to the generalized acid equation

$$HB^+ = H^+ + B \tag{13}$$

The anion for HB^+ is accordingly $HO(SO_3)_{n+1}^-$ or to adequate sharpness $HO(SO_3)_n^-$. It is probable that the neighbouring polymers of the family $H_2O(SO_3)_n$ are in fluid equilibrium, since indicator measurements and vapour-pressure measurements are not reported to show time lags until anhydrous SO_3 is reached [B4].

It is obvious that the protons of equations (12) and (13) are suitably solvated. The tremendous range of $-\mathbf{H}_0$ values shows that the free energy of solvation[11] of a proton by H_2O is about 14·5 Kcal per mole lower than the solvation in pure H_2SO_4 to form $H_3SO_4^+$ (i.e., 1·365 × 10·6). Taking the extrapolated Lewis-Bigeleisen $-\mathbf{H}_0$ of 14·1, it is apparent that $H_2O(SO_3)_n$ provides a free energy of solvation[11] of a proton by this acid which (for very large n) is about 4·8 Kcal (i.e., 1·365 × 3·5) higher than by H_2SO_4.

The limiting $-\mathbf{H}_0$ value of 14·1 found by LEWIS and BIGELEISEN is the limit of proton activity produced by equation (12), as n goes to infinity. Here, in pure SO_3, $-\log a_{H^+}$ has a finite value, the highest attainable in the H_2O—SO_3 system, rather than a low value following the maximum at 100 per cent H_2SO_4 indicated in Fig. 1 by the dotted paraboloid curve.

We consider the quantitative measurements of LEWIS and BIGELEISEN [L1] to be such an important extension of the armament of HAMMETT [H1, H2], that we present in Table 1 interpolated numerical values of $\mathbf{H}_0$ at various rounded mole percentage of SO_3 in the systems H_2O—SO_3 and H_2SO_4—SO_3. LEWIS and BIGELEISEN took the vapour pressures of H_2SO_4—SO_3 mixtures from the International Critical Tables [I2] and of pure SO_3 from an extrapolation of the data of BERTHOUD [B2].[12]

[10] This argument, as pointed out by Professor T. F. YOUNG, ignores cyclic polymers of SO_3, especially $(SO_3)_3$. The authors feel that this, if important, would act effectively as an inert diluent.

[11] It should be pointed out that as the component H_2O goes to the vanishing point, $-\mathbf{H}_0$ shows no sign of discontinuity. Thus it is apparent that solvation of H^+ in pure SO_3 is accompanied by virtually the same free-energy decrease as the solvation of H^+ by $H_2O(SO_3)_n$.

[12] A more recent set of vapour pressures of SO_3 at various compositions and temperatures is given by BRAND and RUTHERFORD [B4].

TABLE 1.—INTERPOLATED H_0 VALUES

H_2SO_4—SO_3 % SO_3	H_2O—SO_3 % SO_3	H_0	H_2SO_4—SO_3 % SO_3	H_2O—SO_3 % SO_3	H_0
0	50	−10·60[a]	75	80	−14·0
18	55	−11·1	82	85	−14·0$_3$
33	60	−12·3	89	90	−14·0$_5$
46	65	−13·3	95	95	−14·0$_6$
57	70	−13·7	100	100	−14·1
67	75	−13·9			

[a] Reference value of HAMMETT [H1, H2]; compare footnote (5) in the text.

It is interesting to reverse the treatment to predict that the vapour pressure of pure SO_3 above $1M$ H_2SO_4 is $10^{-14·7}$, since the H_0 of $1M$ H_2SO_4 is 0·09.

It is interesting to note that DENO [D2] has estimated the H_0 of 90% N_2H_4 −10% H_2O as +19, and SCHWARZENBACH [S3] has estimated the H_0 of saturated NaOH solution as +19. CONANT and WHELAND [C1] have measured basicities in ether solution that would correspond to H_0 values in the neighbourhood of +31, while BELL [B1] and SCHWARZENBACH estimated the pK_a of CH_4 as +50. The studies in organic solvents are plagued by problems of low dielectric constant. It might be more profitable for inorganic chemists to work with a witch's broth of a eutectic of $(Li,Na,K,Rb,Cs)_2O$.

The senior author expresses his indebtedness over a period of many years to a large number of colleagues, including particularly Professors LOUIS P. HAMMETT, LEONOR MICHAELIS, LINUS PAULING, GEORGE SCATCHARD, GEROLD SCHWARZENBACH, C. GARDNER SWAIN, and T. FRASER YOUNG, and including former students W. BURTON LEWIS, HAROLD F. PLANK, LIONEL S. GOLDRING, and DAVID J. SHEPHERD.

REFERENCES

[A1] AMBAR, M., DOSTROVSKY, I., SAMUEL, D., and YOFFE, A. D., *J. Chem. Soc.*, **1954**, 3603–11.
[B1] BELL, R. P., *Acids and Bases. Their Quantitative Behaviour*, John Wiley and Sons, Inc., New York, 1952, Table 6.
[B2] BERTHOUD, A., *Helv. Chim. Acta*, **5**, 513 (1922).
[B3] BRAND, J. C. D., *J. Chem. Soc.*, **1950**, 997.
[B4] BRAND, J. C. D., and RUTHERFORD, A., *J. Chem. Soc.*, **1952**, 3916.
[C1] CONANT, J. B., and WHELAND, G. W., *J. Amer. Chem. Soc.*, **54**, 1217 (1932).
[C2] CORYELL, C. D., and SHEPHERD, D. J., unpublished work, University of California at Los Angeles (1941–2).
[D1] DEANE, C. W., *J. Amer. Chem. Soc.*, **67**, 329 (1945).
[D2] DENO, N. C., *J. Amer. Chem. Soc.*, **74**, 2039 (1952).
[D3] DOSTROVSKY, I., Weizmann Institute of Science, Rehovoth, Israel, personal communication, 1954.
[G1] GILLESPIE, R. J., *J. Chem. Soc.*, **1950**, 2492 and 2516; GODDARD, G. R., HUGHES, E. D., and INGOLD, E. K., *J. Chem. Soc.*, **1950**, 2559.
[G2] GOLDRING, L. S., Ph.D. Thesis, Department of Chemistry, Massachusetts Institute of Technology, 1950; see also GOLDRING, L. S., and CORYELL, C. D., Massachusetts Institute of Technology, Laboratory for Nuclear Science and Engineering Progress Report, July 1, 1950.
[G3] GOLDRING, L. S., HAWES, R. C., HARE, G. H., BECKMAN, A. O., and STICKNEY, M. E., *Anal. Chem.*, **25**, 869 (1953).
[G4] GRUNWALD, E., and BERKOWITZ, B. J., *J. Amer. Chem. Soc.*, **73**, 4939 (1951).
[G5] GURNEY, R. W., *Ionic Processes in Solution*, McGraw-Hill Book Co., Inc., New York, 1953, p. 139.

[G6] GUTBEZAHL, B., and GRUNWALD, E., *J. Amer. Chem. Soc.*, **75,** 565 (1953).
[H1] HAMMETT, L. P., *Chem. Revs.*, **16,** 67 (1935).
[H2] HAMMETT, L. P., *Physical Organic Chemistry*, McGraw-Hill Book Co., Inc., New York, 1940, Chapter IX.
[H3] HAMMETT, L. P., and DEYRUP, A. J., *J. Amer. Chem. Soc.*, **54,** 2721 (1932).
[H4] HAMMETT, L. P., and PAUL, A. M., *J. Amer. Chem. Soc.*, **56,** 827 (1934).
[I1] INGOLD, C. K., MILLEN, D. J., and POOLE. H, G., *J. Chem. Soc.*, **1950,** 2576; see also the 22-paper sequence *J. Chem. Soc.*, **1950,** 2400–2684.
[I2] *International Critical Tables*, McGraw-Hill Book Co., Inc., New York, 1928, p. 213.
[K1] KRIEBLE, V. K., and HOLST, K. A., *J. Amer. Chem. Soc.*, **60,** 2976 (1938).
[L1] LEWIS, G. N., and BIGELEISEN, J., *J. Amer. Chem. Soc.*, **65,** 1144 (1943).
[L2] LEWIS, G. N., and RANDALL, M., *Thermodynamics and the Free Energy of Chemical Substances*, McGraw-Hill Book Co., Inc., New York, 1923, p. 207.
[L3] LUDER, W. F., and ZUFFANTI, S., *The Electronic Theory of Acids and Bases*, John Wiley and Sons, Inc., New York, 1946.
[M1] MICHAELIS, L., and GRANICK, S., *J. Amer. Chem. Soc.*, **64,** 1861 (1942).
[R1] REDLICH, O., and BIGELEISEN, J., *J. Amer. Chem. Soc.*, **65,** 1883 (1943).
[S1] SCHWARZENBACH, G., *Z. phys. Chem.*, **176,** 133–53 (1936).
[S2] SCHWARZENBACH, G., *Z. Electrochem.*, **47,** 40–52 (1941).
[S3] SCHWARZENBACH, G., and SULZBERGER, R., *Helv. Chim. Acta*, **27,** 361 (1944).
[S4] SHEPHERD, D. J., M.A. Thesis in Chemistry, University of California at Los Angeles, 1942.
[S5] SWAIN, C. G., Massachusetts Institute of Technology, private communication, 1952.
[Y1] YOUNG, T. F., *Rec. Chem. Prog.*, **12,** 81 (1951).

VOL.
1
1955

J. Inorganic and Nuclear Chemistry, 1955, Vol. 1, pp. 126–142. Pergamon Press Ltd., London

ÜBER ELEKTROMETRISCHE TITRATIONEN IN WASSERFREIER ESSIGSÄURE

Von G. JANDER und H. KLAUS
Aus dem Anorganisch-chemischen Institut der Technischen Universität Berlin—Charlottenburg

Abstract—A special type of electrode ("gebremste Elektrode") has been used to follow neutralization-type reactions in anhydrous acetic acid. As compared with conventional methods, this has the advantage of avoiding an aqueous reference electrode. The apparatus developed on this basis has been tested from various aspects, and there appear to be no restrictions on its application to glacial acetic acid solutions. The best electrode material is gold wire or foil; this can be used over the whole range of hydrogen and acetate ion concentration, and yields reproducible potential measurements. An attempt to replace perchloric acid as standard by some other acid-analogue led to no satisfactory result. As a result of these investigations, objections are raised against the conception that perchloric and sulphuric acid solutions in glacial acetic acid have a superacid character.

1. POTENTIOMETRISCHE TITRATIONSMETHODEN IN WASSERFREIER ESSIGSÄURE

DIE ersten Arbeiten über die potentiometrische Verfolgung neutralisationsanaloger Reaktionen in Eisessig wurden von HALL und CONANT[1, 2] durchgeführt. Ihre Meßanordnung bestand aus einer Chloranil-Elektrode, die sie gegen eine Kalomel-Elektrode schalteten.

	$C_6Cl_4O_2$ (ges.)	Brücke:	KCl, Hg_2Cl_2 (ges.)	
Pt	$C_6Cl_4(OH)_2$ (ges.)	LiCl in	KCl (ges.)	Hg
	HX in CH_3COOH	CH_3COOH	in H_2O	

Die Tatsache, daß die in dieser aus wasserfreiem und wässrigem System bestehenden Anordnung auftretenden Diffusionspotentiale geschätzt werden mußten, läßt keine einwandfreie quantitative Auswertung der gemessenen Potentiale zu. Die Bedeutung dieser Arbeiten liegt in der erstmaligen Titration einer großen Anzahl organischer Basen, womit durch die Bestimmung ihrer relativen Stärke eine breite Grundlage für alle weiteren Untersuchungen geschaffen wurde.

Die von HALL und CONANT entwickelte Chloranil-Elektrode wurde in der Folgezeit von mehreren Forschern mit geringen Abwandlungen übernommen. BLUMRICH und BANDEL[3] erweiterten die Zahl der in Eisessig titrierbaren Basenanalogen erheblich. Darüber hinaus führten sie die ersten Messungen unter Verwendung einer Glas-Elektrode durch, ohne allerdings nähere Angaben über die Versuchsanordnung zu machen.

Zur potentiometrischen Schnellbestimmung von stickstoffhaltigen Basen verwendete WITTMANN[4] eine Glas-Elektrode, die er gegen eine Kalomel-Elektrode

[1] N. F. HALL und J. B. CONANT, *J. Amer. Chem. Soc.* **49**, 3047 (1927).
[2] J. B. CONANT und N. F. HALL, *J. Amer. Chem. Soc.* **49**, 3062 (1927).
[3] K. BLUMRICH und G. BANDEL, *Angew. Chem.* **54**, 374 (1941).
[4] G. WITTMANN, *Angew. Chem.* **60**, 330 (1948).

schaltete. Als Potentiometer benutzte er ein "Pehavi." Mit dieser Methode sind Titrationen bis zu einer Konzentration von N/10 gut durchführbar. Bei größeren Verdünnungen werden die Potentialsprünge sehr flach da der innere Widerstand der Meßkette zu groß wird.

Eine gleiche Elektroden-Anordnung wurde von SEAMAN und ALLEN[5] bei der Erprobung von Kaliumbiphthalat als Urtitersubstanz in Eisessig-Lösungen benutzt.

Der Nachteil des wässrigen Vergleichssystems wurde von FRITZ[6] umgangen, indem er die Glas-Elektrode gegen einen Silberdraht schaltete der mit einer Silberchloridschicht überzogen war. Irgendwelche Absolutmessungen konnte er mit dieser Methode natürlich nicht durchführen.

Eine Anzahl von Forschern hat sich mit dem Problem einer Wasserstoff-Elektrode in wasserfreier Essigsäure befaßt. Die Hauptschwierigkeit dabei lag in der Bestimmung der für eine definierte Wasserstoff-Elektrode unentbehrlichen Wasserstoff-Ionen-Aktivität. Amerikanische Forscher wie DAVIDSON und CHAPPELL[7] oder HUTCHINSON und CHANDLEE,[8] außerdem aber auch LA MER und EICHELBERGER[9] sowie WEBB[10] gingen auf Grund der von Conant und Hall gefundenen Ergebnisse von deren Auffassung aus, daß Perchlorsäure und Schwefelsäure in Eisessig starke Elektrolyte seien. Daher berechneten sie die Ionen-Aktivitäten nach der Debye-Hückelschen Theorie. Bei ihren Messungen verwendeten sie die Kalomel-Elektrode, außer HUTCHINSON und CHANDLEE, die eine Zelle ohne wässrige Lösung entwickelten von der Zusammensetzung

H_2	H_2SO_4 in Eisessig	$HgSO_4$	Hg

für die sie ein Potential von $E_0 = 0{\cdot}338$ extrapolierten.

KILPI und PURANEN,[11] die auch mit einer Kalomel-Elektrode als Vergleichssystem arbeiteten, berechneten die H^+-Ionen-Aktivität aus der Pufferkapazität von o-Aminobenzoesäure am Anfang und am Ende einer Titration mit einer Base.

TOMICZEK und HEYROVSKY[12] benutzten eine gleichartige potentiometrische Meßanordnung.

Durch kryoskopische Molekulargewichtsbestimmungen, die JANDER und MAAß[13] durchgeführt haben, zeigte sich, daß die Säurenanalogen $HClO_4$ und H_2SO_4 in Eisessig weitgehend assoziiert vorliegen und daß selbst bei relativ geringen Konzentrationen kaum Monomere existieren. Dies hat aber zur Folge, daß eine Berechnung der H^+-Ionen-Aktivität an eine Reihe von Voraussetzungen gebunden ist, die diese Ergebnisse als nicht völlig gesichert erscheinen lassen. Ein Vergleich der Äquivalent-Leitfähigkeiten mit den van't Hoffschen Faktoren läßt es wahrscheinlich sein, daß eine Reihe von Elektrolyten in wasserfreier Essigsäure wenigstens teilweise als

[5] W. SEAMAN und E. ALLEN, *Anal. Chem.* **23**, 592 (1951).
[6] J. S. FRITZ, *Anal. Chem.* **22**, 1028 (1950).
[7] A. W. DAVIDSON und W. CHAPPELL, *J. Amer. Chem. Soc.* **55**, 3531 (1933).
[8] A. W. HUTCHINSON und G. C. CHANDLEE, *J. Amer. Chem. Soc.* **53**, 2881 (1931).
[9] W. C. EICHELBERGER und V. K. LA MER, *J. Amer. Chem. Soc.* **54**, 2763 (1932).
[10] T. J. WEBB, *J. Amer. Chem. Soc.* **48**, 2263 (1926).
[11] S. KILPI und M. PURANEN, *Ann. Acad. Sci. Fennicae* Ser. A. **57**, Nr. 3 (1941).
[12] O. TOMICZEK und A. HEYROVSKY, *Chem. Listy Vedu Prumysl* **43**, 193 (1949).
[13] G. JANDER und G. MAAß, Die Grundlagen der Chemie in wasserfreier Essigsäure. *Fortschr. chem. Forsch.* **2**, 619 (1953).

Tripelionen vorliegen, deren Dissoziationsverhältnisse nicht restlos zu durchschauen sind. Diese Überlegungen gaben im wesentlichen den Anlaß, ein Meßsystem für potentiometrische Titrationen in wasserfreier Essigsäure anzuwenden, das nicht auf die Wasserstoff-Ionen, sondern auf die Azetat-Ionen anspricht.

Im Jahre 1951 wurde daher die potentiometrische Titration mit "gebremster Elektrode"[14] in die Chemie der wasserfreien Essigsäure eingeführt,[13] nachdem diese Methode bereits in anderen nichtwäßrigen Lösungsmitteln mit Erfolg angewandt worden war.[15] Im Prinzip handelt es sich dabei um eine Konzentrationskette. Es werden zwei Elektroden gleichen Metalls verwendet, von denen sich die eine in einer Kapillare befindet, die, genau wie die andere Elektrode, in die zu titrierende Lösung eintaucht. Während der Titration ändert sich nun die Zusammensetzung der vorgelegten Lösung laufend, wogegen sie in der Kapillare unverändert bleibt. Diese Methode ist deshalb von so großem Vorteil, weil sie ein wässriges Vergleichssystem wie die Kalomelelektrode überflüssig macht. Es ist anzunehmen, daß sich auf der Elektroden-Oberfläche eine Azetat-Deckschicht bildet, die ein Ansprechen auf die Azetat-Ionen ermöglicht.

Als Elektrodenmaterial wurde zunächst Silber für geeignet befunden, allerdings zeigte sich, daß bei Titrationen mit Perchlorsäure die Potentiale im schwach sauren Gebiet zusammenbrachen. Damit war aber die Silberelektrode insofern Einschränkungen unterworfen, als die Verwendung des in Eisessig stärksten Säurenanalogen unmöglich war.

Um eine Elektrode zu finden, die diesen Nachteil nicht zeigte, wurden mehrere verschiedene Metallproben untersucht. Die entscheidende Bedingung, die ein Elektroden-Metall erfüllen mußte, war, daß es weder in reiner Essigsäure noch in Gegenwart von Säuren- oder Basenanalogen in Lösung ging. Nach Möglichkeit sollte es außerdem nur in einer stabilen Wertigkeitsstufe auftreten können. Auf die an sich notwendige Bedingung, daß das betr. Metall ein in Eisessig unlösliches Acetat bilden kann, das den elektrischen Strom möglichst schlecht leitet, wurde aus Mangel an entsprechenden Literaturangaben keine Rücksicht genommen.

Zur Feststellung der Löslichkeit wurde eine Reihe von Metallproben einmal mit reiner Essigsäure, dann mit 1N basenanaloger und außerdem mit 1N säurenanaloger Eisessiglösung eingeschmolzen. In diese Versuchsreihe wurden folgende Metalle einbezogen:

Cu, Ag, Au
Zn, Cd
Al
Sn, Pb
Sb, Bi
W
Fe, Co, Pd

Das Einschmelzen dieser Proben geschah unter Stickstoff. Nachdem sie etwa 10 Tage sich selbst überlassen waren, wurden die Gewichtsdifferenzen festgestellt. Dabei zeigte sich, daß lediglich die Metalle

Ag, Au, W, Pd

[14] E. MÜLLER, *Die elektrometrische Maßanalyse*, Verl. Steinkopf, 7 Aufl, S.107.
[15] G. JANDER, *Die Chemie in wasserähnlichen Lösungsmitteln*. Verl. Springer (1949).

völlig unangegriffen geblieben waren. Alle übrigen wiesen einen mehr oder weniger großen Gewichtsverlust auf.

Die vier erwähnten Metalle wurden mit der im experimentellen Teil beschriebenen Apparatur praktisch auf ihre Eignung als Elektroden für potentiometrische Titrationen untersucht.

Mit den bereits von JANDER und MAAß[13] erprobten Silberelektroden wurden einige Messungen wiederholt und bestätigt.

Die Verwendung von Palladiumelektroden ergab zwar potentiometrische Meßkurven, die am Äquivalenzpunkt einen deutlichen Sprung aufwiesen, jedoch waren die einzelnen Potentialwerte nicht reproduzierbar. Bei mehrfacher Wiederholung der Titrationen ergaben sich Kurven, die sowohl in ihrer allgemeinen Form als auch in der Höhe der Potentialsprünge stark voneinander abwichen.

Ebenfalls negativ waren die Versuche mit Wolframelektroden. Diese sprachen nur bei relativ hohen Konzentrationen an, außerdem brachen die Potentiale im stärker sauren Gebiet zusammen.

VOL. 1 1955

2. POTENTIOMETRISCHE TITRATIONEN MIT GOLDELEKTRODEN ZUR VERFOLGUNG NEUTRALISATIONSANALOGER REAKTIONEN

(*a*) *Titrationen von Alkaliazetaten mit Perchlorsäure*

Die ersten Vorversuche mit Goldelektroden fielen hinsichtlich der Potentialeinstellung als auch der Ablesbarkeit der Galvanometerausschläge günstiger aus als mit den bisher untersuchten Elektroden-Metallen.

Von den in wasserfreier Essigsäure basenanalogen Alkali-Azetaten ist es bekannt, daß ihre Stärke mit zunehmendem Kationenradius steigt. Es war nun von Interesse, festzustellen, inwieweit sich diese Unterschiede auf die Kurvenformen von potentiometrischen Neutralisations-Titrationen auswirken. In Abb. 1 sind N/4 Lösungen der Azetate von Lithium, Natrium und Kalium mit einer Lösung von N/4 Perchlorsäure in Eisessig titriert worden. Die Endpotentiale dieser drei Kurven stimmen beim Lithium- und beim Natriumazetat ungefähr überein, beim Kaliumazetat liegt es bedeutend höher. Wesentlicher als diese Endwerte sind wegen der in diesem Gebiet immer stärker werdenden Assoziation der Perchlorsäure die Höhen des ungefähr senkrecht verlaufenden Kurvenzuges, der in der angegebenen Reihenfolge laufend zunimmt. Außerdem ist die Stärke der Krümmung vor dem Äquivalenzpunkt von Interesse, die ebenfalls vom Lithium zum Kalium deutlich stärker wird.

Zur Erprobung der Goldelektroden bei Titrationen, die vom säurenanalogen Gebiet zum basenanalogen führten, wurden diese drei neutralisationsanalogen Reaktionen nochmals in umgekehrter Weise potentiometrisch verfolgt. Mit den in Abb. 2 dargestellten Potentialkurven wird bewiesen, daß die Goldelektroden auch im perchlorsauren Gebiet uneingeschränkt verwendbar sind, sodaß der Nachteil, den die Silberelektroden hatten, beseitigt ist. Ein Vergleich der drei Kurven zeigt, daß hier die Verschiedenheit in den Dissoziations-Konstanten ebenso deutlich hervortritt. Nach diesen Titrationskurven hat es den Anschein, daß die Goldelektroden tatsächlich konzentrationsrichtig auf die Azetationen ansprechen. Daß die Titrationskurven exakt reproduzierbar sind, wurde in allen Fällen durch mehrfache Wiederholung festgestellt.

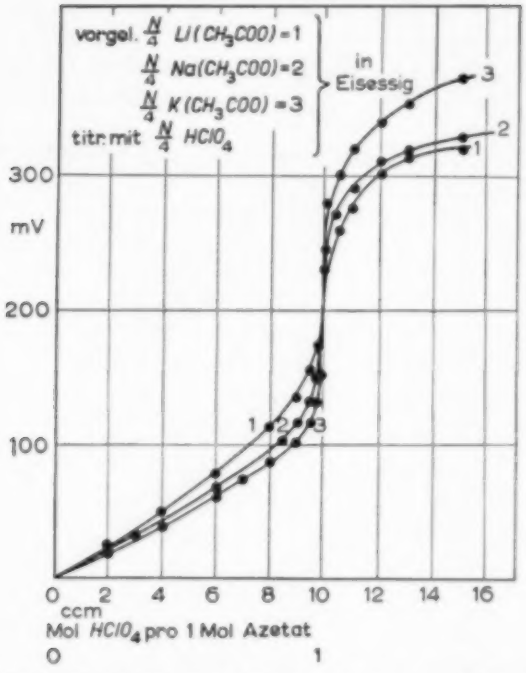

ABB. 1.—Potentiometrische Titration von Li-, Na-, und K-Azetat mit Perchlorsäure in wasserfreier Essigsäure.

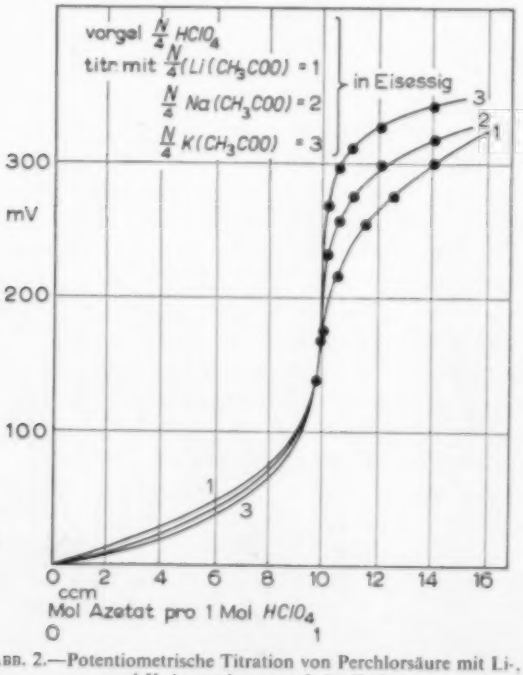

ABB. 2.—Potentiometrische Titration von Perchlorsäure mit Li-, Na-, und K-Azetat in wasserfreier Essigsäure.

(b) Titrationen von organischen potentiellen Basenanalogen

Wegen der praktischen Bedeutung der "Eisessigmethode" zur Bestimmung schwacher Basen war es erforderlich, die potentiometrische Titration mit Goldelektroden an einer Reihe organischer Basenanaloger zu erproben. Als erstes Beispiel dieser Art ist in Abb. 3 die Neutralisation von Diäthylanilin mit Perchlorsäure gezeigt.

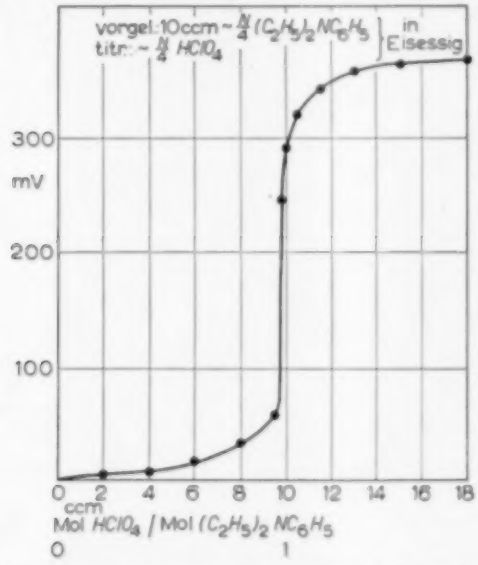

ABB. 3.—Potentiometrische Titration von Diäthylanilin mit Perchlorsäure in wasserfreier Essigsäure.

Die wiedergegebene Potentialkurve weist verschieden starke Krümmungen vor und nach dem Äquivalenzpunkt auf. Dies läßt den Schluß zu, daß die Dissoziationskonstanten von Säuren- und Basenanalogen deutlich verschieden sein müssen. Offensichtlich fungiert Diäthylanilin als starker Elektrolyt. Gleichzeitig zugesetztes Kristallviolett als Farbindikator schlug am Potentialsprung von violett über grün nach rotgelb um. Bläulich-grün gibt bei dieser Titration den Äquivalenzpunkt wieder.

In Abb. 4 ist die Titration von Pyridin mit Perchlorsäure gezeigt. Pyridin ist ein schwächeres Basenanaloges als Diäthylanilin. Daß der Potentialsprung trotzdem so gut ausgebildet ist, liegt an der Schwerlöslichkeit des gebildeten Pyridiniumperchlorates in Eisessig. In der Literatur sind verschiedene sog. anormale Salze des Pyridins beschrieben,[13], [16], [17] die zwei und mehr Pyridinium-Ionen enthalten. Es trat jedoch bei den potentiometrischen Titrationen stets nur ein Sprung beim Molverhältnis 1 : 1 auf.

Die gleiche Umsetzung wurde vom säurenanalogen Gebiet her kommend durchgeführt. Auch hierbei bildet sich bei der ersten Zugabe des Basenanalogen ein dicker Niederschlag des Salzes.

Aus einer Anzahl im einzelnen nicht aufgeführter potentiometrischer Titrationen von organischen Basenanalogen verschiedener Stärke (Anilin, Dimethylanilin,

[16] E. GRIMAUX, *Bull. Soc. Chim. France* [2], **38**, 124 (1882).
[17] H. MANDAL, *Ber. Dtsch. Chem. Ges.* **53**, 2216 (1920).

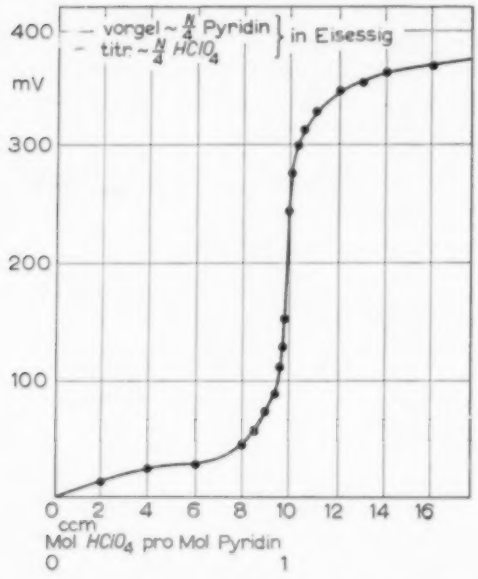

ABB. 4.—Potentiometrische Titration von Pyridin mit Perchlorsäure in wasserfreier Essigsäure.

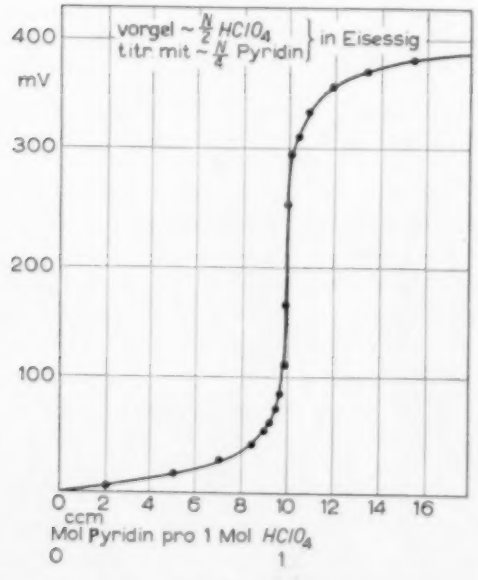

ABB. 5.—Potentiometrische Titration von Perchlorsäure mit Pyridin in wasserfreier Essigsäure.

α-Naphtylamin) bei verschiedenen Konzentrationen mit Perchlorsäure läßt sich folgendes zusammenfassen:

(1) Organische Basenanaloge lassen sich in Eisessiglösung mit Perchlorsäure unter Verwendung von Goldelektroden bis zu einer Konzentration von N/100 potentiometrisch genau titrieren.
(2) Es ist dabei gleichgültig, ob das Basenanaloge oder das Säurenanaloge vorgelegt wird.
(3) Aus den Kurvenformen sind Rückschlüsse auf die relative Stärke der titrierten Verbindungen möglich.
(4) Die Ausbildung des Potentialsprunges im Äquivalenzpunkt wird durch das Auftreten eines schwerlöslichen Salzanalogen begünstigt.
(5) Die Meßergebnisse sind vollkommen reproduzierbar und sie widersprechen nicht der Vorstellung, daß die Goldelektroden konzentrationsrichtig auf die Azetationen ansprechen.

VOL. 1 1955

(*c*) *Titrationen mit Schwefelsäure.*

Mit den beiden auf den Abb. 6 und 7 dargestellten Titrationskurven wurde die neutralisationsanaloge Reaktion von Diäthylanilin mit Schwefelsäure untersucht.

In Abb. 6 ist das Basenanaloge vorgelegt. Die Krümmung der Kurve vor dem Äquivalenzpunkt hat die gleiche Form wie bei der Umsetzung mit Perchlorsäure. Der Umschlag ist aber viel undeutlicher ausgeprägt, was auf die weit geringere Stärke der Schwefelsäure zurückzuführen ist. Außerdem wird bei weitem nicht das Endpotential erreicht, das bei der Titration mit Perchlorsäure auftritt.

Auf der Abb. 7, die die gleiche Reaktion in umgekehrter Anordnung wiedergibt, drückt sich die geringe Stärke der Schwefelsäure ebenfalls recht deutlich in dem unscharfen Potentialsprung aus. Das Endpotential von 345 mV entspricht dem gut dissoziierten Diäthylanilin.

3. SÄURENANALOGE IN WASSERFREIER ESSIGSÄURE

Die Zahl der in wasserfreier Essigsäure bekannten Säurenanalogen ist weitaus geringer als die der Basenanalogen. An Untersuchungen über Verbindungen, die in Eisessig säurenanalogen Charakter haben, liegen Arbeiten einmal von HANTZSCH und LANGBEIN[18] und außerdem von KOLTHOFF und WILLMAN[19] vor.

Auf Grund von Molekulargewichtsbestimmungen ist es erwiesen, daß $HClO_4$ und H_2SO_4 in Eisessig stark assoziiert sind. Um aber die bei den Titrationen gemessenen Potentiale physikalisch-chemischen Berechnungen zugrunde legen zu können, war es erwünscht, ein Säurenanaloges zu finden, daß an Stärke der Perchlorsäure etwa gleichkommt, aber möglichst keine oder nur geringe Assoziationserscheinungen zeigt. Es war selbstverständlich, daß ein derartiges Säurenanaloges auch in wässriger Lösung sehr stark dissoziiert sein mußte. Sehr aussichtsreich schienen in dieser Hinsicht die organischen Sulfonsäuren zu sein. Aus der Chemie der wässrigen Lösungen ist bekannt, daß diese die Schwefelsäure an Stärke erreichen können, außerdem sind sie fast alle gut löslich und schließlich war es vorteilhaft, daß sie einbasisch sind. Hantzsch und Langbein haben bei ihren Arbeiten mit Trichlormethylsulfonsäure und Toluolsulfonsäure nicht die wasserfreien Verbindungen, sondern ihre

[18] A. HANTZSCH und W. LANGBEIN, *Z. anorg. allgem. Chem.* **204**, 193 (1932).
[19] I. M. KOLTHOFF und A. WILLMAN, *J. Amer. Chem. Soc.* **56**, 1016 (1934).

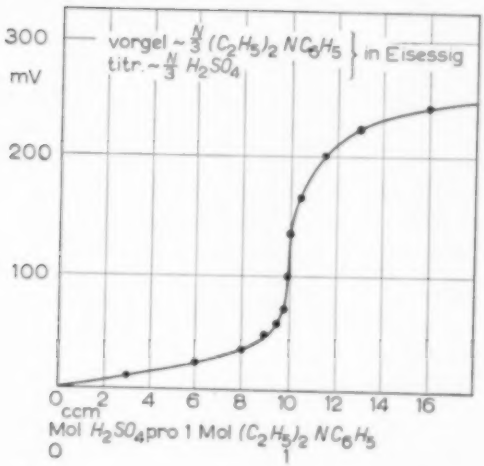

ABB. 6.—Potentiometrische Titration von Diäthylanilin mit Schwefelsäure in wasserfreier Essigsäure.

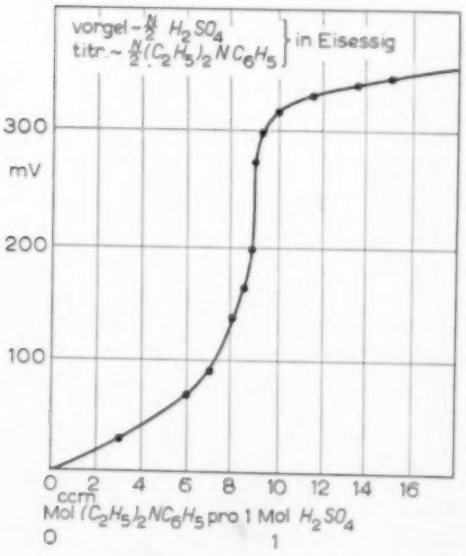

ABB. 7.—Potentiometrische Titration von Schwefelsäure mit Diäthylanilin.

Monohydrate verwendet. Der säurenanaloge Charakter dieser Verbindungen beruhte also auf der starken Solvolyse der betreffenden Hydroniumsalze.

Die Toluolsulfonsäure, die wesentlich stabiler ist als die Trichlormethylsulfonsäure, ist, wie eigene Versuche ergaben, auf normalem Wege, durch vorsichtiges Erwärmen im Vakuum nicht restlos zu entwässern. Sie färbt sich allmählich dunkelbraun und läßt sich in Eisessig nicht mehr klar lösen. Längeres Trocknen über P_2O_5 führt nicht weiter als zum Monohydrat und die Umsetzung dieses mit der berechneten Menge Azetanhydrid führte stets wieder nur zu getrübten Lösungen.

Eine besonders starke Azidität wurde bei der o- und der p-Chlorbenzolsulfonsäure erwartet, aber weder bei diesen noch bei der m-Nitrobenzolsulfonsäure gelang es, sie vollkommen ohne beginnende Zersetzung zu entwässern.

VOL. 1 1955

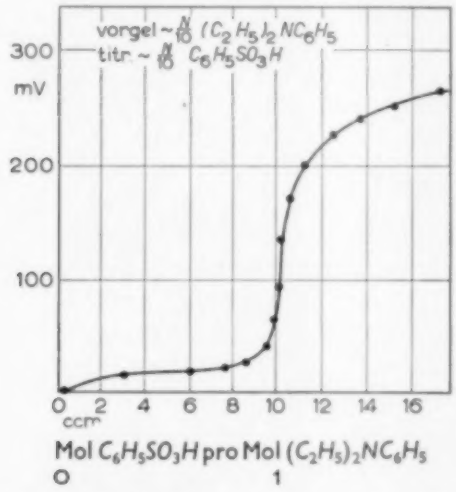

Abb. 8.—Potentiometrische Titration von Diäthylanilin mit Benzolsulfonsäure in wasserfreier Essigsäure.

Die einzige stabile Sulfonsäure, die wasserfrei darstellbar ist, ist die unsubstituierte Benzolsulfonsäure. (Mehrstündiges Trocknen im Vakuum bei 100°C). Ihre wasserfreie Lösung in Eisessig ist zwar schwach rötlich gefärbt, aber sie ist völlig klar.

Die in Abb. 8 gezeigte potentiometrische Titration von Diäthylanilin mit Benzolsulfonsäure läßt schon aus der allgemeinen Kurvenform schließen, daß sie in ihrer Stärke ungefähr der Schwefelsäure entspricht. Gemäß dem Potential von 270 mV scheint sie etwas stärker zu sein als die Schwefelsäure (s. Abb. 6, Endpot. = 245 mV).

Abb. 9 zeigt die konduktometrische Verfolgung der gleichen Reaktion. Die beiden Kurvenäste dieser Titration schließen einen sehr stumpfen Winkel ein. Die schwache Krümmung des ersten Leitfähigkeits-Anstieges sowie die Abrundung des Knickes im Äquivalenzpunkt lassen auf Solvolyse des gebildeten Salzes schließen.

An Säurenanalogen anorganischer Natur wurde als erstes die Perjodsäure untersucht, ob sie die erwähnten Anforderungen erfüllt. Ihre Verwendbarkeit scheiterte jedoch daran, daß sie in wasserfreier Essigsäure praktisch unlöslich ist.

Eine nach den Erfahrungen aus wässrigen Lösungen sehr starke Säure ist die

Borfluorwasserstoffsäure. Sie ist bisher nur in wässriger Lösung bekannt. Beim Versuch, sie zu entwässern, zerfällt sie gemäß

$$HBF_4 = BF_3 + HF.$$

Aus diesem Grunde konnte nur eine Entwässerung durch Umsetzung mit Azetanhydrid erfolgreich sein. Unter Eiskühlung wurde die wässrige HBF_4-Lösung mit der

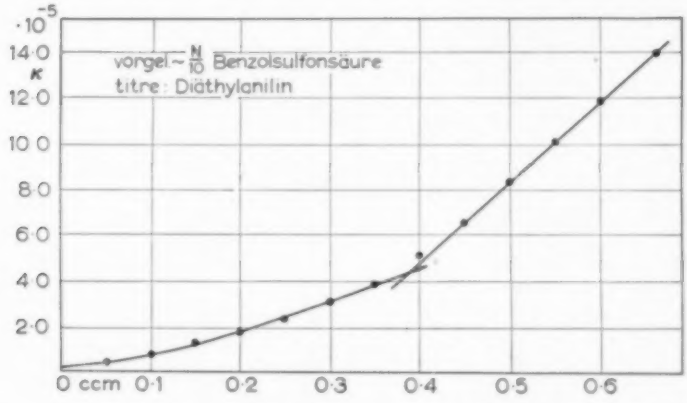

ABB. 9.—Konduktometrische Titration von Benzolsulfonsäure mit Diäthylanilin in wasserfreier Essigsäure.

berechneten Menge Azetanhydrid versetzt. Diese Lösung, die noch mit wasserfreier Essigsäure verdünnt worden war, schied nach einigem Stehen einen farblosen Niederschlag aus. Trotzdem war es möglich, vor der Zersetzung eine konduktometrische

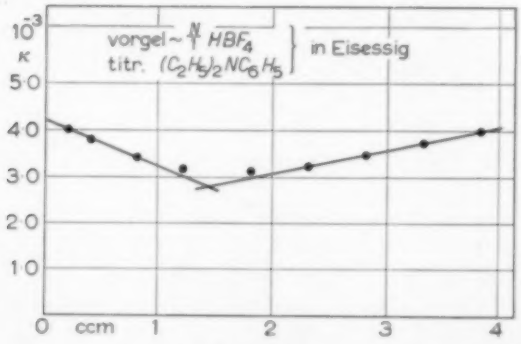

ABB. 10.—Konduktometrische Titration von Borfluorwasserstoffsäure mit Diäthylanilin.

Titration durchzuführen (für eine potentiometrische Titration reichte die Haltbarkeit nicht aus.). Abb. 10 gibt die Leitfähigkeitskurve dieser Titration wieder. Die starke Abrundung im Äquivalenzpunkt läßt auf eine weitgehende Solvolyse des Diäthylaniliniumbortetrafluorids schließen.

Der farblose Niederschlag, der sich nach knapp einstündigem Stehen der wasserfrei essigsauren HBF_4-Lösung ausgeschieden hatte, wurde als SiO_2 identifiziert, das geringe Mengen $NaBF_4$ enthielt.

VOL. 1 1955

4. DIE RELATIVE STÄRKE VON SÄUREN- UND BASENANALOGEN IN WASSERFREIER ESSIGSÄURE

Es ist heute, vor allem durch die Arbeiten BRÖNSTEDS,[20], [21], [22] bekannt, daß der Säurecharakter einer Substanz kein ihr arteigenes Kriterium ist, sondern daß er eine relative Eigenschaft darstellt. BRÖNSTED entwickelte den Begriff des korrespondierenden Säuren- und Basenpaares, die er als Protonendonatoren und -akzeptoren definierte. Diese Auffassung war zunächst für die Chemie in wässrigen Lösungen geschaffen. Wenn BRÖNSTED auch Untersuchungen in nichtwässrigen Lösungsmitteln durchgeführt hat, so geschah dies—er benutzte z.B. Benzol-Lösungen—doch nur unter dem Blickpunkt des Protonenaustauschs. Die Untersuchungen über protonenfreie Lösungsmittel, wie z.B. SO_2, J_2, $HgBr_2$, Azetanhydrid und andere,[15] haben aber gezeigt, daß überhaupt kein bestimmtes Ion schlechthin als Träger der sauren Eigenschaften angesehen werden darf, sondern daß der Säuren- und Basenbegriff immer nur in Relation zum betrachteten Lösungsmittel zu fassen ist. In diesem Sinne ist der von uns und unseren früheren Mitarbeitern eingeführte Begriff der Säuren- und Basenanalogen zu verstehen.

Für die Essigsäure als protonenhaltiges Lösungsmittel ist hinsichtlich der relativen Stärke von Säuren- und Basenanalogen die Protonenaffinität des Solvens von großer Bedeutung. Es darf heute als erwiesen angesehen werden, daß Protonen in Lösung immer solvatisiert vorliegen, in Wasser als H_3O^+-Ionen, in Essigsäure als "Azetacidium-Ionen" $(CH_3COOH \cdot H)^+$.

Betrachtet man einige bereits untersuchte Lösungsmittel in der Reihenfolge abnehmender Protonenaffinität, z.B.

$$NH_3 \qquad H_2O \qquad CH_3COOH \qquad HF$$

dann zeigt die Erfahrung, daß eine in dieser Reihe weiter links stehende Verbindung basenanalog in einer rechts von ihr stehenden, die als Lösungsmittel angesehen sei, reagieren muß, Die Stärke dieses Basenanalogen ist umso größer, je größer der Unterschied in der Protonenaffinität ist. Die umgekehrte Reihenfolge gilt für Säurenanaloge.

Für Eisessig-Lösungen ist diese Überlegung insofern von Interesse, als einige Forscher die Meinung geäußert haben, daß Perchlorsäure- und Schwefelsäure-Lösungen in wasserfreier Essigsäure superaciden Charakter haben[1], [2], [7], [23]. Diese Auffassung entstand zunächst dadurch, daß in wasserfreier Essigsäure auch Basen titrierbar sind, die in Wasser praktisch undissoziiert vorliegen. Nach den oben dargelegten Gedanken ist aber viel eher anzunehmen, daß diese Titrierbarkeit auf die grössere Stärke der Basenanalogen in Eisessig-Lösung zurückzuführen ist.

HALL und CONANT[1], [2] versuchten, die Existenz superacider Lösungen in wasserfreier Essigsäure mit den von ihnen durchgeführten Potentialmessungen zu begründen. Für eine 1N Perchlorsäure-Lösung errechneten sie einen p_H-Wert von −4,4, der einer H^+-Ionenaktivität von etwa 25,000 gval pro Liter entspricht. Eine derartige Protonen-Aktivität kann aber überhaupt nicht realisierbar sein.

Gegen die Existenz der "übersauren Lösungen" ist eine Reihe theoretischer Einwände zu erheben.

[20] J. N. BRÖNSTED, *Ber. dtsch. chem. Ges.* **61**, 2049 (1928).
[21] J. N. BRÖNSTED, *Angew. Chem.* **43**, 229 (1930).
[22] J. N. BRÖNSTED, *Z. phys. Chem.* A. **169**, 52 (1934).
[23] N. F. HALL und W. F. SPENGEMAN, *J. Amer. Chem. Soc.* **62**, 2487 (1940).

1. Der p_H-Begriff ist ein Maß für die Azidität einer wässrigen Lösung. Er ist direkt aus dem Dissoziations-Gleichgewicht des Wassers abgeleitet und gibt das Verhältnis

$$\frac{[H_3O^+]}{[H_2O]} \text{ wieder.}$$

2. Der Nenner dieses Quotienten kann nur dann als konstant angenommen werden, wenn er genügend groß ist, was ausschließlich für verdünnte Lösungen zutrifft.

3. Es dürfte demzufolge nicht statthaft sein, den Wert für H_2O beliebig klein werden zu lassen, wie man es sich beim allmählichen Übergang von einer wässrigen zu einer nichtwässrigen Lösung durch laufende Konzentrationserhöhung vorstellen könnte. Im Gebiet des nichtwässrigen Lösungsmittels ist ja die Azidität dann durch ein völlig anderes Konzentrationsverhältnis gegeben, beim Übergang zum Ammonosystem z.B. durch $\frac{[NH_4^+]}{[NH_3]}$. Daß tatsächlich für jedes Lösungsmittel-System ein eigener Aziditätsbegriff existieren muß, ergibt sich noch klarer bei der Betrachtung protonenfreier Lösungsmittel, wo ein p_H-Wert-Begriff völlig unsinnig geworden wäre.

4. Die Eigengesetzlichkeit eines Lösungsmittel-Systems beruht nicht nur in dem Vorhandensein eines eigenen Aziditätsbegriffes und eigener säuren- und basenanaloger Verbindungen, sondern auch in einer eigenen Spannungsreihe und eigenen Gesetzmäßigkeiten hinsichtlich der Löslichkeit, der Solvatation, der solvolytischen Erscheinungen, der Amphoterie und der Komplexbildung. Ein großer Teil dieser Erscheinungen ist in zahlreichen Solventien experimentell bewiesen.[15]

Der Annahme übersaurer Lösungen, speziell in wasserfreier Essigsäure, ist auf Grund folgender experimenteller Befunde zu widersprechen:

1. Wenn der übersaure Charakter von $HClO_4$- und H_2SO_4-Lösungen in Eisessig auf die geringere Solvatation der Protonen im Vergleich zu wässrigen Lösungen zurückgeführt wird, dann ist es nicht einzusehen, daß andererseits Salpetersäure, Trichloressigsäure oder auch Fluorwasserstoff in wasserfreier Essigsäure fast undissoziiert sind, während sie in Wasser eine bemerkenswerte Azidität[19], [24] besitzen.

2. Konduktometrische und kryoskopische Messungen haben gezeigt[13] daß besonders die Säurenanalogen in wasserfreier Essigsäure stark assoziiert sind. Wenn diese Assoziate auch ihrerseits wieder dissoziieren, so ist doch schwer vorzustellen, daß unter diesen Umständen ein übersaurer Charakter auftritt.

Wenn in Eisessig die Titration schwacher organischer Basen möglich ist, dann folgt das, wie schon erwähnt, aus der Verstärkung ihres basenanalogen Charakters. Die Säurenanalogen sind in wasserfreier Essigsäure weit schwächere Elektrolyte als in wässriger Lösung, immerhin reicht die Stärke der Perchlorsäure noch aus, um Titrationen mit genügender Genauigkeit durchführen zu können.

5. EXPERIMENTELLER TEIL

(a) *Die Entwicklung einer geeigneten Messapparatur.*

Die in der vorliegenden Arbeit zur Durchführung der Potentialmessungen benutzte Apparatur gleicht im wesentlichen der, die JANDER und MAAß[13] bei ihren Untersuchungen verwendet hatten. Abgeändert war sie nur darin, daß die Kapillare am

[24] I. M. KOLTHOFF und A. WILLMAN, *J. Amer. Chem. Soc.* **56**, 1007 (1934).

oberen Ende luftdicht mit einem Stück Vacuumschlauch und einer Schlauchklemme abgeschlossen war. Dadurch war es möglich, mit Substanzlösungen zu titrieren, während im anderen Falle nur feste Substanzen zugesetzt werden konnten, um ein Nachsteigen der vorgelegten Lösung in die Kapillare infolge der Volumenzunahme zu vermeiden. Vor der Abdichtung wurde die Flüssigkeit in der Kapillare leicht angesaugt. Durch den Niveau-Unterschied wurde einer vorzeitigen Diffusion entgegengewirkt.

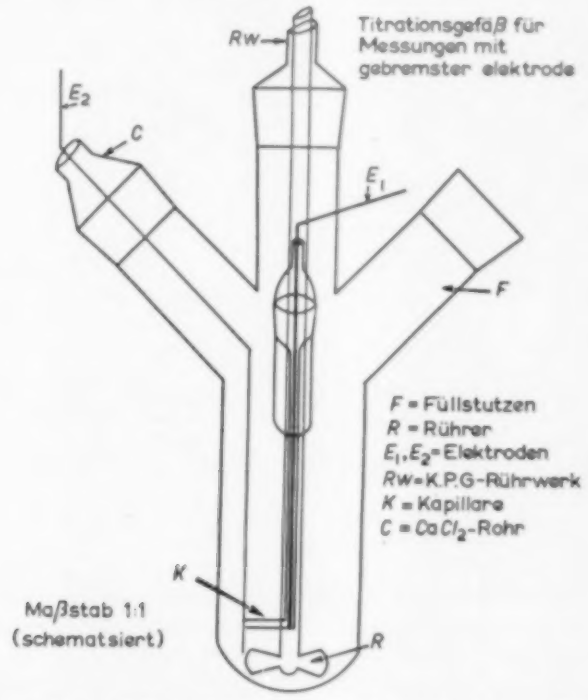

Abb. 11.—Meßgefäß für potentiometrische Titrationen mit gebremster Elektrode.

Bei allen Titrationen mit "gebremster Elektrode" muß das in der Kapillare befindliche Lösungsvolumen von der Ausgangslösung abgezogen werden, da es ja selbst nicht mittitriert wird. Zu diesem Zweck ist es am einfachsten, die Kapillare mit Strichen zu versehen und die damit angegebenen Volumina durch Auswägen mit Wasser zu bestimmen. Das verwendete Titrationsgefäß ist in Abb. 11 wiedergegeben.

Die Meßanordnung bestand in einer Poggendorfschen Kompensationsschaltung. Als Stromquelle diente ein 2 V-Bleiakkumulator, die Meßbrücke hatte einen Widerstand von 53 Ohm. Vor jeder Titration wurde die Spannung des Akku mit einem geeichten "Internationalen West-Element" bestimmt (P.T.R. Berlin-Charlottenburg, Nr. 491/52 $1{\cdot}0183_0$ int. V bei 20°C; $1{\cdot}0186_5$ abs. V.). Als Nullinstrument wurde ein Ruhstrat Spiegelgalvanometer SSG verwendet. Dessen Stromempfindlichkeit betrug $4{\cdot}15.10^{-9}$ Amp/mm bei 1 m Skalenentfernung, die Spannungsempfindlichkeit $6{\cdot}25.10^{-9}$ Volt/mm bei gleicher Skalenentfernung.

Zur Erzielung reproduzierbarer Meßwerte ist es sehr wichtig, der Kapillare die

richtige Form zu geben. Einerseits muß sie so eng sein, daß praktisch keine Diffusion eintreten kann. Andererseits muß sie so weit sein, daß der innere Widerstand der Meßkette nicht zu stark erhöht wird. Die richtigen Dimensionen der Kapillare können nur experimentell bestimmt werden, indem man eine Potential-Einstellungskurve aufnimmt. Bei einer zu weiten Kapillare würden die Potentiale nicht konstant bleiben, sondern nach einer gewissen Zeit wieder absinken. Bei einer zu engen würde es zu lange dauern, bis die Potentiale konstant bleiben, außerdem würden die Galvanometer-Ausschläge so gering werden, daß eine einwandfreie Ablesung nicht mehr

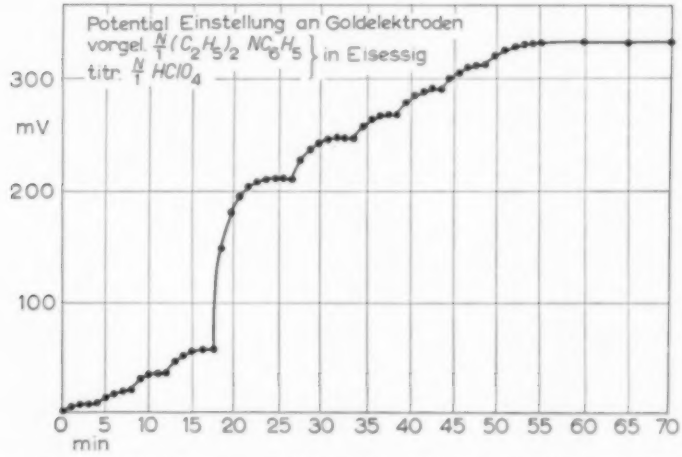

ABB. 12.—Potential-Einstellung an Goldelektroden bei einer Titration von Diäthylanilin mit Perchlorsäure in wasserfreier Essigsäure.

möglich wäre. Abb. 12 gibt die Einstellungs-Kurve unter Verwendung der Kapillare wieder, die bei den beschriebenen potentiometrischen Titrationen benutzt worden war. Zu Beginn jedes Sprunges waren 2 ccm Maßlösung zugesetzt worden.

Die Einstellung des Nullpotentials zu Beginn jeder Titration dauert verschieden lange, maximal 45 min. Die zunächst auftretende Potentialdifferenz wird vermutlich durch einen Temperaturunterschied der beiden Elektroden verursacht, der sich erst ausgleichen muß.

Die Reinigung der Goldelektroden erfolgt durch Abspülen mit konz. Ammoniak, anschließendem Nachspülen mit Wasser und schließlich, zur schnelleren Trocknung, erst Spülen mit Methanol und danach mit Azeton oder Äther.

(*b*) *Die Reinigung und Trocknung des Lösungsmittels.*

Als Ausgangssubstanz diente "Merck: Acidum aceticum glaciale 1·055–1·058 p.A." Diese Essigsäure ist indifferent gegen Chrom(VI)-oxyd, enthält also keine oxydierbaren Bestandteile wie Alkohole oder Aldehyde und hat einen Schmelzpunkt, der zwischen 16·2 und 16·4°C liegt. Nach einigen fraktionierten Destillationen über eine Raschigkolonne wurde sie mehrfach ausgefroren. Die Zahl dieser fraktionierten Kristallisationen richtete sich nach dem erreichten Schmelzpunkt, der wenigstens bei 16·55–16·6°C liegen mußte. Das Ausfrieren wurde so durchgeführt, daß die Säure in eine Eis-Kochsalzmischung gebracht wurde. Durch die starke Abkühlung bildete

sich sofort an der Gefäßwand ein Kristallbeschlag, der langsam nach innen wuchs. Zur Bestimmung des Schmelzpunktes wurde die Säure unterkühlt, indem sie in Eiswasser gestellt wurde. Durch Anschlagen des eingeführten Thermometers an die Kolbenwand wird die Unterkühlung aufgehoben und die Flüssigkeit erstarrt zu einem dicken Kristallbrei. Das Temperaturgleichgewicht hat sich nach wenigen Minuten eingestellt.

Sämtliche Meßgefäße wurden zur Beseitigung der Wasserhaut mindestens eine Stunde im Trockenschrank aufbewahrt. Das Umfüllen der Lösungen geschah ebenso wie das Abgießen von der auskristallisierten Essigsäure unter völligem Ausschluß von Luftfeuchtigkeit.

(*c*) *Darstellung und Reinigung der Reagenzien.*

Die Perchlorsäure-Lösung in wasserfreier Essigsäure wurde nach HALL und WERNER[25] dargestellt. Zunächst wurde der $HClO_4$-Gehalt einer wässrigen ca. 70%igen Perchlorsäure azidimetrisch bestimmt. Unter Eiskühlung wurde diese bei konstantem Rühren gleichmäßig und unter laufender Temperaturkontrolle zu der berechneten Menge Azetanhydrid zugetropft. Solange eine Komponente im Überschuß vorliegt, ist bei Zugabe der anderen ein starker Wärme-Effekt zu beobachten, der im Endpunkt ein Minimum erreicht. Bei langsamer und gleichmäßiger Tropfgeschwindigkeit ist dieser Punkt deutlich zu erkennen. Bei dieser Operation darf die Temperatur nicht über $+15°C$ steigen, da sonst bereits nach kurzer Zeit unter Gelbfärbung eine Zersetzung der Lösung eintritt.

Die absolute, essigsaure Schwefelsäure-Lösung wurde durch Vermischen einer mit SO_3 entwässerten H_2SO_4 mit Eisessig unter Kühlung dargestellt. Die Konzentration der wasserhaltigen und der absoluten Säure wurde azidimetrisch bestimmt, die der essigsauren Lösung gravimetrisch als $BaSO_4$.

Das Natriumazetat wurde durch vorsichtiges Schmelzen der kristallwasserhaltigen Verbindung bis zu einer Temperatur von 330°C getrocknet. Die erstarrte Schmelze wurde dann rasch pulverisiert und mehrere Stunden bei 130°C nachgetrocknet. Das so vorbehandelte Azetat löste sich klar in wasserfreier Essigsäure.

$Li(CH_3COO)$ wurde durch Umsetzung von Lithiumkarbonat mit Essigsäure dargestellt, Die durch Eindampfen gewonnenen Kristalle wurden auf dem Wasserbad im Vakuum getrocknet.

Das $K(CH_3COO)$ wurde durch mehrstündiges Erhitzen des kristallwasserhaltigen Azetats auf über 180°C getrocknet. Beide Basenanaloge sind hygroskopisch.

Die Reinigung und Trocknung erfolgte beim Pyridin und beim Anilin durch dreimalige Destillation über eine Raschig-Kolonne unter Ausschluß von Luftfeuchtigkeit. Das Dimethylanilin wurde nach der Destillation einmal ausgefroren Die Reinigung des α-Naphtylamins erfolgte durch Umkristallisieren aus Alkohol. Die erhaltenen Kristalle wurden durch mehrstündiges Stehen im Vakuum bei Zimmertemperatur getrocknet. Das Diäthylanilin wurde ebenfalls durch wiederholte Destillation unter Luftausschluß entwässert. Die Lösungen in wasserfreier Essigsäure wurden jedesmal frisch bereitet.

Die Durchführung der Untersuchungen wurde uns durch Gewährung von ERP-Mitteln ermöglicht.

[25] N. F. HALL und T. H. WERNER, *J. Amer. Chem. Soc.* **50**, 2373 (1928).

VOL. 1 1955

ZUSAMMENFASSUNG

Die Verwendung einer "gebremsten Elektrode" bei der potentiometrischen Verfolgung neutralisationsnanaloger Umsetzungen in wasserfreier Essigsäure hat gegenüber den bisherigen Versuchsanordnungen den Vorteil, daß keine wässrige Vergleichs-Elektrode benutzt wird. Die Erprobung der entwickelten Meßanordnung nach verschiedenen Gesichtspunkten bestätigt ihre uneingeschränkte Verwendbarkeit in Eisessig-Lösungen. Als Elektrodenmaterial bewährt sich Golddraht bzw. -blech am besten. Es ist über den ganzen Bereich der Wasserstoffionen- bzw. der Azetationen-Konzentration verwendbar und gewährleistet reproduzierbare Potentialmessungen. Der Versuch, die Perchlorsäure als Maßflüssigkeit durch ein anderes Säurenanaloges zu ersetzen, blieb ohne befriedigendes Ergebnis. Auf Grund der durchgeführten Untersuchungen lassen sich Einwände gegen die Vorstellung erheben, daß $HClO_4$- und H_2SO_4-Lösungen in Eisessig superaciden Charakter haben.

J. Inorganic and Nuclear Chemistry, 1955, Vol. 1, pp. 143–148. Pergamon Press Ltd., London

THE THERMAL DECOMPOSITION OF THORIUM OXALATE

By R. W. M. D'Eye and P. G. Sellman
Atomic Energy Research Establishment, Harwell, Berks

(*Received* 8 *October* 1954)

Abstract—The thermal decomposition of thorium oxalate dihydrate has been studied in the temperature region 270–900°C in both air and nitrogen atmospheres. The water of hydration is readily removed at 270°. At 330° decomposition takes place with liberation of CO and CO_2, the quantity of CO being slightly greater than that of CO_2. The results are compatible with formation of a carbonate as an intermediary in the degradation process. Some free carbon is found which is probably formed by disproportionation of CO. The thoria prepared at low temperatures 300–500° from the oxalate has a small crystallite size and is hygroscopic.

VOL. 1 1955

1. INTRODUCTION

The decomposition of thorium oxalate at low temperatures is of interest for the preparation of a reactive form of thoria; other methods involving ignition at high temperatures yield thoria of a large particle size, which is extremely unreactive. There is, however, a danger of impurities in the material prepared from the oxalate.

Beckett and Winfield (1951) found that at 320° the decomposition of thorium oxalate was nearly complete. The weight-loss, after heating at this temperature, was 37·3 per cent of the weight taken, whereas for complete conversion to ThO_2 the percentage loss is 40·8. Above 320° the gradual loss in weight, which continued to temperatures above 600°, was shown to be due to the breakdown of a carbonate. They further found that after heat treatment at 350°, X-ray analysis indicated two phases: ThO_2 and a cubic phase with $a = 13{\cdot}00$ kX. The pattern of this latter phase persisted even after heating at 800°, but with a decreased intensity. No suggestions as to the composition of this phase were put forward. The thoria prepared by the decomposition of the oxalate at low temperature was shown to have a large surface area.

In a paper on the thermal decomposition of oxalates in vacuum, Günther and Rehäag (1938) suggested that $Nd_2(C_2O_4)_3$ first decomposed on ignition to a peroxydioxalate $Nd_2O_2(C_2O_4)_2$ with liberation of CO, which then disproportionated to CO_2 and C. (The O_2 in the formula represents a peroxide grouping.) This accounted for the fact that CO_2 and CO were not liberated at the same rates. They further suggested that the oxalates of Na, Ca, Ba, and Th decomposed in a similar manner.

A report by Yatabe and Pollock (1952) describes the low-temperature thermal decomposition of thorium oxalate dihydrate, which was prepared from acid thorium nitrate solution, using oxalic acid as the precipitant and drying at 105°. The residue, after decomposition in air to constant weight at temperatures in the range 250–320°, suffered a further 2 per cent weight-loss on ignition at 900°. No explanation of this was given.

In view of the existing anomalies it was decided to carry out degradation studies in an inert atmosphere and determine the water, carbon dioxide, and monoxide

evolved. An inert atmosphere, nitrogen, would prevent the oxidation of the CO to CO_2, which might otherwise tend to give misleading data.

Our results substantially confirm the work of BECKETT and WINFIELD, in that thorium oxalate decomposes with some formation of thorium carbonate. The present work differs, however, in the fact that our X-ray studies do not show a cubic phase occurring with the ThO_2.

2. EXPERIMENTAL

(a) *Preparation*

Thorium oxalate when prepared, using ammonium oxalate as the precipitant (SCHOELLER and POWELL, 1940) and dried at 105°, gives the pentahydrate, whereas if oxalic acid is used as the precipitant the dihydrate is formed. Both hydrates were found to be rather hygroscopic.

The dihydrate has been used exclusively in the following work.

(b) *Analysis*

The oxalate radical was determined in the usual manner with standardized potassium permanganate, and the Th determined by ignition to ThO_2. The water contents were found both by difference and by absorption in U-tubes containing magnesium perchlorate (anhydrone).

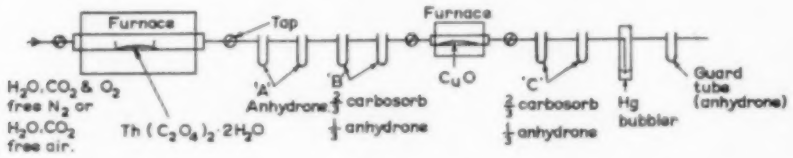

Diagram of apparatus.

(c) *X-ray Analysis*

Diffraction patterns were obtained, using standard X-ray equipment and a 9-cm Unicam camera with filtered Cu$K\alpha$ radiation.

(d) *Degradation Experiments*

The apparatus used is shown in the diagram. A known quantity of the oxalate was placed in a tared quartz boat and heated at known temperatures for known lengths of time in either a stream of air or nitrogen. The water and CO_2 were collected in the U-tubes A and B, which contained "anhydrone" and "carbosorb" respectively. The CO was oxidized to CO_2 by passing it over heated copper oxide and the resulting dioxide collected in traps C.

The nitrogen used in these experiments was first passed over heated reduced-copper turnings to remove oxygen and then through traps to remove any water or CO_2.

3. RESULTS AND DISCUSSION

(a) *Decomposition in Air*

Thorium oxalate dihydrate when heated in air at 270° readily loses its water of hydration. At a higher temperature, 320°, decomposition commences with evolution of CO and CO_2, the ratio moles of CO/moles of CO_2 being slightly greater than unity. After five hours at 320° the weight-loss was 23 per cent of the weight taken, whereas for complete conversion to ThO_2 the weight-loss would be 40·8 per cent. On further heating for sixteen hours at 420° the ratio of CO/CO_2 changed to approximately 0·3. The total amount of carbon now found, calculated from the total amounts of CO and CO_2 evolved, agreed with the theoretical value for C in the oxalate. However, the total mass of CO and CO_2 found exceeded the calculated value. This could be explained if

some C had been formed by the disproportionation of CO ($2CO \rightleftharpoons C + CO_2$); the carbon then being oxidized by the air-stream at 420° giving more CO and CO_2. In order to confirm the presence of free carbon and to prevent any ambiguity in the results due to the oxidation of CO to CO_2, it was decided to carry out further runs in an inert atmosphere, nitrogen.

(b) *Decomposition in Nitrogen* (see Table 1 and runs 2 and 3)

Again the water of hydration was readily removed at 270°, and at 320° the ratio CO/CO_2 was greater than unity. The weight-loss after heating at this temperature for twenty hours was 30 per cent. Evolution of CO then ceased, and at temperatures up to 500° only CO_2 was evolved. The weight-loss at this stage was 39·6 per cent. Even after heating at 500° for twenty-four hours and at 900° for some hours, the total carbon found was not equal to the calculated value. However, heating in an air-stream at 900° caused a further evolution of CO and CO_2, now making the total

VOL. 1 1955

TABLE 1

Temp.	Total moles H_2O per mole Th oxalate	Total moles CO_2 per mole Th oxalate	Total moles CO per mole Th oxalate	Total moles C per mole Th oxalate	Analysis of starting material
		RUN 2 (Nitrogen)			
325°	2·14	1·02	1·25	2·28	
350°		1·25	1·33	2·59	
400°		1·75	1·36	3·11	$Th(C_2O_4)_2 . 2·10\ H_2O$
500°		2·29	1·39	3·67	
900°		2·31	1·52	3·83	
900°*		2·40	1·74	4·13	
		RUN 3 (Nitrogen)			
320°	2·13	0·67	0·94	1·61	
338°		1·41	1·53	2·94	
420°		2·07	1·53	3·60	$Th(C_2O_4)_2 . 2·15\ H_2O$
500°		2·33	1·53	3·86	
900°		2·35	1·62	3·97	
900°*		2·51	1·62	4·13	
		RUN 5 (air)			
320°	2·06	0·78	1·13	1·91	$Th(C_2O_4)_2 . 2·06\ H_2O$
420°		2·51	1·62	4·13	

* Ignited in a current of air.

carbon found equal to the theoretical quantity. The amount of C evolved in this latter stage was 7 per cent of the total C present in the oxalate. It would appear, therefore, that free C is definitely present and as suggested above is probably formed by disproportionation of CO.

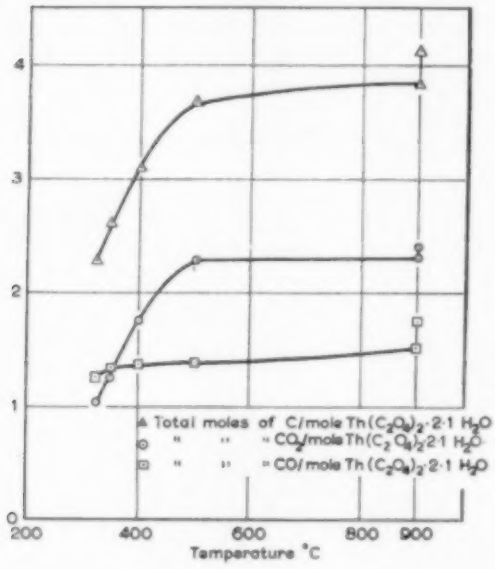

RUN 2.—Nitrogen.

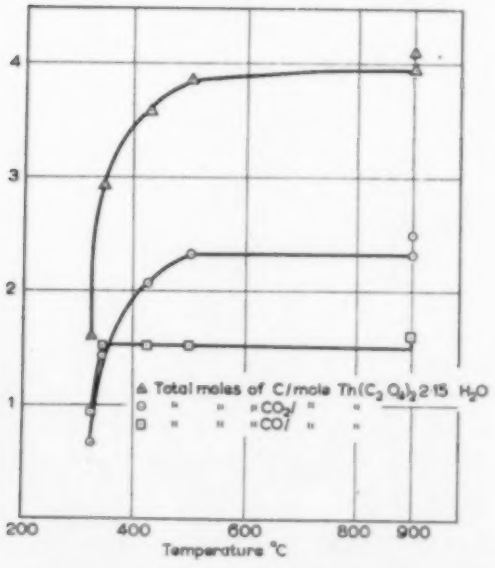

RUN 3.—Nitrogen.

Since the ratio CO/CO_2 is greater than unity, the degradations in air and in nitrogen both indicate that the decomposition reaction is not entirely of the form:

$$Th(C_2O_4)_2 \rightarrow ThO_2 + 2CO + 2CO_2$$

where equimolecular amounts of gaseous products would be expected. The results are consistent with either of two degradation processes. At 330° the oxalate can decompose either simultaneously to thoria and thorium carbonate according to the equation:

$$Th(C_2O_4)_2 \xrightarrow{330°} \begin{cases} ThO_2 + 2CO_2 + 2CO \\ Th(CO_3)_2 + 2CO \end{cases}$$
$$\downarrow$$
$$ThO_2 + 2CO_2$$

or solely to the carbonate. The carbonate then decomposes to thoria, but in either case the decomposition rate must be slower than the rate of formation, as the CO/CO_2 ratio is greater than unity. Above 330° the decomposition of the carbonate continues, as is indicated by the evolution solely of CO_2.

Further evidence in favour of carbonate formation was obtained by degrading a sample of oxalate as above, below 400°, and then analyzing the resulting light-brown product. The thorium oxalate found by permanganate titration was only 30 per cent of the amount that should have been present assuming no carbonate formation. The value of 30 per cent might also well be high, since the carbon formed, presumably by disproportionation of CO, would have a very small particle size and would probably be oxidized by the permanganate.

Thoria prepared at low temperatures ($< 400°$) by oxalate decomposition was hygroscopic. This would be expected from the small crystallite size shown by our X-ray photographs and the large surface area found by BECKETT and WINFIELD. After heating the thoria for some hours at 900° the crystallite size had increased and the water adsorption was correspondingly less. This annealing effect on water adsorption might well have caused the weight-loss of 2 per cent found by YATABE and POLLOCK on igniting thoria prepared at low temperatures. Our results further indicate that carbon could be present in the low-temperature product, which would again cause a weight-loss on ignition.

(c) *X-ray Analysis*

Diffraction photographs of samples heated in air and in nitrogen at temperatures about 350° showed only ThO_2 of small crystallite size. This is not in agreement with BECKETT and WINFIELD, who found a cubic pattern occurring with the thoria. They claimed that this cubic phase persisted even at 800°, but with a decreased intensity.

4. CONCLUSION

Thorium oxalate dihydrate readily loses its water of hydration at 270°. Decomposition of the oxalate occurs at 330° with either simultaneous formation of ThO_2 and $Th(CO_3)_2$ or formation solely of the carbonate. The rate of decomposition of the carbonate to ThO_2 is apparently slightly slower than its rate of formation. Our results, which indicate carbonate formation as an intermediate step in the degradation

VOL. 1 1955

of the oxalate, are compatible with those of BECKETT and WINFIELD. Although all the results could be formally explained by formation of an intermediary compound $ThO_2C_2O_4$, as suggested by GÜNTHER and REHÄAG (1938) the existence of such a compound $ThO_2C_2O_4$ is improbable. (The O_2 again represents a peroxide grouping.)

The thoria prepared at low temperatures ($< 400°$) is of small crystallite size and is hygroscopic.

ACKNOWLEDGMENTS

The authors thank Professor J. S. ANDERSON, F.R.S., for discussion.

REFERENCES

BECKETT, R., and WINFIELD, M. E. (1951) *Australian J. Scient. Res.*, **4**, 644.

GÜNTHER, P. L., and REHÄAG, H. (1938) *Ber.*, **71B**, 1771.

SCHOELLER, W. R., and POWELL, A. R. (1940) *The Analysis of Minerals and Ores of the Rarer Elements* (Griffin and Co., Ltd., London).

YATABE, E., and POLLOCK, L. I. (1952) *Atomic Energy of Canada Ltd.*, CEI-49.

J. Inorganic and Nuclear Chemistry, 1955, Vol. 1, pp. 149–158. Pergamon Press Ltd., London

CHEMICAL EFFECTS IN FISSION PRODUCT RECOIL

By G. N. WALTON and I. F. CROALL
Atomic Energy Research Establishment, Harwell, Didcot, Berks

(*Received November* 1954)

Abstract—Some measurements of I^{131} arising after fission recoil from uranium oxide particles into a surrounding medium of solid potassium iodate show that:

1. The fraction of recoils stopping in the iodate phase increases as the relative amount of iodate to oxide increases.
2. The amount of chemical decomposition in the iodate phase is proportional to the number of fission recoils stopping in the iodate phase. The "G" factor under the conditions in question lies between 2 and 6 molecules of iodate reduced per 100 eV of recoil energy absorbed.
3. The specific activity of the reduced forms of iodine (I_2, I^-) remains fairly constant, whatever the extent of fission, and is always higher than the specific activity of the oxidized form (IO_3^-). Approximately 90 per cent of the I^{131} is retained in the oxidized form.

VOL.
1
1955

INTRODUCTION

SOME studies have been reported on the valency state of elements found after fission (STANLEY and DAVIES, 1951; BURGUS and DAVIES, 1951), but the only observation that appears to have been published on the chemical effect of fission recoil itself, is that large amounts of residual organic matter are decomposed in graphite into which fission fragments recoil (SANGSTER and WRIGHT, 1952).

The chemical state of elements formed in fission might be expected to be linked with the radiation decomposition of the medium in which they are absorbed, i.e., the process may be considered as a reaction between the fission product and its surroundings. In default of information by which preliminary experiments could be planned to illustrate this, a system was chosen in which a wide variety of observations could be made by fairly simple and rapid techniques. It was decided to study the fate of fission-product iodine produced after recoil into potassium iodate. The exchange behaviour of iodine amongst its various valency states is known (BURGUS and DAVIES, 1951; MYERS and KENNEDY, 1950), and its active forms are readily purified and characterized.

Uranium oxide, as a source of fission products, was ground with potassium iodate to form a fine powder and irradiated in BEPO for about twelve hours. The resulting mixture of fission products and iodate decomposition products was then extracted with carbon tetrachloride and water. The activity of the iodine occurring as molecular iodine, as iodide, and as unchanged iodate, was measured.

In the initial experiments attempts were made to study the proportions of the different short-lived iodine isotopes, but, as pointed out by BURGUS and DAVIES (1951), these grow at different times from their parent telluriums, and cannot readily be compared with each other. In subsequent irradiations the irradiation tubes were therefore not opened until only 8-day I^{131} remained of the active isotopes.

The only variables in the different experiments were the amounts of potassium iodate and uranium oxide used, and the pile flux.

EXPERIMENTAL

A.R.-grade black uranium oxide and potassium iodate, kept dry in silica gel desiccators, were weighed out and ground up together in a small mortar to a freely-running uniform grey powder. The irradiation vessels consisted of silica tubes 15 cm long by 2 cm diameter, with stoppers ground to the external surface so that grease was isolated from the contents of the tube. The vessels were irradiated inside 10-in. aluminium cans in vertical BEPO experimental holes in a flux of the order $1{\cdot}6 \times 10^{12}$n/cm^2/sec. After cooling for three weeks the vessels were unstoppered and immediately closed and inverted behind shielding in the apparatus shown in Fig. 1,

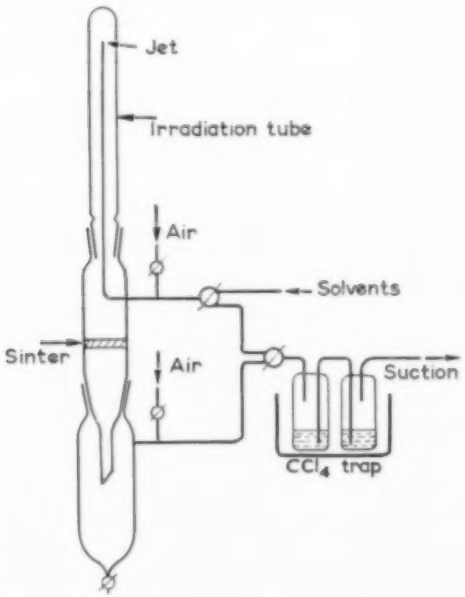

FIG. 1.—Extraction apparatus.

by means of which the contents could be extracted by solvents without further exposure. Free condensed iodine was visible on the walls of the unopened tubes in which the fission rate had been high, and this was extracted with carbon tetrachloride before the admission of water. On wetting the iodate there was considerable effervescence similar to that observed in the radiation decomposition of nitrates and chlorates (HEANIG *et al.*, 1953). The uranium oxide sludge collected on the sintered glass disc, where it was stirred by the suction of air through the sinter, and the solvents containing the iodate and its decomposition products were run off through the filter. The carbon tetrachloride traps, cooled to 0°C, at which the vapour pressure of iodine is very low, were used to detect any iodine activity carried over. In all cases this was negligible, and the solvents were eventually added to the main fractions. Dissolution was continued until no remaining iodate could be detected in the washings. The carbon tetrachloride layer was separated, washed, and made up to 100 ml, and the aqueous layer to 250 ml.

Estimation of Free Iodine

20 ml of the carbon tetrachloride containing the free iodine were titrated direct with aqueous sodium thiosulphate, using acid potassium iodide (iodine-free), and starch indicator (STONE, 1954). A further aliquot was radiochemically purified by repeatedly extracting the iodine with sulphur dioxide into water and back into carbon tetrachloride with nitrous acid (CAMPBELL and BRADY, 1951). After three cycles in which care was taken not to allow the interfaces between solvent and aqueous layers to be carried through, the activity of the iodine showed only an 8-day decay to less than 1 per cent of the initial count. After counting, the iodine was again titrated so as to give the chemical yield of the purification process. The counters used were halogen-filled liquid counters, type M6H CF, made by 20th Century Electronics Ltd. They were calibrated by converting the iodine to silver iodide, which was mounted as a thin film in a 4-π counter. The counting rates of the liquid samples were corrected for background, chemical yield, and decay from the time of removal of the sample from the pile.

VOL. 1 1955

Estimation of Iodide

The aqueous iodate solution was acidified to release iodine equivalent to that present as iodide or as other reduced forms. This was again extracted with carbon tetrachloride, titrated and counted as described above. Care was taken that the organic layer was washed completely free of traces of iodate.

The activity of the original iodide was estimated, knowing (PERLMAN *et al.*, 1941) that one-sixth of the iodine measured came from the original iodate according to the equation:

$$5I^- + IO_3^- + 6H^+ \rightarrow 3I_2 + 3H_2O.$$

As the specific activity of the iodate was relatively low, this involved only a small correction.

The rate of exchange of iodide and free iodine with iodate in solution is mainly dependent on the hydrogen-ion concentration (MYERS and KENNEDY, 1950), and as this was low there would be little opportunity for isotopic exchange. Exchange, however, could occur between iodide and some of the iodine, because not all the latter was extracted with carbon tetrachloride before dissolution of the iodate and iodide in water.

Estimation of Iodate

2 ml of the iodate solution were diluted and reduced to the iodide with sulphur dioxide gas. Excess gas was boiled out and the iodine extracted into carbon tetrachloride with nitrous acid. This was titrated and counted as before. Any periodate present was estimated as iodate. The correction involved in the release of iodine in the original acidification was negligible.

RESULTS

Table 1 shows the results. In each batch the tubes were irradiated together in the same pile position for the same time and therefore received approximately the same neutron dose. In blank runs, potassium iodate irradiated for twelve hours in the absence of uranium oxide showed no detectable decomposition by the methods

TABLE 1.—RESULTS

Original contents of tube			Products in soluble phase						Iodine recovery (%)
			I as I_2		I as I^-		I as IO_3^-		
Batch	Wt. of U_3O_8 (g)	Wt. of KIO_3 (g)	Wt. (mg)	Activity dpm $\times 10^5$	Wt. (mg)	Activity dpm $\times 10^6$	Wt. (g)	Activity dpm $\times 10^7$	
1	0·285	3·940	2	6·75	11	3·14	2·295	3·33	98·6
	0·019	3·963	0·2	0·81	0·9	0·47	2·285	0·47	97·3
	0·067	2·317	0·8	2·54	3·5	0·64	1·352	0·96	98·6
	0·273	1·354	1·8	4·58	11·6	2·03	0·786	3·25	99·2
	0·989	1·021	3·2	11·3	28	3·29	0·552	7·00	96·2
2	0·406	3·975	3·3	17·6	71·2	32·7	2·280	15·7	99·8
	1·996	4·003	6·4	40·3	275	117	2·061	71·5	98·4
3	0·349	2·987	3·8	9·71	56·5	24·5	1·670	17·0	97·6
	1·070	3·518	3·5	20·8	168	65·3	1·892	37·6	98·9
4	1·004	3·747*	2·2	14·0	102	27·3	2·085	23·8	98·6
	1·002	3·743	8·2	57·1	111	43·5	2·050	27·0	97·7
5	0·519	8·875	3·6	20·6	88	22·6	5·080	26·5	98·3
	3·989	0·505	5·9	80	59·5	75·2	0·217	19·1	94·4
6	0·463	4·089	9·6	7·9	80	24·4	2·341	23·2	100·3
	0·462	4·086	12·8	8·6	84	25·6	2·365	23·5	101·6

* Components not ground together.

described, nor was any I^{131} activity detected above background. Mixtures of potassium iodate and uranium oxide maintained at 100°C for twelve hours and extracted without irradiation, similarly showed no decomposition.

Attempts were made in the initial experiments to devise a method of drawing an iodine activity balance analogous to the mass balance shown in the last column of Table 1. Owing to the absorption of neutrons in the varying mass of the potassium iodate, the activity of cobalt foils simultaneously irradiated with the samples did not give a true measure of the total amount of fission. Analyses for another fission product, Ba^{140}, were also carried out, but the barium activity extracted with the aqueous solution of iodate was relatively less than that corresponding to the I^{131}, after allowing for the different fission yields. On the supposition that insoluble barium iodate remained adsorbed on the uranium oxide, the latter was washed with 0·01N nitric acid. This dissolved off the Ba^{140} in amounts corresponding to the I^{131} found in the iodate, but a small amount of uranium was also dissolved, and no precision was possible. Interpretation of the results therefore rests on the supposition that all the I^{131} that was released from the uranium oxide exchanged with the various forms of inactive iodine that were analyzed.

DISCUSSION

The Release of Fission Fragments

In any given batch there is no proportionality between the total amount of I^{131} found outside the uranium oxide and the amount of uranium. Table 2 shows qualitatively that for each batch the amount escaping from the oxide increases with

increasing concentration of iodate phase, i.e., the more potassium iodate present, the more is a fission fragment likely to come to rest in it. Similar observations have been made by JORDAN for *np*-recoil effects in irradiated pastes (JORDAN, 1951). The stopping power of a medium for the major portion of the range of fission fragments is proportional to the electron density (BOHR, 1941), and column 2 of Table 2 is

TABLE 2.—FRACTION OF RECOILS STOPPING IN IODATE PHASE

Batch	Concentration of potassium iodate in total contents of tube (corrected for electron density)	Atoms of I^{131} recoiling into iodate phase per gram of oxide phase
1	99%	$4{\cdot}6 \times 10^{12}$
	94	2·6
	86·5	2·2
	69·7	2·2
	32·4	1·3
2	82·0	8·0
	48·2	7·0
3	79·8	9·9
	60·4	7·0
4	63·4*	4·5
	63·4	5·4
5	88·5	9·3
	5·5	1·2
6	80·4	9·3
	80·4	9·4

* Components not ground together.

therefore expressed in electron density units. If m_1 is the mass, and Z_1 the average atomic number per unit mass of component 1, then the electron concentration C of component 1 in a mixture of components 1 and 2 is given by:

$$C = \frac{m_1 Z_1}{m_1 Z_1 + m_2 Z_2}$$

The average atomic number per unit mass, Z, of a compound is given by:

$$Z = \sum \frac{nAZ_A}{M}$$

where n is the number of atoms of atomic weight A and atomic number Z_A in a molecule of molecular weight M.

Chemical Effect of Fission Recoils

In Fig. 2 the total number of reduced iodine atoms found in each tube ($I_2 + I^-$) is plotted against the total number of I^{131} atoms found outside the oxide phase, to show an approximately linear relationship over a wide range. This holds for very different conditions. For instance, in Batch 4 the iodate phase in the tube in which

the components were ground together had more activity, and also showed correspondingly more decomposition than the tube in which the same weights of components were merely mixed. In the two tubes of Batch 5 the ratio of uranium to iodate varied by a factor of 134, and yet the decomposition per fission fragment only differs by a factor 1·3, being low for the tube containing most uranium.

From Fig. 2 the number of atoms of reduced iodine formed per atom of I^{131} is $1{\cdot}0 \times 10^8$. This enables an estimate to be made of the "G" factor for iodate decomposition by fission-fragment energy, assuming one iodate ion decomposes for every reduced iodine atom found. The range in air (KATCOFF *et al.*, 1948), and in aluminium (SUZOR, 1948; FINKLE *et al.*, 1951), for fission fragments shows extensive straggling according to the different masses, but mass number 131, being near the

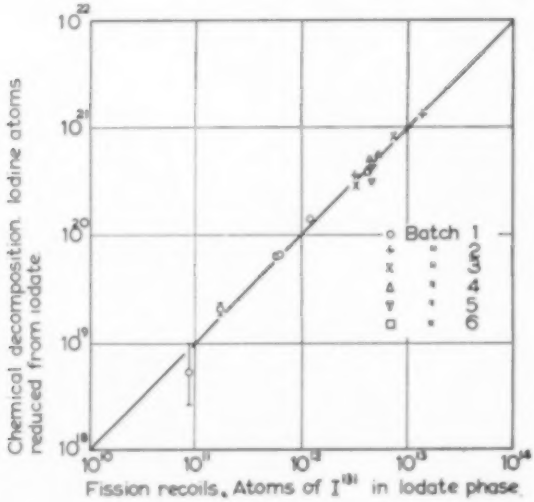

FIG. 2.—Iodate decomposition and iodine activity.

middle of the fission-product series, may be taken as representative of the others as an approximation. The fission yield of mass number 131 is 3·0 per cent (YAFFE *et al.*, 1953), and the molecular decomposition of iodate per fission is therefore 3×10^6 molecules/fission.

The mean range of fission recoils in uranium metal has been reported to be 4·3 microns (OZEROFF, 1949). The uranium oxide used in these experiments consisted of irregular masses 10 to 50 microns in diameter, and there is therefore much uncertainty in considering how the recoil energy is distributed between the oxide and iodate phases. However, this may be calculated for limiting cases. According to the BOHR theory (BOHR, 1941), the energy of fission recoils is lost over the major part of the range by ionization, and only at the end of the range by nuclear collisions. For the first part of the track the ionization per unit-length of track dE/dR is linearly related to the residual range R. For the purposes of our calculation a satisfactory approximation is

$$dE/dR = 2aR$$

where a is a constant, whence

$$E = aR^2 \qquad (1)$$

Using this approximation, the energy of monoenergetic particles escaping from a flat uranium oxide surface in all directions from the interior (neglecting scattering) is distributed in such a way that one-third is absorbed in the surroundings (see Appendix). If the exponent of R in equation 1 is less than 2, as suggested by the work on tracks in photographic emulsions by MATHIEU and DEMERS (1953), this fraction is greater. For recoil atoms escaping from the convex surfaces of small particles the fraction would also be greater, but cannot be greater than unity. If each fission which produces fragments coming to rest in the iodate phase releases 162 MeV of kinetic energy, one-third of which is absorbed in the iodate to decompose 3×10^6 molecules, the "G" factor would be 5·6 molecules per 100 eV absorbed. If all the 162 MeV is absorbed in the iodate phase, the "G" factor is 1·9 molecules/100 eV, and the true value will be expected to lie between these extremes.

VOL. 1 1955

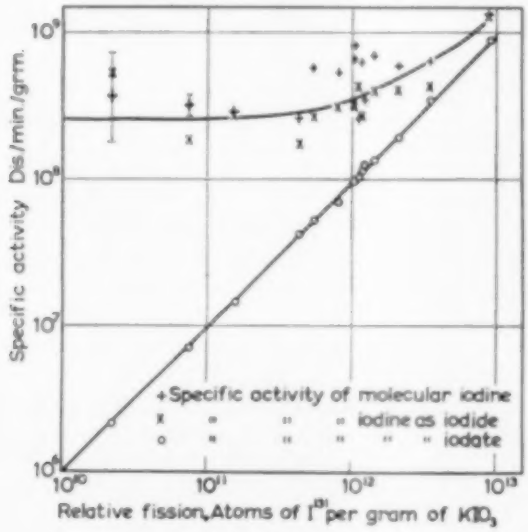

FIG. 3.—Relative specific activity.

"G" values for the decomposition of iodate by photons or light particles do not appear to have been measured. The value for solid potassium chlorate decomposition by pile-neutron irradiation has been reported to lie between 2·0 to 3·0 molecules O_2/100 eV (HEANIG *et al.*, 1953).

The Specific Activity of the Iodine

If the I^{131} were equally distributed throughout all the inactive iodine in the tube, the specific activity of each iodine species would be the same. In Fig. 3 the specific activity observed for each species is plotted against that expected if such complete exchange had taken place. This shows that while the specific activity of the iodine in the iodate varies over a wide range (according to the relative amounts of I^{131} and inactive iodine present), the specific activities of the molecular iodine and iodide remain within a relatively small range. Similar behaviour was observed by BOYD (1952) in his experiments on the neutron irradiation of solid potassium bromate,

where the rate of formation of decomposition products was proportional to the rate of radiobromine formation.

Fission product I^{131} is the daughter of Te^{131}. STANLEY and DAVIES (1951) show that all tellurium formed in fission appears as $TeO_3^{=}$ or $TeO_4^{=}$ after dissolution in water, and these might be expected to be the forms in an iodate medium. WILLIAMS (1951) gives evidence to suggest that in the isomeric transitions that occur in tellurium decay, the atoms which undergo internal conversion of the γ-ray leave the molecule in which they are combined, while those which are not internally converted stay unchanged. This process could result in a constant proportion p of the X atoms of I^{131} present being released from the oxidized state. If, as has been shown above, the number of molecules n of iodate reduced is proportional to X, i.e.,

$$n = kX \tag{2}$$

the specific activity s of the reduced forms will be

$$s = \frac{pX}{n}$$

therefore, from equation 2,

$$s = \frac{p}{k}$$

which is independent of X as observed (to a first-order approximation). From Fig. 2, $k = 1{\cdot}0 \times 10^8$, and from Fig. 3 (converting from disintegrations/min/gram to atoms of I^{131} per atom of inactive iodine) $s \simeq 1{\cdot}1 \times 10^{-9}$, whence $p = 11$ per cent. This value is too small for the internal conversion coefficient, and it is concluded that at least some of the I^{131} in the iodate must have arrived by exchange with the reduced forms.

A similar situation has been observed by BOYD (1952) in the solid bromates, where the active bromine turned out of bromate by the $n\gamma$-reaction was induced to return to the bromate ion form by heating and by γ-irradiation. WILLIAMS (1952) has also observed the same effect for solid sodium iodate irradiated by neutrons. The maximum retention observed in the latter case was 90 per cent, and in the experiments reported here the retention is also about 90 per cent.

If the specific activity of the reduced forms s_R is greater than that of the oxidized form s_0, any effect which promotes isotopic exchange will cause the specific activity of the oxidized form to increase and give rise to apparent retention, i.e., after the exchange of a fraction x of the atoms between the reduced and oxidized forms, the new specific activity of the oxidized form s_0' is given by:

$$s_0' = s_0(1 - x) + xs_R$$

and if $s_R > s_0$

then $s_0' > s_0$

No special oxidizing back reaction therefore need be postulated. The dislocating effect of fission recoil at track ends may be expected to create the conditions for isotopic exchange, and may have contributed to the high apparent retention observed.

In Fig. 3 the specific activity of the iodide is seen to lie in nearly all cases between those of the iodine, which is always the highest, and the iodate. This suggests that

I^{131} must first arise as iodine, and subsequently distribute itself between a small amount of iodide and a large amount of iodate. If the I^{131} arose initially as iodate which then chemically decomposed, there is no way by which the products could become enriched in I^{131}.

REFERENCES

BOHR, N. (1941) *Phys. Rev.*, **59**, 272.

BOYD, G. E., COBBLE, J. W., and WEXLER, S. (1952) *J. Amer. Chem. Soc.*, **74**, 237.

BURGUS, W. H., and DAVIES, T. H. (1951) N.N.E.S. Vol. IV, 9, *The Fission Products*, Paper 19 (McGraw-Hill, New York).

CAMPBELL, G. W., and BRADY, E. L. (1951) N.N.E.S Vol IV, 9, *The Fission Products*, Paper 277 (McGraw-Hill, New York)

CLEARY, R. E., HAMILL, W. H., and WILLIAMS, R. R. (1952) *J. Amer. Chem. Soc.*, **74**, 4675.

FINKLE, B., HOAGLAND, E. J., KATCOFF, S., and SUGARMAN, N. (1951) N.N.E.S. Vol. IV, 9, *The Fission Products*, Papers 45 and 46 (McGraw-Hill, New York).

HEANIG, G., LEES, R., and MATHESON, M. S. (1953) *J. Chem. Phys.*, **21**(4), 665.

JORDAN, P. (1951) *J. Chim. Phys.*, **48**, 179.

KATCOFF, S., MIRKEL, J. A., and STANLEY, C. W. (1948) *Phys. Rev.*, **74**, 631.

MATHIEU, R., and DEMERS, P. (1953) *Can. J. Phys.*, **31**, 97.

MYERS, O. E., and KENNEDY, J. W. (1950) *J. Amer. Chem. Soc.*, **72**, 897.

OZEROFF, L. (1949) AECD, 2973.

PERLMAN, I., MORTON, M. E., and CHAIKOFF, I. L. (1941) *J. Biol. Chem.*, **139**, 433.

SANGSTER, D. F., and WRIGHT, J. (1952) *Nature*, **30**, 368.

STANLEY, C. W., and DAVIES, T. H. (1951) N.N.E.S. Vol. IV, 9, *The Fission Products*, Paper 18 (McGraw-Hill, New York).

STONE, K. G. (1954) *Analyt. Chem.*, **26**, 396.

SUZOR, F. (1948) *C.R. Acad. Sci., Paris*, **226**, 1081.

WILLIAMS, R. R. (1951) N.N.E.S. Vol. IV, 9, *The Fission Products*, Paper 20 (McGraw-Hill, New York).

YAFFE, L. *et al.* (1953) *Can. J. Chem.*, **31**, 120.

VOL. 1 1955

APPENDIX

Distribution of Recoil Energy between Fissile Material and Surroundings

From any point in the fissile material the chance of a recoil atom moving off in the angle increment $\delta\varphi$ in the plane of the surface, and $\delta\theta$ from the normal to the surface, is $\sin\theta\,\delta\varphi\,\delta\theta/4\pi$. The number of fissions in a thin layer of unit area δx cm thick parallel to the surface is $c\delta x$, where c is the number of fissions/cm^3 in the material. The number of recoils δN moving in the solid angle increment is therefore

$$\delta N = c \sin\theta\,\delta x\,\delta\theta\,\delta\varphi/4\pi \tag{1}$$

From Fig. A1 only the recoils of range R_0 within the angle $\cos^{-1} x/R_0$ to the normal will escape from the surface. The total number N of the recoils escaping from the surface is then

$$N = \frac{c}{4\pi}\int_{x=0}^{x=R_0}\int_{\theta=0}^{\theta=\cos^{-1}\frac{x}{R_0}}\int_{\varphi=0}^{\varphi=2\pi}\sin\theta\,dx\,d\theta\,d\varphi$$

$$= \frac{R_0 c}{4} \tag{2}$$

The residual range R when a recoil atom escapes from the surface is from Fig. A1,

$$R = R_0 - x/\cos\theta$$

Using the approximation for the relation between energy E and residual range for each recoil atom

$$E = aR^2 \tag{3}$$

where a is a constant for the material in which the recoil originates, the total energy

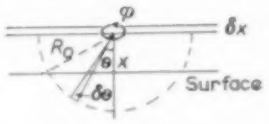

FIG. A1.

E_s expended by all the recoils after escaping from the surface into the surroundings is derived as for equation 1:

$$E_s = \frac{ca}{4\pi} \int_{x=0}^{x=R_0} \int_{\theta=0}^{\theta=\cos^{-1}\frac{x}{R_0}} \int_{\varphi=0}^{\varphi=2\pi} (R_0 - x/\cos\theta)^2 \sin\theta \, dx \, d\theta \, d\varphi$$

$$= \frac{ca\,R_0^3}{12}$$

The total original energy E_0 of the recoils leaving the surface is

$$E_0 = NaR_0^2$$

Hence from (2)

$$E_s/E_0 = \tfrac{1}{3}.$$

J. Inorganic and Nuclear Chemistry, 1955, Vol. 1, pp. 159–162. Pergamon Press Ltd., London

THE HOMOGENEOUS EXCHANGE REACTION BETWEEN MONOVALENT AND TRIVALENT THALLIUM

By F. J. C. Rossotti
Department of Inorganic Chemistry, Royal Institute of Technology,
Stockholm 70, Sweden

(*Received* 13 *November* 1954)

Abstract—Re-examination of the kinetic data on the Tl(I)—Tl(III) exchange, in the light of recent results on Tl(III) hydrolysis, indicates that both the Tl^{3+} and $Tl(OH)^{2+}$ ions play a significant part, the specific rate constants being 0·154 and 1·22 litre/mole/sec respectively.

VOL. 1 1955

The kinetics of the homogeneous exchange reaction between monovalent and trivalent thallium in sodium perchlorate-perchloric acid media have been found to be first-order with respect to the total concentrations of thallium, [Tl(I)], [Tl(III)], in each valency state (Prestwood and Wahl, 1949; Harbottle and Dodson, 1951). Although the results obtained by the different investigators under the same conditions are in good quantitative agreement (Dodson, 1953), widely different interpretations of the measurements have been made (Prestwood and Wahl, 1949; Harbottle and Dodson, 1951). Independent data for the hydrolysis of trivalent thallium (Biedermann, 1953) permit of a choice between the two interpretations (cf. Dodson, 1953, and Amphlett, 1954).

Monovalent thallium may be considered to be completely unhydrolyzed (Bell and George, 1953). If the stoichiometric hydrolysis constants of trivalent thallium be represented by

$$\kappa_n = [Tl(OH)_n^{(3-n)+}]\,[H^+]^n/[Tl^{3+}] \qquad (1)$$

where $\kappa_0 = 1$, the degree of formation, α_n, of the thallic species, $Tl(OH)_n^{(3-n)+}$, is given by:

$$\alpha_n = [Tl(OH)_n^{(3-n)+}]/[Tl(III)] \qquad (2a)$$

$$= \kappa_n[H^+]^{-n}/\sum_0^n \kappa_n[H^+]^{-n} \qquad (2b)$$

With the aid of values of $\kappa_1 = 0{\cdot}073$M, and $\kappa_2 = 2{\cdot}375 \times 10^{-3}$M² obtained by Biedermann (1953) at 25°C in a 3M sodium perchlorate medium, the proportions of the various thallic species have been calculated at some acidities used in the exchange experiments (Prestwood and Wahl, 1949), and are given below. The species $Tl(OH)_3$ was not detected in solution so that $n \leqslant 2$.

Table 1.—Percentages of species $Tl(OH)_n^{(3-n)+}$ at 25°C in a 3M perchlorate medium

H^+	Tl^{3+} $100\alpha_0$	$TlOH^{2+}$ $100\alpha_1$	$Tl(OH)_2^+$ $100\alpha_2$
0·8	91·33	8·33	0·34
1·5	95·26	4·64	0·10
2·5	97·13	2·84	0·04

The overall rate of exchange, R, may be expressed as

$$R = [\mathrm{Tl(I)}] \sum_{0}^{2} k_n [\mathrm{Tl(OH)}_n^{(3-n)+}] \tag{3}$$

where k_n is the specific rate constant for the bimolecular exchange of the hydrated thallous ion with the thallic species $\mathrm{Tl(OH)}_n^{(3-n)+}$. The overall specific-rate constant is defined by:

$$k = R/[\mathrm{Tl(I)}]\,[\mathrm{Tl(III)}] \tag{4}$$

By substituting from equations (2a) and (3) into (4), the general form of this equation is obtained:

$$k = \sum_{0}^{2} k_n \alpha_n \tag{5}$$

Hence from (2b)

$$k \sum_{0}^{2} \kappa_n [\mathrm{H^+}]^{-n} = \sum_{0}^{2} k_n \kappa_n [\mathrm{H^+}]^{-n} \tag{6}$$

If corresponding values of k and $[\mathrm{H^+}]$ are known from exchange data, and the values of κ_n from equilibrium data, the left-hand side of equation (6) is known, so that, in principle, n equations of this form may be solved for the n specific rate constants by the use of determinants. Alternatively, a graphical method of solution may be used. In the latter manner, BIEDERMANN's (1953) values of the hydrolysis constants, and PRESTWOOD and WAHL's (1949) values of k and $[\mathrm{H^+}]$, referring to exchange at 24·9°C in a 3·68M perchlorate medium were correlated. The value of the product $k_2\kappa_2$ obtained as the intercept of the plot of $k \sum_{0}^{2} \kappa_n [\mathrm{H^+}]^{2-n}$ against $[\mathrm{H^+}]$ could not be distinguished from zero. Under these circumstances, equation (6) may be simplified to

$$k(1 + \kappa_1[\mathrm{H^+}]^{-1} + \kappa_2[\mathrm{H^+}]^{-2}) = k_0 + k_1\kappa_1[\mathrm{H^+}]^{-1} \tag{7}$$

and the left-hand side of equation (7) plotted against $[\mathrm{H^+}]^{-1}$. In this manner, the equation

$$k(1 + 0{\cdot}073[\mathrm{H^+}]^{-1} + 0{\cdot}002375[\mathrm{H^+}]^{-2}) = 0{\cdot}088[\mathrm{H^+}]^{-1} + 0{\cdot}154 \pm 0{\cdot}005 \tag{7a}$$

has been obtained by a least-squares treatment. From the slope and intercept of the straight line, values of the specific-rate constants $k_0 = 0{\cdot}154$ and $k_1 = 1{\cdot}22$ litre/mole/sec have been obtained. Equation (5) may be rewritten in the form:

$$k = 0{\cdot}154\alpha_0 + 1{\cdot}22\alpha_1, \tag{8}$$

whence it appears that the participation of the first hydrolysis product, $\mathrm{Tl(OH)^{2+}}$, in the observed exchange decreases from approximately 40 per cent in 1M perchloric acid to approximately 20 per cent in 3M perchloric acid. However, as the second hydrolysis product, $\mathrm{Tl(OH)_2^+}$, formed an insignificant fraction of the total trivalent thallium in the exchange experiments (cf. Table 1), the possibility that this species participates in the reaction cannot be eliminated, and it is possible that the value of k_2 is of the same order as those of k_0 and k_1. Further data for the exchange reaction at lower acidities would be of considerable value.

It is of interest to compare the present results with interpretations of the exchange reaction which were made at a time when the hydrolysis constants of trivalent thallium

were not known. (It should be noted that the subscripts of specific-rate constants used in the present communication differ from those used by other authors.) PRESTWOOD and WAHL (1949) assumed that both the thallic species Tl^{3+} and $Tl(OH)^{2+}$ exchanged at comparable rates, and that hydrolysis was small. Under these conditions ($[H^+] \gg \kappa_1$), equation (6) may be further simplified to

$$k = k_0 + k_1\kappa_1[H^+]^{-1} \tag{9}$$

so that values of k_0 and the product $k_1\kappa_1$ may be obtained from a plot of k against $[H^+]^{-1}$. The equation of the form (9) now obtained by subjecting the exchange data at 24·9°C to a least-squares treatment is

$$k = 0{\cdot}157 + 0{\cdot}0685[H^+]^{-1} \tag{9a}$$

The two functions represented by equations (7a) and (9a) are plotted in Fig. 1.

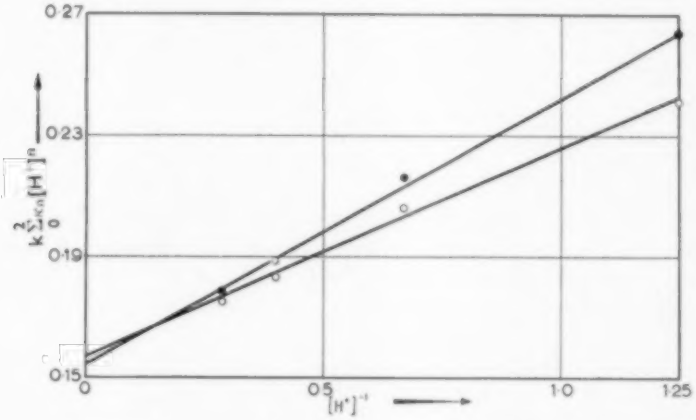

FIG. 1.—Correlation of data for exchange reaction of Tl(I) and Tl(III) with hydrolysis constants of Tl(III).
● $n \leqslant 2$, cf. equation (7a).
○ $n = 0$, cf. equation (9a).

The increasing divergence of the two lines as $[H^+]^{-1}$ increases, emphasizes the importance of the terms neglected in equation (9). The value of k_0 obtained from the approximate equation (9a) is in good agreement with the present value, but the product $k_1\kappa_1$ is underestimated by some 23 per cent, owing to the neglect of the hydrolysis constants on the left-hand side of equation (6). However, the present case must represent an extreme example of the error introduced into an estimate of specific-rate constants by using equation (9), as the thallic ion is hydrolyzed to a greater extent than most other cations which undergo exchange reactions. (See MATTOCK, 1954, for a list of hydrolysis constants.)

If exchange data were available at lower acidities than 0·8M in a 3M perchlorate medium at 25°C, the plot of k against $[H^+]^{-1}$ would probably become convex to the $[H^+]^{-1}$ axis. Such a curvature was shown by the data of HARBOTTLE and DODSON (1951), referring to a 6M medium. However, these investigators rejected the hypotheses made by PRESTWOOD and WAHL, and assumed that the exchange of the hydrated thallic ion was negligible, but that its hydrolysis was considerable. Under these conditions ($k_1 \gg k_0$), equation (6) may be reduced to the form:

$$1/k = [H]/k_1\kappa_1 + 1/k_1 \tag{10}$$

The straight lines obtained as plots of $1/k$ against $[H^+]$ appeared to support these assumptions, but the values of κ_1 so obtained range from 2·8 at 18°C to 5·5 — 10 at 50°C (HARBOTTLE and DODSON, 1951; DODSON, 1953). Although the approximate activity factor, $\gamma^3_{\pm 2-1} \cdot \gamma^2_{\pm 1-1}/\gamma^4_{\pm 3-1}$, of the thermodynamic constant $\kappa_1\gamma'_{Tl(OH)^{2+}} \cdot \gamma'_{H^+}/\gamma'_{Tl^{3+}}$, may be expected to decrease somewhat with increasing ionic strength (cf. DODSON, 1953), it does not seem likely that the stoicheiometric hydrolysis constant at 25°C can increase from a value of 0·073 at an ionic strength of 3M to a value of 3·2 at an ionic strength of 6M. Hence the present treatment suggests that the assumptions of PRESTWOOD and WAHL are substantially correct.

It has generally been assumed that the activity coefficients of the reactants do not alter when sodium ions are replaced by hydrogen ions in the perchlorate medium. Although BIEDERMANN and SILLÉN (1953) have shown that a 20 per cent replacement of sodium by hydrogen ions in a 3M sodium perchlorate medium has a negligible effect on the activity coefficients of cationic reactants, the much larger replacements ($\leqslant$ 95 per cent) used in the exchange experiments must have an appreciable effect. It would appear that the magnitude of this effect is comparable with the magnitude of the variations observed in the overall specific rate constant, so that extreme caution is required in the interpretation of kinetic data in the absence of equilibrium data.

ACKNOWLEDGMENTS

The author thanks Professor L. G. SILLÉN for helpful comments on the manuscript, and the Swedish Natural Science Research Council for financial support.

REFERENCES

AMPHLETT, C. B. (1954) *Quarterly Reviews*, **8**, 219.
BELL, R. P., and GEORGE, J. H. B. (1953) *Trans. Faraday Soc.*, **49**, 619.
BIEDERMANN, G. (1953) *Arkiv Kemi*, **5**, 441.
BIEDERMANN, G., and SILLÉN, L. G. (1953) *Arkiv Kemi*, **5**, 425.
DODSON, R. (1953) *J. Amer. Chem. Soc.*, **75**, 1795.
HARBOTTLE, G., and DODSON, R. (1951) *J. Amer. Chem. Soc.*, **73**, 2442.
MATTOCK, G. (1954) *Acta Chem. Scand.*, **8**, 777.
PRESTWOOD, R., and WAHL, A. (1949) *J. Amer. Chem. Soc.*, **71**, 3137.

VOL.
1
1955

LETTER TO THE EDITORS

The Rapid Separation of Rare-earth Fission Products by Cation Exchange, using Lactic-acid Eluant

FREILING and BUNNEY (1954) have reported the separation of the uranium fission-product rare earths by cation exchange, using lactic-acid eluant of constant *p*H, but varying concentration. With 20-mg quantities of Ce, Pr, Nd, and Sm carriers, a separation of Y, Tb, Gd, Eu, Sm, Pm, Nd, Pr, Ce, and La was obtained in forty-nine hours. The purpose of this investigation was to develop a procedure which would separate these fission products in about four hours or less, when half-lives of greater than about one hour should be detectable. Only Y, Eu, Sm, Pm, Nd, and Pr need to be separated, since Ce can be separated much more quickly by oxidation, and La activities may be grown from Ba.

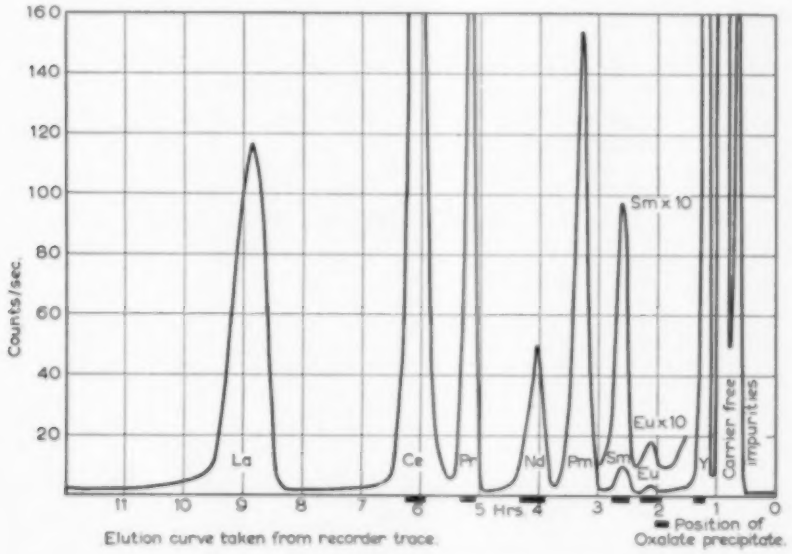

FIG. 1.—Elution curve taken from recorder trace.

Columns of 3–4 mm inside diameter, 20–30 cm long, heated to 87°C, surmounted by a pre-heater at 105°C, were used. The resin used was Zeokarb 225 graded by a flotation method, with a mean particle size of 16–27 μ. It settled in water at a rate of 0·5–1·0 cm/min. The sample, containing 1 mg each of Y, Eu, Sm, Nd, Pr, and Ce carriers, in the minimum volume of 0·01–0·1N HCl, was passed through the column at 10–12 ml/hr, the acid washed through with a little water, and the column topped with a tamper of clean resin. 1M lactic acid, whose strength had been estimated by caustic-soda titration, was adjusted with ammonia to a *p*H of 3·25 ± 0·03, and was used as eluant. A pressure of 5–15 lb/in.^{2} was needed to force the eluant through the column at the operating speed of 10–12 ml/hr.

The eluant passed through a thin glass loop between two thin-window Geiger counters, and on to the automatic fraction collector. Pulses from the counters were fed to a ratemeter and recorded on a Kent recorder, so that the rare-earth peaks were plotted directly on the recorder chart. The activities were identified both by their elution order and by oxalate precipitation and subsequent half-life determinations. A further check was given by the position of the (carrier-free) Pm peak.

The active sample was prepared by dissolution of the irradiated uranium in acid containing the

carriers, followed by one fluoride and two hydroxide precipitations. This procedure, together with the time needed to add the activity to the column took 30–40 min.

A sample elution curve, which has been copied from the recorder trace, is given as Fig. 1. The positions of the oxalate precipitates of the various peaks are shown along the bottom of the figure. The drop-rate was 6 drops/min, corresponding to a flow-rate of 1·75 ml/cm²/min. A total volume of 93 ml of eluant had been used to the end of the Ce peak. This separation was carried out on a 4-mm diameter, 20-cm long column.

The separation is not so sensitive to *p*H changes as the citrate separation. A *p*H of 3·25 with 1M lactic acid separates Y from the impurities which are eluted before it from the column and which are unavoidable unless a much longer initial rare-earth purification is carried out. This *p*H is also advisable for the Eu-Sm separation, and if it is maintained the Pr is eluted approximately five hours from the start of the run. For a good Eu-Sm separation, a flowrate of 10–12 ml/hr is required.

For the examination of short-lived activities it will probably be desirable to study only one element at a time. In this case even more rapid separations should be possible by suitable adjustment of the conditions. Carrier need be added only for the element being studied, thus resulting in sharper peaks for the adjacent elements. The *p*H and flowrate may be arranged so that unwanted elements eluting before the required one are not separated from each other, but are removed quickly from the column. For example, Pr, Ce, and La can be separated from each other in one hour, the Pr being eluted two hours from the beginning of the run, if a flowrate of 50 ml/hr and a *p*H of 4·0 are used. If the chemical yield of the element is not required, no carrier need be added at all, since the initial purification can be carried out using Ce carrier, which can be removed by oxidation before the activity is added to the column.

It should be noted that, while reproducible results may be obtained using the same bottle of resin from the maker, the breakthrough volumes may differ slightly from batch to batch.

The authors wish to thank Dr. J. Milsted of A.E.R.E. for helpful discussions.

Atomic Energy Research Establishment,
Harwell, Berks

J. G. Cuninghame
M. L. Sizeland (Miss)
H. H. Willis.

Atomic Weapons Research Establishment,
Aldermaston, Berks

J. Eakins (Miss)
E. R. Mercer

REFERENCE

Freiling, E. C., and Bunney, L. R. (1954) *J. Amer. Chem. Soc.*, **76**, 1021.

J. Inorganic and Nuclear Chemistry, 1955, Vol. 1, pp. 165–174. Pergamon Press Ltd., London

VOL.
1
1955

CYCLOPENTADIENYL-CARBON MONOXIDE AND RELATED COMPOUNDS OF SOME TRANSITIONAL METALS

By T. S. Piper, F. A. Cotton, and G. Wilkinson
Mallinckrodt Laboratory, Harvard University, Cambridge, Mass.

(*Received* 20 *December* 1954)

Abstract—The preparation of cyclopentadienyl-carbon monoxide compounds of manganese, iron and cobalt, and of cyclopentadienyl-nitric oxide-nickel is described.

The compounds $(C_5H_5Fe)_2(CO)_4$ and $C_5H_5Co(CO)_2$ were prepared by the direct reaction of the metal carbonyl with dicyclopentadiene and cyclopentadiene, respectively. $C_5H_5Mn(CO)_3$ was prepared by the action of carbon monoxide on the reaction mixture of sodium cyclopentadienide with manganous bromide, and C_5H_5NiNO by the reaction of nitric oxide with bis-cyclopentadienyl-nickel.

The cation $[C_5H_5Mn(CO)_2NO]^+$ was isolated as the chloroplatinate from the reaction of $C_5H_5Mn(CO)_3$ with nitrous acid in ethanol. The compounds $C_5H_5Fe(CO)_2Cl$ and $C_5H_5Fe(CO)_2CN$ have been prepared from $(C_5H_5Fe)_2(CO)_4$.

The configurations and structures of the compounds are discussed briefly.

I. INTRODUCTION

The first examples to be described[1] of compounds with only one cyclopentadienyl ring bonded to a transitional metal atom were the cyclopentadienyl-carbon monoxide compounds of molybdenum and tungsten, $C_5H_5Mo(CO)_3MoC_5H_5$ and $C_5H_5W(CO)_3WC_5H_5$ respectively. A binuclear "triple decker sandwich" structure was proposed for these compounds in which all the carbon monoxide groups were located between the metal atoms in a five- or six-membered ring for Mo and W respectively; from the cyclic carbon monoxide system it was suggested that electrons were withdrawn into bonding with the metal atoms.

While the present work was in progress, a second type of cyclopentadienyl-carbon monoxide compound was described; this was the mononuclear compound $C_5H_5V(CO)_4$, which was prepared[2] by the action of carbon monoxide on *bis*-cyclopentadienylvanadium (II)

Certain generalizations can be made regarding the formation of cyclopentadienyl-carbon monoxide compounds of transitional metals. Evidence presented in this paper confirms our view that in the mono- and binuclear cyclopentadienyl-carbon monoxide and associated compounds, the cyclopentadienyl ring is bonded to the metal atom in a manner similar to the bond in the *bis*-cyclopentadienyl compounds.[3, 4] Thus the compounds show only a single C—H stretching frequency in the infrared absorption spectra at 3·20–3·25 μ, a C—C ring breathing absorption at 6·9–7·0 μ, and other bands similar to those in the spectra of *bis*-cyclopentadienyl compounds. It is to be noted, however, that the symmetries of the compounds with only one C_5H_5 ring per metal atom are different from the highly symmetrical *bis*-cyclopentadienyl metal

[1] G. Wilkinson, *J. Amer. Chem. Soc.* **76**, 209 (1954).
[2] E. O. Fischer and W. Hafner, *Z. Naturforsch.* **9b**, 503 (1954).
[3] J. D. Dunitz and L. E. Orgel, *Nature* **171**, 121 (1953).
[4] W. Moffitt, *J. Amer. Chem. Soc.* **76**, 3386 (1954).

compounds. Although the metal-to-ring bond in the former is undoubtedly due to the overlap of a π-electron of the ring with a *d*-electron of the metal atom, the orbitals both having E_1 symmetry with respect to the *local* symmetry of the C_5H_5 ring, the metal orbitals involved need not be exactly the same as in the *bis*-cyclopentadienyl compounds. We shall refer to this type of bond as a "sandwich bond," although the compounds with a single C_5H_5 ring attached to a metal atom are not "sandwich" molecules in the sense that, for example, ferrocene is.[3, 4] Accepting this view of the metal-to-ring bond, and noting further that the cyclopentadienyl-carbon monoxide metal compounds, like the transition metal carbonyls themselves, are diamagnetic, it follows that metals with odd atomic number, *Z*, e.g., V, Mn, and Co, may form mononuclear compounds, but that elements of even *Z* will give binuclear compounds. The substitution of carbon monoxide by nitric oxide may be expected to lead to diamagnetic mononuclear nitric oxide or mixed carbon monoxide-nitric oxide compounds of the types $C_5H_5M_{(even)}(CO)_xNO$ and $C_5H_5M_{(odd)}(CO)_x(NO)_2$. A further possibility is the replacement of carbon monoxide by the nitrosonium ion NO^+, which would lead to cationic species $[C_5H_5M_{(odd)}(CO)_xNO]^+$.

In addition to the cyclopentadienyl-carbon monoxide compounds noted above, we have characterized nitric oxide derivatives illustrating some of the above principles, namely C_5H_5NiNO and the $[C_5H_5Mn(CO)_2NO]^+$ ion.

It appears that the possibilities for the preparation of cyclopentadienyl compounds with only one ring per metal atom are numerous, and the chemistry seems to be rather generally similar to that of the carbonyls, nitrosyls, and similar compounds of transitional metals. Thus one might expect to find mononuclear cyclopentadienyl derivatives with ligands such as pyridine, isocyanides, and trivalent phosphorous compounds. We have observed for example that phosphorous trichloride and triisocyanate replace carbon monoxide from $C_5H_5Co(CO)_2$; with these ligands, substitution products only of nickel tetracarbonyl have previously been characterized.[5] We have also characterized the compounds $C_5H_5Fe(CO)_2Cl$ and $C_5H_5Fe(CO)_2CN$. More extensive studies may lead to cyclopentadienyl-carbon monoxide metal hydrides, complex cyanides, etc.

II. EXPERIMENTAL

Cyclopentadienyl-tricarbon monoxide-manganese (I)

This compound was first produced in low yields (~5 per cent) by passing carbon monoxide at ordinary pressures through the yellow solution from the reaction of manganous chloride and $(C_5H_5)MgBr$ in ether. A better procedure was the following. To a solution of sodium cyclopentadienide (0·6 moles) in tetrahydrofuran (200 ml) was added anhydrous manganous bromide (0·2 moles). After stirring for an hour in a nitrogen atmosphere at room temperature, the solvent was removed and the residue transferred in nitrogen to a steel bomb. Carbon monoxide at a pressure of 800 p.s.i. was admitted and the bomb heated at 250°C for twelve hours, the carbon monoxide pressure being maintained during this time. After opening the bomb, the product was sublimed in vacuum at 50°C. Yields were ~40 per cent based on manganous bromide.

The compound has also been prepared by the action of carbon monoxide under pressure on $(C_5H_5)_2Mn$.[6]

Cyclopentadienyl-tricarbon monoxide-manganese forms pale yellow plate-like crystals with a strong camphoraceous odour, m.p. 76·8–77·1°C. [*Anal.* Found, C 46·8, H 2·5, Mn 26·9; required

[5] J. W. IRVINE and G. WILKINSON, *Science* **113**, 742 (1951).
G. WILKINSON, *J. Amer. Chem. Soc.* **73**, 5501 (1951); *Z. Naturforsch.* **9b**, 446 (1954).
[6] E. O. FISCHER, *Z. Naturforsch.* **9b**, 618 (1954).

for $C_5H_5Mn(CO)_3$, C 47·1, H 2·47, Mn 26·9.† The crystals are stable to air and light, although solutions in organic solvents are slowly oxidized by air; it is decomposed by irradiation with ultraviolet light. The compound is readily soluble in petroleum ether and in other common organic solvents. It is insoluble in and unaffected by water. No oxidation wave could be detected at the dropping mercury electrode in a 50 per cent ethanolic sodium perchlorate supporting electrolyte solution.

The compound sublimes very readily in vacuum at temperatures a little above room temperature. The molecular weight by the freezing-point depression method in benzene is 210; required 204·0. With bromine and aqueous potassium permanganate, rapid decomposition occurs. There is no reaction with iodine in carbon tetrachloride, with hydrogen chloride in ethanol, or with boiling phosphorous trichloride or phosphorous triisocyanate. The compound does not react with maleic anhydride in boiling benzene.

The Cyclopentadienyl-dicarbon monoxide-nitrosonium-manganese (I) Ion.

On heating cyclopentadienyl-tri-carbon monoxide-manganese with hot 3 M nitric acid, considerable decomposition occurs, but a yellow solution is formed. This solution gives precipitates with the large anions which give precipitates with *bis*-cyclopentadienyl-metal cations, e.g. silicotungstic acid and Reinecke's salt, and has been shown to contain the ion $[C_5H_5Mn(CO)_3NO]^+$. The *chloroplatinate* is made as follows. The $C_5H_5Mn(CO)_3$ (0·6 g) is dissolved in absolute ethanol (30 ml) and concentrated hydrochloric acid (6 ml). A concentrated aqueous solution of sodium nitrite (0·21 g) was added dropwise to the solution at 70°C; the sodium chloride which precipitates is removed by centrifugation. Solid platinic chloride (0·5 g) was added and the solution cooled. The orange crystalline precipitate obtained was washed with alcohol; the yield is 30 per cent of the theoretical based on $C_5H_5Mn(CO)_3$. [*Anal.* Found, C 20·7, H 1·4, N 3·55, Mn 13·30, Cl 25·70; required for $[C_5H_5Mn(CO)_3NO]_2PtCl_6$, C 20·5, H 1·23, N 3·42, Mn 13·4, Cl 25·9.] The chloroplatinate is quite soluble in water and decomposes without melting at 165–175°C.

Aqueous solutions of the cation decompose slowly on standing.

The Cyclopentadienyl-carbon monoxide-iron Compound $(C_5H_5Fe)_2(CO)_4$*

Iron pentacarbonyl (10 ml) was refluxed with an excess of dicyclopentadiene (10 ml) for about forty hours; a nitrogen atmosphere was kept above the mixture, and light was excluded. Volatile material was then removed in vacuum, after which chloroform (50 ml) was added and the mixture centrifuged to remove iron enneacarbonyl and other insoluble material. The solution was then chilled in a "Dry-Ice"-acetone bath; the crystals were centrifuged and crystallized again from chloroform. The yield was approximately 30 per cent based on the carbonyl. Cyclopentadienyl-tetracarbon monoxide-iron forms dark reddish-purple crystals; in an evacuated sealed tube m.p. 194° with decomposition. [*Anal.* Found C 47·55, H 2·85, Fe 31·53; required for $(C_5H_5Fe)_2(CO)_4$, C 47·51, H 2·85, Fe 31·56.] The compound dissolves readily in chloroform, pyridine, and alcohol; it is less soluble in carbon tetrachloride and carbon disulphide and is rather sparingly soluble in petroleum ether. The solutions are red. The molecular weight by the isothermal distillation method in benzene is 368 (required 353·9). The compound is unaffected by and is insoluble in water. The solid is stable to air and light, but solutions decompose slowly by the action of these agents. On heating the compound at 210°C, ferrocene is formed in approximately 75 per cent yields based on the C_5H_5 present in the molecule.

Cyclopentadienyl-dicarbon monoxide-chloro-iron (II)

In a mixture of 250 ml ethanol, 50 ml chloroform, and 7·5 ml concentrated hydrochloric acid was dissolved 3·5 g $(C_5H_5Fe)_2(CO)_4$; air was then bubbled through the mixture for three hours.†

The solution was evaporated to dryness in vacuum and the residue extracted with 300 ml water. After filtering, the red solution was extracted with chloroform. The extract was dried and the product crystallized from a mixture of chloroform with 15 per cent petroleum ether. The yield was about

* The structure and formal nomenclature of this compound are discussed later. The stoichiometry previously reported by us (*Z. Naturforsch.* **9b**, 453 (1954)) was incorrect due to inadequate purification.

† It may be noted that it is not necessary to isolate $(C_5H_5Fe)_2(CO)_4$ and air may be bubbled through the crude preparation of this compound in ethanolic acid solution.

75 per cent of the theoretical. The compound forms well-defined red crystals which decompose without melting above 87°C. [*Anal.* Found, C 39·3, H 2·3, Fe 26·06, Cl 16·77; calcd. for $C_5H_5Fe(CO)_2Cl$, C 39·60, H 2·37, Fe 26·26, Cl 16·70.] The molecular weight by the freezing-point method in benzene was 213 (calcd. 212·4).

Cyclopentadienyl-dicarbon monoxide-chloro-iron is very soluble in chloroform, alcohol, and ether, moderately soluble in benzene, carbon disulphide, and carbon tetrachloride, and is sparingly soluble in petroleum ether. It is also moderately soluble in water, giving red solutions which do not give immediate precipitates with silver nitrate, silicotungstic acid, or Reinecke's salt. In acid solutions silver nitrate gives a precipitate within a minute. One may conclude that the compound is essentially undissociated in aqueous solution.

The Cyclopentadienyl-dicarbon monoxide-iron (II) Ion

Removal of chloride from the above compound by silver nitrate in dilute nitric acid or silver perchlorate in dilute perchloric-acid solution leaves an orange cation in solution. The solution gives precipitates with large anions such as silico-tungstic acid, Reinecke's salt, and sodium tetraphenyl-boron. The cation can also be made directly from $(C_5H_5Fe)_2(CO)_4$ by bubbling air through a solution of the compound in aqueous acetone containing perchloric acid, by oxidation with warm 3 N nitric acid, or by bromine water. In ether solution the $(C_5H_5Fe)_2(CO)_4$ is oxidized by quinone in the presence of picric acid to give a brown precipitate of the picrate of the cation. The cation is unstable in aqueous solution and decomposes completely within a few days; it is also quite easily destructively oxidized, and in its formation the yields are low.

The *Reineckate* forms pink crystals from ice cold solutions [*Anal.* Found, Fe 11·30, Cr 10·37, C 26·7, H 2·3, N 16·65; required for $[C_5H_5Fe(CO)_2][Cr(CNS)_4(NH_3)_2]$, Fe 11·20, Cr 10·45, C 26·7, H 2·24, N 16·98.]

Cyclopentadienyl-dicarbon monoxide-cyano-iron (II)

To cyclopentadienyl-dicarbon monoxide-chloro-iron (0·5 g) in methanol (20 ml) was added sodium cyanide (0·46 g), and the mixture refluxed for twenty-four hours. After evaporation of the solvent, the residue was extracted with chloroform, and the product crystallized from a chloroform-ether mixture by cooling in a dry-ice acetone bath. Yield 0·22 g (46 per cent based on the chloride). The cyano derivative forms yellow acicular crystals which decompose without melting at about 120°C. [*Anal.* Found, C 47·4, H 2·5, N 6·93, Fe 27·4; required for $C_5H_5Fe(CO)_2CN$, C 47·35, H 2·48, N 6·94, Fe 27·50.] The compound is soluble in chloroform, benzene, and in water, but is sparingly soluble in petroleum ether.

Cyclopentadienyl-dicarbon monoxide-cobalt (I)

A two-fold excess of dicobalt octacarbonyl (10 g) was treated with cyclopentadiene (3 ml) at room temperature. In an exothermic reaction, a dark-red liquid is produced, which is separated by fractional distillation under reduced pressure in a carbon monoxide atmosphere. The yields are of the order of 80 per cent. The compound has also been prepared[6] by the action of carbon monoxide under pressure on *bis*-cyclopentadienyl cobalt.

Cyclopentadienyl-dicarbon monoxide-cobalt is a dark-red liquid, b.p. 75°C/22 mm, which decomposes slightly on distillation and loses carbon monoxide in vacuum. [*Anal.* Found C 47·2, H 2·9, Co 32·55; calculated for $C_5H_5Co(CO)_2$: C 46·7, H 2·8, Co 32·77.] The compound is miscible with common organic solvents and the solutions are reasonably stable in air. Ultraviolet irradiation causes rapid decomposition and solutions slowly decompose in sunlight. Attempts to prepare a nitrosonium cation by methods similar to those used in the manganese case led to complete destruction of the molecule.

On heating the compound with either phosphorous trichloride or phosphorous tri-isocyanate, carbon monoxide is quantitatively evolved; if the reactions are carried out in solution, insoluble precipitates are obtained. These precipitates are very sparingly soluble in a great variety of solvents, and we have been unable to purify them by crystallization. Analyses, although not entirely satisfactory, indicate that the precipitates are *cyclopentadienyl-bis(phosphorous trichloride)-cobalt* (I) and *cyclopentadienyl-bis(phosphorous tri-isocyanate)-cobalt* (I). The former is dark green and the latter a deep buff; both compounds are hydrolyzed by water and decompose on heating without melting.

Cyclopentadienyl-nitric oxide-nickel (I)

Bis-cyclopentadienylnickel (II) (10 g) in petroleum-ether solution was treated with nitric oxide at atmospheric pressure until no more gas was absorbed. The resulting solution was centrifuged to remove insoluble matter. After stripping the petroleum ether, the product was fractionally distilled under reduced pressure.

A dark-red liquid b.p. 49°/27 mm is obtained in ~45 per cent yield based on $(C_5H_5)_2Ni$. [*Anal.* Found C 39·3, H 3·4, N 9·14, Ni 38·1; required for C_5H_5NiNO, C 39·1, H 3·28, N 9·11, Ni 38·2.] The compound is miscible with common organic solvents and is stable both in the pure state and in solution. On distillation slight decomposition was noted.

Cyclopentadienyl-tetracarbon monoxide-vanadium (I)

This compound was prepared for infrared absorption measurement by FISCHER and HAFNER's method;[8] bis-cyclopentadienylvanadium (II) was heated at 250°C under 800 p.s.i. carbon monoxide for twelve hours and the crude product sublimed in vacuum.

Magnetic Measurements

The measurements were made on the pure compounds as finely ground solids or in solution. The Gouy method using a divided tube was used, and water and ferrous ammonium sulphate (MOHR's salt) were employed as references. Checks were made at several field strengths to show the absence of ferromagnetic impurities. The following compounds were studied and found to be diamagnetic—$C_5H_5Mn(CO)_3$, $[C_5H_5Mn(CO)_2NO]_2PtCl_4$, $(C_5H_5Fe)_2(CO)_4$, $C_5H_5Fe(CO)_2Cl$, $C_5H_5Co(CO)_3$ and C_5H_5NiNO. The susceptibility of the $[C_5H_5Fe(CO)_2]^+$ ion was determined by measurement of the Reineckate, which gave a value of 3·90 ± 0·05 B.M.; this is the same as the value for Reinecke's salt itself, and the $[C_5H_5Fe(CO)_2]^+$ ion is hence diamagnetic. The compound $C_5H_5V(CO)_4$ has been shown[9] also to be diamagnetic.

Infrared Spectra

Infrared spectra of the compounds were taken in chloroform, carbon tetrachloride, and carbon disulphide solutions when solubilities were adequate. In other cases, windows of the compounds in potassium bromide or iodide were prepared by pressure forming as one-inch discs. Spectra were obtained using Perkin-Elmer single- and double-beam recording instruments, and a Baird double-beam recording spectrometer. The spectra of $C_5H_5Mn(CO)_3$, $(C_5H_5Fe)_2(CO)_4$, and $[C_5H_5Mn(CO)_2NO]_2PtCl_4$ are shown in Fig. 1; the major bands of other compounds are presented in Table 1, together with the bands of ferrocene for comparison.

Analyses. C, H, and N analyses by S. NAGY, Massachusetts Institute of Technology. After destruction of organic material by fuming with sulphuric acid, the metals Mn, Co, and Ni were determined by titration with the disodium salt of ethylenediamine tetracetic acid according to SCHWARZENBACH's method,[7] modified by the use of a pH meter to determine the end-point; standardization of the procedure showed that an accuracy of ±0·2 per cent can be obtained. Manganese was also determined colorimetrically.[8]

Iron was determined by reduction in a Jones reductor and titration with permanganate, halogens by the Volhard method, and phosphorus by the ammonium molybdate method, all according to standard procedures.[9]

III. DISCUSSION

There are several interesting and novel features connected with the structure of cyclopentadienyl carbon monoxide and nitric oxide metal compounds, in addition to reasons for the mono- or binuclear character noted above.

(1) The cyclopentadienyl ring is unquestionably bonded to the metal by a "sandwich bond," as in the *bis*-cyclopentadienyl compounds. Experimental evidence in

[7] G. SCHWARZENBACH and W. BIEDERMANN, *Helv. Chim. Acta.* **31**, 460 (1948).
[8] E. B. SANDELL, *Colorimetric Determination of Traces of Metals.* 2nd Ed., 1950. Interscience, New York, p. 430.
[9] *Scott's Standard Methods of Chemical Analysis* (N. H. FURMAN, Ed.), 5th Ed., 1939. D. van Nostrand, New York.

support of this type of bonding in the $(C_5H_5)_2M$ compounds has been summarized elsewhere[10]; additional evidence for the aromatic character of the C_5H_5 rings in ferrocene has been more recently obtained from the metallation reactions with butyllithium[11a,b] and mercuric acetate[11a], from the reaction of ferrocene with

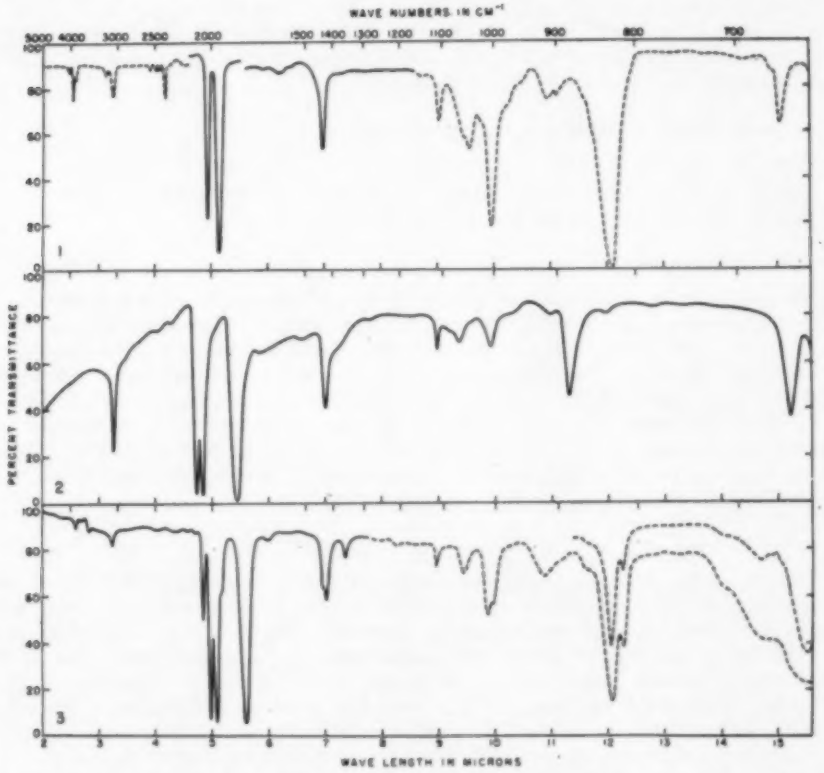

FIG. 1.—Infrared absorption spectra. Top: $(C_5H_5)Mn(CO)_3$, (- - - -) 55 mg/ml in CS_2; (——) 30, 3·0 mg/ml in CCl_4. Middle: $[C_5H_5Mn(CO)_3NO^+]_2[PtCl_6]$: 7·0 mg in KBr window, 1-in. diameter. Bottom: $(C_5H_5Fe)_2(CO)_4$: (- - - - -) 17, 10 mg/ml in CS_2; (——) 17 mg/ml inCCl_4. Perkin-Elmer Model 21 double-beam recording infrared spectrometer.

diazonium salts[11a,12] and from the sulphonation of ferrocene with sulphuric acid in acetic acid solution.[13] The similarity of the infrared spectra of compounds with only one C_5H_5 ring bonded to the metal to the spectra of ferrocene and other *bis*-cyclopentadienyl compounds[14,15] is very noticeable, and provides substantial evidence for the similarity in the metal to ring bonding. Additional

[10] F. A. COTTON and G. WILKINSON, *Z. Naturforsch.* **9b**, 453 (1954).
[11a] A. N. NESMEYANOV, E. G. PEREVALOVA, R. V. GOLOVNYA, and O. A. NESMEYANOVA, *Proc. Acad. Sci. USSR* XCVII (3), 459 (1954).
[11b] R. A. BENKESER, D. GOGGIN, and G. SCROLL, *J. Amer. Chem. Soc.* **76**, 4025 (1954).
[12] G. D. BROADHEAD and P. L. PAUSON, *J. Chem. Soc.* 367 (1955).
[13] M. HUNT, Abstracts, American Chemical Society, New York Meeting, September, 1954 and *J. Amer. Chem. Soc.*, in press.
[14] E. R. LIPPINCOTT and R. D. NELSON, *J. Chem. Phys.* **21**, 1307 (1953).
[15] G. WILKINSON, P. L. PAUSON, and F. A. COTTON, *J. Amer. Chem. Soc.* **76**, 1970 (1954). *Note:* In this reference the *dotted* line in Fig. 1 is the spectrum of ferrocene.

VOL. 1 1955

TABLE 1.—THE MAIN INFRARED ABSORPTION BANDS (IN CM^{-1}) IN THE SPECTRA OF VARIOUS CYCLOPENTADIENYL METAL COMPOUNDS

Compound	C—H stretch	Addenda stretch	Bands characteristic of C_5H_5—M compounds
$C_5H_5V(CO)_4$	3110 (m)	2019 (vs) 1951 (vs)[a] 1919 (vs)	1430 (m) 1370 (w) 1120 (vw) 1060 (w) 1010 (m) 840 (s)
$C_5H_5Fe(CO)_2Cl$	3110 (m)	2050 (vs) 2010 (vs)	1420 (m) 1365 (w) 1118 (w) 1070 (w) 1003 (s) 874 (s) 835 (s)
$C_5H_5Fe(CO)_2CN$	3120 (m)	2060 (vs) 2020 (vs); (C—O) 2125 (vs) (C—N)	1420 (m) 1360 (w) 1115 (w) 1060 (w) 1010 (s) 854 (s) 1003 (s)
$C_5H_5Co(CO)_2$	3110 (m)	2028 (vs) 1967 (vs)	1405 (s) 1360 (w) 1110 (w) 1075 (w) 990 (m) 955 (w) 754 (w) 1016 (w) 917 (w) 726 (m)
C_5H_5NiNO[b]	3105 (m)	1833 (vs) (N—O)	1425 (m) 1110 (w) 1050 (w) 1002 (vs) 803 (vs)
$(C_5H_5)_2Fe$	3085 (m)	1758–1620 (m)[c]	1411 (s) 1108 (s) 1051 (w) 1002 (s) 811 (s)

[a] Occurs in solid only—see following paper.
[b] There are additional bands at ~3600 (m), ~2440 (w).
[c] Converging system possibly characteristic of the two-ring system (see ref. 15).

evidence for the aromatic character of the C_5H_5 rings in these derivatives is that none of them will react with maleic anhydride in benzene solution. The reason for the notable difference between the behaviour of $C_5H_5Mn(CO)_3$ and that of manganese (II) cyclopentadienide $(C_5H_5)_2Mn$, which reacts instantaneously with maleic anhydride, is discussed below.

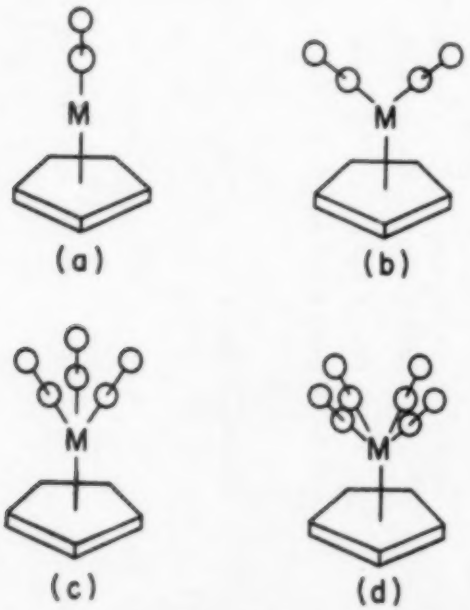

FIG. 2.—Structures proposed for some cyclopentadienyl-carbon monoxide and nitric oxide-metal compounds.
(a) $C_5H_5Ni(NO)$ (b) $C_5H_5Co(CO)_2$ (c) $C_5H_5Mn(CO)_3$ (d) $C_5H_5V(CO)_4$

(2) For the mononuclear carbon monoxide compounds of V, Mn, and Co, the number of associated carbon monoxide groups is respectively four, three, and two. Thus considering the formation of the compounds from the C_5H_5 radical, the neutral metal atom and carbon monoxide, where the first contributes one electron and the last two electrons, the total number of electrons to be allocated in the valence shells of the metals is in all cases fourteen. For example, in the case of $C_5H_5Mn(CO)_3$, we have C_5H_5, 1, Mn, 7, three CO, 6, giving a total of fourteen electrons. The same result is obtained if the compounds are considered to be formed from the metal in its valence state with the cyclopentadienyl anion and neutral carbon monoxide. The same rule holds for the other ligands.

In the subsequent discussion, we shall assume that the structures of the mononuclear cyclopentadienyl compounds are as shown in Fig. 2. In the $C_5H_5MA_3$ and $C_5H_5MA_4$ molecules, the three and four ligands form respectively symmetrical trigonal and square pyramids with the metal at the apices and the principal axis of the molecule is perpendicular to the plane of the C_5H_5 ring. In these diagrams, no fixed configuration of the C_5H_5 ring relative to the ligands is implied for the free molecules. The evidence from infrared absorption studies in the C—O stretching

region on which these proposed configurations are based, is discussed in a following paper. The metal-to-carbon monoxide bond must be similar to the bond in the metal carbonyls themselves, and similar requirements of filled *d* orbitals for the formation of π-bonds between the metal atom and carbon must be fulfilled. We consider the electrons to be allocated $3d^5\ 4s\ 4p$; not all these electrons are used in primary bonding, and some are thus available for multiple bond formation.

On the basis of the proposed structures it is formally possible that there is some contribution to the bonding from all three 4*p* orbitals. However, on the above view of metal-ring bonding, there are only fourteen electrons to be accommodated, all of which, it may be supposed, spend some of their time on the metal atom. It is therefore sufficient in describing the bonding to consider seven orthogonal hybrid orbitals of the metal. The best available orbitals, of course, are the five 3*d* and single 4*s*. The 4*p* orbitals in elements of the first transitional series generally lie some 3 ev higher. Since it is only necessary to use, on the average, one of these in constructing the hybrids, no further promotion of the metal need be invoked, and it may be supposed that the remaining components of the 4*p* band are left unoccupied. The relative contributions to the resultant bonding from the individual 4*p* orbitals cannot be estimated with any certainty, and it would be premature to attempt a unique electronic assignment for these molecules.

VOL. 1 1955

It may be noted that with elements of the second and third transitional series where the relative energies of the *d*, *s*, and *p* levels are different, the cyclopentadienyl-carbon monoxide-metal compounds may not necessarily have the same stoichiometry as in the first transitional series. An example of such a difference is that of $C_5H_5Mo(CO)_5MoC_5H_5$ and $C_5H_5W(CO)_6WC_5H_5$.

(3) The only mononuclear cyclopentadienyl-carbon monoxide-metal compound found to undergo direct substitution with trivalent phosphorus compounds is that of cobalt. The failure to substitute in the other cases may be due either to steric factors or to the decreased number of filled non-bonding orbitals and hence decreased multiple bond character of the metal-carbon monoxide bonds, or to a combination of both factors. It may be noted that, among pure metal carbonyls, only in the case of nickel carbonyl where the multiple bond character of the metal-carbon bond is high, have completely substituted phosphorus derivatives been characterized.

(4) The case of $C_5H_5Mn(CO)_3$ is particularly interesting, since the C_5H_5 ring appears to be bound to the metal by a "sandwich bond." This is not the case with $(C_5H_5)_2Mn$, which has been found[16] to be ionic in nature. The latter compound has a magnetic moment corresponding to five unpaired electrons when magnetically dilute; it forms conducting solutions in liquid ammonia and in tetrahydrofuran, and undergoes an immediate quantitative reaction with ferrous chloride in tetrahydrofuran solution to give ferrocene. The formation of an ionic rather than a covalent "sandwich bonded" compound $(C_5H_5)_2Mn$ may be attributed to be the exceptional stability of the manganous ion, which in a $^6S_{5/2}$ state has the 3*d* shell half filled. The noticeable stability of species containing half-filled *d* and *f* shells is well known and in the case of manganese this fact has often been invoked to explain *inter alia* the paucity of complex compounds of divalent manganese. In $C_5H_5Mn(CO)_3$ the manganous ion cannot arise simply by formation of ionic metal to ligand and ring bonds, and so a

[16] G. WILKINSON and J. M. BIRMINGHAM, *J. Amer. Chem. Soc.* **76**, 6210 (1954).
F. A. COTTON, J. M. BIRMINGHAM, and G. WILKINSON, to be submitted to this Journal.

normal "sandwich" bond is formed as in $(C_5H_5)_2Fe$, the iron atom in the latter being isoelectronic with the manganese atom in $C_5H_5Mn(CO)_3$.

(5) In contrast to the destruction with loss of carbon monoxide of the molybdenum and tungsten cyclopentadienyl compounds, the iron compound $(C_5H_5Fe)_2(CO)_4$ on thermal decomposition gives high yields of ferrocene. This fact ought not to be taken as evidence for the bonding of two C_5H_5 groups to a single iron atom, however. The reaction may be attributed to the great stability of ferrocene and to the fact that the C_5H_5 anion or radical can take part in solid state reactions. Such reactions are known elsewhere; thus *bis*-cyclopentadienyl compounds of chromium, cobalt, and nickel have been prepared by thermal decomposition of the amines $[M(NH_3)_6](C_5H_5)_2$,[17] and we have shown that sodium cyclopentadienide reacts in the solid state at ~200°C with several transitional metal halides to give $(C_5H_5)_2M$ compounds in yields as high as 30 per cent. Quite apart from the serious difficulties which would arise in trying to explain the bonding, a structure for $(C_5H_5Fe)_2(CO)_4$ with essentially a ferrocene group in the molecule cannot be reconciled with other evidence.

The iron compound is oxidized by air in hydrochloric acid-methanol solution almost quantitatively to give the compound $C_5H_5Fe(CO)_2Cl$ and by other oxidizing agents under various conditions, e.g., by picric acid or by iodine to the cation $C_5H_5Fe(CO)_2^+$ or its salts; *no carbon monoxide is evolved in these oxidations*. These reactions are in contrast to the complete destruction with loss of carbon monoxide of the molybdenum and tungsten compounds on oxidation. The oxidation products of the iron compound show that only one C_5H_5 group is bonded to an iron atom.

Comparing the infrared absorption spectrum of $(C_5H_5Fe)_2(CO)_4$ with the spectra of the molybdenum and tungsten compounds,[1] it will be noted that in the iron compound there is a strong C—O stretching frequency at 5·6μ which does not occur in the others. The occurrence of an absorption band of the bridging type exemplified by $Fe_2(CO)_9$, suggests the existence of one or more bridging carbon monoxide groups. The infrared spectra and various possible structures for the molecule, which we formulate tentatively as cyclopentadienyliron(II)-μ-tetra carbon monoxide-cyclopentadienyliron (II), are discussed in a following paper.

It may be noted finally that the diamagnetic $[(C_5H_5Fe(CO)_2]^+$ cation differs from the other mononuclear compounds described here, in that there are only twelve electrons which must be allocated to the 3*d* and 4*s* orbitals.

ACKNOWLEDGMENTS

We wish to thank Prof. W. MOFFITT for his most welcome criticism and advice. Thanks are due to the General Electric Company for a Swope Fellowship (F. A. C.) and to the National Science Foundation for a Predoctoral Fellowship (T. S. P.). The senior author is deeply grateful to the Trustees of the John Simon Guggenheim Foundation for a Fellowship during the tenure of which some of this work was performed, and to Prof. JANNIK BJERRUM, Technical University of Denmark, for his interest and the kind hospitality of his laboratories during this period.

This research was supported in part by the Atomic Energy Commission.

[17] E. O. FISCHER and R. JIRA, *Z. Naturforsch.* **8b**, 217, 327 (1953).

J. Inorganic and Nuclear Chemistry, 1955, Vol. 1, pp. 175–186. Pergamon Press Ltd., London

INFRARED SPECTRA AND STRUCTURES OF CYCLOPENTADIENYL-CARBON MONOXIDE COMPOUNDS OF V, Mn, Fe, Co, Mo, and W

By F. A. COTTON, A. D. LIEHR, and G. WILKINSON
Mallinckrodt Laboratory, Harvard University, Cambridge, Mass.

(*Received* 11 *January* 1955)

Abstract—The infrared absorption spectra in the C—O stretching region of mono- and binuclear transition metal cyclopentadienyl-carbon monoxide compounds are presented. The structures of the molecules are discussed and it is shown that the spectra may be interpreted by consideration of the local symmetry of the carbon monoxide groups only. For the binuclear molybdenum and tungsten compounds the spectra are best explained by puckered five- and six-membered cyclic carbon monoxide systems, respectively. For the iron compound a single bridging carbon monoxide group is postulated. The compounds studied are $C_5H_5V(CO)_4$, $C_5H_5Mn(CO)_3$, $C_5H_5Co(CO)_2$, $C_5H_5Mo(CO)_5MoC_5H_5$, $C_5H_5W(CO)_6WC_5H_5$, and $(C_5H_5Fe)_2(CO)_4$.

VOL.
1
1955

I. INTRODUCTION

THE preparation of several cyclopentadienyl carbonyl compounds of transition metals has now been reported[1, 2, 3] and the structures for some of these have been proposed.[1, 2] In this note, the plausibility of these and other possible structures is examined with respect to the infrared absorption spectra of the compounds in the C—O stretching region. The general characteristics of the spectra of $C_5H_5V(CO)_4$, $C_5H_5Mn(CO)_3$, $C_5H_5Co(CO)_2$, $C_5H_5Mo(CO)_5MoC_5H_5$, $C_5H_5W(CO)_6WC_5H_5$, and $(C_5H_5Fe)_2(CO)_4$ suggest that in all cases the cyclopentadienyl ring is bound to the metal by what we may call the "sandwich bond."[2, 4, 5] This point has been discussed in the previous paper.[2] The proposed structures for these molecules[1, 2] lead one to assume that long-range interaction between the cyclopentadienyl ring and the carbon monoxide groups is small. Thus we assume that *the selection rules for the* C—O *stretching frequencies can be obtained by considering solely the local symmetry of the carbon monoxide groups*, neglecting the influence of the cyclopentadienyl ring. This view provides a consistent explanation for the infrared spectra in the C—O stretching region of the cyclopentadienyl-carbon monoxide metal compounds.

II. EXPERIMENTAL

The cyclopentadienyl compounds studied in this paper were prepared by methods previously described.[1, 2]

The spectra in the region 2,200 cm^{-1} to 1,700 cm^{-1} were taken on a Perkin-Elmer recording double-beam infrared spectrograph Model 21, using a rocksalt prism. The scale was spread to 0·1 micron per inch and the machine was programmed to obtain maximum resolution. In a few cases where resolution greater than that obtainable here was desired, a Perkin-Elmer single-beam recording infrared spectrograph Model 12c was used with a calcium fluoride prism and with double-pass operation.

[1] G. WILKINSON, *J. Amer. Chem. Soc.*, **76**, 209 (1954).
[2] T. S. PIPER, F. A. COTTON, and G. WILKINSON, *J. Inorg. Nucl. Chem.* **1**, 165 (1955).
[3] E. O. FISCHER, W. HAFNER, *Z. Naturforsch.*, **9b**, 503 (1954).
[4] W. MOFFITT, *J. Amer. Chem. Soc.*, **76**, 3386 (1954).
[5] J. D. DUNITZ and L. E. ORGEL, *J. Chem. Phys.* (in press).

Solutions were made in reagent grade chloroform, carbon tetrachloride, or carbon disulphide; the sample thickness was 0·4 mm. Solid samples were ground with potassium iodide (1 g) and pressed into windows 1-inch diameter, ~0·8 mm thickness.

The spectra are shown in Fig. 1.

III. RESULTS AND DISCUSSION

(*a*) *Mononuclear Cyclopentadienyl-carbon monoxide Metal Compounds*

Compounds of this type are $C_5H_5V(CO)_4$, $C_5H_5Mn(CO)_3$, and $C_5H_5Co(CO)_2$. The simplest and most appealing structures for these compounds are those which have a symmetric disposition of the M—C—O axes around the principal axes of the molecules. Thus the metal atom in $C_5H_5V(CO)_4$ would be at the apex of a square pyramid with the CO groups at the corners of the base with the principal axis of the molecule being the principal axis of the pyramid and perpendicular to the C_5H_5 ring. The metal and CO groups in $C_5H_5Mn(CO)_3$ would form a trigonal pyramid and, in $C_5H_5Co(CO)_2$, an isosceles triangle. Sketches of these molecules were presented in the previous paper.[2]

Cyclopentadienyl-tetracarbon monoxide-vanadium (*I*). In Fig. 1a are shown the spectra of this compound in the solid state and in solution. The spectrum of the free molecule can be explained by assuming that all the carbon monoxide groups are located in equivalent sites, i.e., that the interactions between these ligands and the cyclopentadienyl ring are small. We can hence assign a *local* symmetry C_{4v} to the carbon monoxide groups in the free molecule. The C—O stretching motions then have the following symmetry types and activities:

No.	*Symm. Type*	*Activity*
1	A_1	R–IR
1	B_2	R
1	E	R–IR

The observed spectrum of the substance in solution is in accord with the proposed structure. It can be shown that any less symmetrical disposition of the carbon monoxide groups would result in the appearance of more than two C—O bands in the spectrum of the free molecule. In the solid-state spectrum of $C_5H_5V(CO)_4$ a third strong band of approximately the same intensity as the 2,019 cm^{-1} band appears at 1,951 cm^{-1}. This band is probably the "forbidden" B_2 vibration of the free molecule. Strong crystal-field interactions would allow all the C—O stretching motions to be infrared active. However, although the spectrum shows that the B_2 type vibration is allowed in the solid, the E vibration is not split by the crystal field. We must hence assume that these interactions are not strong enough to resolve the degeneracy occurring in the free molecule.

Cyclopentadienyl-tricarbon monoxide-manganese (*I*). The spectrum of this compound in the C—O region is shown in Fig. 1b. Two bands are observed, one of considerably greater intensity than the other, as was the case for $C_5H_5V(CO)_4$ in solution. The structure proposed for the carbon monoxide ligands in $C_5H_5Mn(CO)_3$ has the local symmetry C_{3v}. The carbonyl stretching frequencies for this model are:

No.	*Symm. Type*	*Activity*
1	A_1	R–IR
1	E	R–IR

Thus the observed spectrum satisfies the requirements of the proposed structure.

VOL.
1
1955

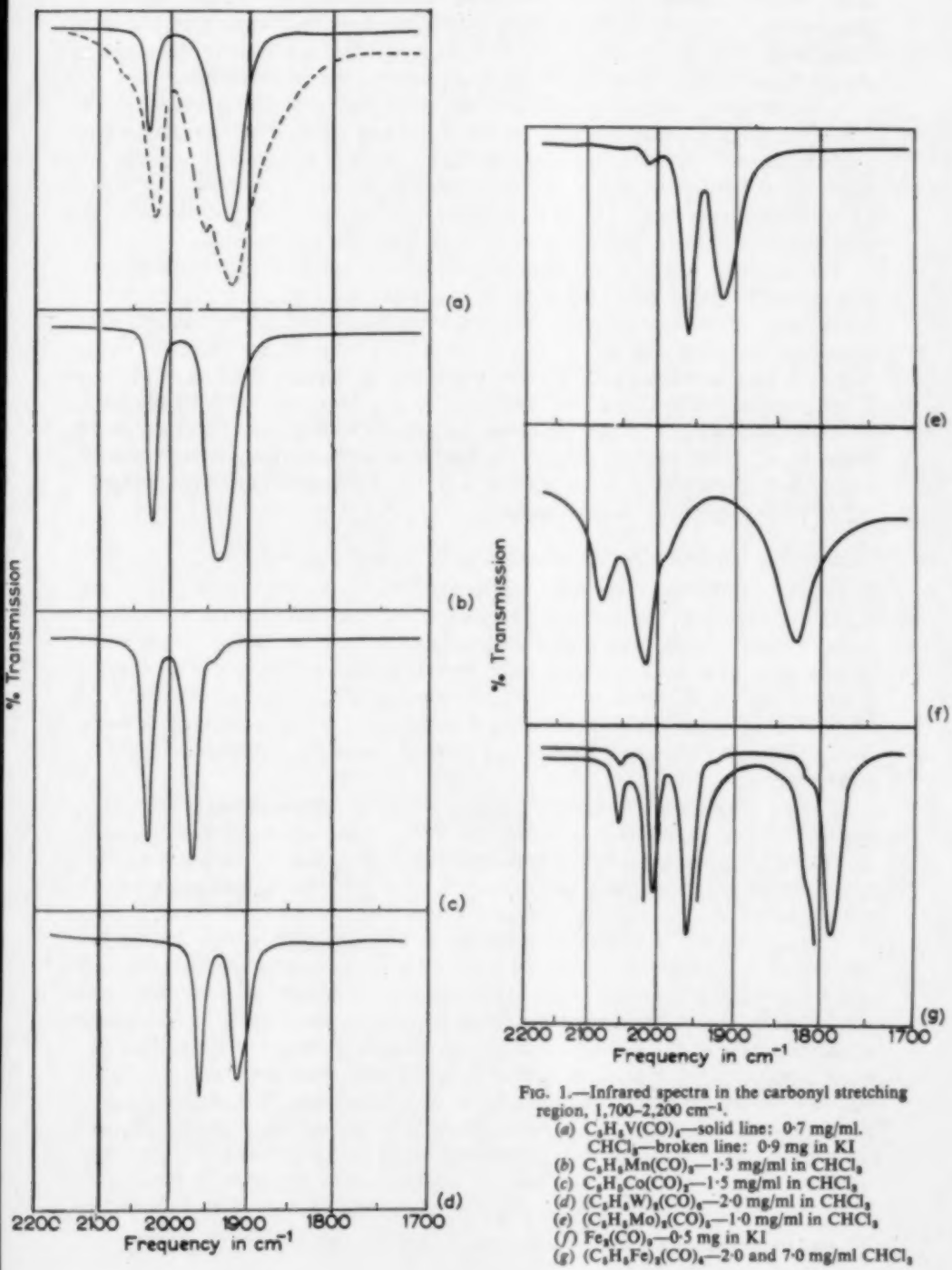

FIG. 1.—Infrared spectra in the carbonyl stretching region, 1,700–2,200 cm^{-1}.
(*a*) $C_5H_5V(CO)_4$—solid line: 0·7 mg/ml. $CHCl_3$—broken line: 0·9 mg in KI
(*b*) $C_5H_5Mn(CO)_3$—1·3 mg/ml in $CHCl_3$
(*c*) $C_5H_5Co(CO)_2$—1·5 mg/ml in $CHCl_3$
(*d*) $(C_5H_5W)_2(CO)_6$—2·0 mg/ml in $CHCl_3$
(*e*) $(C_5H_5Mo)_2(CO)_6$—1·0 mg/ml in $CHCl_3$
(*f*) $Fe_2(CO)_9$—0·5 mg in KI
(*g*) $(C_5H_5Fe)_2(CO)_4$—2·0 and 7·0 mg/ml $CHCl_3$

Any less symmetrical structure would give three infrared active, nondegenerate C—O frequencies. Since solid $C_5H_5Mn(CO)_3$ showed the same two bands with the same intensity ratio, we again must assume that the crystal-field interactions are not great enough to resolve the vibrational degeneracy present in the free molecule.

Cyclopentadienyl-dicarbon monoxide-cobalt (*I*). The proposed structure has the local symmetry C_{2v}. For this model as well as for any other structure there are two infrared active C—O stretching motions. Thus, although no direct information on ring—ligand interaction can be obtained from the spectrum, the similarity of the C—O frequencies to those of the other mononuclear compounds suggests that here too the interaction between the cyclopentadienyl ring and the ligands is small.

The splittings of the C—O stretching frequencies in these mononuclear compounds is of the order of 60–100 cm^{-1}. On the assumption that this splitting can be treated as an effect of the coupling of harmonic oscillators, interaction constants were calculated and found to be of the order of $0{\cdot}5 \times 10^5$ dynes/cm, which is in the proper range for the assumed coupling between equivalent oscillators. Force constants for C—O stretches obtained from this treatment were 16·2, 15·6, and $14{\cdot}9 \times 10^5$ dynes/cm for the cobalt, manganese, and vanadium compounds respectively. These are in the range ($15–16 \times 10^5$) of the constants for the metal carbonyls themselves,[6] but the crudeness of the treatment precludes the attachment of any significance to the progression in magnitude in the three compounds.

(*b*) *Binuclear Cyclopentadienyl-carbon monoxide metal Compounds*

In the structures previously suggested[1] for $C_5H_5Mo(CO)_5MoC_5H_5$ and $C_5H_5W(CO)_6WC_5H_5$, the carbon monoxide groups were located between the metal atoms forming a cyclic system from which electrons were withdrawn into bonding with the metal atoms. This concept, as opposed to ketonic carbon monoxide bridging groups of the type found in iron enneacarbonyl $Fe_2(CO)_9$, was in keeping with the absence of any ketonic C—O stretching frequencies in the infrared, and provided an explanation of the similarities of the two compounds despite the difference in stoichiometry.

We have attempted to interpret the observed infrared spectra of these compounds, making the same assumption as in the case of the mononuclear derivatives, namely that the interactions between the cyclopentadienyl rings and the carbon monoxide ligands are small and that consequently only the *local* symmetry of the ligands need be considered.

There are several possible models for the carbon monoxide system, but we feel that only those having a considerable degree of symmetry need be considered in view of the properties of the compounds. The most obvious models are those with (*a*) a planar symmetrical ring, (*b*) a puckered ring. It is shown below that the planar model is inconsistent with the infrared spectra. The possible puckered ring structures are numerous, but on the basis of the spectra we can limit the models to two types. In the first of these the carbon atoms form a plane with the oxygen atoms extending symmetrically outwards above and below this plane. In the second, provided the puckering is not large, the carbon monoxide groups as a whole form a puckered ring similar to those of saturated cyclic hydrocarbons. A large puckering would be tantamount to complete breakdown of the cyclic carbon monoxide system, some of the ligands then

[6] See for example R. S. NYHOLM and L. N. SHORT, *J. Chem. Soc.* **1953**, 2670.

being so close to a metal atom that they must be considered to be bonded to that particular metal atom.

Cyclopentadienyltungsten (I)-μ-hexacarbon monoxide-cyclopentadienyltungsten (I). X-ray diffraction studies[7] of crystalline $C_5H_5W(CO)_6WC_5H_5$ have confirmed the general features of the proposed structure[1] for this molecule. Thus the carbon monoxide groups lie between the tungsten atoms, the W-W distance being ~3·2 Å, with the cyclopentadienyl groups situated at the extremities of the molecule. It is also certain that the carbon monoxide ring system is nonplanar in the crystal and probably has a puckered structure. It also appears that the molecule may be skewed in the crystal.

TABLE 1.—TABULATION OF C—O STRETCHING FREQUENCIES

Compound	Physical state	Observed bands in cm^{-1}				
$C_5H_5V(CO)_4$	solution and solid	2019(vs)	1951(solid only, vs)			1919(vs)
$C_5H_5Mn(CO)_3$	solution and solid	2023(vs)		1939(vs)		
$C_5H_5Co(CO)_2$	solution	2028(vs)		1967(vs)		
$(C_5H_5Mo)_2(CO)_6$	solution		1960(vs)	1916(vs)		
	solid		1957(vs)	1926(vs)	1904(vs)	1891 (vs)
$(C_5H_5W)_2(CO)_6$	solution		1956(vs)	1910(vs)		
	solid		1958 (vs)	1919 (vs)	1882 (vs)	
$(C_5H_5Fe)_2(CO)_4$	solution	2054 (w)	2005 (vs)	1958 (vs)		1786 (vs)
	solid	2000 (sh, w)	1965 (vs)	1950 (vs)		1782, 1770 (vs)

s = strong; w = weak; v = very; sh = shoulder

No information on the configuration of the free molecule is obtained from X-ray data, however. The spectrum of $C_5H_5W(CO)_6WC_5H_5$ in solution is shown in Fig. 1d, and the absorption maxima for the solid and for dissolved samples are listed in Table 1. Considering once again only the carbon monoxide system, models with symmetrical planar and symmetrical puckered rings would have respectively the symmetries D_{6h} and D_{3d}. The vibration types and activities for these models are:

D_{6h}			D_{3d}		
No.	*Symm. Type*	*Activity*	*No.*	*Symm. Type*	*Activity*
1	A_{1g}	R	1	A_{1g}	R
1	B_{1u}	inactive	1	A_{2u}	I.R.
1	E_{1u}	I.R.	1	E_g	R.
1	E_{2g}	R.	1	E_u	I.R.

Thus it will be seen that for the free molecule a puckered ring is in agreement with the observed spectrum, whereas a planar ring is not. The infrared data thus favours the model with the puckered ring system. Whilst no particular puckered ring system of symmetry D_{3d} can be chosen, the most appealing one is that in which the carbon atoms

[7] D. P. SHOEMAKER and F. C. WILSON, Massachusetts Institute of Technology, Private communication.

are in a plane and the oxygen atoms are alternately directed up and down from this plane at equal angles to it. A representation of such a scheme is shown in Fig. 2. An unequivocal statement of the configuration of the carbon monoxide groups must await more direct evidence such as electron diffraction studies might provide.

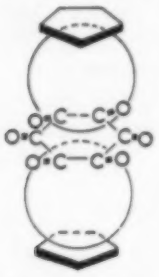

FIG. 2.—Probable structure for the free $(C_5H_5W)_2(CO)_4$ molecule. No fixed rotational orientation of the rings relative to one another is implied.

As noted above, in the crystal the evidence points to a puckered ring. Since three strong C—O bands are observed in the spectrum of the solid compound, we must assume that the crystal field causes at least one of the "forbidden" bands to appear.

The calculation of force constants assuming a coupled harmonic oscillator model for the carbon monoxide system yields values consistent with the above spectral interpretation.

Cyclopentadienylmolybdenum (I)-μ-pentacarbonmonoxide-cyclopentadienylmolybdenum (I). For this compound we have the local symmetry D_{5h} for the carbon monoxide ligands if the system is planar; for a puckered five-membered ring of carbon monoxide groups the symmetry may vary from C_s to no symmetry at all. For the planar and puckered ring systems, respectively, group theory leads to permissible C—O stretching modes with the following symmetry types and activities:

D_{5h} (planar)			C_s or no symmetry (puckered)		
No.	*Symm. Type*	*Activity*	*No.*	*Symm. Type*	*Activity*
1	A_1'	R.	5	—	IR, R
1	E_1'	I.R.			
1	E_2'	R.			

From Fig. 1e, it will be noticed that there are two strong absorption bands in the infrared spectrum of the molecule, and hence the planar model is inconsistent with the data. One is left therefore with a puckered model as the prime possibility. Although group theory predicts that with such a model five bands *may* be observed, the theory yields no information about the intensity of the bands, so that one cannot say whether they will be observable or not. Thus the appearance in the spectrum of the free molecule of only two strong bands may be reconciled with a puckered structure.

The striking similarity of the molybdenum and tungsten compounds suggests that their structures are indeed also similar. A five-membered puckered carbon monoxide ring in the molybdenum compound can be obtained in the following way. We assume that all five of the carbon atoms of the carbon monoxide groups lie in a plane perpendicular to the Mo–Mo axis with one of the oxygen atoms also lying in this plane. The remaining four oxygen atoms extend alternately above and below the plane of the carbon atoms, making equal angles with this plane. Let us call this angle of inclination α.

Assuming that the potential energy of the above structure is similar to that for a planar cyclic carbon monoxide system, and this seems a reasonable assumption, we obtain three infrared active frequencies, one designated "nondegenerate" and two "degenerate." The change of the dipole moment associated with the normal coordinate describing the "nondegenerate" vibration is found to be strongly dependent on the angle of inclination, α, of the out-of-plane oxygen atoms. The "degenerate"

vibration, which in the limit as $\alpha \to 0$ becomes identical with the E_1' stretching mode of the planar D_{5h} model, has normal co-ordinates which have a change in dipole moment which is largely independent of α. On the other hand, the "degenerate" vibration which coincides with the E_2' mode of vibration as $\alpha \to 0$ has normal co-ordinates having a dipole moment gradient of moderate dependence on α. Calculation shows, however, that the change in the dipole moment associated with the latter "degenerate" mode is always larger than that for the "nondegenerate" mode. *Indeed, by suitably choosing a value of the angle α one can make the magnitude of the change in dipole moment, and hence the intensity, of the "nondegenerate" vibration negligible compared to that of the two "degenerate" vibrations.* Also force constants calculated for this model yield small interaction constants, and the C—O stretching frequency is of the correct order of magnitude.

Hence a puckered carbon monoxide ring model is consistent with the observed spectrum of the molybdenum compound. It should be noted, of course, that symmetrically puckered rings different from the one used above can be constructed to explain the observed spectrum. The model used here for the purpose of qualitative calculations therefore has no special significance.

VOL. 1 1955

A preliminary X-ray study[7] of $C_5H_5Mo(CO)_5MoC_5H_5$ shows that the molecule crystallizes in triclinic form, and hence the crystal field has no symmetry. It is quite possible that the molecule is distorted in the crystal, as has been found to be the case with the tungsten analogue. Although only four bands are definitely discernable in the solid state spectrum (Table 1), the existence of a fifth cannot be ruled out because of poor resolution.

Cyclopentadienyliron (II)-μ-tetra carbon monoxide-cyclopentadienyliron (II).

This molecule has a formal resemblance to the binuclear molybdenum and tungsten compounds. That the molecule has a different type of structure, however, is suggested firstly by the fact that its chemical behaviour is quite different, and secondly by the appearance of widely split C—O stretching frequencies in the infrared spectrum (Fig. 1g). An attempt to explain the large splitting of the C—O frequencies by assuming that this is due only to the interaction of coupled harmonic oscillators in a four-membered carbon monoxide ring, similar to the five-membered ring in the molybdenum compound, leads to unrealistic interaction constants. Thus it would seem that the carbon monoxide groups are not all equivalent. The occurrence of a band in the 1,700–1,800 cm^{-1} region in the spectra of $Fe_2(CO)_9$ and $Co_2(CO)_8$ has been attributed[8, 9] to the presence in these molecules of bridging ketonic carbon monoxide groups. For $Fe_2(CO)_9$, the existence of three such bridging groups has been confirmed by X-ray diffraction studies[10] of the crystal. SHELINE and PITZER[8] showed the spectrum of $Fe_2(CO)_9$ obtained using thinly spread powdered material; the spectrum of $Fe_2(CO)_9$ as obtained on a sample pressed in a potassium iodide window is shown for comparison in Fig. 1f. The new technique provides better resolution and clearly shows the presence of two bands in the 2,000 cm^{-1} region, and one in the ketonic region.[11] In Fig. 1g the spectrum of $(C_5H_5Fe)_2(CO)_4$ in solution is shown; the close similarity

[8] R. SHELINE and K. S. PITZER, *J. Amer. Chem. Soc.* **72**, 1107 (1950).
[9] J. CABLE, R. SHELINE and R. S. NYHOLM, *J. Amer. Chem. Soc.* **76**, 3373 (1954).
[10] H. M. POWELL and R. V. G. EWENS, *J. Chem. Soc.* 1939, 286.
[11] The bands occur at 2,082, 2,019 and 1,829 cm^{-1} in very good agreement with the data of SHELINE and PITZER.

of the spectrum to that of $Fe_2(CO)_9$ suggests by analogy that $(C_5H_5Fe)_2(CO)_4$ contains both bridging and nonbridging carbon monoxide groups.

The appearance of a total of four C—O stretching frequencies in the *free* molecule which contains only four carbon monoxide groups implies a low symmetry of the molecule. However, preliminary X-ray diffraction studies[7] of the crystalline compound indicate that the molecule is centrosymmetric. It is possible to reconcile this observation with the infrared spectrum *of the free molecule* if the centrosymmetry which appears to exist in the crystal is not rigorous here but is approximate. The only reasonable, rigorously centrosymmetric models would be either a structure with two ketonic type carbon monoxide bridging groups with the two nonbridging carbon monoxide groups placed one on each iron atom and oppositely directed, or a structure in which the $(C_5H_5)Fe$ moieties are connected by some type of centrosymmetric pseudo-ring of four carbon monoxide groups. The former structure is rigorously excluded by the infrared data, since it allows only one bridging and one nonbridging C—O stretching frequency. The second possibility is excluded for two reasons. Firstly, a strictly centrosymmetric system could not give rise to a sufficient number of frequencies, and secondly, the wide splitting observed does not seem reasonable for a system of equivalent oscillators.

The only type of model consistent with the infrared data is one in which there is one bridging carbon monoxide group which is essentially ketonic in nature and which gives rise to the band at $\sim$1,800 cm^{-1}, together with three nonbridging groups which would account for the three frequencies in the neighbourhood of 2,000 cm^{-1}. A reasonable approach to centrosymmetry can be obtained if the following conditions are fulfilled: (a) the centres of the axes between opposite carbon atoms coincide at the approximate centre of the molecule, (b) the C—O axes of the nonbridging carbon monoxide groups make small angles with the median plane of the carbon atoms. These angles cannot, however, be zero, since the system of carbon monoxide groups would then have rigorous centrosymmetry. Two variants of this general, approximately centrosymmetric model have been considered in detail. These are shown diagrammatically in Fig. 4. In each case we make the convenient assumption that the four carbon atoms are planar. This is not strictly necessary, but wide deviations from planarity are unlikely. The first variant (4a), in which the nonbridging groups have their C—O axes alternately above and below the median plane of the four carbon atoms may have a plane of symmetry if, as is possible, other parts of the molecule are symmetrically placed with respect to the x-z plane. In the second, two *adjacent* nonbridging carbon monoxide groups are deflected from the median plane towards one iron atom and the third nonbridging carbon monoxide group is deflected the opposite way (4b).

Calculations of the relative intensities of the absorption bands for these two models have been made in the same manner as for the puckered five-membered ring in the case of the molybdenum compound. The relative intensities, when $\alpha = 30°$, based on the intensity of the 1,800 cm^{-1} band as 1·00 are given in Table 2.

It may be seen that when the angle α is 30°, the more symmetric model (a) is in qualitative agreement with the observed spectrum, whereas model (b) is not. Furthermore, in model (b), to the degree of approximation made in the calculations, the intensities of ν_0 and ν_2 (both nonbridging) are identical and those of ν_{1a} and ν_{1b} remain in an approximately 1 : 1 ratio over the entire range of α from 0° to 60°. Even

when α is 60°, the intensities of both ν_0 and ν_2 are an order of magnitude lower than those of ν_{1a} and ν_{1b} in model (b). Thus for any choice of α between 0° and 60°, model (b) would require the ~1,800 cm^{-1} band and one of the ~2,000 cm^{-1} bands to have at least ten times the intensity of the other two ~2,000 cm^{-1} bands. Model (b) may hence be considered unsatisfactory.

TABLE 2

Model (a)		Model (b)	
Vibration	Approximate relative intensity	Vibration	Approximate relative intensity
ν_0	0·036	ν_0	0·036
ν_{1a}	1·00	ν_{1a}	1·00
ν_{1b}	0·80	ν_{1b}	1·07
ν_2	0·30	ν_2	0·036

VOL. 1 1955

As Table 1 indicates, the crystalline compound also exhibits widely separated absorption in the carbonyl stretching region. There are two strong bands at ~1,776 cm^{-1} split by only 12 cm^{-1}, two strong bands at ~1,957 cm^{-1} split by only 15 cm^{-1} and a shoulder at 2,000 cm^{-1}. Such a spectrum is not compatible with centrosymmetric molecules in a lattice of equally high symmetry.

With the present knowledge, it is impossible to say whether the nonbridging carbon monoxide groups are to be regarded as primarily bonded by localized bonds two to one iron atom and one to the other iron atom, or rather as forming with the ketonic bridging group a puckered four-membered ring. For nomenclatural purposes only, we have used the second case. It is unlikely that any one simple "canonical" bonding structure will be completely adequate to explain the configuration and stability of the compound—or indeed of the similar "triple decker sandwiches" of molybdenum and tungsten. It may be noted that any of the structures discussed above can account for the observed diamagnetism of the molecule.

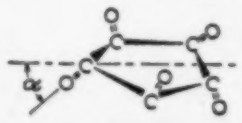

FIG. 3.—Structure of the puckered ring of five carbonyl groups used in calculation.

It is interesting to note[12] that recent electron diffraction studies of gaseous $(C_5H_5)_2Fe$ and $(C_5H_5)_2Ni$ indicate free, or only slightly hindered rotation of the C_5H_5 rings in these molecules. Such free rotation is in accord with the molecular orbital theory of the "sandwich bond" and probably occurs in the cyclopentadienylmetal carbon monoxide compounds also.

In this paper we have treated the infrared spectra of various molecules in the C—O stretching region on the assumption that, to a good approximation, only the local symmetry of the carbon monoxide groups need be considered; consistent results were obtained. Free rotation of the C_5H_5 rings in these compounds would make this assumption even more satisfactory.

[12] V. SCHOMAKER *et al.*, "Chemistry and Chemical Engineering at California Institute of Technology 1953–54," Pasadena, Calif.

APPENDIX

For the molybdenum compound $C_5H_5Mo(CO)_5MoC_5H_5$ we have considered a puckered five-membered carbon monoxide cyclic stysem (Fig. 3) on the basis of a coupled harmonic oscillator model. The calculations involved are outlined briefly here.

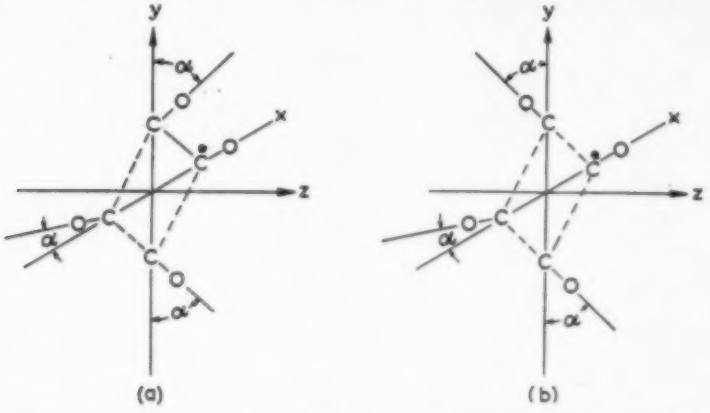

FIG. 4.—Possible structures for four carbon monoxide groups in $(C_5H_5Fe)_2(CO)_4$.

Let us assume that the potential function for the five-membered cyclic system is of the same form as that for a planar cyclic carbon monoxide system, i.e.,

$$V = \tfrac{1}{2}K\sum_{r=0}^{4}\eta_r^2 + \tfrac{1}{2}K'\sum_{r=0}^{4}\eta_r\eta_{r+1} + \tfrac{1}{2}K''\sum_{r=0}^{4}\eta_r\eta_{r+2} \tag{1}$$

The kinetic energy is assumed to be that of five linear oscillators

$$T = \frac{1}{2\mu}\sum_{r=0}^{4}\dot{\eta}_r^2 \tag{2}$$

where η_r is the change in bond length of the rth carbon monoxide ligand and μ is its reduced mass. Equations (1) and (2) can be brought into simple harmonic oscillator form by the co-ordinate transformation

$$\eta_r = \sqrt{\frac{2}{5}}\left(\frac{1}{\sqrt{2}}Q_0 + \cos\frac{2\pi r}{5}Q_{1a} + \sin\frac{2\pi r}{5}Q_{1b} + \cos\frac{4\pi r}{5}Q_{2a} + \sin\frac{4\pi r}{5}Q_{2b}\right) \tag{3}$$

where

$$\begin{aligned}
Q_0 &= \frac{1}{\sqrt{5}}\sum_{r=0}^{4}\eta_r \\
Q_{1a} &= \sqrt{\frac{2}{5}}\sum_{r=0}^{4}\cos\frac{2\pi r}{5}\eta_r \\
Q_{1b} &= \sqrt{\frac{2}{5}}\sum_{r=0}^{4}\sin\frac{2\pi r}{5}\eta_r \\
Q_{2a} &= \sqrt{\frac{2}{5}}\sum_{r=0}^{4}\cos\frac{4\pi r}{5}\eta_r \\
Q_{2b} &= \sqrt{\frac{2}{5}}\sum_{r=0}^{4}\sin\frac{4\pi r}{5}\eta_r
\end{aligned} \tag{4}$$

Substituting (3) in (1) and (2) yields

$$V = \tfrac{1}{2}\lambda_0 Q_0^2 + \tfrac{1}{2}\lambda_1 Q_{1a}^2 + \tfrac{1}{2}\lambda_1 Q_{1b}^2 + \tfrac{1}{2}\lambda_2 Q_{2a}^2 + \tfrac{1}{2}\lambda_2 Q_{2b}^2$$

$$T = \frac{1}{2\mu}\dot{Q}_0^2 + \frac{1}{2\mu}\dot{Q}_{1a}^2 + \frac{1}{2\mu}\dot{Q}_{1b}^2 + \frac{1}{2\mu}\dot{Q}_{2a}^2 + \frac{1}{2\mu}\dot{Q}_{2b}^2 \qquad (5)$$

where

$$\lambda_0 = K + K' + K''$$

$$\lambda_1 = K + \cos\frac{2\pi}{5}K' - \cos\frac{\pi}{5}K''$$

$$\lambda_2 = K - \cos\frac{\pi}{5}K' + \cos\frac{2\pi}{5}K'' \qquad (6)$$

Using the puckered model described above, we obtain the change of the dipole moments associated with the normal co-ordinates $Q_s (s = 0; 1a, b; 2a, b)$ as

$$\left|\frac{\partial \vec{M}}{\partial Q_0}\right|^2 = \frac{4}{5}\sin^4\frac{\alpha}{2}q^2 \quad \text{along } y\text{-axis}$$

$$\left|\frac{\partial \vec{M}}{\partial Q_{1a}}\right|^2 = \frac{2}{5}q^2\left(4\sin^4\frac{\alpha}{2} + 10\cos\alpha\sin^2\frac{\alpha}{2} + \frac{25}{4}\cos^2\alpha\right) \quad \text{along } y\text{-axis}$$

$$\left|\frac{\partial \vec{M}}{\partial Q_{1b}}\right|^2 = \frac{2}{5}q^2\left(\frac{25}{4}\cos^2\alpha + 16\sin^2\alpha\cos^2\frac{2\pi}{5}\sin^2\frac{\pi}{5}\right) \quad \text{along } x \text{ and } z \text{ axes}$$

$$\left|\frac{\partial \vec{M}}{\partial Q_{2a}}\right|^2 = \frac{8}{5}\sin^4\frac{\alpha}{2}q^2 \quad \text{along } y\text{-axis}$$

$$\left|\frac{\partial \vec{M}}{\partial Q_{2b}}\right|^2 = \frac{32}{5}\sin^2\alpha\sin^2\frac{2\pi}{5}\cos^2\frac{\pi}{5}q^2 \quad \text{along } z\text{-axis}$$

where q is the charge associated with each atom in one of the carbon monoxide ligands. The co-ordinate system has been chosen so that the x-y plane coincides with the plane of the carbon atoms, with the y-axis passing through the C—O group lying in this plane. Considering a numerical example with $\alpha = 30°$, we have

$$\left|\frac{\partial M}{\partial Q_0}\right|^2 \approx 4 \times 10^{-3} q^2$$

$$\left|\frac{\partial M}{\partial Q_{2a}}\right|^2 + \left|\frac{\partial M}{\partial Q_{2b}}\right|^2 \approx q^2$$

$$\left|\frac{\partial M}{\partial Q_{1a}}\right|^2 + \left|\frac{\partial M}{\partial Q_{1b}}\right|^2 \approx 4q^2$$

Since the intensity is proportional to the square of the vector representing the charge in the dipole moment,[13] it follows that (Q_{1a}, Q_{1b}) and (Q_{2a}, Q_{2b}) have approximately the same intensity, while the intensity of Q_0 is about 10^{-2}–10^{-3} smaller.

[13] See, for example, G. HERZBERG, *Infrared and Raman Spectra of Polyatomic Molecules*. D. VAN NOSTRAND, New York, 1945, pp. 240 and 261.

VOL. 1 1955

ACKNOWLEDGMENTS

We are indebted to the General Electric Company for support through a Swope Fellowship (F. A. C.) and to the National Science Foundation for a Predoctoral Fellowship (A. D. L.). Thanks are due to Prof. W. MOFFITT for his advice and criticism.

This work was supported in part by the United States Atomic Energy Commission.

J. Inorganic and Nuclear Chemistry, 1955, Vol. 1, pp. 187–193. Pergamon Press Ltd., London

PHOSPHINE AND ARSINE DERIVATIVES OF MONOSILANE

By B. J. Aylett, H. J. Emeléus, and A. G. Maddock
University Chemical Laboratory, Cambridge.

(*Received* 23 *March* 1955)

Abstract—The reaction of silyl iodide with phosphorus, phosphine, arsenic and the arsenides of potassium and mercury has been studied. The compounds $P(SiH_3)I_2$ and $As(SiH_3)I_2$ have been isolated and characterized. Both decompose below 100°. Evidence is presented for the existence of the compounds $P(SiH_3)_2I$, $P(SiH_3)_3$, $P(SiH_3)_4I$, $As(SiH_3)_2I$, $As(SiH_3)_3$ and $As(SiH_3)_4I$ which, however, have not yet been fully characterized. Silyl iodide forms 1 : 1 addition compounds with trimethylamine, triethylamine, trimethyl phosphine, triethylphosphine and trimethyl arsine. The first four are only slightly dissociated, but the arsenic compound dissociates readily. Silyl iodide also forms a compound $SiH_3I \cdot 1{\cdot}8\ N(CH_3)_3$ in its reaction with trimethylamine under pressure. This compound gives a non-conducting solution in acetonitrile, whereas the compounds with one mole of trimethylamine and triethylphosphine give conducting solutions and are therefore salt-like. These results are related to current theories of the formation by silicon of compounds with co-ordination number in excess of four, and of the utilization of *d* orbitals in bond formation.

VOL. 1 1955

The alteration in the properties of an organic compound on substitution of silicon for one or more of the carbon atoms can often be explained in terms of a few fundamental points of difference between the two elements. Thus the covalently bound silicon atom is larger than the carbon atom and can therefore be thought of as more exposed to attack. Silicon is also more electropositive than carbon. The most far-reaching consequence of this difference is the presumed reversal of the polarity of the bond dipole in the Si—H and C—H bonds, which renders the silanes and their partially substituted derivatives much more liable to polar attack by nucleophilic reagents. In addition, silicon can attain a maximum covalency of six, whereas carbon is restricted to four. This provides a mechanism for the readier reaction of silicon compounds, and also accounts for the formation of some of their adducts.

The above differences are to some extent interdependent and, largely because of the greater size of the silicon atom, p_π—p_π bonding cannot be strong, so that normal double or triple bonds between silicon or silicon and carbon atoms are unknown.[1] There is, however, considerable evidence for the existence of double bond character in bonds involving the silicon atom in certain types of compound. Thus, although the trialkyl silyl group sometimes exhibits an electron releasing effect, as for instance in its influence on the strength of the substituted amines[2, 3] or fatty acids,[4] it may exhibit the opposite behaviour. Thus, electron attraction is found in the nucleophilic substitution of chlorine by iodine in Me_3SiCH_2Cl,[5] and in the reduced dipole moments and ionization constants of compounds such as *p*-trimethylsilyl aniline.[6, 7]

Recently, a new theoretical analysis has confirmed that double bonds of the π type can be formed in some circumstances between silicon and other atoms. Craig, Maccoll, Nyholm, Orgel, and Sutton, have shown[8] that the overlap between a vacant d_π orbital on a silicon atom and a fully occupied p_π on an atom to which the

[1] Pitzer, *J. Amer. Chem. Soc.* **70**, 2140 (1948).
[2] Sommer & Rockett, *J. Amer. Chem. Soc.* **73**, 5130 (1951).
[3] Noll, Daubert, & Speier, *ibid.*, 3871.
[4] Sommer, Gold, Goldberg, & Marans, *ibid.* **71**, 1509 (1949).
[5] Cooper & Prober, *ibid.* **76**, 3943 (1954).
[6] Soffer & de Vries, *ibid.* **73**, 5817 (1951).
[7] Benkeser & Krysiak, *ibid.* **75**, 2421 (1953).

silicon is already bound by a σ bond is sufficient to confer double bond character on the bond. The bonds between silicon and the elements of Groups 5, 6, and 7 can therefore be expected to show a double bond character which will be stronger the more electronegative the element providing the p_π orbital.[9] In many compounds this double bond effect should oppose the effect of the greater electropositivity of silicon.

Hitherto, relatively few compounds have been described which are suitable for estimating the actual importance of this effect. That silicon-halogen bonds possess some double bond character is shown by the fact that the dipole moments of the simple halogenated silanes are generally smaller, rather than larger, than those of the corresponding carbon compounds.[9] The Si—Cl and Si—F bonds are shorter than would be expected for single bonds. On the other hand the Si—I bond is of the same length in SiH_3I as in SiI_4.[10] The silicon-oxygen bond in the silicones is also shorter than is required for a single bond.

The only known compounds containing the Si—N bond which are suitable for testing the extent of double bond character are trisilylamine and the methyl silylamines. The absence of base forming properties in the former was observed by STOCK and SOMIESKI.[11] This was adduced as evidence of double bond character in the Si—N bond by CRAIG *et al.*[8] BURG and KULJIAN[12] also found that boron trifluoride and trichloride gave addition compounds with trisilylamine and methyl disilylamine, whereas diborane did not. Had the donor properties of the nitrogen atom been unimpaired a borine derivative should have been formed, as in the case of trimethylamine. These authors suggest that the unexpectedly high volatility of $(SiH_3)_2NB_2H_5$ and $(SiH_3)(CH_3)NB_2H_5$ may be due to a reduction of the dipole by charge migration associated with the double bond character. Another result of this bonding is the unusual planar configuration of the $(SiH_3)_3N$ molecule (HEDBERG, *vide* CRAIG *et al.*[8] This double bonding is often referred to as back co-ordination.

Notwithstanding this evidence of the reduction in the availability of the electron pair in amines containing a Si—N bond, a quaternary compound, $N(CH_3)_3SiH_3Cl$, containing this linkage has been found.[13] The salt-like character of the compound was demonstrated by showing that its solution in acetone could be electrolyzed. If the silyl chloride-trimethylamine compound were not quaternary in character it would presumably be a compound of penta- or hexa-covalent silicon.[14] The possibility that silicon can exceed a covalency of four in molecules containing Si—Cl bonds has been questioned by SCHUMB and COOK,[15] although similar compounds containing Si—F bonds have long been known. However, the existence of HARDEN's pyridine adduct of silicon tetrachloride[15a] has been confirmed.[16]

[8] *J. Chem. Soc.*, 332 (1954).
[9] BROCKWAY and COOP, *Trans. Faraday Soc.* **34**, 1429 (1938).
LEWIS and SMYTHE, *J. Amer. Chem. Soc.* **61**, 3063 (1939).
MALATESTA and PIZZOTTI, *Gazzetta* **73**, 143 (1943).
SPANSCHUS, MILLS, SCOTT, and MCKENZIE, *J. Amer. Chem. Soc.* **72**, 1377 (1950).
[10] SHARBAUGH, HEATH, THOMAS, and SHERIDAN, *Nature* **171**, 87 (1953).
[11] *Ber.* **54B**, 740 (1921).
[12] *J. Amer. Chem. Soc.* **72**, 3103 (1950).
[13] EMELÉUS and MILLER, *J. Chem. Soc.*, 819 (1939).
[14] SUJISHI and WITZ, *J. Amer. Chem. Soc.* **76**, 4630 (1954).
[15] *J. Amer. Chem. Soc.* **75**, 5133 (1953).
[15a] *J. Chem. Soc.* **51**, 40 (1887).
[16] PIPER and ROCHOW, *J. Amer. Chem. Soc.* **76**, 4318 (1954).

The assessment of the importance of back co-ordination and the question of the existence of derivatives containing penta- and hexa-covalent silicon call for the study of a wider range of silicon compounds, and the purpose of this investigation was the preparation of derivatives containing bonds between silicon and the elements of Groups 5 and 6. Some results on the nitrogen, phosphorus, and arsenic derivatives are described below. The compounds of the elements of Group 6 will be considered in a subsequent paper. At the time when this investigation was commenced no derivatives containing the Si—P and Si—As bonds had been described. FRITZ has, however, recently described the preparation of monosilyl phosphine by the pyrolysis of a mixture of monosilane and phosphine.[17] No details of the chemical properties of this substance have been given. Very recently SUJISHI and WITZ[18] have shown that mono- and dimethyl-phosphine give 1 : 1 adducts with silyl bromide and iodide at low temperatures. Both compounds were extensively dissociated at 0°, much more so than methyl phosphonium iodide and bromide or the compound between triethylamine and silyl bromide. No reaction was observed with phosphine. The authors found that the 1 : 1 dimethyl phosphine adduct reacted with more dimethyl phosphine. Decomposition reactions also occurred with liberation of monosilane. It was concluded that the compounds were not phosphonium salts.

VOL. 1 1955

Silyl iodide was found to react with phosphorus much more readily than does methyl iodide. In a series of experiments at temperatures between 20–100° the only product isolated in a pure state was silyl diiodo phosphine, SiH_3PI_2. There was evidence that $(SiH_3)_2PI$ and $P(SiH_3)_3$ were also produced. The former could not be separated from silylene iodide, SiH_2I_2, which is formed by the disproportionation of silyl iodide, and phosphorus trisilyl appears to have a similar volatility to silyl iodide. It also reacted with silyl iodide to form a readily dissociated 1 : 1 adduct. The reaction of silyl iodide with arsenic gave similar products, but only $As(SiH_3)I_2$ was isolated in a pure state. There was again evidence for the formation of a 1 : 1 arsenic trisilyl-silyl iodide adduct. The compound SiH_3PI_2 and its arsenic analogue both decomposed slowly at room temperature, forming a mixture of products which included hydrogen, hydrogen iodide, silyl iodide and phosphine, or arsine, and decomposition was rapid at 80°. There was evidence that the other silyl derivatives of these two elements were also unstable, and were thus sharply differentiated from the disilyls of sulphur and selenium.[19]

Although it did not prove possible to isolate in a pure state the trisilyls of phosphorus and arsenic and to study in detail the quaternary compounds which they form, several related adducts of silyl iodide were isolated. Thus, solid compounds were obtained by the combination of equimolecular quantities of silyl iodide and trimethylamine or triethylamine. Both had a dissociation pressure at room temperature of <1 mm, compared with the dissociation pressure of 3 cm for the chloro-compound, $N(CH_3)_3SiH_3Cl$. (EMELÉUS and MILLER.[12]) The compound $N(CH_3)_3SiH_3I$ was not spontaneously inflammable in air, underwent only superficial oxidation, and could be handled in a dry-box. The compounds $P(CH_3)_3SiH_3I$ and $P(C_2H_5)_3SiH_3I$ were prepared by reaction of the alkyl phosphines with silyl iodide at room temperature, and had also very low dissociation pressures, the ethyl compounds being

[17] *Z. Naturforsch.* **8b**, 776 (1953).
[18] Rept. No. 1, March 1954, Office of Ordnance Research Control DA-11-OLL. ORD 1264.
[19] EMELÉUS, MCDIARMID, and MADDOCK, *J. Inorg. Nucl. Chem.* **1**, 195 (1955).

less volatile than the methyl compounds. All these compounds lost monosilane very slowly at room temperature and formed involatile products. Trimethyl arsine also formed a 1 : 1 adduct, $As(CH_3)_3SiH_3I$, which dissociated more readily, and reversibly. From measurements of the dissociation pressure the value of ΔH_{273} from liquid SiH_3I and $AsMe_3$ was—9,700 cals.

The action of excess of trimethylamine on the compound $(CH_3)_3NSiH_3I$ led to some decomposition and silane production, but the main product had a composition approximating to the formula $[(CH_3)_3N]_2SiH_3I$. The conductivities of the compounds $(CH_3)_3NSiH_3I$, $(C_2H_5)_3PSiH_3I$, and $[(CH_3)_3N]_2SiH_3I$ were measured in acetonitrile solution. The first two gave readily conducting solutions and were therefore represented as salt-like substituted ammonium and phosphonium compounds. The 2 : 1 compound was likewise readily soluble in acetonitrite but did not give an appreciable increase in conductance. It is likely therefore that this compound differs in type from the quaternary compounds and it may well be a derivative of hexa covalent silicon.

EXPERIMENTAL

Silyl iodide was prepared by the reaction of monosilane with hydrogen iodide in presence of aluminium iodide.[20] Monosilane was prepared by the method of FINHOLT, BOND, WILZBACH, and SCHLESINGER[21] in an apparatus similar to that used by PEAKE, NEBERGALL, and YUN TI CHEN.[22] The separation and characterization of volatile substances was done in an all-glass vacuum apparatus of the type described by STOCK, using taps in place of mercury float valves. In some cases, where it was necessary to avoid contact with tap grease, taps were replaced by thin glass diaphragms, which were broken electromagnetically as required.

Reaction of silyl iodide with phosphorus—In a series of experiments varying quantities of white phosphorus were sealed with measured quantities of silyl iodide in a 500 ml bulb in which the phosphorus had first been heated in vacuum so as to produce a large surface. The bulb was fitted with a diaphragm and magnetic breaker to enable the reaction products to be returned to the vacuum system for separation and identification. Reaction occurred below 0°, giving a red solid. The orange-red liquid gradually disappeared as the reaction proceeded. In most cases the bulb was heated to 100° for a time. In one such experiment silyl iodide (11·076 g) was heated with phosphorus (43·06 g) for 18 hr at 100°. The volatile products identified were hydrogen (63 ml), monosilane (0·35 g), silylene iodide and about 0·6 g of a liquid which was identified as phosphorus silyl diiodide (Found: P, 9·0; Si, 8·8; H, 0·87; I, 81·3 per cent; M, 321, 317. Calc. for $PSiH_3I_2$: P, 9·8; Si, 8·9; H, 0·96; I, 80·4; M, 316). The compound melted sharply at −1·8°. Vapour pressures measured with a spoon-gauge in the range 20–109° gave the following values.

Temp°	0	10·1	19·0	36	52	70	94	109
V.p, mm	1·2	2·2	3·5	75	88	133	207	299

The b.p. was 190° ± 0·5°, the latent heat of vaporisation 9300 cals/g-mol and TROUTON's constant 20·5. The approximate liquid density was 2·9 ± 0·2 g/ml at 20°. Decomposition was fairly rapid above about 80° and appreciable in a few days at room temperature. The decomposition products identified were hydrogen, hydrogen iodide, silyl iodide, and phosphine. A red solid was also formed. In a similar experiment with silyl iodide (10·14 g) and phosphorus (21 g) heated for 12 hr at 80° the above products were again identified and in addition a small liquid fraction (0·15 g), which condensed in the fractional condensation at −46°, was isolated. It had a molecular weight of 256 (SiH_3I_2, 284; $P(SiH_3)_2I$, 220). It was shown by hydrolysis to contain phosphorus, silicon, hydrogen (as Si—H), and iodine and was thought to be a mixture of silylene iodide, SiH_3I_2, and phosphorus disilyl iodide, $P(SiH_3)_2I$. Numerous attempts to obtain this compound in a pure condition were unsuccessful. Fractions such as the above yielded, on standing for several days at room temperature, silyl iodide, phosphine, hydrogen and phosphorus silyl diiodide. The latter was characterized by molecular weight determination and vapour pressure measurements.

[20] EMELÉUS, MADDOCK, and REID, *J. Chem. Soc.* 353 (1941).
[21] *J. Amer. Chem. Soc.* **69**, 2692 (1949).
[22] *Ibid.* **74**, 1526 (1952).

Reaction at room temperature was incomplete, probably because of the limited phosphorus surface available. In a typical experiment silyl iodide (7·615 g) and phosphorus (26·8 g) were allowed to react for 18 hr at 20°. The products were roughly fractionated and all the material condensed in a trap cooled to −96° (i.e. unchanged SiH_3I and reaction products other than hydrogen and monosilane) were resealed with fresh phosphorus (15 g) for a further 18 hr. The products then identified were hydrogen, phosphine, disilane, unreacted silyl iodide, a trace of silylene iodide and a pale buff-coloured solid which had a vapour pressure at 19° of 2 cm. This solid could be distilled in the vacuum apparatus. It passed through a trap cooled to −64° but was held by one at −96°. Approximate determinations of molecular weight at room temperature gave values of 151, 152, and 145 (Calc. for SiH_3I, 158; Calc. for $P(SiH_3)_3$, 124). These approximate values were consistent with the solid being the compound $P(SiH_3)_4I$, which dissociated in the vapour phase. A quantity of the solid was hydrolyzed by 15 per cent alkali. The hydrogen evolved and the iodide in the hydrolysate were measured. (Found: H_2 : I, 12 : 1. Calc. for $P(SiH_3)_4I$. H_2 : I, 12.) The solid did not react with trimethylamine or triethylamine.

Reaction of silyl iodide with phosphine—When silyl iodide (2·993 g) and phosphine (0·950 g) were sealed together in a tube a very small amount of buff-coloured solid was formed; 2·906 g of silyl iodide and 0·921 g of phosphine were recovered, together with 50 mg of a solid (v.p. 2 cm at 20°) which was shown qualitatively to contain phosphorus, silicon, iodine, and hydrogen. The unreacted silyl iodide and phosphine were distilled back to the reaction tube with an excess of triethylamine (which would yield NEt_3SiH_3I, which could react further with phosphine). A white solid was formed at room temperature. The volatile products were H_2 (21·7 ml), unreacted phosphine (160 ml), excess triethylamine and a liquid (0·15 ml) which was spontaneously inflammable and liberated phosphine with water. It was possibly a mixture of phosphorus trisilyl and triethylamine (Found: M, 116. Calc. for $P(SiH_3)_3$, 124. Calc. for $N(C_2H_5)_3$, 101).

In a further experiment silyl iodide (1·901 g) was mixed with excess of trimethylamine to form the quaternary compound $N(CH_3)_3SiH_3I$. Excess of the amine was removed and phosphine (0·842 g) added. The tube was heated for 7·5 hr at 65°. The products were H_2 (24 ml), PH_3 (139 ml) and two small fractions which were held during separation by fractional condensation by baths at −134° and −96°, respectively. The former yielded phosphine on hydrolysis with water and contained phosphorus, silicon, and hydrogen (as Si—H), but no iodine. The molecular weight (67·6) suggested that it was silyl phosphine (M, 64). The substance held at −96° (v.p. at 0°, 8·3 cm) was shown qualitatively by hydrolysis to contain phosphorus, silicon, and hydrogen (as Si—H), but no iodine. It had a molecular weight of 122 (calc. for $P(SiH_3)_3$, 124). The compound was shown not to react with carbon disulphide.

Reaction of silyl iodide with arsenic—Reaction between silyl iodide and powdered arsenic occurred on gently heating. The same type of apparatus was used as in the reaction with phosphorus. Arsenic (30·2 g) and silyl iodide (8·08 g) were kept for 9 weeks at room temperature and then heated for 14 hrs at 72°. The products were hydrogen (176 ml), silyl iodide (1·510 g), and fractions which, from molecular weight determinations, were identified as arsine, hydrogen iodide, monosilane, and silylene iodide. In addition impure arsenic silyl diiodide (0·7 g) was isolated. During purification by repeated fractional condensation this passed a trap cooled to 0° but was held at −36°. (Found: H, 0·79; I, 71·0 per cent; M, 354. Calc. for $AsSiH_3I_2$: H, 0·83; I, 70·6 per cent; M, 360.) Arsenic and silicon were also present in the hydrolysate. The m.p. was −4·0° ± 0·5°. Vapour pressure measurements with a spoon gauge in the range 20°–108° gave the following values:

Temp°	21·0	34·8	59	63	71·7	83·7	100·6	107·9
V.p., mm	4·5	14	50	70	74	109	190	238

The extrapolated b.p. was 210° ± 5°, the latent heat of vaporisation 9200 cals/g-ml and TROUTON'S constant 19.3

In a further experiment arsenic (16·65 g) and silyl iodide (11·37 g) reacted for 5 days at room temperature. The tube contents were red-brown in colour. The volatile products were hydrogen (266 ml), unchanged silyl iodide (4·11 g, 36·1 per cent), disilane, hydrogen iodide and a small amount of a liquid which was held during fractionation by a trap cooled to −64°. It had a molecular weight of 167 (calc. for $As(SiH_3)_3$, 168) and 18·1 mg on hydrolysis with alkali gave 21·6 ml of H_2 and 6·1 mg of AsH_3 (M, 79. Calc. for AsH_3; M, 78). These figures represent 99·5 per cent and 73 per cent respectively of the amounts expected from the hydrolysis of this weight of arsenic trisilyl. In a further

VOL. 1 1955

experiment using arsenic (27·4 g) and silyl iodide (6·94 g) with a reaction time of 7 weeks the products identified were H_2 (181 ml), disilane (0·194 g), hydrogen iodide (0·405 g) and silyl iodide (2·56 g) with a liquid (0·49 g, M, 276–285) which was mainly silylene iodide. A further small fraction which passed a trap cooled to −112° but which was held at −134° had M, 113 and 31·5 mg gave, on hydrolysis with alkali, 10·8 ml of H_2 (Calc. for $As(SiH_3)H_2$: M, 108. Hydrogen on hydrolysis, assuming each Si—H bond gives H_2 is 11.0 ml). The hydrolysate contained silicon and arsenic, but no iodide.

Reaction of silyl iodide with potassium and mercuric arsenides—Potassium arsenide was prepared by the reaction of powdered arsenic (51 g) with molten potassium (55 g). The product was powdered in a nitrogen-filled dry box, and 20 g of it was sealed with silyl iodide (5·562 g) and allowed to react at 20° for 3 days. The products were H_2 (7·4 ml), silyl iodide (2·05 g), SiH_4, Si_2H_6, and a very small less volatile fraction which condensed during the fractionation in a trap at −46°. It was treated with silver powder to remove traces of free iodine. The product (14·0 mg) had M, 168 (Calc. for $As(SiH_3)_3$; M, 168). It was shown qualitatively to contain arsenic, silicon and hydrogen (as Si—H bonds), but no iodine. A similar small fraction was isolated in a repeat experiment during which the reactants were heated at 85° for 5 hrs. It had a v.p. at 0° of 1·7 cm and evolved hydrogen at room temperature.

Mercuric arsenide, prepared by the method of DUMESNIL[33] was dried in vacuum for 48 hrs and 5 g of the dry material was mixed with an equal weight of powdered glass and placed in a horizontal reaction tube (20 mm diam.). Silyl iodide (2·174 g) was streamed repeatedly (12 times) in vacuum through this tube, the contents of which became warm, with production of mercuric iodide. A small amount of hydrogen was removed after each pass. The products included arsine and monosilane, which were separated by fractionation and identified by molecular weight determinations. A volatile cream-coloured solid was also formed (v.p. at 21°, 1·6 cm). This lost silyl iodide and hydrogen at room temperature, the former being characterized by its molecular weight. A fresh sample on hydrolysis with aqueous alkali evolved hydrogen and gave a solution containing arsenic, silicon, and iodide (Found: H_2 evolved: I, 11·2 : 1. Calc. for $As(SiH_3)_4I$: H_2 : I, 12 : 1).

Reaction of silyl iodide with tertiary amines—These reactions were studied in small bulbs (50 ml) attached to the vacuum system. Known weights of the reactants were distilled in and the bulbs were sealed off with the reactants frozen in liquid nitrogen. The volatile reaction products were taken back into the vacuum system for identification. Silyl iodide (0·379 g) reacted with trimethylamine (0·143 g) forming a white solid. Excess trimethylamine (0·069 g) was the only volatile material remaining. There was thus a reaction ratio of SiH_3I : $N(CH_3)_3$ of 1 : 1·01. The v.p. of the solid was very low, since a 50 ml sample required 12 hrs for its complete vaporization in high vacuum at room temperature. When a sample was heated in a sealed tube to 150° the only volatile product was a very small amount of monosilane and hydrogen. The solid was decomposed slowly in moist air. In a second experiment silyl iodide (0·688 g) reacted with trimethylamine (0·216 g). Excess of silyl iodide (0·106 g) was recovered, leading to a reaction ratio, SiH_3I : $N(CH_3)_3$, of 1 : 0·994. A portion (0·448 g) of this solid was hydrolyzed with 15 per cent sodium hydroxide solution (Found: H, 1·30; I, 58·9 per cent. $N(CH_3)_2SiH_2I$ requires: H, 1·39; I, 58·5 per cent). In a similar experiment silyl iodide (0·461 g) reacted with triethylamine (0·273 g), giving a white solid of very low volatility. Silyl iodide (0·030 g) was recovered, giving a reaction ratio, SiH_3I : $N(C_2H_5)_3$, of 1 : 0·992. No other volatile products were formed. [Found: H, 1·12; I, 49·2 per cent. $N(C_2H_5)_2SiH_2I$ requires: H, 1·17; I, 49·0 per cent.]

Reaction of silyl iodide with tertiary phosphines—Silyl iodide (2·534 g) reacted with trimethylphosphine, giving a white solid. Silyl iodide (0·204 g) was recovered, giving a combining ratio, SiH_3I : $P(CH_3)_3$, of 1 : 0·98. The compound was hydrolyzed by aqueous alkali with evolution of hydrogen [Found: H, 1·31; I, 54·8 per cent. $P(CH_3)_2SiH_2I$ requires: H, 1·29; I, 54·2 per cent]. Similarly, silyl iodide (1·308 g) reacted with triethylphosphine (0·882 g) to form a white solid and 0·135 g of silyl iodide was recovered [SiH_3I : $P(C_2H_5)_3$, 1 : 1·01. Found: H, 1·04; I, 46·1 per cent. $P(C_2H_5)_2SiH_2I$ requires: H, 1·10; I, 46·0 per cent]. This compound and that with trimethylphosphine had a very low volatility in vacuum.

Reaction of silyl iodide with trimethylarsine—Silyl iodide (0·770 g) and trimethylarsine (0·795 g) reacted at low temperatures to form a solid which melted just below room temperature. Excess of trimethyl arsine (0·216 g) was pumped off at −64°, giving a combining ratio, SiH_3I : $As(SiH_3)_3$, of 1 : 0·99. The m.p. of the solid was in the range 8·1–9·6°. A sample was analyzed by hydrolysis with 20 per cent sodium hydroxide solution (Found: H, 1·05; I, 45·4 per cent. $As(CH_3)_2SiH_2I$ requires:

[33] *Compt. rend.* **152**, 868 (1911).

H, 1·09; I, 45·7 per cent). The v.p. of three samples of the compound was measured in the range −40° to 21° with a sensitive spoon gauge. Typical data are:

Temp°	−34°	−26·4	−19·7	−15	−9	−0·7	5·1	12·0	15·0	21·0
V.p., mm	6·5	13	24·5	39	64	105	140·5	189	212	665

At temperatures above about 5° these data corresponded with values calculated from the partial pressures of an equimolecular mixture of silyl iodide and trimethyl arsine. At lower temperatures the vapour pressure became progressively lower than those calculated on this basis. Thus at −39·3° the measured vapour pressure was 3·0 mm, whereas an equimolecular mixture of $As(CH_3)_3$ and SiH_3I should have a vapour pressure of 13·8 mm. Approximate determinations of vapour density at −24° and 0° gave values of 131 and 133, compared with calculated values of 136 and 142, assuming complete dissociation of the vapours to $As(CH_3)_3$ and SiH_3I. The slope of a plot of $\log p$ versus $1/T$ showed that the heat of dissociation of the compound was 23,400 cals at 0°. Assuming the vapour was completely dissociated the heat of formation of the complex from the liquid components at 0° must be 9,700 cals, since the heat of volatilization of silyl iodide at 0° is 7,040 cals (EMELÉUS, MADDOCK, and REID[23]) and of trimethyl arsine is 6,600 cals.[24]

Reaction of silyl iodide with excess of trimethylamine under pressure—Two bulbs of approximately 50 ml capacity were connected by a long wide reaction tube. In one bulb was placed 0·986 g of silyl iodide and in the other 1·232 g of trimethylamine ($SiH_3I : N(CH_3)_3 = 1 : 3·5$). The volume of the apparatus was such as to give a pressure of 5 atm if no reaction occurred. The two reactants, each frozen initially in liquid nitrogen, were allowed to warm up so that the two vapours met mainly in the connecting reaction tube. A white solid separated. The apparatus, containing excess of methylamine, was kept at room temperature for 14 hrs. The volatile products were: H_2 (7·9 ml), SiH_4 (6·0 mg, M, 31·3) and residual trimethylamine (0·631 g). Thus the combining ratio $SiH_3I : N(CH_3)_3$, was 1 : 1·63. The tube was filled with dry nitrogen and a sample of the powder was removed in a nitrogen-filled dry box and weighed. This was analysed by hydrolysis with 30 per cent potassium hydroxide solution (Found: H, 1·05; I, 47·8 per cent. $SiH_3I \cdot 1·83\ N(CH_3)_3$ requires: H, 1·13; I, 47·7 per cent). The discrepancy between this result and the experimentally determined combining ratio may be accounted for by the fact that during the mixing process some of the more volatile amine reacted with liquid silyl iodide and the solid product of this reaction was not included in the sample taken. The white solid analyzed was very little changed on exposure for several days to moist air.

Conductivity measurements—Freshly-distilled acetonitrile (boiling range 81–83°) was allowed to stand successively over anhydrous potassium carbonate and phosphorus pentoxide and then further purified by vacuum distillation. The material used as solvent had a resistance of about 1·5 megohms in a cell of constant 4·6 cm^{-1}, corresponding to a specific conductivity of $1·80 \times 10^{-6}$ $ohm^{-1}\ cm^{-1}$.

The 1 : 1 addition compound of silyl iodide and trimethylamine (0·0992 g, 457 micromoles) was transferred to the bulb of the conductivity cell in a nitrogen-filled dry box. Approx. 25 ml of acetonitrile was distilled into the cell in vacuo and the solid dissolved readily. The resistance of the solutions at 25° changed from 630 ohms after 15 mins to 690 ohms after 90 mins, indicating a very slow decomposition. This resistance corresponds to a specific conductivity for the solution of $7·30 \times 10^{-3}$ $ohm^{-1}\ cm^{-1}$. The solvent was distilled out of the cell in vacuum and its specific conductivity was found to be $7·81 \times 10^{-6}$ $ohm^{-1}\ cm^{-1}$.

In a similar way 0·0143 g of the 1 : 1·83 silyl iodide—trimethylamine compound was mixed with approx. 25 ml of acetonitrile. It dissolved readily. The specific conductivity of the pure solvent was $1·24 \times 10^{-6}$ $ohm^{-1}\ cm^{-1}$, that of the solution $1·80 \times 10^{-6}$ $ohm^{-1}\ cm^{-1}$, and that of the solvent after recovery, as before, $3·22 \times 10^{-6}$ $ohm^{-1}\ cm^{-1}$. The 1 : 1 silyl iodide-triethylphosphine compound (0·0623 g, 226 micromoles) was likewise dissolved in 25 ml of acetonitrile, which had an initial specific conductivity of $2·43 \times 10^{-6}$ $ohm^{-1}\ cm^{-1}$. The specific conductivities of the solution and the solvent recovered from it were $4·95 \times 10^{-3}$ and $6·80 \times 10^{-6}$ $ohm^{-1}\ cm^{-1}$, respectively.

One of the authors (B. J. A.) wishes to thank the Department of Scientific and Industrial Research for a Maintenance Grant.

[24] ROSENBAUM and SANDBERG, *J. Amer. Chem. Soc.* **62**, 1622 (1940).

VOL. 1 1955

J. Inorganic and Nuclear Chemistry, 1955, Vol. 1, pp. 194–201. Pergamon Press Ltd., London

SULPHUR AND SELENIUM DERIVATIVES OF MONOSILANE

By H. J. Emeléus, A. G. MacDiarmid, and A. G. Maddock
University Chemical Laboratory, Cambridge

(*Received* 23 *March* 1955)

Abstract—Disilyl sulphide, $(SiH_3)_2S$, and selenide, $(SiH_3)_2Se$, have been prepared and characterized by the measurement of some of their physical properties. A number of the chemical reactions of these compounds, as well as of the previously known disilyl ether, have been studied. Although these reactions were chosen to encourage the compounds to display donor activity they always failed to show such properties.

In this paper the preparation, properties, and reactions of disilyl ether, $(SiH_3)_2O$, disilyl sulphide, $(SiH_3)_2S$, and disilyl selenide, $(SiH_3)_2Se$, are described. These compounds are formally inorganic analogues of dimethyl ether, sulphide, and selenide, and as such might be expected to have somewhat similar properties. In the preceding paper, however, it was shown that the chemistry of silyl compounds containing Group VI elements might be affected by back co-ordination from the oxygen, sulphur, or selenium to the silicon. The reactions studied here have been chosen to display the change in the donor properties of the silicon compounds attributable to back co-ordination.

There are only two volatile silyl compounds known which contain the Si—O—Si linkage, although it is found also in the substituted silicones. Disilyl ether, $(SiH_3)_2O$,[1] has been completely characterized, but very few of its chemical properties are known. Another ether, $(SiH_3SiH_2)_2O$, has also been reported.[2] Silyl alcohol, SiH_3OH, which would contain the Si—O—H linkage, appears to have only a transitory existence and rapidly condenses to form disilyl ether.[3] Two silyl-sulphur compounds have been reported, disilyl sulphide, $(SiH_3)_2S$, and silyl mercaptan, SiH_3SH,[4] but these were obtained only in an impure state and were not characterized in any way. In fact, very little is known about any compounds containing Si—S linkages, though trichlorosilyl mercaptan, $SiCl_3SH$, was prepared many years ago.[5] The thiohalides, $SiSCl_2$ and $SiSBr_2$ have also been described,[6] and more recently a number of thioethers containing the Si—S—C bond system have been made.[7] No volatile compounds containing the Si—Se linkage have so far been described.

Disilyl ether is conveniently obtained by the hydrolysis of silyl iodide[8] or, in higher yields, by the hydrolysis of disilyl sulphide. An attempt to reduce the oxychloride, $(SiCl_3)_2O$, directly to the ether with lithium aluminium hydride failed, even

(1) Stock and Somieski, *Ber.* **56**, 132 (1923).
(2) Stock and Somieski, *Ber.* **53**, 759 (1920).
(3) Stock, Somieski, and Wintgen, *Ber.* **50**, 1754 (1917).
(4) Aylett, Emeléus, and Maddock, *Research* **6**, 14 (1953).
(5) Pierre, *Ann. Chim. Phys.* [3] **24**, 286 (1848); Fridel and Ladenburg, *Compt. Rend.* **64**, 1215 (1861).
(6) Besson, *Compt. Rend.* **113**, 1040 (1891); Blix **36**, 4218 (1903).
(7) See, for example, Backer and Stienstra, *Rec. Trav. Chim.* **51**, 1197 (1932); Wolinski, Tieckelmann, and Post, *J. Org. Chem.* **16**, 1134 (1951).
(8) Emeléus, Maddock, and Reid, *J. Chem. Soc.* 353 (1941).

when the solution of the lithium compound in diethyl ether was added dropwise to a large excess of the oxychloride. Apparently the Si—O and Si—Cl linkages were equally readily reduced to Si—H by this reagent.

Disilyl sulphide was prepared in yields of over 90 per cent by the action of silyl iodide on mercuric sulphide, but disilyl selenide could not be made from mercuric selenide. It was, however, obtained in approximately 60 per cent yields by passing silyl iodide vapour over silver selenide. Silyl mercaptan has not been fully characterized, but its existence seems likely. It is apparently formed by the interaction of hydrogen sulphide and disilyl sulphide.

The reactions above involving silver salts are in general agreement with the replacement series for the alkyl-substituted silyl derivatives, which was first proposed by EABORN[9] and later extended by ANDERSON.[10] The conditions used in preparing disilyl sulphide and selenide, namely the reaction of silyl iodide vapour with the metallic salt, were such that it is unlikely that a heterolytic fission of the Si—X bond was involved, though fission of this type was postulated in the reactions studied by EABORN. The Si—Se bond should probably be inserted in this series between the Si—I and Si—S bonds. A more detailed discussion of this type of reaction will appear in an article which is now in the process of preparation.

VOL. 1 1955

Disilyl sulphide and selenide were both hydrolyzed by water to give disilyl ether and hydrogen sulphide or selenide. There was visual evidence that a solid, intermediate compound was formed in the hydrolysis, though it was not isolated. These observations are consistent with those for the hydrolysis of most silyl compounds, since the ether is obtained in most cases, in varying yields.[3, 8, 11]

Iodine does not form a sulphonium or selenonium compound with $(SiH_3)_2S$ or $(SiH_3)_2Se$ as it does with the methyl analogues. Instead, the sulphide and selenide are decomposed, with deposition of sulphur or selenium and the formation of silyl iodide. The ether undergoes a similar decomposition reaction.

Hydrogen iodide also fails to form sulphonium or selenonium type compounds. The sulphide and selenide are again decomposed, with the formation of silyl iodide and hydrogen sulphide or selenide. No evidence for the formation of a sulphonium compound could be obtained when the sulphide was treated with either silyl or methyl iodide, nor did disilyl selenide react with methyl iodide. Mercuric chloride does not form an addition compound with disilyl sulphide, as it does with some dialkyl sulphides. However, a reaction ensued to give silyl chloride and mercuric sulphide. A very slight reaction occurred between mercuric iodide and disilyl sulphide; the product was silyl iodide.

The above reactions indicate that in their silyl derivatives sulphur and selenium exhibit weaker donor properties than in their methyl compounds. Since silicon is more electropositive than carbon it might be assumed that the donor properties of these elements would be even greater. However, the powerful electron-attracting properties of the silyl group could be explained if there was a considerable amount of π-bonding between the silicon and sulphur or selenium atoms.

In their other reactions, the greater reactivity of these silicon compounds, as compared with their carbon analogues, may be attributed to lower activation energies.

[9] *J. Chem. Soc.* 3077 (1950).
[10] ANDERSON and FISCHER, *J. Org. Chem.* **19**, 1296 (1954); ANDERSON and VASTA, *ibid.*, 1300.
[11] EMELÉUS and MILLER, *J. Chem. Soc.* 819 (1939).

In circumstances where heterolytic reactions are improbable the lowering of the activation energy is probably due to the existence of the vacant *d* orbitals and the greater accessibility of the silicon atom because of its larger size.

The reactions with various boron compounds of the silyl compounds discussed in this paper are being investigated to provide further evidence for the presence or lack of donor properties in the Group VI atom.

It has been reported that the trisilylamine molecule is planar[12] and it is important to know the configuration of the molecules of silyl oxide, sulphide and selenide. Presumably if the double bond character is sufficient, the disilyl ether might prove to be a symmetric top molecule $H_3Si{=}O{=}SiH_3$. For this purpose the infrared spectra of these compounds have been measured. Silyl and silylene iodide have also been examined to facilitate the identification of some of the bonds. The most striking feature of the infrared spectra of these compounds was the intensity of the Si—O stretching absorption at 1106 cm^{-1}. WRIGHT and HUNTER[13] have already observed that this band is more than five times as intense as the corresponding C—O absorption under similar conditions. Thus, great care had to be taken to avoid hydrolysis of the other compounds and production of disilyl ether. Even the traces of water dissolving in the grease initially used to fix the cell windows to the cell produced sufficient ether to give a strong absorption at 1106 cm^{-1}. The difficulty was overcome by using a cell in which the windows were sealed on with glyptal varnish and baked hard in an oven. Nonetheless, both the sulphide and selenide still showed a weak absorption at 1106 cm^{-1}. The infrared spectrum is obviously an extremely sensitive means of detection of the ether.

The parallel ν_1 and perpendicular ν_4 Si—H stretch frequencies occur at 2198 cm^{-1} in silyl iodide and the corresponding ν_1 and ν_6 frequencies in silylene iodide appear at 2205 cm^{-1}. In the ether, sulphide, and selenide the Si—H stretch frequencies appear at 2175 cm^{-1}. Three weak overtones have been found in this region in all the silyl derivatives so far examined. The highest of these lies near 4300 cm^{-1}. Another appears between 3100 and 3150 cm^{-1}, and the third is found between 1876 and 1920 cm^{-1}.

Silyl iodide shows a doublet at 909 and 895 cm^{-1} possibly including the parallel and perpendicular SiH_3 deformation frequencies, ν_2 and ν_5.[14] The perpendicular band shows the strong, weak, weak rotational detail required by the H_3SiI molecule.

A corresponding absorption doublet appears in the ether, sulphide and selenide, the centre of the bands moving from 957 through 911 to 895 cm^{-1}. The ether also shows a strong, but broad, absorption at 760 cm^{-1} which might include the Si—O binding frequency harmonic since the fundamental is believed to lie at about 370 cm^{-1}.[13]

The remaining strong band in the silyl iodide spectrum, lying above 700 cm^{-1}, is a doublet at 1185 cm^{-1} with the same separation of the maxima as the band at 902 cm^{-1}. A detailed analysis of this spectrum will shortly be published by SHEPPARD and DIXON.

The ether shows strong absorption at 1718 and 1222 cm^{-1}. The former might be a combination of the 957 and 760 cm^{-1} frequencies.

[12] HEDBURG *vide* CRAIG *et al.*, *J. Chem. Soc.* 350 (1954).
[13] *J. Amer. Chem. Soc.* **69**, 803 (1947).
[14] MONFILS, *Compt. Rend.* **236**, 795 (1953).

It is not yet possible to distinguish any features due to the Si—S or Si—Se bonds. If the ether molecule were linear the perpendicular band at 957 cm^{-1} should show rotational detail with strong, weak, weak alternations. No such detail was observed. The three compounds are all asymmetric tops.

EXPERIMENTAL

The Reduction of Silicon Oxychloride

A number of attempts were made to reduce $(SiCl_3)_2O$ to $(SiH_3)_2O$ by means of lithium aluminium hydride. In a typical experiment lithium aluminium hydride (0.8 g) suspended in 15 cc of anhydrous ether was added in small portions to a solution of silicon oxychloride (3·07 g) in 10 cc of anhydrous ether. The reaction vessel was maintained at 0° until the reaction was complete. After fractionation of the products, 56 per cent of the silicon used was recovered as monosilane (M, found 32·0, calc. 32·0). No other volatile products were found. The excess silicon oxychloride was recovered. An attempt was made to effect the reduction by hot aluminium in the presence of hydrogen. Hydrogen at atmospheric pressure was bubbled through the boiling oxychloride (0·5 g) contained in a trap and the saturated gas passed through a 90 cm tube packed with aluminium foil and heated to 500°. Immediately beyond the furnace a white deposit was found. Further on a brown film appeared. Fractionation of the products gave a substance (0·228 g) behaving like silicochloroform (M, found 126·0, 129·0, 131·9 on successive samples, calc. 135·5. Vapour pressure 23·5 cm at 0°, calc. 21·8 cm). Silane (0·073 g), probably contaminated with a trace of disilyl ether, was obtained (M, 37·5. calc. 32·0). Disilyl ether (0·051 g) was also obtained (M, 78·2, calc. 78·0. Vapour pressure 8·25 cm/−64·5°, 10·34 cm/−59·7°, 10·73 cm/−58·5°, compared with 5·8 cm/−65°, 8·1 cm/−60°, 10·9 cm/−55.°[3] No traces of silyl chloride or partially reduced Si_2OCl_6 were obtained. This method might be developed to give satisfactory yields.

Production and Reactions of Disilyl Ether, Sulphide, and Selenide

Working quantities of the ether were prepared by the hydrolysis of silyl iodide. Silyl iodide (1·32 g) shaken with 10 cc of ice-cold water gave disilyl ether (0·220 g) (yield 67 per cent).

The reaction with iodine was examined. Disilyl ether (0·0940 g) was sealed up with iodine (0·100 g) in a 70 cc vessel. After leaving overnight at room temperature very little iodine remained. Silyl iodide (0·0387 g) (M, 160, calc. 158) was separated from the products.

Reaction of silyl iodide with mercuric sulphide—The reaction was studied by streaming the vapour of silyl iodide (4·8033 g) through a horizontal tube charged with red mercuric sulphide (20 g). The reaction tube became hot and the flow of silyl iodide was controlled to avoid overheating. The silyl iodide and reaction products were repassed twice through the tube. No hydrogen was formed. A fraction which condensed at −96° during separation of the products by fractional condensation was disilyl sulphide (1·3184 g). Only minute amounts of unchanged silyl iodide were found. The yield of disilyl sulphide was 92·5 per cent of that based on the equation $2SiH_3I + HgS = (SiH_3)_2S + HgI_2$. In a series of runs it was never less than 90 per cent. The material (0·1038 g) was analysed by hydrolysis with 30 per cent sodium hydroxide solution. Hydrogen evolved was measured. The hydrolysate was made strongly acid with hydrochloric acid and the silicon was determined as silica. Sulphur was determined by hydrolysing another sample (0·2352 g). The sulphide in the hydrolysate was oxidised to sulphate with nitric acid and bromine water and determined as barium sulphate (Found: H, 6·15; Si, 59·3; S, 34·1 per cent; M, 94·9. $(SiH_3)_2S$ requires H, 6·38; Si, 59·6; S, 34·1 per cent; M, 94·0).

The m.p. of disilyl sulphide was $-70·0° \pm 0·2°$. Vapour pressures, in the range −40° to 50° were represented by the equation: $\log_{10} P = \frac{-1692}{T} + 7·977$. The calculated vapour pressure at 0° was 6·08 cm. The boiling point was $58·8° \pm 0·7°$, the molar heat of vaporization 7743 cals/mol, and TROUTON'S constant 23·3. Density determinations in the range 5–16° were represented by the equation $d = 1·21211\ (1 - 0·00082350T)$. The refractive index was $1·52 \pm 0·03$. Before use in any experiment the vapour pressure of the disilyl sulphide was checked at 0°.

Disilyl sulphide underwent no detectable decomposition when stored at room temperature in the dark for 5 weeks. When a sample (0.1515 g) was heated at 100° in a sealed tube for 2 hr, 98·8 per

VOL. 1 1955

cent of the starting material was recoverd in a pure state. Irradiation of a sample of disilyl sulphide in a quartz tube for 6 days produced an orange film on the quartz and a sticky yellow residue on evaporating off unchanged disilyl sulphide (0·0816 g, 65 per cent recovery). In addition, an approximately equimolecular mixture of monosilane and hydrogen sulphide was recovered (M, found 33·1, calc. 33·0) which, on hydrolysis, gave 17·4 ml of hydrogen, compared with 18·0 ml expected from a 1 : 1 mixture. The hydrolysate gave qualitative tests for sulphide.

Air, dried by passing through a trap cooled in liquid nitrogen, did not react with disilyl sulphide. On cutting the reaction vessel and exposing the contents to the atmosphere immediate inflammation occurred. There was a very slow reaction between disilyl sulphide and mercury. A dark film was formed on the mercury but the minute amounts of reaction products were not identified.

The hydrolysis of disilyl sulphide—Disilyl sulphide (0·1470 g) was sealed in an evacuated tube with 1 ml of distilled water. The two substances were frozen in liquid nitrogen as they were distilled into the tube prior to sealing. When, after sealing, they were allowed to melt a gelatinous solid floated on top of the water. This disappeared on shaking the tube and minute bubbles of gas were evolved. No hydrogen was formed. The products, other than unchanged water, were disilyl ether (0·1120 g; M, found 77·6, calc. 78·0) the vapour pressure curve of which checked well with that of STOCK, SOMIESKI, and WINGTEN.[8] In addition, a fraction (0·0615 g) which, during separation by fractional condensation, passed through a trap cooled to −134° was identified as hydrogen sulphide containing a little disilyl ether (M, found 36·0, calc. 34·0). Refractionation gave a molecular weight of 34·1. The yield of pure disilyl ether was 92 per cent of that expected for the equation $(SiH_3)_2S + H_2O = (SiH_3)_2O + H_2S$.

Reaction of disilyl sulphide with silyl iodide and methyl iodide—Silyl iodide (0·2242 g) and disilyl sulphide (0·1090 g) were sealed up together and heated for 2 hr at 80° and then left over-night at room temperature. The liquids were miscible but no solid formed, nor was any solid residue left on returning the volatile contents of the tube to the vacuum apparatus. Silyl iodide could not be separated from disilyl sulphide but the amount of material recovered (0·3301 g) was 99·7 per cent of the total material initially taken. The molecular weight was 128, compared with 126 calculated for an equimolecular mixture of the two substances.

A similar experiment with methyl iodide (0·3109 g) and disilyl sulphide (0·1859 g) gave no evidence of reaction in 2 hr at 80° and 98·8 per cent of the mixture of disilyl sulphide and methyl iodide was recovered.

Reaction of disilyl sulphide with iodine—Disilyl sulphide (0·1658 g) was sealed with iodine (0·0985 g). Reaction commenced as soon as the disilyl sulphide melted and a pale coloured precipitate was formed, which, on distilling off all volatile material, remained as a bright yellow powder (0·012 g). It was soluble in carbon disulphide and gave crystals on evaporation which had the characteristic form of sulphur. The volatile material was split into two fractions; the first (0·100 g) had M, 123 and was believed to be a mixture of silyl iodide (M, 158) and disilyl sulphide (M, 94). The second (M, 111) gave, on refractionation, a small sample of almost pure disilyl sulphide of M, 96·0. The amount of iodine taken was sufficient to convert only about one quarter of the disilyl sulphide to silyl iodide. The total weight of material recovered was 97·3 per cent of the initial materials used. If all the iodine had reacted according to the equation $(SiH_3)_2S + I_2 = 2SiH_3I + S$, 0·0387 mols of sulphur should have been formed. In the experiment 0·0353 mols of sulphur were recovered.

Reaction of disilyl sulphide with hydrogen iodide—Disilyl sulphide (0·1746 g) and hydrogen iodide (0·2049 g) were kept together at room temperature for 4 weeks and then heated to 77° for 6 hr. No reaction was apparent. No hydrogen was formed. The volatile products were fractionated and a fraction was obtained (0·3389 g; M, 135) which had the distillation properties of a mixture of disilyl sulphide and silyl iodide. A second fraction (0·026 g) had M, 34·6 (H_2S requires M, 34·0). After treating this fraction with potassium hydroxide solution the hydrolysate gave qualitative tests for sulphide. A further small fraction (9·5 mg) had M, 73·5 and gave hydrogen and a solution of sulphide on hydrolysis. It was not definitely identified. The above results are consistent with the equations $(SiH_3)_2S + HI = 2SiH_3I + H_2S$, which, with the quantities taken should have yielded 0·027 g of H_2S and 0·352 g of a mixture of silyl iodide and unreacted disilyl sulphide.

Reaction of disilyl sulphide with mercuric chloride—Disilyl sulphide (0·1120 g) was condensed in a tube on to mercuric chloride (0·2 g). Reaction occurred at room temperature and the mercuric chloride became black. The products, separated by vacuum fractionation, were disilyl sulphide (0·0346 g; M, found 96·2, calc. 94·0) and silyl chloride (0·0954 g; M, found 66·2, calc. 66·5).

The amount of silyl chloride was 87·5 per cent of that expected for the equation $(SiH_3)_2S + HgCl_2 = 2SiH_3Cl + HgS$. The black residue was insoluble in boiling conc. hydrochloric acid but dissolved readily in boiling aqua regia.

Reaction of disilyl sulphide with mercuric iodide—Disilyl sulphide (0·1416 g) was condensed in a 15 cc tube on to mercuric iodide (1·0 g). No visual reaction could be observed at room temperature, and the tube was then heated at 80° for two hours. The mercuric iodide became very slightly darker in colour. The reaction products could not be completely separated by vacuum distillation but possessed the distillation properties of a mixture of $(SiH_3)_2S$ and SiH_3I (the more volatile fraction had the greater molecular weight; M, 131; M, calc. for SiH_3I, 158. Less volatile fraction M, 102; calc. for $(SiH_3)_2S$, 94). Total weight of mixture recovered (0·1706 g) was greater (by 0·0281 g) than the $(SiH_3)_2S$ initially used which would correspond to the reaction $(SiH_3)_2S + HgI_2 \rightarrow 2SiH_3I + HgS$ proceeding to approximately 8 per cent. The mercuric iodide remaining evolved only very small amounts of hydrogen on treatment with alkali solution, thus indicating that very little, if any, solid addition compound had been formed.

Reaction of disilyl sulphide with sulphur—Disilyl sulphide (0·1299 g) and sulphur (0·15 g) were heated together at 80° for 7 days. On fractionation the main material found in the product was unchanged disilyl sulphide (0·118 g; M, found 94·6, calc. 94·0), representing 91 per cent recovery. A very small volatile fraction (0·005 g) had a volatility consistent with its being a mixture of monosilane and hydrogen sulphide and gave hydrogen and sulphide on hydrolysis. There was also a less volatile fraction (0·003–0·004 g) of M, 130·5, which was possibly $(SiH_3)_2S_2$ (calc. M, 126). The experiment was repeated with similar results.

Reaction of silyl iodide with selenium—Selenium (7 g) was melted and spread on the walls of a long Pyrex reaction tube. Silyl iodide (3·239 g) was then distilled in and the tube sealed and left at room temperature for 32 weeks. There was little evidence of reaction, and the products identified were silane (0·027 g), hydrogen selenide (0·059 g), and silyl iodide (2·657 g), all of which were characterized by molecular weight determinations. Probably a little silylene iodide was also formed.

Reaction of silyl iodide with mercuric selenide—Mercuric selenide was prepared by heating selenium (8 g) with mercury (20 g) for 8 hr in a sealed tube in a furnace at 500–600°. The product was powdered and placed in a 150 ml Pyrex reaction tube and silyl iodide (2 g) distilled in. After heating to 75° for 75 hr and standing at room temperature for several months, the tube gave hydrogen (98·5 ml), silylene iodide (0·588 g), silyl iodide (0·288 g), hydrogen iodide (0·022 g) and monosilane (0·197 g), all characterized by molecular weight determinations.

Reaction of silyl iodide with silver selenide—Hydrogen selenide was prepared from aluminium selenide[15] and to its saturated solution in water silver nitrate solution was added slowly.[16] The precipitated silver selenide was filtered and washed in a dry box filled with nitrogen and dried in vacuum. The dry selenide (8 g) was sealed in a tube with silyl iodide (1·9295 g). The tube became slightly warm when the silyl iodide melted. The tube was opened after 30 min at room temperature and gave 2·2 ml of hydrogen and a condensable product, which was fractionally condensed in the vacuum system and yielded disilyl selenide (0·52 g) as a fraction held in a trap cooled to −64°. Repeated fractionation was necessary to secure tensimetrically homogeneous material. The main difficulty was in the separation from silyl iodide and silylene iodide.

Disilyl selenide (0·1390 g) was hydrolyzed by 15 per cent potassium hydroxide solution and the hydrogen evolved measured. The hydrolysate was freed from selenium by passing sulphur dioxide, acidifying with hydrochloric acid, filtering off selenium and sulphur and determining silicon gravimetrically as silica in the filtrate. Selenium was determined in the hydrolysate from another sample (0·1247 g). Most of the selenium was precipitated by adding hydrogen peroxide. The hydrolysate was then made slightly acid with hydrochloric acid and precipitation of selenium completed by adding a hot concentrated hydrazine sulphate solution. The selenium was weighed as such (Found: H, 4·19; Si, 39·5; Se, 55·6 per cent; M, 141, 142. $(SiH_3)_2Se$ requires: H, 4·25; Si, 39·7; Se, 56·0 per cent, M, 141).

The m.p. of disilyl selenide was $-68·0 \pm 0·2°$. Vapour pressures, in the range −43° to 74·5° were measured with a sensitive spoon gauge. The data in this range were represented by the equation $\log_{10} P = -\frac{1796}{T} + 7·894$. The calculated vapour pressure at 0° was 2·09 cm. The b.p. was 85·2°

[15] *Inorganic Syntheses*, Vol. 2, 184.
[16] MOSER and ATYNSKI, *Monatsh.* **45**, 235 (1924).

VOL. 1 1955

± 1°, the molar heat of vaporization 8219 cals/mol, and TROUTON's constant 22·9. The density at 20° was 1·36. There was slight decomposition of disilyl selenide near its boiling-point as shown by the development of pressures of hydrogen in the apparatus of the order of 2 mm in the course of several hours. Before use in any experiment the vapour pressure of the disilyl selenide was checked at 0°.

Hydrolysis of disilyl selenide—Disilyl selenide (0·0325 g) and water (0·0247 g) were distilled in vacuum into a reaction tube cooled in liquid nitrogen. Reaction was seen immediately the solids were allowed to melt. A colourless gelatinous solid was first formed but this disappeared and gas was evolved at room temperature. No hydrogen was evolved. Fractionation of the condensable products gave 0·0365 g of a mixture of disilyl ether and hydrogen selenide which could not be separated in the vacuum apparatus. The molecular weight of the mixture was 79·5, compared with 78·0 and 81·0 for the two pure compounds. On the assumption that the equation representing the hydrolysis is $(SiH_3)_2Se + H_2O = (SiH_3)_2O + H_2Se$, 0·0325 g of disilyl selenide should form 0·0366 g of mixed products. A small sample of disilyl ether was isolated by refractionating the mixture and was identified tensimetrically.

Reaction of disilyl selenide with iodine—Iodine (0·2304 g) was dried for a minute in vacuum and disilyl selenide (0·1363 g) was distilled onto it and the reaction tube sealed. As soon as the selenide melted the mixture became a dark red colour and a red precipitate was slowly formed and grew in bulk over a period of 17 hr. After a further 6 hr the red precipitate had changed to a black powder. The tube was opened after 9 days and no hydrogen was found. The other volatile product was identified by vapour pressure and molecular weight measurements as silyl iodide (0·2848 g). The black powder (0·0715 g) was identified as selenium. The yields of SiH_3I and Se were respectively 99·7 and 101 per cent of those expected from the equation: $(SiH_3)_2Se + I_2 = 2SiH_3I + Se$.

Reaction of disilyl selenide with hydrogen iodide—Disilyl selenide (0·0619 g) and hydrogen iodide (0·1123 g) were sealed in a small tube and kept for 9 weeks at room temperature and exposed to daylight. No hydrogen was formed. The other products, identified by molecular weight and vapour pressure, were: silyl iodide (0·118 g) and hydrogen selenide (0·040 g). The latter was contaminated with a trace of silyl iodide (evolution of hydrogen on hydrolysis with alkali in glass). There were also very small fractions which, from their distillation properties in vacuum, were probably disilane and silylene iodide. The silyl iodide was 85 per cent of the amount expected from the reaction $(SiH_3)_2Se + 2HI = 2SiH_3I + H_2Se$. The hydrogen selenide fraction was 4·5 mg heavier than expected from this equation. It was shown by peroxide oxidation to contain a trace of hydrogen iodide.

Reaction of disilyl selenide with methyl iodide—Approximately equi-molar quantities of disilyl selenide (0·0610 g) and methyl iodide (0·0684 g) were distilled into a small tube and sealed off. There was no evidence of reaction at room temperature nor did any residue remain on distilling the volatile material into a side arm of the tube. The tube was heated for several hours at temperatures up to 75°. Fractionating of the contents of the tube gave disilyl selenide (0·0510 g).

Reaction of disilyl sulphide with hydrogen sulphide—Disilyl sulphide (0·2164 g) and hydrogen sulphide (0·204 g) were sealed in a 20 cc tube at room temperature for 31 days. No hydrogen was liberated. Fractionation in the vacuum system gave silyl mercaptan (0·0825 g) and disilyl sulphide (0·1323 g) the vapour pressure of which at 0° was 6·18 cm, calc. 6·08 cm. Hydrogen sulphide (0·193 g) was identified by its molecular weight, 34·4, calc. 34·0. No other material was formed. The weight of silyl mercaptan produced accounts for 94 per cent of the disilyl sulphide used up according to the equation

$$(SiH_3)_2S + H_2S \rightarrow 2SiH_3SH.$$

With the amount of mercaptan available it was not possible to carry out a quantitative analysis with great accuracy. Silyl mercaptan (0·0325 g) was hydrolyzed in 30 per cent potassium hydroxide solution and the hydrogen evolved measured. Excess bromine water was added to the hydrolysate to oxidize sulphide to sulphate which was then determined as barium sulphate. (Found: H, 5·07; S, 42·3; M, 64·2. SiH_3SH requires H, 4·68 per cent; S, 50·0 per cent; M, 64·0).

The melting point of silyl mercaptan was approximately −134°. Vapour pressures in the range −75 to −35° were represented by the equation $\log_{10} P = -\frac{1355}{T} + 7{\cdot}596$. The boiling point was 14·2°, the molar heat of vaporization 6201 cals/mol and TROUTON's constant 21·9. Decomposition took place slowly even at −78° as indicated by a slow increase in the vapour pressure, and extensive decomposition set in at temperatures above −30°. The only decomposition product which could be

isolated was disilyl sulphide (vapour pressures at −46·0° and 23·8° were 0·32 cm and 1·59 cm; calc. 0·34 cm and 1·59 cm). Decomposition apparently took the form of condensation to the sulphide and hydrogen sulphide.

Infrared measurements—These were made on a Perkin-Elmer Model 21 double beam recording I–R spectrophotometer. A sodium chloride optical system was used. All measurements were made on the gaseous phase with the sample confined in a 10 cm cell with 5 mm sodium chloride end plates.

Silyl iodide—Measured at 124 mm, 35 mm and 3 mm Hg pressure. Absorption maxima, all in cm^{-1}; 4300, weak; 3100, medium; 2790, weak; 2198, very strong (ν_1 and ν_4 ∥ and ⊥ Si-H frequencies); 1876, weak; 1612, weak; 1494, 1482 doublet, weak; 1192, 1178 doublet, strong (possibly overtone involving ν_3 or ν_5?); 909, 895 doublet and intense broad band (ν_5 and ν_3 ∥ and ⊥ SiH_3 deformation; shows strong, weak, weak rotational detail with separation of ~7 cm^{-1}; compare MONFILS[14].)

Silylene iodide—Measured at 0·11 mm Hg pressure. 2205 cm^{-1}, sharp, ν_1 and ν_6 symmetric and asymmetric Si–H stretch. 928, 921 doublet, ν_2, SiH_2 bending. 793, 799 doublet. ν_6 rocking.[17]

Disilyl ether, sulphide and selenide—The results are shown in Table 1. The ether was measured at 74 mm, 11 mm, 2 mm, and 0·5 mm Hg pressure; the sulphide at 125 mm, 25 mm, 3mm, and 1 mm Hg pressure and the selenide at 40 mm, 4·7 mm and 1·3 mm Hg pressure.

TABLE 1.

$(SiH_3)_2O$	$(SiH_3)_2S$	$(SiH_3)_2Se$	Comments
	All measurements in cm^{-1}		
4290	4290	4290	v.w. Also with SiH_3I
3150	3125	3100	m. Also with SiH_3I
2175	2175	2175	Si–H stretch v.s.
1920	1887	1872	w. Also with SiH_3I
1774 v.w.			
1718 s.			Combination of 760 and 957?
1580 w.			
1465 v.w.			
	1277 m.		
1222 s.	Shoulder here 1218 w.		It is difficult to distinguish weak sulphide or selenide bands from ether impurity here.
1106 v.s.	Some contamination here		
962 d. / 952 v.s.	Some contamination here		
	914 d. / 908 v.s.	899 d. / 892 v.s.	
		887	
760 v.s.		751 d. / 745 m.	Broad bands.
	680 v.s.		

w = weak. m = moderate. s = strong. v = very. d = doublet.

The authors would like to acknowledge the assistance of Mr. ELSLEY in making the infrared measurements, and to thank Dr. N. SHEPPARD for helpful discussions. One of the authors (A. G. McD.) is indebted to The Shell Petroleum Company, Ltd. for a Post-graduate Research Fellowship.

[17] Compare HAWKINS, POLO, and WILSON, *J. Chem. Phys.* **21**, 1122 (1953).

J. Inorganic and Nuclear Chemistry, 1955, Vol. 1, pp. 202–212. Pergamon Press Ltd., London

THE KINETICS OF THE REACTION OF ELEMENTARY FLUORINE WITH COPPER METAL

By P. E. Brown, J. M. Crabtree, and J. F. Duncan*
Atomic Energy Research Establishment, Harwell, Didcot, Berks

(*Received October* 1954)

Abstract—The reaction has been investigated under high vacuum conditions between room temperature and 250°C, and at pressures between 6 mm and 60 mm mercury. The equation

$$x = x_0 \log_{10}(1 + at) + b$$

is obeyed, where x is the thickness of the corrosion film at time t, and x_0, a, and b are constants. The experimental data show that the reaction cannot be controlled by a simple diffusive process. The most satisfactory interpretation is that it is due to random cracking of the corrosion film, but whilst this is not obviously at variance with the facts, it does not explain them precisely.

1. INTRODUCTION

Previous work on the mechanism of the corrosion of metals by oxygen or air has been extensive (Evans *et al.*, 1943 and 1946; Vernon *et al.*, 1939; Wagner and Grunewald, 1938), but with a few exceptions very little work has been reported using other gases. Interest in fluorine corrosion of metals has developed with the current extension of fluorine technology. It has been known for several years that copper and nickel can be used for manipulating elementary fluorine (Leech, 1939; Slesser and Schram, 1953), but no quantitative information about reaction of fluorine with these metals has been published. This paper describes the kinetics of the reaction of fluorine with copper metal.

2. EXPERIMENTAL

Fluorine consumption by copper was measured by the pressure drop obtained in a glass apparatus shown in Fig. 2.1. Glass was chosen in preference to metal because of the difficulty of adequately stabilizing metal. Reproducible results can be obtained with glass apparatus, provided it is carefully dried, first by pumping for an extended period in a high vacuum, and then by prefluorinating the surface of the glass before use. Avoidance of loss of fluorine by reaction with components of the apparatus was essential, and it was therefore necessary to use an unreactive tap grease. Large pressure changes were obtained when Apiezon and silicone greases were used, and in one case the grease even fired at room temperature. A fully fluorinated heavy oil was finally chosen. This oil is obtainable in various consistencies, and it was found that the more viscous the oil, the more suitable it is for tap grease. Thick oils require gentle warming before the taps can be turned, but have the advantage that striae are less readily formed. Also, the tendency for fluorine to dissolve in thick viscous fluorocarbon greases is much less; not more than 0·1 mm mercury change in pressure was obtained per day, which is negligible. The taps remained quite clear and unattacked even after six months of use with fluorine. When they occasionally required regreasing, the old grease was removed with hot carbon tetrachloride or chloroform.

The pressure drop was measured by means of a membrane-type manometer (*A* in Fig. 2.1) described earlier (Duncan and Warren, 1954), using a differential oil manometer (*N*) as the associated pressure-sensitive device. The weight of electrolytic copper powder was 24·022 g. The surface area was 390 ± 20 cm²/g, determined by the B.E.T. method (Brunauer *et al.*, 1938), using ethylene. It was spread as a thin layer over the bottom of the sorption chamber (*B*). Before fluorination it was

* Now at Chemistry Department, University of Melbourne, Australia.

thoroughly degassed and reduced in hydrogen, which was introduced through the palladium thimble (*C*), in the conventional manner. Fluorine obtained from a 10-amp cell, supplied by Imperial Chemical Industries Ltd., was passed through the glass flask (*E*) for about one and a half hours, with taps (*F*) and (*G*) both open. This was sufficient to displace all the air and hydrogen fluoride formed by reaction of the initial fluorine with water. The taps (*F*) and (*G*) were then shut and the vessel fitted into the ground glass joint (*H*). The tap (*V*) was opened, and the apparatus evacuated up to the tap (*G*) and pumped for one hour. Liquid oxygen was placed round the trap (*K*) (to remove any residual

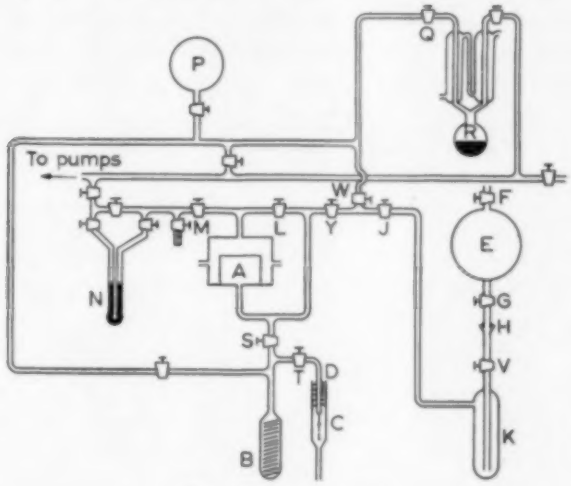

FIG. 2.1—The apparatus.

A Manometer.
B Sorption chamber.
C Palladium thimble.
D Asbestos packing.
E Storage flask.
H Ground glass joint.
K Liquid-air trap.
N Oil manometer.
P Storage flask.
R Mercury reflux still.
F, G, J, L, Q, S, T, V, W, Y Taps.
M Capillary tap.

hydrogen fluoride) and fluorine slowly passed through the tap (*G*) with taps (*W*), (*L*), and (*S*) shut, using the tap (*M*) (connected to a capillary) to balance the pressure across the manometer membrane with air. The air pressure (up to 100 mm oil) was measured on the differential oil manometer (*N*). At this stage the fluorine was at a low enough pressure to give an excitation discharge with a "Tesla" coil. It was found that fluorine of greater than 85 per cent purity always gave a brilliant yellow coloration. A blue or blue-white discharge indicated the presence of hydrogen fluoride, and the gas was in this case discarded. The fluorine could be analyzed (either by a sample initially isolated in the large volume (*P*), or after the experiment) by use of the water-cooled mercury reflux still (*R*). Hot mercury completely absorbs fluorine, but does not react with hydrogen fluoride or oxygen. Purities greater than 97 per cent were in most cases obtained.

When the sorption chamber had been raised to the appropriate temperature, tap (*S*) was opened, with tap (*T*) shut, and the reaction followed by observing the pressure drop during the following few hours. The large volume (*P*) was sometimes included in the apparatus, depending on the sensitivity required in the subsequent experiment. At temperatures above about 300°C the reaction could not be continued for more than twelve hours before the reaction of the fluorine with the glass was sufficiently serious for the yellow excitation discharge to be masked by the blue colour due to impurities. At 100°C and 200°C, about forty-eight hours' and twenty-four hours' exposure respectively were possible. In no case were the results considered reliable unless it was known by analysis that less than 5 per cent of impurities was present at the end of the experiment.

Except for the 250°C isotherm, the same sample of copper was used throughout these experiments. Identical isotherms were obtained in corrosion experiments if the previous fluoride corrosion film were reduced in hydrogen at 400°C until there was no further pressure change. Reduction produces

VOL. 1 1955

hydrogen fluoride, which is reversibly adsorbed on the glass walls of the vessel. No etching of the glass is obtained if the apparatus is quite dry, and the apparatus must be pumped out thoroughly before any subsequent experiment.

3. RESULTS

Pressure changes of 0·01 mm mercury could easily be detected by the technique outlined above. Provided that the apparatus was clean and had been prefluorinated, the reaction of the fluorine with the glass was negligible. This is exemplified by Table 3.1, which gives the pressure changes obtained at various temperatures when the prefluorinated sorption vessel (filled with glass wool) was subsequently exposed to fresh fluorine.

Table 3.1—Pressure changes obtained on exposure of apparatus to elementary fluorine when sorption chamber was filled with glass wool

Time	Temperature (°C)	Pressure (mm Hg after correction for temperature changes)
min.		
0	24·5	0·795
45	24·5	0·785
60	24·5	0·785
90	24·5	0·782
120	24·5	0·774
155	98	0·779
165	102	0·776
180	98	0·776
220	360	0·787
260	355	0·784
290	350	0·784
340	350	0·782
hours		
0	298	0·708
2·1	348	0·697
4·2	350	0·691
5·1	350	0·691
6·3	348	0·688
6·4	348	0·688
9·0	348	0·679
21·5	350	0·682
22·4	22·5	0·687
23·1	22·5	0·682

In order to obtain reproducible isotherms for the corrosion reaction, it was essential that the glass apparatus should be prefluorinated. In practice this required a complete corrosion run to be performed, in order to prefluorinate the glass in the sorption chamber. In this run, large pressure changes were always obtained, but thereafter, all subsequent runs with freshly reduced copper gave reproducible isotherms. If, however, atmospheric air were inadvertently admitted to the apparatus, anomalous results would again be obtained until the glass had been adequately prefluorinated, when isotherms identical with those obtained before the admission of air would again result (see Fig. 3.1). We assume that this was due to the formation

of hydrogen fluoride by reaction of the fluorine with water vapour which was tightly held on the glass. Whenever such anomalous isotherms were obtained, a low-fluorine analysis resulted, and the colour of the excitation discharge was invariably distinctly blue.

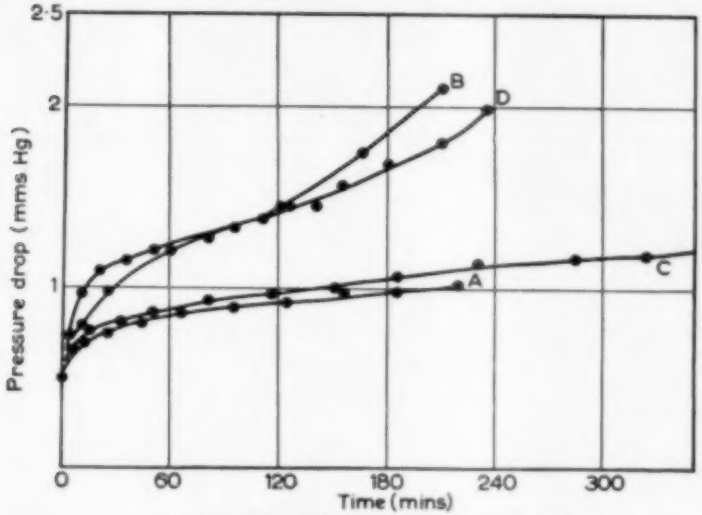

FIG. 3.1.—Effect of impurities on corrosion reaction.
A Isotherm obtained after pre-fluorination of apparatus.
B Isotherm obtained after prior admission of atmospheric air.
C Isotherm obtained immediately after *B*.
D Isotherm obtained subsequent to *C* after prior admission of atmospheric air.

(a) *Pressure dependence*. The rate of reaction was uninfluenced by changes in pressure. This is shown by the isotherms of Fig. 3.2 and Fig. 3.3, in which the pressure was varied widely. Within the limits of experimental error, the isotherms were quite reproducible, provided that the apparatus was not exposed to atmospheric air between runs.

Experiments above 300°C were unreliable, as a wide scatter in the results was obtained, which we believe was due to reaction of the fluorine with the glass and with desorbed impurities from the interior of the glass. We could not be sure, therefore, whether there was any pressure dependence at this temperature.

All isotherms below 250°C were determined without any change in the surface properties of the powder being apparent. Provided the copper fluoride was properly reduced, no change in the 100°C corrosion isotherm was obtained during this series. In fact, we frequently redetermined this isotherm as a means of ascertaining that the surface of the powder was in a reproducible state. Thus, in determining the isotherms at the higher temperatures, it was customary to reduce the sample, to obtain the 100°C corrosion isotherm to check the reproducibility of the surface, to reduce for four hours at 400°C, and then to determine the corrosion isotherm at the appropriate temperature.

(b) *Temperature dependence*. Isotherms determined over the temperature range in which reaction is not influenced by changes in pressure are shown in Fig. 3.4. The monolayer uptake indicated was calculated from the surface area, assuming an

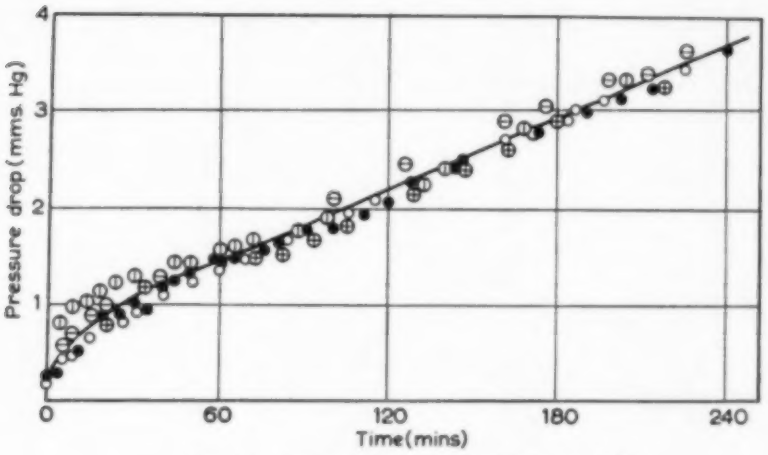

Fig. 3.2.—Reaction of copper with fluorine at 100°C.

⊖ 6·0 mm Hg
◐ 11·9 mm Hg
○ 29·7 mm Hg
● 47·6 mm Hg
⊕ 59·6 mm Hg

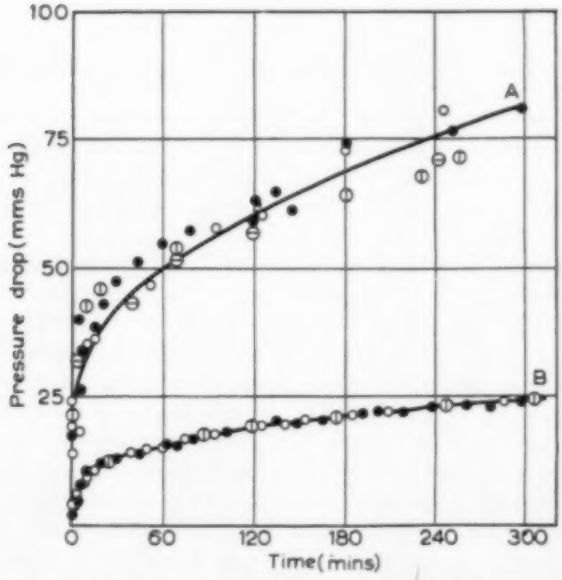

Fig. 3.3.—Reaction of copper with fluorine at (*A*) 250°C and (B) 200°C. These curves refer to specimens of different surface area.

⊖ 29·7 mm Hg
● 29·7 mm Hg (2nd experiment)
◐ 47·6 mm Hg
○ 59·6 mm Hg

area of 5·02 Å² for a copper atom. This leads to a monolayer uptake which is probably accurate to ±30 per cent. Reaction of copper powder with fluorine at 300°C produced an approximately twofold increase in surface area, but the 100°C isotherms were then reproducible, albeit considerably higher than they had been before the temperature had been taken over 200°C.

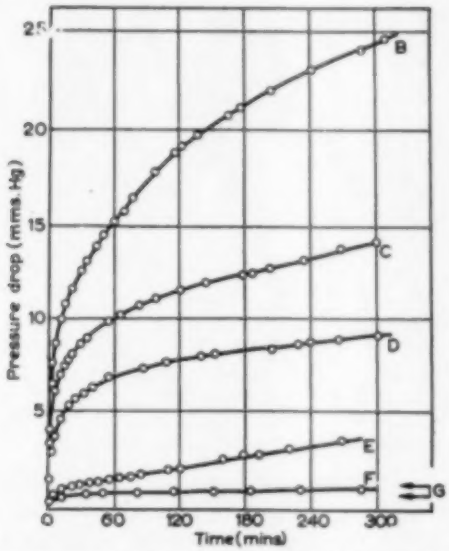

FIG. 3.4.—Reaction of copper with fluorine at (*B*) 200°C, (*C*) 175°C, (*D*) 150°C, (*E*) 100°C, and (*F*) room temperature. (*G*) limits of accuracy of monolayer determination.

All isotherms except that at 250°C (deviations of which may be due to the onset of a parabolic kinetic law at higher temperature) could be described by the relation

$$x = x_0 \log_{10}(1 + at) + b \tag{3.1}$$

where $a = 0{\cdot}05$ when t is expressed in minutes and x is the number of molecular layers of corrosion product. The constants x_0 and b were temperature-dependent, and the values are given in Table 3.2.

TABLE 3.2

Temperature °C	No. of molecular layers	
	x_0	b
22·5	0·55	0·83
100	3·03	1·15
150	5·79	6·07
175	9·38	8·55
200	20·40	9·66

The activation energy for different thicknesses of corrosion layer has been calculated in each case from two of the curves of Fig. 3.5. A near-linear increase in activation energy with thickness is obtained as shown in Fig. 3.6.

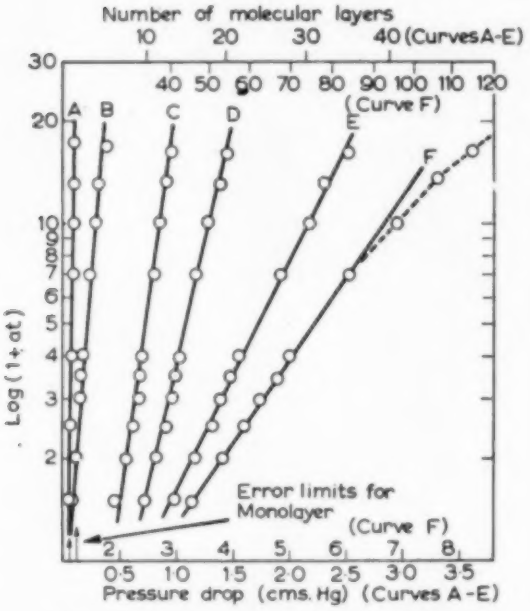
Number of molecular layers
10 20 30 40 (Curves A-E)
40 50 60 70 80 90 100 110 120
(Curve F)
A B C D E F
Log (1+at)
Error limits for
Monolayer
(Curve F)
0·5 1·0 1·5 2·0 2·5 3·0 3·5
Pressure drop (cms. Hg) (Curves A-E)

FIG. 3.5.—Plot of log $(1 + 0{\cdot}05t)$ against pressure drop (where t is in minutes) for the isotherms of Fig. 3.4.

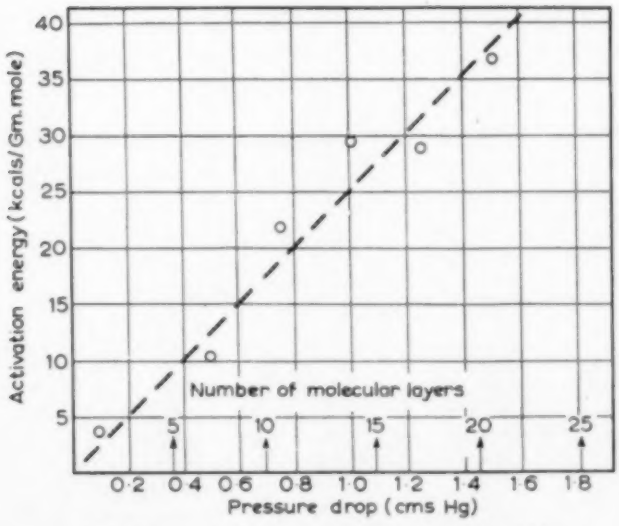

FIG. 3.6.—Activation energy as a function of film thickness.

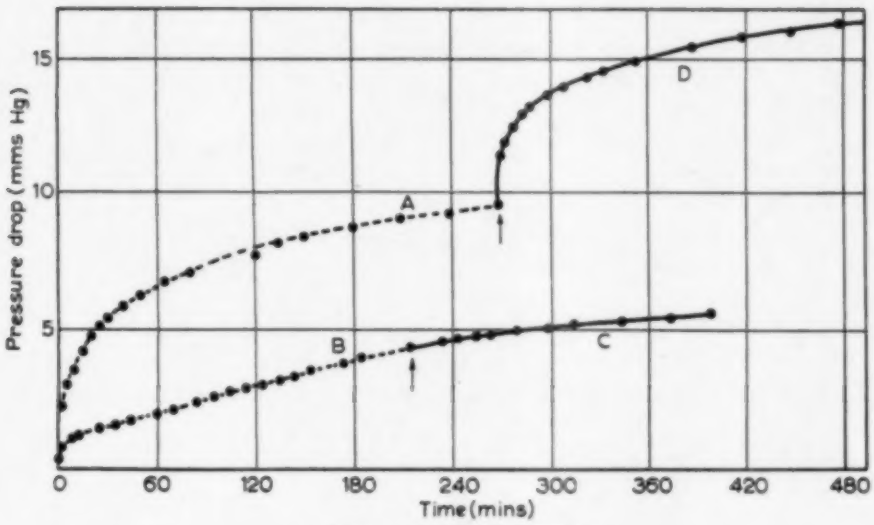

FIG. 3.7.—Interrupted corrosion.

A and *B* Corrosion of clean copper surface at 100°C (different specimens).
C Further corrosion of copper at 100°C after keeping sample in a vacuum at room temperature for about sixty hours.
D Further corrosion of copper at 100°C after heating sample in a vacuum at 300°C for sixteen hours.
The arrows indicate time-intervals for vacuum treatment.

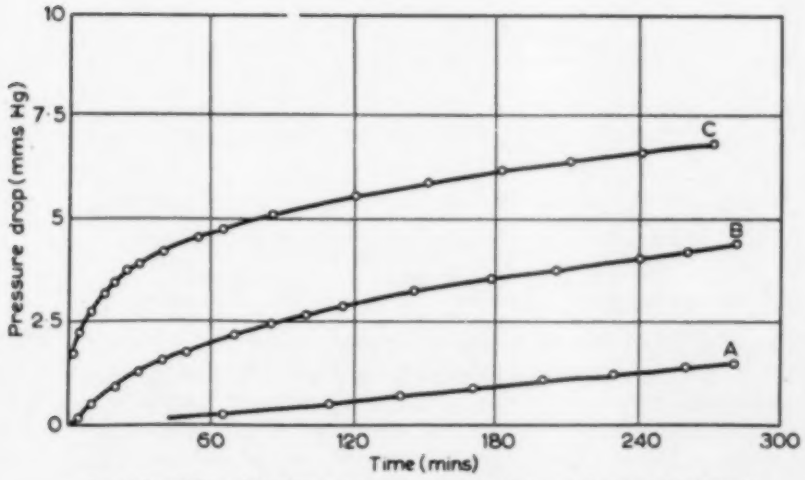

FIG. 3.8.—Effect of heating in a vacuum on the subsequent fluorine-reaction rate.

All samples were prefluorinated at 100°C on a freshly reduced copper surface, and gave identical isotherms. The fluorine was removed and the specimens were heated in a vacuum at (A) 100°C, (B) 200°C, and (C) 300°C for sixteen hours. The curves shown are the subsequent corrosion isotherms at 100°C.

VOL. 1 1955

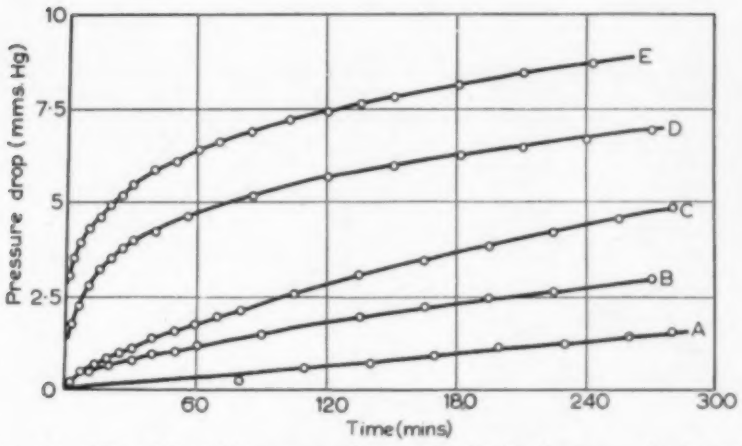

FIG. 3.9.—Effect of film thickness on reaction rate after heating in a vacuum for sixteen hours.

Curve	Temperature of heating	Film thickness (No. of molecular layers)
A	100°C	5·7
B		6·6
C		19·3
D	300°C	13·1
E		31·2

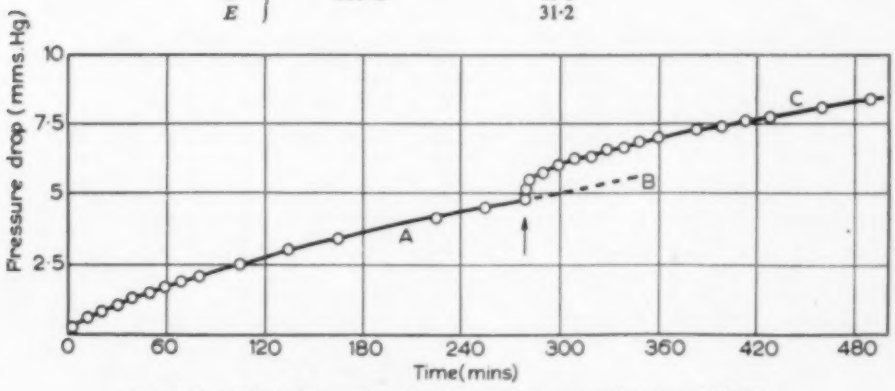

FIG. 3.10.—Effect of time of heating in a vacuum on reaction rate at 100°C.
A Initial reaction rate.
B Extrapolated curve which would be obtained if vacuum heating were continued at 100°C for sixteen hours (see curve *A*, Fig. 3.6).
C Curve obtained after vacuum heating at 100°C for four days.
The arrow indicates a time interval of sixteen hours for vacuum heating.

(c) *Preheating*. The isotherms quoted above were obtained on fresh, clean surfaces of copper. If the fluorination is interrupted, the fluorine gas removed, and fresh fluorine introduced into the sorption chamber, it is found that there is no change in corrosion rate (see curve *C* of Fig. 3.7). If, however, the copper powder is heated after the initial corrosion reaction, and fluorine then introduced at the lower temperature, the corrosion rate is quite seriously increased (see curve *D* in Fig. 3.7). The magnitude of the increase in corrosion rate becomes greater with

(i) the temperature of heating in the absence of fluorine (see Fig. 3.8),
(ii) the thickness of the corrosion film (see Fig. 3.9), and
(iii) the time of heating (see Fig. 3.10).

4. DISCUSSION

In corrosion kinetics there are two commonly-obtained growth laws (MOTT, 1940). The first is expressed by equation 3.1. The other is of the form

$$x^2 = At \tag{4.1}$$

(where A is a constant), which equation can be derived from the assumption that the rate-determining process is the diffusion of one of the components through the corrosion layer. In the present case, it is quite certain that the corrosion reaction is not dependent on such a diffusion process alone, for the following reasons:

(a) The growth law is logarithmic, and not even approximately parabolic.

(b) The activation energy is dependent on the film thickness, whereas for a simple diffusive process one would expect the activation energy to be constant. It would be possible for a variable activation energy to arise when the space charges set up in the corrosion film vary with film thickness, but this would imply some other feature besides simple diffusion.

VOL. 1 1955

(c) The increase in corrosion rate after vacuum degassing increases with the thickness of the film. If the reaction were diffusion-controlled, one would expect the magnitude of this "vacuum effect" to decrease with increasing film thickness.

A growth law of the form

$$x = x_0 \ln\left[\frac{Kt}{x_0} + \text{const.}\right] \tag{4.2}$$

has been predicted by MOTT and CABRERA (1948–9) for diffusion-controlled reactions in which the rate of penetration of the corrosion film by the metal ions is controlled by the quantum-mechanical "tunnel effect." Although equation (4.2) can be mathematically transposed into a form analogous to the observed kinetics (equation 3.1), the "tunnel-effect" mechanism cannot be operative in this case. For not only do objections (b) and (c) above apply with equal force, but also the Mott-Cabrera mechanism is not likely to apply at film thicknesses greater than about 50 Å (say 10–15 molecular layers). Above this thickness the tunnelling mechanism becomes inefficient and corrosion practically ceases (MOTT, 1940), as in the case of the oxidation of chromium and aluminium. The curves of Fig. 3.5 show, however, that equation (3.1) is obeyed very well, even up to film thicknesses of some thirty-five molecular layers.

We are left then with the alternative suggested by EVANS (1929, 1943, and 1946) that the logarithmic growth law is due to random "discrete mechanical breakdown" of the corrosion film, possibly with some recrystallization. None of the observations are at variance with this interpretation, and there is evidence from X-ray and electron-diffraction experiments (CRABTREE, LEES, and LITTLE, 1955) that when these corrosion films are heated in vacuum at 300°C they do break up. But it is difficult on this interpretation fully to understand:

(a) why the activation energy should vary with film thickness.

(b) why the "vacuum effect" should increase with film thickness and also with the time of heating.

(c) why the same kinetic law should hold no matter whether the film is only one or two molecular layers thick (room temperature) or, at the other extreme, some ninety layers thick (250°C). One can hardly expect a film of less than, say, five to

ten layers to behave as a distinct phase, in which case it is not capable of cracking in the sense assumed by this theory. It is therefore surprising that a different kinetic law is not obtained with very thin films.

Thus, whilst the Evans cracking mechanism seems to be the most satisfactory interpretation at present, we do not feel that it adequately explains all the observations, although it is not contrary to them. We prefer therefore to leave the mechanism of this reaction as an open question until the understanding of such systems is more complete. Perhaps a logarithmic expression is merely a convenient way of describing corrosion kinetics in which more than one process is occurring.

5. ACKNOWLEDGMENTS

We should like to thank the following members of the U.K. Atomic Energy Authority: Mr. R. B. HENDERSON (Harwell), for help with the construction of the membrane manometer; Dr. B. A. J. LISTER and Miss M. A. MACDONALD (both of Harwell), for determining the specific surface area of the copper powder; Mr. K. D. B. JOHNSON and Mr. W. R. A. TAYLOR (both of Capenhurst), for supplying the fluorolube used as tap grease.

REFERENCES

BRUNAUER, S., EMMETT, P. H., and TELLER, E. (1938) *J. Amer. Chem. Soc.*, **60**, 309.

CRABTREE, J. M., DUNCAN, J. F., LEES, C. S., and LITTLE, K. (1955) *J. Inorg. & Nucl. Chem.*, **1**, 214.

DUNCAN, J. F., and WARREN, D. T. (1954) *Brit. J. Appl. Phys.*, **5**, 66.

EVANS, U. R., *et al.* (1929) *J. Chem. Soc.*, 2651; (1943) *Trans. Electrochem. Soc.*, **83**, 335; (1946) *J. Chem. Soc.*, 209.

LEECH, H. R. (1939) *Quart. Rev.*, **3**, 22.

MOTT, N. F. (1940) *Trans. Faraday Soc.*, **36**, 472.

MOTT, N. F., and CABRERA, N. (1948–9) *Repts. Progress Phys.*, **12**.

SLESSER, C., and SCHRAM, S. R. (1953) *Preparation, Properties and Technology of Fluorine and Organic Fluoro Compounds* (McGraw-Hill).

VERNON, W. E., *et al.* (1939) *J. Inst. Metals*, **65**, 321.

WAGNER, C., and GRUNEWALD, K. (1938) *Z. Anorg. Chem.*, **236**, 320; (1938) *Z. Phys. Chem.*, **B40**, 455.

J. Inorganic and Nuclear Chemistry, 1955, Vol. 1, pp. 213–217. Pergamon Press Ltd., London

THE COPPER FLUORIDES

PART I—X-RAY AND ELECTRON MICROSCOPE EXAMINATION

By J. M. CRABTREE, C. S. LEES, and K. LITTLE
Atomic Energy Research Establishment, Harwell, Didcot, Berks

(*Received* 14 *April* 1955)

Abstract—X-ray diffraction powder photographs have been used to study the fluorides of copper. Both anhydrous copper fluoride and the dihydrate are slowly converted into a green basic fluoride in atmospheric air. In addition, one other basic fluoride has been observed which is unstable in air. No trace of any compound which might be cuprous fluoride has been obtained, in spite of numerous attempts to make it.

Electron diffraction and electron microscope photographs of the corrosion film formed by the action of elementary fluorine on copper at temperatures between 100°C and 500°C have been taken. There is good evidence that the film has a cupric fluoride structure rapidly changing to the basic fluoride on exposure to air. Electron microscope investigations show that copper metal can migrate and crystallize as bulk copper at temperatures as low as 300°C.

VOL.
1
1955

INTRODUCTION

IN most textbooks and works of reference there appears to be considerable confusion concerning the identity and properties of the copper fluorides. A paper[1] is usually quoted in which it was claimed that CuF and CuF_2 were produced by treatment of copper with mixtures of chlorine and fluorine, the red layer next to the metal being considered to be CuF. The figures quoted for the lattice dimensions were, however, close to those of cupric chloride and cuprous oxide ("CuF," 4·255 kX; "CuF_2," 5·406 kX; Cu_2O, 4·252 kX; $CuCl_2$, 5·4075 kX). In each pair, "CuF" and Cu_2O, "CuF_2" and $CuCl_2$, the crystal structure quoted was the same cubic type. Recently WHEELER and HAENDLER[2] have established the X-ray diffraction data for the compounds $CuF_2 \cdot 2H_2O$ and CuF_2 and have shown earlier data for $CuF_2 \cdot 2H_2O$[3] to be in error, and to refer to a mixture of basic fluorides.

In the present work X-ray diffraction methods have been used to identify the various compounds which can be formed in the copper-fluorine system.

EXPERIMENTAL

(a) *Cupric Fluorides*

(i) Black hydrated cupric oxide was prepared by boiling a 2M solution of cupric nitrate in excess dilute caustic soda for a half-hour. It was filtered off, treated in a platinum vessel with just enough dilute hydrofluoric acid to dissolve it, and evaporated almost to dryness until *blue crystals* formed on cooling. The crystals were filtered off, dried on filter paper, and a powdered sample used for X-ray diffraction within twenty-four hours. The diffraction data obtained are quoted in Table 1. It will be seen that the data agree with those quoted by HAENDLER *et al.*[2] for $CuF_2 \cdot 2H_2O$.

(ii) On allowing the hydrated fluoride to stand in air for several days, it passed first into a *blue-green compound*, and later into a green compound. The blue-green

[1] EBERT, F., and WOITINEK, A., *Z. Anorg. Chem.* **210**, 269 (1933).
[2] WHEELER, C. M., and HAENDLER, H. M., *J. Amer. Chem. Soc.* **76**, 263 (1954).
[3] A.S.T.M. index of X-ray Diffraction Data. Amer. Soc. for Testing Materials, Philadelphia, Pa.

intermediate compound was never isolated, since at no time in the process of conversion from the blue dihydrate to the green basic fluoride did it become a dominant component of the mixture. It was, however, readily identified by its X-ray diffraction

TABLE 1.—X-RAY DIFFRACTION DATA FOR BLUE DIHYDRATE

This work		Reference 2		This work		Reference 2	
d	Intensity	*d*	Intensity	*d*	Intensity	*d*	Intensity
4·82	vs	4·78	100	1·582	w	1·58	5
3·72	s	3·71	25	1·557	w	1·55	5
3·17	m	3·15	12	1·53	mw	1·53	5
3·14	m	3·10	12	1·493	w	1·49	5
2·99	m	2·98	12	1·456	vw		
2·74	vs	2·71	45	1·439	vw	1·43	6
		2·55	18	1·382	vvw		
2·36	m	2·35	15	1·366	w		
2·30	ms	2·29	18	1·358	w		
2·19	m	1·18	9	1·347	vw		
2·02	s	2·02	15	1·332	m	1·33	8
1·97	m	1·96	12	1·318	vvw		
1·92	m	1·92	17	1·295	w		
1·855	m	1·85	13	1·276	w		
1·75	m	1·75	8	1·248	w		
1·704	m	1·70	8	1·235	w		
1·652	vw			1·224	w		
1·631	vw			1·211	w		
1·605	s	1·60	20	1·202	mw		

TABLE 2.—X-RAY DIFFRACTION DATA FOR BLUE BASIC COPPER FLUORIDE

This work		Reference 2		This work		Reference 2	
d	Intensity	*d*	Intensity	*d*	Intensity	*d*	Intensity
4·31	s	4·22	100	1·89	mw	1·87	12
		3·54	85			1·84	18
3·46	s	3·46	70	1·79	w	1·79	6
2·82	w	2·71	70	1·75	w	1·77	45
2·56	ms	2·61	30	1·72	w	1·72	30
2·49	w	2·47	12			1·63	6
2·34	w	2·34	45			1·55	25
2·27	w	2·25	12	1·47	w	1·51	12
		2·20	25	1·44	w	1·43	6
2·14	m	2·10	3			1·4	3
		1·99	3				

pattern. The diffraction data (see Table 2) showed it to be the same compound as that judged by HAENDLER *et al.*[2] to be $Cu(OH)F \cdot CuF_2$.

(iii) On further standing in air, the *green compound* was obtained almost pure (as judged by X-ray diffraction). The X-ray diffraction data (Table 3*a*) agreed with the basic cupric fluoride reported by WHEELER and HAENDLER. In every case this green compound appears to be the one that is stable in the presence of air.

(iv) Blue hydrated cupric fluoride, as originally prepared, was heated to 500°C for

several hours in a copper tube in flowing fluorine at atmospheric pressure. The white product was then cooled in the presence of fluorine. The same product was also formed by passing anhydrous hydrogen fluoride over copper heated to 500°C, and cooling in the presence of hydrogen fluoride. Small differences of lattice spacing, probably along one axis only, were noticed in samples prepared by the two methods.

TABLE 3*a*.—X-RAY DIFFRACTION DATA FOR GREEN BASIC COPPER FLUORIDE

This work		Reference 2		This work		Reference 2	
d	Intensity	*d*	Intensity	*d*	Intensity	*d*	Intensity
4·69	vs	4·68	100	1·538	w	1·54	10
2·67	w	2·65	8	1·506	w	1·51	5
2·56	s	2·55	40	1·490	vw	1·49	3
2·44	m	2·43	25	1·477	vw	1·48	3
2·34	w	2·34	5	1·447	vw	1·44	3
2·28	vvw					1·43	1
2·14	w	2·14	15	1·357	vvw	1·36	1
1·97	ms	1·97	35	1·332	vw	1·33	1
1·89	w	1·88	20	1·304	vw	1·30	2
1·79	vw			1·283	vvw	1·28	1
1·63	w	1·63	5	1·265	vvw	1·26	1
1·604	w			1·24	vw	1·24	1
1·591	w	1·59	15			1·21	2
1·562	vw	1·56	3			1·17	1

The diffraction data for the sample prepared from the hydrate (Table 4) agreed with that of HAENDLER *et al.*[2] for *anhydrous cupric fluoride*. On allowing to stand in atmospheric air, the white anhydrous fluoride changes into green basic fluoride.

(b) *Cuprous Fluorides*

The following attempts were made to prepare cuprous fluoride:—

(i) Cuprous iodide was heated in hydrogen fluoride at 550°C for two hours. The sample still contained large quantities of iodide afterwards (X-ray diffraction and chemical analysis).

(ii) Cuprous iodide was treated with fluorine at room temperature. The surface of the powder turned red owing to liberation of iodine, but the bulk was unchanged. Heating to 100°C resulted in white cupric fluoride (X-ray diffraction and chemical analysis).

(iii) The blue hydrated cupric fluoride was heated in a copper boat at 800°C for two hours in flowing hydrogen fluoride. This method is due to POULENC,[4] who used higher temperatures. After heating, the furnace was cooled rapidly. A white powder with red agglomerates resulted and was shown by X-ray diffraction to be mainly anhydrous cupric fluoride with traces of copper.

(iv) A cupric fluoride solution in aqueous hydrogen fluoride was boiled with excess copper turnings in a copper tube closed by a Bunsen valve. After cooling, the solution remained clear even on dilution. On evaporation to dryness at 40°C under reduced pressure, a blue solid was obtained which was shown by X-ray diffraction to be a mixture of the three cupric compounds.

[4] POULENC, C. *Ann. Chim. Phys.* (7) **2**, 58, 68 (1894).

VOL. 1 1955

(c) *The Corrosion Film formed by Fluorine on Copper*

The corrosion reaction was carried out in fluorine at atmospheric pressure, and at a range of temperatures, under conditions for which the kinetics had previously been determined.[5] The specimens used included solid pieces of copper about ¼-inch

Table 3*b*—Green compound

d from X-ray	*d* from electron diffraction	*d* from X-ray	*d* from electron diffraction
4·69	4·68 s	1·562	
4·57	2·635 vvw	1·538	1·545m
2·56		1·506	
2·44	2·507 s	1·490	
2·34	2·338 w	1·477	1·467
2·28	—	1·447	
2·14	2·137 vw	1·357	—
1·97		1·332	
1·89	1·942 m (broad ring.)	1·304	1·318 w
1·79	—	1·283	—
1·63		1·265	—
1·604	1·609 m	1·241	1·244 w
1·591	—		

square, and copper films about 500 Å thick, made by evaporation of copper metal in vacuum, and placed on copper electron microscope grids with a spacing of 80 per cm. Similar diffraction patterns were obtained when either type of specimen was fluorinated under similar conditions, but the thin films gave clearer rings, and they were therefore used in most of the experiments.

A few copper films were also treated with chlorine trifluoride for comparison. This is a fluorinating agent which always converts metallic compounds to the fluoride of the highest valency state.

Temperatures of fluorination ranged from 100°C to 500°C. The best diffraction patterns were obtained at temperatures in the region of 300°C. At 500°C diffraction patterns showed that large copper grains had formed. At 100°C and 200°C the rate of fluorination was slow, and was not much better with chlorine trifluoride than with fluorine. The thin films were all examined by diffraction in the electron microscope. When accurate measurements of spacing were required, a separate diffraction apparatus was used, and a calibrating specimen of thallous chloride or sodium chloride was recorded immediately afterwards on the same photographic plate without changes in applied potential or filament current.[6] This apparatus was also used to obtain reflection photographs from the copper blocks.

Copper metal is normally covered by a very thin layer of cuprous oxide. Whether this was removed by hydrogen reduction or not, the fluorination product remained the same. In every case the presence of green basic fluoride was established (see Table 3*b*) in films which had been exposed to the air for a few hours. When a sample was transferred to the electron diffraction apparatus within two minutes of exposure to fluorine at 300°C, only the diffraction lines of the anhydrous cupric fluoride were

[5] Brown, P. E., Crabtree, J. M., and Duncan, J. F., *J. Inorg. Nucl. Chem.* **1**, 203 (1955).
[6] Lees, C. S. *J. Sci. Inst.* **51**, 84 (1954).

VOL.
1
1955

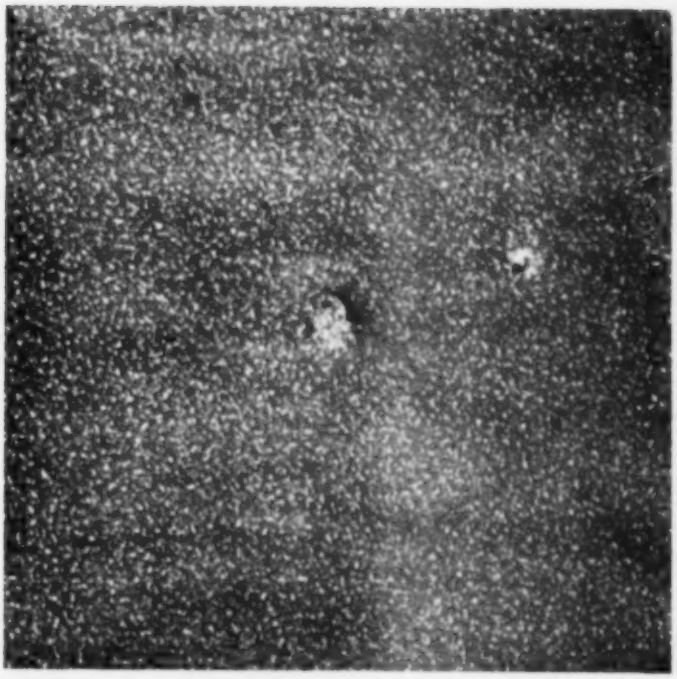

PLATE 1.—Thin copper film treated with fluorine at 300°C for four hours
Magnification × 12,000

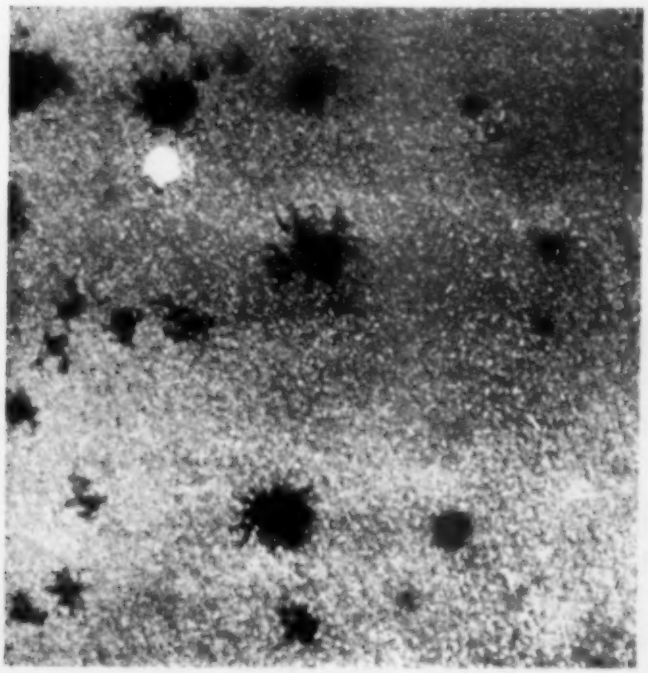

PLATE 2.—Fluorinated film; heated in vacuo at 300°C for two hours
Magnification × 12,000

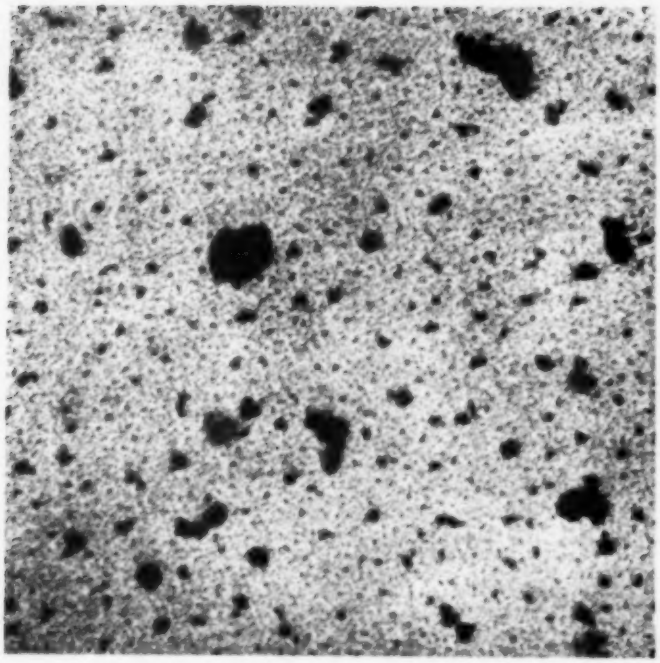

PLATE 3.—Fluorinated film, heated in vacuo at 300°C (another area)
Magnification × 12,000

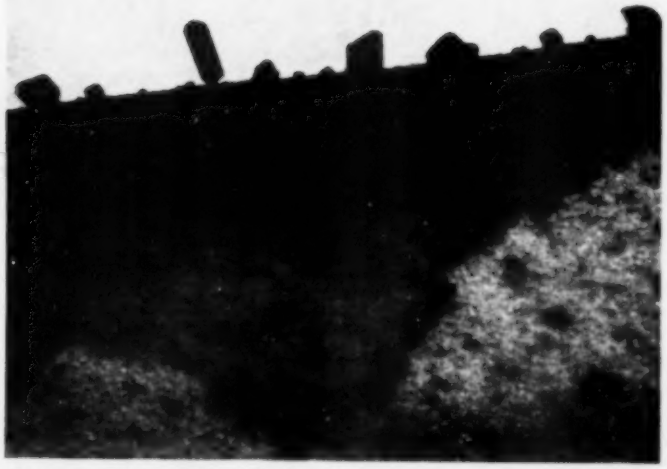

PLATE 4.—Portion of film folded over, showing silhouettes of copper crystals
Magnification × 12,000

present. On standing the sample in air, the corrosion film was converted to the green fluoride (as shown by subsequent electron diffraction).

(d) *Vacuum Heating*

A thin film of the green compound, mounted on a copper grid, with diffraction pattern similar to that quoted in Table 3*b*, was heated in a vacuum of 10^{-4} mm mercury for two hours at 300°C. It was transported in air and inserted again into the

TABLE 4.—X-RAY DIFFRACTION DATA FOR ANHYDROUS CUPRIC FLUORIDE

This work		Reference 2		This work		Reference 2	
d	Intensity	*d*	Intensity	*d*	Intensity	*d*	Intensity
3·23	vs	3·22	100	1·61	s	1·61	20
2·83	m	2·82	25	1·51	m	1·51	3
2·67	ms	2·66	35	1·444	m	1·44	13
2·535	w	2·53	8	1·439	w	1·42	8
2·47	vvw			1·414	m		
2·40	ms	2·39	15	1·370	m	1·38	10
2·28	w	2·28	8	1·322	w	1·32	8
2·21	m	2·21	8	1·264	vw		
2·03	w	2·04	3	1·218	w		
1·82	s	1·82	18	1·197	mw		
1·77	s	1·77	15	1·152	vvw		
1·69	s	1·69	18	1·144	vw		
1·66	ms	1·66	15	1·133	vvw		
1·64	ms	1·64	13	1·101	mw		

electron microscope. The film was found to have become heterogeneous, and to contain crystals of copper which could be identified by electron diffraction, and were clearly visible in the electron microscope (see Plates 1–4). Plates 2 and 4 provide evidence that copper can not only migrate, but also form discrete crystals at quite low temperatures.

RESULTS

At every stage of the experiments which have been described, X-ray or electron diffraction photographs have been taken. All the lines on these photographs have been identified, there being four sets which can correspond to diffraction patterns of copper-fluorine compounds. These compounds appear to be the anhydrous cupric fluoride, blue cupric fluoride dihydrate, and two basic compounds. The green basic compound is the only one of these which appears to be stable under ordinary atmospheric conditions. No single crystal photographs have been obtained, but from the powder photographs it is evident that all four cupric fluorides have complex structures. At no time, either in experiments with bulk chemicals or corrosion films, have any lines been observed which could be interpreted as belonging to a cuprous compound.

The chemical identity of the four cupric compounds and the relations between them will be discussed in Part 2 of this paper.

ACKNOWLEDGMENT

The authors wish to thank Dr. J. F. DUNCAN, now at the Chemistry Department, Melbourne University, for suggesting this problem, and for helpful discussions at all stages of the work.

VOL. 1 1955

J. Inorganic and Nuclear Chemistry, 1955, Vol. 1, pp. 218–227. Pergamon Press Ltd., London

SUR L'ABSENCE D'EFFET ISOTOPIQUE DANS LA RÉACTION D'ÉCHANGE ENTRE L'ION CARBONATE ET L'ION COMPLEXE COBALTI-CARBONATO-TÉTRAMMINE

par E. SAITO et B. LAZARD
Commissariat à l'Energie Atomique, Section des Isotopes Stables, Paris

(*Received October* 1954; *in final form, January* 1955)

Abstract—We have looked for isotope effects in the exchange of carbonate ion with the cobalti-tetrammino-carbonato complex ion, a reaction for which STRANKS and HARRIS, using C^{14} labelling, have found a very strong effect. We used normal carbon, as well as samples labelled, separately or together, with C^{13} and C^{14}. Apparent contradictions can be reconciled by the assumption that the reaction shows no true isotopic effect, and that the complex ion preparation contains a non-exchanging impurity. While varied indirect arguments (in particular the polarographic evidence) and the absence of any effect with normal carbon preparations, strongly support this assumption, attempts to identify the impurity have failed so far. Our results fit with the fact that no isotope effect was detected in the case of cobalti-carbonato-bisethylenediamine, neither with C^{13} (YANKWICH and MCNAMARA) nor with C^{14} (this investigation).

INTRODUCTION

PARMI les nombreux cas d'effet isotopique publiés depuis quelques années[1] notre attention a été attirée sur celui de la réaction d'échange

$$(Co(NH_3)_4{}^{12}CO_3)^+ + {}^{14}CO_3^{=} \rightleftharpoons (Co(NH_3)_4{}^{14}CO_3)^+ + {}^{12}CO_3^{=}.$$

En effet, STRANKS et HARRIS[2, 3] ont attribué à cette réaction un effet isotopique considérable. La constante d'équilibre serait d'après eux, entre 0° et 30°C

$$K_{14} = \frac{(Co(NH_3)_4{}^{14}CO_3)^+/(Co(NH_3)_4{}^{12}CO_3)^+}{({}^{14}CO_3^{=})/({}^{12}CO_3^{=})} = 0{\cdot}89$$

A l'équilibre, le complexe serait ainsi fortement appauvri en ^{14}C par rapport à l'ion carbonate libre.

Notre but initial était de vérifier cet effet et de mettre éventuellement à profit son importance pour en étudier la variation suivant que le carbone est marqué par l'isotope radioactif ^{14}C ou par l'isotope stable ^{13}C.

Entre temps, YANKWICH et MCNAMARA[4] n'ont pas observé d'effet isotopique sur le carbone 13 dans l'échange entre l'ion CO_3H-et l'ion complexe [Co(diéthylène-diamine)$_2CO_3$]$^+$. Cette différence flagrante entre deux réactions que l'on peut croire comparables rendait encore plus nécessaire de reprendre la question, malgré les efforts de HARRIS[5] pour expliquer cette divergence par une différence de mécanisme entre les deux réactions.

[1] G. A. ROPP, *Nucleonics* **10**, 22 (1952).
[2] G. M. HARRIS, *J. Chem. Phys.* **18**, 764 (1950).
[3] D. R. STRANKS et G. M. HARRIS, *J. Chem. Phys.* **19**, 257 (1951).
[4] P. E. YANKWICH et J. E. MCNAMARA, *J. Chem. Phys.* **20**, 1325 (1952).
[5] F. BASOLO, *Chem. Rev.* **52**, (3) 472 (1953).

L'expérimentation semble particulièrement facile sur la réaction de STRANKS et HARRIS. En effet, si l'isotope 14 donne un effet mesuré par la constante $K_{14} = 0{\cdot}89$ on doit s'attendre avec l'isotope 13 à un effet environ moitié $K_{13} \sim 0{\cdot}95$, aisément décelable en partant de produits non marqués, étant donné la précision de l'analyse de CO_2 au spectromètre de masse.

En principe, la méthode d'étude employée (détaillée plus loin) consiste à mettre en présence le complexe et l'ion $CO_3^=$, en solution légèrement alcaline, à laisser l'échange se poursuivre, et à séparer ensuite les deux constituants à l'aide de chlorure de baryum qui précipite l'ion $CO_3^=$ libre sans agir sur celui du complexe. Ce dernier est décomposé par l'acide phosphorique; on recueille le CO_2 dégagé et le transforme en $BaCO_3$. La teneur en ^{14}C est mesurée par comptage; celle en ^{13}C par spectrométrie de masse.

Soit A la composition isotopique du carbone provenant de l'ion $CO_3^=$ libre.

B celle du carbone provenant du complexe.

Ces lettres sont affectées d'un indice inférieur représentant le temps de contact entre complexe et solution carbonatée, et d'un indice supérieur égal au nombre de masse de l'isotope considéré. Ainsi, B_0^{13} représente le rapport $(^{13}C)/[(^{13}C) + (^{12}C)]$ dans le complexe au moment de sa dissolution dans la solution carbonatée. On peut toujours négliger (^{14}C) devant (^{13}C) et (^{12}C).

Il est alors clair que l'on a

$$K_{14} = B_\infty^{14}/A_\infty^{14} \qquad K_{13} = B_\infty^{13}/A_\infty^{13} \tag{1}$$

Toutes nos expériences utilisant complexe et carbonate ayant à l'origine l'abondance naturelle en ^{13}C ont conduit à une valeur de

$$K_{13} = 1{\cdot}00 \pm 0{\cdot}01 \text{ (voir tableau 1).}$$

Si la valeur $K_{14} = 0{\cdot}89$ donnée par STRANKS et HARRIS provenait d'un effet isotopique réel, on aurait pu s'attendre à une valeur de K_{13} voisine de 0·95.

TABLEAU 1

pH	t	K_{13}
9·2	48 h	0·993
9·2	48 h	1·000
9·3	48 h	0·993
9·65	160 min	0·991
	255	0·990
	400	1·000
	1,000	0·995
	1,400	0·996
	1,420	0·998
	2,700	0·994
9·8	48 h	1·000

Employant ensuite ^{14}C nous avons trouvé $K_{14} = 0{\cdot}89 \pm 0{\cdot}02$. Puis nous avons essayé le double marquage en enrichissant le carbonate en ^{14}C et en ^{13}C.

Le tableau 2 donne les résultats d'un série d'expériences portant sur divers échantillons du complexe, avec simple ou double marquage. Les valeurs de K_{14} varient de 0·85 à 0·97 et celles de K_{13} de 0·94 à 1·00, suivant la préparation. La contradiction

entre les échanges avec et sans enrichissement en ^{13}C ressort nettement de la comparaison avec le tableau 1. La troisième colonne indique le constituant le plus actif au début de l'échange.

Parmi les différents échantillons de *A* à *L*, *B* est le produit brut de British Drug House, *G* et *H* le même après recristallisation. Les autres échantillons proviennent de préparations diverses effectuées à partir de nitrate cobalteux.

TABLEAU 2

Exp. No.	Echantillon	Constituant initialement actif	Enrichissement en	K_{14}	K_{13}	A_∞^{13}	B_∞^{13}
1	*A*	carbonate	^{14}C	0·87			
2	*A*	carbonate	^{14}C	0·90			
3	*A*	complexe*	^{14}C	0·90	1·009	1·091	1·101
4	*A*	complexe*	^{14}C	0·89	0·995	1·091	1·087
5	*A*	carbonate	^{14}C	0·92	1·005	1·070	1·075
6	*B*	carbonate	^{14}C	0·86	1·00	1·110	1·112
7	*A*	carbonate	^{14}C ^{13}C	0·89	0·955	1·652	1·573
8	*A*	carbonate	^{14}C ^{13}C	0·93	0·962	3·310	3·185
9	*A*	complexe*	^{14}C ^{13}C	0·89	0·960	2·000	1·922
10	*A*	carbonate	^{14}C ^{13}C	0·91	0·956	3·637	3·447
11	*B*	carbonate	^{14}C ^{13}C	0·85	0·943	2·020	1·904
12	*C*	carbonate	^{14}C	0·89			
13	*D*	carbonate	^{14}C	0·94			
14	*E*	carbonate	^{14}C	0·94			
15	*F*	carbonate	^{14}C	0·975			
16	*G*	carbonate	^{14}C	0·952			
17	*H*	carbonate	^{14}C	0·97			
18	*I*	carbonate	^{14}C	0·945			
19	*J*	carbonate	^{14}C	0·91			
20	*K*	carbonate	^{14}C	0·92			
21	*L*	carbonate	^{14}C	0·87			
22	*M*	carbonate	^{14}C	0·91			

* Complexe rendu actif par échange en solution.

La seule hypothèse qui nous paraisse lever cette contradiction consiste à supposer que l'effet isotopique de la réaction d'échange est nul ou extrêmement faible, mais qu'il existe, dans nos préparations, comme dans celles de STRANKS et HARRIS, au moins une impureté dans laquelle le groupement carbonate fortement lié n'échange que très lentement avec l'ion carbonate libre. Les *K* mesurés sont alors des constantes d'équilibre "apparentes," tandis que les vraies valeurs de *K* sont 1·00.

Désignons pour abréger le complexe $(CO(NH_3)_4CO_3)^+$ par *X* et l'impureté supposée par *Y*. D'après notre hypothèse *X* échange avec l'ion carbonate sans effet isotopique; à l'équilibre leurs activités spécifiques sont égales $A_X = A_{CO_3^=}$; *Y* n'échange pas et conserve l'activité spécifique initiale $A_Y \ll A_{CO_3^=}$.

Lorsque après séparation de l'ion carbonate, on décompose le complexe, le CO_2 provenant de *Y* vient diluer celui qui provient de *X*. Ainsi, l'activité observée et attribuée au groupement carbonate du complexe *X*, est-elle inférieure à celle de l'ion

$CO_3^{=}$. Ce raisonnement est valable *mutatis mutandis* dans le cas où on part de complexe marqué et d'ion carbonate inactif, car alors $A_Y > A_{CO_3^{=}}$.

En fait, des expériences utilisant un complexe marqué à l'état solide ont donné des valeurs de K_{14} supérieures à 1·00 et respectivement égales à 1·03, 1·06 et 1·08 dans trois essais indépendants effectués avec des aliquotes d'un même échantillon dans les mêmes conditions que les expériences rassemblées dans le tableau 1. Le CO_2 de l'impureté Y étant actif, vient augmenter l'activité spécifique de X. Mais ceci n'est pas le cas pour les expériences No. 3, 4 et 9 où le complexe est rendu actif par échange en solution avec l'ion carbonate actif. Comme Y n'échange pas son carbonate, il vient diluer l'activité du complexe et nous obtenons des valeurs de K_{14} inférieures à 1·00.

Dans les expériences utilisant l'ion carbonate marqué par ^{14}C, la contamination par Y entraîne une dilution par du CO_2 totalement inactif. Dans le cas de ^{13}C, on dilue CO_2 contenant de 2 à 3 pour cent de ^{13}C par CO_2 contenant 1·1 pour cent de ^{13}C (abondance naturelle). Il y a donc dans les deux cas un effet isotopique apparent. Par contre, à l'abondance naturelle, le diluant a la même teneur en ^{13}C que les constituants qui participent à l'échange et la constante d'équilibre doit être égale à 1·00; c'est ce qui se produisait dans notre première série d'expériences.

VOL. 1 1955

Si l'impureté supposée contient une fraction x du carbone renfermé dans l'ensemble complexe plus impureté, les valeurs des constantes d'équilibre "apparentes" se calculent aisément. Le carbone venant de l'impureté a toujours la composition isotopique B_0, et à l'équilibre le carbone venant du complexe a la même composition que le carbonate, soit A_∞. La composition mesurée de l'ensemble complexe plus impureté est alors

$$B_\infty = xB_0 + (1 - x)A_\infty.$$

D'où:
$$K = B_\infty/A_\infty = xB_0/A_\infty + (1 - x) \tag{2}$$

Lorsqu'on utilise le carbone 14 et qu'on part du complexe inactif, $B_0 = 0$ et

$$K_{14} = 1 - x. \tag{3}$$

Dans le cas du carbone 13 la composition isotopique du complexe est, à l'origine, la composition naturelle ($B_0 = 0{\cdot}011$) d'où, compte tenu de (3):

$$K_{13} = K_{14} + (1 - K_{14})\,0{\cdot}011/A_\infty^{13}. \tag{4}$$

TABLEAU 3

Exp. No.	K_{14}	A_∞	$K_{13\,obs}$	$K_{13\,calc}$	Δ
7	0·89	1·613	0·955	0·965	−0·010
8	0·93	3·247	0·962	0·954	+0·008
9	0·89	1·965	0·960	0·952	+0·008
10	0·91	3·557	0·956	0·938	+0·018
11	0·85	1·962	0·943	0·944	−0·001

Enfin, A_∞ s'obtient par un simple calcul de mélange puisque nous supposons la discrimination isotopique apparente. Dans le cas le plus général si le complexe contient c atomes de carbone et s'il y en a un dans l'ion libre, on voit que:

$$A_\infty = (cB_0 + A_0)/(c + 1) \tag{5}$$

La cinquième colonne du tableau 3 rassemble, pour les expériences à double

marquage, les valeurs de K_{13} calculées à l'aide des équations (4) et (5), en prenant la valeur de K_{14} comme mesure de la pureté du complexe. Nous voyons que, pour des valeurs assez variables de K_{14} et du pourcentage final en ^{13}C, il y a un bon accord entre les valeurs de K_{13} observées et calculées.

Enfin, la comparaison des échantillons *B*, *G* et *H* (tableau 2) nous paraît importante. Le produit brut *B* donne $K_{14} = 0{\cdot}85$ tandis que, après recristallisation, on obtient 0·95 et 0·97. La purification fait donc disparaître la plus grande partie de l'effet.

Nous avons aussi vérifié notre technique en effectuant un échange entre l'ion cobalti-carbonato bisdiéthylène-diamine et l'ion $CO_3^=$ marqué au ^{14}C. Comme YANKWICH et MCNAMARA (utilisant ^{13}C), nous n'avons pas observé d'effet isotopique.

Ces divers faits expérimentaux étant expliqués par l'absence d'effet isotopique et par la présence d'une impureté n'échangeant que lentement avec l'ion $CO_3^=$ libre, il fallait chercher à mettre cette dernière en évidence.

Avant d'exposer nos tentatives d'identification—jusqu'ici infructueuses—nous allons rapporter les expériences polarographiques qui soutiennent, indirectement, notre hypothèse.

POLAROGRAPHIE

Les échantillons soumis à la polarographie ont été préparés soit par le procédé habituel, à partir de nitrate de Co, soit par recristallisation du produit fourni par British Drug House.

Les complexes cobaltiques donnent deux ondes, la première attribuée à la réduction du complexe de Co-III en complexe de Co-II, et la deuxième due à la destruction de l'ion et à la réduction à l'état de cobalt élémentaire.[6] Les potentiels de demi-onde se placent respectivement de −0·1 à −0·4 V (E.C.S.) suivant le complexe pour la première onde, et au voisinage de −1·3 V (E.C.S.) pour la seconde.

Les mesures préliminaires ont montré que nos échantillons donnaient deux ondes. La première a un potentiel de demi-onde de −0·4 V (E.C.S.). La deuxième vers −1·3 V, est accompagnée d'un maximum que nous n'avons pu supprimer et qui rend moins précise la détermination de la hauteur de la deuxième onde. A concentrations égales, la hauteur de la première onde varie d'un échantillon à l'autre. On peut donc supposer que l'impureté n'est pas électroréductible et que l'onde appartient au complexe tétrammino seul. Dans cette hypothèse, la hauteur *h* de la première onde fournit une indication sur la pureté du produit.

Un graphique de K_{14} en fonction de *h*, montre une variation linéraire. Extrapolant à $K_{14} = 1{\cdot}00$, on a la valeur $h_0 = 172$ qui serait la hauteur de l'onde correspondant au produit pur. Nous pouvons alors calculer la fraction $F = h/h_0$ du produit pur dans les différents échantillons. Le tableau 4 rassemble la hauteur *h* de la première onde, la fraction *F* et K_{14}. Nous voyons qu'il y a presque égalité entre *F* (que nous supposons indiquer la pureté de l'échantillon) et la constante "apparente" K_{14}. Ces résultats, s'ils n'indiquent rien de précis sur la nature de l'impureté,* viennent à l'appui de notre hypothèse.

[6] I. M. KOLTHOFF et J. J. LINGANE, *Polarography*, 2nd Ed., p. 480, Interscience, New York, 1952. J. B. WILLIS, J. A. FRIEND et D. P. MELLOR, *J. Amer. Chem. Soc.* **67**, 1680 (1945).

* L'impureté supposée serait donc non réductible, vers −0·4 V, à la cathode de mercure. Elle pourrait donc être un complexe cobalteux, mais ceux-ci sont trop labiles pour ne pas échanger avec l'ion carbonate libre. Ce pourrait être aussi un complexe cobaltique non électrolyte.

RECHERCHE DE L'IMPURETE

Un certain nombre de complexes s'obtiennent dans des conditions voisines de celles du tétrammino. Ainsi, le cobalti-carbonato-pentammino avait de fortes chances de souiller le tétrammino.

Des mesures cinétiques avec le pentammino ont montré un échange très rapide ($T_{1/2} \sim 14$ minutes contre 450 minutes pour le tétrammino) et éliminent ce produit

TABLEAU 4.—CONSTANTE K_{14} ET HAUTEUR h DE L'ONDE POLAROGRAPHIQUE À $E_{1/2} = -0{\cdot}4$ V (E.C.S.) (h en unités arbitraires par mg de complexe, à 25°C, en tampon ammoniaque-chlorure d'ammonium à pH = 9·5).

Echantillon	Exp. No.	h	F	K_{14}
		(172)*	(1·00)	(1·00)
B	11	147 ± 1·5	0·855 ± 0·01	0·85 ± 0·02
K	20	149	0·87	0·92
L	21	151	0·88	0·87
M	22	155	0·90	0·91
D	13	158	0·92	0·94
J	19	160	0·93	0·91
E	14	164	0·95	0·94
H	17	165	0·96	0·97

* Valeur obtenue par extrapolation.

comme impureté hypothétique. D'ailleurs. le pentammino présente dans le visible une bande d'absorption avec maximum à 5060 Å qui ne se retrouve pas dans le spectre d'absorption du tétrammino (maximum à 5200 Å) et n'apparait pas dans nos produits.

Un autre complexe de composition voisine est le dicobalti-tricarbonato-hexammine. Ce produit est difficile à obtenir pur et les différentes échantillons ont donné des résultats variables pour l'échange. Le spectre d'absorption dans le visible présente un maximum à 5600 Å et la présence de 10 à 15 pour cent de ce produit aurait modifié la bande du tétrammino. Il en est de même dans les domaines U.V. et I.R. et nous pouvons éliminer ce complexe de la liste de complexes hypothétiques.

Les différents échantillons du complexe tétrammino ont des spectres d'absorption presque identiques dans le visible avec un maximum à 5200 Å, bien dégagé dans les échantillons donnant des constantes K_{14} élevées. Pour les produits que nous considérons comme impurs, la bande à 3600 Å n'est plus qu'une bosse. La présence aux courtes longueurs d'ondes d'une bande qui ajoute une composante de hauteur importante mais indéterminée au maximum de 3600 Å ne nous fournit que des renseignements qualitatifs sur la pureté du produit.

Ni les spectres d'absorption dans les domaines infrarouge visible et ultraviolet, ni les diagrammes de rayons X des différents échantillons n'ont pu orienter la recherche de l'impureté.

D'autres complexes du type binucléaire[7]

I $^{++}[Co(NH_3)_5—O—CO—O—Co(NH_3)_5]^{++}$

II $^{0}[Co(NH_3)_3CO_3—O—CO—O—Co(NH_3)_3CO_3]^{0}$

III $^{++}[Co(NH_3)_5—O—CO—O—Co(NH_3)_3CO_3]^{0}$

ou du type carbaminato[8]

IV $[Co(NH_3)_5—O—CONH_2]^{++}$

V $[Co(NH_3)_3—OH—OCONH_2]^{+}$

[7] J. KRANIG, *Ann. de Chim.* **11**, 85 (1929).
[8] M. LINHARD et H. FLYGARE, *Z. Anorg. Chem.* **251**, 25 (1943).

peuvent être considérés. III et IV ont même formule brute que le complexe tétrammino et seraient donc indécelables par analyse chimique en mélange avec ce dernier. Mais leurs propriétés chimiques et leurs modes de préparation, que l'on trouve dans la littérature, rendent peu probable qu'ils constituent l'impureté cherchée.

DETAILS EXPERIMENTAUX

Mesure des concentrations isotopiques

Notre technique est légèrement différente de celle de STRANKS et HARRIS. Pour les comptages, nous avons préféré opérer en couche "infiniment épaisse" ce qui exigeait avec notre dispositif expérimental, au moins 140 mg de $BaCO_3$ dans les coupelles. Nous avons donc utilisé des volumes plus importants de solution (100 ou 200 ml, 0·010 M en ion carbonate et en complexe). La séparation des deux constituants est effectuée en précipitant l'ion carbonate par simple addition de chlorure de baryum et d'ammoniaque à la solution, réaction qui ne touche pas le carbonate du complexe.

Le $BaCO_3$ provenant de l'ion est toujours souillé par des oxydes de cobalt. Pour éviter l'erreur due à cette surcharge dans le calcul de l'activité spécifique, le précipité brut est décomposé par l'acide phosphorique et CO_2 absorbé par de la soude décarbonatée. De cette solution on précipite de nouveau $BaCO_3$ qui est centrifugé, lavé, puis filtré sur verre fritté, séché, pesé et enfin soumis au comptage (cf. infra).

Pour obtenir le carbonate du complexe, on ajoute de l'acide phosphorique à sa solution. Celle-ci est chauffée à ébullition. Un courant d'azote, exempt de CO_2, balaie l'appareil et assure le transfert du CO_2 libéré à de la soude décarbonatée.

Toutes ces opérations sont effectuées dans une boîte à gants sous atmosphère d'azote pour éviter la contamination par le CO_2 atmosphérique. Des expériences de contrôle utilisant ^{14}C ont montré l'absence de contamination: on retrouve la même activité spécifique avant et après un essai à blanc.

Les échantillons de $BaCO_3$ sont placés dans les coupelles de comptage, broyés sous acétone et étalés uniformément. Après évaporation lente à l'air, on achève le séchage sous une lampe infrarouge: un séchage trop brutal provoque des fissures qui augmentent la surface totale et de ce fait, le taux de comptage.

Les comptages sont effectués avec un compteur Geiger à fenêtre mince (2·5 mg/cm^2) et en se référant à un étalon de résine marquée au ^{14}C. On compte au moins 10,000 impulsions pour avoir un écart type inférieur à 1 pour cent.

Les appareils fournissant le CO_2 pour analyses au spectromètre de masse sont montés sur une rampe à vide. Le $BaCO_3$ est décomposé par l'acide sulfurique, CO_2 s'échappe tandis que l'eau est retenue par l'excès d'acide. Le CO_2 est condensé dans une trappe refroidie par l'azote liquide puis transféré dans le tube qui sera adapté au spectromètre de masse, analogue à celui de GRAHAM, HARKNESS et THODE.[9] [10]

Réactions d'échange

Les échanges ont été effectués à 25° et en solution 0·010 M. Ne cherchant pas à répéter l'étude de mécanismes de réactions de STRANKS et HARRIS, nous n'avons fait varier ni les concentrations, ni le pH, qui était maintenu à 9·5. Quelques échanges effectués à d'autres pH (8·5, 9·0 et 9·8) n'ont pas montré de différences notables.

[9] R. L. GRAHAM, A. L. HARKNESS et H. G. THODE, *J. Sci. Instr.* **24**, 119 (1947).
[10] G. NIEF et E. ROTH, *Electricité* **181**, 45 (1952); **182**, 183 (1952).

En général, nous avons utilisé des solutions de complexe inactif et de carbonate actif. Dans quelques cas, nous avons utilisé au départ le complexe actif en présence de carbonate inactif. Pour ce faire, on pouvait soit effectuer une préparation de complexe solide marqué, ou procéder par échange. Nous avons fait l'un et l'autre. Après 60 à 80 pour cent d'échange, on précipite l'ion carbonate actif, libre; par le chlorure de baryum. On a ainsi une solution de complexe marqué et, en ajoutant du carbonate inactif, on renverse le sens de l'échange. L'activité du complexe décroît, l'activité de l'ion carbonate augmente et à l'équilibre devient supérieure à celle du complexe.

Décomposition du complexe

En même temps que l'échange, se produit une certaine décomposition du complexe. STRANKS et HARRIS n'ont trouvé que quelques pour cent de décomposition. Ils la déterminaient par mesure spectrophotométrique, sur la bande d'absorption à 5200 Å. Nous avons pu déterminer le taux de décomposition par l'augmentation relative du poids de $BaCO_3$ provenant de l'ion carbonate. La décomposition atteint facilement 10 pour cent dans nos mesures. Utilisant les spectres d'absorption, nous avons constaté que l'absorption augmente en fonction du temps par suite de la formation d'une suspension de particules d'hydroxyde de cobalt. Ce n'est qu'après centrifugation de la solution que la courbe d'absorption décroît proportionnellement à la concentration. L'article de STRANKS et HARRIS n'indique pas de détails à ce sujet et il se peut que le faible pourcentage de décomposition qu'ils calculent reflète simplement une compensation entre la diminution d'absorption due au complexe proprement dit et une augmentation d'absorption due à la turbidité. Nous avons utilisé un Unicam SP 500 (et des cellules en silice) pour obtenir nos courbes d'absorption.

Durée de demi-échange

Quelques échanges ont été suivis en fonction du temps. Les durées de demi-échange calculées pour le ^{14}C et le ^{13}C pour la même expérience ont donné à 25°C,

$$^{14}C \qquad T_{1/2} = 425 \pm 25 \text{ min.}$$

$$^{13}C \qquad T_{1/2} = 400 \pm 30 \text{ min.}$$

Ces valeurs sont un peu plus faibles que celle calculée par interpolation des résultats de STRANKS et HARRIS, obtenus à d'autres températures (580 min. pour 25°C).

Échange entre l'ion carbonate et l'ion cobalti-carbonato-bis-éthylène-diamine

Cet échange a été effectué dans des conditions analogues à celles de l'étude sur le complexe tétrammino. La réaction d'échange n'est pas accompagnée de décomposition du complexe et, à l'équilibre, les activités spécifiques des carbonates sont pratiquement égales $A_{CO_3} = 1{,}500$ cpm $A_{complexe} = 1{,}500$ cpm. Il n'y a pas d'effet isotopique, en accord avec les résultats trouvés avec ^{13}C par P. E. YANKWÎCH et J. E. MCNAMARA.[4]

Mesures polarographiques

Les polarogrammes ont été obtenus avec des appareils du type manuel: le Cambridge Voltamoscope et le Polarographe Système Du Bellay (AOIP). Les solutions de complexes étaient environ 0·010 M. Les polarogrammes présentaient deux ondes, la première ayant un potentiel de demi-onde de $-0{\cdot}41 \pm 0{\cdot}01$ V par

rapport à l'électrode à calomel saturée, la deuxième aux environs de −1·3 V. La deuxième onde est perturbée par la présence d'un maximum difficile à éliminer par addition de gélatine ou de rouge de méthyle. L'électrolyte de fond utilisé est une solution ammoniacale de chlorure d'ammonium −0·1 n, pH 9·5. Les résultats sont indiqués dans le tableau 4.

PREPARATIONS

Nitrate de cobalti-carbonato-tétrammine

Ce produit est préparé selon la méthode de JÖRGENSEN[11, 12] et cristallisé soit par précipitation par l'alcool ou par évaporation sous vide.

Sur les différents échantillons nous avons dosé Co, NH_3, CO_3, H_2O. Le Co a été déterminé par oxydation à l'état de Co_3O_4, NH_3 par la décomposition par la soude et distillation de NH_3 dans une solution titrée d'acide chlorhydrique. Le CO_3 a été obtenue par la décomposition du complexe par l'acide phosphorique et absorption du CO_2 dégagé, dans une solution de soude décarbonatée. L'eau de cristallisation a été déterminée par chauffage à 120° du complexe dans un courant d'azote sec et absorption de l'eau dégagée par le perchlorate de magnésium.

Les quelques résultats suivants montrent que les valeurs obtenues sont voisines de celles calculées pour $[Co(NH_3)_4CO_3]NO_3H_2O$.

Echantillon	*B*	*D*	*J*	Théor.
Co	22·2	22·0	22·85	22·9%
CO_3	23·9	23·8	23·8	23·35
NH_3	26·6	28·0	26·3	26·5
H_2O	5·2	3·7	4·9	3·5

Nitrate de cobalti-carbonato-pentammine

Ce complexe a été préparé dans des conditions analogues à celles du tétrammino[12] à cela près que les concentrations en ammoniaque et en carbonate d'ammonium sont très élevées. Le produit est soluble à 1 pour cent à 0°, ce qui permet par refroidissement, d'obtenir de beaux cristaux rouges. L'analyse chimique a donné:

	Trouvé	Théor.
Co	20·7%	21·5%
CO_3	21·3%	21·1%
NH_3	30·2%	30·0%

L'échange avec l'ion carbonate actif est compliqué par l'aquation qui l'accompagne. Cette aquation rapide rend difficile la séparation de l'ion carbonate par le chlorure de baryum. Le carbonate de baryum de l'ion est accompagné par le carbonate provenant

[11] S. M. JÖRGENSEN, *Z. Anorg. Chem.* **2**, 291 (1892).
[12] Gmelins Handbuch der anorganischen Chemie, *Kobalt-Teil B.* **58**, p. 198 (1930).

de l'aquation ou de l'attaque de l'ion complexe par le chlorure de baryum. Malgré ces difficultés, nous avons pu suivre l'échange en fonction du temps à 25° et calculer approximativement la durée de demi-échange qui est de 14 ± 4 min. L'échange est très rapide en comparaison avec celui du complexe tétrammino (425 ± 25 min) et par conséquent le complexe pentammino ne peut pas être l'impureté que nous cherchons.

A l'équilibre, les valeurs des activités des ions carbonate libre et du carbonate du complexe n'ont pas de valeurs reproductibles. Ceci est dû probablement à un effet isotopique dans la décomposition du complexe en présence des ions baryum. Les valeurs de "K" ne dépendent plus seulement de l'équilibre, mais aussi de la vitesse avec laquelle on effectue la séparation des constituants. Nous n'avons pas poussé plus loin les essais avec ce complexe.

Cobalti-tricarbonato-hexammine

Ce complexe[13] est un sous-produit de la préparation du carbonate carbonato-tétramminocobaltique. Le carbonate de cobalt en solution ammoniacale est oxydé par un courant d'oxygène. En même temps, on envoie un courant de gaz carbonique à travers la solution. Par addition d'alcool, le cobalti-tricarbonato-hexammine se sépare sous forme d'une huile qui, étalée en couche mince sur des verres de montre, durcit sans former de cristaux. Ce complexe est relativement instable dans l'eau et ses solutions se décomposent de façon nettement plus rapide que celles du nitrate carbonato-tétrammino cobaltique.

Nitrate de cobalti-carbonato biséthylène diamine

Il a été préparé et purifié suivant la méthode indiquée dans la littérature.[14]

[13] Gmelins Handbuch der anorganischen Chemie, *Kobalt-Teil B.* 58, p. 312 (1930)
[14] Gmelins Handbuch der anorganischen Chemie, *Kobalt-Teil B.* 58, p. 283 (1930)

VOL. 1 1955

J. Inorganic and Nuclear Chemistry, 1955, Vol. 1, pp. 228 to 237. Pergamon Press Ltd., London

ÜBER DEN ZUSTAND GELÖSTER VERBINDUNGEN IN WASSERFREIER ESSIGSÄURE

von G. JANDER und H. KLAUS
Aus dem Anorganisch-chemischen Institut der Technischen Universität Berlin-Charlottenburg

(*Received* 30 *January* 1955)

Abstract—Cryoscopic measurements in glacial acetic acid show that acetates and amines, which are analogues of bases, are both associated and electrolytically dissociated in concentrated solution. In dilute solution the equilibria shift towards the monomer and the ionized state. Only diethylaniline, the strongest base-analogue, is completely ionized at 0·004 N. Acid-analogues are more strongly associated and less ionized than base-analogues. Even the strongest, perchloric acid, is still partially associated and by no means fully ionized at 0·01 N.

These conclusions are confirmed by potentiometric titrations, in which it appears that gold electrodes can be used to follow the acetate ion concentration.

1. KRYOSKOPISCHE MOLEKULARGEWICHTSBESTIMMUNGEN IN WASSERFREIER ESSIGSÄURE

IN wasserfreier Essigsäure sind bisher nur wenige Molekulargewichtsbestimmungen durchgeführt worden. Die kryoskopische Konstante sowie die ebullioskopische Konstante der Essigsäure wurde bereits von BECKMANN[1] erstmalig bestimmt. Der Wert der kryoskopischer Konstanten wurde in der Folgezeit von mehreren Forschern bestätigt;[2] er beträgt 3·9. In Eisessiglösung sind bisher an Säuren- und Basenanalogen nur Schwefelsäure von EICHELBERGER[3] und Natriumacetat von WEBB[4] untersucht worden. Beide Forscher betrachten die betreffenden Elektrolyte als stark dissoziierend, weshalb sie die Aktivitätskoeffizienten nach der Debye-Hückelschen Theorie berechneten. Weitere Molekulargewichtsbestimmungen an Nichtelektrolyten wurden von Hess und Mitarbeitern[5][6] an Glykosiden durchgeführt. Dabei wurde vor allem sehr sorgfältig die Methodik der Molekulargewichtsbestimmungen in Eisessig ausgearbeitet. In jüngster Zeit wurde eine Anzahl Säuren- und Basenanaloge von G. JANDER und G. MAAß[7] untersucht. Dabei wurde festgestellt, daß in basenanalogen Lösungen bis zu Konzentrationsbereichen von etwa N/100 in keinem Falle vollständige Dissoziation stattfindet. In säurenanalogen Lösungen wurde äußerst starke Assoziation beobachtet. Auf Grund des Vergleichs dieser Messungen mit den entsprechenden Äquivalentleitfähigkeiten ergab sich, daß die assoziierten Moleküle ihrerseits wieder dissoziieren müssen.

Zur Erweiterung dieser Untersuchungen durch eigene Arbeiten wurde zunächst mit Benzil und mit Benzoesäure, die beide in wasserfreier Essigsäure als Nichtelektrolyte fungieren, die kryoskopische Konstante festgelegt; sie betrug 3·9° pro Mol, gelöst in 1000 g Lösungsmittel. Es sei betont, daß die zu Molekulargewichts-Bestimmungen

[1] E. BECKMANN, *Z. anorg. Chem.* **74**, 291 (1912).
[2] K. HESS u. H. HABER, *Ber.* **70**, 2209 (1937).
[3] W. C. EICHELBERGER u. V. K. LA MER, *J. Amer. Chem. Soc.* **54**, 2763 (1932).
[4] WEBB, *J. Amer. Chem. Soc.* **48**, 2263 (1926).
[5] K. HESS, *Ber.* **63**, 518 (1930).
[6] K. HESS, *Ber.* **64**, 882 (1931).
[7] G. JANDER u. G. MAAß, Die Grundlagen der Chemie in wasserfreier Essigsäure, *Fortschr. chem. Forsch.* **2**, 619 (1953).

verwendete Essigsäure völlig wasserfrei und absolut rein sein muß. Es wurde nur Essigsäure verwendet, deren spezifische Leitfähigkeit $2{\cdot}0 \cdot 10^{-8}$ rez. Ohm beträgt.

Abb. 1 zeigt die Werte der van't Hoff'schen Faktoren i von Basenanalogen in Abhängigkeit vom Logarithmus der Verdünnung. Die Waagerechte beim Wert 1 wurde zur Bestimmung der kryoskopischen Konstanten aufgenommen. Da die i-Werte definiert sind durch die Beziehung

$$i = \frac{\text{theor. berechenbares einfaches Molekulargewicht}}{\text{praktisch gefundenes Molekulargewicht}}$$

bedeutet der Wert von $i = 1$ Nichtelektrolytcharakter, ein Wert größer als 1 Dissoziation, ein Wert von 2 bei ein-einwertigen Elektrolyten völlige Dissoziation, ein

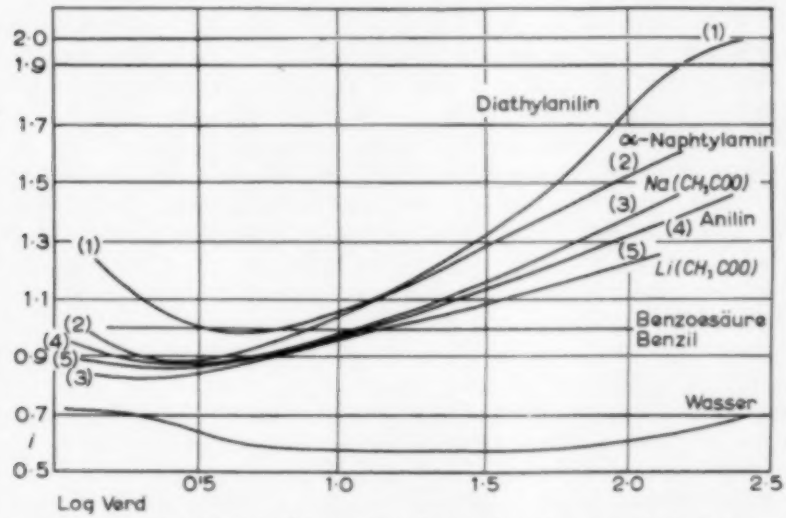

Abb. 1.—Van't Hoffsche Faktoren i von Basenanalogen in wasserfreier Essigsäure.

Wert kleiner als 1 teilweise Assoziation. Wie die Abb. 1 beweist, ist Diäthylanilin das einzige Basenanaloge, das völlige Dissoziation erreicht, und zwar bei einer Konzentration von etwa 0·004 N. Das von G. Maaß[7] bestimmte Tetramethylammoniumacetat ist unter allen bisher bekannter Basenanalogen als das zweitstärkste zu bezeichnen. Es erreicht bei der genannten Konzentration einen i-Wert von etwa 1·8. Das nächststarke Basenanaloge ist das α-Naphthylamin. Diese drei Verbindungen zeichnen sich dadurch aus, daß sie ein relativ großes Kation besitzen. Damit wird eine Regel bestätigt, die aus der Chemie der wässrigen Lösungen bekannt ist und die sich auch in den potentiometrischen Titrations-Kurven der Alkaliacetate ausprägt. Mit der i-Kurve des Natriumacetats wird eine Messung von Maaß[7] wiederholt und bestätigt. Nachdem er festgestellt hatte, daß Kaliumacetat stärker dissoziiert, war es interessant, festzustellen, daß das Lithiumacetat eine geringere Dissoziation zeigt. Die gesamte Kurvenschar der organischen Basenanalogen und der Alkaliacetate sinkt mit zunehmender Konzentration unter den Wert von 1. Die daraus folgernde Assoziation ist bereits Gegenstand mehrerer Untersuchungen[2][8] gewesen.

[8] M. Dole, *Trans. electrochem. Soc.* (1940).

Es ist bekannt, daß die Karbonsäuren eine große Tendenz zur Assoziation haben, was auf den stark polaren Charakter ihrer Moleküle zurückzuführen ist. BECKMANN und LIESCHE[9] haben festgestellt, daß das Molekulargewicht des Essigsäuredampfes bei 760 mm 102 beträgt. Daraus folgt ein Assoziationsgrad von 1·7. Dieser ändert sich bei Variierung des Druckes kaum.

Diese starke Assoziationsneigung der Essigsäure läßt es verstehen, daß auch Verbindungen wie Pyridin in Eisessiglösung assoziiert erscheinen, obwohl ein derartiges Verhalten des reinen Pyridins sonst nicht bekannt ist. Es muß wohl angenommen verden, daß die Assoziation unter Beteiligung von Essigsäuremolekülen stattfindet. Wenn auch in diesem Fall die Bezeichnung einer "assoziierenden Solvatation" treffender wäre, soll doch die Bezeichnung "Assoziation" für diesen Vorgang beibehalten werden.

KRAUS und FUOSS[10] haben dieses Problem mit der Annahme von Tripelionen zu erklären versucht, G. JANDER und G. MAAß[7] haben für deren Dissoziation ein theoretisch mögliches Dissoziationsschema auf Grund der Erfahrungen in anderen nichtwässrigen Lösungmitteln entworfen; es muß aber bemerkt werden, daß der Nachweis eines derartigen Vorganges noch nicht möglich gewesen ist.

Auf Grund dieser Erkenntnisse könnte man annehmen, daß auch die zur Bestimmung der kryoskopischen Konstanten verwendeten Nichtelektrolyte solvatisieren und daraufhin assoziieren. Dem sei ertgegnet, daß in der vorliegenden Arbeit Benzoesäure und Benzil und in der Arbeit von MAAß[7] Benzoesäure und Benzol zu diesen Messungen verwendet wurden. Die drei verschiedenen Verbindungen gehören völlig verschiedenen Typen an, denn es handelt sich dabei um ein α-Diketon, um eine aromatische Karbonsäure und um einen aromatischen Kohlenwasserstoff. Auf Grund der verschiedenen Bindungsverhältnisse und der daraus folgenden unterschiedlichen Polaritäten ist auch eine verschieden starke Solvatation und Assoziation zu erwarten und damit differierende Werte bei den Molekulargewichtsbestimmungen. Eine derartige Abweichnung wurde in keinem Falle festgestellt. In Abb. 2 zeigt der Verlauf der *i*-Wert-Kurven der Säurenanalogen, daß bei diesen eine noch stärkere Assoziation bestehen muß als bei den Basenanalogen. Daraus ist im Anschluß an das eben erörterte Problem zu folgern, daß für einen Assoziationsvorgang die Anwesenheit von Ionen in der Lösung notwendig ist, und zwar ungeachtet der Art der Ladung.

Die *i*-Werte von Säurenanalogen in Abhängigkeit von der Konzentration lassen bis zu einer Verdünnung von N/100 bei keinem der 4 Säurenanalogen eine normale Dissoziation erkennen. Während die Kurve der Schwefelsäure gut mit der Bestimmung von MAAß[7] übereinstimmt, zeigen die Werte für die Perchlorsäure eine Abweichung von den früher gefundenen Resultaten, für die keine Erklärung gegeben werden kann. Hinsichtlich des molekularen Zustandes der Perchlorsäure in Eisessiglösungen nimmt KOLTHOFF[11] die Möglichkeit an, daß sie z.T. in "Ionenpaaren" vorliegt, die er mit den von HANTZSCH[12] angenommenen Acet-Acidium-Verbindungen und mit den Hydroniumperchlorat vergleicht. Außerdem nimmt er die Existenz von undissoziierten Ionen an. Er zog diese Schlüsse aus konduktometrischen Messungen.

Auf Grund der bei den Säurenanalogen in wasserfreier Essigsäure viel stärkeren

[9] E. BECKMANN u. O. LIESCHE, *Z. phys. Chem.* **88**, 442 (1914).
[10] CH. A. KRAUS u. R. F. FUOSS, *J. Amer. Chem. Soc.* **55**, 2387 (1933).
[11] I. M. KOLTHOFF u. A. WILLMAN, *J. Amer. Chem. Soc.* **56**, 1007 (1934).
[12] A. HANTZSCH u. W. LANGBEIN, *Z. anorg. Chem.* **204**, 193 (1932).

Assoziation im Vergleich zu den Basenanalogen ist zu verstehen, welche Problematik für die genaue Definition einer Wasserstoffelektrode in Eisessig besteht. Praktisch ist die Bestimmung der $[H^+]$-Ionenaktivität nur extrapolatorisch möglich, und so ist das auch nur in allen Fällen geschehen.

Tabelle 1 gibt die einzelnen Meßwerte wieder, aus denen die in den Abbildungen 1 und 2 gezeigten Kurven entstanden sind. Es sei hinzugefügt, daß bei flüssigen Substanzen Additivität der Volumina angenommen wurde, nachdem experimentell festgestellt worden war, daß in keinem Fall die Abweichung von der Additivität mehr

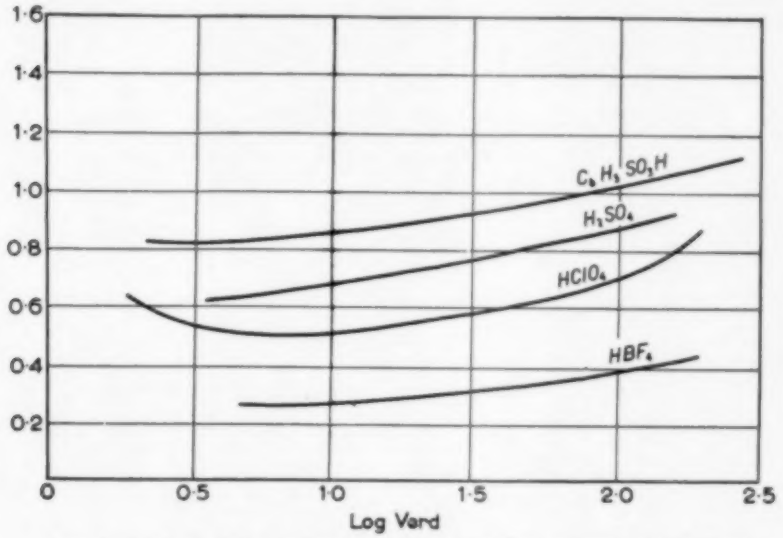

Abb. 2.—Van't Hoffsche Faktoren *i* von Säurenanalogen in wasserfreier Essigsäure.

als 0·5% betrug. Bei festen Substanzen wurden Volumkontraktionen und -dilatationen nicht berücksichtigt.

Die Berechnung der Molekulargewichte erfolgte nach der Formel

$$M_s = \frac{E \,.\, K \,.\, 1000}{L \,.\, \Delta T}$$

Darin bedeuten
E = Einwaage in g
K = Kryoskopische Konstante = 3·9
L = Gewicht des Lösungsmittels in g
ΔT = Gefrierpunktsdepression.

Aus den auf diese Art ermittelten M_s-Werten ergeben sich die van't Hoff'schen Faktoren aus der Formel, die auf Seite 230 angeführt ist.

2. DIE KONZENTRATIONSABHÄNGIGKEIT DER POTENTIOMETRISCHEN TITRATIONSKURVEN

Die kryoskopisch nachgewiesene starke Assoziation der Säurenanalogen läßt es nicht ohne weiteres zu, die potentiometrischen Meßwerte zu physikalisch-chemischen Berechnungen heranzuziehen. Die Anwendung der Nernstschen Gleichung zur

TABELLE 1

A. Nichtelektrolyte

Benzoesäure	$L = 36{\cdot}6$	Benzil	$L = 36{\cdot}6$
E	i	E	i
50·5	1·01	98·3	1·00
123·5	1·01	176·7	1·00
234·8	0·99	363·5	1·01
410·4	0·99	821·6	1·01
1138·1	1·00	1420·3	0·98
1922·4	1·00	2501·3	1·01
		4283·8	0·99

B. Basenanaloge

Diäthylanilin	$L = 36{\cdot}6$	Natriumacetat	$L = 36{\cdot}6$
E	i	E	i
21·8	1·99	25·2	1·40
49·3	1·79	67·8	1·22
111·2	1·42	177·9	1·08
269·8	1·19	458·5	0·91
499·7	1·07	806·3	0·84
646·0	1·04	1351·3	0·84
1213·1	0·98	1869·0	0·84
1816·8	1·02		
2843·1	1·15		
α-Naphthylamin	$L = 36{\cdot}6$	Lithiumacetat	$L = 36{\cdot}6$
E	i	E	i
38·9	1·59	22·3	1·22
71·2	1·45	44·7	1·15
174·2	1·36	156·3	1·04
360·4	1·11	397·9	0·92
841·6	0·96	949·2	0·86
1547·1	0·90	1561·4	0·89
2298·4	0·89		
3364·7	0·95		
Anilin	$L = 36{\cdot}6$	Wasser	$L = 36{\cdot}6$
E	i	E	i
19·7	1·42	6·2	0·60
43·1	1·22	14·3	0·58
125·8	1·0	36·6	0·57
183·4	1·04	79·6	0·58
404·6	0·96	160·1	0·62
915·9	0·87	226·3	0·67
2018·6	0·90	332·8	0·70
2668·7	0·94	513·7	0·72

C. Säurenanalogen

Perchlorsäure	$L = 36{\cdot}6$	Schwefelsäure	$L = 36{\cdot}6$
E	i	E	i
21·2	0·80	33·8	0·87
38·2	0·69	104·2	0·79
71·6	0·60	194·4	0·71
189·4	0·53	705·0	0·63
528·9	0·50		
1168·2	0·54		
Benzo-sulfonsäure	$L = 36{\cdot}6$	Borfluorwasserstoffsäure	$L = 36{\cdot}3$
E	i	E	i
33·7	1·06	10·6	0·40
94·4	0·97	44·9	0·34
213·3	0·91	83·8	0·32
423·2	0·87	141·7	0·29
1202·1	0·83	419·5	0·25
2112·7	0·82		

Die Werte für E sind in mg angegeben.

Ermittlung des Ionenprodukts des Lösungsmittels setzt die genaue Kenntnis derjenigen Ionenaktivität voraus, die für den Elektroden-Vorgang maßgebend ist. Bei Veränderung der Konzentration der Lösungen um eine Zehnerpotenz ist dann theoretisch zu erwarten, daß sich die jeweiligen Endpotentiale um 58 mV unterscheiden, wenn man bei Zimmertemperatur arbeitet. Da die in den folgenden Abbildungen gezeigten Titrationen bei 23°C durchgeführt wurden, würde der genaue Potentialunterschied, der durch einen Konzentrationsunterschied von einer Zehnerpotenz hervorgerufen

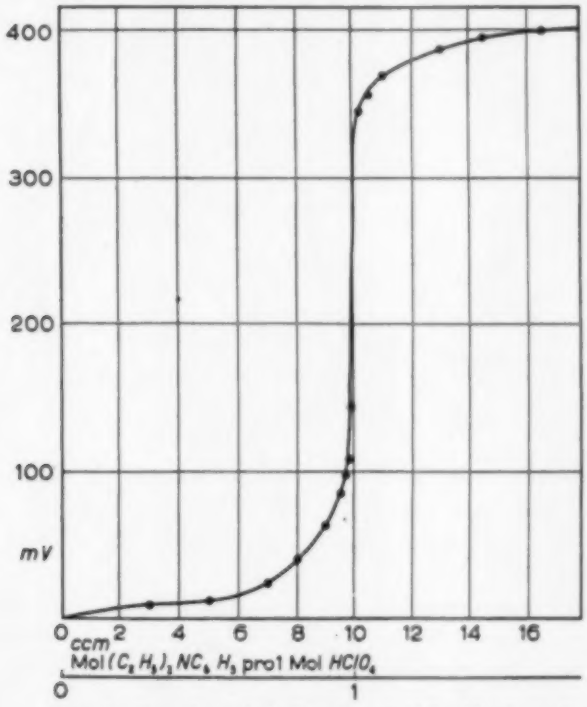

Abb. 3.—Potentiometrische Titration von N Perchlorsäure mit N Diäthylanilin in wasserfreier Essigsäure.

wird, 58·7 mV betragen Dieser Wert müßte, da in das Endpotential der Titrationskurve die Konzentration des Säuren- und des Basenanalogen eingeht, verdoppelt werden, wodurch sich 117·4 mV ergeben.

Um nun die diesbezüglichen Verhältnisse in wasserfreier Essigsäure zu ermitteln, wurden drei Titrationen von Diäthylanilin mit Perchlorsäure durchgeführt. Dazu wurden N, N/10, und N/100, Lösungen verwendet. Die vorgelegten säurenanalogen Lösungen hatten jeweils die gleiche Konzentration wie die Diäthylanilin-Lösungen. Die Einstellung der Perchlorsäurelösungen erfolgte nach SEAMAN und ALLEN mit "Merck Kaliumbiphthalat p.a." Mit diesen Säurenanalogen Lösungen wurden dann die Basenanalogen eingestellt.

In den Abb. 3, 4, und 5 sind die gemessenen Potentialkurven wiedergegeben. Ein Vergleich ergibt, daß das allgemeine Kurvenbild völlig den früher gezeigten entspricht. Das Endpotential der N-Lösung beträgt 400 mV, das der N/10-Lösung 370 mV, und das der N/100-Lösung 288 mV. Es zeigt sich, daß die Potentialdifferenzen vom

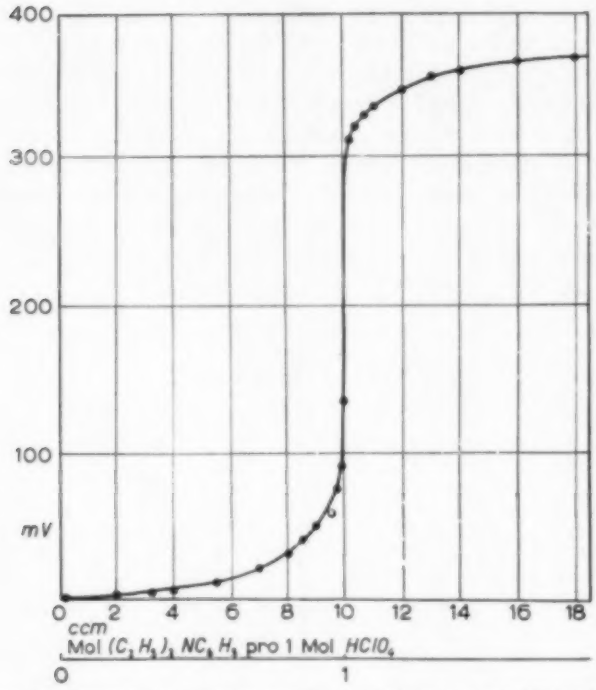

ABB. 4.—Potentiometrische Titration von N/10 Perchlorsäure mit N/10 Diäthylanilin in wasserfreier Essigsäure.

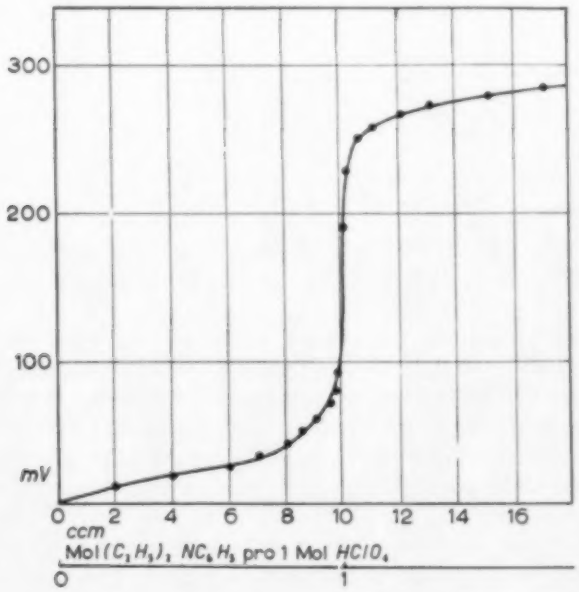

ABB. 5.—Potentiometrische Titration von N/100 Perchlorsäure mit Diäthylanilin in wasserfreier Essigsäure.

VOL.
1
1955

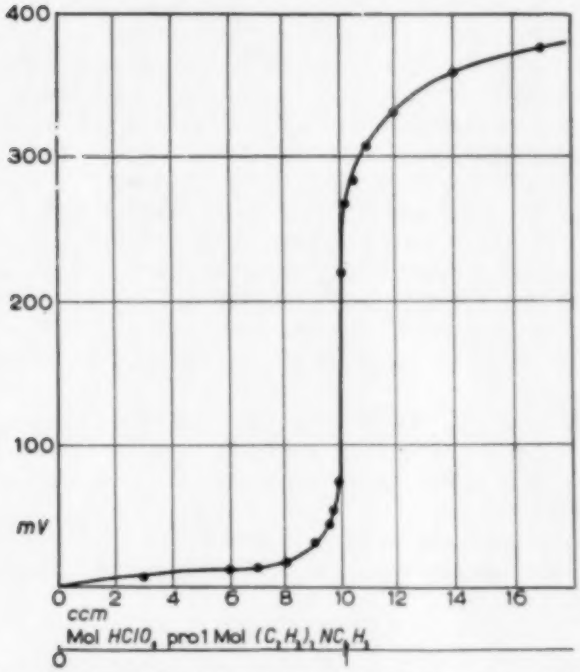

Abb. 6.—Potentiometrische Titration von N Diäthylanilin mit N Perchlorsäure in wasserfreier Essigsäure.

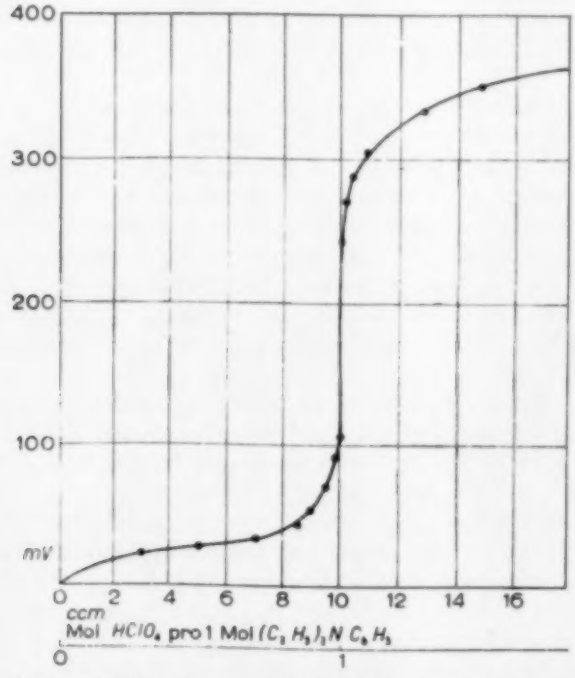

Abb. 7.—Potentiometrische Titration von N/10 Diäthylanilin mit N/10 Perchlorsäure in wasserfreier Essigsäure.

theoretisch geforderten Wert von 117·4 mV abweichen. Am geringsten ist diese Abweichung noch zwischen der N/10- und der N/100-Lösung, wo die Differenz 82 mV beträgt. Verursacht wird diese Abweichung höchstwahrscheinlich durch die Assoziation der Säurenanalogen und die nicht vollständige Dissoziation der Basenanalogen in diesen Konzentrationsbereichen.

Durch die in Abb. 1 und 2 gezeigten Kurven der van't Hoffschen Faktoren der Säuren- und der Basenanalogen wird dieser Sachverhalt bestätigt. Der Versuch, auch N/1000-Lösungen mit in dieser Reihe aufzunehmen, mißlang, da die Messung der sich einstellenden Potentiale durch den zu hohen inneren Widerstand der Meßzelle zu unsicher war. Es konnte zwar der Potentialsprung im Äquivalenzpunkt noch festgestellt werden, aber höchstens mit einer Genauigkeit von ± 30 mV. Bei den N/100-Lösungen betrug die Ablesegenauigkeit ± 5 mV, bei den konzentrierteren Lösungen ± 1 mV.

Es ist leider nicht möglich, einen exakten Schluß aus diesen Messungen auf das konzentrationsrichtige Ansprechen der Goldelektroden zu ziehen. Da diese gemessenen Potentialwerte aber vollkommen reproduzierbar sind, darf dies mit einer gewissen Sicherheit angenommen werden.

Die Abb. 6 und 7 geben die analogen Titrationen in umgekehrter Anordnung wieder. Beide Kurven zeigen, wie zu erwarten, gegenüber den Abb. 3 und 4 ein etwas erniedrigtes Potential.

3. EXPERIMENTELLER TEIL

Die zur Messung verwendete Apparatur ist in Abb. 8 wiedergegeben. Das dabei benutzte Beckmann-Thermometer war nicht gegen eine absolute Temperatur eingestellt, da vor jeder Meßreihe zunächst die Gefriertemperatur des reinen Lösungsmittels bestimmt wurde und zur Berechnung der Molekulargewichte bekanntlich nur die Erniedrigung des Gefrierpunktes erforderlich ist. (Beckmann-Thermometer PTR 605/43 III-T.)

Experimentell wurde dabei so vorgegangen, daß zu jeder Messung die Lösung unterkühlt wurde und bei Erreichen der jeweils gewünschten Unterkühlungstemperatur mit Eisessigkristallen angeimpft wurde. Diese Impfkristalle wurden dadurch erhalten, daß das ganze Meßgefäß mit reinem Lösungsmittel vor der ersten Messung jeder Versuchsreihe in Eis-Kochsalz-Mischung gebracht wurde. Dadurch wurde an der Gefäßwand eine spontane Kristallisation erzielt. Der gesamte Kristallbeschlag, der unter dem Flüssigkeitsspiegel war, wurde durch Eintauchen in warmes Wasser weggetaut, sodaß nur im oberen Gefäßteil ein geringer Kristallbeschlag verblieb. Von diesem wurden bei den Messungen jeweils einige Impfkristalle mit dem Rührer in Lösung befördert.

Sehr wesentlich für das Erzielen reproduzierbarer Ergebnisse ist die genaue Einstellung der Unterkühlungstemperatur und der Badtemperatur. Aus der Schmelzwärme der wasserfreien Essigsäure von 49·5 cal/g und der spezifischen Wärme von 0·46 cal/g ergibt sich, daß bei einer Unterkühlung von 1° knapp 1% des Lösungsmittels gefriert. Daraus folgt, daß bei der in der vorliegenden Arbeit angewandten Unterkühlung von 0·5° eine Konzentrationsänderung von maximal 0·5% bewirkt wird. Dieser Fehler spielt keine Rolle, wenn bei jeder einzelnen Messung völlig die gleichen Bedingungen in dieser Hinsicht gehalten werden. Damit ergab sich, daß immer die erste Messung einer bestimmten Konzentration dazu diente, den Gefrierpunkt grob festzustellen und bei der zweiten die notwendige Unterkühlung eingestellt wurde.

Das gleiche gilt für die Badtemperatur. Die dritte Messung wurde zur Kontrolle durchgeführt.

Um jede Bestimmung unter völlig gleichen Bedingungen durchführen zu können, mußte auch die Badtemperatur von Messung zu Messung variiert werden. Nach den Untersuchungen von RAOULT[13] ist dazu notwendig, daß die Badtemperatur nicht tiefer liegt als 0·1° unter dem Gefrierpunkt der betreffenden Lösung. Es ist außer

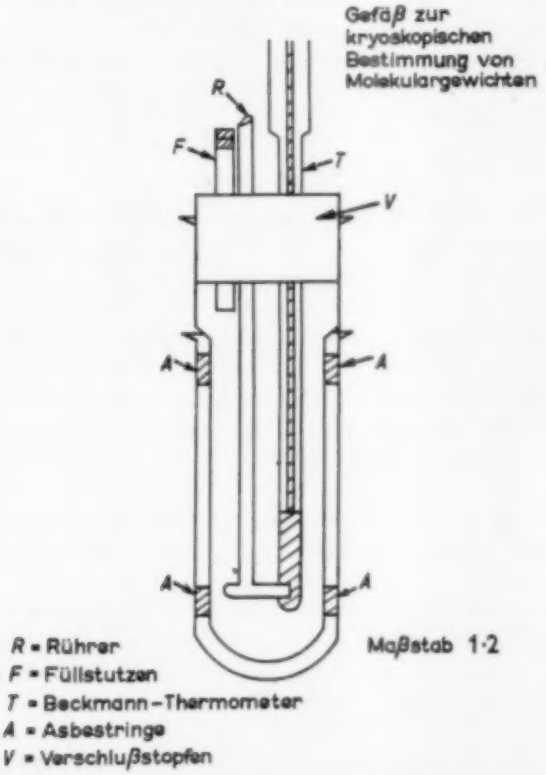

ABB. 8.—Meßgefäß zur kryoskopischen Bestimmung von Molekulargewichten.

diesen Bedingungen notwendig, daß die Rührgeschwindigkeit absolut konstant gehalten wird. In der vorliegenden Arbeit geschah das Rühren mit der Hand. Der Grund dafür war ein technischer. Unmittelbar nach dem Impfen muß das Meßgefäß unter ununterbrochenem Rühren in das Temperaturbad gebracht werden. Bei einer etwaigen Unterbrechung des Rührens zetzten sich die Kristalle sofort an der Gefäßwand fest, wodurch ein normaler Temperaturausgleich zwischen Meßgefäß und Bad gestört worden wäre. In Vorversuchen wurde festgestellt, daß bei Einhaltung dieser Bedingungen vollkommen reproduzierbare Ergebnisse erhalten werden, die in einer Fehlerbreite von 0·005° übereinstimmen. Die Raumtemperatur wurde nach Möglichkeit auf gleicher Höhe oder wenig unter der Badtemperatur gehalten.

Die Arbeit der Verfasser wurde durch Gewährung von ERP-Mitteln in großzügiger Weise gefördert.

[13] F. M. RAOULT, *Z. phys. Chem.* **27**, 617 (1898).

J. Inorganic and Nuclear Chemistry, 1955, Vol. 1, pp. 238–240. Pergamon Press Ltd., London

DOSAGE DE $^{14}CO_2$ DANS UN COMPTEUR G.M.

Mme. GEORGETTE DELIBRIAS
Centre d'Etudes Nucleaires de Saclay, B.P. No. 2, Gif sur Yvette (S et. O)

(*Received February* 1955)

Abstract—The author describes a method for the measurement of small amounts of CO_2 in a Geiger counter, with an addition of ethyl alcohol (1 cm Hg). With an electronic time constant of 10^{-5} s, one obtains plateaux of many hundred volts. The minimum activity one can detect is about $5 . 10^{-13}$ curies of ^{14}C in a CO_2 volume varying from 3 to 30 cm³ N.T.P.

INTRODUCTION

DANS les mesures de carbone-14 effectuées en biologie, les quantités de cet isotope sont, en général, comprises entre 10^{-7} et 10^{-12} curie. Diverses méthodes peuvent être utilisées pour doser de telles quantités de carbone-14.

Il peut être dosé sous forme de carbonate, à l'aide d'un compteur cloche à paroi mince.[1] Le mouvement propre d'un tel compteur est de l'ordre de dix impulsions par minute. Un échantillon de carbonate de baryum ayant une activité de 10^{-9} curie et une surface de 6 cm², placé au plus près sous la paroi mince (2 mg/cm²) d'un compteur donne environ vingt impulsions par minute, en plus du mouvement propre.

Les méthodes de dosages du carbone-14 sous forme gazeuse atteignent une meilleure sensibilité.

Les rayons β mous du ^{14}C sont émis au sein même du gaz de remplissage, dans un angle de 4π et ne subissent pas d'absorption. De ce fait, ils sont détectés avec un rendement maximum.

Le gaz à doser est habituellement introduit dans une chambre d'ionisation, dont le volume est de 250 cm³ environ. Dans ce cas, un échantillon gazeux d'activité 10^{-9} curie donne un courant de $5 . 10^{-15}$ A. Ce courant est mesuré facilement à l'aide d'un amplificateur à condensateur vibrant. Le mouvement propre est de $5 . 10^{-16}$ A environ.[2]

Une autre méthode consiste à utiliser du $^{14}CO_2$ comme gaz de remplissage de compteurs. C'est cette méthode que nous décrivons ici. Le mouvement propre du compteur utilisé, protégé par 5 cm de plomb et 2 mm d'aluminium est de vingt impulsions par minute. Un échantillon ayant une activité de 10^{-9} curie introduit dans ce compteur donne lieu à 1,200 impulsions par minute. Le rapport de ce taux de comptage à celui dû au bruit de fond est alors de soixante.

DOSAGE DE $^{14}CO_2$ DANS UN COMPTEUR G.M.

Plusieurs auteurs ont signalé le bon fonctionnement, dans la région de Geiger, de compteurs remplis avec du gaz carbonique additionné d'une petite quantité d'une vapeur de coupure.[3–5]

Le type de compteur utilisé par nous pour ces dosages est un compteur en verre, à

[1] D. R. SMITH, Carbon 14 Sample Preparation and Counting Techniques, *Atomics* 1953 **4**, 29.
[2] O. KENTON NEVILLE, *Atomics* 1952 **3**, 309.
[3] J. LABEYRIE, *J. Phys. Radium* 1951 **12**, 146.
[4] E. BRODA and O. FELDSTEIN, *Nature* 1951 **168**, 599.
[5] A. F. HENSON, *Brit. J. Appl. Phys.* 1953 **4**, 217.

cathode métallique interne, en dilver 0,* poli électrolytiquement. L'anode est un fil de tungstène de 1/10 de mm de diamètre (Fig. 1). Le volume total du compteur est de 30 cm³ environ.

Remplissage du compteur

Le gaz de remplissage est le gaz carbonique dont on veut mesurer l'activité, additionné de vapeur d'alcool éthylique (pression de celle-ci: 1 cm Hg).

Le gaz carbonique utilisé pour ces différents remplissages et les différentes mesures

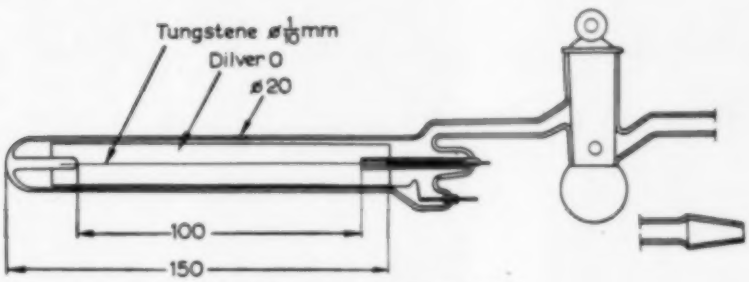

FIG. 1.—Schéma du compteur utilisé.

effectuées ici, provenait de l'attaque, sous vide, de carbonate de baryum par l'acide sulfurique. —carbonate et acide ayant été soigneusement dégazés sous vide avant l'attaque—.

Le gaz carbonique dégagé est desséché par passage dáns un serpentin plongé dans la glace; il est ensuite piégé dans un mélange réfrigérant vers —120°C. Toute trace d'air qui a pu se dégager au moment de l'attaque du carbonate par l'acide est évacuée par pompage, et le gaz carbonique peut alors être utilisé pour le remplissage du compteur.

Fonctionnement du compteur

La pression du gaz à l'intérieur des compteurs peut être variable; à la pression atmosphérique, le fonctionnement du compteur est encore satisfaisant. Les figures 2 et 3 montrent les courbes de "palier" de compteurs remplis à des pressions variables de CO_2.†

La présence de vapeur organique à l'intérieur du compteur est insuffisante pour éviter les coups multiples, avec les constantes de temps habituellement utilisées pour restituer le potentiel d'anode.

Il suffit d'augmenter cette constante de temps de restitution pour obtenir un fonctionnement correct du compteur. La constante de temps utilisée ici est de l'ordre de 10^{-3} s. Elle est obtenue en alimentant l'anode du compteur à travers une résistance de 10 MΩ.

La perte de comptage‡ qui résulte de cette constante de temps est de 1 pour cent

* Ferro-chrome à environ 20 pour cent de Cr.
† La pression d'alcool étant toujours de 1 cm Hg.
‡ Calculée par la formule $n = n_0 (1 - T_m . n)$.
T_m est le temps de résolution utilisé.
n le taux de comptage obtenu avec un temps de résolution T_m.
n_0 le taux de comptage obtenu si $T_m = 0$.

VOL. 1 1955

pour des taux de comptage de l'ordre de 600 impulsions par minute. Dans ces conditions de remplissage et d'utilisation, la courbe du taux de comptage du compteur en fonction de la tension présente un palier de plusieurs centaines de volts; la pente de ce palier varie de 0 à 4 pour cent environ suivant la pression.

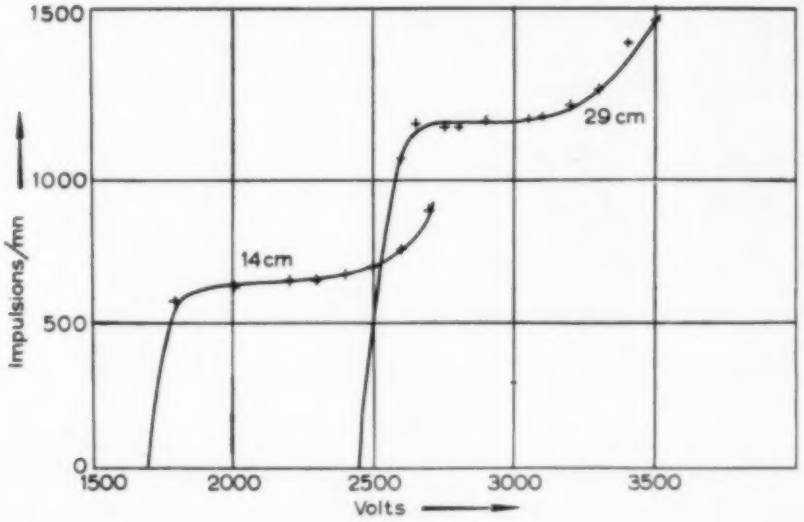

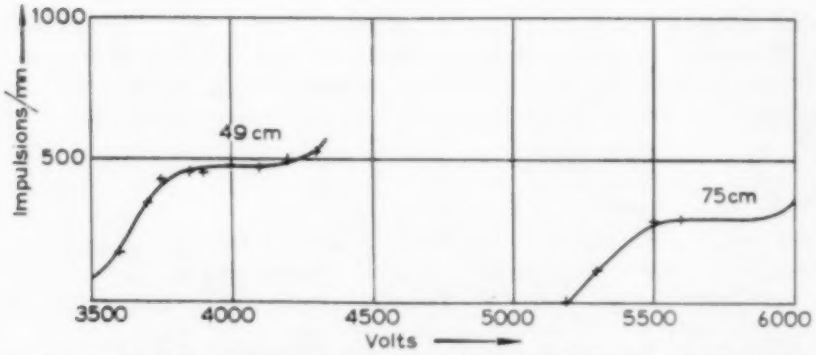

FIGS. 2 et 3.—Paliers de compteurs remplis à pression variable de CO_2 (les activités spécifiques du CO_2 ne sont pas constantes d'un remplissage à l'autre).

Les taux de comptage obtenus lors de différents remplissages sont strictement proportionnels à la quantité de carbone-14 introduite à l'intérieur du compteur; les taux de comptage sont indépendants de la pression de remplissage.

Le rendement* des compteurs utilisés ici pour les dosages de ^{14}C est de 55 pour cent. Ce rendement peut être augmenté en diminuant le volume mort des extrémités du compteur.

Je remercie M. J. LABEYRIE qui a suggéré l'utilisation d'un compteur G.M. et qui m'a encouragée au cours de l'exécution de ce travail.

* Rendement: rapport entre le nombre de rayons β comptés et le nombre de rayons β émis par la totalité du gaz introduit dans le compteur.

J. Inorganic and Nuclear Chemistry, 1955, Vol. 1, pp. 241–247. Pergamon Press Ltd., London

THE HALF-LIFE OF Cs^{137}

By F. Brown, G. R. Hall, and A. J. Walter
Atomic Energy Research Establishment, Harwell, Didcot, Berks

(*Received* 16 *June* 1955)

Abstract—The β-decay half-life of Cs^{137} has been obtained from a specific activity measurement. The disintegration rate was measured in a "4π"-type proportional counter. The number of atoms of Cs^{137} was measured by mass spectrometry, using the isotopic dilution method. The result is $30{\cdot}0^{+0{\cdot}3}_{-0{\cdot}4}$ years. No allowance is made in this error for uncertainties in the decay scheme used.

VOL. 1 1955

The nuclide Cs^{137} occurs as a fission product. The β-decay half-life is too long to be measured conveniently by observing the decay of its activity. Early estimates[1] of the half-life were therefore made indirectly by measuring the Cs^{137} activity produced in fission, and combining this with an estimate of the fission yield. More recently the decay of Cs^{137} has been observed,[2] using a mass spectrometer to measure the Cs^{137}/Cs^{133} ratio in a sample over a period of five years. This latter experiment gave a value of 33 ± 2 years.

This paper describes how the half-life has been obtained by means of a specific activity determination. The Cs^{137}, as caesium sulphate in solution, was obtained from the Radiochemical Centre, Amersham, Bucks. This caesium was of fission-product origin, and therefore besides the Cs^{137} it contained Cs^{133} (stable), Cs^{135} (3×10^6 yrs), and a small quantity of Cs^{134} (2·3 yrs). The radiochemical purity was such that not less than 99·9 per cent of the activity was due to Cs^{134} Cs^{137}, and Ba^{137m} (the daughter of Cs^{137}); Cs^{135} contributed to the mass, but hardly at all to the activity. A "master" solution of this material was prepared, containing about 10 μg/ml of caesium and made slightly acid with sulphuric acid. From this solution a number of dilutions were prepared, using water containing various concentrations of natural caesium (Cs^{133}) as carrier. Aliquots from these, measured by a calibrated micro-pipette, were counted in a 4π-type proportional counter. The observed activity (per ml of master solution) was corrected for the various counting losses, for the presence of the Ba^{137m} (in equilibrium with the Cs^{137}), and for the small quantity of Cs^{134} (measured mass-spectrometrically). The concentration of Cs^{137} in the master solution was determined by the mass spectrometer method of isotopic dilution. Three solutions containing known concentrations of natural Cs^{133} were prepared, henceforward referred to as spike solutions, one from caesium nitrate and two from caesium chloride, each being made slightly acid with sulphuric acid. The master solution was mixed in known proportions with each of these three solutions, and the isotopic compositions of the master and the various mixtures were measured. From these measurements the concentration of Cs^{137} in the master solution was calculated. Hence the specific activity of the Cs^{137} was now known, and the half-life could be obtained, using the relationship $-dN/dt = N\lambda$, where $-dN/dt$ is the corrected activity per ml of master, N is the number of atoms of

[1] L. E. Glendenin and R. P. Metcalf, N.N.E.S. Vol. IV, 9, The Fission Products, p. 1067, McGraw-Hill, New York (1951).
[2] D. R. Wiles, B. W. Smith, R. Horsley, and H. G. Thode, *Canad. J. Physics*, **31**, 419 (1953).

Cs^{137} per ml of master, and λ is the decay-constant related to the half-life in the usual manner.

DETERMINATION OF THE DISINTEGRATION RATE

A methane-flow type of counter of conventional "4π" design was used, the source being supported on a thin aluminium foil of 250 $\mu g/cm^2$. A paralysis time of 5 μsec was imposed in the scaling circuit, so that the dead-time losses could be calculated with reasonable accuracy. Since the counting rates were of the order of 10^3/sec, the

TABLE 1.—POSSIBLE VARIATION OF OBSERVED COUNTING RATE WITH CONCENTRATION OF Cs^+

Cs^+ concentration (μg/ml)	Observed count $\times 10^{-7}$ (counts/sec per ml of master)
50	1·687
25	1·696
10*	1·703
10	1·704
5*	1·693
5	1·702
2·5*	1·703
2·0	1·710
1·0	1·702

* These dilutions of the master solution were made volumetrically; the others were made gravimetrically.

dead-time corrections were of the order of 0·5 per cent. The background corrections of about 1 count/sec were also very small. The efficiency of the counter for Cs^{137} was checked by comparing it with a 4π Geiger counter used in the Isotopes Division of A.E.R.E., Harwell. The counters agreed within 0·25 per cent, which is within the expected statistical fluctuations of the counts ($\pm$0·3 per cent).

Two other counting losses are important, the self-absorption in the source and the absorption in the supporting film. In order to obtain information on self-absorption losses, a number of solutions were prepared, each containing the master solution in accurately known dilution, but containing various concentrations of natural caesium carrier. Each solution was counted, using several sources, the standard deviation between sources being about 0·3 per cent. The results are summarized in Table 1, where the observed count-rate is corrected for dead-time losses and background.

With the exception of the result for 50 μg/ml, there is no significant variation of counting rate with Cs^+ concentrations. This indicates that the self-absorption correction for the solutions of Cs^+ concentration in the range 10–1 μg/ml is very small. It is not necessarily zero, since even the most dilute solutions produce crystals of finite size on evaporation. The mean of the results for the 10–1 μg/ml solutions is $1{\cdot}702 \times 10^7$ counts/sec per ml, with a standard deviation of 0·3 per cent. No correction for self-absorption has been applied, but a possible error of +1 per cent has been allowed.

Some estimate of the film-absorption losses can be made by mounting a source on varying thicknesses of aluminium and extrapolating the observed counting rate to zero film thickness. In order to increase the accuracy of this extrapolation, a few

measurements were made of sources mounted on thin aluminized plastic films of weight 30 $\mu g/cm^2$, as well as on aluminium films of 250 $\mu g/cm^2$ and heavier. In the case of Cs^{137} this procedure indicates a film loss of a little less than 1 per cent for the films used. SMITH[3] used a similar procedure to estimate the loss for Co^{60} on similar aluminium films. He also measured the film loss by comparing the count for an electroplated Co^{60} source in a 4π counter with the disintegration rate for the same source as measured by the $\beta\gamma$-coincidence method. The extrapolation method indicated a film loss of 2·6 per cent, and the $\beta\gamma$-coincidence method a film loss of ~5 per cent. The former method is likely to give a lower limit for the loss and the latter method (as discussed by SMITH) an upper limit. The assumption has been made in this paper that the film loss for Cs^{137} is not less than that measured by the extrapolation method, and not greater than twice this quantity, i.e., not less than 1 per cent, and not greater than 2 per cent. This view is supported by SMITH's $\beta\gamma$-coincidence measurements on Na^{22}, which has a similar β-energy to Cs^{137}. A correction of $1{\cdot}5 \pm 0{\cdot}5$ per cent has been applied.

VOL. 1 1955

The Ba^{137m} (2·6 min), which is in equilibrium with the parent Cs^{137}, contributes to the counting rate mainly through the conversion electrons of the 660 keV γ-ray and to a lesser extent by direct counting of the unconverted γ's. The following data have been used in calculating the contribution due to conversion electrons: fraction of Cs^{137} decaying via $Ba^{137m} = 92$ per cent; ratio of $e_K/e_L/e_{(M+N)}$ in conversion of Ba^{137m} γ-ray = 5·5/1·0/0·27; ratio of $e_K/\gamma = 0{\cdot}097$. These data were taken from the *Table of Isotopes* of HOLLANDER, PERLAMN, and SEABORG.[4] It is calculated that the Ba^{137m} contributes 0·098 conversion electrons per decay of Cs^{137}. No error has been placed on this figure, since it can readily be changed should new data make this necessary. The contribution from the unconverted γ-rays was measured to be approximately 0·002 counts per β-decay, making the total contribution from Ba^{137m} equal to 0·100 counts per β-decay. Thus the apparent disintegration rate must be divided by 1·100 (multiplied by 0·9091).

The caesium in the master solution contained 31·79 atoms per cent of Cs^{137} and 0·039 atom per cent of Cs^{134}. If the half-life of Cs^{137} is taken as 30 years, and that of Cs^{134} as 2·3 years, the contribution to the counting rate from the Cs^{134} comes to $1{\cdot}5 \pm 0{\cdot}3$ per cent, where the error takes account of the error in the atom per cent Cs^{134} and the uncertainty in the half-life of Cs^{134} ($2{\cdot}3 \pm 0{\cdot}3$ yrs).[5]

The mean of the observed counting rates for the 10–1 $\mu g/ml$ solutions, corrected for dead-time losses and background, must be multiplied by the following correction factors:

Correction for film absorption	1·015
Correction for Ba^{137m} contribution	0·909
Correction for Cs^{134} contribution	0·985

The following errors are involved:

Standard deviation of measurements	$\pm 0{\cdot}3$ per cent
Self absorption correction	$+1$ per cent -0 per cent
Film absorption correction	$\pm 0{\cdot}5$ per cent
Cs^{134} correction	$\pm 0{\cdot}3$ per cent

[3] D. B. SMITH, *Atomic Energy Research Establishment Report* I/R 1527.
[4] J. M. HOLLANDER, I. PERLMAN, and G. T. SEABORG, *Rev. Mod. Physics* **25**, 469 (1953).

Since these errors are mainly estimates, they cannot be treated strictly by the methods of statistics. However, if the root of the sum of the squares is taken as a measure of the combined error, the Cs^{137} activity of the master solution is $1{\cdot}546 \times 10^7$ disintegrations/sec per ml with an error of $+1{\cdot}2$ per cent and $-0{\cdot}6$ per cent. These errors do not include any allowance for uncertainties in the decay scheme.

DETERMINATION OF CAESIUM-137

It is necessary to measure the isotopic abundances of the caesium isotopes in the master solution, so that the counting rate may be corrected as above for the Cs^{134} activity, and to determine the concentration of Cs^{137} in the master solution to obtain N (number of atoms of Cs^{137} per ml of master). The latter was measured by isotopic dilution experiments.

Mass Spectrometer Analysis

The isotopic abundance measurements were made with a 60° sector field mass spectrometer with a 6-in. radius analyzing tube. This had a multiple filament source[6] in front of an ion gun which accelerated the ions to 2000 V. In the source the sample is evaporated from a relatively cool side filament on to a hot central filament. In this way the ratio of charged to neutral particles is much greater than if a single thermal ionization filament had been used. Scanning is by variation of the magnetic field.

It was found in preliminary experiments that satisfactory ion beams could be obtained from 10^{-8} g of caesium. The sample, in about 2 μl of solution just made acid with sulphuric acid, was pipetted on to the centre of a side filament. This was evaporated to dryness by passing a small current through the filament.

The analysis was carried out by slowly increasing the current through the centre filament until it was at about 2200°C. The sample filament was just warmed by passing a small current, and large but controllable Cs^+ ion beams were readily produced. Measurements of the ratio Cs^{133}/Cs^{137} for about forty separate scans showed a standard deviation of <1 per cent. This indicated the overall stability of the ion beams.

After each analysis the multiple filament mounting was removed from the mass spectrometer. It was washed with dilute acid and three new filaments were inserted. A blank run was then carried out. It was always found that, under the operating conditions which have been described, there was no caesium memory effect. If, however, the currents through the sample and centre filaments were increased until their temperatures were greater than ~500° and ~2400°C respectively, then small Cs^+ ion beams were often formed, due to contamination from previous samples. This contamination might either be at the top plate of the ion gun, or might be due to caesium which had not been washed off the sides and supports of the filament mounting. The memory effect was very much worse if samples of caesium chloride were used, because of the greater volatility of the halide. It was thought that the multiple filament source, because it is more efficient than the single thermal ionization filament for any particular temperature, would reduce the memory troubles due to deposition of caesium on the walls of the ion source.

During the periods of analysis (several hours) there was no indication of isotopic fractionation, as would have been shown by a progressive decrease in the ratio Cs^{133}/Cs^{137}.

[5] L. E. GLENDENIN, N.N.E.S. Vol. IV, 9, The Fission Products, p. 1931, McGraw-Hill, New York (1951).
[6] M. G. INGHRAM and W. C. CHUPKA, *Rev. Sci. Instrum.* **24**, 518 (1953).

Isotopic Dilution Method

Let the ratio (atoms Cs^{133} per ml)/(atoms Cs^{137} per ml) in the master solution be x.

To a g of master solution add b g of spike solution, and let the concentration of Cs^{133} in the spike solution be c atoms per ml (i.e., of natural caesium). Determine the ratio atoms Cs^{133}/atoms $Cs^{137} = y$ in the mixed solution.

Then, if $[Cs^{133}]_m$ and $[Cs^{137}]_m$ represent the concentrations of caesium isotopes in the master solution, we have:

$$y = (a[Cs^{133}]_m + bc)/a[Cs^{137}]_m = x + bc/a[Cs^{137}]_m$$

and

$$[Cs^{137}]_m = bc/a(y - x) \tag{1}$$

Isotopic Constitution of the Master Solution

The relative abundances of the caesium isotopes in the master solution are given in atom per cent in Table 2. The result is the mean of two separate analyses, and for each analysis about fifty scans were actually measured. The errors represent the standard errors of these measurements.

VOL. 1 1955

TABLE 2.—ISOTOPIC COMPOSITION OF THE MASTER SOLUTION

Cs^{133}	Cs^{134}	Cs^{135}	Cs^{137}
39·68 ± 0·05	0·039 ± 0·003	28·49 ± 0·05	31·79 ± 0·05

Determination of the Concentration of Cs^{137} *in the Master Solution*

Four separate isotopic dilution experiments were carried out. For two of these, the spike solution was prepared from dried caesium nitrate, and for the others from dried caesium chloride. The reagents were checked by spectrographic analysis, and the only impurities observed were those given in Table 3.

TABLE 3.—ANALYSIS OF CAESIUM SALTS

Impurity	Caesium chloride	Caesium nitrate
Sodium	0·05 ± 0·02 per cent	0·05 ± 0·02 per cent
Rubidium	<0·05	0·05 ± 0·02
Calcium	~0·001	0·05 ± 0·02

The weights of caesium chloride and caesium nitrate were corrected for these impurities.

A sample of the redistilled water used to prepare all the solutions was checked in the mass spectrometer, and no caesium was detected from it.

The required mixtures of master and spike solutions were prepared by weighing the solutions. This is more accurate than a pipetting procedure for the small quantities involved.

The results of the isotopic dilution experiments are given in Table 4. Spiked solutions I and II were both prepared from the same spike solution of caesium nitrate. However, spiked solutions III and IV were each prepared from different spike solutions of caesium chloride. Two samples from each spiked solution were analyzed, and for each analysis about forty measurements of the caesium isotopic ratios were made. As the mass spectrometer measurements extended over three months, it was necessary to apply small corrections for the decay of Cs^{137}. In Tables 2 and 4 all results are corrected to the date of the β-counting, assuming a half-life of 30·0 years.

TABLE 4.—RESULTS OF THE ISOTOPIC DILUTION EXPERIMENTS

Spiked solution	*a* Weight of master solution (g)	*b* Weight of spike solution (g)	*c* Concentration of Cs^{133} in spike solution atoms/ml ($\times 10^{16}$)	*x* Cs^{133}/Cs^{137} master solution	*x* Repeat analysis	Mean value of *x*	*y* Cs^{133}/Cs^{137} spiked solution	*y* Repeat analysis	Mean value of *y*	Concentration of Cs^{137} in master solution $bc/a(y-x)$ atoms/ml ($\times 10^{16}$)
I $CsNO_3$	4·9851	4·8338	5·3041	1·248 ± 0·001	1·255 ± 0·002	1·251 ± 0·002	3·659 ± 0·007	3·664 ± 0·007	3·661 ± 0·007	2·134 ± 0·007
II $CsNO_3$	3·7546	2·4947	5·3041			1·251 ± 0·002	2·928 ± 0·007	2·921 ± 0·007	2·926 ± 0·007	2·104 ± 0·010
III CsCl	2·0071	0·7782	5·5665			1·251 ± 0·002	2·277 ± 0·004	2·284 ± 0·004	2·280 ± 0·004	2·097 ± 0·010
IV CsCl	1·2776	1·0352	9·3620			1·251 ± 0·002	4·830 ± 0·006	4·856 ± 0·012	4·842 ± 0·010	2·112 ± 0·006

Mean value for $[Cs^{137}]_m = 2·112 \pm 0·016 \times 10^{16}$ atoms/ml.

The errors quoted for each ratio are standard errors. The errors given for each result in the last column (Table 4) are also standard errors, computed from the standard errors of the mean values of x and y. As would be expected, the largest error occurs where $(y - x)$ is smallest. These considerations do not take into account any errors which may have occurred in the preparation of the solutions. Hence the error quoted on the mean value for $[Cs^{137}]_m$ is the standard deviation of the four results in the last column. This error is about twice the standard error which is calculated from the four standard errors given in the last column.

HALF-LIFE OF Cs^{137}

If the values for Cs^{137} concentration and activity in the master solution are inserted into the equation $\lambda = -dN/Ndt$, the decay constant λ and hence the half-life are obtained.

$$\lambda = -dN/Ndt = 1·546 \times 10^7/2·112 \times 10^{16}\ \text{sec}^{-1}$$

$$= 7·320 \times 10^{-10}\ \text{sec}^{-1}.$$

$$\text{Half-life} = 0·69315/7·320 \times 10^{-10} \times 3·156 \times 10^7\ \text{yrs.}$$

$$= 30·0\ ^{+0·3}_{-0·4}\ \text{yrs.}$$

The errors on this half-life are calculated from the errors $^{+1·2}_{-0·6}$ per cent assigned to the β-counting and the error $\pm 0·8$ per cent due to the determination of $[Cs^{137}]_m$.

ACKNOWLEDGEMENT

The authors wish to thank Mr. R. P. THORNE for the spectrographic analysis of the caesium chloride and caesium nitrate.

Note added in Proof

A recent publication by PATE and YAFFE[7] gives a full account of how film absorption corrections in 4π counters may be determined by counting a source on films of various thicknesses and extrapolating to zero thickness. By means of a graph presented in this publication a rough estimate can be made of the film correction for a β emitter of given energy on a film of given thickness. The correction obtained from this graph for Cs^{137} on 250 $\mu g/cm^2$ film is approximately 1·5 per cent which agrees with that used in the present work.

[7] *Canad. J. Chem.* **33**, 929 (1955).

VOL.
1
1955

J. Inorganic and Nuclear Chemistry, 1955, Vol. 1, pp. 248–252. Pergamon Press Ltd., London

THE YIELD OF Cs^{137} IN THE PILE NEUTRON FISSION OF NATURAL URANIUM

By F. Brown
Atomic Energy Research Establishment, Harwell, Didcot, Berks

(*Received* 30 *June* 1955)

Abstract—When natural uranium is irradiated with pile neutrons the fission yield of Cs^{137} is $0{\cdot}985 \pm {}^{0{\cdot}03}_{0{\cdot}02}$ of the yield of Ba^{140}.

INTRODUCTION

The ratios of the fission yields for the chains of mass 131 to 137 in the pile neutron fission of natural uranium have been measured accurately by Thode and co-workers.[1] These yields are important partly because they constitute the main evidence for the "fine structure" of the fission yield curve, and partly because they include the technologically important nuclides Xe^{135} and Cs^{137}. Since these yields are measured relative to each other, it is necessary to "normalize" them by choosing an actual yield value for one of the chains. The value used may either be an absolute value or may be measured relative to some other nuclide whose yield has been measured absolutely. Two procedures can be used, both based upon fairly recent measurements. In the first case one takes the absolute yield of Ba^{140} measured by Yaffe *et al.*[2] as 6·32 per cent. The ratio of the I^{131}/Ba^{140} yields has been measured by Bartholomew

Table 1.—Fission yields for masses 131–137

Mass	Element measured	(1) Ba^{140} = 6·32% I^{131} = 3·21%	(2) Ba^{140} = 6·32% I^{131} = 3·09%	(3) Xe^{133} = 6·62%	(4) Ba^{140} = 6·32% Cs^{137} = 6·225%
		%	%	%	%
131	Xe	3·21	3·09	2·97	$3{\cdot}04_4$
132	Xe	4·81	4·63	4·45	$4{\cdot}56_3$
133	Xe and Cs	7·15	6·89	6·62	$6{\cdot}78_9$
134	Xe	8·44	8·13	7·81	$8{\cdot}00_9$
135	Cs	6·92	6·66	6·40	$6{\cdot}56_3$
136	Xe	6·94	6·68	6·42	$6{\cdot}58_4$
137	Cs	6·56	6·32	6·07	$6{\cdot}22_5$

Notes

(1) The ratios of the yields for masses 131–137 are those given by Katcoff and Rubinson,[6] and differ slightly from those originally given by Thode,[1] since a small correction has been applied for the Xe^{133m} (2·3 days) which was not known at the time of Thode's publication.

(2) The normalization carried out at mass 131 assumes that the yields of I^{131} and Xe^{131} are equal (i.e., that the independent yield of Xe^{131} is negligible). Similarly Thode assumed that the yields of Xe^{133} and Cs^{133} are equal (independent yield of Cs^{133} negligible) in order to relate the ratios for xenon isotopes to those for caesium isotopes. These assumptions are justified by any reasonable postulates for the distribution of charge in fission (e.g., see ref. (4)).

[1] D. R. Wiles, B. W. Smith, R. Horsley, and H. G. Thode, *Canad. J. Phys.*, **31**, 419 (1953).
[2] L. Yaffe, H. G. Thode, W. F. Merritt, R. C. Hawkings, F. Brown, and R. M. Bartholomew, *Canad. J. Chem.*, **32**, 1017 (1954).

et al.[3] to be 0·508 and by PAPPAS[4] to be 0·489. Combining these, one obtains the yield of I^{131} as either 3·21 per cent or 3·09 per cent. The results of normalizing THODE's ratios to these values for mass 131 are shown in columns 1 and 2 of Table 1. In the second case one takes the absolute yield of Xe^{133} measured by KATCOFF and RUBINSON[5] as 6·62 per cent and normalizes at this mass; the results are shown in column 3.

The agreement between columns 1, 2, and 3 is not so good as might be hoped for, although it should be noted that a combination of the errors ascribed to all the relevant measurements is enough to cover the discrepancies. In view of this rather unsatisfactory situation it seemed worthwhile to measure the yield of Cs^{137} relative to Ba^{140}. This provides another normalization point, although the same absolute yield (Ba^{140}) is involved. No accurate radiochemical yield measurements for Cs^{137} have been possible until recently, because the half-life of this nuclide was not known with sufficient accuracy.* This half-life has recently been measured by BROWN, HALL, and WALTER[6] to be $30{\cdot}0\ ^{+0{\cdot}3}_{-0{\cdot}4}$ yr.

VOL. 1 1955

The method used to determine the yield ratio was very simple in principle. Uranium metal was irradiated in BEPO and then dissolved in nitric acid together with measured quantities of Ba and Cs carriers. The Ba and Cs were separated and purified, the chemical yields measured, and the activities determined by 4π counting. Full details are given in the following section.

EXPERIMENTAL

Irradiations and Dissolution of Metal

Four pieces of uranium rod, approximately 2 mm in diameter and about 1 g weight, were used. Two pieces were irradiated in BEPO for two weeks and two pieces for four weeks. Each piece was treated separately as follows. The metal was allowed to "cool" for about a week, dissolved in nitric acid containing 2·24 mg of Ba^{++} and 2·46 mg of Cs^{+}, and the solution made to 100 ml in 3N nitric acid. Exactly one-tenth of this solution was used for the barium determination and nine-tenths for the caesium.

Determination of Ba^{140}

A further 56·10 mg of Ba^{2+} were added to the uranium solution, and the barium was separated and purified by a conventional procedure involving the following steps:

(1) Precipitate $BaCl_2$ with HCl in ether and discard the supernatant liquor.
(2) Dissolve $BaCl_2$ in water and scavenge with $Fe(OH)_3$.
(3) Repeat $BaCl_2$ precipitation.
(4) Scavenge with $La(OH)_3$.
(5) Scavenge with $Fe(OH)_3$.
(6) Repeat $BaCl_2$ precipitation.
(7) Wash $BaCl_2$ with alcohol.
(8) Make $BaCl_2$ to standard volume in water (100 ml).

A portion of the $BaCl_2$ solution was diluted ten times for counting purposes and a further portion used for gravimetric determination of barium as $BaSO_4$.

* The half-life of Cs^{137} was first estimated by GLENDENIN[7] to be 33 ± 3 yr by combining a measurement of the Cs^{137} activity produced in fission with an estimate of the fission yield for mass 137. Later a value of 33 ± 2 yr was obtained by THODE *et al.*[1] by observing changes in Cs^{137}/Cs^{133} ratios during various periods up to five years.

[3] R. M. BARTHOLOMEW, F. BROWN, R. C. HAWKINGS, W. F. MERRITT, and L. YAFFE, *Canad. J. Chem.*, **31**, 120 (1953).
[4] A. C. PAPPAS, Technical Report No. 63, Massachusetts Institute of Technology.
[5] S. KATCOFF and W. RUBINSON, *Phys. Rev.*, **91**, 1458 (1953).
[6] F. BROWN, G. R. HALL, and A. J. WALTERS, *J. Inorg. Nuc. Chem.*, in press.
[7] L. E. GLENDENIN and R. P. METCALF, N.N.E.S., Vol. 9, 1067 (1951). McGraw-Hill Book Company Inc.

The Ba^{140} activity was measured by means of a 4π type, methane flow, proportional counter. Sources were made by evaporating aliquots from calibrated micropipettes on to 250 $\mu g/cm^2$ aluminium films. The weights of these sources were 1–2 μg. Growth and decay curves were followed over 4–5 half-lives, the observed counts being corrected for counting losses (not greater than 0·5 per cent) and background (not greater than 1 per cent). No significant deviation from a Ba^{140} half-life of 12·8 days was observed. The growth curves were extrapolated to the time of the last separation of Ba from La (taken as the end of step 6 above), the growth between separation and the first count being in the order of 2 per cent. This gives the Ba^{140} activity, uncorrected for self-absorption in the sources or losses in the mounting film, at the time of the last Ba-La separation.

This result was corrected for the aliquots used and for the chemical yield to give the total Ba^{140} activity in the uranium rod at the time of separation.

Determination of Cs^{137}

On account of its long half-life, the activity of Cs^{137} formed in fission is small compared to that of the other fission product with which it is mixed. The radiochemical purity cannot be checked by means of a decay curve. Thus it is essential to use a separation of proved efficiency. The procedure, outlined below, was an extension of that recommended by GLENDENIN.[8] A further 61·45 mg of Cs^+ were added to the uranium solution before starting.

(1) Remove the bulk of uranium by extracting with tri-butyl phosphate in kerosene.
(2) Evaporate to dryness twice with fuming nitric acid.
(3) Separate caesium as $CsClO_4$ (see ref. (8)).
(4) Dissolve the $CsClO_4$ in water. Scavenge twice with Fe^{3+}, two drops of saturated $(NH_4)_2CO_3$, and the minimum of NH_4OH. Scavenge again with Fe^{3+} and minimum of NH_4OH only.
(5) Add six drops of 6N NaOH and boil to remove ammonia.
(6) Repeat the perchlorate separation (step 3).
(7) Evaporate the $CsClO_4$ to dryness with one drop conc. HNO_3 and 1 ml of 100-vol H_2O_2. Repeat twice.
(8) Repeat the scavengings, using Fe^{3+} and La^{3+} for the first two and Fe^{3+} alone for the third (step 4).
(9) Remove ammonia as before (step 5).
(10) Repeat the perchlorate separation (step 3).
(11) Dissolve $CsClO_4$ in 3 ml water, 1 ml conc. HNO_3, and 15 ml alcohol. Add 0·5M H_2PtCl_6. Separate the Cs_2PtCl_6, and wash with alcohol.
(12) Boil the Cs_2PtCl_6 with 15 ml water and a few drops conc. HNO_3. Cool, separate the $CsPtCl_6$ (which remains largely undissolved), wash with alcohol and ether. Dry in oven at 110°C.

The chemical yield was obtained by weighing the Cs_2PtCl_6, which was then dissolved in water containing a few drops of conc. HNO_3 and made to a standard volume (100 ml). Note that Cs_2PtCl_6 is not readily soluble, cf. step 12 above. Sources for the 4π counter were prepared from the solution by evaporating aliquots on to 250 $\mu g/cm^2$ aluminium film, the weights of the sources being in the range 10–20 μg.

This procedure was tested and found to give a decontamination of at least 10^6 from Sr^{90}—Y^{90}, Ce^{144}, and Zr^{95}. As a further precaution, the procedure was varied slightly for each of the four pieces of uranium:

First piece: as above.
Second piece: an additional precipitation of $Fe(OH)_3$ by NaOH (modification of step 9).
Third piece: the Cs_2PtCl_6 from step 11 was fumed with perchloric acid and the procedure repeated from step 6 onwards.
Fourth piece: two additional precipitations of $Fe(OH)_3$ with NaOH (modification of steps 5 and 9).

The Cs^{137} fission yields obtained in the four cases were in good agreement (Table 2), which would be unlikely if the Cs^{137} were not radiochemically pure. A period of about three months elapsed between the end of the irradiation and the counting of the Cs^{137}.

The Ba^{137m} (2·6 min), which is equilibrium with Cs^{137} contributes to the counting rate. The correction was calculated using the same data as in reference,[8] as follows. Fraction of Cs^{137} decaying

[8] L. E. GLENDENIN and C. M. NELSON, N.N.E.S., Vol. 9, 1642 (1951). McGraw-Hill Book Company Inc.

via Ba^{137m} = 92 per cent, ratio of $e_K/e_L/e_{(M+N)}$ in internal conversion of the Ba^{137m} γ-ray = 5·5/1·0/0·27, ratio of e_K/γ = 0·097. Whence number of counts due to internal conversion of Ba^{137m} = 0·098 per decay of Cs^{137}. Number of counts due to unconverted γ-rays of Ba^{137m} = 0·002 per β decay of Cs^{137}. Total counts per β decay of Cs^{137} = 1·000 + 0·098 + 0·002 = 1·100.

After applying this correction and those for the aliquots used, the chemical yield, and the decay between end of irradiation and measurement, one obtains the total Cs^{137} activity in the uranium rod at the end of irradiation, uncorrected for absorption losses.

Relative Ba^{140} and Cs^{137} Activities

True disintegration rates would be obtained only if corrections were made for self-absorption in the sources and for absorption in the aluminium films. Both these corrections are small under the conditions of this experiment. The β energies of Ba^{140} and Cs^{137} are not greatly different and the corrections should be similar for these nuclides, in which case, since only relative activities are required, the corrections may be neglected. An estimate of the film absorption can be made by counting a source on a series of films of varying thickness and extrapolating the counting rate to zero film thickness. These measurements were made for Cs^{137} and Ba^{140} (freshly separated from La^{140}), and the results showed that the activities observed on 250 μg/cm² films should not be in error relative to each other by more than $\pm$0·5 per cent due to film losses.

The self-absorption will probably be greater in the Cs^{137} sources than in the Ba^{140}, since the former were approximately ten times heavier. Some experiments were carried out by counting sources prepared from solutions of fixed activity but varying solid content. There was some scatter in the results, partly due to statistical fluctuations and partly due to the difficulty of preparing exactly reproducible sources when the solid content was appreciable. However, of the sources in the weight range 10–20 μg, none showed a loss of more than 2 per cent compared to the weightless source; whereby it was concluded that the observed Cs^{137} activities were not in error relative to the observed Ba^{140} activities by more than -2 per cent due to self-absorption. No corrections have been applied for film or source absorption, but errors in the Cs^{137}/Ba^{140} ratio of $\pm$0·5 per cent and $^{+2\cdot0}_{-0\cdot0}$ per cent have been allowed for these respective causes.

RESULTS

The ratio of the Cs^{137} to Ba^{140} fission yields was calculated in the usual manner. The growth of Ba^{140} during irradiation and its subsequent decay prior to separation were calculated using a half-life of 12·8 days. Due allowance was made for the effect of pile "shut-downs" on the growth during irradiation. No allowance was made for the decay of Cs^{137} during irradiation, but as mentioned above, the Cs^{137} activities were corrected for decay between end of irradiation and measurement. A half-life of 30·0 yr was used for Cs^{137}. The results are shown in Table 2.

TABLE 2.—RATIOS OF Cs^{137} AND Ba^{140} FISSION YIELDS

Experiment	Irradiation time (weeks)	Cs^{137}/Ba^{140} yield
1	2	0·966
2	2	0·985
3	4	0·987
4	4	1·003
	Mean	0·985 $\pm$ 0·010

The error shown for the mean is the average deviation of the four results from their mean.

The errors associated with the measurements are estimated to be as follows:—

(i) Random errors:

Statistical fluctuations in counting	$\pm 0{\cdot}3$ per cent
Deviation between sources	$\pm 0{\cdot}5$ per cent
Chemical yield of barium	$\pm 0{\cdot}5$ per cent
Chemical yield of caesium	$\pm 0{\cdot}5$ per cent
Aliquots and dilutions	$\pm 0{\cdot}5$ per cent

If these are compounded as though they were probable errors, the total is $\pm 1{\cdot}1$ per cent, in good agreement with the average deviation of 1 per cent observed in the four experiments.

(ii) Systematic errors:

Relative activities due to (a) self-absorption	$^{+2{\cdot}0}_{-0{\cdot}0}$
(b) film absorption	$\pm 0{\cdot}5$ per cent

In addition there is an error associated with the half-life of Cs^{137} ($30{\cdot}0 \pm^{0{\cdot}3}_{0{\cdot}4}$ yr), which introduces a further uncertainty of approximately 1 per cent into the fission yield. It would seem therefore that an overall error of $\pm\frac{3}{2}$ per cent is a reasonable estimate. The gives an answer of $0{\cdot}985 \pm^{0{\cdot}03}_{0{\cdot}02}$ for the ratio of the Cs^{137}/Ba^{140} yields. The chain yield for mass 137 is of course somewhat higher than the Cs^{137} yield, because of the delayed neutron emission from Xe^{137}.

DISCUSSION

Using the value of YAFFE *et al.*[2] for the Ba^{140} yield = 6·32 per cent, one obtains $6{\cdot}22_5$ per cent for yield of Cs^{137}. The result of normalizing THODE's ratios to this value for Cs^{137} are shown in column 4 of Table 1. The difference between these values and those obtained by normalizing at $Xe^{133} = 6{\cdot}62$ per cent (column 3) is 2·6 per cent. Thus on the basis of the present value for Cs^{137}/Ba^{140} the absolute yields of Ba^{140} [2] and of Xe^{133} [5] are in fairly good agreement.

ACKNOWLEDGEMENT

The author wishes to thank Mr. I. G. SWAINBANK for his assistance in counting.

J. Inorganic and Nuclear Chemistry, 1955, Vol. 1, p. 253. Pergamon Press Ltd., London

THE THERMAL NEUTRON-CAPTURE CROSS-SECTION OF RADIUM-223*

By GARMAN HARBOTTLE
Department of Chemistry, Brookhaven National Laboratory,
Upton, Long Island, New York

(*Received* 19 *January* 1955)

VOL.
1
1955

RADIUM-223, a member of the naturally-occurring actinium series, is an alpha emitter of half-life 11·685 days.[1] By neutron capture the isotope radium-224 is formed; it has a half-life of 3·64 days and is also an alpha emitter. In order to determine the neutron-capture cross-section of radium-223, a sample of about a millicurie of this isotope (carried on barium nitrate) was irradiated in the Brookhaven reactor for ten days. The neutron flux at the irradiation site was monitored by a weighed portion of potassium cobalticyanide. The disintegration rate of the cobalt in this sample was afterwards determined by coincidence counting. A cross-section of 35 barns was assumed for cobalt.[2] The irradiated material was dissolved, and when secular equilibrium had been attained between radium-223, radium-224, and their daughters, a lead fraction was removed by extraction with a benzene solution of thenoyl trifluoroacetone (TTA). The lead fraction was highly purified by repeated TTA extractions, followed by precipitation with carrier barium nitrate from concentrated nitric acid and as lead sulphide. The purified lead fraction was dissolved, evaporated to dryness, and alpha-counted continuously for several days. The alpha activity of the lead fraction (arising from the short-lived bismuth daughters) clearly showed two, and only two, periods, one of 36 minutes (Pb^{211} arising from Ra^{223}) and one of 10·6 hours (Pb^{212} arising from Ra^{224}). The 10·6-hour period was completely absent in lead fractions removed from the original, unirradiated radium-223. The alpha activity of the daughters of the 10·6-hour lead was approximately 20,000 counts per minute, while that of the 36-minute lead was nearly 1,600 times larger in the equilibrium mixture. From the ratio of the Pb^{211} to Pb^{212} activity and a knowledge of the neutron flux the capture cross-section was calculated by straightforward procedures.[3] The results of two experiments gave 121 and 129 barns. Taking all errors into account, the neutron-capture cross-section may be stated as 125 ± 15 barns.

The author wishes to thank Dr. M. SALUTSKY of the Mound Laboratory for supplying the sample of radium-223.

* Research carried out under the auspices of the U.S. Atomic Energy Commission.

(1) M. SALUTSKY; private communication.
(2) Neutron Cross Sections, AECU 2040 (1952).
(3) W. RUBINSON; *J. Chem. Phys.* **17**, 542 (1949).

J. Inorganic and Nuclear Chemistry, 1955, Vol. 1, pp. 254–261. Pergamon Press Ltd., London

THE DECAY CHAIN Pu^{245}—Am^{245}—Cm^{245} *

By C. I. Browne, D. C. Hoffman, W. T. Crane, J. P. Balagna, G. H. Higgins, J. W. Barnes, R. W. Hoff, H. L. Smith, J. P. Mize, and M. E. Bunker
University of California, Los Alamos Scientific Laboratory, Los Alamos, New Mexico

(*Received* 20 *May* 1955)

Abstract—Two nuclides not previously reported in the literature, Pu^{245} and Am^{245}, have been produced by neutron irradiation methods. The study of the radiations of these nuclides is described and a preliminary decay scheme for Am^{245} is presented.

1. INTRODUCTION

In the region of high atomic number, study of the radiation of beta emitters is of particular interest in that determination of the disintegration energy affords additional data for the closing of cycles of alpha and beta modes of decay. The requirement of internal consistency of these cycles provides a very powerful method of evaluation of data, prediction of decay characteristics of new nuclides, and recognition of such variations as decay from isomeric states.

The decay chain under discussion contains two new nuclides, Pu^{245} and Am^{245}, not previously reported in the literature.

2. CHEMICAL METHODS

The activity present in samples obtained by neutron irradiation of transthorium elements is overwhelmingly that of the fission products. Since the purification of multicapture products requires decontamination factors of the order of 10^{10}, the chemical techniques employed constitute one of the most important aspects of the work. The chemistry used in this study was aimed at the purification of the plutonium, since the americium could be "milked" from the plutonium after purification had been achieved.

The original sample was brought into solution through the action of nitric, perchloric, and hydrochloric acids, and contained finally in a solution some 6N in HCl. As a convenience step, lanthanum carrier was added, and the solution made alkaline with ammonium hydroxide and centrifuged. The precipitate was washed, redissolved, and reprecipitated several times. The final hydroxide was dissolved in concentrated HCl to which concentrated HNO_3 had been added in the ratio of about 30 microliters per 5 milliliters of HCl. This solution was passed through a column of Dowex 1 anion exchange resin which had been previously washed, graded, and equilibrated with HCl and HNO_3 in the concentrations present in the active solution. After extensive washing with the HCl-HNO_3 mixture, the plutonium was eluted from the column by passing through a solution 10M in HCl and 0.25M in HI. Further purification was accomplished by repeating three or four times a cycle of oxidation of the plutonium with $KMnO_4$, precipitation of LaF_3, reduction of the plutonium with hydroxylamine, reprecipitation of LaF_3, dissolving of the fluoride in H_3BO_3, precipitation of the hydroxide with NH_4OH, putting the plutonium on a Dowex-1 column with HCl-HNO_3, and elution with HCl-HI. Such cycles utilize the ability of plutonium to

* This work was performed under the auspices of the U.S. Atomic Energy Commission.

form 3^+, 4^+, and 6^+ valence states, and provide very high decontamination factors ($\sim 10^5$ from fission products) per cycle performed.

Throughout the chemistry, samples were withdrawn to test the alpha-to-beta ratio as the decontamination proceeded. The chemistry was considered complete when this ratio remained essentially constant with further cycles. In the final cycle, the plutonium was not eluted from the column, but was retained as a "cow" from which daughter activities could be "milked" by passing through the HCl-HNO_3 mixture.

VOL. 1 1955

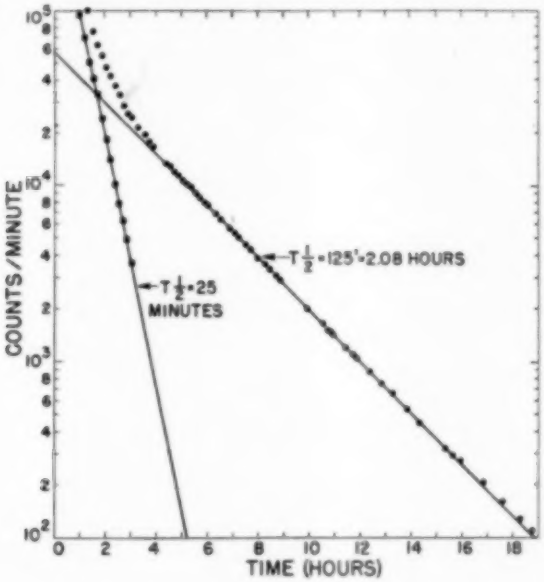

FIG. 1.—Gross decay.
Am fraction milked from Pu.
Am^{245} after subtraction of 2.08-hour component.

3. AMERICIUM

The Half-life

At times early in the history of the sample, activity "milked from the cow" exhibited beta activity with only one discernible half-life, measured as 2.08 hr. The amount of activity in successive milks decreased fairly rapidly with time, and after the sample was a day or two old there could be observed a second component in the half-life of the milk. Repeated determinations of the half-lives of these activities led to a value of 25 min for the second component, taken to be the Am^{246} activity described in an earlier report[1] and 2.08 ± 0.08 hr for the new activity (Fig. 1).

The Atomic Number

The atomic number of the 2-hour emitter was established by eluting milked activity from a Dowex-50 column with 0.25M lactic acid. The elution peaks were marked with Am^{241} and Cm^{242} to establish location of the individual atomic numbers. The 2.08-hour activity was observed to elute identically with the Am^{241}, which established its atomic number conclusively as 95.

[1] S. FRIED *et al.*, *J. Inorg. Nuc. Chem.* (to be submitted).

The Mass Number

Consideration of the properties of known nuclides reveals that, in activities formed by neutron capture in uranium or plutonium, any americium beta-active nuclide must be either the 16-hour Am^{242m} (formed by n, γ on the Am^{241} which will grow into the plutonium if appreciable Pu^{241} is present), or of mass number 245 or greater. It seems likely, also, that in such a process the number of atoms formed will decrease with increasing mass number, since an extreme variation in capture cross-section would be necessary to offset this trend. Accordingly, the first indication of the mass number of the new activity was obtained from the datum that more atoms of the parent were present than of the known Pu^{246}, leading to a tentative mass assignment of 245.

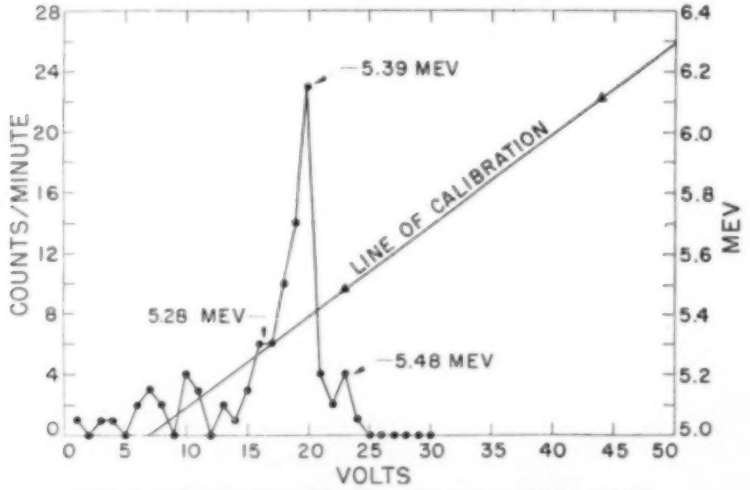

FIG. 2.—Alpha spectrum of Cm^{245} and Cm^{246} from Pu^{245} and Pu^{246}.

To establish the mass number conclusively, samples milked from the plutonium were allowed to decay for several days and separated into two gross samples, the first of which contained the milk gathered over the first thirty-six hours of the sample history, and the second those samples gathered on the third and following days. These two samples were eluted from a Dowex-50 column with hot lactic acid, and alpha pulse analyses were made of the curium peaks. The spectra showed the presence of Cm^{245} and Cm^{246} (Fig. 2). Since these alpha spectra overlap, determination of the relative abundance was made on the basis of the high energy (5.48 MeV) component of the Cm^{245} alpha spectrum, and its abundance relative to its other components, as determined by HULET[2] from samples from the decay of Bk^{245}. The abundance of the Cm^{245} alpha activity relative to the Cm^{246} decayed by a factor of at least 7 from the early to the late sample, establishing its growth from the shorter-lived plutonium activity. The half-life of Cm^{245} calculated from these data was 14,300 years, with some 20 per cent uncertainty, and the half-life of Cm^{246} 2300 years, with the same uncertainty.

The Beta Radiation

The beta spectrum was studied with a thin lens magnetic spectrometer, using a sample aged for some six hours after milk-time to permit decay of the 25-min Am^{246}

[2] E. K. HULET, UCRL-2283, July, 1953 (unpublished).

activity. The observed spectrum is shown in Fig. 3. Two conversion lines were observed at energies of 126.7 and 226.9 keV, corresponding to the K and L lines, respectively, of a gamma-ray of 255 keV. The K/L ratio was determined to be 5 ± 1, which lies closest to the values for an $M1$ or an $E1$ transition, as calculated from ROSE's tables of K and L conversion coefficients.[3] The K conversion coefficient was calculated as 0.19 on the basis of e^- intensity, gamma-ray intensities, beta intensity, and the decay scheme of Fig. 7. This value is in poor agreement with ROSE's $E1$ value of 0.04, but is far too low to permit the possibility of magnetic transition types. Consideration of both of these data leads to the assignment of $E1$ as the transition type.

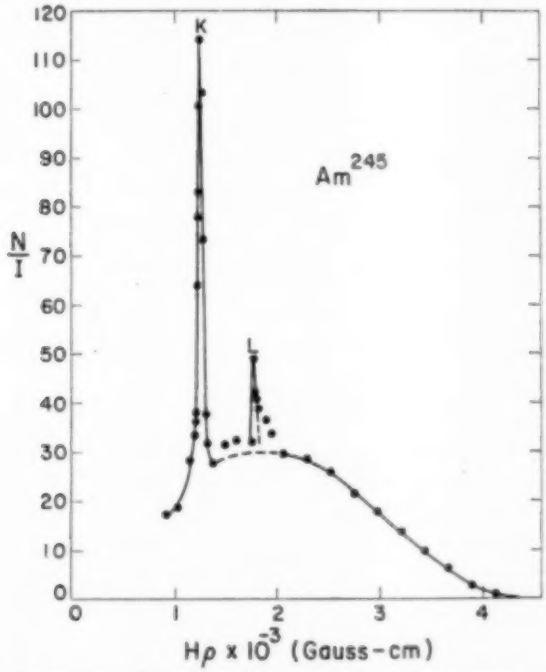

FIG. 3.—Beta spectrum. The points which do not lie on the spectrum as drawn indicate the presence of additional conversion lines which were not completely analyzed due to the relatively short half-life of Am^{245}.

Fermi analysis of the beta continuum showed only one component, of end-point energy 905 ± 5 keV, but the data do not permit the exclusion of low-abundance components of energy greater than 900 keV or less than 250 keV. The Fermi plot was linear in the range 250 to 900 keV (Fig. 4), implying an allowed or first forbidden transition. Computation of the log ft-value for the transition led to a figure of 6.2, again indicating an allowed or first forbidden transition since the extent of knowledge of ft-values in the heavy region is not sufficient to permit distinction of these two types from this datum.

The Gamma Radiation

The gamma radiation was analyzed with multichannel pulse-height analyzers and NaI(Tl) scintillation crystals mounted on DuMont 6292 photomultiplier tubes. In

[3] M. E. ROSE, private communication.

VOL. 1 1955

the coincidence work, a Los Alamos Model-300 coincidence unit was used, with a resolving time of 0.2 microsecond. Each channel of the Model-300 unit has provisions for setting upper and lower bounds; the procedure followed was to set the bounds of

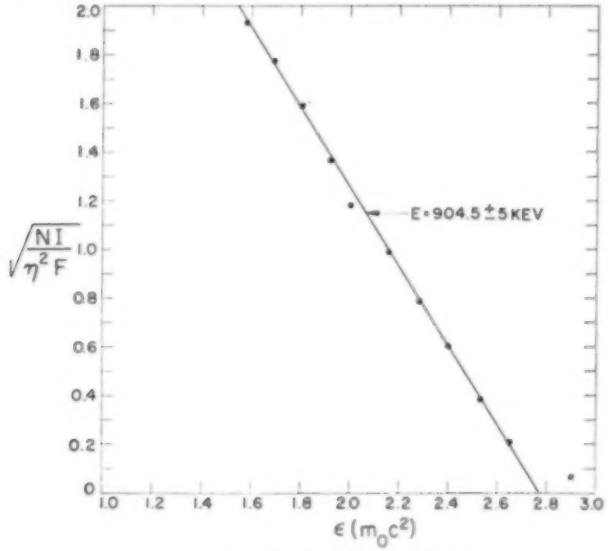

FIG. 4.—Fermi plot of Am^{245}.

one channel over a narrow energy region (called the "trigger" region) and to operate the other channel with bounds at minimum and maximum values. The signal to the latter channel also fed a 10-channel analyzer (after appropriate delay of about

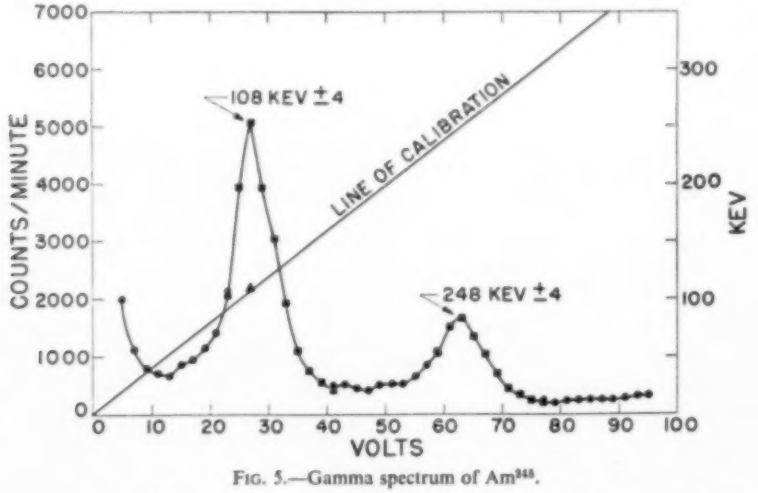

FIG. 5.—Gamma spectrum of Am^{245}.

1 microsecond), which was gated with the coincidence pulse from the Model-300 circuit.

Fig. 5 presents the gamma "singles" spectrum, with peaks at 108 and 248 keV.

The indication of rising intensities at low energies comes about through the presence of strong *L* X-radiation, not visible on Fig. 5 because of the gain settings in this particular run. The similarity to the spectrum reported by HULET[2] for Bk^{245} is very striking, and implies very similar beta and electron capture modes of decay to Cm^{245}.

The coincidence spectra revealed several additional gamma-rays. Table 1 summarizes the energies and coincidence data of these gamma-rays, and Fig. 6 illustrates the spectrum observed in coincidence with the 100-keV region.

TABLE 1.—GAMMA-GAMMA COINCIDENCE DATA

Energy region of trigger radiation (keV)	Energy and relative intensity of coincident radiation* (keV)	
260–280	153 ± 5	1.2
	123 ± 5	3
	108 (X-ray, ?)	7
	78 (?)	2.5
	60 (?)	2.2
	36 ± 5	4.5
239–260	140 ± 5	2.2
	111 ± 5	6
	78 (?)	2.8
	60 (?)	1
	36 ± 5	7
98–118	255 ± 5	5.5
	230 ± 5	3.3
	140 ± 5	55
	111 ± 5	35
	(*L* X-rays)	120

* Relative intensities apply only within a given trigger.

The Decay Scheme

Fig. 7 presents a preliminary decay scheme consistent with the main features of the data. It should be noted that beta-gamma coincidences have not been studied.

The decay scheme of Fig. 7 leads to a disintegration energy of 1.32 MeV, which leads in turn to a discrepancy in energetics. The "closed" cycle in which the Bk^{249}

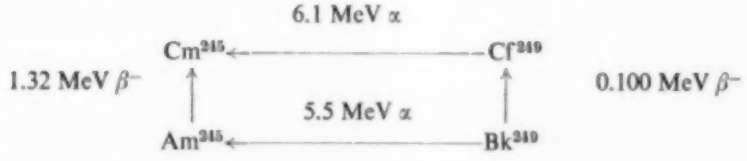

and Cf^{249} data are those of DIAMOND *et al.*[4] and GHIORSO *et al.*[5] does not close. The 600-keV discrepancy is not completely removed even if the assumption is made that the decay scheme of Fig. 7 is in error, since the beta energy alone gives rise to a

[4] H. DIAMOND, L. B. MAGNUSSON, J. F. MECH, C. M. STEVENS, A. M. FRIEDMAN, M. H. STUDIER, P. R. FIELDS, and J. R. HUIZENGA, *Phys. Rev.* **94**, 1083 (1954).
[5] A. GHIORSO, S. G. THOMPSON, G. R. CHOPPIN, and B. G. HARVEY, *Phys. Rev.* **94**, 1081 (1954).

200 keV inequality. The abundance of the gamma-rays, and the fair limits which can be placed on the presence of other beta components, make it doubtful that the principal beta transition is to the ground state. In explaining this discrepancy, GHIORSO and

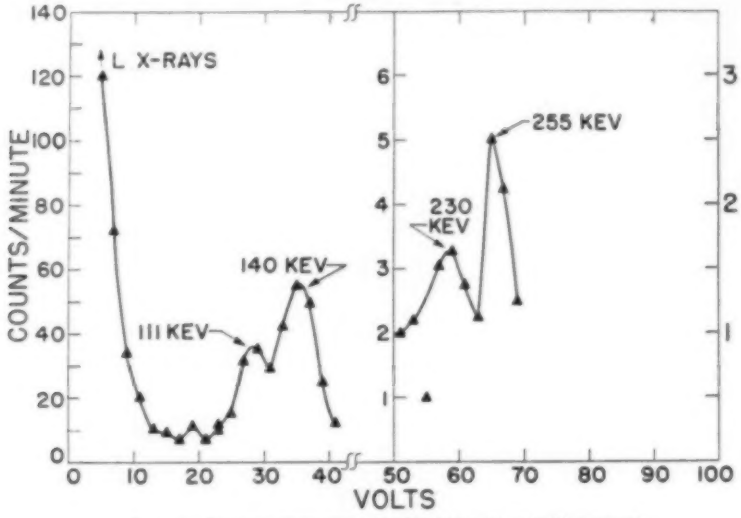

FIG. 6.—Gamma spectrum using 98–118 keV coincidence gate.

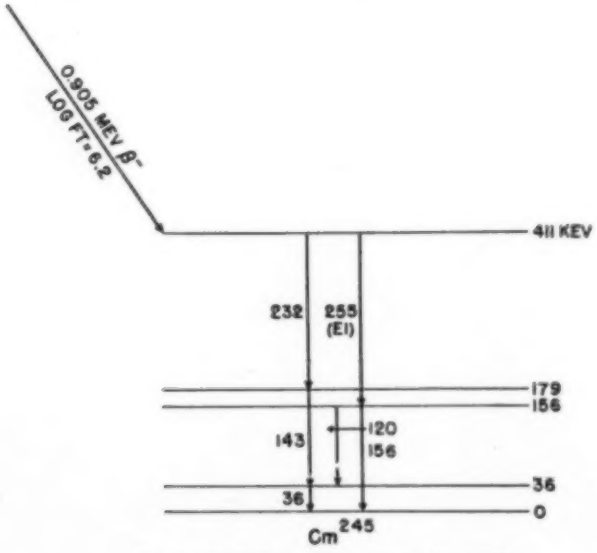

FIG. 7.—Preliminary decay scheme for Am^{245}.

THOMPSON[6] have proposed an isomeric state in Am^{245}. Further studies on this point, as well as on the beta-gamma coincidences and low-abundance decay modes, are in progress.

[6] A. GHIORSO and S. G. THOMPSON, private communication.

4. PLUTONIUM

Study of the Pu^{245} decay was complicated by the presence in the sample of large quantities of the 5-hr Pu^{243} and the 11-day Pu^{246}. The gamma radiation of these nuclides and the daughter Am^{246} made it impossible to assign with confidence any gamma-ray to Pu^{245}, even on a difference or decay basis. By the same token, the beta radiation of Pu^{245} could not be measured directly, though it seems unlikely that its beta spectrum end-point energy is larger than the 0.8 MeV observed in the $Pu^{243-245}$ mixture at a time early in the history of the sample.

The half-life of Pu^{245} was measured by resolving the gross decay curve of a plutonium sample, and by measuring the activity of its "equilibrated" daughter at successive times. The two methods lead to inconsistent values; direct decay gives a half-life of 12.8 hr, while methods based upon daughter activity lead to a value of 11.0 hr. Until further data are available, the best value to be taken is 12 ± 1 hr.

VOL.
1
1955

ACKNOWLEDGEMENTS

It is a pleasure to acknowledge the indebtedness of the authors to Dr. R. W. SPENCE and Dr. KENNETH STREET for their continued interest and encouragement. We are also indebted to MELVIN COOPS and FRANCINE J. LAWRENCE for assistance in the chemistry, and RICHARD D. HIEBERT and HARRY BOWMAN for invaluable aid with the electronic apparatus employed.

J. Inorganic and Nuclear Chemistry, 1955, Vol. 1, pp. 262–266. Pergamon Press Ltd., London

PRODUCTION OF Pu^{245} AND Am^{245} BY NEUTRON IRRADIATION OF Pu^{244}

By P. R. Fields, M. H. Studier, A. M. Friedman, H. Diamond, R. Sjoblom, and P. A. Sellers
Chemistry Division, Argonne National Laboratory, Lemont, Illinois, U.S.A.

(*Received* 20 *May* 1955)

Abstract—Pu^{245} and Am^{245} were prepared by neutron irradiation of Pu^{244}. The beta-decay half-lives of Pu^{245} and Am^{245} were found to be 10·1 ± 0·5 hours and 119 ± 1 minutes, respectively. The beta-decay energy of Am^{245} was found to be 0·86 MeV by absorption methods, and γ-rays of 260, 121, and 70 keV* were resolved with a sodium iodide crystal spectrometer. The thermal neutron capture cross-section of Pu^{244} was determined to be 1·4 barns.

In a search for Pu^{245} and Am^{245}, an early bombardment in the Argonne CP-3 reactor of plutonium containing a small amount of Pu^{244} yielded a two-hour activity in the americium fraction separated after bombardment.[1] The activity could not be positively assigned to Am^{245}. The experiment was not repeated, and no information was obtained about a possible plutonium parent. Values of 2·08 hours[2] and 120 min[3] have been reported for the Am^{245} beta half-life, and a half-life of 12[2] and 11·0 hours[3] for Pu^{245}. Since the programme of irradiating plutonium in a very high neutron flux reactor (MTR) had yielded large amounts of plutonium containing Pu^{244}, it was possible to repeat the early neutron irradiation of Pu^{244} and prepare larger quantities of Pu^{245} and Am^{245}. The present bombardments yielded a 119 ± 1 min beta-emitting Am^{245}, and a 10·1 ± 0·5 hour Pu^{245} parent. The Pu^{245} beta particle was not observed directly, but its half-life was measured by repeated separations of its Am^{245} daughter over a period of time. A pile neutron-capture cross-section of 1·4 barns was found for Pu^{244}.

A plutonium sample containing all isotopes from mass 238 to 244 with a $\frac{244}{242}$ ratio of 0·000384 was bombarded twice in the new Argonne heavy-water pile. The first irradiation was about two and one-half hours and the second irradiation about twelve hours in duration. A gold foil was included in the second sample as a flux monitor. The irradiated plutonium was separated from fission products by solvent extraction, using hexone as the solvent, followed by a Dowex-1 anion resin column, and finally a TTA (thenoyltrifluoracetone) extraction.

In the first irradiation Am^{245} was characterized as a 119 ± 1 min beta emitter (Fig. 1). The Pu^{245} betas were obscured by the larger amount of Pu^{243} formed from the Pu^{242} present in the target material, so its half-life had to be determined by successive separations of its daughter Am^{245} over a period of time. Five separations were carried out over a period of twenty-one hours, and the Am^{241} which grew in from Pu^{241} served as an internal tracer for the americium separations. Table 1 shows the decay times and

* The 70 keV γ-ray is probably due to fluorescence of the platinum backing.

[1] M. H. Studier, P. R. Fields, S. M. Fried, G. L. Pyle, and H. Diamond, unpublished data.
[2] C. I. Browne, private communication.
[3] S. Fried, H. Selig, and G. Pyle, private communication.

VOL.
1
1955

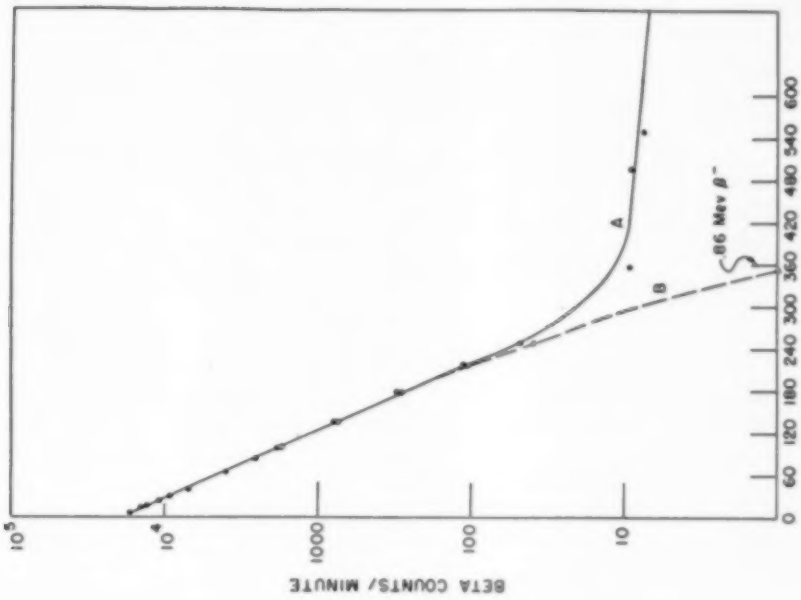

FIG. 2.—Aluminium absorption curve of Am^{245}. Curve *A* is the original absorption curve. Curve *B* is the absorption curve corrected for the γ-tail.

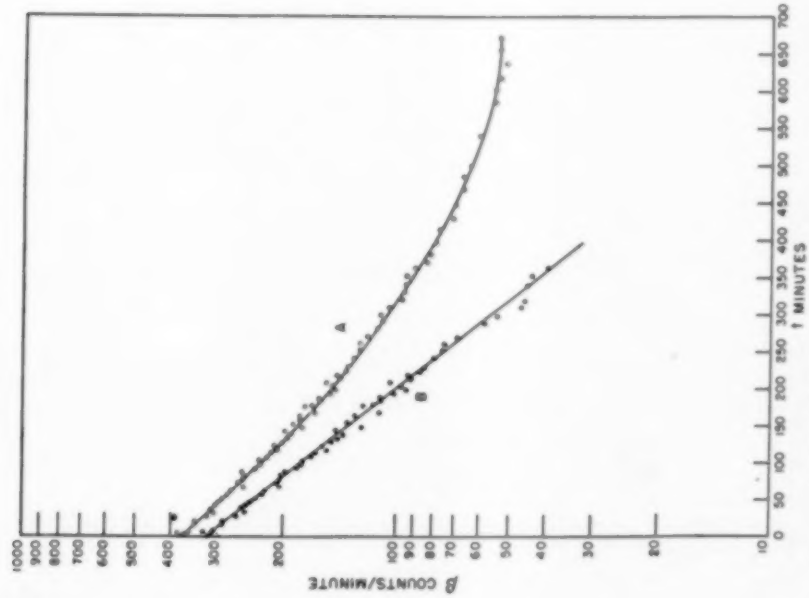

FIG. 1.—β^- decay of Am^{245}. Curve *A* is the uncorrected decay curve. Curve *B* is the decay curve corrected for counter background and the Am^{241} alpha particles.

the beta-to-alpha ratios due to Am^{245} and Am^{241}, corrected to the time of each separation. Decay time is the time from the original purification of plutonium to the beginning of the growth interval. Growth time is the time the americium was allowed to grow into the plutonium fraction before it was separated again.

TABLE 1

Separation No.	$\frac{\beta}{\alpha}$	Growth time t (min)	Decay time t' (min)
1	29·718	110	0
2	13·021	216	404
3	8·181	321	620
4	5·643	287	941
5	0·846	875	1228

The number of Am^{245} betas was normalized to a unit Am^{241} alpha count, thus removing the necessity of determining the chemical yield of the americium. From any

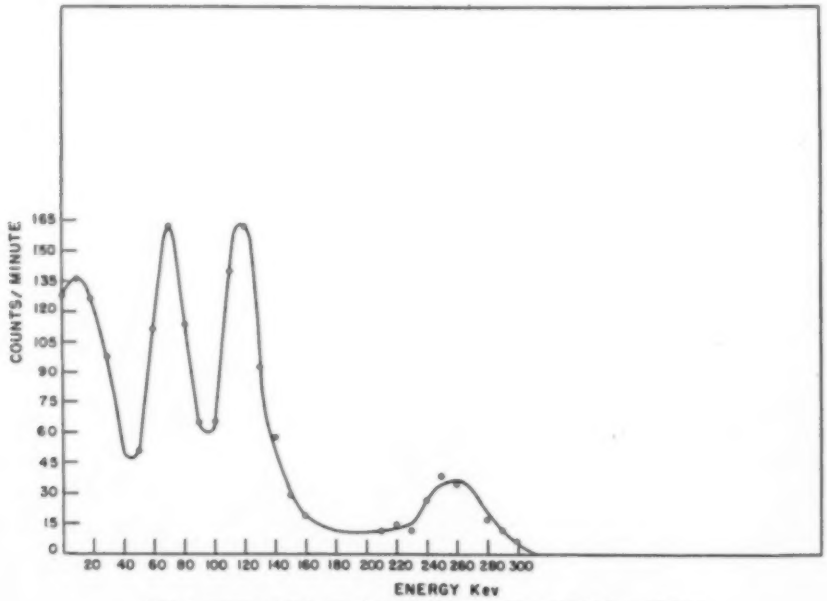

FIG. 3.—γ-ray spectrum of Am^{245} decay. Channel width = 10 keV.

two ratios of americium separations, the half-life of Pu^{245} could be calculated by successive approximations from the relationship

$$\frac{\left(\frac{\beta}{\alpha}\right)_m \cdot t_m}{\left(\frac{\beta}{\alpha}\right)_n \cdot t_n} = \frac{(e^{-\lambda_1 t_m} - e^{-\lambda_2 t_m})e^{-\lambda_1 t'_m}}{(e^{-\lambda_1 t_n} - e^{-\lambda_2 t_n})e^{-\lambda_1 t'_n}}$$

λ_1 = decay constant of Pu^{245}.

λ_2 = decay constant of Am^{245}.

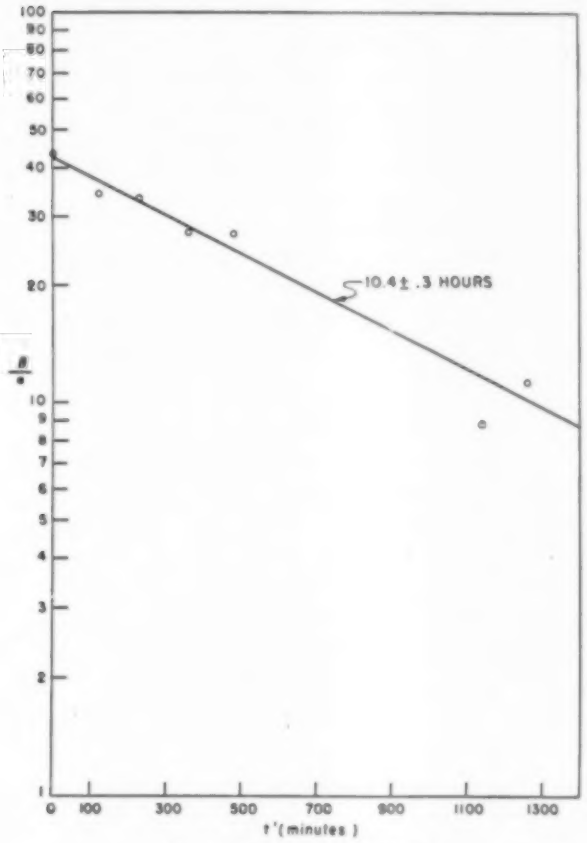

Fig. 4.—Pu^{245} β^- decay half-life.

Subscripts m and n refer to the separation numbers.

Enough ratios were considered so that the consistency of the data was demonstrated. Table 2 shows the results of some of the calculations.

TABLE 2.—Pu^{245} HALF-LIFE VALUES FROM VARIOUS PAIRS OF AMERICIUM SEPARATIONS

Separations	Pu^{245} half-life (hours)
1, 2	9·63
1, 3	10·6
1, 4	9·34
2, 4	9·74
1, 5	9·61
Average	9·78 ± 0·43

A much larger amount of activity was generated in the second bombardment, and sufficient Am^{245} was separated to obtain an aluminium absorption curve (Fig. 2) and to outline the γ-ray energies with a NaI scintillation spectrometer (Fig. 3). The beta-particle energy obtained from the absorption curve was approximately 0·86 MeV and the γ-rays observed were 260 keV, 121 keV, 70 keV,* and some unresolved lower energies. The 121-keV and lower-energy photons are probably X-rays. The pile neutron-capture cross-section of Pu^{244} was determined as 1·4 barns. The early CP-3 irradiation results yielded a neutron-capture cross-section for Pu^{244} which is in rough agreement with the 1·4 barns calculated from the present work.[1]

The half-life of Pu^{245} was redetermined graphically (Fig. 4) from the second bombardment by allowing the Am^{245} to grow in from its plutonium parent over equal time intervals, so the amount of Am^{245} isolated is directly proportional to the amount of Pu^{245} present at the time of separation. A least-squares analysis of the data yielded a value of $10{\cdot}4 \pm 0{\cdot}3$ hours, in good agreement with the half-life determined in the earlier irradiation. A half-life of 10·1 hours for Pu^{245} was somewhat surprising, in that it is longer than that of Pu^{243}, which has a five-hour half-life.[4] The systematics of beta emitters in this region of the heavy elements would predict a beta half-life shorter than five hours for Pu^{245}.

ACKNOWLEDGEMENTS

The valuable assistance in these experiments by R. F. BARNES, S. W. MOLINE, J. E. GINDLER, and M. PETHERAM is gratefully acknowledged.

* See footnote, p. 262

(1) J. C. SULLIVAN, G. L. PYLE, M. H. STUDIER, P. R. FIELDS, and W. M. MANNING, *Phys. Rev.*, **83**, 1267 (1951).

J. Inorganic and Nuclear Chemistry, 1955, Vol. 1, pp. 267–273. Pergamon Press Ltd., London

EXACT ALPHA-PARTICLE ENERGIES FOR THE ISOTOPES Em^{211}, Em^{210}, Em^{209}, Em^{208}, and Fr^{212} *

By F. F. MOMYER, Jr., F. ASARO, and E. K. HYDE
Radiation Laboratory and Department of Chemistry, University of California, Berkeley, California

(*Received* 18 *April* 1955)

Abstract—Using the glow-discharge technique of sample preparation, some wire-mounted sources of emanation isotopes were prepared and exposed in the magnetic alpha-particle spectrograph. Em^{211} has alpha groups of 5·847 ± 0·002 MeV (33·5 per cent), 5·779 ± 0·003 MeV (64·5 per cent), and 5·613 ± 0·007 MeV (2 per cent). Em^{210} emits alpha particles of 6·037 ± 0·003 MeV (100 per cent). Em^{209} emits alpha particles of 6·037 ± 0·010 MeV (100 per cent). Em^{208} and Em^{212} emit alpha particles of 6·141 ± 0·004 (100 per cent), and 6·262 ± 0·005 MeV (100 per cent), respectively. In addition, a measurement of the alpha spectrum of Fr^{212} was made. Fr^{212} has alpha groups of 6·411 MeV (37 per cent), 6·387 (39 per cent), and 6·342 MeV (24 per cent).

VOL.
1
1955

1. INTRODUCTION

IN a companion paper, MOMYER and HYDE[1] have discussed the preparation and study of a whole new series of isotopes of francium, emanation, and radium. A primary goal of their study was the determination of the alpha-decay characteristics of these isotopes to show the pronounced effect of the 126-neutron shell on their properties. The measurement of alpha-particle energies was carried out in an argon-filled ionization chamber coupled to a multichannel pulse-height analyzer. This widely-used method has several pronounced advantages: energies of alpha-particle groups can be obtained on weak sources, half-lives of specific alpha groups can be determined by repeated analyses of the alpha spectrum, and genetic relationships can be explored by observing the growth of alpha-particle groups associated with daughter activity. However, the ionization chamber method is fundamentally incapable of giving results as accurate as those obtained on a magnetic spectrograph. Hence, when the orientation and genetic studies, discussed in the above paper, had been completed, it was considered desirable to redetermine the alpha-particle energies in the magnetic spectrograph.

The magnetic spectrograph has been described previously[2] and a number of papers have been published on the alpha spectra determined with the instrument.[3] Basically it is a large mass spectrograph which uses a 60°-sector magnet with the normal mass spectrograph ion source replaced by a thin radioactive source. The alpha particles emitted by the source pass through a slit system and then through the magnetic field with a radius of curvature of about 75 cm, and impinge on a photographic emulsion. A microscope and a mechanical stage are used to count individual tracks in the developed plate.

In the present study the principal difference in the use of the spectrograph from

* This research was performed under the auspices of the U.S. Atomic Energy Commission.

[1] F. F. MOMYER, Jr., and E. K. HYDE, *J. Inorg. Nucl. Chem.* **1**, 274 (1955)

[2] F. L. REYNOLDS, *Rev. Sci. Instrum.* **22**, 749 (1951).

[3] ASARO, REYNOLDS, and PERLMAN, *Phys. Rev.* **87**, 277 (1952); F. ASARO and I. PERLMAN, *Phys. Rev.* **88**, 129 (1952); F. ASARO and I. PERLMAN, *Phys. Rev.* **88**, 828 (1952); ASARO, THOMPSON, and PERLMAN, *Phys. Rev.* **92**, 694 (1953).

the research studies cited above[3] was in the preparation of the sources. The spectrograph requires source strengths of the order of 10^6 to 10^7 alpha disintegrations per minute for isotopes with half-lives of an hour or less. To prepare such samples mounted on a solid backing and covered with no absorbing material was a severe experimental problem in the case of the short-lived isotopes of the rare-gas element emanation. The invention of the glow-discharge method for the deposition of gaseous isotopes on metallic foils or wires, as discussed by MOMYER and HYDE,[1] made it possible to solve the source problem.

2. DISCUSSION OF EXPOSURES ON EMANATION SAMPLES

Two strips of thorium foil 0·005 in. in thickness were bombarded for fifty minutes with 340-MeV protons in the 184-in. cyclotron at a beam intensity of roughly 0·1 microampere. Immediately after the bombardment the foils were dissolved in a closed

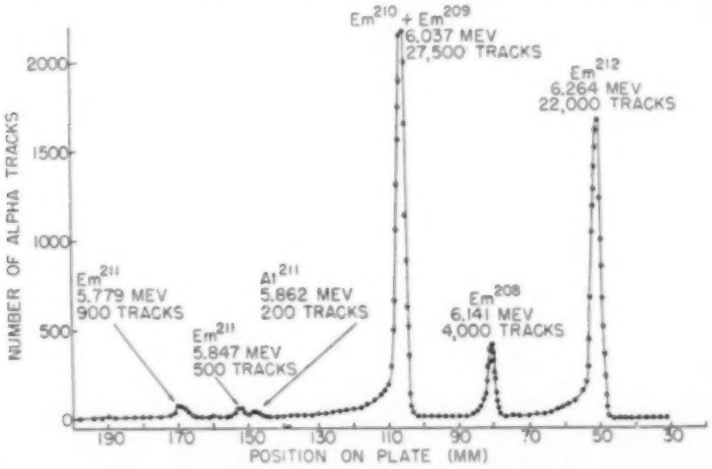

FIG. 1.—Alpha spectrum of mixture of emanation isotopes. Fifteen-minute exposure started 65 minutes after the end of a 50-minute bombardment of thorium with 340-MeV protons.

system. The evolved gases were purified according to the methods previously discussed and the emanation radioactivity was deposited on a 0·01-in. diameter monel wire, using the glow-discharge method.[1]

Sixty-five minutes after the end of the bombardment the wire source was mounted in the alpha-particle spectrograph and exposed for a 15-minute period. It was known from the previous work that this sample would consist of a mixture of 23-minute Em^{212}, 16-hour Em^{211}, 2·7-hour Em^{210}, 30-minute Em^{209}, and 23-minute Em^{208}. Furthermore, the energies of the principal alpha groups of all these isotopes were known to about 15 keV from previous measurements in the ionization chamber. Fig. 1 shows the results of this run. The number of individual alpha-particle tracks per $\frac{1}{4}$ mm of distance on the plate is plotted versus distance. The peaks are identified from the properties previously determined in the ionization chambers. The energies quoted in the figure are determined by assigning Em^{211} the exact energy of 5·847 MeV and using it as an internal standard. The Em^{211} alpha groups were related to At^{211} as an intermediate standard, as discussed below. The dispersion was taken to be 4·11 keV per mm. The half-widths of the peaks are about 10 keV.

It was considered desirable to obtain corroborative evidence on the assignment of the peaks by making successive short exposures, and thus checking to see that the peaks decayed with the expected half-lives. There was an additional reason for doing this in the case of the 6·037 ± 0·003-MeV peak, because it was almost certain that this was a double peak, i.e., that Em^{210} and Em^{209} with half-lives of 2·7 hours and 30 minutes,

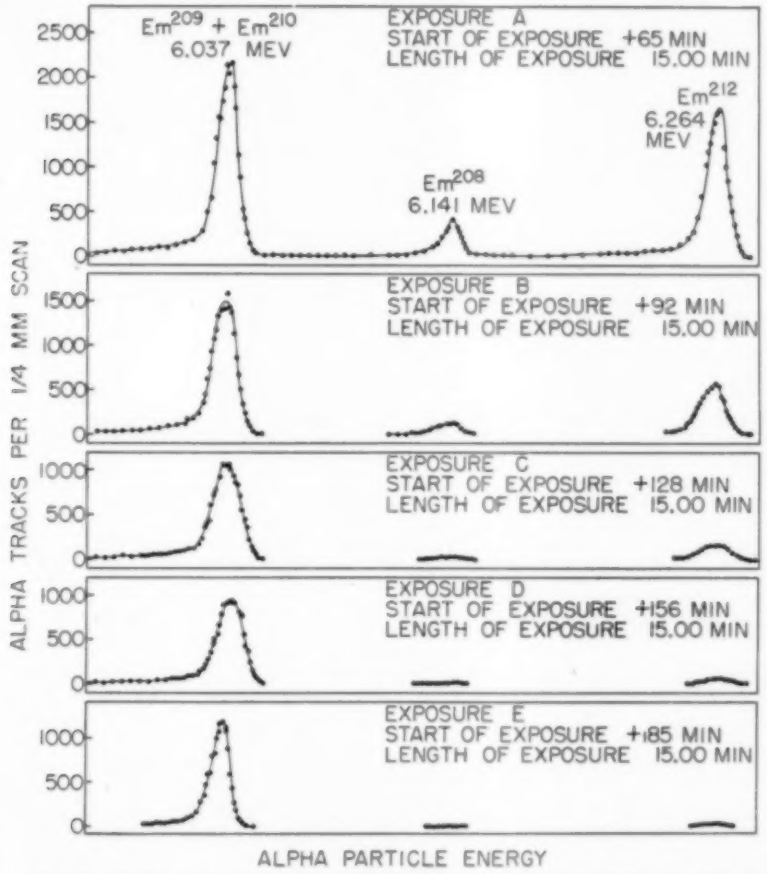

FIG. 2.—Alpha spectra from successive fifteen-minute exposures of mixture of emanation isotopes. The time elapsed since the end of the bombardment of the thorium target in the cyclotron to the start of the exposure of the film is recorded. To prevent overcrowding of the figure, some data were not plotted.

respectively, were contributing alpha particles of almost identical energy to this peak. Hence, when the 15-minute exposure represented by Fig. 1 was completed, the emulsion was replaced and a second 15-minute exposure was made. This procedure was repeated three times more to give a series of five exposures, as shown in Fig. 2. The top curve (exposure *A*) is identical with the high-energy portion of Fig. 1. The expected changes occurred in the alpha spectra of exposures *B*, *C*, *D*, and *E*. This is shown more clearly by the curves in Fig. 3, which represent the decay of the area under the peaks. The decay curve of the 6·037-MeV peak is resolvable into a 2·7-hour component due to Em^{210} and a 20-minute component which we are certain is due to 30-minute

Em^{209}. The 6·141-MeV peak and the 6·264-MeV peak decay with a 20-minute half-life, which is within experimental error of the 23-minute half-life of Em^{208} and Em^{212}, respectively.

In Fig. 1 alpha peaks due to Em^{211} are observed, but the exposures were too short for accurate measurement of this 16-hour activity. Hence, the separate runs displayed in Figs. 4 and 5 were made.

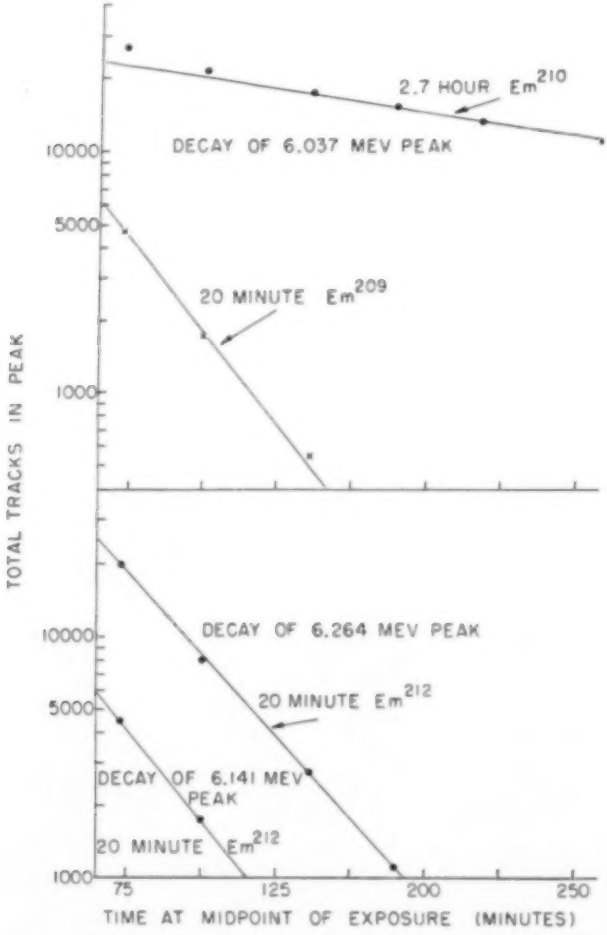

Fig. 3.—Decay curves for the alpha peaks of Fig. 2. The contribution of Em^{209} and Em^{210} to the alpha group at 6·037 MeV is shown.

In this case thorium metal strips were bombarded for 2 hours with 340-MeV protons. The target was processed 2 hours later, and part of the Em^{211} activity was mounted on a 0·010-in. monel wire. The exposure in the spectrograph started 4·25 hours after the bombardment and continued for 4 hours. The results are shown in Fig. 4. The At^{211} peak represents daughter activity grown into the sample from the electron-capture branch decay. The overlapping of the 5·862 $\pm$ 0·002-MeV At^{211} peak

with the most energetic Em^{211} peak is not serious, and the At^{211} peak served as an excellent internal standard. The At^{211} alpha-particle energy was taken from the work of HOFF and ASARO.[4]

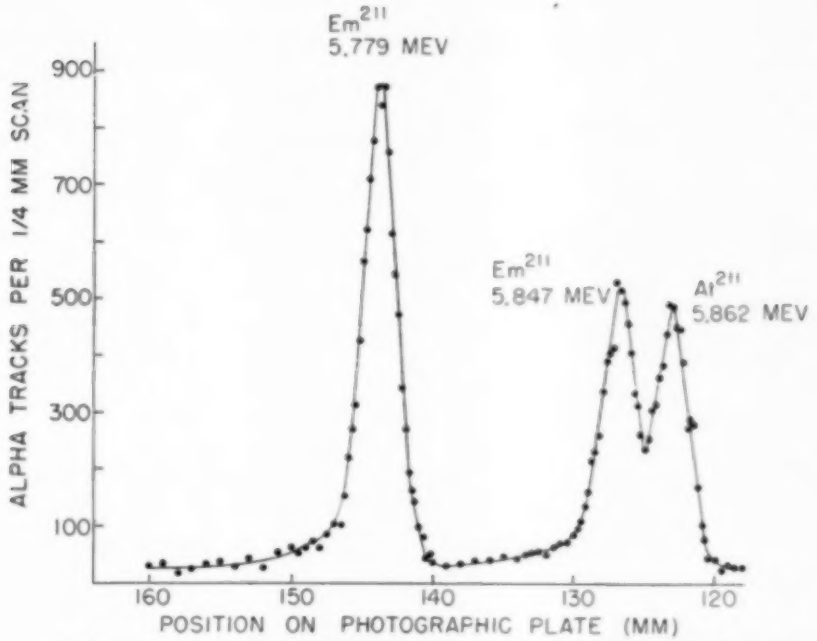

FIG. 4.—Alpha spectrum of Em^{211}. The At^{211} daughter activity grown in during the four-hour exposure serves as the standard. The dispersion was 4·03 keV/mm.

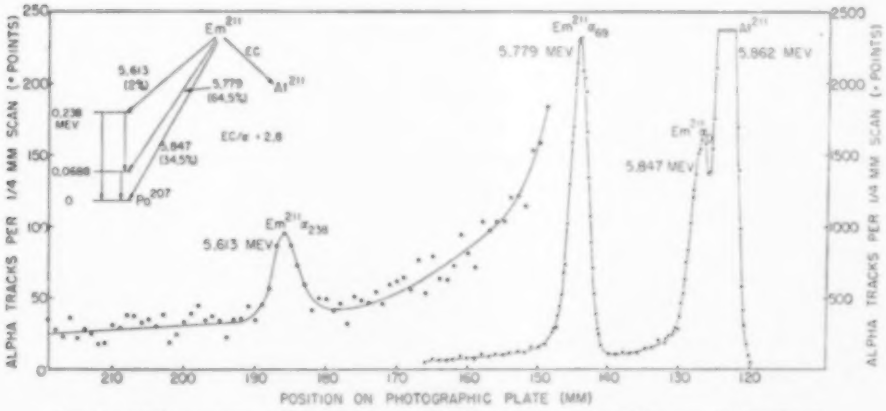

FIG. 5.—Alpha spectrum and decay scheme of Em^{211}. Exposure started 8·4 hours after bombardment, and lasted 20 hours. The 2 per cent group at 5·613 MeV is shown on an expanded scale.

Some unpublished alpha-gamma coincidence work carried out in this laboratory by A. W. STONER and F. ASARO had shown that gamma rays of 70, 169, and 234 keV

[4] R. HOFF and F. ASARO, private communication as reported by HOLLANDER, PERLMAN, and SEABORG, *Revs. Mod. Phys.* **25**, 465 (1953).

are in coincidence with the alpha particles of Em^{211}. These results could be explained by postulating another alpha group about 169 keV lower in energy than the 5·779-MeV group, as shown in the decay scheme of Fig. 5. This group was looked for and found. The same Em^{211} sample which had been run in the spectrograph to obtain the data for Fig. 4 was re-exposed for 20 hours, starting 8·4 hours after the end of the bombardment. The results are shown in Fig. 5. The daughter At^{211} peak is much larger relative to the Em^{211} peaks, but the 5·847- and 5·779-MeV peaks are still clearly resolved. The expected low-intensity group is observed at 5·613 MeV.

From the data of Figs. 4 and 5, using At^{211} as a standard, the following values were obtained for the Em^{211} alpha groups: α_0, 5·847 ± 0·002 MeV (33·5 per cent); α_{69}, 5·779 ± 0·003 (64·5 per cent); and α_{238}, 5·613 ± 0·007 MeV (2 per cent).

Redetermination of the Em^{211} spectrum, using a sample prepared from an entirely different thorium bombardment target, confirmed the results. A precise value of 68·8 keV was determined for the gamma transition connecting the Po^{207} levels reached by the two principal alpha groups of Em^{211} by measuring the conversion electrons from this transition in a permanent magnet spectrograph.[5]

3. THE ALPHA-PARTICLE GROUPS OF Fr^{212}

The 19-minute isotope Fr^{212} was reported originally by HYDE, GHIORSO, and SEABORG.[6] It was prepared by bombarding thorium with 340-MeV protons and extracting a chemically pure francium fraction. Fr^{212} decays 44 per cent by alpha-particle emission, and ion chamber measurements indicated an alpha-particle energy of 6·36 MeV.

Improvement in chemical techniques[7] for isolating carrier-free samples of this short-lived francium isotope made it possible to attempt the measurement of the alpha-particle energy in the magnetic spectrograph. After several futile attempts, the successful run shown in Fig. 6 was made.

Three strips of thorium foil 1·75 × 0·5 × 0·005 inches were bombarded for forty minutes with 340-Me . protons in the 184-in. cyclotron. Immediately after the bombardment the foils were dissolved in hot concentrated HCl containing NH_4SiF_6 catalyst. The francium was coprecipitated on silicotungstic acid from saturated hydrochloric acid. In the final step the francium was separated from the carrier on a cation-exchange column. Complete details of the method are given elsewhere.[7] The chemical separations were completed fifty-seven minutes after the end of the bombardment. At this point the sample intensity was 2×10^5 alpha disintegrations per minute.

The final solution was evaporated to dryness, taken up in 25 microlitres of water, and evaporated on a tungsten filament. This filament was placed in a vacuum system and heated by passing a current through it. The francium was volatilized and collected through a collimating slit on a special collector plate to form a line source. This sample was placed in the spectrograph one hundred minutes, or 5·2 Fr^{212} half-lives after the end of the bombardment. It was exposed for three hours in the spectrograph.

In Fig. 6 the largest peak is due to Em^{212}, which grew into the sample as the Fr^{212} decayed. It was used as an internal standard, assigning it the value 6·264 ± 0·005 MeV

[5] A. W. STONER, W. G. SMITH, and J. M. HOLLANDER, unpublished results.
[6] E. K. HYDE, A. GHIORSO, and G. T. SEABORG, *Phys. Rev.* **77**, 765 (1950).
[7] E. K. HYDE, *J. Amer. Chem. Soc.* **74**, 4181 (1952).

obtained from Fig. 2. The Fr^{212} alpha spectrum is seen to be complex. Resolution of the data according to the curves in the figure give the following energies and intensities: α_0, 6·411 ± 0·009 MeV (37 per cent); α_{25}, 6·387 ± 0·009 MeV (39 per cent); α_{70}, 6·342 ± 0·007 (24 per cent). The rather large limits of error are the result of the

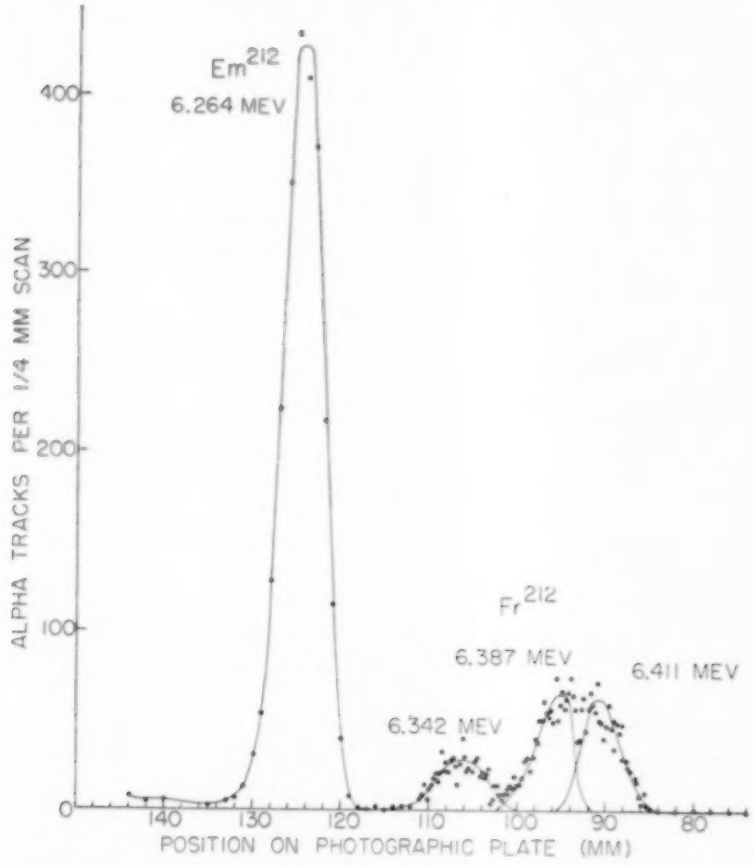

FIG. 6.—Alpha spectrum of Fr^{212}, using daughter Em^{211} as an internal standard.

cumulative errors in standardization. The Em^{212} energy is four steps removed from the primary standard.

ACKNOWLEDGEMENTS

We wish to thank JAMES VALE, LLOYD HOUSER, and members of the 184-in. cyclotron crew for carrying out the cyclotron bombardments. We are indebted to A. W. STONER, W. G. SMITH, and J. M. HOLLANDER for permission to quote from their unpublished results. The very considerable labour of counting the alpha tracks was carried out with the assistance of HELEN VAUGHN.

VOL. 1 1955

J. Inorganic and Nuclear Chemistry, 1955, Vol. 1, pp. 274–295. Pergamon Press Ltd., London

THE INFLUENCE OF THE 126-NEUTRON SHELL ON THE ALPHA-DECAY PROPERTIES OF THE ISOTOPES OF EMANATION, FRANCIUM, AND RADIUM*

F. F. MOMYER, Jr., and E. K. HYDE

Radiation Laboratory and Department of Chemistry, University of California, Berkeley, California

(*Received* 19 *April* 1955)

Abstract—A consideration of alpha systematics indicated that it might be possible to prepare a number of new isotopes of emanation, francium, and radium with half-lives sufficiently long to permit radio-chemical isolation and identification. These isotopes were predicted to lie below the neutron number 126, or much lighter in mass number than the naturally occurring isotopes of these elements. The new isotopes were looked for and found in various cyclotron bombardments, including the bombardment of thorium with high-energy protons, the bombardment of lead with high-energy carbon ions, and bombardment of gold with high-energy nitrogen ions. Data are presented for 16-hour Em^{211}, 2·7-hour Em^{210}, 30-minute Em^{209}, 23-minute Em^{208}, 11-minute Em^{207}, 6·2-minute Em^{206}, 2·7-minute Ra^{213}, and 19-minute Fr^{212}. The complete data are summarized in Table 2.

The methods of chemical purification, the measurements of the energy of the radiations, and the experiments proving genetic relationships are discussed in detail. Of particular interest is the development of a glow-discharge method for the deposition of rare-gas radioactivity on metallic counting foils.

1. INTRODUCTION

SINCE the very early days of the study of natural radioactivity the question of the inter-relationship of alpha-particle energies, half-lives, and neutron and proton numbers, has engaged the attention of those interested in the systemization of the empirical facts, so that clues to their basic meaning would be more readily apparent and unknown data more readily predicted. Such correlations have in recent years come to be known as "alpha systematics." One of the chief generalizations, that having to do with the relationship of the alpha disintegration energy and the mass number of the isotopes of a particular element, stated that the disintegration energy decreased in a nearly linear fashion with increasing mass number.

This generalization holds quite well for most of the heavy elements, as an inspection of Fig. 1 will show. However, in those elements having alpha emitting isotopes covering the region above and below the neutron number 126 this linear relationship breaks down, and a very sharp discontinuity of about 4 MeV occurs in the alpha disintegration energy. The curve of the polonium isotopes in Fig. 1 indicates this discontinuity most dramatically. The break is quite understandable in terms of the MAYER,[1] and HAXEL, JENSEN, and SUESS[2] single-particle model of the nucleus, and is related to the closed shell at 126 neutrons as is discussed more fully by PERLMAN, GHIORSO, and SEABORG.[3] This reference also cites considerable past and recent literature bearing on the general subject of alpha systematics. Recent developments in alpha radioactivity up to mid-1954 are reviewed by ASARO and PERLMAN.[4]

The chief purpose in undertaking the work to be discussed here was to show the

* This work was carried out under the auspices of the U.S. Atomic Energy Commission.

[1] M. G. MAYER, *Phys. Rev.* **75**, 1969 (1949).
[2] O. HAXEL, J. H. D. JENSEN, and H. E. SUESS, *Z. Phys.* **128**, 295 (1950).
[3] I. PERLMAN, A. GHIORSO, and G. T. SEABORG, *Phys. Rev.* **77**, 26 (1950).
[4] F. ASARO and I. PERLMAN, Annual Reviews of Nuclear Science **4**, 157 (1954).

extent of the influence of the closed shell of 126 neutrons on the alpha-decay characteristics of the lighter isotopes of emanation, francium, and radium. It can be considered an extension of some research for the same general purpose on the isotopes Fr^{212} and Em^{212} reported earlier by HYDE, GHIORSO, and SEABORG.[5] The sharp lowering of the alpha disintegration energy in those isotopes containing 126 or fewer neutrons is reflected in a marked lengthening of the alpha half-lives, so that it was thought

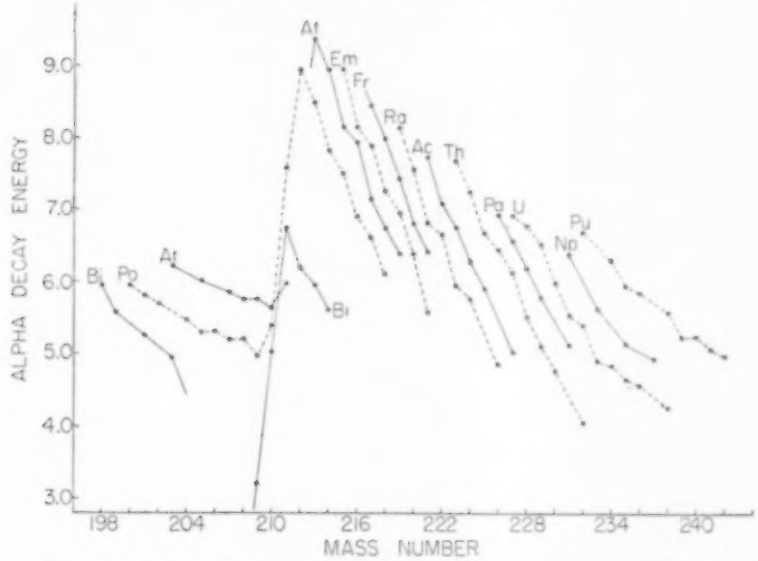

FIG. 1.—Alpha disintegration energy versus mass number. Energies include recoil energy of daughter nucleus.

possible to prepare such isotopes by cyclotron bombardment and to have time for radiochemical purification and measurement of their properties. It was hoped that an island of isotopes with appreciable half-life would be found much lower in mass number than the familiar isotopes in the mass region of the naturally occurring radioactive isotopes. It should be noted, however, that the low point in the alpha disintegration energy curve occurs at an increasingly higher value as one goes from bismuth up through the elements to emanation, francium, and radium, and at some point the alpha half-lives even with the large stabilization due to the shell effect must become too short for experiments involving chemical separation. Furthermore, with increasing atomic number these isotopes are dropping increasingly to the neutron-deficient side of stability, and in some cases the shortness of the orbital electron capture half-life should make it difficult to observe the alpha decay.

The search for isotopes in this region is not one that can be carried out by examination of naturally occurring radioactivities, nor can these isotopes be prepared by cyclotron reactions with low-energy beams. In most of the cases covered in this report it was possible to prepare them by high-energy cyclotron reactions, and the most successful approach was the bombardment of 5-mil thorium metal foils in the 184-inch cyclotron with 340-MeV protons. Spallation reactions produced the isotopes of interest directly.

[5] E. K. HYDE, A. GHIORSO, and G. T. SEABORG, *Phys. Rev.* 77, 765 (1950).

VOL. 1 1955

or produced other neutron deficient isotopes which decayed immediately into them. At the same time, of course, a large number of other spallation products as well as high-energy fission products were also produced, and chemical purification was obligatory before any significant measurements could be made.

Another approach, which was used somewhat in the present study, was the bombardment of lead targets with beams of carbon ions accelerated to high energy in the 60-inch cyclotron. Reactions of the type $Pb^{206}(C, 5n)Ra^{213}$ resulted in the production of some of the isotopes under study. This method has the advantage that none of the previously known high mass number isotopes can be produced to interfere with the search for new activities. Recently this approach has been exploited in an interesting fashion to extend the results of this paper by using accelerated beams of nitrogen ions to bombard gold foils. Very light emanation isotopes are produced in high yields by such reactions as $Au^{197}(N^{14}, 4n)Em^{207}$. A study of this type has recently been carried out by BURCHAM at the University of Birmingham.[6] An independent study carried out simultaneously by A. W. STONER and E. K. HYDE of our laboratory will be summarized at the end of this report and published in detail later.

It was mentioned above that the properties of Fr^{212} and Em^{212}, which constituted the initial study of this problem, have been published.[5] Mention should also be made of some preliminary work of MEINKE, GHIORSO, and SEABORG[7] on the emanation isotopes herein identified as Em^{210} and Em^{212}. In the sections which follow, our detailed studies on the isotopes Em^{211}, Em^{210}, Em^{209}, Em^{208}, and of Ra^{213} will be presented. It will then be discussed how closely the measured properties of these emanation and radium isotopes resemble the bismuth, polonium, and astatine isotopes in reflecting the 126-neutron shell effect. The chemical methods and instruments are described in a section at the end of the report. Of particular interest is the section on the deposition of gaseous emanation activity on metallic foils by a glow-discharge technique. Without this novel method it would not have been possible to measure the alpha-particle energies of the emanation activities, and much of the purpose of the investigation would have been defeated.

The initial measurements of the alpha-particle energies were made in an ionization chamber coupled to a multichannel pulse-height analyzer.[8] Later in the work it was possible to prepare intense sources and to remeasure many of these values much more accurately in a magnetic alpha-particle spectrograph.[9] These measurements were carried out with the collaboration of Dr. FRANK ASARO, and are reported in a companion paper.[10] The properties of Em^{221} were measured during the course of this research, but as they have nothing to do with the central purpose here they are to be discussed in a separate paper.[11] All of these results were presented earlier in the Ph.D. thesis of one of us (F. F. M),[12] and some details are discussed there more fully. Some of the results were published in a preliminary note.[13]

[6] W. E. BURCHAM, *Proc. Phys. Soc.* **A67**, 555 (1954).
[7] A. GHIORSO, W. W. MEINKE, and G. T. SEABORG, *Phys. Rev.* **76**, 1414 (1949).
[8] GHIORSO, JAFFEY, ROBINSON, and WEISSBOURD, *National Nuclear Energy Series, Plutonium Project Record*, Vol. 14B, "The Transuranium Elements: Research Papers." Paper No. 16·8 (1949). (McGraw-Hill Book Company, Inc., New York.)
[9] F. L. REYNOLDS, *Rev. Sci. Instrum.* **22**, 749 (1951).
[10] F. F. MOMYER, Jr., F. ASARO, and E. K. HYDE, *J. Inorg. Nucl. Chem.* **1**, 267 (1955).
[11] F. F. MOMYER, Jr., and E. K. HYDE, paper in preparation.
[12] F. F. MOMYER, Jr., Ph.D. Thesis, University of California Radiation Laboratory Unclassified Report UCRL-2060 (February, 1953).
[13] F. F. MOMYER, Jr., E. K. HYDE, A. GHIORSO, and W. E. GLENN, *Phys. Rev.* **86**, 805 (1952).

VOL. 1 1955

2. EMANATION-211

When the daughter activity left in U-tube traps by the decay of the gaseous fraction was examined, 7·3-hour At^{211} was found as identified by its chemical properties, half-life, and the presence of alpha particles of 5·85 and 7·43 MeV in the ratio of 40/60, corresponding to At^{211} and its Po^{211} daughter.

In this connection there was some confusion as to the proper energy of the At^{211} alpha particle. At the beginning of our experiments we were accepting the value of

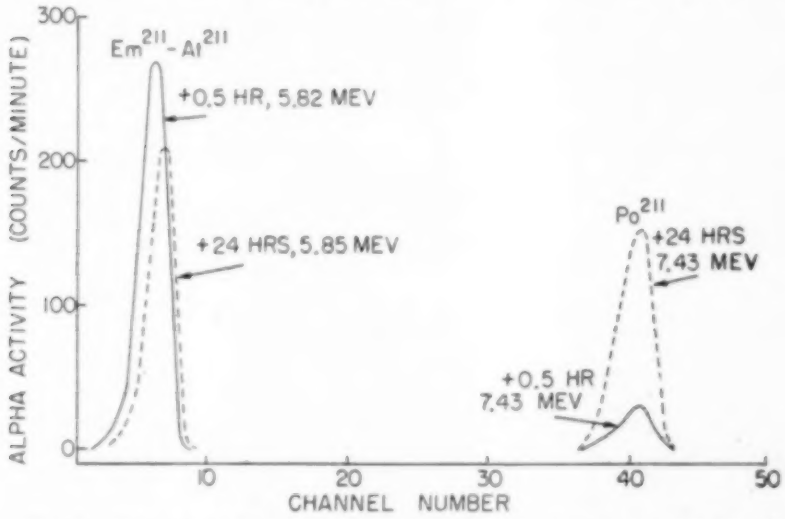

FIG. 2.—Alpha pulse-height analysis of activity in initially pure sample of Em^{211}. Solid curve-data taken 0·5 hour after preparation of sample. Broken curve-data taken twenty-four hours after preparation of sample.

5·89 ± 0·02 MeV given by BARTON *et al.*,[14] but our own determinations consistently gave the lower value of 5·85 ± 0·02 MeV. Later a precise value of 5·862 ± 0·002 MeV was determined on the magnetic alpha-particle spectrograph by HOFF and ASARO.[15]

When a freshly purified emanation sample was placed in one of the special brass ionization chambers described later in the Experimental Part, the growth of the At^{211} alpha activity could be observed. When the glow-discharge method was used twenty-four hours after bombardment to deposit a sample of the emanation fraction on a platinum foil, considerable information was derived from repeated analysis of the alpha spectrum in the 48-channel pulse-height analyzer over a period of a few days.

Alpha spectrum analysis immediately after preparation of the sample showed one peak of energy 5·82 ± 0·02 MeV. As time passed, another peak corresponding to the 7·43-MeV alpha particles of Po^{211} was observed to grow in, indicating that At^{211} was growing in from the electron capture branching of Em^{211}. Both of these peaks eventually decayed with a 16 ± 1 hour half-life, indicating that this was the half-life of Em^{211}. Fig. 2 shows two such spectra taken twenty-four hours apart. In the solid curve taken 0·5 hour after the preparation of the sample, the main alpha group at

[14] G. W. BARTON, JR., A. GHIORSO, and I. PERLMAN, *Phys. Rev.* **82**, 13 (1951).
[15] R. W. HOFF and F. ASARO, private communication (August, 1952) as reported by HOLLANDER, PERLMAN, and SEABORG, *Revs. Mod. Phys.* **25**, 465 (1953).

5·82 is assigned to Em^{211}. A little Po^{211} alpha activity is present because of the At^{211} grown into the sample by the electron-capture decay of Em^{211}. The At^{211} peak could not be resolved from the Em^{211} alpha peak. In the dotted curve taken a day later the growth of the Po^{211} peak is evident, and the lower-energy peak which is now largely At^{211} has shifted to a slightly higher energy.

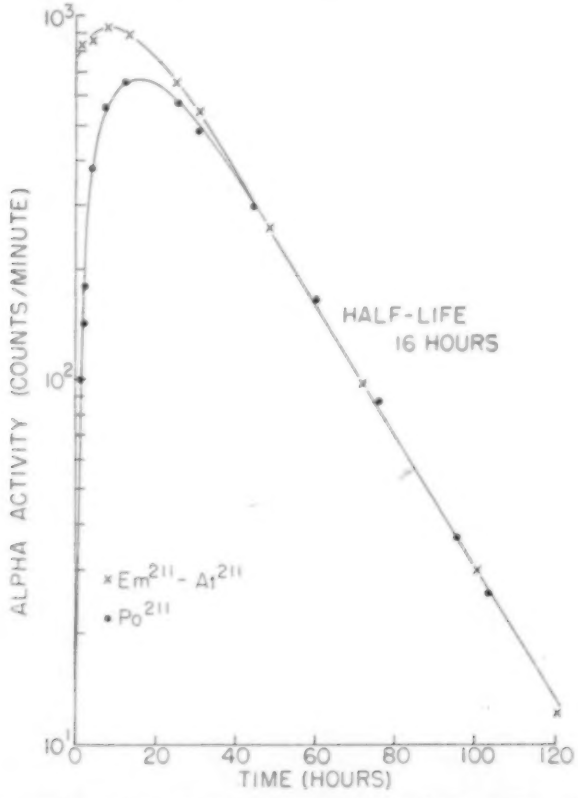

FIG. 3.—Growth and decay of combined alpha activity in Em^{211}—At^{211} peak (unresolved), and growth and decay of Po^{211} alpha peak in initially pure sample of Em^{211}. Points are experimental. Curves are theoretical for the decay chain:

$$Em^{211} \xrightarrow[EC/\alpha = 2{\cdot}8]{16{\cdot}0\ hr} At^{211} \xrightarrow[EC/\alpha = 1{\cdot}5]{7{\cdot}3\ hr} Po^{211}.$$

From the ratio of the Po^{211} to the Em^{211}-At^{211} peak after transient equilibrium was reached, from the half-lives of Em^{211} and At^{211}, and from the known branching ratio of At^{211}, the branching ratio of Em^{211} was calculated. The ratio of the Po^{211} to the Em^{211}-At^{211} peak at equilibrium was $1{\cdot}0 \pm 0{\cdot}1$. The branching ratio of At^{211} had previously been determined as $1{\cdot}5(EC/\alpha)$ to within 5 per cent.[16] The half-life of At^{211} was taken as 7·3 hours and that of Em^{211} as 16 hours. A value of $2{\cdot}8 \pm 0{\cdot}3$ for the orbital electron capture to alpha-particle emission ratio of Em^{211} results. The orbital electron capture half-life of Em^{211} is then 22 ± 2 hours, and the alpha half-life is 62 ± 6 hours. Using the above half-lives and branching ratios, theoretical curves for

[16] H. M. NEUMANN and I. PERLMAN, *Phys. Rev.* **81**, 958 (1951).

the alpha activity in the Em^{211}-At^{211} and Po^{211} peaks as functions of time elapsed after preparation of the sample were constructed and compared with the empirical curves obtained from the data taken on the 48-channel pulse-height analyzer. Fig. 3 shows the fit of the empirical points in one run to the theoretical curves.

The shape and half-width of the pure Em^{211} peak in alpha pulse analyses at high-gain settings (channel width 15 to 20 keV) suggested that the alpha spectrum of Em^{211} might contain two groups in comparable abundance with an energy separation of the order of 50 keV. The resolution of the ionization chamber pulse-height analyzer was not great enough to determine definitely whether this was the case. The alpha spectrum of Em^{211} was later determined much more precisely with the magnetic alpha-particle spectrograph.[10] With the much higher resolution of this instrument, the broad peak at 5·82 MeV reported above could be resolved into two peaks with energies of $5{\cdot}847 \pm 0{\cdot}002$ (33·5 per cent abundance) and $5{\cdot}779 \pm 0{\cdot}003$ (64·5 per cent abundance). An additional low-intensity group was found at $5{\cdot}613 \pm 0{\cdot}007$ (2 per cent abundance).

The gamma spectrum of Em^{211} was studied on the sodium iodide scintillation spectrometer. The most prominent feature was the X-radiation of about 80-keV energy. This was the K-radiation of astatine from the electron capture process. Later, as the At^{211} grew in, the K-radiation of polonium from the electron-capture decay of At^{211} contributed to the 80-keV peak. From the growth and decay of this X-radiation the half-life of sixteen hours for Em^{211} could be confirmed.

A number of additional gamma rays were found by using a sodium iodide crystal spectrometer coupled to a 50-channel pulse-height analyzer. In some curves taken for us by B. RABY and by A. W. STONER, gamma rays of 30, 240, 430, 890, 970, 1130, and 1340 keV were found. A typical curve is shown in Fig. 4. It was established that these gamma rays decayed with a 16-hour half-life. These gamma rays arise in the electron-capture branch of Em^{211} decay. Some alpha-gamma coincidence studies carried out by STONER and reported in another paper[10] showed that gamma-rays of 70, 169, and 234 keV were in coincidence with the alpha particles of Em^{211}. Further work has been done on this complex gamma spectrum of Em^{211} and will be prepared for publication later.

The properties of Em^{211} and of its daughters are presented for reference in Fig. 5. These properties are well established and the mass assignment of Em^{211} may be regarded as certain.

3. EMANATION-210

An emanation activity with half-life of $2{\cdot}7 \pm 0{\cdot}2$ hours and an alpha-particle energy of $6{\cdot}02 \pm 0{\cdot}02$ MeV was observed in alpha-spectrum analyses of emanation fractions from 340-MeV proton bombardments of thorium when the emanation fraction was isolated within a few hours of the end of the bombardment. Decay curves showing straight-line decay over more than six half-lives were obtained. This activity is probably to be identified with the 2·1-hour alpha activity reported previously by MEINKE and GHIORSO in the gross alpha decay of such samples.[7]

It was not possible to prepare pure samples of this activity, but in emanation fractions collected approximately four hours after bombardment about 90 per cent of the alpha activity belongs to this isotope, the remainder being Em^{211} along with a few tenths of 1 per cent of Em^{222}. After decay of the emanation, such samples were found to contain Po^{206} and smaller amounts of Po^{210} (no Po^{208}) as identified by their alpha energies of 5·22 and 5·30 MeV, and half-lives of 9 days and roughly 140 days.

VOL. 1 1955

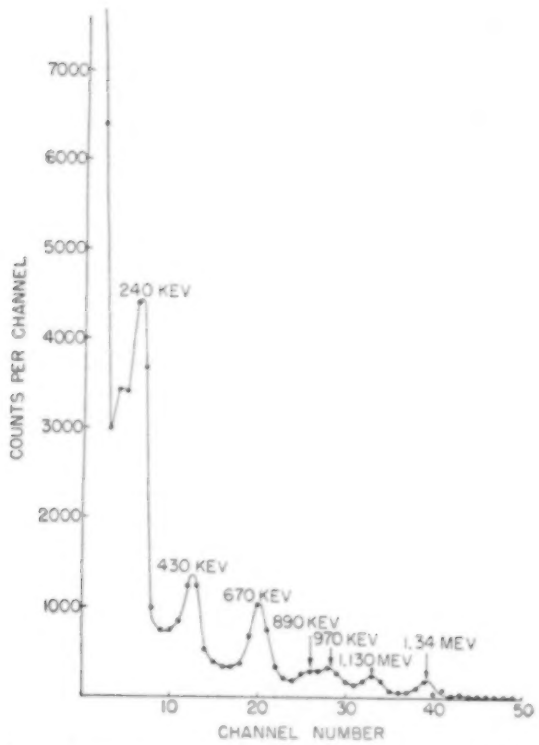

FIG. 4.—Gamma spectrum of Em^{211} taken by the sodium iodide scintillator pulse-height analysis technique (A. W. STONER, unpublished results).

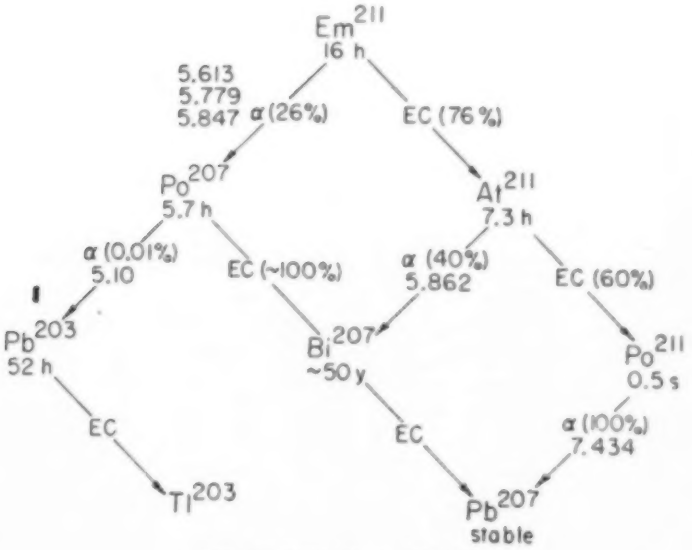

FIG. 5.—Decay scheme of Em^{211}.

respectively. The amount of Po^{206} present indicated that the original samples must have contained a large amount of Em^{210} alpha activity. The 2·7-hour, 6·02-MeV alpha activity was the only such unassigned activity present, and was thus assigned to Em^{210}.

On the basis of this assignment, attempts were made to determine the percentage of alpha branching in the decay of Po^{206}. From the half-lives of Em^{210} and of Po^{206}, and from the ratio of the initial alpha activity due to Em^{210} to the amount of Po^{206} alpha activity present after decay of the emanation, this branching could be calculated in a straightforward fashion. This is one of the few cases in the heavy region in which an orbital electron capture branching ratio can be determined directly without recourse to chemical yield corrections or X-ray counting efficiencies. The fact that the Po^{206} alpha activity amounts only to about 0·1 per cent of the initial Em^{210} activity causes one complication which was overcome by doing alpha-spectrum analysis on two separate samples. A small aliquot of Em^{210} was counted accurately for total alpha activity, and analyzed in the ionization chamber to determine the percentage of the activity to be assigned to Em^{210}. A much larger aliquot was accurately counted for total alpha activity, and allowed to sit until the Em^{210} had decayed. Then the amount of Po^{206} alpha activity was measured on the alpha pulse-height analyzer.

VOL. 1 1955

The average of several determinations gave 5 ± 1 per cent as the percentage decay of Po^{206} by alpha emission. A previous estimate[17] based on estimates of X-ray counting efficiency was 5 to 10 per cent.

In our measurement we gave consideration to the error which would arise if an appreciable fraction of the Po^{206} were lost from the plate by alpha recoil. Experiments designed to check the extent of this loss indicated that it was low. Hence error due to recoil loss has been neglected in the calculations and is probably substantially less than the limits of error placed on the alpha branching of Po^{206}.

The electron-capture branching of Em^{210} can be calculated from the amount of Po^{210} found after decay of an accurately measured sample. In only three of the runs was enough Po^{210} present to make reasonably accurate counting possible. In these the counting rate was a few counts per minute. The expected accuracy is low, especially since there was considerable difficulty in resolving accurately the Po^{210} from the Po^{206} peak, which was initially twenty times larger. The average value of the EC/α decay for Em^{210} was $0{\cdot}04 \pm 0{\cdot}01$. It appears that Em^{210} decays by alpha emission to an extent greater than 95 per cent. As recoils from electron capture have very low energy, there will be no significant loss of the electron-capture decay products of Em^{210} by recoil.

The question might arise as to whether the Po^{206} and Po^{210} observed in the samples could not have resulted from At^{206} and At^{210} present in the emanation fraction as contamination. Judging from the amount of At^{211} present initially in the samples, an upper limit of 0·1 per cent by activity can be set for At^{210} and At^{206} contamination, assuming equal cross-sections for these three isotopes in the bombardment. This means that no appreciable amount of the Po^{206} observed could have resulted from At^{206} contamination, and at most 10 per cent of the Po^{210} could have resulted from At^{210}. The actual contamination is probably considerably less than 0·1 per cent, as the observed amount of At^{211} represents just about the amount expected to have grown in from Em^{211} at the time of pulse analysis. It thus seems certain that the electron-capture

[17] D. H. Templeton, J. J. Howland, Jr., and I. Perlman, *Phys. Rev.* **72**, 758 (1947).

branching of Em^{210} has been observed, and the genetic relationship of this activity to Po^{210} established.

Later, the alpha-particle energy of Em^{210} was determined more accurately on the magnetic alpha-ray spectrograph as 6·037 ± 0·003 MeV.[10]

In summary, Em^{210} has been identified by its genetic relationship to Po^{206} and Po^{210}. The mass assignment is thus considered as good as the assignments of these two

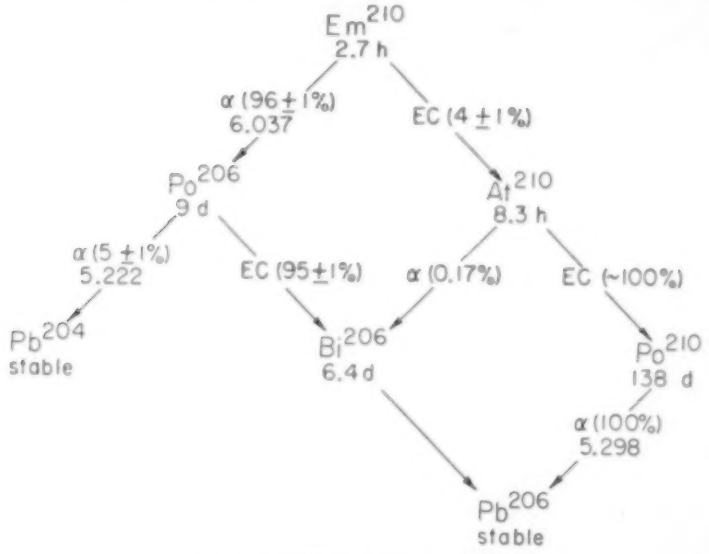

FIG. 6.—Decay scheme of Em^{210}.

activities. The half-life of Em^{210} is 2·7 ± 0·2 hours, and the alpha-particle energy is 6·037 ± 0·003 MeV. The ratio of orbital electron decay to alpha decay is about 0·04, and the partial alpha and electron-capture half-lives are thus 2·7 ± 0·2 hours and greater than 50 hours, respectively. The alpha branching of Po^{206} was determined to be 5 ± 1 per cent. Fig. 6 summarizes the decay scheme for Em^{210}.

4. EMANATION-209

Early in this work it was found that if a radium fraction were isolated from a thorium target within a few minutes after bombardment with 340-MeV protons, and if emanation daughter activity growing into the radium fraction were isolated, then radiochemically pure At^{209} could be observed as an end-product in the emanation fraction. At^{209} was identified by its alpha-particle energy of 5·65 MeV and its half-life of 5·7 hours obtained both from alpha and beta-gamma activity decay. This was considered evidence that the radium fraction isolated directly from the thorium target contained an alpha-emitting Ra^{213} with a half-life of at least several minutes. With the advent of the glow-discharge technique, one of the obvious experiments was to separate emanation daughter activity from radium fractions and subject this to the glow discharge in an attempt to obtain pure samples of Em^{209}. More information on Ra^{213} itself is given in a later section of this report.

When this experiment was performed, it was found that pure samples of a new alpha activity were obtained. This activity was studied on the alpha-pulse analyzer

VOL.
1
1955

and found to have a half-life of 30 ± 2 minutes and an alpha particle of energy $6{\cdot}02 \pm 0{\cdot}02$ MeV (identical with that of Em^{210} to within experimental error). As the sample decayed, an alpha activity identified as At^{209} by its 5·65-MeV alpha particle, and final 5·7-hour decay was observed to grow in. The fit of the empirical points to the theoretical curves for the amounts of Em^{209} and At^{209} activity as a function of time (5·7-hour daughter from a 30-minute parent) is shown in Fig. 7.

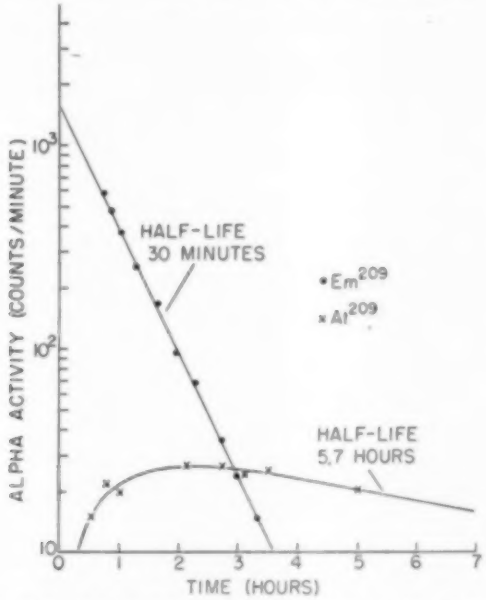

FIG. 7.—Half-life of Em^{209} from decay of 6·02-MeV peak on alpha pulse-height analyzer. Growth and decay of At^{209} alpha activity (5·65-MeV peak) in initially pure sample of Em^{209}. Points are experimental. At^{209} curve is theoretical for the decay chain,

$$Em^{209} \xrightarrow{30\ min} At^{209} \xrightarrow{5{\cdot}7\ hr} Po^{205}.$$

The samples initially contained a few hundred alpha counts per minute of Em^{209} and the amount of At^{209} growing in was of the order of 10 counts per minute. If the electron-capture to alpha-decay branching ratio of At^{209} were known accurately, the branching ratio of Em^{209} could be calculated. Unfortunately, the At^{209} branching is not well known, but three runs were nonetheless made in an attempt to determine the order of magnitude of the Em^{209} branching. The ratio of the At^{209} alpha activity at five hours after preparation of the sample to the initial Em^{209} alpha activity was found to be $0{\cdot}013 \pm 0{\cdot}002$. As any At^{209} resulting from the decay of Em^{209} during the preparation of the sample might be expected to collect along with the emanation if it were transferred into the glow chamber, there is some uncertainty as to where to choose the zero of time (the time at which one can consider At^{209} to start growing into an initially pure sample of Em^{209}). This error was minimized by transferring the emanation into the glow chamber from a dry-ice trap which should have retained any astatine present. The limits on the value quoted allow for the uncertainty in the zero time. No other appreciable errors are apparent if one makes the plausible assumption that astatine collects at most only as efficiently as emanation in the glow-discharge.

Calculations then yield an electron-capture to alpha-decay ratio of 5 ± 1 for Em^{209}, assuming 5 per cent alpha branching[14] for At^{209}. The greatest uncertainty in this calculation is in the 5 per cent figure for the alpha branching of At^{209}. The derived partial half-life for electron-capture decay of Em^{209} is 36 ± 3 minutes and the partial alpha half-life is $3 \pm 0{\cdot}5$ hours. This is about the value predicted, as one expects the partial alpha half-life of Em^{209} to be greater than or equal to that of Em^{210} ($2{\cdot}7 \pm 0{\cdot}2$ hours). This consideration would set a lower limit of about 5 on the expected branching ratio. A cross-check was also carried out later by observing the amount of Em^{209} growing into a sample of Ra^{213}. The branching ratio calculated in this case for Em^{209} was 6 ± 2. The greatest significance of the preceding is that the branching ratios

FIG. 8.—Decay scheme of Em^{209} and Ra^{213}.

obtained by assuming the $Ra^{213} \rightarrow Em^{209} \rightarrow At^{209}$ genetic relationship for the activities in question are consistent within themselves, and compatible with other data and estimates. This makes it rather certain that the mass assignments are correct.

When emanation samples were removed directly from thorium targets bombarded with 340-MeV protons, it was not easy to distinguish Em^{209} in the mixture of isotopes produced. In the curves run on the alpha pulse-height analyzer the alpha group of Em^{209} was unresolved from that of Em^{210}, so that a single peak appeared at 6·02 MeV.

If the decay of the 6·02-MeV peak were carefully measured, however, it was apparent that the alpha activity of Em^{209} was $0{\cdot}8 \pm 0{\cdot}2$ times that of Em^{210} immediately after a 20-minute bombardment.

When the alpha-particle energies of Em^{209} and Em^{210} were studied[10] with high resolution on the magnetic alpha-particle spectrometer, it still was not possible to resolve the peaks, and the energy of both groups is 6·037 MeV within a few kilovolts.

In summary, Em^{209} has a half-life of 30 ± 2 minutes and an electron-capture to alpha-decay ratio of about 5, assuming 5 per cent alpha branching in At^{209}. The alpha-particle energy is $6{\cdot}02 \pm 0{\cdot}02$ MeV from pulse-analyzer measurements, and from runs on the magnetic alpha-ray spectrograph, appears to be $6{\cdot}037 \pm 0{\cdot}010$ MeV. The genetic relationship of this activity to At^{209} has been well established, and the mass assignment is thus considered as good as that of At^{209}. The decay scheme for Em^{209} is shown in Fig. 8.

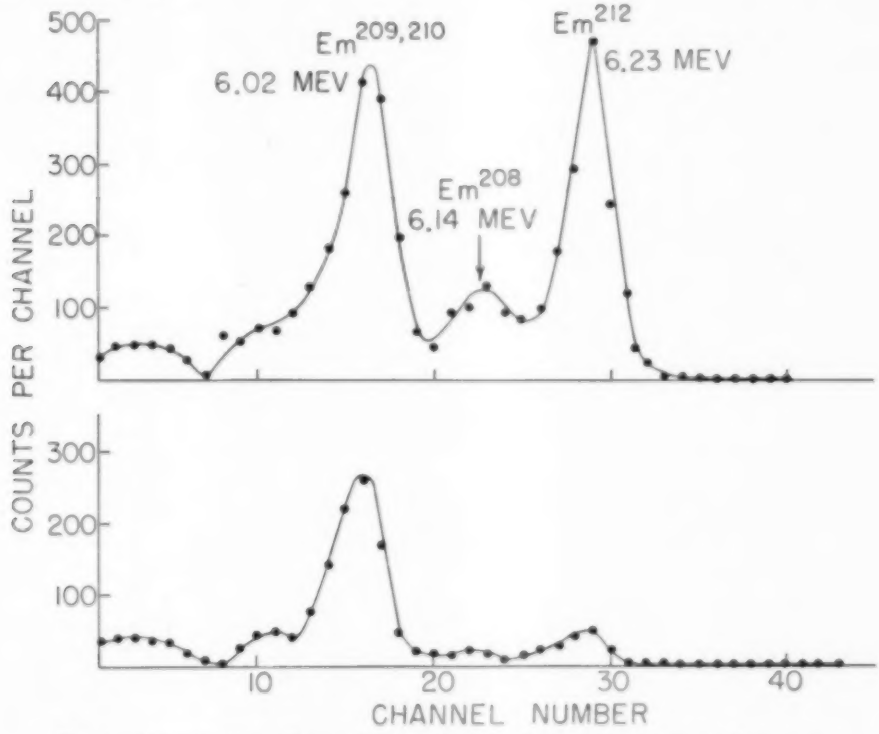

FIG. 9.—Alpha spectrum of emanation sample isolated from thorium target. Upper curve taken 75 minutes and lower curve 140 minutes after end of bombardment.

5. EMANATION-208

Fig. 9 shows an analysis of the alpha spectrum of an emanation fraction isolated directly from a thorium target and affixed to a platinum plate by the glow-discharge method about thirty minutes after bombardment. Three alpha-particle groups account for the greater part of the activity. The group at 6·02 MeV is the unresolved combined peak of Em^{209}-Em^{210}. The group at 6·23 MeV decaying with a 23-minute half-life is Em^{212}. The intermediate peak at $6{\cdot}14 \pm 0{\cdot}02$ MeV decayed with a half-life of 23 ± 2 minutes. This activity is assigned to Em^{208} for reasons to be discussed below.

The fact that the half-life of this activity is the same as that of Em^{212} to within experimental error would at first suggest that this might be an alpha group belonging to Em^{212}. Pure samples of Em^{212} isolated from Fr^{212} contain no such group, however.[5] Furthermore, the ratio of the two alpha groups is different for emanation isotope

mixtures prepared in different ways. For example, in thorium targets bombarded with 340-MeV protons the ratio of the 6·32-MeV to the 6·14-MeV alpha activity is $4{\cdot}7 \pm 0{\cdot}5$. In the case of a target of enriched lead (Pb^{204}—15 per cent, Pb^{206}—50 per cent, Pb^{207}—15 per cent, and Pb^{208}—20 per cent) bombarded with carbon ions in the 60-inch cyclotron, pulse analysis of the emanation activity ejected from the lead and caught on a tantalum collector foil showed that the ratio of the two alpha activities under discussion was about unity. It thus appears established that the 6·14-MeV alpha particle belongs to a new and distinct alpha activity.

Traps which had contained this activity for ten to twenty minutes were found to contain Po^{204} as identified by its alpha-particle energy of 5·37 MeV and measured half-life of about four hours.[18] The presence of alpha-emitting Em^{208} in the original sample was thus indicated. The 6·14-MeV activity was the only activity observed which

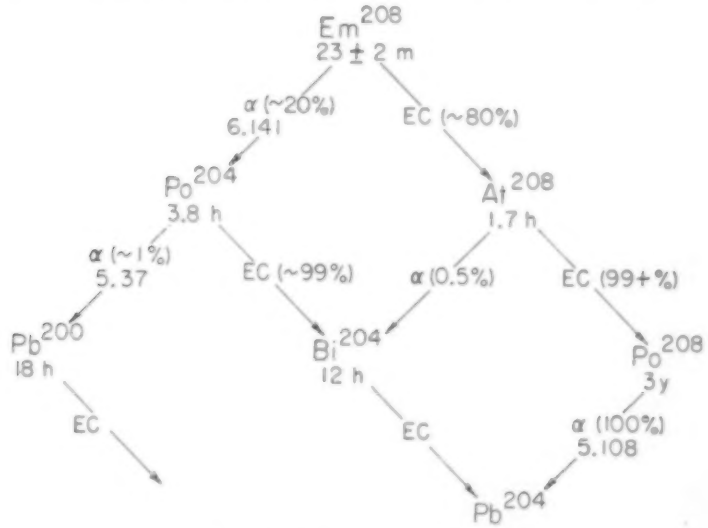

FIG. 10.—Decay scheme of Em^{208}.

was not definitely assigned, and the most logical assignment was Em^{208}. This assignment is in agreement with the alpha systematics, as will be shown in the discussion below.

It was possible to estimate the electron-capture branching of Em^{208} by measuring the amount of three-year Po^{208} present after decay of the Em^{208} and of its immediate daughter At^{208}. That part of the Po^{208} arising from the alpha decay of Em^{212} was subtracted. The calculation yielded an orbital electron-capture to alpha-decay ratio of 4 for Em^{208}, a value which is probably trustworthy to about 25 per cent. The amount of Po^{208} isolated was much larger than could be accounted for by decay of Em^{212}, making it certain that Em^{208} was present in the original sample.

It is possible to cross-check the branching ratio roughly by making the reasonable assumption that the atom yield of Em^{208} is equal to or less than that of Em^{212} in the thorium bombardments, and from the observed alpha-particle ratios to calculate an upper limit for the Em^{208} branching ratio. The upper limit so calculated is 4. Using this branching ratio, the partial alpha half-life of one to two hours is obtained.

The alpha-particle energy of Em^{208} was determined accurately on the magnetic alpha-ray spectrograph to be 6·141 ± 0·004 MeV.[10]

In summary, Em^{208} appears to be a 23 ± 2-minute activity with alpha-particle energy 6·141 MeV. There is some evidence for a genetic relationship between this activity and Po^{204} and Po^{206}. The mass assignment is still considered somewhat tentative, however, especially as the assignment of Po^{204} is not a certainty.[18] The electron-capture to alpha-decay ratio appears to be approximately 4. Fig. 10 shows the decay scheme of Em^{208}.

6. EMANATION ISOTOPES LIGHTER THAN 208

Any emanation isotope having a mass number smaller than those reported above and having a half-life of fifteen minutes or longer would surely have been observed in this study. No determined effort was made to work up thorium targets quickly enough to look for isotopes of shorter half-life. A few very preliminary bombardments of lead targets with accelerated carbon ions were carried out to look for lighter emanation isotopes. In one case a target of lead enriched in Pb^{204} (Pb^{204}—15 per cent, Pb^{206}—50 per cent, Pb^{207}—15 per cent, Pb^{208}—20 per cent) was bombarded with carbon ions, and the activity collected by recoil during the bombardment on a tantalum foil was subjected to alpha-spectrum analysis within a few minutes of the end of the bombardment. An activity of roughly 10-minute half-life was found, and this was tentatively assigned to Em^{206}.

TABLE 1.—EMANATION ISOTOPES PRODUCED BY BOMBARDMENT OF GOLD WITH NITROGEN IONS (DATA TAKEN FROM UNPUBLISHED WORK OF A. W. STONER AND E. K. HYDE)

Isotope	Half-life (min)	Alpha-particle energy (MeV)	Branching ratio
Em^{209}	21	6·12	—
Em^{207}	11	6·12	4% α, 96% EC[c]
Em^{206}	6·2	6·22	—
Em^{205}?	3	6·27–6·30	70% α, 30% EC[d]

[a] Identified by growth and decay of 5·75-MeV alpha particles of 103-minute At^{207} daughter.
[b] Identified by growth of 5·59-MeV alpha particles of 52-minute Po^{202} daughter and by observation of Po^{206} alpha activity of 5·21-MeV energy. An incidental result was a new estimate of 2 per cent for the alpha branching of Po^{206}.
[c] Determined by measuring alpha activity of At^{207} growing in and assuming 10 per cent alpha branching for At^{207}. The number of alpha disintegrations of Em^{207} was obtained from resolution of decay curve of 6·12-MeV alpha peak.
[d] Determined by comparing initial alpha counting rate of 6·2-minute Em^{206} to the final amount of 9-day Po^{206}. Calculation assumes 5 per cent alpha branching in Po^{206}.

Sometime later a beam of nitrogen ions of sufficient energy and intensity to carry out nuclear reactions was produced in the Berkeley 60-inch cyclotron.[19] A. W. STONER, working with one of us (E. K. H.), carried out a series of experiments in which gold targets were bombarded with nitrogen ions. In such bombardments nuclear reactions of the type $At^{197}(N^{14}, 3n)Em^{208}$ occur. The number of neutrons

[18] D. G. KARRAKER and D. H. TEMPLETON, *Phys. Rev.* **81**, 510 (1951).
[19] G. B. ROSSI, W. B. JONES, J. M. HOLLANDER, and J. G. HAMILTON, *Phys. Rev.* **93**, 256 (1954).

VOL. 1 1955

ejected is 3 or higher, so that only those emanation isotopes of mass number 208 or less are produced in appreciable yield. This, of course, greatly facilitates the search for these lighter isotopes. STONER and HYDE identified Em^{208}, Em^{207}, Em^{206}, and another activity tentatively assigned to Em^{204}. A complete report will be given later, but the essential results are summarized in Table 1.

These results are in good agreement with the published results of a similar study of BURCHAM.[6] Other than minor details, the main point of difference lies in the respective values for the alpha-branching of Em^{207}, for which BURCHAM gets a somewhat larger value than do STONER and HYDE.[20]

7. SEARCH FOR NEW ISOTOPES OF FRANCIUM

Determined efforts were made to isolate francium fractions quickly after bombardment and to look directly for evidence of new isotopes of francium in the alpha spectra of such samples. In addition to the previously reported Fr^{212}, it was hoped that evidence could be found for Fr^{211} and Fr^{213}, although it was expected that these half-lives would be shorter. No evidence for these was found, however. A previous tentative statement about Fr^{211} is withdrawn.[5] The amounts of Fr^{212} isolated were large, and Fr^{211} and Fr^{213} should have been seen easily if their half-lives were five minutes or longer.

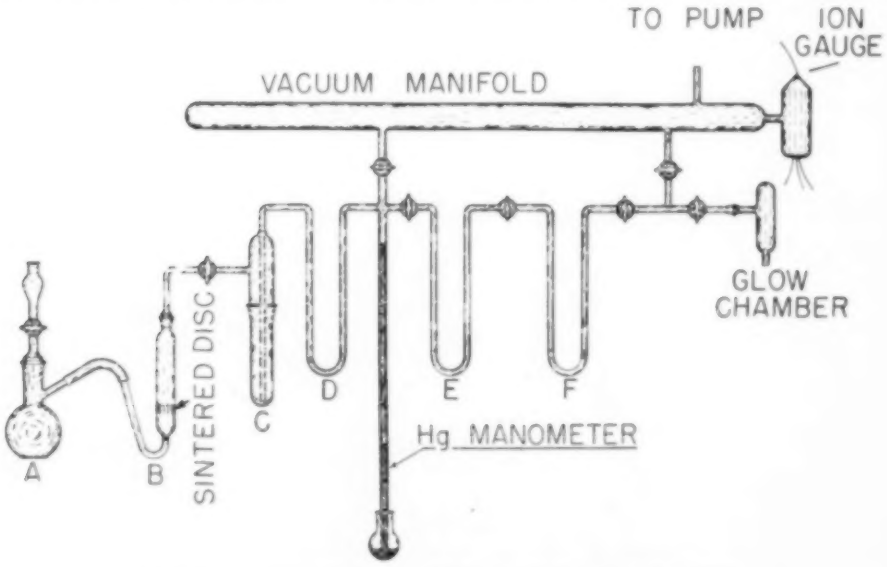

FIG. 11.—Vacuum system used in the isolation of emanation fractions.

Experiments were performed in which an emanation daughter fraction was separated from francium fractions isolated five to ten minutes after bombardment, in attempts to get information on electron-capturing francium isotopes of appreciable half-life. In these experiments the target was dissolved quickly in hot HCl, and silicotungstic acid was precipitated from the solution after saturating it with gaseous HCl. This precipitate with its coprecipitated francium was washed only once, dissolved in water and inserted in vessel *B* of Fig. 11. The gaseous daughter-activity was swept

[20] A. W. STONER and E. K. HYDE, unpublished results.

from the solution after a few minutes, and mounted on platinum foils by the glow-discharge method. There was no reliable evidence from these experiments for francium isotopes other than Fr^{212}. Any isotope with a half-life greater than five minutes should have been detected.

It will be difficult to search for francium isotopes with half-lives shorter than five minutes among the high-energy spallation products of thorium, because of the necessity for extensive decontamination from interfering activities. There is hope, however, that bombardments with heavy ion beams on different targets will reveal more information about these isotopes.

8. RADIUM-213

Radium fractions isolated from thorium targets bombarded with high-energy protons consist mainly of the higher-mass isotopes. The alpha activity of these isotopes and of their decay products makes it difficult to search directly for new alpha-particle groups from unreported low-mass isotopes of short half-life. It was only by the indirect approach of identifying daughter-activity growing into such radium fractions that evidence for Ra^{213} was found, as was mentioned in the section on Em^{209}.

VOL. 1 1955

Further information on Ra^{213} was obtained in carbon-ion bombardments. Several runs were made in which lead targets were bombarded for five to ten minutes by carbon ions and then subjected to radiochemical procedures to remove radium. In three such radium fractions alpha particles of about 6·9 MeV energy and half-life of a few minutes were observed. In one run several hundred counts per minute of this activity were observed on the alpha pulse-analyzer. The half-life of the activity was $2{\cdot}7 \pm 0{\cdot}3$ minutes, and the energy of the alpha particle was $6{\cdot}90 \pm 0{\cdot}04$ MeV. After decay of the short-lived activity, several counts per minute of Em^{209} were observed on the plate (identified by its alpha-particle energy of 6·02 MeV and measured 30-minute half-life). No other activities were observed in significant amounts. The short-lived activity was identified as radium through the chemical separation, and the presence of Em^{209} free of other emanation activities on the plate suffices to assign the activity to Ra^{213} with a certainty equal to that of the assignment of Em^{209}. The alpha-pulse analyses showed only the single peak assigned to Ra^{213}, but the possibility of appreciable electron capture is not ruled out as the alpha-particle energy of Fr^{213} is expected to be nearly the same as that of Ra^{213}, and the two peaks may not have been resolved under the conditions of the pulse-height analysis.

Other low-mass isotopes of radium with half-lives greater than one minute probably do not exist. Activities with half-lives as short as a minute or slightly less may eventually be detectable, so that there is at least a chance of finding Ra^{212} in addition to getting a better determination of the properties of Ra^{213}. Attention should be called to the fact that Ra^{213} and Fr^{212}, the only light isotopes of radium and francium identified in our studies, have 125 neutrons. This is in keeping with the fact that the longest-lived isotope of emanation, astatine, and polonium is that one with 125 neutrons.

9. SUMMARY OF RESULTS

Table 2 summarizes all data presently available on the isotopes of radium, francium, and emanation at or below the 126-neutron shell.

Fig. 12 plots the alpha-disintegration energy (defined in this case as the kinetic energy of the most energetic alpha-particle group plus the recoil energy of the recoiling

TABLE 2.—SUMMARY OF NUCLEAR DATA ON LOW MASS ISOTOPES OF RADIUM, FRANCIUM, AND EMANATION

Isotope	Half-life	Alpha-particle energy (MeV)		Alpha branching	Gamma-rays (keV)
Ra^{213}	2·7 ± 0·3 min	6·90 ± 0·04		—	—
Fr^{213}	19 min[5]	6·342 ± 0·007[10]	24%	44% α[5]	—
		6·387 ± 0·009	39%	56% EC	—
		6·411 ± 0·009	37%	—	—
Fr^{211}, Fr^{213}	<3 min	—		—	—
Em^{212}	23 min	6·264 ± 0·005[10]		100% α	—
Em^{211}	16 hr	5·847 ± 0·002[10,20]	33·5%	26% α	70-, 169-, and 234-keV γ-rays in coincidence with α's.[20]
		5·779 ± 0·003	64·5%		
		5·613 ± 0·007	2·0%		
				74% EC	30, 240, 430, 890, 970, 1130, and 1340 keV
Em^{210}	2·7 ± 0·2 hr	6·037 ± 0·003[10]		96% α 4% EC	—
Em^{209}	30 ± 2 min	6·037 ± 0·010[10]		17% α 83% EC	—
Em^{208}	23 ± 2 min	6·141 ± 0·004[10]		20% α 80% EC	—
Em^{207}	11 min[6,20]	6·09 ± 0·05[6] 6·12[20]		4% α 96% EC[20]	—
Em^{206}	6·2 min[6,20]	6·25 ± 0·05[6] 6·22[20]		70% α 30% EC[20]	—
$Em^{204(?)}$	~3 min[20]	6·27–6·30[20]		—	—

heavy nucleus) versus the neutron number for these same nuclides. In addition, Fig. 12 includes data on isotopes of bismuth, polonium, and astatine. In the case of bismuth, polonium, and radium, data on heavier isotopes are included to illustrate the sharp increase in alpha energy in crossing the closed shell. The corresponding points for heavy isotopes of astatine, emanation, and francium fall between the curves for polonium and radium and are omitted to avoid cluttering the figure. It will be noted that the shape of the curve for emanation at and below 126 neutrons is almost identical with the shapes of the astatine and polonium curves. On the assumption that this similarity holds for radium, francium, and emanation isotopes as yet undiscovered, portions of the figure are filled in with broken lines to indicate estimated alpha-decay energies.

It is noteworthy that the maximum alpha-decay energy appears to occur in the 128-neutron isotopes. This is as expected, as these decay into isotopes having 126 neutrons. The minimum alpha energy, however, occurs at 125 neutrons for polonium, astatine, and emanation, and apparently also for francium and radium, as the 125-neutron isotopes seem to have the longest alpha half-lives for these elements. Alpha energies increase rather slowly below 126 neutrons, the decay energy actually remaining less than that of the 126-neutron isotope for several lower neutron numbers. The slope of the mass surface in this region is much more gentle than in the heavier region.

The position of the minimum in the alpha-disintegration energy curve is determined by the binding energies of the last few neutrons before shell completion. The

empirical results indicate a higher binding energy for the 124th neutron than for the 126th. There is no way to predict details of this nature from shell theory in its present state of development.

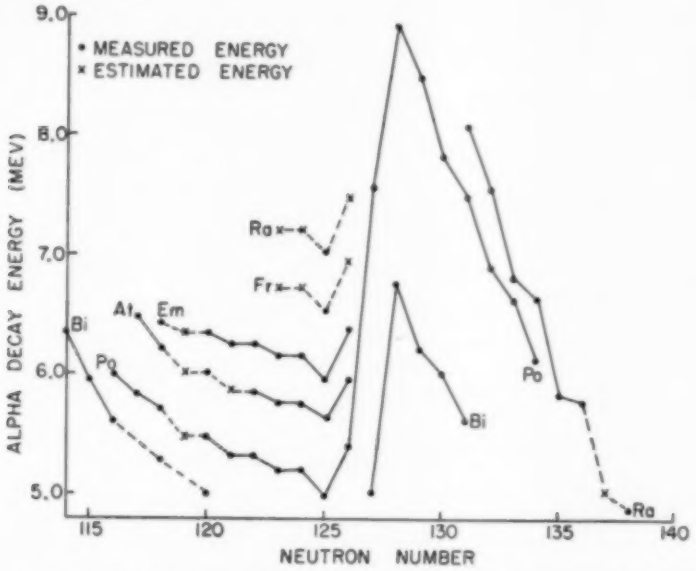

FIG. 12.—Alpha-disintegration energy versus neutron number for isotopes of elements 83–88.

10. EXPERIMENTAL

(a) *Bombardment Techniques*

The great majority of the experiments involved the bombardment of thorium metal foils with 340-MeV protons in the 184-inch cyclotron. Two or three pieces of 0·005-inch thick foils 0·5 × 1·75 inch were bombarded on edge. These foils were uncooled. After bombardment the foils were dissolved and treated as discussed below.

In the bombardment of lead or bismuth with C^{+6} ion beams in the 60-inch cyclotron some precautions against target melting had to be taken because of the nature of the C^{+6} beam.[21] The beam intensity was of the order of 0·1 microampere, but the energy distribution of the beam was continuous, apparently because complete stripping of the carbon ions occurred at various distances from the centre of the cyclotron. In addition, the C^{+6} beam was accompanied by a much larger beam of C^{+3} ions accelerated on the third harmonic up to an energy (about 10 MeV) insufficient to cause nuclear reactions, but troublesome as far as energy dissipation in the target is concerned. This heating was avoided by shielding the target with a 19-mg/cm² tantalum foil which stopped the C^{+3} ions but passed the C^{+6} beam with but slight energy degradation.

The lead-target material was cooled by welding it to a water-cooled stainless-steel backing plate. The steel surface was first cleaned with a special flux,* after which the lead was melted onto it.

(b) *Techniques Used for Gaseous Fractions*

The basic instrument used in the measurement of alpha-particle energies was an argon-filled gridded ionization chamber. Nearly weightless radioactive samples mounted on platinum counting discs were inserted in an ionization chamber. Pulses produced in this chamber due to ionization caused by alpha particles were applied to a linear amplifier. The output of this amplifier was proportional to the energy of the original alpha particle, and it was applied to a forty-eight channel differential

* Ruby's Stainless Steel Soldering Flux, Ruby Chemical Company, Columbus, Ohio.

[21] J. F. MILLER, J. G. HAMILTON, T. M. PUTNAM, H. R. HAYMOND, and G. B. ROSSI, *Phys. Rev.* **80**, 486 (1950).

VOL. 1 1955

pulse-height analyzer. The data registered by the forty-eight channels allowed the construction of the energy spectrum of the alpha particles. Resolution expressed in terms of width at half-maximum for mono-energetic peaks was about 40 keV. Repeated analysis allowed determination of the decay rate of specific alpha groups. A very early model of this alpha-analysis equipment has been published.[8] The equipment used in this research was developed by A. GHIORSO,[22] and we are indebted to him for considerable assistance in its use.

This method requires that the material to be analyzed be deposited on a metallic plate, which is a severe limitation for rare-gas radioactive samples. In the case of Em^{212} the problem was circumvented by evaporating samples of Fr^{212} on a platinum plate and allowing the Em^{212} to grow into the sample. For the other lower-mass emanation isotopes the parent half-lives were unfavourable for this approach.

In the beginning the goal of energy analysis was given up and the alpha-disintegration rates of the gaseous samples were measured in a closed counter. GHIORSO, MEINKE, and SEABORG constructed such a counter to measure the gross alpha activity in emanation samples directly isolated from thorium targets.[7] This counter was simply a brass ionization chamber with an insulated charged wire and a stopcock to allow introduction of the gaseous sample and of argon counter gas. This counter was described by HYDE, GHIORSO, and SEABORG.[6]

When electromagnetic radiations were to be studied, it was satisfactory in many of the preliminary studies to condense the gas in a small glass bubble blown on the end of a piece of capillary tubing and to seal off the tubing with a torch. The bubble could then be mounted on a piece of cardboard and analyzed in a scintillation spectrometer.

In some of the bombardments with accelerated carbon ions emanation samples were collected suitable for alpha-energy analysis by a recoil technique. A thin layer of lead or bismuth (about 1 mg/cm²) was volatilized onto a ¼-mil tantalum foil. This foil was bombarded with the lead or bismuth facing away from the beam and with another ¼-mil tantalum foil placed adjacent to the target material. Recoils from the target were collected on the second tantalum foil and could be counted in the differential alpha pulse analyzer or any of the usual alpha-counting devices. Nuclei recoiling from C^{12} collisions could have energies as high as several MeV, so that emanation atoms collected in the foil would be expected to be quite firmly affixed. This appeared to be the case. The first alpha-particle spectrum analyses of emanation isotopes with mass number less than 212 were obtained in this fashion. The total initial alpha activity in these samples was of the order of a few hundred counts per minute, and the resolution on the pulse analyzer was poor, due largely to beta-gamma activity induced in the tantalum foil itself. This resulted in straggling on the high-energy side of the peaks, due to beta-alpha coincidences. Also, this method did not allow manipulation of the emanation so as to isolate and identify daughter activities and at the same time study the emanation activities present in order to make mass assignments, or in fact even to identify positively the element to which a given activity belonged. Nonetheless, valuable preliminary information on half-lives and approximate alpha-energies was obtained in this way to guide future investigations.

The Glow-Discharge Method

After considerable preliminary work had been done using the above methods, a far superior technique was found. This new method made it possible to deposit emanation activities on a metallic foil or wire and to study the radioactivity so deposited in any manner applicable to normal non-gaseous samples. The technique is so simple and potentially so widely applicable to the study of other gaseous activities that it will be discussed here in some detail. The method was suggested by the success of KOCH[23] and of BERGSTRÖM[24] in collecting samples of noble gases on metallic foils in a mass spectrograph. It was also an outgrowth of some anomalous unpublished results obtained by W. E. GLENN, Jr., and E. K. HYDE during the course of some runs on mixed samples of Fr^{212}-Em^{212} in the time-of-flight mass spectrometer developed by GLENN.[25]

Briefly, the method consists of transferring the emanation radioactivity together with 100- to 1000-microns pressure of some carrier gas such as nitrogen or ordinary air into a glass tube equipped with two electrodes. A d.c. potential of a few hundred volts is placed across the electrodes to cause

[22] A. GHIORSO and A. E. LARSH, to be published.
[23] J. KOCH, *Nature* **161**, 566 (1948).
[24] I. BERGSTRÖM, *Arkiv för Fysik* **5** (14), 191 (1952).
[25] W. E. GLENN, Ph.D. Thesis, University of California Radiation Laboratory Unclassified Report UCRL-1628 (February, 1952).

formation of a glow-discharge. In this discharge the rare-gas atoms are ionized and the resulting ions are collected on the negative electrode.

Several tubes were built and tested. In some designs a counting disc was attached to the negative electrode to collect the activity on a flat surface most suitable for ionization chamber methods. In the design shown in Fig. 13 the cathode was a thin wire centred in a spiral anode. This type of collection was particularly suited for preparation of line sources for the magnetic alpha-particle spectrograph.[9, 10]

Several points are worth mentioning. First, in order to determine half-lives and alpha energies satisfactorily, it was, of course, necessary that the emanation remain affixed to the plate after being deposited. It was found that no appreciable fraction was lost at atmospheric pressure or in a vacuum if the plate was not raised above room temperature. Trial runs were made on Rn^{222}, and the correct half-life of 3·8 days was determined on samples so deposited. Secondly, the fraction of the activity deposited is appreciable. In our runs the collection efficiency as checked on measured amounts of

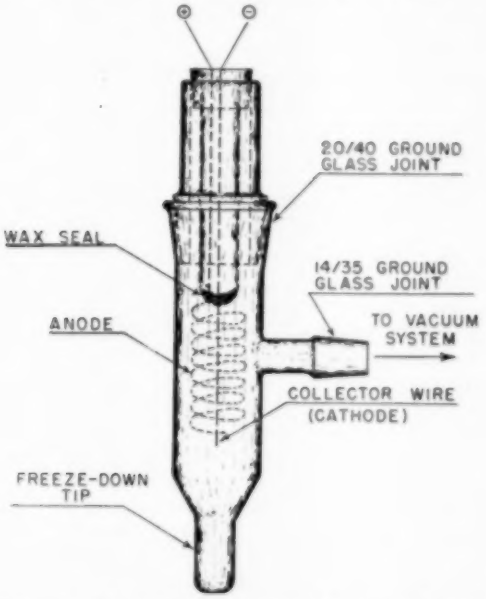

FIG. 13.—Glow-discharge tube used in the deposition of emanation activity on metal wires.

Rn^{222} ranged from 1 to 10 per cent. It is believed that suitable redesign should permit nearly quantitative collection. Heating of the electrodes by the ion current is a major factor, reducing the amount of emanation activity retained on the electrode. Hence the potential was kept as low as was consistent with maintenance of the discharge, and a large resistance was placed in the external circuit. Lastly, the penetration of the electrode surface was so slight that no widening of the alpha peaks due to self-absorption was observed. In fact, the half-widths of the alpha peaks determined in the magnetic alpha-particle spectrograph[10] were close to the lowest ever achieved in this high-resolution instrument.

In the glow-discharge tube shown in Fig. 13 the electrodes were inserted through small holes in the end of the inner glass tube and sealed with wax. The collector wire of 10-mil chromel or platinum wire could be clipped off after each run, the seal loosened by heating, and more of the wire pushed through to serve as the electrode in the next run.

Fig. 11 is a schematic drawing of the elements of the vacuum system used in connection with the glow-discharge method. A Cenco-Hyvac forepump and a mercury diffusion pump were used to obtain a base pressure in the system of between 10^{-6} and 10^{-5} mm of mercury. This allowed rapid and quantitative transfer of the gaseous samples from one trap to another.

In experiments involving direct removal of emanation from targets, the target foil was placed in the flask *A* and a concentrated solution of sodium hydroxide was placed above the sintered disc in

B. Trap *C* was immersed in a dry-ice–acetone mixture and traps *D*, *E*, and *F* were cooled in liquid-nitrogen filled Dewar flasks. The system was evacuated and the dissolver solution (hot concentrated HCl with ammonium fluosilicate catalyst for the dissolution of thorium) was added in several portions from the separatory funnel. The evolved gases were pumped off through *B*, *C*, *D*, *E*, and *F*. *A* and *B* were then closed off and the system was pumped down to base pressure. The emanation was next concentrated in trap *F*, and was transferred from there to the glow-discharge tube. The discharge was then run, and any emanation not collected was transferred back to trap *F* for use in possible later runs.

The sodium hydroxide bath was included to remove HCl from the evolved gases. The sintered disc insured the completeness of the cleansing operation by causing the gas stream to flow through the solution in the form of fine bubbles. Also, astatine has been found to behave as a gas at low pressure and room temperature, and it was desired to remove this contaminant. In analogy to iodine, astatine vapour can be removed by a hydroxide solution.[36] The dry-ice bath removed water vapour from the evolved gases, and also served as further insurance against astatine reaching the system beyond. The liquid-nitrogen baths thus trapped emanation, along with krypton and xenon fission product activity and small amounts of oxygen present in the system. Three successive liquid-nitrogen traps were used, since, because of the initial high pressure and high rate of flow of the evolved gases through the traps not all of the emanation was condensed in the first.

In cases where it was desired to remove emanation from solutions of francium or radium (see sections 4 and 7), the solution of parent activity took the place of the hydroxide solution in *B*, and *B* was connected to a nitrogen line instead of to the flask *A*. The emanation was then swept from the solution by a slow stream of nitrogen gas, the rest of the procedure being the same as that outlined above.

When the emanation activity was transferred into the glow-discharge tube of Fig. 13 by cooling the freeze-down tip with liquid nitrogen, and then allowed to warm up after isolating the discharge tube from the system by closing the stopcock, it was usually found that enough inert gas had been brought along, because of the crudeness of the fractionation process, to raise the total pressure to the range of 100 to 1000 microns. When this was not the case, nitrogen was introduced to raise the pressure to this range. The electrode potential difference was raised slowly until a discharge was achieved. This discharge was run for five minutes, but was frequently interrupted by dropping the voltage so that the cathode did not warm up and hence lose emanation. After five minutes the gas was pumped back into the vacuum system and collected in trap *F*. The glow tube was removed from the line and opened so that the wire could be cut.

Part of the reason for describing this method in detail is that it should have considerable usefulness in the preparation of samples of other gaseous radioactive elements. MATHUR and HYDE,[37] for example, have been able to measure conversion electrons in a beta-ray spectrometer from xenon isotopes deposited on thin aluminium foil by this method.

(c) *Chemical Procedure for the Isolation of Francium*

The removal of francium from thorium was effected by using an improved procedure of HYDE's[38] previously described. This involved coprecipitation of francium with free silico-tungstic acid from cold saturated HCl solution. To obtain carrier-free samples of francium, the silico-tungstic acid precipitate was dissolved in water and passed through a Dowex-50 column. The francium adheres to the column and can later be removed with 6 *M* HCl. This procedure results in carrier-free samples radiochemically pure except for cesium fission-product activities.

(d) *Chemical Procedures for the Isolation of Radium*

To remove radium from thorium targets, the usual method of coprecipitation with $BaCl_2$ was used. The target was dissolved in HCl (with ammonium fluosilicate catalyst added), the solution was saturated with HCl gas and cooled in ice, and the $BaCl_2$ precipitate was brought down within five to ten minutes after the end of bombardment. The precipitation was made from about 10 ml of HCl using about 1 mg of barium carrier. Because of the presence of large amounts of higher mass radium isotopes and their daughters, it was not possible to subject such samples to alpha-spectrum analysis

[36] C. F. JOHNSON, R. F. LEININGER, and E. SEGRÈ, *Phys. Rev.* **76**, 18 (1949).
[37] H. B. MATHUR and E. K. HYDE, *Phys. Rev.* **96**, 126 (1954).
[38] E. K. HYDE, *J. Amer. Chem. Soc.* **74**, 4181 (1952).

directly to obtain information on neutron-deficient radium isotopes. The emanation daughters of such activities could be studied by dissolving the $BaCl_2$, transferring it to tube *B* (Fig. 11), and later sweeping the emanation daughter activity from the solution.

A fast method was also developed for removing radium from lead targets bombarded with carbon ions in the 60-inch cyclotron. The lead was dissolved in a minimum amount of hot 2 to 3 *M* HNO_3, and the solution was saturated with HCl gas and cooled in ice. In saturated HCl the lead forms a soluble chloride complex. Barium carrier (a few tenths of a milligram) was then added to precipitate $BaCl_2$ to carry the radium. With sufficient barium carrier and time to complete the precipitation, one would expect quantitative yields. The precipitation is not instantaneous, however, and $BaCl_2$ is slightly soluble even in saturated HCl. To obtain thin samples for pulse analysis in a short time, incomplete precipitation of the barium chloride was tolerated, and yields were sometimes as low as 20 per cent, judging from tracer runs with Ra^{226}. Samples could be prepared in five to ten minutes, but the time required for transport of the sample to the pulse-height proportional counter equipment located at a five-minute drive from the 60-inch cyclotron, made it impossible to start pulse analyses sooner than about fifteen minutes after the end of the bombardment.

VOL.
1
1955

ACKNOWLEDGEMENTS

We are indebted to Drs. GLENN T. SEABORG and I. PERLMAN for many helpful suggestions. ALBERT GHIORSO was generous with his time and expert assistance, particularly during the orientation stage of this research. For the heavy ion bombardments at the 60-inch cyclotron we owe thanks to G. BERNARD ROSSI, ALBERT GHIORSO, and to Dr. JOSEPH G. HAMILTON. The numerous thorium-foil bombardments were carried out at the 184-inch cyclotron by JAMES T. VALE, LLOYD B. HOUSER, and the 184-inch crew. We wish to thank A. W. STONER and B. A. RABY for permission to quote from their unpublished work.

J. Inorganic and Nuclear Chemistry, 1955, Vol. 1, pp. 296–300. Pergamon Press Ltd., London

CHEMICAL STATE OF NITROGEN-13 FORMED BY THE (*n*, 2*n*) REACTION IN SOLID NITROGEN COMPOUNDS

By R. D. SMITH* and A. H. W. ATEN, JUN.
Instituut voor Kernphysisch Onderzoek, Ooster Ringdijk 18, Amsterdam-O.

(*Received* 22 *April* 1955; *in final form* 21 *June* 1955)

Abstract—The distribution of N^{13} over different chemical states after irradiation with fast neutrons is investigated for $NaNO_2$, $NaNO_3$, NH_4NO_3, KNO_3, and $LiNO_3$.

INTRODUCTION

WHEN nitrogen atoms are exposed to a flux of fast neutrons, N^{14} is partly, but only for a very small fraction, converted to N^{13} as a result of an $n,2n$-reaction. The half-life of the product is 10·1 min, and the radiation emitted consists of positrons. The nuclear process causes a change in the chemical state of the nitrogen atoms involved, similar to the Szilard-Chalmers effect in the case of the n,γ-process. A study of the chemical form of N^{13} in the irradiated material should provide some information concerning the chemical reactions which take place between highly energetic nitrogen ions and the target material.

We have investigated the chemical state of N^{13} after fast neutron irradiation of several salts containing nitrogen.

EXPERIMENTAL

The salts were of analytical reagent purity, except for the lithium nitrate. This was made from lithium carbonate, the product being melted *in vacuo*, and dried over phosphorus pentoxide. The nitrate content was 98 per cent of the theoretical, and the discrepancy was presumably due to water. The salts were powdered and (except for the lithium nitrate) air-dried at 110°. They were exposed at the ordinary ambient temperature of the cyclotron to the neutrons emitted from a beryllium target bombarded with deuterons of energy 26 MeV.

The N^{13} in the irradiated material and in the analytical products was determined either by means of a thin window counter using thin layers of solid or by means of a liquid counter, which registered the annihilation radiation from solutions. In the former case corrections were applied for self-absorption.[1] Activities induced in oxygen and sodium in the salts differed sufficiently in half-life not to interfere with the N^{13} determination, but a strong Cl^{38} activity induced on bombardment of potassium nitrate had to be removed by precipitating with silver nitrate. Experiments with the ammonium halides failed because of the difficulty of removing the activities induced in the halogens.

The proportion of N^{13} activity in the ammonium ion was found by precipitating a sample of ammonium hydrogen tartrate. Nitrate was isolated as nitron nitrate, after removal of nitrite with hydrazine sulphate, and nitrite as silver nitrite precipitated slowly from the hot dilute solution. Carriers and hold-back carriers were employed in the usual way. The proportion of N^{13} in gaseous forms was measured by comparing the activities of two solutions, one of which had been made up in a stoppered tube without loss of gas, and the other of which had been boiled or bubbled through with nitrogen until there was no further loss in activity.

In the sodium and ammonium salts, the fraction of the total N^{13} activity in any particular chemical form could be reproduced to within a few percent of the total activity. In the case of lithium nitrate, however, the reproducibility was much poorer. All experiments, except a few concerning ammonium nitrate, were performed at least in duplicate. The results are quoted as the range of values actually

* Present address: I.C.I., Nobel Division, Stevenston, Ayrshire.
[1] A. H. W. ATEN, JUN. *Nucleonics* **6**, No. 1, 68 (1950).

found; where only one figure is quoted, only one determination was made. Experimental errors cause the totals to differ from 100 per cent since the analysis was not done by difference.

RESULTS

The values found in the main experiments are given in the table.

TABLE—PART OF TOTAL N^{13}-ACTIVITY FOUND IN DIFFERENT FRACTIONS OF VARIOUS NITROGEN COMPOUNDS

Compound	NO_3^-	NO_2^-	NH_4^+	Recrystallized material	Gases
$NaNO_3$	0·44 ± 0·02	0·46 ± 0·01		0·52 ± 0·02	0·07 ± 0·02
$NaNO_2$	0·02 ± 0·01	0·45 ± 0·01			0·58 ± 0·02
NH_4NO_3	0·44 ± 0·01	0·01 ± 0·01	0·03 ± 0·00	0·43 ± 0·01	0·57 ± 0·02
$LiNO_3$	0·51 ± 0·04	0·47 ± 0·08			0·07 ± 0·00

VOL. 1 1955

Attempts, which were only partially successful, were made to extend this series in different directions. When KNO_3 was irradiated, the total activity of the N^{13} could not be determined, owing to the large quantity of Cl^{38} which was formed. We did, however, determine the ratio $[N^{13}O_3^-]/[N^{13}O_2^-]$, for which we found 0·41 ± 0·04. We repeated the experiment with a sample recrystallized from water through which hydrogen was bubbled, and found 0·39 ± 0·05 for this ratio. With a sample similarly treated with oxygen we found 0·29 ± 0·02.

It would have been very interesting to obtain similar data on the distribution of N^{13} in ammonium halides. With these compounds we were, however, unable to measure the total nitrogen activity owing to the presence of strong radio-halogen periods, although it was possible to detect $N^{13}H_4^+$ among the products.

Special attention was paid to the case of the ammonium nitrate. It was ascertained that the fraction of the activity found as gases was essentially unchanged if the ammonium nitrate had been recrystallized in the presence of hydrogen (0·50) or in the presence of oxygen (0·52 ± 0·02) (these samples had been dried at 120° after recrystallization). We also made sure that the fraction of the activity retained in the ammonium nitrate on recrystallization was not notably affected if the irradiated crystals were dissolved in 0·1 N sulphuric acid (0·44 ± 0·01), dilute sodium hydroxide (0·42), or a solution of potassium permanganate (0·43).

An attempt was made to determine the constituents of the active gas fraction. Oxidizable forms were sought by adding a little acidified permanganate solution before boiling to remove dissolved gases. The permanganate had no effect on the retention of activity by the solution, showing that there could be no appreciable amount of NO or NO_2 originally among the active dissolved gases: free NO_2 is in any case unlikely at very low concentrations. Similarly, the loss in activity was no less when nitrogen was passed through a cold mixed solution of the irradiated ammonium nitrate and concentrated ferrous sulphate than when it was passed through the simple solution of the nitrate in water. Molecular nitrogen and nitrous oxide are the only two remaining likely constituents of the active gas. Nitrous oxide was sought by dissolving the irradiated ammonium nitrate in water saturated with nitrous oxide as carrier, and then drawing nitrogen through until all gaseous activity had been swept out of the solution and through a liquid air-trap, where the nitrous oxide condensed. The contents of this trap were later allowed to evaporate into one of the stoppered tubes generally used for liquid counting. 8 per cent of the total N^{13} activity was isolated in this way. Although separation of nitrous oxide was probably not complete, this figure does suggest that a considerable part of the active products consists of nitrous oxide inside ammonium nitrate crystals.

DISCUSSION

With most compounds the radiochemical separation seems to give satisfactory results. In this connection it should be realized that in the case of sodium nitrate the recrystallized fraction would be expected to give the NO_3^--activity, and in the case of the ammonium nitrate the sum of the NO_3^--activity and the NH_4^+-activity.

The fact that in all irradiated compounds the sum of the activities of nitrate, nitrite, and the gaseous compounds amounts to about 100 per cent indicates that nitrate and nitrite are the only non-volatile reaction products which are important.

With lithium nitrate the reproducibility is not nearly so good as it is in the other cases. A possible explanation might be found in the extremely hygroscopic nature of this substance, but the fact that it was handled in a dry box detracts from the weight of this consideration.

In view of the fact that the chemical state of radio-sulphur formed by fast neutron irradiation of potassium chloride is strongly dependent[2] on the presence of oxygen in the crystal lattice, it seemed worth while to test for a similar influence in our experiments. Our results with ammonium nitrate indicated that with N^{13} such an influence could not be clearly recognized.

However, the ratio $[N^{13}O_3^-]/[N^{13}O_2^-]$, which was about unity in $NaNO_3$ and iNO_3, proved to be appreciably lower in KNO_3, so we had to reconsider the possibility of such an oxidation in the crystal. Although for the latter salt we were unable to exclude wholly such an interference (though we are not certain that the difference actually exceeds the possible error), we consider that the $[N^{13}O_3^-]/[N^{13}O_2^-]$ ratio is definitely lower in this compound than it is in the two other alkali nitrates investigated.

An even more serious question was whether the valences found for N^{13} are uniquely determined by the processes which take place in the crystal, or whether the final distribution is influenced by processes taking place during solution, as seems to be the case with neutron-irradiated $KMnO_4$.[3] For this reason the experiments were undertaken in which irradiated ammonium nitrate was dissolved in the presence of H^+-, OH^--, or MnO_4^--ions. The fact that these additions did not influence the activity distribution makes it almost certain that the final form in which the N^{13}-atoms will be found is already determined entirely in the crystal. This does not, of course, mean that radioactive nitrate and nitrite ions are necessarily present in the solid as such. It is not impossible that they are formed by hydration of radioactive nitrogen atoms or oxides carrying the appropriate charge at the moment these go into solution.

Neutrons must have an energy around 10 MeV to form N^{13} from N^{14} by the $n,2n$-process. Under these circumstances they have also an excess energy, which is on the average of the order of 1 MeV. Most of this excess energy will be dissipated as kinetic energy of the two neutrons formed, but an appreciable fraction will turn up as recoil energy of the N^{13}-atoms. This energy not only enables the N^{13}-atoms to break their chemical bonds, but also to strip off some of their electrons and to adopt a positive charge. Similar circumstances occur in n,p- and n,α-processes.[4] For this reason it is to be expected that if different nitrogen compounds are irradiated with fast neutrons the primary condition of N^{13} will be a highly oxidized one, and presumably one which depends very little on the nature of the irradiated substance. This state of affairs does not, of course, determine by itself the results of the chemical analysis, as the highly charged positive N^{13} will be able to react chemically with the components of the crystal lattice after it has lost most of its excess energy. The activity measurement indicates therefore the results of the chemical processes which have taken place between N^{13}-atoms or ions in essentially similar conditions and the ions which make up the different solids.

[2] W. S. KOSKI, *J. Amer. Chem. Soc.* **70**, 4251 (1948).
[3] W. F. LIBBY, *J. Amer. Chem. Soc.* **62**, 1930 (1940).
[4] A. H. W. ATEN, JUN., *Recueil Trav. Chim. Pays-Bas* **61**, 467 (1942); *Phys. Rev.* **71**, 641 (1947).

It is to be expected that the composition and the structure of the target material will exert a strong influence on the activity distribution. A very striking example is presented by the difference between $NaNO_3$ and $NaNO_2$. The lack of radioactive NO_3^--ions in the latter solid may perhaps be taken as an argument for the assumption that the complex radioactive anions, or at least the nitrate ions, are already formed in the crystal lattice before the material is dissolved, but it certainly does not definitely disprove the opposite. In any case this difference shows clearly the influence of the target material on the chemical form of the reaction products, in agreement with the observations made with n,p- and n,α-processes.[4] As KNO_3 gives results which are quite different from those found with $NaNO_3$ and $LiNO_3$, it is clear that even the cation can make a difference.

It is worth pointing out that, in all the materials studied, an important fraction of the N^{13} is found in an oxidized state, as is to be expected if the N^{13} passes through a stage in which it is positively charged. It should be kept in mind, however, that in the ordinary Szilard-Chalmers process the n,γ-reaction sometimes leads to a similar situation, as in the case of the iodates.[5]

VOL.
1
1955

We want to make it quite clear that, although the N^{13} is found in an oxidized state to an important degree, the three alkali nitrates and sodium nitrite all show a partial loss of oxygen during the nuclear reaction, relative to the combination state of nitrogen in the substrate. The only compound which does not suffer a reduction during activation is ammonium nitrate. This substance constitutes a more complicated case, for the medium can exert both an oxidizing and a reducing influence on the N^{13}. It should be kept in mind that in this case secondary reactions may be possible with radioactive ions in an excited state. If an intermediate formation of active NO_2^--ions has occurred, these have disappeared by the reaction $NO_2^- + NH_4^+ \rightarrow 2H_2O + N_2$ before the energy liberated by the nuclear process has been dissipated. Similarly, excited radioactive ions of NH_4^+ and of NO_3^- may have been lost by the reaction $NO_3^- + NH_4^+ \rightarrow 2H_2O + N_2O$. The uncertainty of the determination of N_2O in the reaction products makes it impossible to reach quantitative conclusions concerning these possibilities. It must be stated clearly, however, that the radioactive gases N_2 and N_2O may very well have been formed "directly," that is, from a mixture of highly energetic atoms (one of which was radioactive) without passing through an intermediate stage in which they had the composition of stable ions or compounds.

The abundance of NO_3^- relative to NH_4^+ in the active products from ammonium nitrate is noteworthy. It suggests, without proving it, that NO_3^- is indeed a more favoured first product of the reaction of energetic N^{13} atoms with the substrate, for if the relative lack of $N^{13}H_4^+$ is to be ascribed solely to the secondary reaction postulated above, it is difficult to explain why the $N^{13}O_3^-$ has not disappeared to a corresponding degree. In any case, by making the extreme assumption that all the active gases are the reaction products of active ammonium ions, one is led to the conclusion that the original concentration of the latter cannot have appreciably exceeded the combined concentrations of active nitrate and nitrite ions.

Discussion of a more quantitative nature, e.g., of the difference between the $[N^{13}O_3^-]/[N^{13}O_2^-]$ ratios in $NaNO_3$ and $LiNO_3$ on the one hand and KNO_3 on the other, is at present hardly possible. Interpretation of the observations on ammonium nitrate would have been greatly helped by a knowledge of the processes in ammonium

[5] R. E. Cleary, W. H. Hamill, and R. R. Williams, *J. Amer. Chem. Soc.* **74**, 4675 (1952).

salts with stable anions, but experiments with this aim were unsuccessful for the reasons given above.

ACKNOWLEDGEMENTS

The authors wish to thank Miss A. C. KLOPPER for carrying out some of the analyses. We also wish to express our thanks to the personnel of the Philips' cyclotron for the irradiations. This investigation forms part of the Research Programme of the Foundation for Fundamental Research of Matter (F.O.M.). It was carried out with financial aid from the Netherlands Organization for Pure Research (Z.W.O.). Grateful acknowledgement is also made to Imperial Chemical Industries Limited (Nobel Division) for allowing one of the authors (R. D. S.) to take part in this work.

J. Inorganic and Nuclear Chemistry, 1955, Vol. 1, pp. 301–308. Pergamon Press Ltd., London

FFFECTIVE QUANTUM NUMBERS IN *d*- AND *f*-SHELLS

By Chr. Klixbüll Jørgensen
Chemistry Department A, Technical University of Denmark, Copenhagen

(*Received* 5 *May* 1955)

Abstract—The behaviour of the effective nuclear charge Z_* and the effective principal quantum number n_* is investigated, with special emphasis on the beginning of the 3*d*-, 4*f*-, and 5*f*-periods. The screening constants are seen to be so dependent on the net charge of the atom that the value of the concept is impaired. The available data on deviations from the hydrogen model, as derived from atomic spectroscopy and the absorption spectra of metal ions in solution, lead to some conclusions of chemical interest.

VOL.
1
1955

INTRODUCTION

The line spectra of atoms with one (or a few) electrons outside the closed shell configurations are usually described by means of the parameters from the treatment of the hydrogen atom. In the present paper, these parameters are obtained for several transition group ions with different external charge, and compared with the current theories of screening by internal electrons, which have been developed for *s*- and *p*-electrons. The nature of the electronic configurations in the lanthanide and actinide ions will be shown to be highly dependent on their net external charge, contrary to the usual opinion that *f*-electrons are highly shielded. Actually, the beginnings of the *d*- and *f*-transition groups are more similar in behaviour than might be expected.

Much of the discussion to follow will relate to the parameters of the following equations:

$$E = -\frac{Z_*^2}{n_*^2}\,109{,}737\ \text{cm}^{-1} \tag{1}$$

$$\zeta_{nl} = \frac{Z_*^4}{n_*^3 l(l+\tfrac{1}{2})(l+1)}\,5{\cdot}822\ \text{cm}^{-1} \tag{2}$$

$$F_k = f((nl),(n'l'))\,.\,Z_* \tag{3}$$

Equation (1) gives the energy of a level in terms of the Rydberg constant, equation (2) the Lande multiplet splitting factor ζ_{nl} for an electron with quantum numbers n and l, and equation (3) the expression for the Condon-Shortley[1] parameters F_k ($k = 2, 4, \ldots$) for the electrostatic interaction between two electrons (nl) and $(n'l')$.

In equations (1), (2), (3), the quantity Z_* is termed the effective nuclear charge and n_* the effective principal quantum number. In some cases, one of these two quantities is regarded as fixed, while the other is made responsible for the deviations from the hydrogen case. Thus, in atomic spectroscopy, it has been customary to take Z_* equal to Z_0 (the external charge of the atom or ion, plus one). Sommerfeld[2] and many X-ray spectroscopists have chosen to define n_* equal to n, the real principal quantum number, and then to take $Z_* = Z - \sigma$, where Z is the atomic number and σ the screening constant. Finally, Slater[3] considers both Z_* and n_* as free parameters.

[1] E. U. Condon and G. H. Shortley, Theory of Atomic Spectra, Cambridge, 1953.
[2] A. Sommerfeld, Atombau und Spektrallinien. 4. Aufl. 1924.
[3] J. C. Slater, *Phys. Rev.*, **36**, 57 (1930).

The need for empirical definitions for Z_* and n_* is, for example, clearly demonstrated by the large increase of ζ_{nl} with Z observed in the alkali metals. LANDÉ[4] proposed a model where the valency electron is attracted in the outer parts of its orbit by an effective nuclear charge $Z_* = Z_0$, while in the inner parts of the orbit $Z_* = Z$. Further, LANDÉ assumed a value of n_* known from the energy expression (1) (where other authors also applied the $Z > Z_* > Z_0$ model) and wrote:

$$\zeta_{nl} = \frac{Z_0^2 Z^2}{n_*^3 l(l+\frac{1}{2})(l+1)} \, 5{\cdot}822 \text{ cm}^{-1} \tag{4}$$

This simple model is more satisfactory for electrons with high values of $(n - l)$ than for 3*d*- and 4*f*-electrons, which are the main subject of the present paper. The radial hydrogen eigenfunctions have $(n - l)$ maxima corresponding to the electron being present in regions of highly different Z_*, when $(n - l)$ is large. But when this quantity is unity, the square of the radial functions is highly concentrated around a single maximum, viz.:

$$r_{\max} = \frac{n^2}{Z_0} \, 0{\cdot}528 \text{ Å} \tag{5}$$

This results in a low electron density near the nucleus.

NUMERICAL RESULTS

In Table 1 are given values of ζ_{nd} obtained from ^2D-terms of *d*-, ^3F and ^3P-terms of d^2-, ^4F, and ^4P-terms of d^3- and ^5D-terms of d^4-systems. The multiplet levels are

TABLE 1.—VALUES OF ζ_{nd} AND ζ_{nd}/Z_0^2 FOR SYSTEMS WITH ONE, TWO, THREE, AND FOUR *d*-ELECTRONS, ALL IN UNITS OF CM^{-1}

	3*d*			3*d*²			3*d*³			3*d*⁴	
	ζ_{nd}	ζ_{nd}/Z_0^2		ζ_{nd}	ζ_{nd}/Z_0^2		ζ_{nd}	ζ_{nd}/Z_0^2		ζ_{nd}	ζ_{nd}/Z_0^2
K	−0·9	(−0·9)	Ca	26·5	26·5	Sc	46	46·0			
Ca^+	23·9	6·0	Sc^+	53·5	13·4	Ti^+	95	23·7	V^+	135	33·9
Sc^{+2}	79·0	8·8	Ti^{+2}	123	13·7	V^{+2}	169	18·8	Cr^{+2}	229	25·4
Ti^{+3}	153·7	9·6	V^{+3}	217	13·6	Cr^{+3}	275	17·2	Mn^{+3}	352	22·0
V^{+4}	248	9·9	Cr^{+4}	348	13·9	Mn^{+4}	406	16·2	Fe^{+4}	514	20·6
Cr^{+5}	383	10·6	Mn^{+5}	520	14·4	Fe^{+5}	574	15·9	Co^{+5}	714	19·8
Mn^{+6}	542	11·1	Fe^{+6}	742	15·1				Ni^{+6}	952	19·4
	4*d*			4*d*²							
Rb	−0·2	(−0·2)	Sr	136·6	136·6						
Sr^+	112·2	28·0	Y^+	194	48·5						
Y^{+2}	290	32·2	Zr^{+2}	468	52·0						
Zr^{+3}	500	31·2	Nb^{+3}	804	50·2						
Nb^{+4}	748	29·9	Mo^{+4}	1210	48·4						
	5*d*										
Cs	39·0	39·0									
Ba^+	320·4	80·1									
La^{+2}	641	71·1									
Ce^{+3}	996	62·2									
	6*d*										
Ra^+	663·5	165·9									
Th^{+2}	2117	132·3									

[4] A. LANDÉ, *Z. Phys.*, **25**, 46 (1924).

taken from the compilations of MOORE[5] and (especially for $Z > 41$) from Landolt-Börnstein tables,[6] and the average values of ζ_{nd} were obtained by the method of CONDON and SHORTLEY.[1] It can be seen that ζ_{nd} is approximately proportional to Z_0^2.

From the values given for ζ_{nd}/Z_0^2, it is seen that irregularities occur mainly in the neutral atoms with $Z_0 = 1$. The probably nearly constant error in ζ_{nd} due to interaction with other terms would, of course, make the relative error in ζ_{nd} much larger for the small values associated with the case $Z_0 = 1$. The special case of a negative, small value of ζ_{3d} in K is due to perturbation from highly-excited levels with other electron configurations.[1] With increasing Z, the values of ζ_{nd} increase so much that LANDÉ's interval rule is not obeyed, and therefore ζ_{nd} cannot be found directly from the multiplet splitting. The matrices of intermediate coupling cannot reliably be applied to the atoms with more electrons in unfilled shells because not all the other states with a given J are known. It can be seen from the energy levels[5, 6] that P-terms usually give more irregularities in ζ_{nd} than do F-terms. This corresponds to larger non-diagonal elements for small values of J, and smaller distances to the perturbing terms of lower multiplicity. The interaction between the even electron configurations d^n, $d^{n-1}s$, and $d^{n-2}s^2$ is considerable, as contrasted with the f^n configurations which have not the same parity as $f^{n-1}d$.

Even if LANDÉ's equation[4] is supported by the approximate proportionality of ζ_{nd} to Z_0^2, one sees from the results above that a comparison with the hydrogen case is not very successful. It is of interest to consider the general expression of ζ_{nl} (ref. 1, p. 122):

$$\zeta_{nl} = \frac{h^2}{8\pi^2 m^2 c^2} \int_0^\infty R^2(nl) \frac{1}{r} \frac{\partial U(r)}{\partial r} \, dr \tag{6}$$

$R^2(nl)$ is the square of the radial function, U is the electrostatic potential of the electron. If U formally is expressed as $U = -Z_* e^2/r$, where Z_* is a function of r,

$$\zeta_{nl} = \frac{h^2 e^2}{8\pi^2 m^2 c^2} \int_0^\infty R^2(nl) \frac{Z_*}{r^3} \, dr \tag{7}$$

The anomalous high values of ζ_{nd} for $n = 4$ and 5 are therefore caused by large contributions of the integrand of (7) near $r = 0$, as in LANDÉ's more classical explanation.

GOBRECHT[7] applied equation (2) to the ζ_{4f} of trivalent lanthanide ions with $n_* = 4$ to find effective charges Z_*, which he defined as $Z - \sigma$, where the screening constant σ slowly varies from 28 to 36 in the series from Ce^{+3} to Yb^{+3}. GRUEN[8] has extended this concept to the actinide ions, where σ is assumed to be 58. The present author[9] stressed the importance of external charge $(Z_0 - 1)$ and found[10] several more ζ_{nf}-values. While the Z_0 equals 4 for all the cases studied by GOBRECHT, considerable variations of σ (if this quantity is related to equation (2)) is observed in these actinide ions, which have different oxidation states of the elements, thus giving rise to iso-electronic series.

[5] C. E. MOORE, Atomic Energy Levels., *Nat. Bur. Stand. Circ.* No. 467, Parts 1 and 2.
[6] LANDOLT-BÖRNSTEIN, 6. Auflage, Vol. 1, Part 1.
[7] H. GOBRECHT, *Ann. Phys.* (*Leipzig*) (5), **31**, 755 (1938)
[8] D. M. J. GRUEN, *Chem. Phys.*, **20**, 1818 (1952).
[9] C. KLIXBÜLL JØRGENSEN, *J. Chem. Phys.*, **23**, 399 (1955).
[10] C. KLIXBÜLL JØRGENSEN, *K. Danske Vidensk. Selsk., Mat-fys. Medd.*, **29**, No. 11 (1955).

VOL. 1 1955

Table 2 gives all the published values of ζ_{4f} and ζ_{5f}. The values for Cs, Ba^{+}, La^{+2}, Ce^{+3}, La^{+}, Ra^{+}, Th^{+3}, and Th^{+2} are derived from atomic spectroscopy while the others are inferred from absorption spectra of aqueous solutions.

It would be interesting to determine ζ_{5f} in the one-electron systems Pa^{+4}, U^{+5}, and Np^{+6}, but the infra-red absorption spectra will probably be perturbed by crystal fields. In the special case of La^{+2}, ζ_{4f} was inferred[11] from the series limits of La^{+}.

The influence of Z_0 on ζ_{4f} and ζ_{5f} is evident from Table 2, and the dependence seems to be of a higher power than 2 for small values of Z_0[2]. Thus contrary to the opinion of many chemists 4*f*- and 5*f* electrons should be more hydrogen-like in these ions than *nd*-electrons in the normal transition group ions. This viewpoint is supported by the energy values, treated by equation (1). The ionization potentials for the

TABLE 2.—VALUES OF ζ_{nf} IN UNITS OF CM^{-1} FOR LANTHANIDE AND ACTINIDE PERIODS

		ζ_{4f}	Ref. No.			ζ_{5f}	Ref. No.
f	Cs	−0·1	6	f	Ra^{+}	81·2	14
f	Ba^{+}	64·1	6	f	Th^{+3}	1236	15
f	La^{+2}	410	11	f^{1}	Th^{+2}	1035	16
f	Ce^{+3}	644	12	f^{1}	U^{+4}	1600	19
f^{1}	La^{+}	280	13	f^{2}	Np^{+5}	1900	8
f^{2}	Pr^{+3}	800	17	f^{3}	Pu^{+6}	2200	8
f^{3}	Nd^{+3}	900	18	f^{3}	U^{+3}	1700	10
f^{5}	Sm^{+3}	1200	7	f^{3}	Np^{+4}	2100	10
f^{6}	Eu^{+3}	1450	7	f^{3}	Pu^{+5}	2700	10
f^{6}	Tb^{+3}	1700	7	f^{4}	Np^{+3}	1900	10
f^{9}	Dy^{+3}	1850	7	f^{4}	Pu^{+4}	2300	10
f^{10}	Ho^{+3}	2050	7	f^{4}	Am^{+5}	3000	10
f^{11}	Er^{+3}	2350	7	f^{5}	Pu^{+3}	2500	10
f^{12}	Tm^{+3}	2800	17	f^{6}	Am^{+3}	3500	10
f^{13}	Yb^{+3}	3000	7				

typical lanthanide and actinide ions, giving the absolute term values, are regrettably only known for Ce^{+3} and Th^{+3}. Table 3 gives the values of n_* of 4*f*- and 5*f*-terms, respectively, when $Z_* = Z_0$ in equation (1).

LANTHANIDE AND ACTINIDE GROUPS

It is seen in Table 3 that the energy of the 4*f*-electron in Cs also corresponds very nearly to $n_* = 4$, while this quantity decreases in the isoelectronic Ba^{+} and Ce^{+3}. In the latter ion, $Z_* = 6{\cdot}56$ if n_* is defined $= 4$. Thus the 4*f*-electron seems to eventually be screened slightly by the kernel. It can be connected with the radius of the

TABLE 3.—VALUES OF n_* FROM ENERGY LEVELS OF IONS WITH Z_* DEFINED $= Z_0$

Z		$4f\,^2F_{5/2}$	$4f\,^2F_{7/2}$	$5f\,^2F_{5/2}$	$5f\,^2F_{7/2}$
55	Cs	3·977	3·977	4·974	4·974
56	Ba^{+}	3·679	3·692	4·341	4·363
58	Ce^{+3}	2·435	2·444	3·966	3·969
80	Hg^{+}			3·968	3·950
88	Ra^{+}			3·655	3·671
90	Th^{+3}			2·752	2·778

[11] T. L. DE BRUIN, P. F. A. KLINKENBERG, and PH. SCHUURMANS, *Z. Phys.*, **118**, 58 (1941).
[12] R. J. LANG, *Canad. J. Res.*, **14A**, 127 (1936).
[13] H. N. RUSSELL and W. F. J. MEGGERS, *Res. Bur. Stand.*, **9**, 625 (1932).
[14] E. RASMUSSEN, *Z. Phys.* **86**, 24 (1933).
[15] P. F. A. KLINKENBERG and R. J. LANG, *Physica*, **15**, 774 (1949).
[16] G. RACAH, *Physica*, **16**, 651 (1950)
[17] F. H. SPEDDING, *Phys. Rev.*, **58**, 255 (1940).
[18] R. A. SATTEN, *J. Chem. Phys.*, **21**, 637 (1953).
[19] C. KLIXBÜLL JØRGENSEN, *Danske Vidensk. Selsk. Mat-fys. Medd.*, **29**, No. 7 (1955).

kernel, viz., the xenon configuration. From equation (5) it is concluded that the maximum density of the 4f-electron occurs at 8·45 Å for $Z_0 = 1$, at 2·82 Å for $Z_0 = 3$ and at 1·69 Å for $Z_0 = 5$. Since the radius of Cs^+ is 1·65 Å, Ba^{+2} 1·22 Å, and La^{+3} 1·02 Å, as determined by crystallography,[20] or of Cs^+ 2·5 Å, as determined by Hartree's self-consistent field methods,[21] it is clearly understood why considerable deviations from the hydrogen model begin to occur for $Z_0 \sim 4$, i.e., in the trivalent ions. The chemical paradox that 4f-electrons have only $Z_* = 1$ in cesium, but are quite shielded in the lanthanide ions, is thus mainly explained by the difference in external charge. The neutral lanthanide atoms all have two, and in some cases three valency electrons (6s and 5d) besides their 4f-electrons[22] and show no tendency to have groundstates with 4f-electrons alone, which would correspond to "inert gases." The latter type of states would have $Z_0 = 1$ and correspondingly hydrogen-like values (only $-6{,}858\ cm^{-1}$) for the energy of 4f-electrons. On the other hand, the trivalent lanthanide ions do not show any tendency to give up more electrons, because with $Z_0 = 4$, the 4f-electrons have received sufficient shielding by the kernel. This results in smaller values of r_{max} than given directly by equation (5).

VOL. 1 1955

In the case of 5f-electrons, the deviation of n_* from 5 is initiated much earlier as a function of the atomic number Z; for example, even in Ce^{+3} and Hg^+, n_* is decreased to ~4. This fact is explained by the two maxima of the radial 5f-function; a part of this function is necessarily placed nearer to the nucleus giving a larger Z_*. While a fixed oxidation state of +3 prevails in the lanthanides with only small irregularities at the beginning of the series (+4 in Ce and Pr), greater variations of oxidation state are found in the actinides.[23] The higher oxidation states +6, +5, and +4, which can persist up to Am, cannot fruitfully be discussed in connection with the ground states of the neutral atoms. Rather, the ionization potentials and energy differences in the ionized species must be compared with the empirically known potentials for removing electrons in chemical reactions, where the higher oxidation states are stabilized by solvation effects and complex formation.

While the principal reason for the chemical variation of the actinide elements is the slow variation of n_* of 5f-electrons as a function of Z_0, the finer details can be found from the energy difference between 5f and 6d electrons. This is known from atomic spectroscopy for several oxidation states of Ra and Th, and can be inferred from the absorption spectroscopy of compounds of many of the later elements. BUTEMENT[24] proposed the broad, intense bands of lanthanide ions (different from the usual narrow bands due to internal $4f^n$-transitions) to be due to transitions to $4f^{n-1}5d$-states, which have the opposite parity and thus make direct electric dipole radiation possible according to LAPORTE's rule. STEWART[25] has collected much experimental material on the similar $5f^n - 5f^{n-1}6d$ bands in the actinides and calculated oscillator strengths P for these bands, $P \sim 10^{-2}$ to 10^{-1}, while the maximum values of P are 10^{-3} in the actinides[25] and 10^{-5} in the lanthanides[26] in the case of ordinary bands. The importance of Z_0 for the energy difference between the lowest

[20] V. M. GOLDSCHMIDT, *Ber.*, **60**, 1263 (1927).
[21] D. R. HARTREE, *Proc. Roy. Soc.* **A143**, 506 (1934).
[22] W. F. MEGGERS, *Science*, **105**, 514 (1947).
[23] G. T. SEABORG and J. J. KATZ, The Actinide Elements, Nat. Nuc. Energy Ser. *Div. IV*, Vol. 14A (1954)
[24] F. D. S. BUTEMENT, *Trans. Faraday Soc.*, **44**, 617 (1948).
[25] D. C. STEWART, Absorption Spectra of Lanthanide and Actinide Rare Earths. II. Transition Probabilities for +3 Ions in the two Series. ANL-4812 (1952).
[26] J. HOOGSCHAGEN and C. J. GORTER, *Physica*, **14**, 197 (1948).

terms of the two electron configurations $5f^{n-1}6d$ and $5f^n$ was discussed in a previous publication.[10] This behaviour can be compared to the mechanism of an ordinary transition group, where *s*- and *d*-electrons are competing for the lowest energy. Table 4 gives some representative values of the energy difference $6d - 5f$ in the lowest terms for $Z > 87$.

The material of Table 4 can be represented by the equation

$$E(5f^{n-1}6d) - E(5f^n) = (Z - 96)\ 7{,}000\ \text{cm}^{-1} + (Z_0 - 1)\ 18{,}000\ \text{cm}^{-1} \qquad (8)$$

showing the strong dependence on the external charge $(Z_0 - 1)$ of the ion. The energy differences, determined from absorption spectra, may very well be 10,000 cm^{-1}

TABLE 4.—ENERGY DIFFERENCES BETWEEN THE LOWEST TERMS OF THE TWO ELECTRON CONFIGURATIONS $5f^{n-1}$ $6d$ AND $5f^n$ IN UNITS OF 1000 CM^{-1}

$n = 1$	$n = 2$	$n = 3$	$n = 4$	$n = 5$
$Ra^+ - 37$				
	$Th^{+3} - 15$			
$Th^{+3} + 9$		$U^{+3} + 26$	$Np^{+3} + 33$	$Pu^{+3} + 40$
$Pa^{+4} + 35$	$U^{+4} > 40$	$Np^{+4} > 45$	Pu^{+4} ?	

too low, due to crystal field splitting of the atomic energy levels. Thus, ^2D of Ce^{+3} is situated[12] at 49,737 and 52,226 cm^{-1} while bands are observed at 39,500, 42,000, and 45,200 cm^{-1} of the aqueous solution of trivalent cerium.

CONDON and SHORTLEY[1] demonstrated that the electrostatic interaction parameters between 3*d*-electrons, F_2 and F_4, were very nearly proportional to Z_0 in the d^2-systems from Sc^+ to Ni^{+8}. SATTEN[18] assumed that the parameters F_2, F_4, and F_6 for 4*f*-electrons varied in the trivalent lanthanides proportional to $(Z - \sigma)$, where σ is the screening constant, given by GOBRECHT[7]. In this way SATTEN satisfactorily explained the increase of F_k of about three per cent by increasing Z one unit in the trivalent lanthanide ions. However, it is believed that this corresponds only to a variation of Z_* in equation (3) from, e.g., 8 to 8·2, the most important contribution of Z_* being a monotonous function of Z_0. One of the reasons that Z_* does not increase very steeply during the entrance of the 4*f*-electron in the kernel is the "external screening" effect. While electrons in a distance from the nucleus r_0 less than that of the considered electron r cause complete screening, outer electrons with $r_0 > r$ each have the screening effect r/r_0. This effect is considerable when r_0 is not much larger than r. The external screening is especially important for radial functions with only one maximum, as, e.g., 4*f*-electrons.

CHEMICAL IMPLICATIONS

Many chemical conclusions can be drawn from the energy levels given by atomic and chemical spectroscopy. While the crystal field splitting[27] of the levels amounts to only some hundred cm^{-1} in the lanthanide ions,[18] in the first transition group it is $\sim$10,000 cm^{-1} for the divalent and $\sim$20,000 cm^{-1} for the trivalent ions.[28] This quantity is increased *inter alia* 60 per cent in the second transition group.[29] Since the magnetic properties of chemical complexes are mainly determined by the total spin quantum number S, complexes of anomalous magnetism (S lower than the

[27] H. BETHE, *Ann. Phys.* (*Leipzig*) (5), **3**, 133 (1929).
[28] C. KLIXBÜLL JØRGENSEN, *Acta Chem. Scand.*, **8**, 1502 (1954).
[29] C. KLIXBÜLL JØRGENSEN, *Acta Chem. Scand.*, **9** (1955).

maximum value) occur when the energy decrease due to crystal fields of an excited state with lower value of S causes the state to have lower energy than the original groundstate. According to HUND's rule the original ground state always has a maximum value of S. The crystal field theory has recently[28–35] been applied to the transition group complexes with d^n-configurations. Since the distances between the terms in the free ion generally decreases in $4d^n$- and $5d^n$-configurations, compared to $3d^n$-configurations, and since the crystal field perturbations to overcome these differences in magnetic anomalous complexes increases, the second and third transition groups have a much larger tendency to show these low values of S. It has not been possible to prepare complexes of the platinum metals, which show the same S as the gaseous ion. Since ζ_{4d} and ζ_{5d} are much larger *inter alia* than ζ_{3d}, the departures from Russell-Saunders coupling are more pronounced than in the first transition group, giving larger intensities to the weak bands, caused by transitions[28, 30] between states of different S. The latter case is exemplified by the low bands in the red,[29] due to $S(\frac{3}{2} - \frac{1}{2})$ transitions in the d^3-systems Cr^{+3}, Mo^{+3}, and Re^{+4}. The tendency of higher oxidation states in the later transition groups seems to be explained along the same lines as the differences between actinides and lanthanides, discussed above. In the fundamental equations for crystal field energy differences,[36] an effective nuclear charge Z_* also occurs, which was given the value proposed by SLATER.[3] Here, the most appropriate choice of Z_* will be important. A hydrogen-like $3d$-wave function with $Z_* = 4$ has $r_{max} = 1{\cdot}18$ Å, while Ti^{+3} is assumed to have the radius 0·7 Å. This special case of chemical entities being smaller than known from atomic spectroscopy demonstrates the uncertainty of quantitative crystal field calculations, except of the group-theoretically derived ratios between the energy differences.[28, 30, 35, 37]

It would be of great interest to find the wave-functions of the electrons of a metal ion in a potential box, representing the repulsion from the electron clouds of the neighbouring atoms. The relatively small radius of the metal ion and some features of the absorption spectra of compounds might thus be explained. The highly different ionization potentials in vacuo (where only neutral atoms are stable at room temperature) and in aqueous solution must be treated by more macroscopic methods, taking into account the polarization of solvent molecules around the central ion. As an empirical rule, it will be possible for a metal to attain at least the oxidation state +1, if the first ionization potential in vacuo is less than 10 eV (= 80,700 cm^{-1} = 230 kcal/mole), and at least +2 or +3, if the second and the third ionization potentials are less than 20 eV and 30 eV, respectively. The only known exception from this rule (excluded deviations less than 1 eV) is the anomalously small hydrogen ion. Since there is only a two volt potential difference between evolving hydrogen or oxygen molecules from water, the hydration must stabilize the metal ions to a similar amount for the same oxidation state (cf. the investigations by LATIMER[38]). This

[30] F. E. ILSE and H. HARTMANN, *Z. Naturforschg.*, **6a**, 751 (1951).
[31] J. S. VAN SANTEN and J. S. VAN WIERINGEN, *Rec. Trav. chim. Pays-Bas*, **71**, 420 (1952).
[32] L. E. ORGEL, *J. Chem. Phys.*, **23** (1955)
[33] J. OWEN, *Proc. Roy. Soc.*, **A227**, 183 (1955).
[34] C. J. BALLHAUSEN, *K. Danske Vidensk. Selsk. Mat-fys. Medd.*, **29**, Nos. 4 and 8 (1955).
[35] C. J. BALLHAUSEN and C. KLIXBÜLL JØRGENSEN, *K. Danske Vidensk. Selsk. Mat-fys. Medd.*, **29**, No. 14 (1955).
[36] F. E. ILSE and H. HARTMANN, *Z. phys. Chem.*, **197**, 239 (1951).
[37] C. KLIXBÜLL JØRGENSEN, *Acta Chem. Scand.*, **9**, 116 and 715 (1955).
[38] W. M. LATIMER, *J. Chem. Phys.*, **23**, 90 (1955).

VOL. 1 1955

stabilization is *inter alia* proportional to external charge $Z_0 - 1$ and must increase slightly with Z_0 due to smaller ionic radii. The usual formation constants for complexes correspond to much smaller changes in free energy, expressing the difference between bonding of water and of the other ligands to the metal ion.[39]

CONCLUSIONS

1. Just as LANDÉ found for *p*-electrons, ζ_{nl} is roughly proportional to Z_0^2 in *d*-shells and *f*-shells. If ζ_{nl} is defined to be proportional to $(Z - \sigma)^4$, the screening constant σ is highly dependent on Z_0 and seems to have no physical significance. Analogous results are valid for the parameters of electrostatic interaction.

2. The behaviour of *d*- and *f*- shells is very similar for the first few electrons, and the screening by internal electrons is of equal importance. The number of maxima, $(n - l)$, of the radial wave function determines several characteristic properties of the transition groups.

3. The higher oxidation states of 4*d*- and 5*d*-elements, compared to 3*d*-elements, and of 5*f*-compared to 4*f*-elements, are explained by means of atomic spectroscopy, as well as the increased tendency towards lower total spin moments in the 4*d*- and 5*d*-complexes.

ACKNOWLEDGEMENTS

I am very much indebted to Professor JANNIK BJERRUM for valuable discussions. Further, I thank Professor ARTHUR W. ADAMSON, University of Southern California, for several interesting comments.

[39] J. BJERRUM, Metal Ammine Formation—Thesis, Copenhagen 1941.

J. Inorganic and Nuclear Chemistry, 1955, Vol. 1, pp. 309–312. Pergamon Press Ltd., London

A CUBIC FORM OF URANIUM TRIOXIDE

By E. WAIT
Atomic Energy Research Establishment, Harwell, Didcot, Berks

(*Received* 7 *March* 1955)

Abstract—The crystal structure of a uranium oxide phase of composition $UO_{2.82}$ has been determined by X-ray powder diffraction techniques using a Guinier-type focusing camera. The unit cell is cubic with $a = 4{\cdot}138 \pm 0{\cdot}005$ kX. A uranium atom is located at (000) and oxygens at ($\frac{1}{2}$00), (0$\frac{1}{2}$0), and (00$\frac{1}{2}$) with some anion vacancies. The compound is isostructural with ReO_3. The U—O bond distance of 2·073 Å agrees with that predicted by ZACHARIASEN for a bond strength $S = 1$.

VOL.
1
1955

THE formation of non-stoichiometric uranium oxide phases as a consequence of the easy variability of valency of uranium has been observed for compounds of ideal composition UO_2, U_3O_8, and UO_3. In each case, the crystal structure is essentially unchanged over a limited range of composition near the ideal.[1]

The compound to be described has the composition $UO_{2.82}$. It is, however, convenient to describe its crystal structure in terms of the ideal UO_3.

A number of different crystalline modifications of uranium trioxide have been reported,[2, 3, 4] but in only one case has a detailed crystal structure analysis been carried out.[5] Many methods of preparation are reputed to give an amorphous product, and most of the work in this field has been handicapped by the small crystallite size of the preparations, which results in very diffuse X-ray diffraction patterns. A considerable improvement on the ordinary Debye-Scherrer powder photograph may be obtained by means of a Guinier-type focusing powder camera using monochromatic radiation.[6] The work to be described was possible only with the aid of such a camera.

EXPERIMENTAL

Preparation and Analysis. The specimen examined was prepared by the thermal decomposition of one of several available crystalline modifications of uranium trioxide monohydrate in air at 415°C. It was deep brick-red in colour.

Oxygen in excess of $UO_{2.00}$ was determined by reducing a weighed sample of the material in carbon monoxide at 800°C and measuring the carbon dioxide produced by a gas volumetric method. The composition as determined by this method corresponded to a formula $UO_{2.82}$. Attempts to prepare samples with compositions nearer to the ideal UO_3 by decomposing the hydrate at lower temperatures were unsuccessful. The hydrate had lost no appreciable amount of water after heating for one hour at 375°C.

Morphology and Optics. Under the microscope in unpolarized light, the trioxide appeared to consist of tablets about 20 μ in length. This was, however, the habit of the monohydrate precursor. A more detailed examination under a linear magnification of 1000 showed the pitted surface and translucent appearance characteristic of a mass of disordered crystallites. The bulk of the material appeared to be optically isotropic. A few fragments of birefringent material, different in colour from the main phase, were present and may have been formed by the rehydration of the anhydrous oxide.

(1) J. J. KATZ and E. RABINOWITCH, p. 227, *The Chemistry of Uranium*, National Nuclear Energy Series, McGraw Hill, New York (1951).
(2) I. SHEFT, S. FRIED, and N. R. DAVIDSON, *J. Amer. Chem. Soc.*, **72**, 2172 (1950).
(3) J. J. KATZ and D. M. GRUEN, *J. Amer. Chem. Soc.*, **71**, 2106 (1949) and **73**, 1475 (1951).
(4) P. PERIO, *Bull. Soc. Chim. Fr.*, p. 776 (1953).
(5) W. H. ZACHARIASEN, *Acta Cryst.*, **1**, 265 (1948).
(6) R. W. M. D'EYE, Harwell Report A.E.R.E. C/R 1524 (1954).

X-ray Photography. A thin layer of the oxide was mounted on a base of "Sellotape" and protected from atmospheric moisture by a further layer of the same material. The resulting "sandwich" was mounted in the specimen holder of the Guinier camera. Before processing, a scale graduated at 0·1 mm intervals was printed along one edge of the film so as to correct for film shrinkage errors.[6]

The X-ray diffraction photograph obtained after an exposure of twenty-four hours using CuK_α radiation is reproduced in Fig. 1.

THE DETERMINATION OF THE STRUCTURE

The most prominent lines on the photograph are very diffuse and correspond to a crystallite size of less than 0·1 μ. For comparison purposes, the diffraction photograph of aluminium foil is also presented in Fig. 1 as an example of the type of line to be expected from a well crystallized specimen. The very faint sharp lines on the trioxide photograph may be attributed to the hydrate phase which was noticed in the optical examination. They are also present in the diffraction pattern of the monohydrate precursor.

The lines of the trioxide phase may be indexed on the basis of a simple cubic cell with the cell constant:—

$$a_0 = 4{\cdot}138 \pm 0{\cdot}005 \text{ kX.}$$

$$= 4{\cdot}146 \pm 0{\cdot}005 \text{ Å.}$$

The calculated and observed values of $\sin^2\theta$ are compared in Table 1.

TABLE 1.—CALCULATED AND OBSERVED VALUES OF $\sin^2\theta$ AND THE REFLECTION INTENSITIES

hkl	$\sin^2\theta_{obs}$	$\sin^2\theta_{calc}$	I_{obs}	$I_c(1)$	$I_c(2)$	$I_c(U)$
100	0·0346	0·0346	S	27	19	23
110	0·0691	0·0691	M	15	15	18
111	0·1027	0·1036	W−	4	10	7
200	0·1385	0·1382	W	5	5	4
210	0·1728	0·1728	M	11	8	10
211	0·2069	0·2073	M	7	7	8
220	0·2740	0·2765	VW	3	3	3
300 and 221	0·3113	0·3110	W−	7	5	6
310	0·3452	0·3456	VW	3	3	4
311	0·3798	0·3802	VW	2	5	3

The volume of the unit cell $V_c = 71{\cdot}27$ Å^3. This corresponds to a cell content of one formula unit UO_3 on the reasonable assumption of an oxygen packing volume of 20 Å^3. The calculated density $\rho_c = 6{\cdot}663$ g/cc.

The uranium atoms must lie in positions of one-fold and the oxygens in positions of three-fold multiplicity, respectively. In the cubic system there are one-fold positions at (000) and $(\frac{1}{2}\frac{1}{2}\frac{1}{2})$ and three-fold positions at $(\frac{1}{2}00)$, $(0\frac{1}{2}0)$, and $(00\frac{1}{2})$, and at $(0\frac{1}{2}\frac{1}{2})$, $(\frac{1}{2}0\frac{1}{2})$, and $(\frac{1}{2}\frac{1}{2}0)$. These latter correspond to the midpoints of the cube edges and faces respectively. The uranium atom may be arbitrarily assigned to the (000) position by a suitable choice of origin. There are then two alternative sets of three-fold positions for the oxygens.

The values of the X-ray intensities to be expected in the two cases were now calculated.

VOL.
1
1955

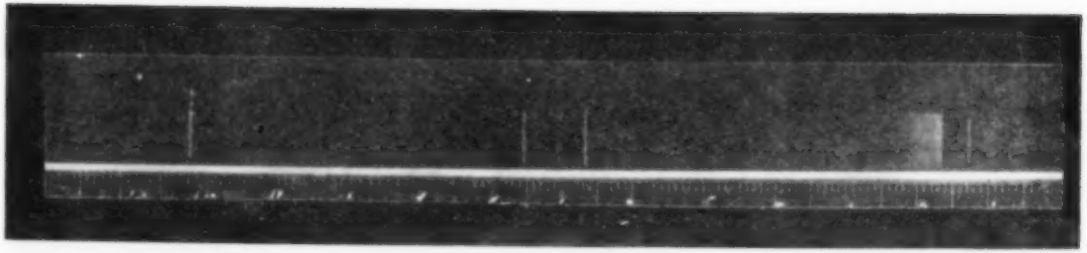

(i)

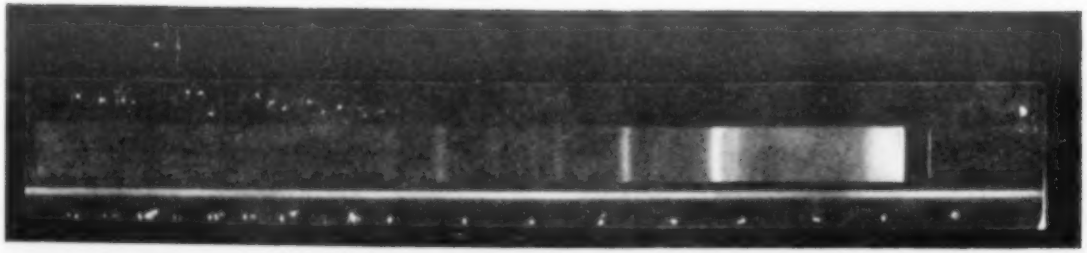

(ii)

Fig. 1. UO_3 and AL

We have

$$I \propto ALp\,|F|^2$$

where I is the intensity, A the absorption factor, L the combined Lorentz and polarization factor, p the number of crystal planes co-operating in a given reflection, and F the structure factor. The constant of proportionality is independent of the Bragg angle θ.

The absorption factor A was assumed to be near unity for the thin powder specimen used. The Lorentz-polarization factor used was the approximate form quoted by D'EYE.[6] The simplified structure factors for the two sets of atomic positions considered, are set out in Table 2 for the observed reflections.

TABLE 2.—SIMPLIFIED STRUCTURE FACTORS FOR THE ALTERNATIVE SETS OF ATOMIC POSITIONS

hkl	1	2
100	$f_u + f_o$	$f_u - f_o$
110	$f_u - f_o$	$f_u - f_o$
111	$f_u - 3f_o$	$f_u + 3f_o$
200	$f_u + 3f_o$	$f_u + 3f_o$
210	$f_u + f_o$	$f_u - f_o$
211	$f_u - f_o$	$f_u - f_o$
220	$f_u + 3f_o$	$f_u + 3f_o$
300	$f_u + f_o$	$f_u - f_o$
221	$f_u + f_o$	$f_u - f_o$
310	$f_u - f_o$	$f_u - f_o$
311	$f_u - 3f_o$	$f_u + 3f_o$

The atomic scattering factors used were those of THOMAS and FERMI for uranium[7] and of MCWEENEY for oxygen.[8] No correction was made for the effects of thermal vibration.

In Table 1, the observed intensities are compared with those calculated for the two alternative sets of oxygen positions and with the values given by the uranium alone with no oxygen contribution. The overall agreement, and in particular the relative intensities of 111 and 200, are best represented by the first set of intensities, from oxygen positions ($\frac{1}{2}00$), ($0\frac{1}{2}0$), and ($00\frac{1}{2}$). Hence we may conclude that the cell has uranium at (000) and oxygens at ($\frac{1}{2}00$), ($0\frac{1}{2}0$), and ($00\frac{1}{2}$).

DISCUSSION

Fig. 2 is a diagram of the proposed structure in isometric projection.

Each uranium is octahedrally co-ordinated by oxygen and each oxygen linearly by uranium. The compound is isostructural with rhenium trioxide.[9] A feature of this structure is the "hole" at ($\frac{1}{2}\frac{1}{2}\frac{1}{2}$). In the related perowskite structure ABX_3 this position is occupied by the larger cation A.

The bond length U—O is equal to $a/2 = 2{\cdot}073$ Å. This is not significantly different from the value 2·08 Å obtained by ZACHARIASEN for the U—O_1 distance in

[7] "Internationale Tabellen zur Bestimmung von Krystallstrukturen." Bd. II p. 571. Borntraeger, Berlin (1935).
[8] R. MCWEENEY, *Acta Cryst.*, **4**, 513 (1951).

hexagonal UO_3 (*loc. cit.*). The close agreement between these bond lengths is consistent with ZACHARIASEN's observation[10] of a monotonic increase in bond length with decreasing bond strength over a series of oxygen compounds of hexavalent uranium. Each oxygen forms two bonds only to adjacent uranium, so that the bond strength S = 1 as in the primary U—O_1 bonds in hexagonal UO_3.

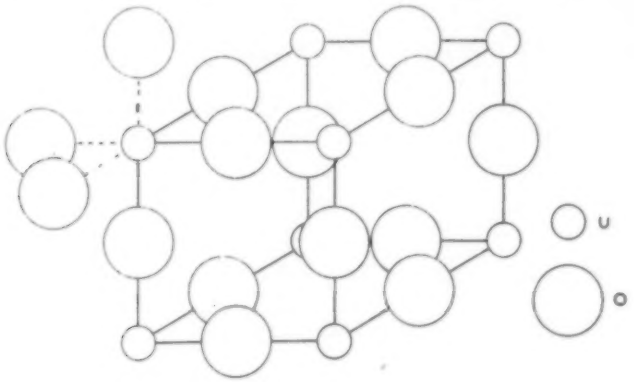

FIG. 2.

The chemical analyses indicate an oxygen content corresponding to the formula $UO_{2.82}$. The structure is one of considerable rigidity, and it would easily be possible to remove an occasional oxygen at random without causing the collapse of the lattice. The net charge balance would be maintained by a diminution of the average uranium valency.

ACKNOWLEDGEMENTS

The author is greatly indebted to Drs. R. W. M. D'EYE and J. K. DAWSON for many valuable discussions.

[9] R. W. G. WYCKOFF, "Crystal Structures," Vol. I. Interscience Publishers Inc., New York, 1948.
[10] W. H. ZACHARIASEN, *Acta Cryst.*, **7**, 795 (1954).

J. Inorganic and Nuclear Chemistry, 1955, Vol. 1, pp. 313–316. Pergamon Press Ltd., London

DICYCLOPENTADIENYLDIIRONTETRACARBONYL

By B. F. HALLAM, O. S. MILLS, and P. L. PAUSON
The Staveley Laboratories, Department of Chemistry, University of Sheffield

(*Received* 14 *March* 1955)

Abstract—It has been shown by X-ray crystallographic examination that the product obtained from iron pentacarbonyl and dicyclopentadiene possesses a centrosymmetric structure with the formula $(C_5H_5Fe)_2(CO)_4$ and with an Fe—Fe bond. Analytical evidence in support of the new formulation is given.

VOL. 1 1955

THE preparation of ferrocene directly from cyclopentadiene and iron carbonyl has been reported.[1] It has become known that this process has been used since 1952 in several industrial laboratories in a modified form in which the purple intermediate cyclopentadienyl iron carbonyl is isolated. The first published information concerning the latter compound is contained in two communications by COTTON and WILKINSON[2] in which the compound is referred to as $(C_5H_5Fe)_2(CO)_5$, although no preparative method or analytical data are given.

We were able to prepare the compound in satisfactory yield by heating a mixture of iron pentacarbonyl and dicyclopentadiene. Good crystals of the product could be obtained from ligroin solution. When these were subjected to X-ray examination, to determine the detailed structure, it soon became evident that the above formulation must be incorrect.

The crystals are monoclinic with space group $P2_1/c$ ($a = 7{\cdot}0$ A; $b = 12{\cdot}4$ A; $c = 7{\cdot}9$ A (all $\pm 0{\cdot}1$ A); $\beta = 108\frac{1}{4}^\circ \pm \frac{1}{4}^\circ$) and their density is $1{\cdot}77 \pm 0{\cdot}01$ g-cc^{-1}. It follows that there are two molecules per unit cell, that each molecule must possess a centre of symmetry, and that the molecular weight is approximately 357. The two latter deductions are clearly incompatible with the formula $(C_5H_5Fe)_2(CO)_5$ and suggest the alternative $(C_5H_5Fe)_2(CO)_4$.

While this work was in progress, Dr. G. WILKINSON kindly sent us a manuscript copy of his paper[3] containing the detailed evidence for his formulation. This is largely based on the magnetic data and apparently supported by analytical and molecular weight determinations. While we have been able to confirm that the compound is diamagnetic, this finds an alternative explanation in the presence of an iron–iron bond. This is clearly evident, even at this stage, from the X-ray work which shows the two iron atoms to be 2·5 A apart—a distance close to that observed in iron enneacarbonyl.[4]

We have now obtained analytical evidence in excellent agreement with the tetracarbonyl formulation shown at top of page 309.

The Van't Hoff *i*-factor of a solution of the compound in sulphuric acid has been measured by Dr. J. A. LEISTEN of this department. An immediate value of 3 (corresponding to the uptake of two protons per molecule) is obtained when calculated on

(1) G. WILKINSON, P. L. PAUSON, and F. A. COTTON, *J. Amer. Chem. Soc.* **76**, 1970 (1954).
(2) F. A. COTTON and G. WILKINSON, *Z. Naturforschung* **9b**, 417, 453 (1954).
(3) T. S. PIPER, F. A. COTTON, and G. WILKINSON, *J. Inorg. Nucl. Chem.*, **1**, 165 (1955)
(4) H. M. POWELL and R. V. G. EWENS, *J. Chem. Soc.* 286 (1939).

	Carbon %	Hydrogen %	Oxygen %	Iron %	Mol. Wt. in C_6H_6	Mol. Wt. X-ray
$(C_5H_5Fe)_2(CO)_5$ requires	47·2	2·6	20·9	29·25	382	382
WILKINSON *et al.*[3]	47·6	2·8	—	29·2	395	—
$(C_5H_5Fe)_2(CO)_4$ requires	47·5	2·8	18·1	31·6	354	354
Our work	47·4 47·5	3·2 3·1	18·5	31·8 31·2 31·3 31·2	357 365 347	357 ± 5

the basis of a molecular weight of 354. The stability to concentrated sulphuric acid is in striking contrast to the behaviour of the three iron carbonyls which rapidly evolve carbon monoxide. The *i*-factor slowly increases to a maximum value of approximately 10 as a result of oxidation of the molecule by the sulphuric acid. This oxidation has been studied under different conditions by WILKINSON,[3] who has isolated the product $(C_5H_5Fe(CO)_2)^+$ in the form of various "salts," notably the chloride. We have repeated this oxidation quantitatively using pure oxygen gas in a closed system. Under these conditions the uptake of oxygen was almost complete after two hours, and after sixteen hours corresponded (within the limits of experimental error) accurately to the absorption of one half molecule of oxygen per molecule of iron compound. The volume of the remaining gas did not decrease measurably when allowed to stand over an alkaline silver pyridinium chloride solution,[5] showing the absence of carbon monoxide. These facts are in good agreement with the formulation of the reaction as:

$$(C_5H_5Fe)_2(CO)_4 + \tfrac{1}{2}O_2 + H_2O = 2(C_5H_5Fe(CO)_2)^+ + 2HO^-$$

whereas $(C_5H_5Fe)_2(CO)_5$ would evolve two volumes of carbon monoxide for every volume of oxygen absorbed.

The reverse reaction also becomes possible, and we have isolated some dicyclopentadienyldiiron tetracarbonyl from the reaction of cyclopentadienyliron dicarbonyl chloride with sodium phenylacetylide.

By employing hydrogen bromide in the oxidation in place of the hydrogen chloride we have prepared the bromide $C_5H_5Fe(CO)_2Br$, and brown crystals of the corresponding iodide are obtained by refluxing the chloride with potassium iodide in acetone. These show the expected increase in reactivity over the chloride, reacting rapidly with, e.g., silver nitrate.

The chloride and bromide are isomorphous, crystallizing from ligroin in the orthorhombic system, space group $P2_12_12_1$ with four molecules in the unit cell. The detailed work on the crystal structure of these halides and on dicyclopentadienyldiiron tetracarbonyl is being continued by one of us (O. S. M.) and will be published in full

(5) W. MANCHOT and O. SCHERER, *Ber.* **60**, 326 (1927).

in *Acta Crystallographica*. We already have good reason to believe, however, that the latter substance is correctly represented as:

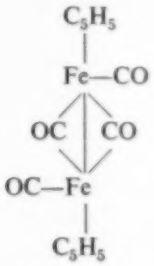

In this formulation the iron atoms together with the two bridging carbonyl groups may be considered to define a plane with which the planes of the cyclopentadiene rings as well as the (nonbridging) Fe—C—O bonds are approximately at right angles. The presence of two bridging and two nonbridging carbonyl groups is in excellent agreement with both the position and intensities of the carbonyl stretching frequencies in the infrared spectrum.[3] That the two five-membered rings must possess the staggered configuration as in ferrocene[6] follows from the presence in the molecule of a centre of symmetry.

Our investigations of the interesting transformation of dicyclopentadienyldiiron tetracarbonyl to ferrocene[3] and its other reactions are continuing.

EXPERIMENTAL

Preparation—The following method is much simpler than the published method[3] and gives consistently twice the yield.

A mixture of dicyclopentadiene (70 g) and iron pentacarbonyl (15 g) is heated under reflux in an oilbath maintained at 145–150°C for three hours. The mixture is cooled to room temperature and the product is filtered and recrystallized from methanol or aqueous pyridine (yield: 8·1 g). Dicyclopentadiene is recovered from the filtrate by vacuum distillation. For analysis the product was further crystallized from aqueous pyridine and dried in a vacuum over phosphorus pentoxide; m.p. 192° (uncorr.).

When iron ennea- or dodecacarbonyls were reacted with dicyclopentadiene under the same conditions the same product was formed, but in yields of only 5 and 2 per cent respectively.

Analysis—Attempted dissolution of the compound in nitric acid was accompanied by such violent reaction, that loss of material frequently could not be avoided and very variable results were obtained. For iron determination the compound was therefore heated in perchloric acid until completely dissolved. The solution was then evaporated to small bulk, diluted, and iron precipitated as hydroxide and ignited to Fe_2O_3 in the usual manner.

Molecular Weights—These were carried out in "ANALAR" benzene with careful exclusion of atmospheric oxygen, which causes rapid decomposition. Even under these conditions the solutions are not stable and measurements had to be made rapidly. The figures given in the above table are three consecutive values obtained with solutions containing 0·2008, 0·4006, and 0·5985 g of solute respectively in 17·5 g benzene. The molal depression constant (5·07°) for the sample of benzene used was determined with pure naphthalene as solute.

The authors wish to thank Dr. J. A. LEISTEN for permission to quote his cryoscopic measurements, the B.S.A. Group Research Centre for the kind loan of a Weissenberg

(6) (*a*) P. F. EILAND and R. PEPINSKY, *J. Amer. Chem. Soc.* **74**, 4971 (1952).
(*b*) J. D. DUNITZ and L. E. ORGEL, *Nature* **171**, 121 (1953).
(*c*) W. PFAB and E. O. FISCHER, *Z. anorg. Chem.* **274**, 317 (1953).

VOL. 1 1955

camera, and the Mond Nickel Company for the gift of a sample of iron pentacarbonyl. They are also grateful to the University of Sheffield for a grant from the Research Fund towards X-ray apparatus and the award of a Henry Ellison Fellowship to B. F. H.

Added in proof:

We have recently been informed by Dr. G. WILKINSON that, as a result of independent X-ray investigation by Dr. D. P. SHOEMAKER, he has abandoned his original formulation. His revised paper[3] therefore contains analytical data in agreement with the correct formula, whereas the values quoted in the above table are taken from his original manuscript. No explanation for the earlier results has been offered.

J. Inorganic and Nuclear Chemistry, 1955, Vol. 1, pp. 317–325. Pergamon Press Ltd., London

THE PREPARATION OF SODIUM AND CALCIUM ALUMINUM HYDRIDES[1]

By A. E. Finholt, Glen D. Barbaras, Geraldine K. Barbaras, Grant Urry, Thomas Wartik, and H. I. Schlesinger

The George Herbert Jones Laboratory of the University of Chicago
and St. Olaf College

(*Received* 16 *March* 1955)

Abstract—The difficulties encountered in the preparation of sodium and calcium aluminum hydrides and the methods of overcoming them are described, as are some of the properties of these compounds.

VOL.
1
1955

Sodium aluminum hydride was first prepared by the reaction between sodium hydride and aluminum bromide at room temperature in the presence of dimethyl ether as a solvent.[2] Although this procedure gave a product of satisfactory purity, it has numerous disadvantages, for which reason publication was deferred. Thus the yield, in terms of aluminum bromide used, approximated only about 60 per cent. Furthermore, it is inconvenient and somewhat hazardous to carry out the reaction, and to filter the reaction product under the high vapour tension of dimethyl ether at room temperature, in the glass vessels available for small-scale laboratory preparations. For large-scale production for which metal apparatus could be employed, the use of aluminum bromide is undesirable because of its cost. The analogous procedure using aluminum chloride gave unsatisfactory yields and impure products.

Calcium aluminum hydride was prepared similarly, i.e., by the reaction of calcium hydride on aluminum bromide in dimethyl ether. The product was an etherate, $Ca(AlH_4)_2 \cdot O(CH_3)_2$. Not only did the procedure have the disadvantages mentioned above, but the etherate obtained was only moderately pure.

Some improvement in the preparation of the calcium salt was achieved by evaporating the dimethyl ether from the reaction mixture before the latter was filtered. The calcium aluminum hydride was then extracted from the residue by tetrahydrofuran and isolated by evaporation of the filtrate. Aluminum chloride instead of the bromide had to be used for this modification of the procedure, since calcium bromide is sufficiently soluble in tetrahydrofuran seriously to contaminate the calcium aluminum hydride. The latter is obtained as a moderately pure etherate of the formula $Ca(AlH_4)_2 \cdot O(CH_2)_4$.[3] The corresponding procedure for the sodium salt has not been carried out successfully.

Numerous modifications of the original procedure for the preparation of sodium aluminum hydride have been studied to avoid the use of dimethyl ether, and to make

[1] A portion of this paper is taken from a thesis presented by Glen D. Barbaras to the Department of Chemistry of the University of Chicago in part fulfilment of the requirements for the Ph.D. degree.

[2] Final Report for the period July 1, 1946, to June 30, 1947, on contract N6ori-20 (NRL Report No. C3147). The procedure is also described in U.S. patent No. 2,576,311, which deals primarily with the use of metal aluminum hydrides as reducing agents.

[3] In this procedure the calcium salt is apparently first produced as a dimethyl etherate. The addition of tetrahydrofuran drives off all of the dimethyl ether. Evidently the tetrahydrofuranate is more stable than the dimethyl etherate. A successful procedure employing tetrahydrofuran as the liquid medium in the preparation of calcium aluminum hydride has been described by W. Schwab and K. Wintersberger, *Z. Naturforsch* **8b**, 690 (1953).

possible the substitution of aluminum chloride for the bromide. Most of the modifications involved the use of tetrahydrofuran as the reaction medium, but other solvents were tested. These included diethyl ether, methyl ethyl ether, methyl isopropyl ether, the dimethyl ethers of ethylene glycol, of triethylene glycol, and of tetraethylene glycol, etc. In diethyl, methyl ethyl, and methyl isopropyl ethers, in which the desired sodium salt appears to be insoluble, no reaction was observed; none of the other solvents proved superior to tetrahydrofuran, and most of them had less favorable physical properties (e.g., volatility).

In the course of the investigation it became evident that at least one source of the difficulties encountered was the slowness of the reactions involved. Because of this slowness, cleavage of the solvents occurred and gave rise, not only to decreased yields and purity of the end product, but also to the formation of gelatinous deposits which made filtration difficult and sometimes impossible. Another possible effect of the slowness of the reactions may be that some of the aluminum hydride, formed as an intermediate product, polymerizes and precipitates out of solution.

Presumably the formation of metal aluminum hydrides occurs in steps which may be represented by the overall equations:[4]

$$3MH + AlX_3 \rightarrow 3MX + AlH_3 \quad (1)$$

$$AlH_3 + MH \rightarrow MAlH_4 \quad (2)$$

Reaction (1) is slow in the case of sodium hydride; furthermore, aluminum chloride reacts more slowly with either sodium or lithium hydrides than does aluminum bromide.[5] The slowness of the overall reaction:

$$4NaH + AlCl_3 \rightarrow NaAlH_4 + 3NaCl \quad (3)$$

is, therefore, probably due largely to the slowness of reaction (1), especially when aluminum chloride is the halide used.

Of the numerous modifications of the reaction investigated by us, only two are described here. The first is one of several attempts to accelerate reaction (1);[6] the second is a procedure which avoids step (1) entirely.

The only procedure for accelerating step (1) which appeared at all effective consisted of the addition of small amounts of lithium bromide to mixtures of aluminum chloride, with suspensions of sodium hydride in tetrahydrofuran. This procedure was based on the hypothesis that ions of the type, AlX_4^- (in which X is a halide) react more rapidly with sodium hydride than does aluminum chloride.[7] In the absence of lithium bromide, the reaction produced either no sodium aluminum hydride or only small yields of impure products. The mixtures containing lithium bromide invariably gave moderate amounts of fairly pure sodium aluminum hydride, as is shown in the experimental part.

[4] These equations do not represent mechanisms. Intermediates such as AlX_yH_{3-y} or ions such as $(AlX_yH_{4-y})^-$ are probably involved.

[5] There is some indirect evidence that the presence of aluminum chloride also retards the reactions of aluminum hydride.

[6] Experiments to accelerate the reaction by mechanical means, e.g., by increasing the rate of stirring or continuous grinding of the sodium hydride, were unsuccessful. Ultra-high-speed stirring was not tested.

[7] Both sodium chloride and lithium chloride, like lithium bromide, are soluble in solutions of aluminum chloride in tetrahydrofuran, but lithium bromide is the most soluble, and was used for that reason. The chlorides proved much less, if at all, effective.

The procedure nevertheless proved not to be a satisfactory one. The reactions were still relatively slow, and still led to cleavage of the tetrahydrofuran. The filtration difficulty was again so great that it was impossible in most cases to obtain reliable data about the yields. Attention is furthermore called to the fact that the partial success attending the use of lithium bromide cannot be considered as evidence of the correctness of the hypothesis on which the use was based.

The method which avoids reaction (1) entirely, and which ultimately led to a satisfactory means of preparing sodium aluminum hydride, is based on the sequence of reactions[8]

$$3NaAlH_4 + AlCl_3 \rightarrow 3NaCl + 4AlH_3 \quad (4)$$

$$4AlH_3 + 4NaH \rightarrow 4NaAlH_4 \quad (5)$$

Both of these reactions are rapid when carried out in tetrahydrofuran and with pure materials. Furthermore, the sequence represents a production of sodium aluminum hydride, since from 3 moles of the compound 4 are theoretically obtainable.

VOL. 1 1955

In principle this sequence might be achieved by adding to a mixture of an excess of sodium hydride with a small amount of sodium aluminum hydride a quantity of aluminum chloride just enough to convert the sodium aluminum hydride to aluminum hydride. After the latter had then reacted with some of the excess sodium hydride to produce fresh sodium aluminum hydride, a second portion of aluminum chloride, 4/3 as large as the first, could then be added. Because reaction (4) is very rapid, the procedure avoids contact of aluminum chloride with the sodium hydride. Repetition of the steps described could lead to the production of any desired amount of sodium aluminum hydride.

In practice, however, the reaction became slower with each addition of aluminum chloride, and the formation of gummy deposits and the filtration difficulties previously mentioned were again encountered. It seems likely, though not proven, that the cause is the coating of the solid sodium hydride by sodium chloride, which is precipitated in very finely divided form by reaction (4).

Whatever the cause, the difficulty is overcome by physically separating steps (4) and (5), i.e. by treating a solution of sodium hydride free from solid sodium hydride with an equivalent amount of aluminum chloride (or slightly less), and then adding the sodium hydride. It is not necessary to filter the mixture before the addition of the sodium hydride, although it may be desirable to do so if the amount of sodium chloride is large.[9] After the addition of the sodium hydride and completion of the reaction, the mixture is filtered. The filtrate may then be evaporated to isolate the sodium aluminum hydride, or it may be treated with an enlarged amount of aluminum chloride to repeat the cycle of reactions. Yields of 98 per cent of the theoretical, and purity of 95 per cent, may be attained by the procedure, which is described in detail in the experimental part.

If no sodium aluminum hydride is on hand to start the cycle, it may be prepared from lithium aluminum hydride, which is commercially available. All that is necessary is to substitute lithium aluminum hydride for the corresponding sodium salt in reaction (4) and then to proceed with reaction (5).[10]

[8] A. E. Finholt, A. C. Bond, Jr., and H. I. Schlesinger, *J. Amer. Chem. Soc.* **69**, 1199 (1947).

[9] In terms of the explanation suggested above, one must make the further, reasonable assumption that the sodium chloride coats the hydride only when the chloride is freshly precipitated on the hydride.

[10] The first portion of sodium aluminum hydride may, of course, be made from sodium hydride and aluminum bromide in dimethyl ether, but this procedure is much less convenient.

More important is the fact that lithium aluminum hydride may be readily made from the sodium salt. The advantage of doing so is seen by a comparison of equation (6) with equations (7) and (8):

$$4LiH + AlCl_3 \rightarrow 3LiCl + LiAlH_4 \quad (6)$$

$$\begin{cases} \frac{3}{4}NaAlH_4 + \frac{1}{4}AlCl_3 \rightarrow \frac{3}{4}NaCl + AlH_3 & (7) \\ AlH_3 + LiH \rightarrow LiAlH_4 & (8) \end{cases}$$

For the manufacture of $\frac{3}{4}$ mole of sodium aluminum hydride, 3 moles of sodium hydride are required. As shown by equations (7) and (8), for conversion of this $\frac{3}{4}$ mole of sodium aluminum hydride to one mole of lithium aluminum hydride, one mole of lithium hydride is needed. In other words, the preparation of lithium aluminum hydride from the corresponding sodium salt requires 3 moles of sodium hydride plus only 1 mole of lithium hydride per mole of lithium aluminum hydride, whereas in the direct process (equation (6)) 4 moles of the relatively expensive lithium hydride are needed.

The corresponding procedure has been employed for the preparation of calcium aluminum hydride, but, as shown in the experimental part, has not produced as satisfactory results as have been obtained with the sodium salt.

Properties of Sodium Aluminum Hydride

Sodium aluminum hydride reacts much as does the corresponding lithium salt, except that it is not soluble in diethyl ether and that it is somewhat more stable thermally and, in some respects, somewhat less reactive. It is soluble in tetrahydrofuran and in the dimethyl ethers of ethylene glycols. When the dry salt is slowly heated, barely detectable decomposition occurs at temperatures between 145 and 183°C. At the latter temperature the solid begins to melt, but decomposition does not become rapid till about 230–240°C. At these temperatures the decomposition occurs according to the equation:

$$NaAlH_4 \rightarrow NaH + Al + 1.5H_2 \quad (9)$$

As an example of the reactivity of sodium aluminum hydride, one may cite the fact that it reacts much more slowly than does lithium aluminum hydride with boron trichloride or trifluoride in the presence of diethyl ether to generate diborane. The difference may be largely due to a difference in solubility. Treatment of the sodium salt with liquid ammonia or liquid isopropylamine generates a quantity of hydrogen gas corresponding to complete replacement of the hydrogen of the compound by amine groups, i.e., by NH_2 or $(CH_3)_2CHNH$ groups.

The behavior of sodium aluminum hydride toward organic compounds will be described in a forthcoming paper by A. E. FINHOLT.

EXPERIMENTAL

Materials

Sodium hydride was first obtained from the du Pont Company, later from Metal Hydrides, Inc., from which calcium hydride was also obtained. Lithium hydride was a product of the Maywood Chemical Co.; all of the hydrides were in powdered form of better than 100-mesh fineness. The aluminum halides were commercial samples resublimed *in vacuo*. Dimethyl ether was freed from carbon dioxide by condensing a sample (MATHESON) in a small bulb and pumping on it at −80°C for

a short time. Tetrahydrofuran was a technical sample purified by distillation from sodium or sodium hydride, or from lithium aluminum hydride and lithium hydride. The lithium halides were reagent-grade samples dried by heating them *in vacuo*.

Preparation of Sodium Aluminum Hydride in Dimethyl Ether

A typical preparation of sodium aluminum hydride from sodium hydride and aluminum bromide in dimethyl ether was as follows. After the apparatus (Fig. 1) had been evacuated and filled with nitrogen, 4.470 g (16.75 mmoles) of molten aluminum bromide was poured into the reaction bulb, *B*, from a container having a long spout. The apparatus was re-evacuated to remove any hydrogen bromide formed during the transfer, and was refilled with nitrogen. Sodium hydride (3.34 g or 139.5 mmoles)

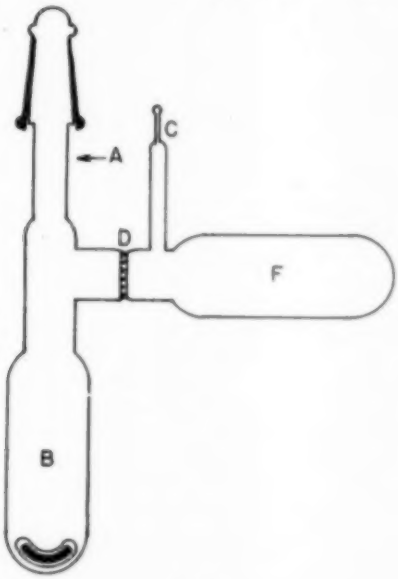

FIG. 1.

was then introduced into *B*. A constriction was then made at *A* to facilitate later sealing of the apparatus. Bulb *B* was cooled with a −196°C bath and evacuated to permit the condensation of an amount of dimethyl ether equal to about 15–20 ml of liquid. It is important that the ether be freed from all but small amounts of carbon dioxide, as described above, since the presence of the latter may give rise to explosions when the reaction product is evaporated.[11]

When the reaction bulb was warmed to −25°C rapid reaction occurred, presumably due to the formation of an etherate of aluminum bromide. Any hydrogen generated was removed with *B* at −196°C, whereupon the apparatus was sealed at *A*. It was then warmed to room temperature and there maintained for about three hours with magnetic stirring. The resulting mixture was filtered through the fritted disk, *D*, into bulb *F*, from which the ether was then recondensed in *B*. After another repetition of this step, the apparatus was connected to the vacuum system through a tube opener and break-off side arm *C*.

Evaporation of the solvent left a white powder weighing 0.54 g, a yield of about 60 per cent based on the aluminum bromide used.[12] Analyses by the usual methods gave the values: Na, 42.1 and 41.8 per cent; Al, 49.2 and 49.1 per cent; H_2, 7.5 per cent; theory for $NaAlH_4$: 42.6, 49.9, and 7.5 per cent, respectively.

[11] GERALDINE BARBARAS, GLEN D. BARBARAS, A. E. FINHOLT, and H. I. SCHLESINGER, *J. Amer. Chem. Soc.* **70**, 877 (1948).

[12] In spite of the fact that only 60 per cent of the aluminum was recovered as sodium aluminum hydride there was no bromine left in the solution or in the final product.

Preparation of Calcium Aluminum Hydride

(a) A preparation involving 2.64 g of aluminum bromide and3.02 g of calcium hydride (85 per cent pure) was carried out in about 25 ml of dimethyl ether, using the apparatus and techniques as for the preparation of sodium aluminum hydride. The product weighed 243.4 mg. It contained 87.3 mg (3.23 mmoles) of aluminum, 58.2 mg (1.45 mmoles) of calcium, and 6.7 mg (0.084 mmole) of bromine, and generated 282 cc (12.6 mmoles) of hydrogen. Assuming that the bromine was present as unchanged aluminum bromide, the aluminum so bound amounted to 0.028 mmole, leaving 3.23 − 0.028 or 3.20 mmoles of aluminum as calcium aluminum hydride. Furthermore, the sum of the calcium, aluminum, bromine, and hydrogen (atomic) was only 164.3 mg, whereas the weight of sample was 243.4 mg. Assuming that the discrepancy is due to retained dimethyl ether, the quantity of the latter was 79.1 g, or 1.71 mmoles. On the assumption made above about the source of the bromine, 0.03 mmole of the ether would have been bound to the aluminum bromide, leaving 1.71 − 0.03 = 1.68 mmoles present in the calcium aluminum hydride. The ratio of constituents in the latter then is $Ca : Al : H : (CH_3)_2O = 1.46 : 3.20 : 12.6 : 1.68 = 0.9 : 2.0 : 7.9 : 1.05$ mmoles, thus corresponding satisfactorily to the formula $Ca(AlH_4)_2 \cdot O(CH_3)_2$. A somewhat purer sample was obtained as described in paragraph (b).

(b) An experiment involving 3.916 g of aluminum chloride, 6.624 g of calcium hydride, and 70 ml of dimethyl ether was carried out as described above, except that the apparatus was opened and the dimethyl ether was distilled away before the reaction mixture was filtered. The fact that eight days of vigorous stirring was required before any noticeable change had occurred (e.g., change in volume of the solid) illustrates the fact that aluminum chloride reacts more slowly than aluminum bromide, the reaction of which was complete in less than two days.

After removal of the dimethyl ether, about 70 ml of tetrahydrofuran was condensed into the reaction vessel, the resulting mixture shaken and then filtered through the fritted disk. Evaporation of the solvent left behind a white powder. A 0.0826-g sample of the latter contained 0.0035 g of hydrogen (generated by hydrolysis), 0.0173 g of calcium, and 0.0240 g of aluminum, a total of 0.0448 g. If the 0.0378 g unaccounted for is assumed to have been retained tetrahydrofuran, the atomic (and molecular) ratios $Ca : Al : H : O(CH_2)_4$ are 1 : 2.07 : 8.14 : 1.2 moles. The result is in satisfactory agreement with the formula $Ca(AlH_4)_2 \cdot [O(CH_2)_4]$, especially if one takes into consideration the fact that the solid was not heated to drive off mechanically retained solvent.

The best yield obtained in several similar experiments was 63.5 per cent, but the results were erratic, probably because it is difficult to extract all of the desired product from the residue left after evaporation of the dimethyl ether. It was noted that addition of a little preformed calcium aluminum hydride to the mixture of calcium hydride and aluminum chloride appeared to accelerate the reaction somewhat.

Reaction of Sodium Hydride with Aluminum Chloride in the Presence of Lithium Bromide and Tetrahydrofuran

Eight experiments were carried out to study the effect of lithium bromide on the reaction between aluminum chloride and sodium hydride in tetrahydrofuran. In all of these a large excess of sodium hydride (from nine- to fifteen-fold the theoretical amount) was used. The amount of lithium bromide was varied from 0.015 to 0.045 mole per mole of aluminum chloride. In each case the reaction mixture was stirred at room temperature under an atmosphere of nitrogen until a small sample of the solution, withdrawn from the reaction vessel, was free from halide. The time required for attaining this condition varied from three to six days. The reaction mixture was then filtered, the filtrate was evaporated to dryness, and the resulting solid was hydrolyzed to determine the amount of hydrogen generated per gram.[12] Judged by this criterion the purity of the products obtained varied from 80 to 85 per cent. Because of the difficulty of filtration (as mentioned in the earlier discussion of this reaction) the yield could be determined in only four of the eight experiments: in these it varied from about 55 to 65 per cent. Such moderately good results were not obtained by this type of procedure without the use of lithium bromide.

[12] The ratio of hydrogen to aluminum was also determined, but the results were considered unreliable, since in a number of cases the ratio exceeded the theoretical value 4. This observation was apparently the result of the precipitation, during hydrolysis, of a white, aluminum-containing but active hydrogen-free solid which could be completely redissolved in acid only with great difficulty.

No relation between the amount of lithium bromide and yield or purity was detected; probably because the smallest amount employed was sufficient to produce the maximum effect. For this reason it seemed unnecessary to report the details of the eight experiments involved.

Preparation of Sodium Aluminum Hydride by Successive Additions of Aluminum Chloride to Sodium Hydride

Increasing portions of a solution of 19 mmoles of aluminum chloride in 30 ml of tetrahydrofuran were added at room temperature to a mixture of 3.65 mmoles of sodium aluminum hydride with 170 mmoles of sodium hydride (a large excess). The first portion of solution contained about 1.1 mmole of aluminum chloride, i.e., about 10 per cent less than required to react with all of the initial sodium aluminum hydride. Each of the six succeeding portions was about 33 per cent larger than the preceding one. Between each of the additions the mixtures were stirred for about forty minutes to allow the aluminum hydride formed to react with sodium hydride.

After all of the aluminum chloride had thus been added, the mixture was subjected to filtration. Even though nitrogen pressure was used, only about one-half of the liquid could be forced through the filter plate. Consequently the total yield could not be determined. Evaporation of the filtrate obtained left a solid which consisted of sodium aluminum hydride of 92 per cent purity, as judged by the amount of hydrogen generated by hydrolysis.

VOL. 1 1955

Preparation of Sodium Aluminum Hydride by the "Cyclic Process"

(a) To a solution of 1.44 g (26.7 mmoles) of sodium aluminum hydride, dissolved in 52 g of tetrahydrofuran, 1.19 g (8.91 mmoles) of aluminum chloride was added. The white precipitate, formed immediately, was removed by filtration, and 3.0 g (125 mmoles) of sodium hydride was added to the solution. After fifteen minutes of agitation the mixture became warm, and remained so for another fifteen minutes. After four hours of stirring the mixture was filtered. All manipulations were carried out under an atmosphere of nitrogen.

The 52 g of filtrate was divided into several portions. From an 11.8-g portion most of the tetrahydrofuran was removed at room temperature *in vacuo*. Hydrolysis of the residue generated 718 cc (S.T.P.) of hydrogen. Sodium was determined in the hydrolysate by use of the flame attachment of a Beckman Model DU Quartz spectrometer.[14] The amount of sodium found in the aliquot was 182 mg (7.91 mmoles), corresponding to an atomic H/Na ratio of 4.05. The amount of hydrogen generated corresponded to a total of 35.43 mmoles of sodium aluminum hydride. Theoretically the initial 26.7 mmoles of the latter should have produced 35.6 mmoles by the procedure used: the yield was, therefore, 99 per cent.

From another portion of the final solution, the solvent was removed by evaporation. The residue was heated for forty-five minutes under nitrogen at 110°C. The purity, as determined by hydrolysis and measurement of the hydrogen generated, was only 87 per cent. Whether the impurity was retained tetrahydrofuran or a product of decomposition of the latter was not ascertained.

(b) A preparation was carried out with very nearly the same quantities of reactants and in the same manner as was the preceding one, except that the sodium chloride precipitated in the first step was not removed by filtration before addition of the sodium hydride. The amount of hydrogen generated by hydrolysis showed that from 27.2 mmoles of sodium aluminum hydride 35.1 mmoles had been obtained, a yield of 96.6 per cent. The H/Na ratio was 4.06. The sodium aluminum hydride was not isolated from the solution.

It was also shown that aluminum chloride may be replaced by aluminum bromide. Since no advantage results therefrom, the experimental data are not further reported herein.

Preparation of Lithium Aluminum Hydride from Sodium Aluminum Hydride

To demonstrate the feasibility of preparing lithium aluminum hydride from the corresponding sodium salt, a tetrahydrofuran solution of aluminum hydride was prepared from sodium aluminum hydride by the addition of aluminum chloride. To a portion of this solution, containing 1.80 g (60.0 mmoles) of the solute in 64 g of the solvent, an excess of powdered lithium hydride (of about 90 per cent purity) was added. The mixture, which became warm almost immediately, was stirred for several hours and then filtered.

[14] P. T. Gilbert, Jr., R. C. Hawes, and A. O. Beckman, *Anal. Chem.* **22**, 772 (1950).

The solvent was removed from an aliquot of the filtrate by heating it for an hour *in vacuo* at 80°C. The amount of hydrogen generated by hydrolysis of the residue indicated that the total amount of lithium aluminum hydride obtained was 61 mmoles, in other words, was 100 per cent of the expected 60 mmoles, within the limit of accuracy of the analysis. However, the solid was only about 86 per cent pure, since 0.433-g sample generated only 882 instead of the 1020 cc of hydrogen by hydrolysis. The impurity in this case also was probably retained tetrahydrofuran or a product of decomposition of the latter.

Preparation of Sodium Aluminum Hydride from Lithium Aluminum Hydride

This application of the method under discussion would be used only to start the "cyclical" procedure when sodium aluminum hydride is not available. Furthermore, it is in all respects analogous to the preceding case, and gives equally good results. For this reason the example chosen is one which also illustrates that the same solvent need not be used for both steps of the procedure.

To a solution of 4.87 g (122 mmoles) of lithium aluminum hydride in 159 g of diethyl ether, 5.39 g (40.3 mmoles) of aluminum chloride were added. After removal of the precipitated lithium chloride by filtration, the solvent was evaporated from a portion of the filtrate to give a solid etherate which was shown to contain 1.70 g (56.6 mmoles) of aluminum hydride. The latter was dissolved in 60 g of tetrahydrofuran. After addition of 1.82 g (75.8 mmoles) of sodium hydride to the resulting solution, the mixture was stirred for four hours.

The solvent was evaporated at room temperature *in vacuo* from a 14.05-g portion of the 62 g of filtrate. The resulting solid, which was not entirely free from tetrahydrofuran, generated 1130 cc (50.2 mmoles) of hydrogen, indicating a yield of 98 per cent. The H : Na ratio in the solid was shown to be 4.00. In another similar experiment, in which the residual solvent was removed at 150°C *in vacuo*, the purity of the product was 95 per cent.

The Reaction of Calcium Hydride with Aluminum Hydride

The statement in the introductory section that the two-step procedure had proved less successful for the preparation of calcium aluminum hydride than of the sodium salt, is based on experiments in which a tetrahydrofuran solution of aluminum hydride (prepared by the action of an equivalent amount of aluminum chloride on a solution of sodium aluminum hydride) was treated with an excess of calcium hydride. The best yield of calcium aluminum hydride was only 20 per cent of the theoretical. For this reason it seems unnecessary to present details of the experiments.

Composition of Sodium Aluminum Hydride

The temperature of a 0.2650-g sample of sodium aluminum hydride (prepared in dimethyl ether solution) was raised to between 230 and 240°C during a period of two hours. Care was taken that in removing the hydrogen by means of a Toepler pump, the pressure in the heated zone did not fall below 2 mm, since at 240°C the dissociation pressure of sodium hydride is 0.06 mm. The amount of hydrogen recovered by this pyrolysis was 158.9 cc (S.T.P.), or 98.4 per cent of that corresponding to equation (8). Treatment of the residue with water and acid produced 262.9 cc more of hydrogen, which is 97.9 per cent of that corresponding to the equation:

$$NaH + Al + 4HCl \rightarrow NaCl + AlCl_3 + 2.5H_2 \qquad (8)$$

Reaction of Sodium Aluminum Hydride with Ammonia and with Isopropylamine

When sodium aluminum hydride is treated with sufficient ammonia or isopropylamine to assure the presence of liquid reactant, an amount of hydrogen corresponding to equations (9) and (10) is evolved.[15]

$$NaAlH_4 + 4NH_3 \rightarrow NaAl(NH_2)_4 + 4H_2 \qquad (9)$$

$$NaAlH_4 + 4(CH_3)_2CHNH_2 \rightarrow NaAl[(CH_3)_2CNH]_4 + 4H_2 \qquad (10)$$

Thus a 0.1843-g sample of sodium aluminum hydride of 94.2 per cent purity at −33°C evolved 278.4 cc (S.T.P.) of hydrogen; at room temperature another 5.2 cc was obtained, thus bringing the total to 98.4 per cent of that demanded by equation (9). The total amount of ammonia consumed was

[15] When lithium aluminum hydride is treated with gaseous ammonia the reaction appears to take a somewhat different course (ref. 4), but the lithium salt behaves with liquid ammonia as does the sodium salt.

283.2 cc (gas at S.T.P.) or 98.3 per cent of the theory. Similarly a 0.3926-g sample of the sodium salt (95.3 per cent purity) consumed 620 cc of isopropyl amine (reported as a gas at S.T.P.) and generated 621 cc of hydrogen. These quantities are 99.6 and 99.7 per cent respectively of the requirements of equation (10).[18]

ACKNOWLEDGEMENTS

We gratefully acknowledge the financial support and interest of the Office of Naval Research, under whose auspices most of the work described was done. We also wish to express our indebtedness to EUGENE JACOBSON, ALLAN OGARD, and PHILLIP THOMPSON, who performed some of the experiments on the cyclic process in the laboratories of St. Olaf College.

[18] A solid having the composition $NaAl(NH_2)_4$ was obtained by F. W. BERGSTROM (*J. Amer. Chem. Soc.* **45**, 2788 [1923]) but differs from ours in that it melts at 90°C with evolution of one mole of ammonia, whereas our product could be heated without melting to 95°C. At this temperature ammonia was evolved. The evolution became very slow after 4.5 hours, by which time about one mole of ammonia had been generated. But loss of ammonia did not cease. By raising the temperature slowly to 295°C, another mole of ammonia could be driven off. The product obtained appeared to be inhomogeneous, and was not further investigated.

VOL.
1
1955

J. Inorganic and Nuclear Chemistry, 1955, Vol. 1, pp. 326–333. Pergamon Press Ltd., London

THE HYDRATES OF THORIUM TETRAFLUORIDE

R. W. M. D'Eye and G. W. Booth
Atomic Energy Research Establishment, Harwell, Didcot, Berks

(*Received* 29 *April* 1955)

Abstract—From a chemical, tensimetric, and X-ray crystallographic study three hydrates of thorium tetrafluoride have been identified. The highest hydrate found, $ThF_4 . 2{\cdot}5\text{–}3{\cdot}0H_2O$, is pseudo-tetragonal, and can be thermally degraded to $ThF_4 . 0{\cdot}25H_2O$. The intermediate hydrate has a composition varying from $ThF_4 . 0{\cdot}5\text{–}2{\cdot}0H_2O$, and is orthorhombic with sixteen molecules per unit cell. The water molecules in this structure are not all crystallographically equivalent. This hydrate can be thermally degraded to $ThF_4 . 0{\cdot}25H_2O$. The lowest hydrate, $ThF_4 . 0{\cdot}25H_2O$, when heated in air or vacuum at 300°C, gives anhydrous ThF_4. X-ray crystallographic data are given for ThF_4 and $UF_4 . 2{\cdot}5H_2O$.

The tetrafluorides of uranium and plutonium form two hydrates, the higher hydrate having 2·5 molecules of water per metal atom and the lower, between 0·5 and 2·0 molecules of water.[1] The higher hydrate $XF_4 . 2{\cdot}5H_2O$(X = U or Pu) is orthorhombic,[2] whereas the lower hydrate $XF_4 . nH_2O$, where n varies between 0·5 and 2·0, is pseudo-cubic.[1] The hydrates of thorium tetrafluoride might be expected to be analogous to those of uranium and plutonium, since the anhydrous tetrafluorides are all isostructural.[3] This, however, is not the case.

An early study of the hydrates of thorium tetrafluoride led Chauvenet[4] to postulate three hydrates: $ThF_4 . 8H_2O$, $ThF_4 . 4H_2O$ and $ThF_4 . 2H_2O$. Recently Asker, Segnit, and Wylie[5] found that, after air-drying, the precipitate formed by the addition of aqueous hydrofluoric acid to a thorium nitrate solution, a tetrafluoride hydrate was obtained whose water content varied in the range 2·5 to 3·5 molecules per metal atom. If this hydrate was heated in an air-oven, the water content dropped to the range 1·0 to 2·0 water molecules per metal atom. Further heating at 300°C for some hours gave the anhydrous fluoride. The freshly precipitated hydrate, after air-drying, was amorphous, but after it was aged in hydrofluoric acid overnight a fibrous anisotropic substance with a long spacing of 17 Å was formed.

We have found three hydrates: $ThF_4 . 2{\cdot}5\text{–}3{\cdot}0H_2O$, $ThF_4 . 0{\cdot}5\text{–}2{\cdot}0H_2O$ and, $ThF_4 . 0{\cdot}25H_2O$, designated $ThF_4 . xH_2O$, $ThF_4 . yH_2O$, and $ThF_4 . zH_2O$, respectively. The intermediate hydrate is not isostructural with $XF_4 . nH_2O$ (X = U or Pu), nor with $ZrF_4 . H_2O$.[6]

EXPERIMENTAL

Preparation of Hydrates

The hydrated tetrafluoride was precipitated by the addition of a slight excess of 40 per cent aqueous hydrofluoric acid to thorium nitrate and chloride solutions in acid-resistant plastic tubes. The precipitates were centrifuged and thoroughly washed with water. The precipitates were dried by

[1] Dawson, J. K., D'Eye, R. W. M., and Truswell, A. E. (1954) *J. Chem. Soc.*, 3922.
[2] Zachariasen, W. H. (1949a) The Transuranium Elements N.N.E.S. IV, **14B**, 1469.
[3] Zachariasen, W. H. (1949b) *Acta. Cryst.* **2**, 388.
[4] Chauvenet, E. (1911) *Ann. Chim. Phys.* **23**, 425.
[5] Asker, W. J., Segnit, E. R., and Wylie, A. W. (1952) *J. Chem. Soc.*, 4470.
[6] D'Eye, R. W. M. (1955) to be published.

the following methods: washed with acetone and allowed to dry in air; dried in a vacuum desiccator with "anhydrone" as the desiccant; dried *in vacuo* and in air at various temperatures.

Analysis

The water present was determined by degrading the sample *in vacuo* and absorbing the resulting water vapour in "anhydrone" traps. The fluorine in the residue was estimated by pyrohydrolytic removal as hydrofluoric acid with steam at temperatures up to 1000°C, condensation of the steam/acid mixture, and titration with standard alkali. The steam-jet was removed and the residual oxide ignited in air up to 1000°C, and weighed as ThO_2. In this way a complete balance sheet Th : F : H_2O was obtained. The water content was also obtained by difference after determining the thorium and fluorine in the sample as above.

X-ray Diffraction Analysis

The diffraction photographs, which we obtained using Debye-Scherrer type powder cameras and standard X-ray equipment were of extremely poor quality due to the small crystallite size and the low order of symmetry of the substances under investigation. Attempts to increase the crystallite size by ageing in hydrofluoric acid and precipitation at temperatures higher than room temperature produced no appreciable improvements in the diffraction patterns. It was necessary therefore to use throughout this study a Guinier-type focusing camera[7] which employs monochromatized and focused Cu$K\alpha$ radiation from a bent quartz crystal. The $\sin^2\theta$ values are thus free from absorption and eccentricity errors. By photographing a 0·1-mm scale on to the film before processing, shrinkage errors are also eliminated. Even with the Guinier camera a large number of specimens were found to be X-ray amorphous.

The complete X-ray data for ThF_4 and $UF_4 . 2{\cdot}5H_2O$ are so far unpublished, although the structures have been determined by ZACHARIASEN.[2, 3] To make this information available, the $\sin^2\theta$ values and observed intensities obtained by the present authors from diffraction patterns of ThF_4 and $UF_4 . 2{\cdot}5H_2O$, are given in an appendix.

Tensimetric Studies

(i) The application of a method for measuring low dissociation pressures, using a quartz helix-type balance, to the determination of the phases present in a two-component system, was discussed in recent papers on the nickel-sulphur and thorium-tellurium systems.[8] The method was satisfactory when the sample was in the form of a thin foil with a high surface area/unit mass ratio. It would, however, be difficult to have the thorium tetrafluoride in such a form; so a powder must be used. The rate of evaporation, μ, instead of being controlled solely by the true dissociation pressure, is then also controlled by the rate of diffusion of the vapour phase through a layer of dissociated material. The results can therefore not be as unequivocal as those for the former case.

If the temperature T, instead of μ, is plotted against N, the number of water molecules per metal atom, the resulting graph should be just as useful, provided the temperature is raised in fairly small steps (10° to 30°C) from room temperature, that it is never increased before the weight-loss from the sample has become negligible over a period of hours, and that the ambient pressure in the apparatus is maintained at 10^{-4} mm. These expectations were confirmed by experiment. A typical degradation run is shown in the following diagram. Vertical lines on the graph indicate regions where two solid phases are present and the system is univariant. Similarly horizontal lines indicate a bivariant region. The weight of sample used in these runs was 100 mg, and the time taken was of the order of days for a degradation from 2·0 to zero molecules of water per metal atom. A trap cooled by liquid nitrogen was near to the sample to remove the water vapour, thus preventing errors due to adsorption on the silica spring.

(ii) A sample of $ThF_4 . 2{\cdot}0H_2O$ was degraded to the approximate composition $ThF_4 . 1{\cdot}0H_2O$ by pumping at 10^{-5} mm. The apparatus was isolated from the vacuum system, and the liquid nitrogen removed, allowing the apparatus to fill with water vapour. The sample slowly increased in weight as water was absorbed. After several hours the water content of the sample had risen to its initial value.

[7] D'EYE, R. W. M. (1954) A.E.R.E. C/R 1524.
[8] D'EYE, R. W. M., and SELLMAN, P. G. (1953) A.E.R.E. C/R 1077; (1954) *J. Chem. Soc.*, 3760.

VOL. 1 1955

Experiments showed that water could be absorbed and desorbed readily in the region of from one to two molecules of water per metal atom. Similar experiments with anhydrous thorium tetrafluoride showed only slight weight increases which could be attributed to surface adsorption.

RESULTS AND DISCUSSION

The Hydrates and Their Inter-relations

$ThF_4 . 2{\cdot}5–3{\cdot}0H_2O$ ($ThF_4 . xH_2O$). Samples precipitated from thorium nitrate solution (0·005*M* to 0·4*M*), when dried by washing with acetone and allowed to dry in air, gave compositions which varied from 2·5 to 3·0 molecules of water per metal atom. The X-ray diffraction photographs of these samples were all identical. The X-ray data would seem to indicate that this was the hydrate found by Asker *et al.*,[5] who gave the composition limits as $ThF_4 . 2{\cdot}5–3{\cdot}5H_2O$.

On pumping the samples at 10^{-5} mm, the water content dropped, the decrease in water content depending on the time of pumping. X-ray diffraction photographs of samples which had degraded to the composition $ThF_4 . 1{\cdot}5H_2O$ showed mainly the lines ascribed to $ThF_4 . xH_2O$. It was difficult, however, to determine the appearance of a new phase, because the photographs of $ThF_4 . xH_2O$ were complex and of poor quality. Further pumping and heating at 50°–80°C reduced the water content to $ThF_4 . 0{\cdot}6H_2O$. The X-ray photographs now showed mainly a new phase, $ThF_4 . zH_2O$, but again due to the poor photographs it was impossible to say whether or not this was single or multiphase. The probable true value of z and the thermal degradation of this phase are discussed below.

$ThF_4 . 0{\cdot}5–2{\cdot}0H_2O$ ($ThF_4 . yH_2O$). The samples which were precipitated from thorium nitrate (0·004*M* to *M*) and tetrachloride solutions and dried in a vacuum desiccator or by heating in air in platinum dishes at 100°C, had compositions ranging from 1·1 to 2·0 molecules of water per thorium atom. The X-ray diffraction photographs of those samples which were not X-ray amorphous were all identical, but quite different from the photographs of $ThF_4 . xH_2O$ and $ThF_4 . zH_2O$.

The hydrate degrades to the anhydrous tetrafluoride when heated in air for some hours at 300°. Above this temperature the tetrafluoride starts to decompose, decomposition to thoria being complete after heating overnight at 500°.

To determine the lower limit of existence of this phase designated $ThF_4 . yH_2O$, samples with a known composition ($ThF_4 . ca.1{\cdot}5H_2O$) and giving fair diffraction photographs were heated *in vacuo* at known temperatures for known lengths of time. Heating *in vacuo* prevents any ambiguity in the results due to atmospheric hydrolysis. The samples were pumped *in vacuo* at 80°, 100°, 130°, 190°, and 250°, both for one and four days. The analytical data showed that the time of heating, provided it was greater than a certain minimum time, had little effect on the final compositions, which were 1·1, 1·0, 0·8, 0·5, 0·3, and 0·3 molecules of water per thorium atom respectively. The X-ray diffraction photographs of those samples with a water content greater than 0·5 molecules per thorium atom were identical with those of samples in the range 1·1 to 2·0. The photograph of $ThF_4 . 0{\cdot}5H_2O$ was of poor quality, with the lines rather diffuse. Although the film was basically similar to those of samples of higher water content, it was apparent that at this composition the lattice was starting to break up.

These results on the degradation of $ThF_4 . yH_2O$ are in accord with the thermal degradation studies carried out *in vacuo* using a quartz spiral spring balance. In these tensimetric studies, breaks were observed in the graphs of composition N (where

N is the number of molecules of water per metal atom) against temperature, for the following values of N: 2·0, *ca.*1·0, 0·75, 0·5, 0·2, and 0·0. The breaks at 2·0 and 0·5 agree well with the upper and lower limits for the hydrate $ThF_4 . yH_2O$, and the break at 0·2 corresponds to the lower hydrate $ThF_4 . zH_2O$. However, the breaks at $N = 0·75$ and *ca.*1·0 cannot be accounted for on the basis of phase changes. They can, however be satisfactorily explained if the water molecules in the structure are not all structurally equivalent, as in the case of thomsonite $NaCa_2Al_5Si_5O_{20} . 6H_2O$.[9]

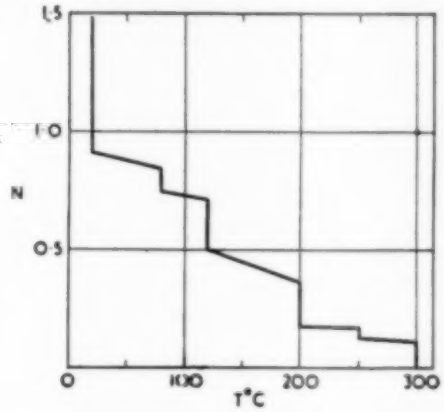

FIG. 1.—Degradation of $ThF_4 . yH_2O$.

$ThF_4 . 0·25H_2O$(?) ($ThF_4 . zH_2O$). The photographs of $ThF_4 . 0·3H_2O$ were identical with those of $ThF_4 . zH_2O$. This phase decomposes to the anhydrous tetrafluoride when heated at 300° both in air and *in vacuo*. The actual composition of this hydrate has not been accurately determined owing to the small weight of the water compared to the weight of the metal atom and the uncertainty caused by surface adsorption of water. The true composition might well be $ThF_4 . 0·25H_2O$.

Miscellaneous

According to ZACHARIASEN,[10] a compound of composition $ThF_4 . 0·25H_2O$ is obtained when thorium fluoride is precipitated from hot concentrated hydrofluoric acid, and under slightly different conditions ThF_4 is obtained. We have carried out precipitations over the temperature range 80° to 100°, but the resulting precipitates did not differ from those obtained at room temperature.

Our X-ray diffraction results showed that no reaction occurred between small particle size thorium tetrafluoride and hydrofluoric acid of varying concentration, under the conditions used in the precipitation.

To obtain an idea of the stability of anhydrous thorium tetrafluoride, prepared by thermal degradation of the hydrate, it was heated at 100° in water both for a number of hours and a number of days. After centrifuging and washing, the residues were dried in a vacuum desiccator overnight. No change was observed in the diffraction photograph after heating the specimen for a number of hours. The samples heated for a

[9] HEY, M. H. and BANNISTER, F. A. (1932) *Min. Mag.* **23**, 51.
[10] ZACHARIASEN, W. H. (1954) The Actinide Elements, N.N.E.S. IV **14A**, 83.

VOL. 1 1955

longer period of time had compositions about $ThF_4 . 0{\cdot}5H_2O$, and their diffraction patterns, although similar to those of the anhydrous compound, were not exactly the same. No trace of the dioxide or oxyfluoride was observed in these diffraction photographs. This reaction is being further investigated. It is of interest to note that the monoclinic unit cell of thorium tetrafluoride, which has a volume of 1002 kX^3, could, on volume considerations, accommodate some water molecules. This might be analogous to the incorporation of fluorine into the uranium tetrafluoride lattice giving rise to a "distorted UF_4" diffraction photograph. As with thorium tetrafluoride, there are twelve voids in the uranium tetrafluoride unit cell which are almost but not quite large enough to accommodate fluorine ions. However, a slight distortion of the lattice can allow three of the holes in the unit cell to be filled by fluorine, giving a sample of composition U_4F_{17} which has a "distorted UF_4" type photograph.[11]

X-ray Crystallographic Results

$ThF_4 . 2{\cdot}5–3{\cdot}0H_2O$. A typical set of data for this hydrate is given in the following table for a hydrate of composition $ThF_4 . 2{\cdot}8H_2O$. The photographs were rather weak even after long exposures.

The $\sin^2\theta$ values for the diffraction lines 1, 2, 3, 4, 6, 9, and 11 are in the ratios 1 : 2 : 4 : 5 : 8 : 16 : 20. This indicates that the symmetry is tetragonal.[12] Taking $\sin^2\theta = 0{\cdot}0021$ as the 100-plane, giving $a = 16{\cdot}75$ kX, the agreement between the calculated and observed $\sin^2\theta$ values for the *hk*0 planes is very fair. However, in the authors' opinion an unambiguous indexing of the diffraction pattern is not possible until better photographs are obtained.

	I_o	$\sin^2\theta_o$	$\sin^2\theta_c$ for *hk*0 planes	*hk*0
1	m	0·0021	0·0021	100
2	vvw	0·0041	0·0042	110
3	vvw	0·0083	0·0084	200
4	vvw	0·0104	0·0105	210
5	vvw	0·0122		
6	vvw	0·0175	0·0168	220
7	vvw	0·0287		
8	vvw	0·0317		
9	w⁻	0·0337	0·0336	400
10	w⁻	0·0349		
11	vw	0·0420	0·0420	420

The $\sin^2\theta$ values and the observed intensities do not vary with changing water content in the range 2·5 to 3·0 molecules of water per thorium atom. Thus at least part of the water in this structure is not necessary to the stability of the lattice, and is probably located in channels running through the structure. This would account for the easy removal of some of the water when the samples were pumped at 10^{-4} mm.

$ThF_4 . 0{\cdot}5–2{\cdot}0H_2O$. The $\sin^2\theta$ values and intensities I_0 for samples with varying water content are shown in the following table.

[11] Burbank, R. D. (1951) AECD.-3216.
[12] Hesse, R. (1948) *Acta Cryst.* **1**, 200.

I_o	$\sin^2\theta_o$ (1) $ThF_4 . 1{\cdot}6H_2O$	(2) $ThF_4 . 1{\cdot}4H_2O$	(3) $ThF_4 . 1{\cdot}2H_2O$	(4) $ThF_4 . 0{\cdot}8H_2O$	$\sin^2\theta_c$	*hkl*
s⁻	0·0171	0·0171	0·0172	0·0172	0·0171	020
m+	0·0233	0·0232	0·0233	0·0232	0·0232	112
w+	0·0278	0·0279	0·0279	0·0278	0·0277	121
					0·0283	022
m+	0·0312	0·0312	0·0312	0·0315	0·0312	200
s	0·0383	0·0383	0·0383	0·0384	0·0383	211
vvw	—	—	0·0426	—	0·0424	202
s⁻	0·0446	0·0448	0·0446	0·0449	0·0448	004
vvw	0·0484	0·0484	0·0485	0·0486	0·0483	220
vvw	0·0496	0·0501	0·0505	0·0497	0·0501	123
m	0·0579	0·0579	0·0579	0·0579	0·0574	132
m+	0·0607	0·0607	0·0605	0·0613	0·0607	213
w	0·0618	0·0621	0·0618	0·0620	0·0619	024
vvw	0·0688	0·0690	0·0690	0·0688	0·0683	040
vvw	0·0759	0·0759	0·0759	0·0765	0·0760	204
vvw	0·0796	—	0·0794	0·0793	0·0795	042
					0·0789	141
vw	0·0905	0·0901	0·0901	0·0903	0·0901	321
vvw	—	—	0·0930	—	0·0931	224
vvw	0·0951	0·0952	0·0952	—	0·0949	125
vvw	0·1056	0·1057	0·1051	—	0·1056	215
m	0·1127	0·1128	0·1127	0·1133	0·1131	044

(1) Precipitated from $Th(NO_3)_4$ solution, dried in vacuum desiccator.
(2) Precipitated from $ThCl_4$ solution, dried in vacuum desiccator.
(3) Precipitated from $Th(NO_3)_4$ solution, dried in air at 120°.
(4) Precipitated from $Th(NO_3)_4$ solution, dried *in vacuo* at 100°.

The diffraction pattern has been successfully indexed on the basis of an orthorhombic cell, using the mathematical methods of HESSE[12] and HENRY, LIPSON, and WOOSTER,[13] with the cell constants $a = 8{\cdot}71 \pm 0{\cdot}01$ kX, $b = 11{\cdot}77 \pm 0{\cdot}01$ kX, $c = 14{\cdot}54 \pm 0{\cdot}01$ kX, and a calculated volume of 1490 kX³. The agreement between the observed and calculated values of $\sin^2\theta$ is seen from the table to be good, considering the rather poor quality of the photographs. On volume considerations, the unit cell will just contain sixteen molecular units of $ThF_4 . yH_2O$, giving calculated densities of 6·09, 5·78, and 5·62 for $ThF_4 . 2H_2O$, $ThF_4 . H_2O$, and $ThF_4 . 0{\cdot}5H_2O$, respectively. A consideration of the observed indices of the reflections shows that they exhibit the following relationships:—

hkl present only when $h + k + l = 2n$ where n is an integer
hko present only when $h = 2n$ ($k = 2n$)
hol present only when $h = 2n$ ($l = 2n$)
okl present only when $k = 2n$ ($l = 2n$)
*h*00 present only when $h = 2n$
0*k*0 present only when $k = 2n$
00*l* present only when $l = 2n$

The first relationship requires a body-centred space group and the others indicate that the space group is $D_2^9 - I2_12_12_1$. If this is the case, the thorium atoms will be

[13] HENRY, N. F. M., LIPSON, H., and WOOSTER, W. A. (1951) *Interpretation of X-ray Diffraction Photographs* (Macmillan).

distributed on the fourfold special positions which all have one variable parameter. Intensity calculations are needed to confirm this structure.

It is apparent from the $\sin^2\theta$ values that the volume of the unit cell does not vary with water content. This is in direct contrast to the behaviour of the lower tetrafluoride hydrates of uranium and plutonium.[1] As was shown above, the water molecules in the hydrate cannot all be structurally equivalent. With sixteen molecules per unit cell the water contents of the three groups would be 32–16, 16–12, and 12–8. The first group can be readily desorbed and absorbed, whereas the latter two groups are more firmly held. Both the chemical and X-ray data indicate that the rigidity of the lattice of $ThF_4 . yH_2O$ depends on there being sixteen Th atoms, sixty-four F atoms, and eight H_2O molecules in the unit cell. The remaining twenty-four water molecules which do not contribute to the strength of the structure, must be accommodated in channels and/or interstices in the lattice. The behaviour of the water in this hydrate is perhaps analogous to that in $AlF_3 . 3{\cdot}5H_2O$, which also loses water in stages, and whose last half molecule of water is removed only at red heat.[14]

$ThF_4 . 0{\cdot}25H_2O$. The diffraction photographs of this phase were extremely poor, and so far no quantitative studies have been undertaken.

APPENDIX

(i) X-ray diffraction patterns of $UF_4 . 2{\cdot}5H_2O$ were indexed on the basis of an orthorhombic cell with $a = 12{\cdot}82 \pm 0{\cdot}01$, $b = 11{\cdot}10 \pm 0{\cdot}01$, and $c = 7{\cdot}05 \pm 0{\cdot}01$ kX. The agreement between the observed and calculated values of $\sin^2\theta$ is seen from the following table to be good. Zachariasen[2] gave the cell constants as $a = 12{\cdot}75$, $b = 11{\cdot}12$, and $c = 7{\cdot}05$ kX, which are in close agreement with those found above.

hkl	$\sin^2\theta_o$	$\sin^2\theta_c$	I_o
110	0·0084	0·0084	s
200	0·0145	0·0144	vw
011	0·0167	0·0167	s−
020, 210	0·0192	0·0192	vw
120	0·0228	0·0228	m
201	0·0265	0·0263	m
211	0·0313	0·0311	s−
220	0·0336	0·0336	m−
221	0·0456	0·0455	m−
130	0·0467	0·0468	w−
002	0·0476	0·0476	m
311	0·0495	0·0491	s
320	0·0519	0·0516	vw
112	0·0562	0·0560	m
131	0·0588	0·0587	s−
022, 212	0·0669	0·0668	vw
122	0·0704	0·0704	m
330	0·0751	0·0756	m−

(ii) Thorium tetrafluoride is monoclinic with $a = 13{\cdot}1 \pm 0{\cdot}1$, $b = 11{\cdot}0 \pm 0{\cdot}1$, $c = 8{\cdot}6 \pm 0{\cdot}1$ kX, and $\alpha = 126° \pm 1°$.[3] The observed values of $\sin^2\theta$ and the

[14] Ketelaar, J. A. A. (1933) *Z. Krist.* **85**, 119.

intensities are given below for a sample of ThF_4 prepared from the hydrate by thermal degradation.

$\sin^2\theta$	*I*	$\sin^2\theta$	*I*
0·0102	w	0·0690	vvw
0·0131	w	0·0731	vvw
0·0210	vvw	0·0784	m+
0·0321	s	0·0803	vw
0·0367	m	0·0926	w−
0·0412	s−	0·0954	vw
0·0453	m	0·1279	w−
0·0503	w−	0·1308	w
0·0524	s−		

VOL. 1 1955

ACKNOWLEDGEMENTS

The authors thank Dr. J. K. DAWSON for the sample of $UF_4 \cdot 2{\cdot}5H_2O$, and Mr. E. A. HARPER for some of the analytical results.

J. Inorganic and Nuclear Chemistry, 1955, Vol. 1, pp. 334–339. Pergamon Press Ltd., London

DIE BESTIMMUNG DES IONENPRODUKTS DER WASSERFREIEN ESSIGSÄURE AUS POTENTIALMESSUNGEN

Von G. Jander und H. Klaus
Aus dem Anorganisch-chemischen Institut der Technischen Universität Berlin-Charlottenburg

(*Received* 30 *January* 1955)

Abstract—The ionic product of anhydrous acetic acid was determined from the e.m.f. of a cell comprising a gold electrode in a capillary containing very pure acetic acid, and a second gold electrode immersed in diethylaniline of various concentrations—diethylaniline being known to be completely dissociated into ions at great dilution in absolute acetic acid. The value $c_H \cdot c_{Ac} = 0{\cdot}95 \times 10^{-13}$ was obtained.

1. POTENTIALMESSUNGEN VON BASENANALOGEN LÖSUNGEN IN EISESSIG GEGEN DAS REINE LÖSUNGSMITTEL

Es soll der Versuch unternommen werden, das Ionenprodukt der wasserfreien Essigsäure auf Grund von Potentialmessungen neu zu bestimmen. Erstmalig wurde dieses von Kolthoff und Willman[1] auf Grund konduktometrischer Messungen berechnet. Sie mußten die vereinfachende Annahme machen, daß die Leitfähigkeit einer wasserfreien, essigsauren Perchlorsäure-Lösung ausschließlich durch die Anwesenheit von Acetacidiumionen, Perchlorat-Ionen und Acetat-Ionen bedingt ist und daß außerdem die Beweglichkeit der beiden Anionen gleich groß ist. Unter diesen Voraussetzungen ergab sich für das Ionenprodukt ein Wert von $2{\cdot}5 \cdot 10^{-13}$ bei 25°C. Berücksichtigt man dabei die Waldensche Regel, nach der das Produkt aus Leitfähigkeit und Viskosität konstant ist, dann ergibt sich ein Wert von $1 \cdot 10^{-15}$ bei 20°C. Zur Berechnung benutzte Kolthoff Werte für die Leitfähigkeit bei unendlicher Verdünnung, die durch graphische Extrapolation ermittelt worden waren.

Zum Vergleich hat Kolthoff[1] das Ionenprodukt der Essigsäure aus den potentiometrischen Titrationskurven berechnet, die von Hall und Conant[2] veröffentlicht worden sind. Er erhielt daraus einen Wert von $3 \cdot 10^{-10}$.

Mehrere Jahre später haben Kilpi und Puranen[3][4] aus potentiometrischen Messungen mit einer Wasserstoffelektrode, die gegen eine Kalomelelektrode geschaltet war, einen Wert von $2{\cdot}8 \cdot 10^{-13}$ errechnet. Als Verbindung mit bekannter H^+-Ionen-Aktivität wurde o-Aminobenzoesäure benutzt. Deren Dissoziationskonstante bestimmten sie aus der Pufferkapazität einer basenanalogen Lösung am Anfang einer Titration. (Aus den so gemessenen Werten hatte sich die Dissoziationskonstante der o-Aminobenzoesäure durch Extrapolation zu $3{\cdot}5 \cdot 10^{-7}$ ergeben.)

In den letzten Jahren wurde dieses Problem des Ionenprodukts von wasserfreier Essigsäure nochmals von Tomiczek und Heyrovsky[5] aufgegriffen. Aus einer potentiometrischen Titration, die ebenfalls mit einer Wasserstoffelektrode unter Verwendung einer Kalomelelektrode als Vergleichssystem durchgeführt worden war,

[1] J. M. Kolthoff u. A. Willman, *J. Amer. Chem. Soc.* **56**, 1007 (1934).
[2] N. F. Hall u. J. B. Conant, *J. Amer. Chem. Soc.* **49**, 3047 (1927).
[3] S. Kilpi u. M. Puranen, *Ann. Acad. Sci. Fennicae*, Ser. A **57**, Nr. 3 (1941).
[4] S. Kilpi u. M. Puranen, *Z. phys. Chem.* **187** A, 276 (1940).
[5] O. Tomiczek u. A. Heyrovsky, *Chem. Listy Vedu Prumysl* **43**, 193 (1949).

ergab sich durch Schätzung ein Wert in der Größenordnung von 10^{-13}. Sie setzten dabei völlige Dissoziation des bei der Titration verwendeten Säuren—und des Basenanalogen voraus.

Dieser kurze Überblick über die bisherigen Arbeiten, die zur Bestimmung des Ionenprodukts der wasserfreien Essigsäure durchgeführt wurden, zeigt, daß in jedem Falle Annahmen gemacht werden mußten, deren Richtigkeit noch nicht bewiesen werden konnte. Bei den potentiometrischen Messungen liegt diese Unsicherheit darin, daß das in jedem bisher benutzten Meßsystem vorhandene Diffusionspotential zwischen wässriger und absolut essigsaurer Lösung nicht bekannt ist. Bei der konduktometrischen Bestimmung mußte eine ungewisse Annahme gemacht werden, die die wahren Dissoziationsvorgänge und die Ionenbeweglichkeiten in Eisessig betraf. Da die potentiometrischen Messungen ausschließlich auf Potentialbestimmungen mit einer Wasserstoffelektrode beruhen, bestanden in allen diesen Fällen Schwierigkeiten in der genauen Bestimmung der H^+-Ionenaktivitäten.

VOL. 1 1955

Bei den eigenen Untersuchungen wurden die Potentiale mit einer gebremsten Goldelektrode[6] gemessen. Hinsichtlich der Wirkungsweise der Goldelektroden wird angenommen, daß sich an der Elektrodenoberfläche eine Acetatdeckschicht ausbildet, die ein Ansprechen auf die Acetationen ermöglicht. Wenn es auch, wie eigene Versuche ergaben, nicht möglich war, diese Arbeitshypothese durch präparative Darstellung von Gold (I)-acetat und die Bestimmung von dessen Löslichkeitsprodukt zu untermauern, so läßt sie sich doch durch die Auswertung der im folgenden gezeigten Potentialkurven stützen. Dies soll bei der Berechnung des Ionenproduktes eingehender behandelt werden.

Bei Untersuchungen über die Abhängigkeit der gemessenen Potentiale von der Konzentration der titrierten Lösungen hatte sich ergeben, daß beim Übergang von einer N/10 Lösung zu einer N/100 Lösung nicht ganz die von der Nernstschen Gleichung geforderte Potentialdifferenz erreicht wird. Auf Grund von kryoskopischen Molekulargewichtsbestimmungen in Eisessig kann diese Tatsache auf Assoziationserscheinungen beim Übergang zu konzentrierteren Lösungen, besonders bei den Säurenanalogen, erklärt werden. Infolge der Unübersichtlichkeit dieser Verhältnisse wäre es nicht exakt gewesen, eine Neutralisations-Titration zur Berechnung des Ionen-Produktes auszuwerten. Es soll deshalb versucht werden, Potentiale zwischen basenanalogen Lösungen größtmöglicher Verdünnung und reiner wasserfreier Essigsäure zu messen.

Die ersten Vorversuche dazu ergaben, daß auf Grund der geringen Eigenleitfähigkeit der absoluten Essigsäure der innere Widerstand der Meßzelle zu groß war. Es mußte also eine andere Kapillare verwendet werden als bei potentiometrischen Titrationen. Zur Messung des Potentials einer N/100 Lösung gegen das reine Lösungsmittel mußte diese aber so weit gehalten werden, daß bereits nach etwa 12–15 min Diffusion eintrat. Das machte es unmöglich, eine Reihe Lösungen zunehmender Konzentration hintereinander zu untersuchen. Es mußte also das Potential jeder einzelnen Konzentration für sich gemessen werden. Aus diesen Einzelpotentialen wurde dann die Potentialkurve von Diäthylanilin gegen reines Lösungsmittel konstruiert. Um nun diese resultierende Kurve nicht durch zufällige Meßungenauigkeiten zu verfälschen, wurden sämtliche Einzelpotentiale mehrfach bestimmt und daraus der Mittelwert genommen.

[6] E. MÜLLER, *Die elektrometrische Maßanalyse*, Verl. Steinkopf, 7. Aufl. S. 107.

In der Abb. 1 ist die Einstellung der Potentiale von einer N/20, basenanalogen Lösung gegen reine Essigsäure in Abhängigkeit von der Zeit dargestellt. Ähnliche Resultaten ergaben sich mit N/50, N/100, und N/300 Lösungen.

Die vier Kurvenscharen, die sich aus diesen Messungen ergeben haben, verlaufen im allgemeinen gleichartig. Sie zeigen einen allmählichen Anstieg und darauf etwa nach 6 bis 10 min ein mehr oder weniger breites Maximum. Der durch die eintretende Diffusion bedingte Potentialabfall ist gewöhnlich etwas steiler.

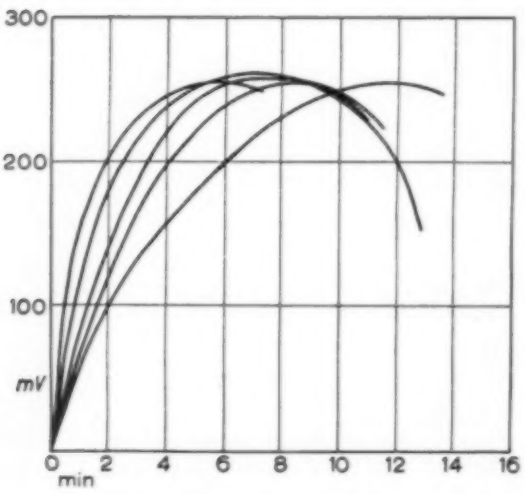

ABB. 1.—Potential einer N/20 basenanalogen Lösung von Diäthylanilin gegen reine Essigsäure.

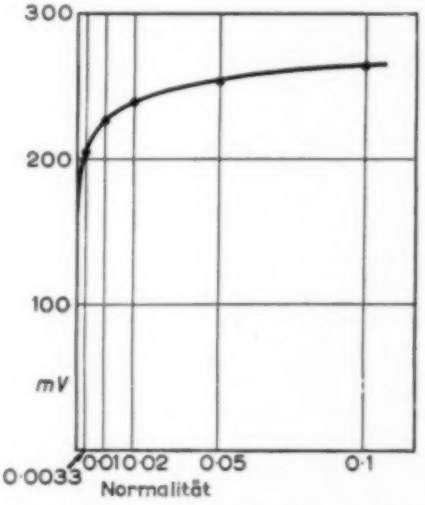

ABB. 2.—Aus den Einzelmessungen konstruierter Potentialverlauf einer Titration von reiner Essigsäure mit Diäthylanilin.

Die aus den einzelnen Maxima gemittelten Werte ergaben für

N/300	205 mV
N/100	227
N/50	240
N/20	254
N/10	265

Aus diesen Werten wurde die Titrationskurve der Abb. 2 konstruiert. Der Wert für die N/10 Lösung stammt aus einer früheren Messung, die mit der Titrations-Kapillare durchgeführt worden war. Es ist bemerkenswert, daß diese unter anderen Bedingungen erhaltene Messung ein Potential wiedergibt, das sich in die Kurve der Abb. 2 gut einfügt.

Die in dieser Versuchsreihe gemessenen Elektrodenpotentiale dienten in Verbindung mit den van't Hoffschen Faktoren dazu, das Ionenprodukt der wasserfreien Essigsäure zu berechnen.

2. EXPERIMENTELLER TEIL

Die verwendete Essigsäure hatte einen Schmelzpunkt von 16·62°C. Sie war durch zahlreiches Ausfrieren entwässert worden. Bei der Bestimmung der Einzelpotentiale

wurde ein Lösungsmittel verwendet, das in zwei voneinander getrennten Ansätzen entwässert worden war, da geringe Verunreinigungen das Ionenprodukt stark beeinflussen können und völlige Reproduzierbarkeit gewährleistet sein mußte.

Das als Basenanaloges verwendete Diäthylanilin war frisch destilliert. Durch Einwägen war eine 1N Lösung bereitet worden, die durch Verdünnen auf die gewünschte Konzentration gebracht wurde. Zu jeder Messung wurden genau 10 cc Essigsäure in das Meßgefäß einpipettiert und davon ein kleiner Teil in die Kapillare gesaugt. Diese Menge wurde abgezogen und dann die berechnete Menge Diäthylanilin-Lösung zugesetzt.

Während der Potentialmessungen wurde nicht ununterbrochen gerührt. Es hatte sich nämlich bei früheren Titrationen herausgestellt, daß dadurch die Potentialwerte beeinträchtigt werden, indem Abweichungen bis zu 5 mV beobachtet wurden.

Vor dem Zusatz des Basenanalogen mußte natürlich die Einstellung des Nullpotentials erreicht werden. Diese war aber deshalb schwer zu kontrollieren, da infolge der schlechten Leitfähigkeit eine ziemlich große Veränderung der Brückeneinstellung (bis zu 30 Teilstrichen) notwendig war, um überhaupt einen Ausschlag zu erhalten. Da aber von den früheren potentiometrischen Titrationen bekannt war, daß diese Einstellung nach höchstens ca. 45 min erfolgt war, wurde hier mindestens 2 Stunden gewartet, ehe mit der eigentlichen Messung begonnen wurde. Zur Kontrolle, daß auch hierdurch die Reproduzierbarkeit der Ergebnisse nicht beeinflußt wurde, wurde auch diese Wartezeit variiert; sie betrug aber nie weniger als 2 Stunden.

VOL. 1 1955

3. DIE BERCHNUNG DES IONENPRODUKTES

Die Berechnung des Ionenproduktes der wasserfreien Essigsäure erfolgt nach der Nernstschen Gleichung

$$E = \frac{RT}{nF} \ln \frac{c}{c_{Ac}}$$

Darin ist die Konzentration der Acetationen des reinen Lösungsmittels c_{Ac} die einzige Unbekannte. Die Messung von E wurde soeben beschrieben, c ist durch die kryoskopischen Molekularge-wichtsbestimmungen bekannt, Bei einer N/300 Lösung herrscht völlige Dissoziation (Abb. 1), sodaß die Nernstsche Gleichung nach Einsetzen aller bekannten Größen lautet:

$$0{\cdot}205 = \frac{0{\cdot}861 \,.\, 10^{-4} \,.\, 293}{1} \,.\, \ln \frac{0{\cdot}0033}{c_{Ac}}$$

Für die Acetationenkonzentration des reinen Lösungsmittels ergibt sich daraus ein Wert von

$$c_{Ac} = 9{\cdot}7 \,.\, 10^{-7}$$

Auf Grund des Dissoziationsschemas der Essigsäure muß die H^+-Ionenkonzentration den gleichen Wert haben, sodaß sich für das Ionenprodukt ein Wert von

$$c_H \,.\, c_{Ac} = 0{\cdot}94 \,.\, 10^{-12} \text{ bei } 20°C$$

ergibt.

In der gleichen Weise wurde das Ionenprodukt aus den übrigen angegebenen Potentialen berechnet. Die Ergebnisse sind im folgenden zusammengestellt:

Aus N/100: $E = 227$ mV (20°C), $c = 0{\cdot}0076$
$c_{Ac} = 9{\cdot}8 \cdot 10^{-7}$
$c_H \cdot c_{Ac} = 0{\cdot}96 \cdot 10^{-13}$

Aus N/50: $E = 240$ mV (20°C), $c = 0{\cdot}0092$
$c_{Ac} = 6{\cdot}8 \cdot 10^{-7}$
$c_H \cdot c_{Ac} = 0{\cdot}46 \cdot 10^{-13}$

Aus N/20: $E = 254$ mV (20°C), $c = 0{\cdot}00105$
$c_{Ac} = 4{\cdot}5 \cdot 10^{-7}$
$c_H \cdot c_{Ac} = 0{\cdot}20 \cdot 10^{-13}$

Aus N/10: $E = 265$ mV (20°C), $c = 0{\cdot}007$
$c_{Ac} = 1{\cdot}9 \cdot 10^{-7}$
$c_H \cdot c_{Ac} = 0{\cdot}36 \cdot 10^{-13}$

Wenn auch der aus einer N/20 Lösung berechnete Wert dem von KOLTHOFF und WILLMAN[1] einerseits und von KILPI und PURANEN[4] andererseits bestimmten am nächsten kommt, ist nach den hier durchgeführten Messungen und Berechnungen der Mittelwert aus den beiden verdünntesten Lösungen als zuverlässiger anzusehen. Damit ist das Ionenprodukt der Essigsäure neu bestimmt mit einem Wert von

$$0{\cdot}95 \cdot 10^{-13}.$$

Die oben zusammengestellten Werte zeigen bei zunehmender Konzentration eine Abnahme und gleichzeitig eine Konvergenz zu den bereits in der Literatur beschriebenen Werten. (Eine Ausnahme zeigt der letzte Wert, was wahrscheinlich darauf zurückzuführen ist, daß das angegebene Potential einer früheren Messung entnommen ist, die unter etwas veränderten Bedingungen durchgeführt wurde.) Setzt man voraus, daß dieser Gang in den einzelnen Werten auf die bei steigender Konzentration zunehmende Assoziation zurückzuführen ist, dann liegt der Schluß nahe, daß auch bei den in der Literatur beschriebenen Messungen nicht die tatsächlichen Ionenaktivitäten benutzt worden sind.

Der Vorteil der Potentialmessungen, die dieser Berechnung zugrundeliegen, besteht darin, daß kein wässriges Vergleichssystem herangezogen zu werden braucht. Hinsichtlich des Elektrodenvorganges wurde zunächst angenommen, daß die Goldelektroden auf die Acetationen konzentrationsrichtig ansprechen. Aus der größenordnungsmäßigen Übereinstimmung der Werte für das Ionenprodukt, die aus Potentialmessungen bei verschiedenen Konzentrationen erhalten wurden, folgt, daß die Elektroden tatsächlich konzentrationsrichtig ansprechen. Daß sie auch wirklich auf die Acetationen ansprechen, läßt sich damit wahrscheinlich machen, daß zur Berechnung der Ionenprodukte ausschließlich mit den Acetationenaktivitäten gerechnet wurde, die den Messungen der van't Hoffschen Faktoren entnommen waren. Damit kann man mit einiger Sicherheit annehmen, daß diese beiden Voraussetzungen erfüllt sind.

Außer diesen wurden aber moch einige Annahmen gemacht, die nicht kontrollierbar sind. Es wurde nicht berücksichtigt, daß auch in der hier verwendeten potentiometrischen Meßanordnung ein Diffusionspotential enthalten ist, dessen Wert unbekannt ist. Da es sich bei diesem Diffusionspotential aber nur um die Berührungsstelle zweier verschieden konzentrierter Lösungen des gleichen Lösungsmittels

handelt, ist hier bei genügend geringer Konzentration eine Vernachlässigung eher gestattet als an der Grenzfläche von zwei verschiedenen Lösungsmitteln.

Daß bei der Bestimmung des Ionenproduktes größeres Gewicht auf die aus verdünnten Lösungen erhaltenen Werte gelegt wurde, hatte noch einen anderen Grund. Sowohl das Raoultsche Gesetz, das den Molekulargewichtsbestimmungen zugrunde liegt, als auch die Nernstsche Gleichung, mit deren Hilfe die letzten Berechnungen durchgeführt wurden, gelten streng nur in ideal verdünnten Lösungen. Dieser Zustand ist aber bei N/300 und sicher auch noch bei N/100 Lösungen am ehesten gewährleistet. Die Gültigkeit der Nernstschen Gleichung wurde bei steigender Konzentration in der obigen Form noch dadurch beeinträchtigt, daß in den Lösungen offenbar assoziierte Moleküle existieren, die ihrerseits wieder dissoziieren. Dabei ist aber nicht zu übersehen, ob der Wert 1 für den Faktor n überhaupt noch gerechtfertigt ist.

Wenn auch die Größenordnung des Ionenproduktes der Essigsäure als gesichert angesehen werden kann, so ist damit zu rechnen, daß bei genauer Kenntnis der in Eisessiglösung bestehenden Dissoziationsverhältnisse und bei Kenntnis der Ionenbeweglichkeiten die Wertangabe noch kleine Verbesserungen erfahren kann.

VOL. 1 1955

Die Arbeiten der Verfasser wurden durch Bewilligung von E.R.P.-Mitteln in großzügiger Weise gefördert.

Anionic Vacancies in Fluorite-type Oxides

(*Received* 26 *April* 1955)

SEVERAL cases have been reported of anomalous mixed crystals of MO_2 oxides having the fluorite structure, and M_2O_3 oxides having the closely-related rare-earth "C" structure.[1, 2, 3] There is general agreement that these contain vacancies in the anion sub-lattice. Recent work on the uranium dioxide-yttria system has shown that such vacancies are very easily filled by oxygen if one of the cations can be oxidized.

The mixed-crystal phases were made by co-precipitation of the hydroxides from a solution containing known quantities of yttrium and uranyl nitrates with excess ammonia, drying and igniting in

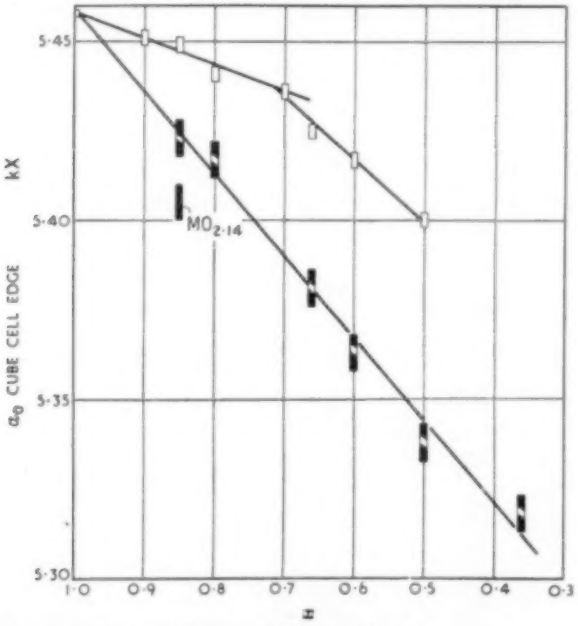

FIG. 1.—Variation of cell edge with composition of $U_xY_{1-x}O_y$.

After heating with uranium metal (fully reduced) (precision probably ±0·002 kX).

After heating in vacuum or carbon monoxide or after heating with uranium metal and oxidizing at room temperature to composition MO_2 (precision probably ±0·005 kX).

Sample oxidized beyond MO_2, to $MO_{2\cdot14}$ (precision probably ±0·005 kX).

carbon monoxide at ~1200° or in vacuum at ~2000°. The resulting products were black and were usually single, fluorite phases, particularly when the uranium content was high. Reduction of these products with uranium metal in a double-walled silica tube at 900°–1000° yielded brown oxides with a much expanded unit cell. These oxidized vigorously at temperatures of −20° to +20°. The final compositions reached after a long exposure to oxygen at room temperature are noted below, expressed

[1] MCCULLOUGH, J. D., and BRITTON, T. D. (1952) *J. Amer. Chem. Soc.* **74**, 5225.
[2] HUND, F., and MEZGER, R. (1952) *Z. physikal. Chem.* **201**, 268.
[3] HUND, F. (1951) *Z. Elektrochem.* **55**, 363.

as the value reached by y in the formula MO_y (M = metal), on the assumption that the reduced mixed crystal contained only U^{IV} and Y^{III}, and could therefore be formulated as $U_xY_{1-x}O_{1\cdot5+0\cdot5x}$.

x:	0·85	0·80	0·67	0·60
Final value of y:	1·98(B)	1·98(A)	1·985(A)	1·932(B)

The values denoted A were obtained by analysis of the final product for U^{VI} and U^{IV}; those denoted B were calculated by direct measurement of the amounts of oxygen absorbed.

As a result of this oxidation a_{100}, the cube cell edge, decreased to the value measured before reduction with uranium metal and the brown oxides became again black. The cell edge is plotted as a function of the composition of the mixed crystal $U_xY_{1-x}O_y$ in Fig. 1. The nonlinear variation of a_{100} with composition in the case of the fully-reduced phases is very similar to that found for the ceria-yttria system.[4] This result, the analytical results, and the colour changes, indicate that the fully reduced phases contain U^{IV} and Y^{III}, with anionic vacancies, a large proportion of which are filled with oxygen by a rapid oxidation process at low temperatures, which brings the phases close to the $MO_{2\cdot0}$ structure.

A different type of oxidation process occurs with uranium dioxide itself, and with uranium dioxide-thoria mixed crystals, where the anion sub-lattice is initially intact and the extra oxygen enters interstitial positions in the lattice; such oxidation is confined to the surface layers at 20° and bulk oxidation occurs at 150°–200°, if the particle size is $0\cdot5 - 2\mu$[5, 6]. The preparation of $U_{0\cdot85}Y_{0\cdot15}O_{1\cdot925}$, which consisted of particles of mean diameter 3μ, absorbed oxygen in excess of the $MO_{2\cdot0}$ composition when heated to 300° in oxygen, finally reaching $MO_{2\cdot14}$, causing further contraction of the lattice. This additional oxygen could be removed by carbon monoxide at 600°, and was probably interstitial oxygen.

Fully reduced phases having $x < 0\cdot5$ did not show the same tendency to oxidize rapidly at room temperature, and the lattice expansion caused by the uranium reduction stage was not so marked. It may be significant that traces of the Type "C" lines occurred in the X-ray diffraction patterns when $x < 0\cdot4$, implying some degree of ordering of the anionic vacancies in this region.

It is hoped to publish a fuller account of this system when more detailed results are available.

Atomic Energy Research Establishment,
Harwell, Berks

J. S. Anderson.*
I. F. Ferguson.
L. E. J. Roberts.

VOL. 1 1955

[4] Martin, R. L., private communication.
[5] Anderson, J. S., Edgington, D. N., Roberts, L. E. J., and Wait, E. (1954) *J. Chem. Soc.*, 3324.
[6] Anderson, J. S., Roberts, L. E. J., and Harper, E. A., to be published.
* Present address: Chemistry Dept., Melbourne University, Victoria.

Mechanism of Basic Hydrolysis of Cobalt(III) Complexes

(*Received* 13 *July* 1955)

The mechanism of the reaction between hydroxide ion and cobalt(III) complexes containing easily replaceable ligands is uncertain. It is believed to involve either a direct nucleophilic displacement (S_N 2) or a dissociation from the conjugate base of the complex ion (S_N 1 C B).[1] A critical test is to examine the behaviour in alkali of complex ions containing no replaceable protons.

It is known[2] that $[Co(CN)_5Br]^{=}$ and $[Co(CN)_5I]^{=}$ hydrolyze at a fixed rate in water independent of pH. These results may be due to electrostatic repulsion between the complex ions and hydroxide ion, and hence are not definitive. We have prepared *trans*-dichlorotetrakis (pyridine) cobalt(III)

[1] F. Basolo, *Chem. Rev.*, **52**, 459(1953).
[2] B. D. Stone, Ph.D Thesis, Northwestern University, 1952; A. W. Adamson and F. Basolo, in press.

nitrate according to the procedure of WERNER.[3] *Anal.* Calcd: Cl 13·95, N 13·78. Found: Cl 13·77, N 14·08. We have also made the β- and γ -picoline analogues.

These three compounds were found by titration to release ionic chloride in a first-order process and with identical rates at pH 1–2 and 9·18 (borate buffer). For comparison, *trans*-dichlorobis-ethylenediamine cobalt(III) chloride forms ionic chloride 1400 times faster at pH 9·18 than at pH 1–2. Similar large ratios have been found for other complexes containing replaceable protons.[4]

The first-order rate constants found above were

	k(min^{-1}), 25°C.	
	pH 1–2	pH 9·18
$[Copy_4Cl_2]^+$	$4{\cdot}9 \times 10^{-4}$	$5{\cdot}0 \times 10^{-4}$
$[Co(\beta\text{-pic})_4Cl_2]^+$	15×10^{-4}	15×10^{-4}
$[Co(\gamma\text{-pic})_4Cl_2]^+$	$9{\cdot}1 \times 10^{-4}$	$9{\cdot}1 \times 10^{-4}$[a]

[a] pH 8·5 because of decomposition at 9·18.

Higher pH's could not be studied because of the complete decomposition of the complex ions.

Trans-dichlorobis (dipyridyl) cobalt(III) chloride was prepared by the method of JAEGER and VAN DIJK.[5] This compound aquated instantaneously, as does the *cis* isomer, and was not suitable for kinetic studies. It was converted into the dinitro*bis* (dipyridyl) cobalt(III) chloride by treating with two equivalents of sodium nitrite in hot water. On cooling, a yellow salt separated which was recrystallized from absolute alcohol and dried at 115° for twenty-two hours. *Anal.* Calcd.: Cl 6·92. Found: 6·77, as ionic chloride.

The first nitro group in this complex was very labile, coming off in acid and in alkaline solution in a few minutes. The acid solution was not convenient for kinetic study because of the further reactions of nitrous acid. The rate of reaction in the presence of hydroxide ion was studied conductimetrically at 25°C. In four runs with complex ion and hydroxide ion equimolar between 1×10^{-4} M and 1×10^{-3} M, the nitrite ion was released in a *first-order* process with identical rate constants of $9{\cdot}1 \times 10^{-5}$ min^{-1}. Hence hydroxide ion had no effect on the rate.

The three pyridine complexes[6] were also found to show a normal enhancement of rates of chloride ion release in the presence of Hg^{++}. The second-order rate constant for the tetrakis (pyridine) complex was 11 M^{-1} min^{-1} at a concentration of 0·001 M in complex ion and mercuric nitrate.

These results are believed to provide strong evidence that the normal mechanism for the rapid basic hydrolysis of cobalt(III) complexes involves prior formation of the conjugate base of the complex ion.

R. G. PEARSON
R. E. MEEKER
F. BASOLO

Chemistry Department,
Northwestern University,
Evanston, Illinois

[3] A. WERNER and R. FEENSTRA, *Ber.* **39**, 1538(1906).
[4] R. G. PEARSON, R. E. MEEKER, and F. BASOLO, unpublished results.
[5] F. M. JAEGER and J. A. VAN DIJK, *Z. anorg. allgem. Chem.* **227**, 317 (1936).
[6] Compare BRÖNSTED and TEETER, *J. Phys. Chem.* **28**, 579 (1924).

The Half-life of Emanation-220*

(*Received* 20 *June* 1955)

CURRENTLY the accepted value for the half-life of thoron (Em^{220}), 54·5 seconds, was chosen[1] by the International Radium Standards Commission in 1930, based on measurements of PERKINS[2] and SCHMID.[3]

Previous measurements have been made, using a leaf electroscope method involving the insertion

* Supported in part by the U.S. Atomic Energy Commission.
[1] M. CURIE A. DEBIERNE, A. S. EVE, H. GEIGER, O. HAHN, S. C. LIND, St. MEYER, E. RUTHERFORD, and E. SCHWEIDLER, *Rev. Mod. Phys.*, **3**, 427 (1931).
[2] P. B. PERKINS, *Phil. Mag.* (6), **27**, 720 (1914).
[3] R. SCHMID, *Mitt. Rad Inst.*, **103**, Wien. *Ber.* IIa, **126**, 1065 (1917).

TABLE 1.—VALUES OF THE HALF-LIFE OF THORON (Em^{220}).

Value (seconds)	Investigator
60	E. RUTHERFORD, *Scientific Papers*, Vol. I, p. 235
51	C. LEROSSIGNOL and C. T. GIMINGHAM, *Phil. Mag.* **8,** 107 (1904).
53·3	O. HAHN, *Jahrbuch d. Radioakt.*, Vol. II, p. 233 (1905).
54	H. L. BRONSON, *Amer. J. Sci.* **19,** 185 (1905).
54·3	M. S. LESLIE, *Phil. Mag.* **24,** 647 (1912).
54·53 ± 0·041	P. B. PERKINS, *Phil. Mag.* **27,** 720 (1914).
54·5	R. SCHMID, *Mitt. Ra. Inst.* **103,** Wien *Ber.* IIa, **126,** 1065 (1917).
51·5 ± 1·0	Present authors.

of suitable capacitance in parallel.[5] The various values reported in the literature are listed in Table 1, along with our value.

Instead of observing ionization current, as was done in the early studies, the decay in this experiment was followed by recording counts per unit time from an alpha-proportional counter. Tank

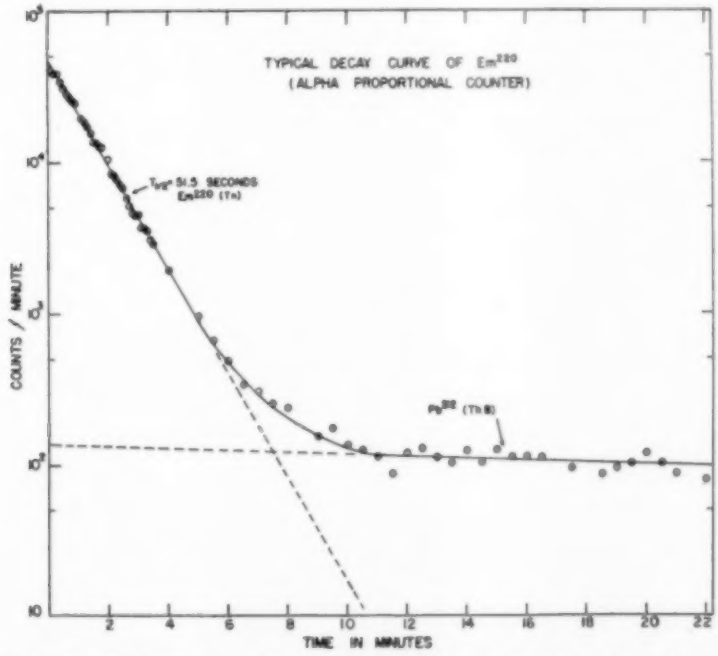

FIG. 1—A typical decay curve of thoron gas from alpha-proportional counting, using argon at 1-atm pressure. The half-life was obtained by a least-squares analysis of the original data in eight runs, not from the decay curve itself.

argon was used at atmospheric pressure both as a carrier for thoron and as the counting gas. To eliminate electronegative quenching gases such as oxygen, water vapour, etc., it was found that prolonged evacuation (up to as much as ten days at better than 10^{-4} mm) of the counting chamber was adequate. The chamber was checked frequently with a standard source of Po^{210} to make certain that quenching gases were absent. Thoron was swept into the evacuated chamber from an aged anhydrous thorium oxide source which had been flushed previously with dried tank argon. Pulses from the

chamber were amplified and fed into a scaler. The scaler and timer were photographed every six seconds with a Bolex Model H-16 cinecamera with Stevens time-lapse attachment. A typical decay curve is shown in Fig. 1. The data obtained from the first three minutes of decay (when the level of activity was approximately 30,000 counts/minute) were subjected to a least-squares analysis giving a final value for the half-life of

$$T^{\frac{1}{2}} = 51{\cdot}5 \pm 1.0 \text{ seconds}$$

representing an average of eight runs.

This value is probably more accurate than the early values in so far as photographic recording of the decay is free of the possible error introduced in reading a leaf electroscope by eye. Another error which is eliminated is the possible time-lag of the electroscope needle due to the capacitance effect (time-constant) which would cause the half-life to appear longer. Although the small error limits on the previously accepted value[2] are hardly justified, it nevertheless remains a tribute to the early workers that they achieved such high accuracy with a relatively primitive technique.

H. Schmied*
R. W. Fink*
B. L. Robinson†

University of Arkansas,
Fayetteville,
Arkansas

* Department of Chemistry.
† Department of Physics.

J. Inorganic and Nuclear Chemistry, 1955, Vol. 1, pp. 345–351. Pergamon Press Ltd., London

THE NEW ISOTOPES Pu^{246} AND Am^{246}

D. Engelkemeir, P. R. Fields, S. Fried, and G. L. Pyle;[1] C. M. Stevens;[2] L. B. Asprey;[3] C. I. Browne, H. Louise Smith, and R. W. Spence[4]

Argonne National Laboratory and Los Alamos Scientific Laboratory

(*Received* 30 *June* 1955)

Abstract—The beta-emitting isotopes Pu^{246} and Am^{246} were found in the debris of a thermonuclear test. These isotopes have half-lives of 11·2 ± 0·2 days and 25 ± 0·2 minutes, respectively. The chemical evidence for the existence of these isotopes is described. The final mass assignment was made on the basis of mass spectrographic evidence. The beta and gamma energies were obtained from scintillation spectrometer studies. The total disintegration energy of Am^{246} was found to be 2·29 MeV, which is in fair agreement with that estimated by Seaborg from closed decay cycle considerations.

VOL.
1
1955

In the course of an examination of the plutonium fraction isolated from the debris of November 1952 thermonuclear test, the new isotope Pu^{244} was detected by mass spectrometric methods.[5] It was naturally of interest to determine the mode of decay of this isotope, since systematic considerations indicated that it would be near the borderline of beta stability.

Examinations of the radiations of the plutonium fraction indicated the presence of two beta activities; one of approximately 0·15 MeV and the other of 1·2 MeV. It was possible by means of chemical separation procedures to show that the less-energetic beta was associated with plutonium, while the more-energetic was attributable to an americium isotope. The beta-emitting plutonium isotope decayed with a half-life of 11·2 ± 0·2 days, while the half-life of the americium isotope was 25 ± 0·2 minutes. The two betas appeared to be present in equal amounts.

This agreement of the values for the half-life and beta energy of the americium isotope with the previously determined values for Am^{244} might point to the assignment of the observed plutonium beta activity to mass 244.[6]

Several considerations, however, indicated that, if Pu^{244} is beta-unstable, it could account for only a small fraction of the beta activity observed. The amount of beta activity and its short-lived decay were clearly inconsistent with the total quantity of mass 244 present in the sample. Calculations indicated that easily detectable amounts of the Cm^{244} daughter of the beta-emitting "Am^{244}" would have appeared in the "milkings" of the plutonium if the 25-minute beta activity were indeed Am^{244}, and if the 10- to 40-year 5·8 MeV alpha is correctly assigned to Cm^{244}.

Alpha pulse analyses of the "milkings" have set an upper limit to the presence of an 18-year Cm^{244} of less than 0·1 per cent of that expected if the decay chain belonged to the 244 mass. In addition, the abundance of Pu^{244} taken in conjunction with the half-life observed for the gross beta decay would require a beta activity

[1] Chemistry Division, Argonne National Laboratory.
[2] Special Materials Division, Argonne National Laboratory.
[3] CMR Division, Los Alamos Scientific Laboratory.
[4] J Division, Los Alamos Scientific Laboratory.
Work performed under the auspices of the U.S. Atomic Energy Commission.
[5] D. C. Hess, G. L. Pyle, S. Fried, M. Inghram, ANL-MGI-48, November 25, 1952.
[6] K. Street, Jr., A. Ghiorso, and G. T. Seaborg, *Phys. Rev.*, 79, 530 (1950).

many times that actually observed. Further indication that the 11·2-day beta half-life cannot be attributed to Pu^{244} is the constant value of the abundance of the 244 mass in two mass spectrometric measurements made about one month apart.

The chemical evidence indicating that the 0·15 MeV beta is due to a plutonium isotope is as follows:

1. Extractability by ether from an oxidized solution.
2. Complete carrying on precipitated lanthanum fluoride.
3. Extractability into TTA-benzene from 0·5M HNO_3.
4. Comparison of behaviour with plutonium on a Dowex A-1 anion column (the alpha-to-beta ratio remained constant in these procedures).

It was possible to "milk" the 1·2-MeV 25-minute beta activity away from the plutonium fraction repeatedly and then to observe its growth back into that fraction.

A series of experiments was carried out to prove the identity of the 25-minute daughter activity. The following evidence is considered as indicative of americium.

1. It could be milked away from the plutonium activity by extraction from TTA-benzene by washing with 0·5M HCl.
2. It could be precipitated with lanthanum fluoride.
3. It precipitated with lanthanum fluoride from a solution containing plutonium which had been oxidized to the VI state.
4. The activity was "spiked" with Am^{241} and Cm^{242} and oxidised with ammonium persulphate. Lanthanum fluoride was precipitated. Less than 10 per cent of the beta activity was carried on the lanthanum fluoride. The solution was then reduced and a second lanthanum fluoride precipitation made. Pulse analyses showed that approximately 5 per cent of Am^{241} was present in the precipitation from the oxidized solution, and about 5 per cent of the Cm^{242} was present in the precipitate from the reduced solution. On this basis, the activity could not be curium, and must have been either americium or an activity of atomic number 97 or higher. The latter is improbable on the basis of systematic considerations, and also because it was very doubtful that two short-lived beta activities would escape undetected in either the equilibrium mixture or the daughter activity.

The decay of the beta activity in the plutonium fraction was followed for some 60 days, and led to a half-life value 11·2 $\pm$ 0·2 days for the parent plutonium. The half-life of the daughter was measured to be 25 $\pm$ 0·2 min by following the decay of 6×10^4 c/m through approximately thirteen half-lives. No deviation from straight-line decay was observed over that interval.

Aluminium absorption measurements were made on the equilibrium mixture, freshly purified plutonium, and separated daughter activity. The half-thickness for the purified plutonium fraction was about 3·5 mg Al/cm², and for the daughter activity about 63 mg Al/cm², corresponding to energies of 0·15 MeV and 1·2 MeV respectively.

MASS ASSIGNMENT

From consideration of the known beta activities of plutonium isotopes and the elimination of Pu^{244} as indicated previously, it seemed quite likely that the activity was due to either Pu^{245} or Pu^{246}. Mass spectrometric examination of the plutonium fraction from a subsequent experiment did indeed show the presence of these

isotopes.[7] Re-examination of the Pu^{246} content of this plutonium after 10 days disclosed a decrease in 246 mass consistent with a half-life of $11{\cdot}2 \pm 0{\cdot}2$ days. On this basis, the mass number was conclusively shown to be 246.

SCINTILLATION SPECTROMETER STUDIES

Analysis of the gamma radiation from the plutonium activities was undertaken, using the usual techniques of analysis of pulses from a scintillation counter. The observed peak positions were translated into energy by making corrections for channel width and zero level of the analyzer. The energy calibration was obtained by measuring the pulse heights of 14 X-ray and gamma-ray lines of known energy, covering the energy range from 22·5 to 1332 keV. The sample of the equilibrium

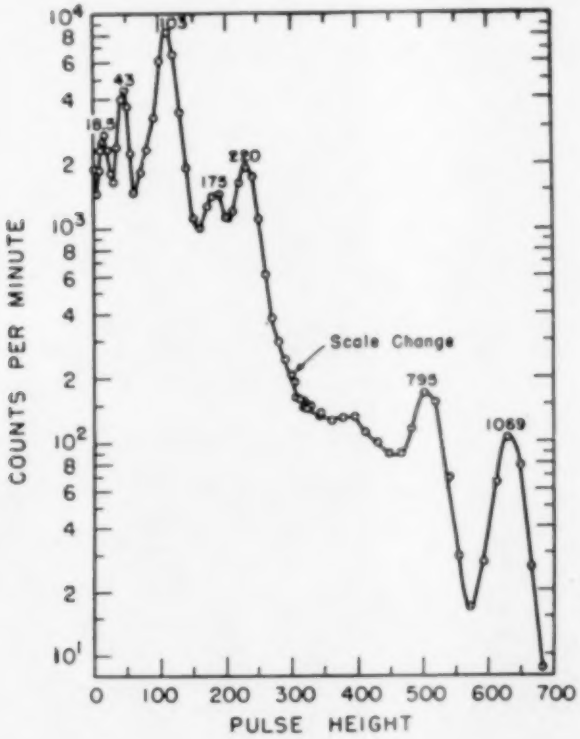

FIG. 1.

mixture, which contained about 5 μg of plutonium, consisted of a 1-ml volume of solution in a 2-ml volumetric flask inserted in a hole drilled in a $\frac{1}{2}$-in. plastic holder. A 245-mg/cm^2 aluminium absorber was placed over the counter, which had a 17S-T aluminium window weighing 95 mg/cm^2. In several determinations, the average values of the energies of the observed gamma-rays were 18·5, 43, 103, 175, 220, 795, and 1069 keV. A representative spectrum is shown in Fig. 1.

Fig. 2 presents the gamma-ray spectrum of Am^{245} separated from Pu^{246}. Gamma-rays are identified which have energies of 18·5, 103, 795, and 1069 keV, with the

[7] P. R. FIELDS, M. H. STUDIER, A. FRIEDMAN, H. DIAMOND, R. SJOBLOM, and P. A. SELLERS, to be published.

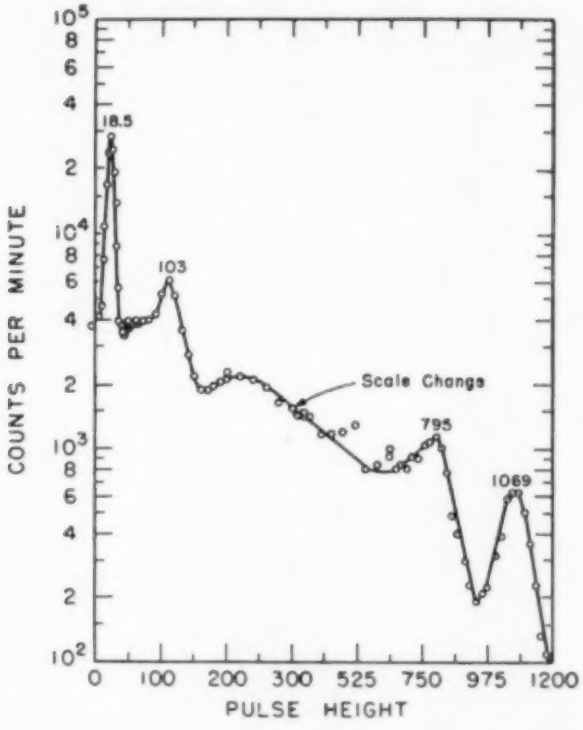
COUNTS PER MINUTE
PULSE HEIGHT
18.5
103
Scale Change
795
1069
0
100
200
300
525
750
975
1200

FIG. 2.

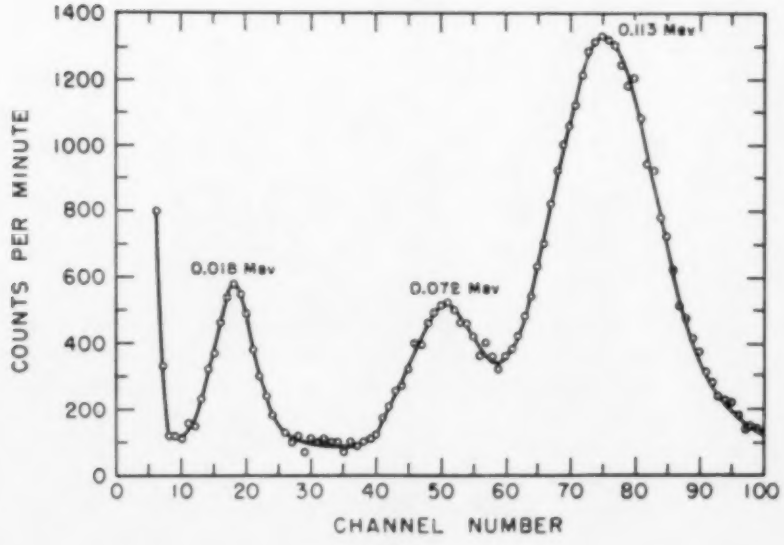
COUNTS PER MINUTE
CHANNEL NUMBER
0.018 Mev
0.072 Mev
0.113 Mev

FIG. 3.

intensity of the 103-line greatly diminished from that obtained with the equilibrium sample. By difference, gamma-rays with energies of 43, 103, 175, and 220 keV may be assigned to the plutonium fraction. In the determination of the americium spectrum, the 245-mg/cm² aluminium absorber was not used, and consequently the absorption of the 18·5-keV line was greatly diminished.

The contribution of the plutonium isotopes with masses less than 244 to any of the peaks observed above was no more than 10 per cent in the case of the 18·5-keV peak, and less than 1 per cent for any of the others. It was also observed that the shape of the spectrum did not change appreciably over a period of one month.

The lower-energy spectrum of the equilibrium mixture was also studied closely. A linear relation between channel and energy was obtained in the region below 200

VOL. 1 1955

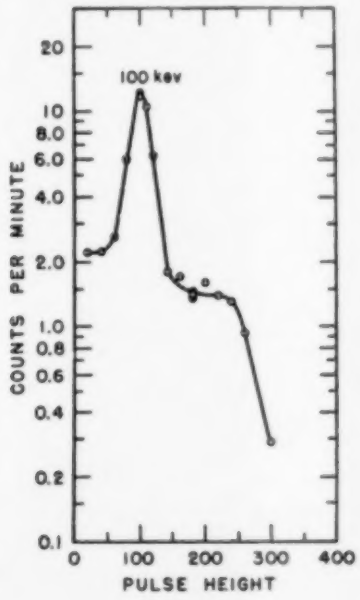

FIG. 4.

keV by calibrations using the gamma-rays and X-rays emitted by Lu^{177}, Am^{241}, and Hg^{203}. The sample used consisted of some 90,000 c/m of plutonium on a platinum plate covered with 0·0005 in. of nylon; the only absorbers present, in addition to several centimetres of air, were 0·005 in. of Al and 1/16 to 1/32 in. of MgO. Repeated observations of this sample led to average values for the gamma-ray energies of 224 ± 10, 111 ± 3, and $18 \pm 0{\cdot}5$ keV. Fig. 3 presents a representative low-energy spectrum.

Two sodium iodide scintillation spectrometers were used in coincidence to measure the spectrum of gammas in coincidence with the 1069-keV gamma. Spectrometer B was set to select only the photopeak pulses of the 1069-keV gamma, whereas the pulse-height channel of spectrometer A was varied. A peak at approximately 100 keV, followed by a low shoulder at approximately 200 keV was observed (Fig. 4). The relative intensity of the 100-keV radiation may be obtained from the ratio of the

integrated coincidence rate over the 100-keV peak divided by the counting rate of the 1069-keV gamma in spectrometer A. The value of this ratio is found to be 0·013, and, since the ratio should equal the efficiency of counter A for a 100-keV photon (about 0·30, if every 1069-keV gamma were in coincidence with a 100-keV photon), it may be concluded that approximately 4 per cent of the 1069-keV gamma-rays are accompanied by a 100-keV photon.

The Kurie plot (Fig. 5) of the beta spectrum taken from an equilibrium mixture of plutonium and americium shows a curvature in the high-energy region which is characteristic of a complex spectrum. The spectrum was taken with an anthracene scintillation spectrometer, and only those beta particles were counted which were in coincidence with the 1069-keV gamma. This counting was accomplished by placing

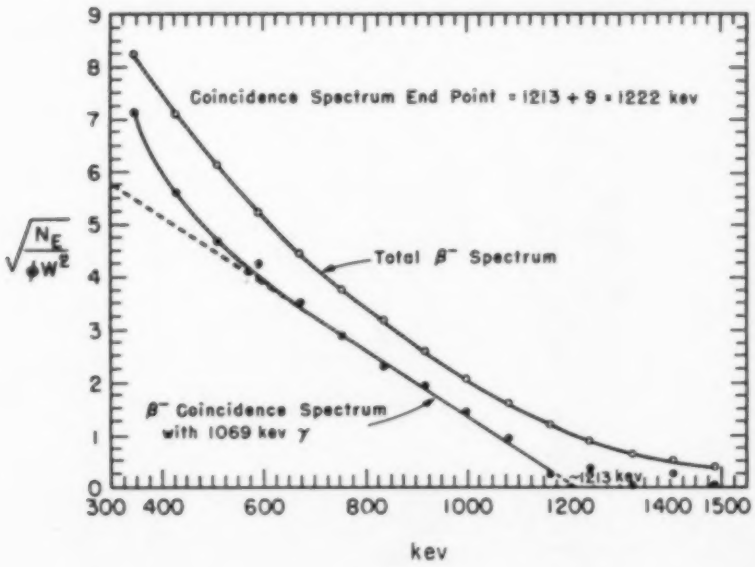

FIG. 5.

the sodium iodide spectrometer behind the sample and selecting only those pulses in the photopeak of the 1069 gamma. The coincidence circuit had a resolving time (2τ) of 0·14 μsec. The Kurie plot of the coincidence spectrum shows a straight-line portion which extrapolates to a maximum energy of 1213 keV. Correction for window absorption increases this energy to 1222 keV. The upswing at about half the maximum energy is characteristic of the instrument, and is due to the scattering of electrons out of the crystal before they have expended all their energy. This upswing makes it impossible to obtain the energy of any possible lower energy components and also masks the spectrum of the plutonium. The large tail on the total β^- spectrum above 1222 keV indicates that betas with an energy greater than 1222 keV are present. However, the low intensity did not permit a determination of their energy. Further evidence for the presence of a higher-energy component is shown in Fig. 5, in which the beta-gamma coincidence rate per beta is plotted as a

function of beta energy. The gamma detector was set to detect all gammas with energies greater than 400 keV, and the beta detector was set to count all betas with energies greater than the abscissa value plotted. For a simple beta spectrum followed by a gamma, the value of $\beta\gamma/\beta$ will remain constant. The decrease of $\beta\gamma/\beta$ at the higher beta energies indicates that betas are present having a higher energy than those in coincidence with the 795- and 1069-keV gammas. The decrease of $\beta\gamma/\beta$ at lower beta energies is probably due to the low-energy betas of plutonium.

The radiation of energy of about 100 keV and that of 18 keV were interpreted as probable K and L X-rays, since these energies roughly correspond to the expected values for the X-rays of americium and curium. The 100-keV photon in coincidence with the 1069-keV radiation could be either a curium K X-ray or a gamma-ray. The total disintegration energy of Am^{246} was interpreted to be the sum of the energy of the 1222-keV beta-ray and that of the coincident 1069-keV gamma-ray, or 2·29 MeV, in fair agreement with the 1·94 MeV estimated by SEABORG[8] from considerations of closed decay cycles.

VOL. 1 1955

[9] R. A. GLASS, S. G. THOMPSON, G. T. SEABORG, *J. Inorg. Nucl. Chem.*, **1**, 3-44 (1955).

J. Inorganic and Nuclear Chemistry, 1955, Vol. 1, pp. 352–356. Pergamon Press Ltd., London

THE VIBRATIONAL FREQUENCIES OF DIBORANE

D. A. BROWN and H. C. LONGUET-HIGGINS
Department of Theoretical Chemistry, University of Cambridge

(*Received* 1 *June* 1955)

Abstract—The vibrational frequencies of diborane have been calculated from a simple model in which the electron distribution is represented as the superposition of two rigid spherical distributions of negative electricity centred on the boron atoms.

It is shown that this model yields a reasonable form of potential function, and is consistent with the observed geometry. The non-totally symmetric vibration frequencies are determined by three unknown parameters: by assigning suitable values to these the fourteen observed frequencies can be reasonably well fitted. The worst discrepancy relates to a frequency about whose assignment there has been most difference of opinion.

THE VIBRATIONAL FREQUENCIES OF DIBORANE

THE relative success of an electrostatic model[1] in accounting for the vibrational frequencies of the hydrides XH_n prompted us to carry out a similar treatment of diborane B_2H_6. The only previous vibrational analysis of this molecule is that due to BELL and LONGUET-HIGGINS,[2] who employed a valence force potential function. The various terms in this potential function could not, however, be given a direct physical interpretation, so we have attempted an alternative, if less sophisticated, analysis of the problem. We represent the electron distribution in the molecule as the superposition of two rigid spherical charge distributions centred on the boron nuclei. The total electron density at a point in the molecule may then be represented as

$$\rho(R_1) + \rho(R_2)$$

where R_1, R_2 are the distances of the chosen point from the two boron nuclei.

The Molecular Geometry

The diborane molecule is known to have the bridged structure shown in Fig. 1, where the four protons 1, 2, 3, 4 lie in a plane perpendicular to the plane of the boron atoms 7, 8 and the bridge hydrogens 5, 6. The various bond lengths and angles were determined by HEDBERG and SCHOMAKER,[3] and are given in Table 1. The electrostatic model described above is represented mathematically by an intramolecular potential of the form

$$\begin{aligned} V = \sum_{i<j}^{8} \frac{e^2}{r_{ij}} &+ \phi_1(r_{17}) + \phi_1(r_{27}) + \phi_1(r_{38}) + \phi_1(r_{48}) \\ &+ \phi_2(r_{57}) + \phi_2(r_{58}) + \phi_2(r_{67}) + \phi_2(r_{68}) \\ &+ \phi_3(r_{15}) + \phi_3(r_{25}) + \phi_3(r_{37}) + \phi_3(r_{47}) \\ &+ \phi_4(r_{78}), \end{aligned}$$

[1] LONGUET-HIGGINS, H. C., and BROWN, D. A., *J. Inorg. Nucl. Chem.* **1**, 60 (1955).
[2] BELL, R. P., and LONGUET-HIGGINS, H. C., *Proc. Roy. Soc.* **A183**, 357 (1945).
[3] HEDBERG, K., and SCHOMAKER, V., *J. Amer. Chem. Soc.* **73**, 1482 (1951).

where

$$\frac{d\phi_1}{dr} = \frac{e^2(Q_1 - Z)}{r_1^2}, \qquad \frac{d^2\phi_1}{dr^2} = e^2\left\{4\pi\rho_1 - \frac{2(Q_1 - Z)}{r_1^3}\right\}$$

$$\frac{d\phi_2}{dr} = \frac{e^2(Q_2 - Z)}{r_2^2}, \qquad \frac{d^2\phi_2}{dr^2} = e^2\left\{4\pi\rho_2 - \frac{2(Q_2 - Z)}{r_2^3}\right\}$$

$$\frac{d\phi_3}{dr} = \frac{e^2(Q_3 - Z)}{r_3^2}, \qquad \frac{d^2\phi_3}{dr^2} = e^2\left\{4\pi\rho_3 - \frac{2(Q_3 - Z)}{r_3^3}\right\}$$

In these equations r_1, r_2, and r_3 represent the equilibrium values of the three B—H distances. Q_1, Q_2, Q_3 are defined as

$$Q_1 = \int_0^{r_1} 4\pi\rho(r)r^2dr, \quad Q_2 = \int_0^{r_2} 4\pi\rho(r)r^2dr, \quad Q_3 = \int_0^{r_3} 4\pi\rho(r)r^2dr\ ;$$

ρ_1, ρ_2, ρ_3 are abbreviations for $\rho(r_1)$, $\rho(r_2)$, $\rho(r_3)$.

VOL. 1 1955

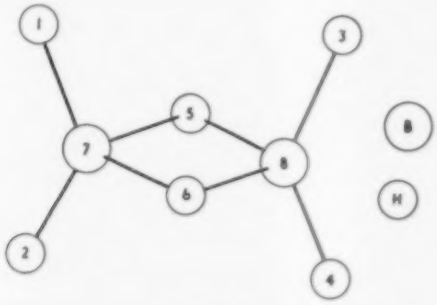

FIG. 1.

In this potential function the only term requiring explanation is the last, which represents the interaction between the two boron nuclei and their associated spherical electron distributions. The equilibrium conditions are obtained by differentiating the potential function with respect to the distances r_1, r_2, r_3, r_{78} and setting the first derivatives equal to zero. These conditions are sufficient to determine Q_1, Q_2, Q_3 and $\frac{d\phi_4}{dr_{78}}$. The values of these parameters obtained in this way are also given in Table 1.

TABLE 1.—MOLECULAR CONSTANTS OF DIBORANE

Internuclear distances (Å)	Q values (units of e)	ρ values (electrons/Å^3)
r_1 1·187	5·6188	1·752
r_2 1·334	5·8330	1·059
r_3 2·518	7·1354	0·300
r_{78} 1·715	—	—

The Vibrational Frequencies

In order to evaluate frequencies it is necessary to assign values to the three unknown density terms ρ_1, ρ_2, ρ_3. At this point we should draw attention to our further assumption that during vibration the centre of each spherical cloud remains in coincidence

with its boron nucleus. This may be justified by the fact, demonstrated in the previous paper, that the effective force constant for displacing a nucleus X from the centre of a spherical electron distribution is given by $\frac{4}{3}\pi\rho_x Ze^2$, where ρ_x is the electron density at the X nucleus; and since both Z and ρ_x are large, this force constant will also be large.

The frequencies of diborane are eighteen in number, falling into the eight representations of the symmetry group V_h. Since the forms of the normal vibrations have already been given by BELL and LONGUET-HIGGINS,[2] they need not be described here. Of the above eighteen frequencies only the totally-symmetric (A_{1g}) involve a first-order change in the distance r_{78}. Consequently the other frequencies do not involve the quantity $\frac{d^2\phi_4}{dr_{78}^2}$, which would be impossible to evaluate without assumptions additional to those already described.

TABLE 2.—SYMMETRY CLASSIFICATION OF VIBRATIONAL FREQUENCIES

Symmetry class	Frequencies occurring	Determining parameters
A_{1u}	ν_5	—
B_{2g}	ν_6 ν_7	ρ_2
B_{2u}	ν_8 ν_9 ν_{10}	ρ_1 ρ_3
B_{1g}	ν_{11} ν_{12}	ρ_1 ρ_3
B_{1u}	ν_{13} ν_{14}	ρ_2
B_{3g}	ν_{15}	—
B_{3u}	ν_{16} ν_{17} ν_{18}	ρ_1 ρ_2 ρ_3

The fourteen non-totally symmetric frequencies, ν_5 to ν_{18}, fall into seven symmetry classes, as indicated in Table 2. The frequencies of species A_{1u} and B_{2g} are found not to depend on ρ_1, ρ_2, or ρ_3, but only on Q_1, Q_2, and Q_3, which have already been determined from the molecular geometry. The density parameters on which the other frequencies depend are indicated in the last column of the table.

Determination of the Electron Density Terms

The algebraic relations between the vibrational frequencies and the parameters ρ_1, ρ_2, ρ_3 are somewhat complicated. To minimize risk of error, we obtained them by two independent methods, using respectively cartesian and internal displacement co-ordinates.

The parameter ρ_2 was determined from the observed value of $\nu_{13}^2 + \nu_{14}^2$, and the resulting value of ρ_2 then used to calculate ν_{13} and ν_{14} separately. It is of course equally possible to calculate ρ_2 from the observed frequencies of the B_{2g} group but the B_{1u} group was preferred because of the uncertainty in the observed values of ν_6 and ν_7.

It should be possible to obtain the parameters ρ_1 and ρ_3 from the B_{1g} symmetry class. The frequency of the vibration ν_{12} is experimentally uncertain, and we assigned it a compromise value of 800 cm^{-1}. However, it was found impossible to obtain in this way consistent values for the parameters ρ_1 and ρ_3. If, for example, ρ_3 is evaluated from the observed sum $\nu_{11}^2 + \nu_{12}^2$, then an exact fit of the product $\nu_{11}\nu_{12}$ requires a negative value of ρ_1. (The expedient of setting ρ_3 equal to zero was tried, but leads to imaginary frequencies.) For these reasons the values of ρ_1 and ρ_3 were adjusted

so that the calculated values of ν_{11} and ν_{12} contained equal and approximately minimal errors. This procedure, which determines ρ_1 more accurately than ρ_3, is appropriate in view of the experimental uncertainty in the value of ν_{12}. The value 606 cm^{-1} chosen by ANDERSON and BARKER[4] is definitely disproved by the polarization measurements of LORD and NIELSEN;[5] but the value 920 cm^{-1} given by the latter authors is not very reliable either, as it was determined from the combination $\nu_{10} + \nu_{12}$.

The values that we eventually adopted for ρ_1, ρ_2, ρ_3, are shown in the last column of Table 1; the resulting values for the non-symmetrical frequencies are given in the last column of Table 3.

TABLE 3.—OBSERVED AND CALCULATED FREQUENCIES OF DIBORANE

Frequency number	Spectroscopic activity	Assignment*					Calculated frequency
		B.L.-H.	P	W.N.P.	A.B.	L.N.	
ν_6	inactive	(890)†	—	613	1013	829	726
ν_6	Raman depolarized	(1540)	—	1745	1321	1768	1876
ν_7		1008	—	1013	764	1035	837
ν_8	Infrared	2625	2614	2614	2609	2612	2362
ν_9		1405	1283	1283	369	950	1813
ν_{10}		412	430	369	1857	368	438
ν_{11}	Raman depolarized	2489	—	2591	2591	2591	2231
ν_{12}		821	—	764	606	920	689
ν_{13}	Infrared	1816	1984	1861	1988	1920	1728
ν_{14}		981	974	974	973	973	1284
ν_{15}	Raman depolarized	(1505)	—	1321	1745	1012	1440
ν_{16}	Infrared	2558	2522	2522	2520	2525	2677
ν_{17}		1608	1604	1604	1604	1602	1792
ν_{18}		1178	1175	1175	1174	1177	1350

* *Key to Table 3*:

B.L.-H. = BELL, R. P., and LONGUET-HIGGINS, H. C., *Proc. Roy. Soc.* **A183,** 357 (1945).
P. = PRICE, W. C., *J. Chem. Phys.* **19,** 1 (1948).
W.N.P. = WEBB, A. N., NEU, J. T., and PITZER., K. S., *J. Chem. Phys.* **17,** 1007 (1949).
A.B. = ANDERSON, W. E., and BARKER, E. F., *J. Chem. Phys.* **18,** 698 (1950).
L.N. = LORD, R. C., and NIELSEN, E., *J. Chem. Phys.* **19,** 1 (1951).

† Bracketed values were estimated theoretically.

DISCUSSION

In general, the agreement between the calculated and observed frequencies is unexpectedly good. Probably the most interesting results are those obtained for the B_{2u} class. It will be seen that our treatment gives a low value of ν_{10}, and a rather high value of ν_9. This lends support to the view that the out-of-plane vibration ν_{10} of the bridge has a low frequency, as most previous workers have thought. On the other hand the discrepancy between the calculated value of ν_9 and the assignment of LORD and NIELSEN[5] is very noticeable; but it is obvious from Table 3 that there has been a good deal of disagreement over this frequency. We think it likely that the strong

[4] ANDERSON, W. E., and BARKER, E. F., *J. Chem. Phys.* **18,** 698 (1950).
[5] LORD, R. C., and NIELSEN, E., *J. Chem. Phys.* **19,** 1 (1951).

Type B band at 1860 cm^{-1}, considered by LORD and NIELSEN as an overtone but assigned by ANDERSON and BARKER to ν_{10}, may be ν_9 itself. We also suggest that, in view of our calculations, ν_{15} may have a considerably higher value than has hitherto been regarded as likely.

The general agreement between calculated and observed frequencies indicates that the above type of potential function gives a fair account of the dynamics of diborane. It remains to consider whether the values of the various parameters employed are reasonable or not. First of all, it will be observed that Q_1, Q_2, Q_3, which are determined by the molecular geometry alone, are in ascending order of magnitude. Since the total number of electrons is sixteen, one would expect Q_3 to lie near 8 as atom 3 lies far from the electron centre 7. This is found to be the case, though the precise value of Q_3 cannot, of course, be given much weight. As to the electron density terms ρ_1, ρ_2, ρ_3, they fall in decreasing order, and this is entirely reasonable physically.

It would, of course, be a mistake to regard our crude model of B_2H_6 as giving an accurate account of the electron distribution in this molecule. However, it does appear that the electron distribution can be reasonably well approximated as the superposition of two spherical distributions on the B atoms, and that as the protons move this distribution is relatively little disturbed.

J. Inorganic and Nuclear Chemistry, 1955, Vol. 1, pp. 357–370. Pergamon Press Ltd., London

VOL. 1 1955

HIGH-TEMPERATURE X-RAY STUDY OF URANIUM OXIDES IN THE UO_2-U_3O_8 REGION

FREDRIK GRØNVOLD
Kjemisk Institutt A, Universitetet i Oslo, Blindern, Norway

(*Received* 18 *May* 1955)

Abstract—Uranium oxides in the UO_2-U_3O_8 range have been studied by the X-ray powder method at temperatures between 20° and 969°C after annealing at 1000°C. The following phases were found:

1. UO_{2+x} with no detectable range of homogeneity at room temperature. The homogeneity range extends to about $UO_{2\cdot17}$ at 950°C. The lattice constant of UO_2 is $a = 5{\cdot}4704$ Å at 20°C, and the average linear thermal coefficient of expansion α is $10{\cdot}8 \cdot 10^{-6}$ °C^{-1} between 20° and 946°C. The observed density of $UO_{2\cdot00}$ is 10·793 g.cm^{-3} at 25°C.

2. $UO_{2\cdot25}$ or U_4O_9 with a narrow range of homogeneity. The lattice constant decreases from $a = 5{\cdot}4411$ Å at 20°C to 5·4397 Å at 86°C. From then on it increases linearly to 960°C with $\alpha = 11{\cdot}6 \cdot 10^{-6}$ °C^{-1}. The high density observed, 11·159 g.cm^{-3}, shows that oxygen atoms are taken up interstitially in the UO_2-like structure.

3. U_3O_{8-z} with a range of homogeneity between $UO_{2\cdot62}$ and $UO_{2\cdot667}$ at room temperature. The lattice constants vary between these limits;

$$UO_{2\cdot632}: \; a = 6{\cdot}735 \text{ Å}, \quad b = 3{\cdot}966 \text{ Å}, \quad c = 4{\cdot}144 \text{ Å}.$$

$$UO_{2\cdot667}: \; a = 6{\cdot}720 \text{ Å}, \quad b = 3{\cdot}983 \text{ Å}, \quad c = 4{\cdot}146 \text{ Å}.$$

The observed density of $UO_{2\cdot632}$ is 8·408 g.cm^{-3}, and of $UO_{2\cdot667}$, 8·378 g.cm^{-3}. The homogeneity range of the U_3O_{8-z} phase extends to about $UO_{2\cdot55}$ at 500° and 750°C.

THE phase relationships in the uranium-oxygen system have been studied by many investigators, and the results up to 1948 are well summarized by KATZ and RABINOWITCH.[1] Extensive bibliographies have been published by CROXTON,[2] ALLEN,[3] and LANG.[4] Only a short account of the most important results will therefore be given here.

According to vapour pressure studies by BILTZ and MÜLLER,[5] the phase relationships in the UO_2-U_3O_8 region are comparatively simple at high temperatures, where only the two oxides UO_2 and U_3O_8 exist. UO_2 has a range of homogeneity from the stoichiometric composition UO_2 to $UO_{2\cdot3}$ at 1160°C. The composition of the U_3O_8 phase in equilibrium with $UO_{2\cdot3}$ at this temperature is $UO_{2\cdot61}$.

RUNDLE *et al.*[6] found that the lattice constant of UO_2 diminished with increasing oxygen content up to approximately the composition $UO_{2\cdot25}$ in heated mixtures of UO_2 and U_3O_8. Indications that $UO_{2\cdot25}$ might not be the end-point of a continuous

[1] KATZ, J. J., and RABINOWITCH, E. *The Chemistry of Uranium, National Nuclear Energy Series*, Div. VIII, Vol. 5, New York, 1951.

[2] CROXTON, F. E. Uranium and its Compounds; *A Bibliography of Unclassified Literature*, K-295, Part 2. U.S. AEC, Oak Ridge, 1951.

[3] ALLEN, R. E. Uranium and its Compounds; *A Bibliography of Unclassified Literature*, TID-3041. U.S. AEC, Oak Ridge, 1953.

[4] LANG, S. M. An Annotated Bibliography of Selected References on the Solid-State Reactions of the Uranium Oxides. *National Bureau of Standards Circular* 535, Washington, 1953.

[5] BILTZ, W., and MÜLLER, H. *Z. anorg. Chem.* **163** (1927), 257.

[6] RUNDLE, R. E., BAENZIGER, N. C., WILSON, A. S., and MCDONALD, R. A. *J. Amer. Chem. Soc.* **70** (1948), 99.

series of solid solutions of oxygen in UO_2 were found by ALBERMAN and ANDERSON,[7] who reported that oxides in the range UO_2–$UO_{2\cdot2}$ disproportionated, when annealed at high temperature, into two well-defined cubic phases, UO_2 and a phase (the β-UO_2 phase) with composition close to $UO_{2\cdot19}$. (See, however, footnote on p. 360.)

Thus annealed UO_2 seems to have no appreciable solid solubility of oxygen, a conclusion also reached by HERING and PERIO.[8] These authors found that the composition limit of the β-UO_2 phase as given by ALBERMAN and ANDERSON[7] was in error, and assigned the composition $UO_{2\cdot25}$ or U_4O_9 to this phase. Recently, however, PERIO[9] studied quenched samples, and concluded that the range of homogeneity of the U_4O_9 phase extended to $UO_{2\cdot21}$ at 1000°C.

Regarding the composition of the U_3O_8 phase, there have been considerable differences in opinion as to both the uranium-rich and the oxygen-rich limits, but in this study we shall be concerned only with the uranium-rich limit. RUNDLE *et al.*[6] claimed, in contrast to BILTZ and MÜLLER,[5] that the U_3O_8 phase extended to the composition U_2O_5, and they obtained single crystals to which they assigned this composition. GRØNVOLD and HARALDSEN[10] found that U_2O_5 prepared by the method of LYDÉN[11] had a composition in the region of $UO_{2\cdot60}$. Reduction of U_3O_8 with hydrogen gas at 330°C indicated the slightly lower value $UO_{2\cdot56}$ as the uranium-rich limit of the U_3O_8 phase.

ALBERMAN and ANDERSON[7] confirmed the results of RUNDLE *et al.*[6] concerning the existence of U_2O_5, while HERING and PERIO[8] found that the composition limit of the U_3O_8 phase varied, as a result of different annealing temperatures, from $UO_{2\cdot64}$ at 100°C to $UO_{2\cdot52}$, i.e., almost U_2O_5, at 650°C. Recently, HOEKSTRA *et al.*[12] reported that the uranium-rich limit of the U_3O_8 phase was $UO_{2\cdot56}$ in samples that had been heated at 1200°C for several weeks.

In most of these investigations, the high temperature phase relationships have been inferred from measurements made at room temperature. It therefore seemed of interest to the author to extend the X-ray investigations to higher temperatures, and a report of that work will be given here.

EXPERIMENTAL

Since it is of the utmost importance to work with oxides of high purity and well-defined composition, special care was taken in this respect. The purification process followed in the main the procedure used by HÖNIGSCHMID[13] to obtain pure U_3O_8. This U_3O_8 was reduced to UO_2 by heating it in dried hydrogen gas in alumina boats: the furnace temperature was kept at about 500°C until water formation ceased, then raised to 1200°C and maintained there for four hours. To inhibit oxidation, the samples were allowed to cool until the next day in hydrogen or vacuum. Preparations richer in oxygen than UO_2 were made by mixing UO_2 and U_3O_8, and the U_3O_8 used for this purpose was made by oxidizing UO_2 to constant weight at 800°C. Mixtures were prepared in steps of 0·05 atom O/U from $UO_{2\cdot05}$ to $UO_{2\cdot65}$ (plus $UO_{2\cdot632}$), annealed in evacuated and sealed quartz tubes at 1000°C for seven days, and then cooled slowly down to room temperature over a period of two months.

In order to study the UO_2-U_3O_8 interconversion, several oxidation-reduction experiments were carried out, and the results are listed in Table 1. Instead of agreeing with the theoretical U_3O_8/UO_2 weight ratio 1·03951, based on the accepted atomic weights for uranium and oxygen, the observed

[7] ALBERMAN, K. B., and ANDERSON, J. S. *J. Chem. Soc.* **1949**, S.303.
[8] HERING, H., and PERIO, P. *Bull. Soc. Chim.* **1952**, 351.
[9] PERIO, P. *Bull. Soc. Chim.* **1953**, 256.
[10] GRØNVOLD, F., and HARALDSEN, H. *Nature* **162** (1948), 69.
[11] LYDÉN, R. *Finska Kemistsamf. Medd.* **48** (1939), 124.
[12] HOEKSTRA, H. R., SIEGEL, S., FUCHS, L. H., and KATZ, J. J. *J. Phys. Chem.* **59** (1955), 136.
[13] HÖNIGSCHMID, O. *Z. anorg. Chem.* **226** (1936), 289.

values in Series I are slightly lower. During the experiments it became evident that the weight of UO_2 increased when the sample had access to air. The approximately constant weight which was found after thirty minutes to one hour indicated that the rapid surface oxidation was complete and that the oxidation process from then on was controlled by diffusion.

TABLE 1.—EXPERIMENTAL DETERMINATION OF THE U_3O_8/UO_2 WEIGHT RATIO

Series	Treatment	g UO_2	g U_3O_8	U_3O_8/UO_2
I	Ox. 4 h 800°C	13·8162	14·35805	1·03922
	Red. 4 h 1000°C	13·8117	14·35241*	1·03915
	Ox. 50 h 800°C	13·8117	14·35232	1·03914
II	Red. 2 h 1000°C	35·5302	36·94106	1·03971
	Ox. 120 h 800°C	35·3326	36·75177	1·04017
	Red. 4 h 900°C	35·3316	36·75119	1·04018
	Ox. 24 h 800°C	35·3316	36·75132	1·04018

The low results compare favourably, however, with those from the classical experiments by ZIMMERMANN,[14] their mean value being 1·03927. RICHARDS and MERIGOLD[15] tried to explain the high atomic weight of uranium (U = 239·6 on the O = 16 scale) resulting from ZIMMERMANN's experiments as due to incomplete oxidation of UO_2 to U_3O_8. In view of the present experiments, a more reasonable interpretation is perhaps that ZIMMERMANN's UO_2 was slightly oxidized.

In Series II, the possibility of oxygen and water uptake was substantially reduced by carrying out the weighings in a dry-box. Dried nitrogen gas served as an inert atmosphere, and nitrogen containing less than 0·001 per cent oxygen was kindly provided by Norsk Hydro = Elektrisk Kvælstofaktieselskab. The precision weights used had recently been calibrated at the National Bureau of Standards, and the masses were corrected for buoyancy.

The U_3O_8/UO_2 weight ratio now found was somewhat higher than the theoretical value of 1·03951, which means that at least one of the oxides is non-stoichiometric under the present conditions. In order to conform to common practice, all results in this paper are based upon an assumed composition $UO_{2\cdot667}$ for the U_3O_8 phase when oxidized to constant weight in oxygen at 800°C. The composition of the most completely reduced oxide is then $UO_{1\cdot999}$, while the composition of the oxides weighed in air (Series I) is $UO_{2\cdot005-2\cdot006}$.

The possibility of preparing UO_2 with less oxygen than corresponds to the stoichiometric formula has been studied by some earlier investigators. BILTZ and MÜLLER[5] were able to prepare $UO_{1\cdot992}$ by reduction of UO_2 with hydrogen at 1300°C, and similar results were obtained by PAPPAS.[16]

An illustration of the instability of UO_2 in air is given in Fig. 1. The oxide had been reduced at 1200°C for four hours, and was not exposed to the air before the next day. The sample weighed 40·6872 g, and increased 0·03352 g during four weeks, standing in air (average conditions: 20°C 40 per cent relative humidity). After four hours the oxidation process followed an approximate parabolic law. To check the moisture content, the sample was dried for two days in a desiccator with P_2O_5. This caused a reduction in weight of only 0·00394 g, and after three hours in air the oxide had regained its weight. The statement by PERIO[9] that the slightly hygroscopic UO_2 may take up 0·4 per cent water during long exposure to the atmosphere, and that this gain in weight disappears on standing over P_2O_5, is not supported by the present experiments, since the major weight increase seems to be due to chemisorbed oxygen.

* Experiments performed to test the stability of U_3O_8 showed a weight decrease of 2·85 mg (0·003 atom O/U) as a result of heating at 900°C for three hours and cooling in air. Heating at 600°C for four days produced no weight increase above the 800°C value.

[14] ZIMMERMANN, C. *Annalen* **232** (1886), 273.

[15] RICHARDS, T. W., and MERIGOLD, B. S. *Z. anorg. Chem.* **31** (1902), 325.

[16] PAPPAS, A. Private communication.

VOL. 1 1955

X-ray photographs of the oxides were taken in a 19-cm Unicam high-temperature camera, with the samples sealed in thin-walled quartz capillaries. By means of a voltage regulator the registered temperature was kept constant within ±3°C. The Pt-PtRh thermocouples of the furnace were calibrated with a standard couple located at the position of the specimen.

Lattice constants are given in Ångström units ($\lambda CuK\alpha_1 = 1{\cdot}54051$ Å), and values from earlier investigations, actually expressed in *kX*, have been transformed to Ångströms by multiplication by the factor 1·00202.

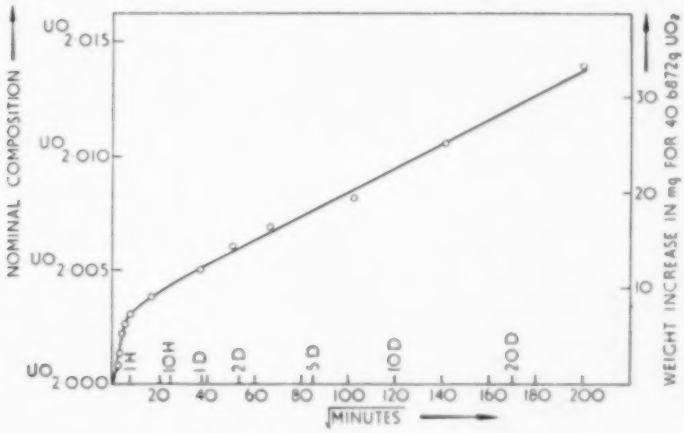

FIG. 1.—Weight increase of UO_2 in air.

The mean error in the lattice constants at room temperature is judged to be ± 0·02 per cent for the cubic phases and ± 0·05 per cent for the orthorhombic phase, unless otherwise stated. Above room temperature the accuracy of the determinations decreases owing to possible variations in oxygen content of the samples and uncertainty regarding their true temperature. In view of these circumstances, the mean error in the high-temperature results is estimated to be ± 0·04 per cent for the cubic phases and ± 0·12 per cent for the orthorhombic phase.

Density determinations were carried out pycnometrically at 25°C. Approximately 2·5 g of oxide was used in each experiment, and the pycnometer was filled with kerosene *in vacuo*.

RESULTS

Room Temperature

X-ray photographs taken at room temperature of samples in the UO_2-U_3O_8 region revealed the presence of three phases: UO_2, U_4O_9, and U_3O_{8-z}.

The UO_2 *and* U_4O_9 *Phases.* These phases both have cubic structure, and exist together in the samples $UO_{2\cdot05}$, $UO_{2\cdot10}$, $UO_{2\cdot15}$, and $UO_{2\cdot20}$. From the change in relative amounts of the phases with the composition, it is concluded that the system is homogeneous close to the composition $UO_{2\cdot25}$ or U_4O_9. HERING and PERIO'S[8] result is thus completely confirmed, and the formula $UO_{2\cdot19}$ given by ALBERMAN and ANDERSON[7] for this oxide is probably in error.*

The lattice constants found for UO_2 and U_4O_9 are listed in Table 2, together with some newer determinations taken from the literature. In general, the agreement between values found by the different investigators is good. A slight variation in lattice constant for U_4O_9 has been found in the present study, depending upon whether the phase is in equilibrium with UO_2 or U_3O_8. A similar effect was observed for

* According to PERIO[9], ANDERSON has indicated that the starting material used by ALBERMAN and ANDERSON[7] had the composition $UO_{2\cdot04}$ instead of $UO_{2\cdot000\pm0\cdot002}$, as stated in their paper.

UO_2 by RUNDLE *et al.*[6] who assumed that the increase in lattice constant observed when UO_2 was heated together with uranium at 2000°C was due to introduction of some uranium atoms into vacant cubic interstices in the UO_2 structure, causing expansion of the lattice.

According to HERING and PERIO,[8] the U_4O_9 structure is closely related to the UO_2 structure, the only difference being that the one excess oxygen atom per unit cell in U_4O_9 is taken up interstitially in the $(\frac{1}{2}\frac{1}{2}\frac{1}{2})$ position. Since the positions of the oxygen atoms cannot be determined by X-ray powder photographs, this problem will not be discussed further here.* It may, however, be pointed out that the uranium atoms in U_4O_9 do not seem to occupy exactly face-centred positions, since

TABLE 2.—LATTICE CONSTANTS OF THE UO_2 AND U_4O_9 PHASES

Author	Composition	a in Å	t°C
Present	$UO_{2\cdot00}$	5·4704 ± 0·0008	20 ± 2
RUNDLE *et al.*[6]	UO_2 + U	5·4720 ± 0·0007	
RUNDLE *et al.*[6]	UO_2	5·4691 ± 0·0005	
SWANSON and FUYAT[17]	$UO_{2\cdot03}$	5·4682	26
PERIO[9]	$UO_{2\cdot000\pm0\cdot003}$	5·4688 ± 0·0001	
ROSENBAUM and PEDERZANI[18]	UO_2	5·4678 ± 0·0005	
Present	$UO_{2\cdot30}$	5·4462 ± 0·0008	20 ± 2
Present	$UO_{2\cdot25}$	5·4411 ± 0·0008	20 ± 2
RUNDLE *et al.*[6]	$UO_{2\cdot3}$	5·4407 ± 0·0008	
ALBERMAN and ANDERSON[7]	"β-UO_2"	5·441 ± 0·003	
PERIO[9]	$UO_{2\cdot25}$	5·438 ± 0·003	

many weak, additional interferences are observed, especially in the high-angle region.

The U_3O_{8-x} Phase. Even at compositions as low as $UO_{2\cdot30}$, weak interferences from the U_3O_{8-x} phase can be observed on the photographs, and with increasing oxygen content the U_3O_{8-x} phase gradually becomes predominant. At the composition $UO_{2\cdot60}$, lines from the U_4O_9 structure are no longer visible.

The structure of U_3O_8 has been studied by several investigators—see KATZ and RABINOWITCH[1]—and according to GRØNVOLD[19] it is orthorhombic with lattice constants: $a = 6{\cdot}717$ Å, $b = 3{\cdot}977$ Å, $c = 4{\cdot}144$ Å. These values seem to refer to a uranium subcell, and by tripling of the b-axis a unit cell is obtained which contains six uranium and sixteen oxygen atoms. Probable positions of the oxygen atoms have been suggested by KIRSCHENBAUM.[20]

During the present study it was observed that the lattice constants of the U_3O_{8-x} phase varied with composition, as can be seen from the values listed in Table 3. The lattice constants of $UO_{2\cdot60}$ and $UO_{2\cdot633}$ are almost equal, but differ appreciably from

* The structure of U_4O_9 is now being studied by means of neutron diffraction by A. F. ANDRESEN at Jener, Lillestrøm.

[17] SWANSON, H.E., and FUYAT, R. K. Standard X-ray Diffraction Powder Patterns, *National Bureau of Standards Circular* 539, Vol. II, Washington, 1953.

[18] ROSENBAUM, B., and PEDERZANI, G. *Report CP*-1168, May 25, 1943, according to ref. 1.

[19] GRØNVOLD, F. *Nature* **162** (1948), 70.

[20] KIRSCHENBAUM, I. *Summary Report SAM Lab.*, according to ref. 1.

those of $UO_{2\cdot65}$ and $UO_{2\cdot667}$. The composition of the U_3O_{8-x} phase in equilibrium with the U_4O_9 phase is therefore judged to be very close to $UO_{2\cdot64\pm0\cdot01}$.

In Table 3 several earlier results are also listed, and if the variations in cell dimensions of the U_3O_{8-x} phase are taken as indications of the variations in oxygen content of the samples, these variations must be small. Only the value $a = 6\cdot76$ Å which HERING and PERIO[8] found for $UO_{2\cdot58}$* and the value $a = 6\cdot752$ Å which HOEKSTRA *et al.*[12] found for $UO_{2\cdot6}$ indicate a lower oxygen content for the U_3O_{8-x} phase than has been found here.

It is worthwhile noticing that the lattice constants of the sub-cell found by RUNDLE *et al.*[6] for U_2O_5 agree extremely well with those of the present $UO_{2\cdot633}$ sample. The superstructure ascribed by RUNDLE *et al.* to their U_2O_5 cell as a result of single-crystal studies might therefore be expected to apply to $UO_{2\cdot633}$. The same superstructure is reported by HOEKSTRA *et al.*, who noted indications that the cell size of the $UO_{2\cdot6}$ phase increases with increasing oxygen content in the range $UO_{2\cdot56}$ to $UO_{2\cdot65}$.

TABLE 3.—LATTICE CONSTANTS OF THE U_3O_{8-x} PHASE

Author	Composition	a in Å	b in Å	c in Å
Present	$UO_{2\cdot60}$	6·734	3·966	4·144
Present	$UO_{2\cdot633}$	6·735	3·966	4·144
Present	$UO_{2\cdot65}$	6·726	3·975	4·145
Present	$UO_{2\cdot667}$	6·7198 ± 0·0012	3·9831 ± 0·0015	4·1462 ± 0·0008
KIRSCHENBAUM[20]	U_3O_8	6·7165 ± 0·0006	3 . 3·9890 ± 0·0004	4·1486 ± 0·0006
HERING and PERIO[8]	$UO_{2\cdot58}$	6·76	3·96	4·15
HERING and PERIO[8]	U_3O_8	6·722 ± 0·005	3·988 ± 0·002	4·149 ± 0·002
HOEKSTRA *et al.*[12]	$UO_{2\cdot6}$	6·752	8 . 3·970	2 . 4·143
HOEKSTRA *et al.*[12]	U_3O_8	6·718	3 . 3·990	4·150
RUNDLE *et al.*[6]	U_2O_5	6·73 ± 0·02	8 . 3·964 ± 0·1	2 . 4·143 ± 0·02
ZACHARIASEN[21]	U_3O_8	6·71 ± 0·01	3·99 ± 0·01	4·15 ± 0·01
MILNE[22]	U_3O_8		3·87 3·94	4·15 4·15

As regards the precision determinations by KIRSCHENBAUM[20] on U_3O_8 (the mean value of three observations is given in Table 3), his samples seem to have been slightly richer in oxygen than $UO_{2\cdot667}$. This may be due to the fact that in his experiments equilibrium was approached from the UO_3 side, while in the present work it was approached from the U_4O_9 side.

The orthorhombic structure of U_3O_8 is not accepted by MILNE[22] or BROOKER and NUFFIELD,[23] who claim that the majority of U_3O_8 samples show two hexagonal structures with identical c-axis and slightly different b-axes. One of these structures is said to contain more oxygen, the other less, than corresponds to the formula U_3O_8. If the two phases exist in equilibrium, one would expect slowly cooled samples in the intermediate range to be mixtures of the two phases in variable proportions, with no

* This sample was made by oxidizing UO_3 at 280°C and annealing it for twenty-four hours at 300°C and two hours at 330°C.

[21] ZACHARIASEN, W. H. *Report CP*-1249, 22 Jan. 1944, according to ref. 1.

[22] MILNE, I. H. *Amer. Miner.* **36** (1951), 415.

[23] BROOKER, E. J., and NUFFIELD, E. W. *Amer. Miner.* **37** (1952), 363.

variation in the lattice constants of either phase. The present measurements show clearly that variations in position of the U_3O_{8-x} reflections with composition do occur in very slowly cooled samples. No reversal in line intensities was observed that could be associated with a change in relative amounts of two phases in the U_3O_{8-x} region. The author therefore concludes that the hexagonal two-cell interpretation of MILNE,[22] and BROOKER and NUFFIELD,[23] is not valid for the very pure and carefully annealed samples that have been studied here.

Densities. Density determinations in the UO_2-U_3O_8 region provide another check on the compositions of the phases. The results are listed in Table 4. By analogy with earlier results obtained by GRØNVOLD and HARALDSEN[10] on UO_2 samples oxidized at low temperatures, the densities of samples heated at high temperatures were also

VOL. 1 1955

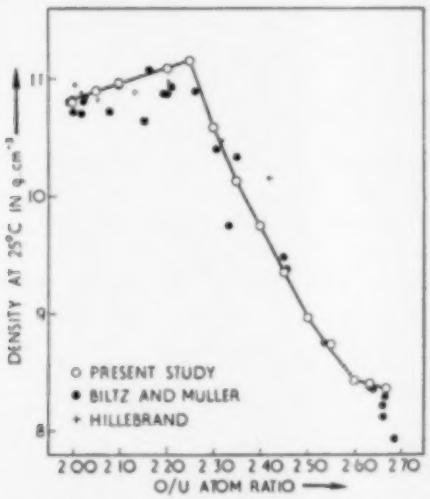

FIG. 2.—Density of uranium oxides as a function of composition.

found to increase with increasing oxygen content. From Fig. 2 it is seen that a sharp break occurs in the density-composition curve close to the composition $UO_{2\cdot25}$, giving an excellent confirmation of the X-ray results. From then on the density falls rapidly* until the composition $UO_{2\cdot60}$ is reached when it levels off to some extent. The density determinations thus indicate a slightly lower oxygen content for the U_3O_{8-x} phase in equilibrium with U_4O_9 than do the lattice parameter measurements. Combining the results, the author concludes that the probable uranium-rich composition limit of the U_3O_{8-x} phase is $UO_{2\cdot62\pm0\cdot02}$.

In Fig. 2 are also included the density values found by HILLEBRAND[24] and BILTZ and MÜLLER[5] in the UO_2-U_3O_8 region. They show the same general trend, but the spread is much larger. This may be due in part to differences in the history of the samples and uncertainties as to their composition.

* It is remarkable that the densities in the two-phase region $UO_{2\cdot25}$-$UO_{2\cdot60}$ fall below the additive values. A straight-line relationship was expected in Fig. 2 owing to the approximate linearity between atomic and weight per cent scales in this region. A possible explanation of the low densities for the two-phase mixture is that the samples consist of small one-phase domains, and that these are intergrown (i.e., they form mixed crystals in the strict sense of the word) as a result of the heat treatment. This might lead to an increase in specific volume compared to that of a coarse mixture.

[24] HILLEBRAND, F. W. *Z. anorg. Chem.* 3 (1893), 243; *U.S. Geol. Surv. Bull.* 113 (1893), 37.

It is of interest to compare the observed density values with those calculated from the lattice constants in combination with a plausible cell content. Such a comparison is shown in Table 5, and fairly satisfactory agreement is found.

TABLE 4.—DENSITIES OF URANIUM OXIDES IN THE UO_2-U_3O_8 RANGE. THE DETERMINATIONS WERE CARRIED OUT AT 25°C AND THE RESULTS ARE GIVEN IN G.CM^{-3}

Sample	Density	Sample	Density	Sample	Density
$UO_{2\cdot00}$	10·793	$UO_{2\cdot20}$	10·586	$UO_{2\cdot55}$	8·739
$UO_{2\cdot05}$	10·891	$UO_{2\cdot25}$	10·132	$UO_{2\cdot60}$	8·436
$UO_{2\cdot10}$	10·959	$UO_{2\cdot40}$	9·735	$UO_{2\cdot633}$	8·408
$UO_{2\cdot20}$	11·077	$UO_{2\cdot45}$	9·349	$UO_{2\cdot667}$	8·378
$UO_{2\cdot25}$	11·159	$UO_{2\cdot50}$	8·987		

TABLE 5.—OBSERVED AND CALCULATED DENSITIES FOR THE UO_2, U_4O_9, AND U_2O_{5-x} PHASES IN G.CM^{-3}. THE ATOMIC WEIGHT UNIT IS TAKEN AS $1{\cdot}6600 \cdot 10^{-24}$ G.

Composition	Cell content	D_{calc}	D_{obs}
$UO_{2\cdot00}$	U_4O_8	10·954	10·793
$UO_{2\cdot25}$	U_4O_9	11·297	11·159
$UO_{2\cdot633}$	$U_2O_{5\cdot267}$	8·405	8·408
$UO_{2\cdot667}$	$U_2O_{5\cdot333}$	8·399	8·378

This is especially gratifying since RUNDLE *et al.*[6] and ALBERMAN and ANDERSON[7] judged density determinations by liquid displacement to be unsuitable for deciding the cell content, and recommended the helium method instead. An evaluation of the correctness of their statement is now possible, since ANDERSON[25] has determined the densities of some uranium oxides by the latter method. His results were $d = 10{\cdot}88$ for α-UO_2 ($=UO_2$) and $d = 11{\cdot}18$ for β-UO_2 ($=UO_{2\cdot25}$). These values are higher than those found here, but still appreciably below the calculated densities. Some density values determined by the helium compression method are also given by PERIO.[9] The result for $UO_{2\cdot000\pm0\cdot003}$ was $d = 10{\cdot}87 \pm 0{\cdot}05$ and for U_4O_9, $d = 11{\cdot}3 \pm 0{\cdot}2$. Measurements of higher precision are needed to show the superiority of the helium method over the vacuum pycnometric method.

High Temperatures

X-ray photographs have been taken at up to 969°C of samples in the $UO_{2\cdot00}$-$UO_{2\cdot30}$ region to study the ranges of homogeneity of the UO_2 and U_4O_9 phases. Results of the lattice-constant determinations are found in Table 6 and Fig. 3. They show that the UO_2 phase takes up rapidly increasing amounts of oxygen (or U_4O_9) in solid solution

[25] ANDERSON, J. S. *Bull. Soc. Chim.* (1953). 781.

above 300°C, and the phase is therefore more aptly described as a UO_{2+x} phase. The limit is judged to be $UO_{2\cdot05}$ at 450°C, $UO_{2\cdot10}$ at 550°C, and $UO_{2\cdot15}$ at 850°C. Between 850° and 950°C the oxygen-rich limit of the UO_2 phase seems to increase from $UO_{2\cdot15}$ to $UO_{2\cdot17}$, but further data are needed.

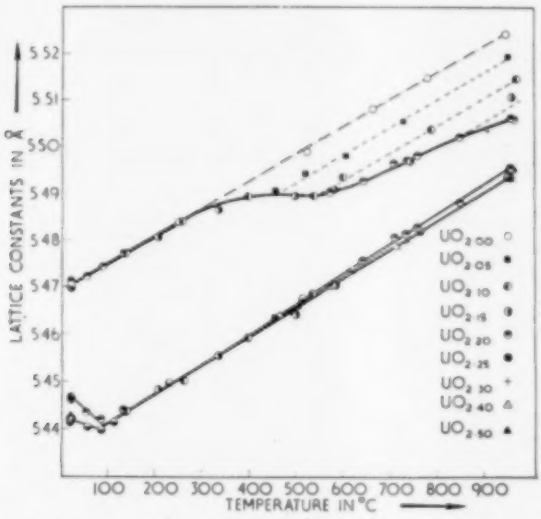

FIG. 3.—Lattice constants of the UO_2 and U_4O_9 phases at different temperatures.

$UO_{2\cdot00}$ is a single-phase product in the temperature range 20° to 946°C. The temperature dependence of the lattice constant is well reproduced with a constant linear expansion coefficient $\alpha = 10{\cdot}8 \,.\, 10^{-6}$°C; the lattice constant at t°C is

$$a_t = 5{\cdot}4704[1 + 10{\cdot}8 \,.\, 10^{-6}(t - 20)] \pm 0{\cdot}0004^{*}\ \text{Å}.$$

$UO_{2\cdot05}$ consists of two phases below and one phase above 460°C. Between 460° and 951°C its lattice constant is

$$a_t = 5{\cdot}4900[1 + 10{\cdot}8 \,.\, 10^{-6}(t - 460)] \pm 0{\cdot}0005\ \text{Å}.$$

$UO_{2\cdot10}$ contains two phases up to 550°C and is homogeneous above. Between 550° and 969°C its lattice constant is

$$a_t = 5{\cdot}4902[1 + 10{\cdot}8 \,.\, 10^{-6}(t - 550)] \pm 0{\cdot}0004\ \text{Å}.$$

$UO_{2\cdot15}$ and $UO_{2\cdot20}$ are two-phase preparations in the temperature range between 20° and 850°C or 960°C respectively.

$UO_{2\cdot25}$ is a one-phase preparation within the whole temperature range. From room temperature to 86°C the lattice constant decreases slightly, probably because of a transformation in the solid state. Between 100° and 960°C the lattice constant is

$$a_t = 5{\cdot}4410[1 + 11{\cdot}6 \,.\, 10^{-6}(t - 100)] \pm 0{\cdot}0007\ \text{Å}.$$

It is here assumed that the composition of the phase does not change with temperature and that the mean values of the lattice constants on both sides of the homogeneity range represent those of $UO_{2\cdot25}$.

* Mean deviation.

Above 600°C the lattice constants of the U_4O_9 phase in equilibrium with the UO_{2+x} phase are consistently higher than those of U_4O_9 in equilibrium with the U_3O_{8-z} phase. The homogeneity range is judged to have a width of about 0·02 atoms O/U at 900°C and to extend between $UO_{2\cdot24}$ and $UO_{2\cdot26}$.

The unit-cell dimensions and composition of the co-existent UO_2 and U_4O_9

phases have been computed from the experimental data at 100° intervals, and are listed in Table 7.

$UO_{2\cdot30}$, $UO_{2\cdot40}$, and $UO_{2\cdot50}$ are all two-phase preparations in the range from room temperature to 950°C, one phase being U_4O_9, the other U_3O_{8-x}. The lattice constants of the U_4O_9 phase are given in Table 5.

TABLE 6.—LATTICE CONSTANTS OF THE UO_{2+x} AND U_4O_9 PHASES AT DIFFERENT TEMPERATURES

t°C	a in Å	t°C	a in Å	t°C	a in Å	t°C	a in Å
$UO_{2\cdot00}$		$UO_{2\cdot10}$		$UO_{2\cdot20}$		$UO_{2\cdot25}$	
20	5·4704	20	5·4696	20	5·4708	20	5·4411
250	5·4839		5·4468		5·4462	52	5·4403
522	5·4988	138	5·4769	20	5·4711	86	5·4397
661	5·5087		5·4438		5·4468	115	5·4413
778	5·5153	260	5·4841	52	5·4722	230	5·4497
946	5·5246		5·4503		5·4432	513	5·4676
		397	5·4896	86	5·4741	623	5·4737
$UO_{2\cdot05}$			5·4591		5·4417	760	5·4821
		536	5·4896	132	5·4772		
456	5·4907		5·4686		5·4442	$UO_{2\cdot30}$	
	5·4635	599	5·4936	573	5·4903		
520	5·4943	785	5·5038		5·4704	496	5·4651
607	5·4980	969	5·5148	643	5·4925	732	5·4796
724	5·5052				5·4756	956	5·4938
951	5·5194	$UO_{2\cdot15}$		706	5·4967		
					5·4807	$UO_{2\cdot40}$	
		20	5·4698	731	5·4973		
			5·4463		5·4814	20	5·4416
		204	5·4807	755	5·4981	464	5·4639
			5·4483		5·4828	710	5·4787
		334	5·4866	847	5·5022	945	5·4941
			5·4554		5·4883		
		498	5·4896	955	5·5062	$UO_{2\cdot50}$	
			5·4639		5·4959		
		584	5·4910	960	5·5059	20	5·4423
			5·4704		5·4952	494	5·4647
		740	5·4970			950	5·4936
		959	5·5109				

The lattice constants of the U_3O_{8-x} phase were determined for $UO_{2\cdot50}$, $UO_{2\cdot60}$, and $UO_{2\cdot667}$, and the results are listed in Table 8. It is seen that the lattice constants of $UO_{2\cdot50}$ and $UO_{2\cdot60}$, which are equal within the limits of experimental error at room temperature, differ slightly at 250°C and markedly at 500° and 750°C. The uranium-rich limit of the homogeneity range of the U_3O_{8-x} phase is close to the composition $UO_{2\cdot60}$ at 250°C. The amount of U_4O_9 present in $UO_{2\cdot50}$ at about 500° and 750°C is

of the order of 20 per cent, and the composition of the U_3O_{8-x} phase is judged to be close to $UO_{2.55}$ at these temperatures.

The change in length of the cell edges with temperatures is rather different along the three axes of the U_3O_{8-x} crystals, and only the *a*-axis increases with increasing temperature for all three samples. Even so, the change is rather abrupt for $UO_{2.667}$

TABLE 7.—LATTICE CONSTANTS AND COMPOSITION OF THE CO-EXISTENT UO_{2+x} AND U_4O_9 PHASES AT 100° INTERVALS

t°C	a_1 in Å	Comp.	a_2 in Å	Comp.
100	5·4750	$UO_{2.00}$	5·4410	$UO_{2.25}$
200	5·4809	$UO_{2.00}$	5·4473	$UO_{2.25}$
300	5·4860	$UO_{2.01}$	5·4536	$UO_{2.25}$
400	5·490	$UO_{2.03}$	5·460	$UO_{2.25}$
500	5·490	$UO_{2.07}$	5·466	$UO_{2.25}$
600	5·491	$UO_{2.11}$	5·473	$UO_{2.25}$
700	5·496	$UO_{2.13}$	5·480	$UO_{2.25}$
800	5·500	$UO_{2.14}$	5·486	$UO_{2.24}$
900	5·505	$UO_{2.16}$	5·492	$UO_{2.24}$

TABLE 8.—LATTICE CONSTANTS OF THE U_3O_{8-x} PHASE AT DIFFERENT TEMPERATURES

Sample	*t*°C	*a* in Å	*b* in Å	*c* in Å	*V* in Å³
$UO_{2.50}$	20	6·734	3·966	4·145	110·7
	250	6·752	3·970	4·144	111·1
	494	6·753	3·979	4·143	111·3
	728	6·764	3·981	4·146	111·7
	950	6·788	3·983	4·140	111·9
$UO_{2.60}$	20	6·734	3·966	4·144	110·7
	246	6·749	3·961	4·141	110·7
	522	6·783	3·959	4·138	111·1
	773	6·799	3·961	4·136	111·4
$UO_{2.667}$	20	6·720	3·983	4·146	111·0
	205	6·772	3·952	4·145	110·9
	495	6·787	3·938	4·135	110·5
	743	6·796	3·960	4·139	111·4

from 20 to 205°C. The results found for $UO_{2.667}$ are, however, in reasonable agreement with those of HOEKSTRA *et al.*[12] for U_3O_8, as estimated from the graph in their paper At 200°C the lattice constants are fairly close to those presented here, with values $a = 6{\cdot}80$ Å, $b = 3\ .\ 3{\cdot}96$ Å, and $c = 4{\cdot}144$ Å. According to HOEKSTRA *et al.*, the structure of U_3O_8 becomes hexagonal above 400°C, and the lattice constants are $a = 6{\cdot}82$ Å and $c = 4{\cdot}136$ Å at 500°C. This is not the case with the $UO_{2.667}$ sample studied here, but the deviation from hexagonal symmetry is rather small.

VOL. 1 1955

DISCUSSION

An interesting result of the present study is that the UO_{2+x} and U_4O_9 phases have a solubility loop extending to at least 950°C, although the lattice constants differ by less than 1 per cent. The causes of the immiscibility are not yet understood, but one possibly important factor is the relatively small lattice constant of U_4O_9. From a linear extrapolation of the lattice constant for the UO_{2+x} phase at 800°C, one would expect to find $a = 5{\cdot}488$ Å for U_4O_9 instead of the actual value $a = 5{\cdot}485$ Å. Complete miscibility might, however, be expected at higher temperatures, since the thermal expansion of U_4O_9 is greater than that of UO_2, so that their lattice constants become more nearly equal as the temperature is increased.

That equilibrium had been attained for the UO_{2+x} phase in the high-temperature study is shown by the constancy with time of the phase boundary and its independence of whether equilibrium was approached from the high-temperature or the low-temperature side. The numerous runs in the UO_2 region indicated equilibrium conditions in the temperature range above 300°C. Regarding the U_4O_9 phase, the results were less conclusive because of its narrow range of homogeneity.*

The broad range of homogeneity which is found for the UO_{2+x} phase at 950°C does not appear on room-temperature photographs of rapidly cooled samples, and shows the danger of assuming that high-temperature phase relationships can be deduced from quenched samples. The slight differences in lattice constants between the various UO_2 samples may, at least in part, have been caused by differences in oxygen content of the UO_{2+x} phase due to the heat treatment and cooling conditions.

Very few thermal expansion measurements have been carried out on uranium oxides, and in the case of UO_2 the only published value is that by THEWLIS.[26] He determined the lattice constant of UO_2 at 720°C as $a = 5{\cdot}512$ Å in samples of β-U and CrU alloys. On the assumption that the lattice constant of UO_2 at room temperature was $a = 5{\cdot}468$ Å, as given by ALBERMAN and ANDERSON, THEWLIS computed the average thermal expansion coefficient as $\alpha = 11{\cdot}5 \cdot 10^{-6}$ °C^{-1} in this range. THEWLIS's high-temperature value fits well with the present results, and the higher expansion coefficient found by him is due primarily to the smaller lattice constant assumed for UO_2 at room temperature.

From the results so far obtained, little can be said about the composition limits and the thermal expansion of the U_3O_{8-x} phase. It is reasonably certain, however, that $UO_{2{\cdot}60}$ is a one-phase product in the temperature range 246° to 773°C, and its average coefficient of linear expansion is $4{\cdot}2 \cdot 10^{-6}$ °C^{-1} in this range. In the case of $UO_{2{\cdot}667}$, the volume of the unit cell decreases slightly from 20° to 205°C, the average linear expansion coefficient being $-1{\cdot}0 \cdot 10^{-6}$ °C^{-1}.

Negative coefficients of expansion were also found by DAY[27] for two polycrystalline U_3O_{8-x} samples that had been heated in air at high temperatures (one hour at 1400°C, and eight hours at 1430°C, respectively). Dilatometric measurements from room temperature to 375°C gave the value $-1{\cdot}0 \cdot 10^{-6}$ °C^{-1} as the linear expansion coefficient of the first sample and $-10 \cdot 10^{-6}$ °C^{-1} for the second. Above 375°C the expansion coefficients became positive, and from the figure in DAY's paper they are estimated as $+2 \cdot 10^{-6}$ °C^{-1} and $+1 \cdot 10^{-6}$ °C^{-1}.

* Some X-ray high-temperature photographs of oxides prepared by low-temperature oxidation of UO_2 indicate that the approach to equilibrium in U_4O_9 is sluggish below 500°C.

[26] THEWLIS, J. *Acta Cryst.* **5** (1952), 790.

[27] DAY, J. *Bull. Soc. Sci. Bretagne* **24** (1949), 13.

Some of the high-temperature photographs showed reflections that did not belong to any known uranium oxide. These reflections are probably due to cristobalite formed by crystallization of the silica specimen tubes. No reflections were found that could be attributed to the uranium oxide "X" which BROOKER and NUFFIELD[23] obtained by heating some pitchblendes. Neither was the new orthorhombic U_3O_8 modification of HOEKSTRA *et al.*,[12] with $a = 7{\cdot}05$ Å, $b = 11{\cdot}42$ Å, and $c = 8{\cdot}29$ Å, observed.

Phase Relationships. During the present study it was confirmed that the phase relationships in the UO_2-U_3O_8 region were comparatively simple for samples heated to high temperatures. These samples did not show the additional phases which GRØNVOLD and HARALDSEN[10] discovered on oxidizing UO_2 in the temperature region 100–265°C. In that investigation the oxygen-rich composition limit for a phase with pseudocubic, UO_2-like structure and lattice-constant $a = 5{\cdot}41$ Å, was found to be $UO_{2{\cdot}34}$.* In addition, a new tetragonal phase with lattice constants $a = 5{\cdot}38$ Å, $c = 5{\cdot}55$ Å, and composition around $UO_{2{\cdot}40}$, was observed. The tetragonal structure was confirmed by ALBERMAN and ANDERSON,[7] but these authors disagreed with the composition ascribed to it by GRØNVOLD and HARALDSEN, and stated instead that it existed in the region $UO_{2{\cdot}20}$ to $UO_{2{\cdot}30}$ with continuously changing lattice constants. The compositions found for these phases by GRØNVOLD and HARALDSEN were, however, fully confirmed three years ago by HERING and PERIO.[8]

More recently, PERIO[9] succeeded in determining the structure of the pseudocubic $UO_{2{\cdot}32}$ (U_3O_7) phase as tetragonal with $a = 5{\cdot}447 \pm 0{\cdot}003$ Å, $c = 5{\cdot}400 \pm 0{\cdot}002$ Å. ANDERSON[25] has lately modified his earlier conclusions, and says that there are some indications that the phase γ' (our $UO_{2{\cdot}34}$) has a composition close to $UO_{2{\cdot}33}$, and that the titre of γ'' (our $UO_{2{\cdot}40}$) is not much higher than that of γ'. The phase relationships of these compounds are rather obscure, and PERIO[28] has recently found a third tetragonal phase in the $UO_{2{\cdot}30}$-$UO_{2{\cdot}40}$ region.

Regarding the stability of these tetragonal phases with respect to UO_2, U_4O_9, and U_3O_8, PERIO[9] noted that samples in the $UO_{2{\cdot}00}$-$UO_{2{\cdot}25}$ region, which consisted of a mixture of the cubic and tetragonal phases, contained only cubic UO_2 and U_4O_9 after heating for about twenty hours at 700°C or for four months at 140°C. The U_3O_7 phase is therefore metastable with regard to the U_4O_9 and U_3O_8 phases at these temperatures. On the other hand, HERING and PERIO[8] stated that the phase reaction: $UO_2 + U_3O_8 \underset{470°}{\overset{300°}{\rightleftarrows}} UO_{2{\cdot}40}$ (tetr.) was reversible, but this has not been verified by the present author. ANDERSON[25] is also of the opinion that the γ' ($UO_{2{\cdot}34}$) and γ'' ($UO_{2{\cdot}40}$) phases are metastable with regard to the β-$UO_2 + U_3O_8$ phases. In the light of the information available at the present time, it seems that U_4O_9 is the only stable intermediate compound between UO_2 and U_3O_8 in the synthetic samples.

As a result of the present and earlier studies, a tentative phase diagram can be constructed for the UO_2-U_3O_8 region. This is done in Fig. 4, where the solid lines represent results from the present study and the dotted lines refer to the oxidation experiments by GRØNVOLD and HARALDSEN.[10] It can be seen that the homogeneity range of the UO_{2+x} and U_3O_{8-x} phases broadens at higher temperature, while that of the U_4O_9 phase is limited to a rather narrow range.

* It was not possible at that time to conclude with certainty whether this structure belonged to a phase different from UO_2 or to the oxygen-rich part of the UO_{2+x} phase.

[28] PERIO, P. *Bull. Soc. Chim.* (1953), 840.

The phase relationships below 300°C are rather uncertain because of the long time required to reach equilibrium, and the dotted horizontal lines only indicate the temperatures at which transformations take place at an appreciable rate. The homogeneity ranges of the $UO_{2\cdot34}$ and $UO_{2\cdot40}$ phases are tentatively drawn to a width of 0·01 atom O/U. There are indications that the oxidation of UO_2 can take

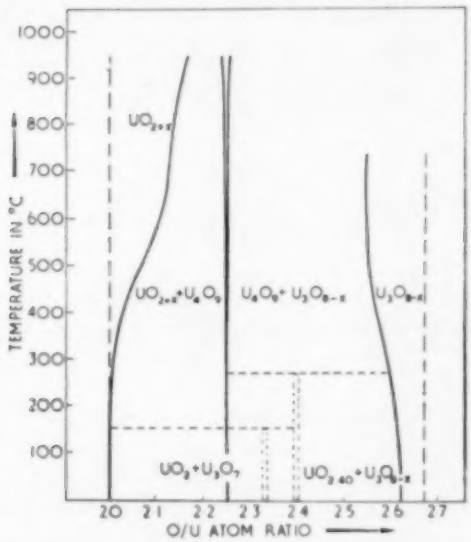

FIG. 4.—Tentative phase diagram for uranium oxides in the UO_2-U_3O_8 region.

place without deformation of the cubic structure when the temperature is low enough. Such a result was obtained by PERIO[9] on heating $UO_{2\cdot32}$ at 140°C for 2000 hours. The tetragonal deformation then disappeared, and the structure became cubic with $a = 5{\cdot}425$ Å.

ACKNOWLEDGEMENTS

The author wishes to express his appreciation to Professor HAAKON HARALDSEN for his interest in this study, and for making laboratory facilities available. He would also like to thank OLAF HAGBERG for his help in carrying out density determinations on the oxides.

J. Inorganic and Nuclear Chemistry, 1955, Vol. 1, pp. 371–377. Pergamon Press Ltd., London

RUTHENIUM(IV) NITRATES

J. S. ANDERSON* and J. D. M. MCCONNELL.
Atomic Energy Research Establishment, Harwell, Didcot, Berks

(*Received* 11 *March* 1955; *in final form* 20 *June* 1955)

Abstract—A solution of ruthenium tetroxide in nitric acid is reduced by hydrogen peroxide to give a deep red solution. On evaporation to dryness, a dark red solid is obtained, which decomposes fairly rapidly. The properties of solutions of this solid, which are strongly acidic, are consistent with the hypothesis that it contains a series of hydroxo-aquo ruthenium complexes of quadrivalent ruthenium of the general formula $[Ru(OH)_x(H_2O)_{6-x}](NO_3)_{4-x}$. On neutralization with alkali there appears to be a slow polymerization process after $[Ru(OH)_3(H_2O)_3]NO_3$ has been formed, leading finally to a precipitate, probably hydrated RuO_2.

VOL.
1
1955

HYDROGEN peroxide reduces ruthenium tetroxide in nitric acid to give a deep red solution containing a complex salt of ruthenium(IV). On evaporation under reduced pressure, excess nitric acid is removed, and a deep red vitreous solid is formed, which can be redissolved in water. The characterization of the species in the final solution is discussed in the present paper. The solid material was not studied directly, because it is both extremely hygroscopic and unstable in air, yielding ruthenium dioxide. Similar solutions in perchloric acid have been examined from a somewhat different point of view by WEHNER and HINDMAN,[1] while SMITH[2] has studied various ruthenium(IV) chlorides.

EXPERIMENTAL

Preparative

Ruthenium tetroxide was prepared by oxidation of potassium ruthenate with periodic acid.[3] It was collected in an ice-cooled receiver containing hydrogen peroxide and 2–5M nitric acid. A solution of the red ruthenium(IV) nitrate complex was obtained, at concentrations in the range 0·01–0·05M.

The red solution was evaporated at 10^{-2} mm Hg at room temperature, losing nitric acid, and yielding finally a deep red vitreous solid. With water this sometimes, but not always, gave a cloudy solution, owing to the presence of ruthenium dioxide as a decomposition product. In such cases a clear solution was obtained by ultrafiltration through collodion membranes supported on filter paper These were prepared by immersing discs of filter paper first in a 5 per cent glacial acetic acid solution of collodion, and then in water to gel the collodion.

Analysis

Ruthenium was determined (i) by the method of MARSHALL and RICKARD,[4] in which the optical density of a ruthenate solution is measured spectrophotometrically, and (ii) in the ion exchange experiments, by radioactive assay using ^{106}Ru. Nitrate was determined by precipitation with "Nitron." Total nitrogen was determined by a micro method using DEVARDA's alloy, the apparatus being a model of that due to PREGL.[5]

Ion Exchange

Equilibrations of solution and resin were carried out by mechanical stirring in 15-ml centrifuge cones.

* Present address: Chemistry Department, University of Melbourne, Victoria, Australia.

[1] WEHNER, P., and HINDMAN, J. C. (1950), *J. Amer. Chem. Soc.* **72**, 3911.
[2] SMITH, A. J. (1954), Thesis, University of London.
[3] MARTIN, F. S. (1952), *J. Chem. Soc.*, 3055.
[4] MARSHALL, E. D., and RICKARD, R. R. (1950), *Anal. Chem.*, **22**, 795
[5] PREGL, F. (1937), *Quantitative Organic Micro-Analysis* (Churchill, London).

RESULTS

The following facts have been established for all the solutions studied:

(1) The ruthenium is quadrivalent. This was demonstrated by titration of the iodine liberated from potassium iodide solution, which reduces ruthenium to the tervalent state.

(2) All the ruthenium is cationic, and is removed from solution by equilibration with a cation exchange resin (Zeocarb-225). It is recovered, apparently unchanged, by elution with dilute sulphuric acid, when the eluate contains no nitrogen. The ruthenium is not retained at all by an anion exchange resin (Deacidite-FF). These results are in agreement with the observation of WEHNER and HINDMAN,[1] that ruthenium(IV) migrates exclusively to the cathode in 6M perchloric acid solution.

(3) None of the nitrate is so tightly complexed that it cannot be precipitated directly by "Nitron" in the cold. If any nitrate complexes are formed, they must be labile ones.

TABLE 1.—ANALYSES OF SOLUTIONS CONTAINING RUTHENIUM(IV) NITRATES

Nitrogen		Acidity
As nitrate	Total	
0·431M	0·411M	0·400M
0·170	0·171	0·177
0·173	0·173	0·174

TABLE 2.—EFFECT OF SUCCESSIVE EVAPORATIONS ON THE $[NO_3]$: [Ru] RATIO

	$[NO_3]$: [Ru]
Original solution	2·56
After evaporating to dryness and taking up in water once	1·73
Do. do. do. three times	1·60
Do. do. do. five times	1·47
After evaporating to dryness and heating in vacuo at 60°C	1·26
After evaporating to dryness and heating in vacuo at 100°C	1·10

(4) The nitrate present accounts for the whole of the nitrogen: the analytical values for nitrate (by "Nitron" precipitation) and for total nitrogen (by reduction with DEVARDA'S alloy) are identical (Table 1). This excludes nitrosylruthenium and all other nitrogen-containing complexes from consideration.

(5) The acidity due to the ruthenium compound, as determined by alkali titration, is equivalent to the nitrate ion concentration (Table 1). The ruthenium is all precipitated as dioxide towards the end of the titration.

Different preparations are characterized by different values of the $[NO_3]$: [Ru] ratio. For the initial material this usually lies between 2 and 3. The ratio can be reduced slowly by successive evaporations with water, and markedly by heating the dry material *in vacuo* at 60° or 100°C (Table 2). This reduction of the $[NO_3]$: [Ru] ratio is accompanied by the production of much ruthenium dioxide.

The apparent cationic charge, as determined by the ion exchange method of STRICKLAND,[6] also usually lies between 2 and 3; Fig. 1 shows a typical set of results.

[6] STRICKLAND, J. D. H. (1952), *Nature*, **169**, 620.

The conclusion may be drawn that nitrate complexing is weak or non-existent, since otherwise the cationic charge would be appreciably smaller than the $[NO_3]$: [Ru] ratio. In view, however, of the simplifications involved in applying STRICKLAND'S method, this conclusion should be accepted with some reserve.

Titration curves for samples of different [No. 3] : [Ru] ratios are shown in Fig. 2.

The earlier stages of titration with alkali appear to be reversible. It is possible,

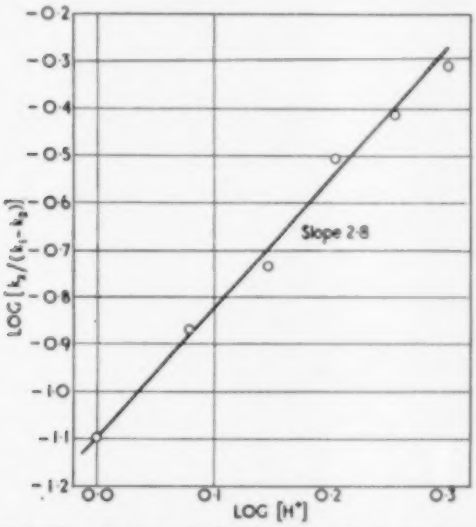

FIG. 1.—Determination of valency by Strickland's method. In the expression $k_2/(k_1 - k_2)$, k_1 is the concentration of solute initially present in solution, k_2 is the concentration present in solution after equilibration with resin.

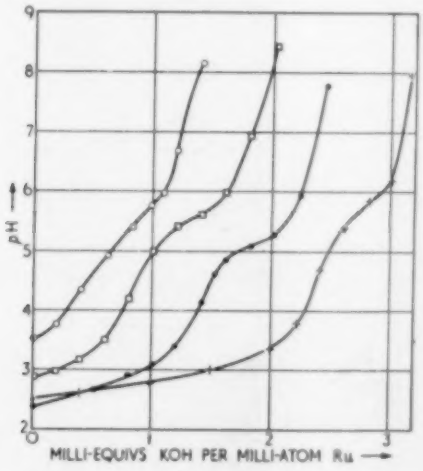

FIG. 2.—Titration curves for various $[NO_3]$: [Ru] ratios. The Ru concentrations differ from one curve to another.

$[NO_3]$: [Ru]

○ 1·3, □ 1·9, ● 2·3, + 3·0.

for example, to take a solution from its natural pH to pH 4·5 and back again, and to obtain the same apparent cationic charge at the end of the process as at the beginning. For increments of alkali above a pH of 3·7, however, a downward drift of pH was observed after the initial rise consequent upon each addition. This is indicated by the short vertical dotted lines in Fig. 3. Fig. 4 (for which we are indebted

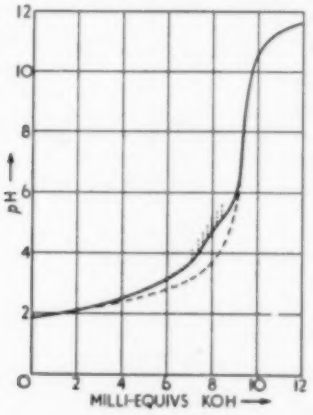

FIG. 3.—Titration curve of ruthenium complex ion against KOH. The solution contained ca. 9·5 milliequivs. Ru. Ratio $[NO_3]$: [Ru], 2·0.

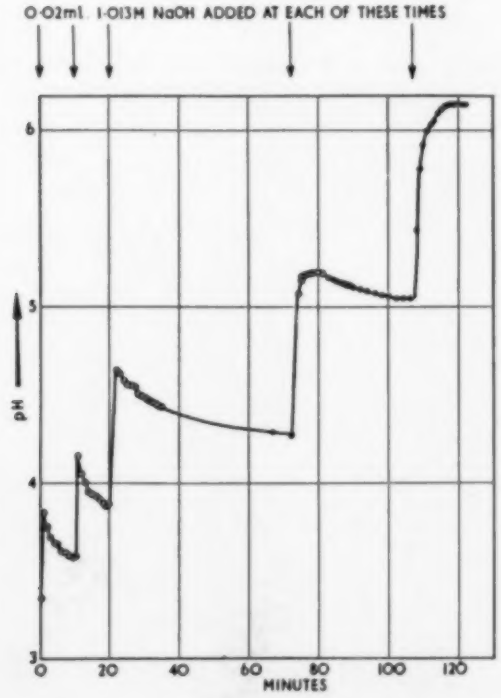

FIG. 4.

to A. C. JACOBS) shows the same effect in greater detail. Furthermore, reverse titration with acid from pH 5 gave the broken curve in Fig. 3, again showing that the titration curves do not correspond to an immediately reversible process. On the other hand, reverse titration from pH 2·8, up to which point no drift occurs, gave a curve exactly coincident with that for the forward titration. The drift only occurs in the final stages of the titration, when less than one equivalent of alkali per atom of ruthenium remains to be added. SMITH[6] has observed similar drifting pH-values in ruthenium(IV) chloride solutions.

VOL. 1 1955

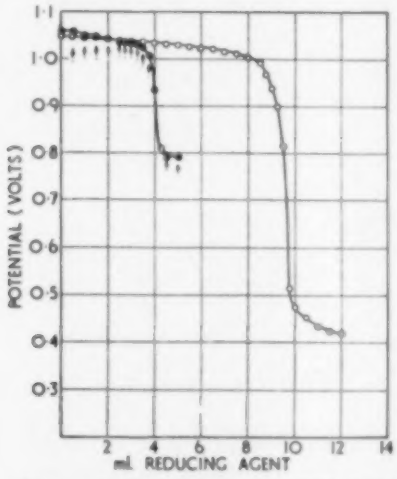

FIG. 5.—Reduction of RuO_4 in HNO_3 (2–5 M).
• Reductant H_2O_2, 0·0815 N; Ru, 0·01 M. Consumption 6·7 equivs. per atom Ru.
▫ Reductant N_2H_4, 0·0824 N; Ru, 0·006 M. Consumption 26 equivs. per atom Ru.
The drifts indicated by arrows were observed in the reduction with H_2O_2.
Electrodes: Saturated calomel, platinum.

When the reduction of ruthenium tetroxide in nitric acid by hydrogen peroxide was followed potentiometrically, there was no evidence of any intermediate stage, e.g., corresponding to ruthenium(VI) (Fig. 5). The same was true of hydrazine reduction, which appeared to yield the same product.

DISCUSSION

In general, a cation in aqueous solution may undergo:—

(1) Hydrolysis, which is best regarded as a loss of protons from the water in the inner hydration shell, i.e., as the dissociation of an acid.

(2) Condensation of mononuclear to polynuclear hydrolysis products, e.g., by formation of oxygen bridges:

(3) Anion complexing, which is usually a form of ligand substitution, the anion replacing a molecule of hydration water.

The relations between these processes are shown in the scheme in Fig. 6, where they are formulated for a quadrivalent metal M of co-ordination number 6, in presence of a univalent anion X. The extent to which one process or another predominates depends on both cation and anion.

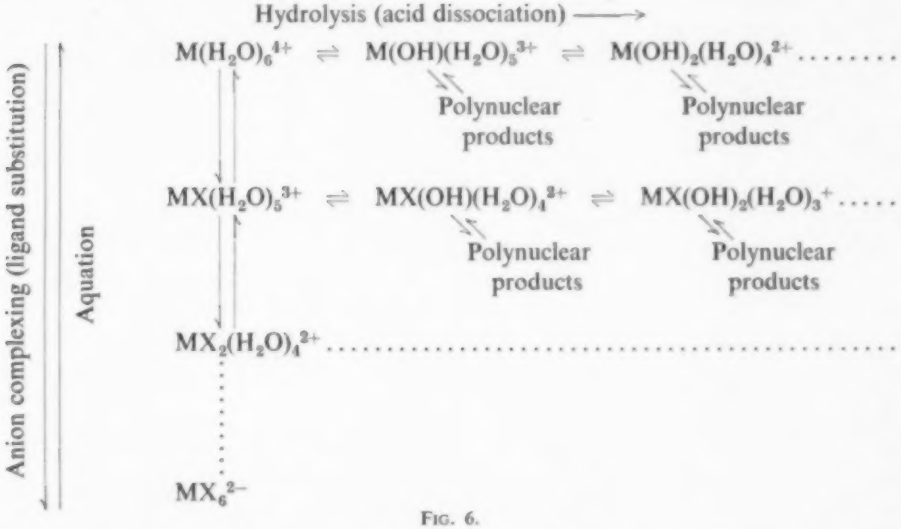

FIG. 6.

In the case of ruthenium(IV) in nitric acid, mononuclear hydrolysis is much the most important process. Most of the experimental results are explicable in terms of the following series of mononuclear complexes:

$$\begin{array}{ll} \text{I} & [Ru(OH)(H_2O)_5]\,(NO_3)_3 \\ & \Downarrow\Uparrow \\ \text{II} & [Ru(OH)_2(H_2O)_4]\,(NO_3)_2 + HNO_3 \\ & \Downarrow\Uparrow \\ \text{III} & [Ru(OH)_3(H_2O)_3]\,NO_3 + 2HNO_3 \\ & \Downarrow \\ \text{IV} & [Ru(OH)_4(H_2O)_2] + 3HNO_3 \end{array}$$

(The Formula IV represents hydrated ruthenium dioxide.) The initial product, as judged by the $[NO_3]$: [Ru] ratio and by the apparent cationic charge, must be mainly I with some II. Removal of nitric acid by evaporation or by addition of alkali increases the proportions of the later products, and ultimately yields IV irreversibly.

The parent member of the series ought logically to be $[Ru(H_2O)_6](NO_3)_4$, but no evidence for this has been found. The deep purple colour obtained on continued evaporation of the red solution with concentrated nitric acid, is likely to be due to a nitrosylruthenium complex.[7] Similarly in perchloric acid, even at concentrations as high as 6M, there is evidence[1] for hydrolysis products of Ru^{4+}, while hydrochloric acid solutions, again at high acid concentrations, yield $Ru(OH)Cl_3$ (aquated?) on evaporation.[8]

[7] FLETCHER, J. M., JENKINS, I. L., LEVER, F. M., MARTIN, F. S., POWELL, A. R., and TODD, R. (1955), *J. Inorg. Nucl. Chem.*, **1**, 378.

[8] REMY, H., and LÜHRS, A. (1928), *Ber.*, 61B, 917; (1929), *Ber.*, 62B, 200.

The prevalence of hydrolysis, even at high acidities, may be attributed to the high charge and small radius (0·67 Å) of the Ru^{4+} ion. All quadripositive ions are indeed readily hydrolyzed, and there is a general tendency towards greater hydrolysis at the smaller ionic radii.

The formation of polynuclear products, with a slow release of hydrogen ions, is the probable cause of the drift in pH observed during the final stages of alkali titration. The process evidently involves compound III, rather than II or I. This is in contrast to other quadripositive ions, which yield condensed species much more readily. It is doubtful, for example, whether Zr^{4+} and Th^{4+} form any detectable mononuclear products,[9, 10] while the first hydrolysis product of U^{4+}, UOH^{3+}, readily gives place to polynuclear species.[11] The existence of a solid compound $K_4[Ru_2Cl_{10}O]$ with an oxygen-bridged structure indicates a definite binuclear step.[12]

Nitrate complexing, and perhaps anion complexing generally, also appears to be weak with Ru^{4+}, again in contrast to other quadripositive ions. There are, for example, no anionic complexes comparable to say $Pu(NO_3)_6^{2-}$, which exists both in the solid state and in solution. Indeed, no nitrate complexing of Ru^{4+} has been detected at all. With chloride, on the other hand, K_2RuCl_6 can be prepared from very concentrated hydrochloric acid solutions.[12]

VOL. 1 1955

ACKNOWLEDGEMENT

We should like to thank H. A. C. McKay for discussions during the preparation of this paper.

[9] Zeilen, A. J. (1953), Thesis, University of California, UCRL-2268.
[10] Hietanen, S. (1954), *Acta. Chem. Scand.*, **8**, 1626.
[11] Hietanen, S. (1955). International Conference on Co-ordination Compounds, Amsterdam.
[12] Mathieson, A. M., Mellor, D. P., and Stephenson, N. C. (1952), *Acta. Cryst.*, **5**, 185.

J. Inorganic and Nuclear Chemistry, 1955, Vol. 1, pp. 378–401. Pergamon Press Ltd., London

NITRATO AND NITRO COMPLEXES OF NITROSYLRUTHENIUM

J. M. FLETCHER, I. L. JENKINS, F. M. LEVER, F. S. MARTIN, A. R. POWELL, and R. TODD
Atomic Energy Research Establishment, Harwell, Didcot, Berks.
Johnson, Matthey & Co. Ltd., Wembley

(*Received* 11 *March* 1955; *in final form* 6 *July* 1955)

Abstract—A series of nitratoaquo nitrosylruthenium complexes, of general formula $[RuNO(NO_3)_x(OH)_{3-x}(H_2O)_2]$, has been identified. In aqueous solution they give rise to anionic and cationic ruthenium species; the higher nitrato complexes are hydrolysed at room temperature at a rapid but measurable rate to lower nitrato complexes; condensation to polynuclear species accompanies these reactions. The trinitrato complex has been prepared by the action of boiling 8M HNO_3 on nitrosylruthenium hydroxide or the nitro complex $Na_2[RuNO(NO_2)_4OH]$ (hitherto considered a nitro complex of Ru(III)), both of which are conveniently made from ruthenium chloride. Nitro and nitrato complexes of nitrosylruthenium are also formed from ruthenium tetroxide and ruthenium alloys by the action of oxides of nitrogen or nitric acid.

The stronger complexing of nitrosylruthenium by NO_2^- than by NO_3^-, as well as the degree of complexing of $RuNO^{3+}$ by ligands such as F^-, Cl^-, point to the general similarity of these coordination complexes to those of Co(III) and Pt(IV). The nitrosylruthenium complexes are converted by sulphides to an insoluble nitrosylruthenium hydrosulphide.

1. INTRODUCTION

THE occurrence of the relatively long-lived isotopes of ruthenium, ^{103}Ru and ^{106}Ru, amongst the fission products, and hence their presence in solutions of irradiated fissile material dissolved in nitric acid, has drawn attention to extensive gaps in the knowledge of ruthenium chemistry. Such solutions contain tervalent nitrosylruthenium complexes in which the ligands are nitrato, nitro, hydroxo, and aquo groups. Although a large number of RuNO complexes (containing the ligands

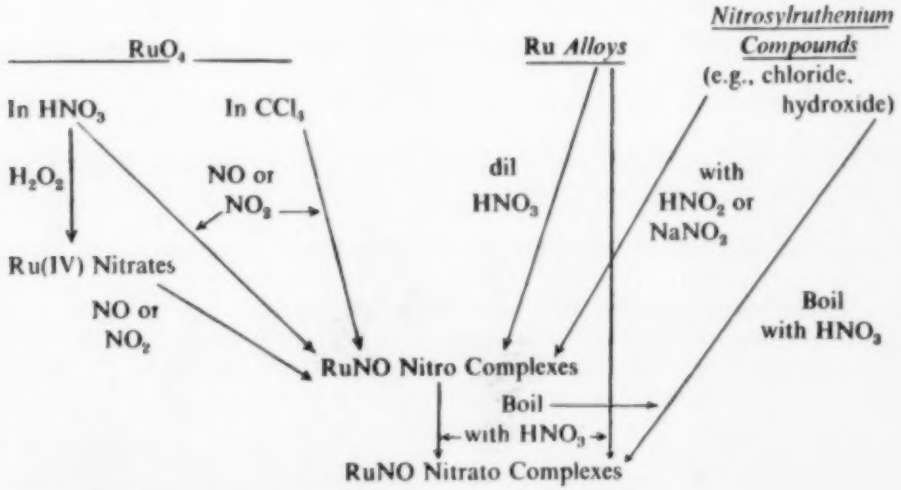

(1) JOLY, A. (1889) *Compt. rend.*, **108**, 854.

NH_3, halide ions, OH^-, SO_4^{2-}, $C_2O_4^{2-}$, and in a few cases NO_3^-) have been identified, the aquo-nitrato complexes have been neglected since JOLY[1] prepared them in solution; furthermore, in spite of the general similarity of RuNO complexes to those of Co(III) and Pt(IV), amongst which nitro complexes are well known, no nitro complex of RuNO has hitherto been formulated: this has partly arisen from the tetranitro complex having hitherto been regarded as a pentanitro complex of Ru(III). The scheme appearing on page 378 summarizes the ways in which aqueous solutions of nitro and nitrato complexes of RuNO are formed.

TABLE 1.—NITROSYLRUTHENIUM COMPLEXES

Substance	Description
Nitrosylruthenium Hydroxide	Dark brown solid. When freshly precipitated readily peptised by water, acids, and alkalis.
Nitrosylruthenium Hydrosulphide	Dark brown solid. Insoluble in water and in dilute acids and alkalis.
$[RuNO(NO_3)_2(H_2O)_2].2H_2O$	Rose-red deliquescent solid. Soluble in water, ethers, ketones, alcohols, esters, etc.
$[RuNO(NO_3)_2OH(H_2O)_2]$	Reddish brown deliquescent solid. Soluble in water, ethers, ketones, etc.
$[RuNO \cdot NO_3 \cdot (OH)_2(H_2O)_2]$	Brown hygroscopic solid. Soluble in water and lower ketones, but not in ethers.
$(RuNO)_2NO_3(OH)_5$	Brown solid. Soluble in water but not in ethers and lower ketones.
Polynuclear aquo-nitrato complexes	Brown solids. Solubility in water and in ketones dependent on composition and method of preparation.
$Na_2[RuNO(NO_2)_4OH].2H_2O$	Orange crystalline salt. Soluble in water, ketones, alcohols, etc.
$Ru_2N_6O_{15}$	Orange-brown deliquescent solid only formed under anhydrous conditions. Soluble in ketones, ethers, alcohols, etc.
$RuNO \cdot NO_3 \cdot C_2O_4 \cdot H_2O$	Pink crystalline solid. Soluble in water, insoluble in organic solvents.
$[RuNO \cdot NO_3 \cdot SO_4(H_2O)_3]$	Orange hygroscopic solid. Soluble in water.
$H_2[RuNOCl_4OH].2H_2O$	Purple deliquescent solid. Soluble in water and alcohols.
Nitrosylruthenium Fluoride	Dark brown powder, containing no complexed fluoride.

VOL. 1 1955

The particular nitrosylruthenium compounds prepared are given in Table 1. These are formulated on the assumption that, as in the ammino-nitrosylruthenium complexes, the ruthenium atom has a co-ordination number of 6, one position being occupied by the nitrosyl group: thus the mononuclear nitrato complexes are represented by the general formula $[RuNO(NO_3)_y(OH)_{3-y}(H_2O)_2]$. Their identity as nitrosylruthenium complexes has been established by their conversion to nitrosylruthenium hydroxide or hydrosulphide, in both of which the ratio [N] : [Ru] is unity.

2. PREPARATION AND IDENTIFICATION

Nitrosylruthenium Hydroxide, $RuNO(OH)_3$.

This substance is the most convenient starting-point for making the nitrato complexes. Joly[1] obtained a dark brown gelatinous precipitate by boiling a solution of nitrosylruthenium chloride with alkali; the product, after drying at 150°C, was originally formulated as the hydrated sesquioxide, $(RuNO)_2O_3,2H_2O$. We prefer to consider both the gelatinous precipitate and products dried from it up to 200°C as a hydroxide; when slowly heated from room temperature to 190°C, there is a continuous loss of water with no evidence for the separate existence of hydrates or for a sharp decomposition from a hydroxide to oxide. Samples dried at various temperatures from 45° to 210°C are glassy fragments showing conchoidal fractures which give diffuse X-ray diffraction patterns, with no evidence for any crystalline species.

To obtain it with a high yield, free from entrained ions, and to overcome the tendency of the precipitate to form colloidal solutions on being washed with water, the following method was employed.

Nitrosylruthenium chloride was prepared by passing a $NO\text{-}NO_2$ mixture into a solution of 10 g commercial ruthenium chloride in 100 ml water, boiling, removing any RuO_2 present, and evaporating with excess HCl until nearly dry. The material was dissolved in 50 ml water, HCl being added if necessary to complete the dissolution of the chloride, and the last traces of RuO_2 were removed by centrifugation. This solution of plum-coloured $RuNOCl_3$ was boiled and NaOH added to maintain the pH > 11; nitrosylruthenium hydroxide was formed, but remained in colloidal solution. The best pH for its complete precipitation was found to be 6·4, adjustment to this pH being made with a non-complexing acid (2 M $HClO_4$) (starting with quantities down to 0·2 g Ru, we have obtained nearly quantitative yields by retaining the suspension at pH 6·4 for several days prior to its separation). The precipitate was separated by centrifugation and repeatedly stirred with 200 ml portions of an acetone-water (9 : 1) mixture, which were decanted after centrifuging. Washing was continued until there was only a trace of chloride ion present in the wash liquor. The precipitate, after drying in a current of air at room temperature, contained Ru 45·4, N 6·1, Na 0·12, Cl 0·3 per cent. The bulk of the precipitate was redissolved in 100 ml dilute NaOH to give a pH > 11. The solution was reboiled, cooled, and the hydroxide reprecipitated and washed with acetone-water, until there were no traces of salts on evaporating the washings. After drying at room temperature to constant weight, there were found Ru 49·8, N 6·9, Na < 0·05, Cl < 0·1 per cent. In a similar preparation, in which traces of acetone were removed by drying at 80°, there were found Ru 49·7, N 7·05 per cent. $RuNO(OH)_3 \cdot H_2O$ requires Ru 50·6, N 7·0 per cent. When dried in vacuo at 210°C, there were found Ru 54·5, N 7·2 per cent. $RuNO(OH)_3$ requires Ru 55·6, N 7·7 per cent. The loss in weight of 170 mg of the hydroxide, dried at room temperature, was measured at temperatures up to 190°C, using a quartz spiral thermobalance. There was a continuous decrease in weight amounting to 9·6 per cent at 100°C and 17·3 per cent at 190°C.

This hydroxide has also been precipitated from acid solutions of other nitrosylruthenium complexes by the addition of alkali (Section 4). From 0·05 M Ru solutions of weak, e.g., nitrato, complexes the hydroxide is first precipitated at pH 4·2, and

re-solution is complete at pH 8·6: from solutions of stronger, e.g., nitro, complexes boiling at pH > 11 is necessary to produce the hydroxide (in colloidal solution).

Nitrosylruthenium Hydrosulphides

Aqueous solutions of the chloro, nitrato, and nitro complexes of nitrosylruthenium form, with hydrogen sulphide, dark brown precipitates in which the ratio [N] : [Ru] is unity. By employing conditions which give quantitative precipitation of all the ruthenium in solution, we have used this reaction not only to identify the presence of the (RuNO) group, but also (Section 5) for determinations of ruthenium and for estimations of the nitrato groups present in nitrosylruthenium complexes.

>0·1 g of a nitrosylruthenium complex was dissolved in water, acidified to pH ~ 2 with sulphuric acid, and saturated with hydrogen sulphide. A precipitate in which [N] : [Ru] = 1 was formed, but to achieve quantitative precipitation of ruthenium, the solution was made alkaline, resaturated with hydrogen sulphide, boiled, and reacidified. (Found for precipitate dried by acetone washing: Ru 43·4, N 6·0, S 34·1 per cent. $RuNO(SH)_{2\cdot4}(OH)_{0\cdot3}(H_2O)_{0\cdot67}$ requires Ru 43·3, N 5·9, S 34·1 per cent). Differences, in the range 2·0 to 3·0, or the ratio [S] : [RuNO] were found, depending on the conditions used for precipitation from nitrato complexes. The precipitates are therefore interpreted as containing OH as well as SH groups. The precipitates obtained from nitro complexes contained free sulphur (extractable by carbon disulphide) due to the interaction of oxides of nitrogen and hydrogen sulphide.

Trinitrato Nitrosylruthenium, $[RuNO(NO_3)_3(H_2O)_2],2H_2O$

The solids prepared by slow evaporation of the solutions (in nitric acid) described below have consistently been found to contain $[NO_3]$: [RuNO] = 3. As with other nitrosylruthenium compounds, part or all of the ligand can theoretically be complexed: the three species possible—$[RuNO \cdot NO_3(H_2O)_4](NO_3)_2$, $[RuNO(NO_3)_2(H_2O)_3]NO_3$, and $[RuNO(NO_3)_3(H_2O)_2]$—are indistinguishable by the analytical methods used for Ru, N, (NO_3), etc., and the conditions necessary for the quantitative formation of nitron nitrate prevent the use of nitron for distinguishing between complexed and uncomplexed (NO_3) groups. A considerable increase in the extractability from aqueous solutions by organic solvents is to be expected as the ratio [complexed NO_3] : [RuNO] increases; this increase has been found experimentally (Section 5, and JENKINS and WAIN[7]). Freshly prepared solutions in nitric acid of a number of preparations—of analysis almost identical to that given in (a) below—have been extracted with organic solvents. The observed degree of extraction indicates that the solids are substantially the trinitrato complex (and are henceforth so described), but that there is 5–20 per cent of lower (cationic) nitrato complexes also present. Small differences in the evaporation procedure from one batch to another are likely to affect the exact percentage of the trinitrato complex in any particular preparation.

(a) *From Nitrosylruthenium Hydroxide*

The hydroxide, after being freed from acetone by drying at 80°C, was boiled with sufficient nitric acid to leave the solution ~8 M HNO_3 (boiling with concentrated nitric acid gives slow oxidation to ruthenium tetroxide). By evaporating the solution to dryness at room temperature in a vacuum desiccator over solid caustic soda, the trinitrato complex was obtained as a dark red mass. (Found: Ru 26·0, N 14·5, NO_3 47·2 per cent; 0·4195 g dissolved in 15·7 g diethyl ether elevated the boiling point by 0·128°C, hence M.Wt., 420. Calc. for $[RuNO(NO_3)_3(H_2O)_2],2H_2O$: Ru 26·1, N 14·4, (NO_3) 47·8 per cent; M.Wt., 389.)

VOL. 1 1955

(b) *From Ruthenium Tetroxide*

When the trinitrato complex is prepared by the action of nitric oxide on a solution of ruthenium tetroxide in nitric acid,[8] relatively large amounts of nitric acid must be removed. This has been avoided by first forming a suspension of $Ru_2N_6O_{15}$ (see below) in carbon tetrachloride. This was extracted into a small volume of concentrated nitric acid, which, after separation from the organic phase, was heated to 80°C for ~15 min. The trinitrato complex was obtained by evaporation at room temperature as in (a).

(c) *From* $Na_2[RuNO(NO_2)_4OH]$

When heated with dilute nitric acid, this was decomposed to a lower (orange) nitro complex with evolution of oxides of nitrogen. On prolonged boiling with more concentrated acid, a solution of the trinitrato complex was formed.

Di- and Mononitrato Nitrosylruthenium Complexes

A number of reddish-brown solids, in which the ratio z of $[NO_3]$: [RuNO] has values from 1·7 to 2·7, have been prepared by the evaporation at 100°C of solutions of the nitrato complexes in nitric acid. These have been entirely soluble in diethyl ether. They are interpreted as mixtures of mononuclear compounds in which there are three, two, or one complexed nitrato groups and some uncomplexed nitrate; in them the mononitrato complex can exist in cationic forms such as $[RuNO \cdot NO_3(H_2O)_4](NO_3)_2$ and $[RuNO \cdot NO_3OH(H_2O)_3]NO_3$ and also as the uncharged molecule $[RuNO \cdot NO_3(OH)_2(H_2O)_2]$. The relative instability of the dinitrato complex (Section 3) makes it unlikely that it is a major constituent of these mixtures, even when z happens to be 2.

(a) *From Trinitrato Nitrosylruthenium*

Evaporation at 100°C of a solution of the trinitrato complex in nitric acid gave a product in which $y = 2·7$. (Found: Ru 29·9, N 15·4, NO_3 48·6 per cent. $[RuNO(NO_3)_{2·7}(OH)_{0·3}(H_2O)_2]$ requires Ru 29·9, N 15·3, NO_3 49·8 per cent). Further evaporations on a water bath to dryness after re-solution in water reduced the value of y to 1·9 after two and to 1·7 after five evaporations.

(b) *From Nickel Ruthenium Alloys* (*with* N. R. W. BENWELL)

Nickel alloys containing up to 8 per cent ruthenium were prepared by melting the two metals together, using a small amount of magnesium as a deoxidizer. The alloy was granulated, the average particle diameter being of the order of a few millimetres. The alloy was dissolved by boiling with 7 M nitric acid under reflux for several hours, the amount of nitric acid used being calculated to leave a definite acidity (0·5, 1, or 3 M) in the final solution. From this solution, a considerable proportion of the ruthenium was extractable by shaking with diethyl ether, dibutyl carbitol, or the higher ketones, none of which solvents extract nickel nitrate. After repeated extractions by one of these solvents, methyl ethyl ketone extracted a further quantity of ruthenium compounds and a small proportion of the nickel nitrate. Products were prepared according to the scheme appearing on page 383.

The solvent extracts (A and C) contained some nitric acid by extraction from the aqueous phase; the procedures adopted for obtaining the solid products involved the presence of this nitric acid during the final evaporation of aqueous phases. Direct evaporation of solvent phases such as (A1) led to violent decomposition.

The chromatographic purification of the methyl ethyl ketone phase (C) was carried out by passing the solution (containing nitric acid, nitrosylruthenium, and nickel nitrates) through a simple cellulose column. The nickel nitrate was strongly adsorbed at the top of the column; the ruthenium complexes passed through with the ketone.

When the final acidity of the nitric-acid solution of the Ni/Ru alloy was 3 M, approximately equal quantities of (II) and (III) were obtained. When the acidity was reduced below 3 M, the proportion of (II) diminished and that of (III) increased; thus, when it was 1 M, relatively little (I) or (II) was produced from ethereal extracts.

For these nitrato complexes, analyses other than for Ru, N, NO, and NO_3 were attempted: the

[8] MARTIN, F. S. (1953) *Chem. and Ind.*, 824.

VOL. 1 1955

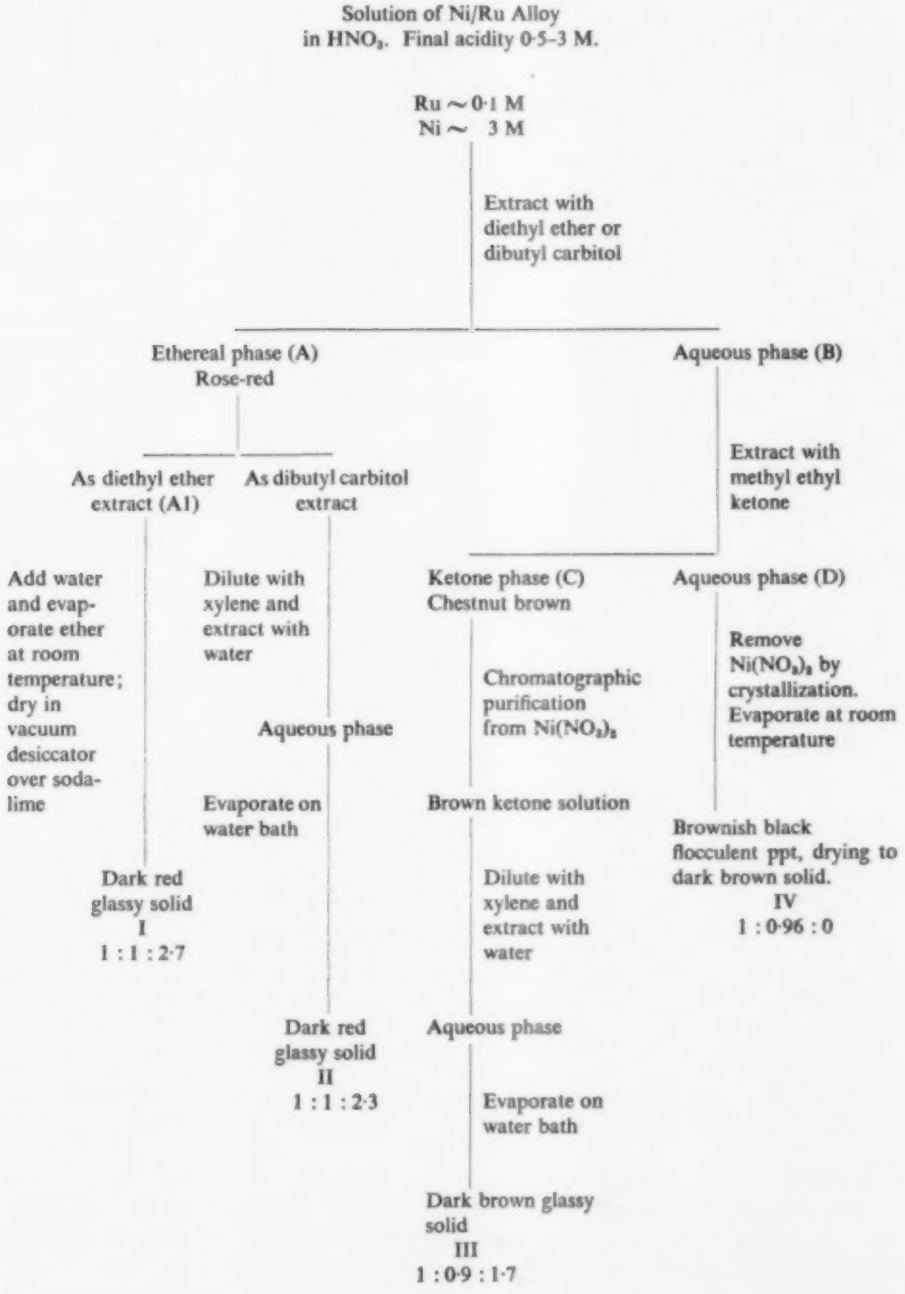
Solution of Ni/Ru Alloy
in HNO_3. Final acidity 0·5–3 M.
Ru ~ 0·1 M
Ni ~ 3 M
Extract with diethyl ether or dibutyl carbitol
Ethereal phase (A)
Rose-red
Aqueous phase (B)
As diethyl ether extract (A1)
As dibutyl carbitol extract
Extract with methyl ethyl ketone
Add water and evaporate ether at room temperature; dry in vacuum desiccator over soda-lime
Dilute with xylene and extract with water
Ketone phase (C)
Chestnut brown
Aqueous phase (D)
Remove $Ni(NO_3)_2$ by crystallization. Evaporate at room temperature
Chromatographic purification from $Ni(NO_3)_2$
Aqueous phase
Evaporate on water bath
Brown ketone solution
Brownish black flocculent ppt, drying to dark brown solid.
IV
1 : 0·96 : 0
Dark red glassy solid
I
1 : 1 : 2·7
Dilute with xylene and extract with water
Dark red glassy solid
II
1 : 1 : 2·3
Aqueous phase
Evaporate on water bath
Dark brown glassy solid
III
1 : 0·9 : 1·7

The ratios shown for the products (I), (II), (III), and (IV) are typical values of [Ru] : [NO] : [NO_3].

estimation of hydrogen and oxygen proved difficult owing to the very hygroscopic nature of the complexes, and because they often decomposed violently on ignition, or exploded when combustion in oxygen or hydrogen was attempted. The most satisfactory procedure was to determine (i) hydrogen as water, either (a) by heating in a current of dry carbon dioxide, oxides of nitrogen being reduced by heated copper turnings and any reduced hydrogen reoxidized by heated copper oxides, or (b) using PENFIELD's method with anhydrous lithium carbonate as an inert diluent; and (ii) oxygen, by reduction with hydrogen in the presence of copper powder. A preparation with Ru 32·1, N 13·9 per cent gave H by (a) 1·09, by (b) 1·53, O 53·5 per cent. $[RuNO(NO_3)_{2\cdot12}(OH)_{0\cdot97}(H_2O)_2]$ requires Ru 32·4, N 14·0, H 1·56, O 52·0 per cent.

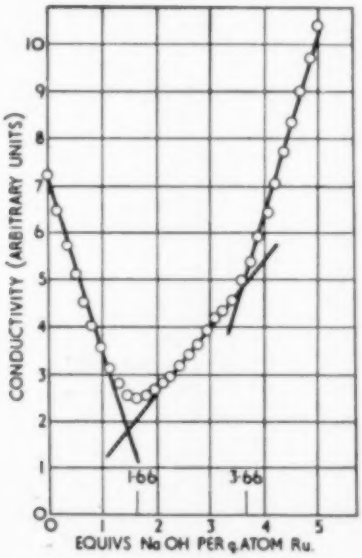

FIG. 1.—0·0078 g of complex $[RuNO(NO_3)_{2\cdot56}(OH)_{0\cdot24}\cdot 2H_2O]$ dissolved in 100 ml of water conductimetrically titrated with 0·1008 N NaOH at 20°C

All the (NO_3) present was precipitated as nitron nitrate after warming solutions of (I), (II), and (III) with nitron. For freshly prepared solutions titrated conductimetrically with sodium hydroxide, the minimum conductivity (Fig. 1) occurred when $(z - 1)$ equivalents of strong acid per gram-atom of ruthenium were neutralized. This result, however, gives no indication of the degree of complexing beyond the mononitrato stage, since hydrolysis of the trinitrato complex itself occurs sufficiently rapidly during conductimetric titration to give a similar result ($[H^+] : [RuNO] = 2$ at the minimum conductivity).

The apparent M.Wt., calculated from the depression of the freezing-point of water of a freshly prepared solution (10 g/litre) of a solid, prepared as for II, with $z = 2·1$, was 155. This result is consistent with essentially mononitrato complexing—$[RuNO(NO_3)_{1\cdot1}(OH)_{0\cdot9}(H_2O)_3]NO_3$ requires apparent M.Wt. = 165.

Polynuclear Nitrato Complexes

Between the mononuclear nitrato complexes and nitrosylruthenium hydroxide, there are brown polynuclear complexes in which some complexed (NO_3) is present. They are distinguishable from the mononuclear complexes by their insolubility in ethers. When the total ratio (z) of $[NO_3] : [RuNO]$ is >1, the products obtained have been soluble in methyl ethyl ketone; as z decreases below unity, the products have been completely soluble in water until the value of z becomes $<0·5$.

By repeatedly moistening substances I or II with water and drying at 100°C, products in which the value of z was reduced to 1·9 after two, and to 1·7 after five evaporations were obtained. These were partly soluble in diethyl ether, the residue being soluble in methyl ethyl ketone. Repetition of the process firstly gave a product insoluble in ether but completely soluble in methyl ethyl ketone, and finally after 20–30 evaporations a non-hygroscopic residue with $z = 0·5$, insoluble in methyl ethyl ketone (Found: Ru 48·1, N 10·3, N as (NO_3) 3·3 per cent. Apparent M.Wt., by depression of the F.P. of water, using a freshly prepared solution, 408. [Uncomplexed (NO_3)]: [RuNO] from minimum in a conductimetric titration, ~0·25. The empirical composition $[(RuNO)_4NO_3(OH)_{11}]NO_3$ requires Ru 46·5, N 9·6, N as (NO_3) 3·2 per cent: apparent M.Wt., assuming complete ionisation, 418).

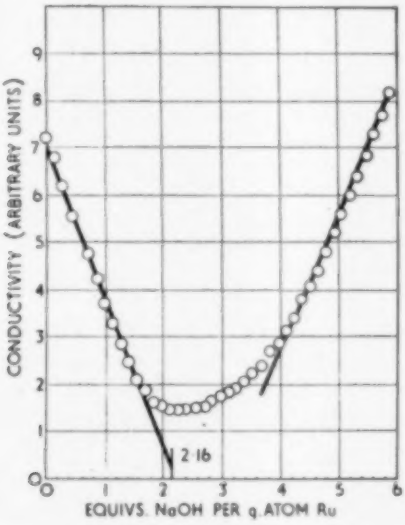

FIG. 3.—0·0086 g of complex $[RuNO(NO_3)_{2\cdot66}(OH)_{0\cdot34}\cdot 2H_2O]$ dissolved in 100 ml of water boiled and cooled, conductimetrically titrated with 0·1008 N NaOH at 20°C.

The potentiometric titration of a freshly precipitated slurry of the hydroxide with 1 M nitric acid at room temperature gave no break in the pH curve although solution of the hydroxide occurred: evaporation of the resulting solutions produced polynuclear mixtures of nitrates; thus one solid, with $y = 2·23$ (32 per cent Ru) was brown (not reddish) in colour, was insoluble in ethers but soluble in ketones, and had a M.Wt. in acetone of 610. (0·194 g dissolved in 17·4 g acetone elevated the boiling point by 0·029°C), corresponding to species with an average value of about two ruthenium atoms per molecule. For a second solid, with $y = 1·2$, (39·2 per cent Ru) the M.Wt. in acetone (810) was more than double the value of 272 required by the empirical formula $[RuNO(NO_3)_{1·2}(OH)_{1·8}(H_2O)_2]$. With smaller proportions of nitric acid solids with $y < 0·5$ which were only partly soluble in water were obtained.

Sodium Tetranitronitrosylruthenate(II), $Na_2[RuNO(NO_2)_4OH],2H_2O$

The preparations of this and the corresponding potassium salt from "ruthenium sesquichloride" were described by JOLY *et al.*[3,4], but the salts were formulated as $Ru_2(NO_2)_6,4MNO_2$. Two stages are involved in their formation: (i) the conversion

[3] JOLY, A., and VEZES, M. (1889) *Compt. rend.* **109,** 668.
[4] JOLY, A., and LEIDIE, E. (1894) *Compt. rend.*, **118,** 468.

VOL. 1 1955

of a solution of the chloride in hydrochloric acid to the trichloronitrosylruthenium complex by alkali nitrite, and (ii) the introduction of four nitro groups into the complex by further additions of the appropriate nitrite at 80°C and at pH ~ 7, i.e.,

$$2RuCl_3 + 6HCl + 6NaNO_2 \rightarrow 2RuNOCl_3 + 6NaCl + 3NO_2 + NO + 3H_2O, \text{ and}$$

$$RuNOCl_3 + 5NaNO_2 + H_2O \rightarrow Na_2[RuNO(NO_2)_4OH] + 3NaCl + HNO_2.$$

The yield obtained by JOLY *et al.*, was low (<10 per cent). In the present work, by allowing the reaction to proceed over a period of several hours and with slow additions of the alkali nitrite, yields up to 70 per cent have been obtained.

5 g of ruthenium trichloride were dissolved in 20 ml of 1 N hydrochloric acid. To the solution, maintained at the boil, the stoichiometric amount of sodium nitrite to form the chloronitrosylruthenium complex was added slowly over a period of one hour. The neutral solution was cooled to 80°C, and further additions of sodium nitrite, sufficient to complete the second stage of the reaction, were made over a period of three hours. The resulting bright orange solution showed no visible sign of further reaction with excess nitrite. On slow evaporation at room temperature, the solution deposited the tetranitro complex as orange crystals, which were recrystallized from water. (Found: Ru, 24·4, N 16·5, H_2O, by loss in weight on drying at 110°C, 8·8 per cent. $Na_2RuN_5O_{10}H,2H_2O$ requires Ru 24·5, N 16·9, H_2O 8·7 per cent.

Composition

(a) The presence of a nitrosylruthenium complex was shown by conversion of the salt to nitrosylruthenium hydroxide (found after drying at room temperature: 6·3 per cent N), and to nitrosylruthenium hydrosulphide (found: [N] : [Ru] = 0·97, Ru 22·2 per cent.)

(b) The presence of four-fifths of the nitrogen as complexed (NO_2) was shown by displacement of this group by boiling with sodium hydroxide and its estimation as sodium nitrite. 0·256 g of the dried compound was boiled with 0·2 g of sodium hydroxide in 15 ml water: from the solution, nitrosylruthenium hydroxide was precipitated, separated by centrifugation and washed. Aliquots of the resulting solution were added to excess of ceric sulphate or potassium permanganate in 1 M sulphuric acid, and the excess estimated by ferrous ion. (Found: NO_2 liberated as sodium nitrite, 48·3 per cent. $Na_2[RuNO(NO_2)_4OH]$ requires 48·7 per cent.) With a sample of sodium hexanitrocobaltate(III), the analysis for which after drying at 110°C corresponded to $Na_3Co(NO_2)_6.H_2O$, a similar estimation gave agreement between the NO_2 found (65·5 per cent) and the NO_2 calculated (65·3 per cent).

(c) Conductivity measurements indicate that the compound is a salt of a dibasic anion. The equivalent conductivities of solutions of $Na_4[Fe(CN)_6]$ and $Na_2[FeNO(CN)_5]$ were measured at 20°C at concentrations of $M/32n$ and $M/1024n$, where n is the charge on the anion. Using OSTWALD's empirical ratio $\Lambda_{1024} - \Lambda_{32} = 10{\cdot}8n$, the values of n found were 3·5 for the ferrocyanide ($\Lambda_{1024} = 129$) and 2·15 for the nitroprusside ($\Lambda_{1024} = 111$), in reasonable agreement with their known composition. Similar measurements were made on solutions of two samples of the compound, recrystallized respectively from water and ethyl alcohol and dried at 110°C. Λ_{1024} was 95 and 102, Λ_{32} was 77 and 83, giving values of 1·7 and 1·8 for n, when inserted in the above formula.

(d) Confirmatory evidence for the proposed composition was obtained by examination of the infra-red absorption spectrum.

The compound, dried at 110°C, was ground in a ball-mill with potassium bromide and pressed into discs; the spectrum was plotted on a Hilger H800 double-beam spectrometer, using prisms of quartz, rocksalt, and potassium bromide. The spectrum closely resembles that of $Na_3[Co(NO_2)_6]$. Bands common to both compounds are observed at 1420, 1338, 1270, 841, 826, 636, and 619 cm^{-1}. Further new bands are present in the spectrum of the ruthenium complex which are absent in the cobalt complex. Of these, the strong absorption at 1907 cm^{-1} is undoubtedly due to the N = O stretching vibration of a nitrosyl group, such as occurs[5] at 1800 cm^{-1} in NOCl and at 1925 cm^{-1} in $Na_2[FeNO(CN)_5]$.[6] The two bands observed at 826 and 841 cm^{-1} in the spectra of both compounds can be ascribed to vibrations of the NO_2 groups; the presence of a third band in the spectrum of the ruthenium complex at 835 cm^{-1} probably arises from the splitting of one of the normal frequencies as a result of the lower symmetry of this complex. A number of weak bands appear elsewhere in the spectrum, some of which are explained as overtone or combination bands: one such band at 3617 cm^{-1} can only be attributed to the presence of hydroxyl.

VOL. 1 1955

$Ru_2N_6O_{15}$

Ruthenium tetroxide (1 g) was dissolved in dry carbon tetrachloride (50 ml), and dry nitric oxide (containing some nitrogen peroxide) was bubbled through the solution until precipitation was complete. The orange-brown amorphous precipitate was filtered on to a sintered glass disc (pump), care being taken not to draw moist laboratory air through the precipitate. The pasty mass was partly dried at 80°C and finally freed from carbon tetrachloride in a vacuum desiccator (yield 1·7 g). (Found: Ru 38·6, N 15·7 per cent. M.Wt. 530; 0·2364 g substance dissolved in 7·60 g acetone elevated the boiling-point by 0·101°C. $Ru_2N_6O_{15}$ requires Ru 38·6 per cent, N 15·9 per cent; M.Wt. 527.)

A known volume of pure nitric oxide (62 ml at 20°C and 749 mm Hg pressure = $2{\cdot}53 \times 10^{-3}$ moles) was allowed to react with excess ruthenium tetroxide in carbon tetrachloride. $6{\cdot}36 \times 10^{-4}$ moles of the tetroxide reacted, hence $[NO] : [RuO_4] :: 4 : 1$ and $2RuO_4 + 8NO \rightarrow Ru_2N_6O_{15} + N_2O$; the presence of N_2O was confirmed by the high solubility of the residual gas in water.

The substance dissolved without reaction in oxygen-containing organic solvents such as alcohol, acetone, or tri-*n*-butyl phosphate, and in water with reaction, liberating oxygen and forming a brown solution. This solution was acidic (pH *ca.* 3 for 10^{-2} M solution), and behaved as a nitronitrosylruthenium complex, since it decolourized acidified potassium permanganate, evolved oxides of nitrogen, and formed nitrosylruthenium trichloride when heated with concentrated hydrochloric acid, and was converted to nitrosylruthenium hydroxide when boiled with alkali. $Ru_2N_6O_{15}$ itself is therefore interpreted as being a binuclear oxygen-bridged nitrosylruthenium compound, containing the $RuNO(NO_2)_2$-structure with additional oxygen atoms attached to the ruthenium atoms.

[5] Short, L. N. (1954) *Reviews of Pure and Applied Chem.* **4**, 41.
[6] Miller, F. A., and Wilkins, C. H. (1952) *Anal. Chem.* **24**, 1253.

Other Nitronitrosylruthenium Compounds

In addition to the dinitro complex formed in acid solution from the tetranitro complex (Section 3), solutions of ruthenium tetroxide or Ru(IV) nitrate in nitric acid form solutions of yellow, orange, or light brown nitronitrosylruthenium complexes by reaction with oxides of nitrogen. These complexes are also formed in solution (i) when Ni/Ru alloys are dissolved in <1 M HNO_3 at temperatures rather below the boiling-point, i.e., where the ratio of [oxides of nitrogen] to [HNO_3] is relatively high: and (ii), when a slurry of nitrosylruthenium hydroxide dissolved in 1 M perchloric acid is treated with sodium nitrite. Attempts to isolate individual nitro complexes from the acid solutions by extraction with organic solvents have led to nitrosylruthenium products in which the ratio [N] : [Ru] has varied from 2 to 4.

A solution (*ca.* 0·1 M) of ruthenium tetroxide in 3 M HNO_3 was treated with nitric oxide at room temperature. After excess nitric oxide had been removed by purging with nitrogen, the original yellow colour of the solution had changed to brown; on boiling, solutions of nitrosylruthenium nitrato complexes were obtained.[2] Prior to boiling, ruthenium-containing compounds extractable by methyl ethyl ketone (in the presence of calcium nitrate) were present. Calcium nitrate and nitric acid were removed from the ketone extract by a cellulose column and by Deacidite E respectively. The dark brown solution contained [N] : [Ru] in the ratio of 4 : 1, and with hydrogen sulphide gave a precipitate in which [N] : [Ru] = 1. No nitrate ions were found in the filtrate from the sulphide precipitation.

100 g of a 5 per cent ruthenium alloy to which 600 ml of 8 M nitric acid were added was dissolved over a period of three days at a temperature of *ca.* 80° C, additions of water being made to keep the volume constant. The final value of [HNO_3] was 0·5 M. Ruthenium compounds were extractable from the solution by dibutyl carbitol and methyl isobutyl ketone. From the latter, after dilution with xylene and washing with water, a light brown material was obtained after evaporation on a water bath. (Found: [N] : [Ru] = 3·8. Ru 36·8 per cent.) It was not hygroscopic, and dissolved readily in water and organic solvents. With hydrogen sulphide, a precipitate, typical of other preparations of nitrosylruthenium hydrosulphide, was formed. (Found: Ru 43·6, N 7·3, S 30·8, H_2O 9·6 per cent.) The filtrate from this precipitate did not give a precipitate of nitron nitrate such as was obtained under similar conditions from nitrosylruthenium nitrato complexes. When the material was boiled with nitric acid, oxides of nitrogen were evolved and nitrosylruthenium nitrato complexes were formed.

Oxalatonitratonitrosylruthenium, $RuNO \cdot NO_3 \cdot C_2O_4 \cdot H_2O$

When solutions of nitrosylruthenium nitrates are evaporated with oxalic acid, nitrato groups in excess of one per ruthenium atom are readily displaced. With excess of oxalic acid, the remaining nitrato group is only replaced with difficulty. Oxalatonitratonitrosylruthenium hydrate is a pink crystalline non-hygroscopic solid, soluble in water. No oxalate ions are detectable in cold or hot aqueous solutions of the complex.

Nitratonitrosylruthenium with $y = 2{\cdot}13$ was evaporated to dryness with oxalic acid solution (1 molecule per Ru atom). (Found after drying at 100°C: Ru 34·7, N 9·5, C_2O_4 30·0, H 0·44 per cent. $RuNO \cdot NO_3 \cdot C_2O_4 \cdot H_2O$ requires Ru 33·8, N 9·4, C_2O_4 29·4, H 0·67 per cent.)

Sulphatonitratonitrosylruthenium, [$RuNO \cdot NO_3 \cdot SO_4\,(H_2O)_3$]

The displacements of nitrato groups by evaporation with sulphuric and with oxalic acids are similar. The sulphatonitrato complex is an orange hygroscopic solid from a solution of which sulphate ions are released on warming to 80°C.

Nitratonitrosylruthenium with $y = 2{\cdot}13$ was evaporated to dryness with sulphuric

acid (1 molecule per Ru atom). (Found: Ru 29·8, N 8·4, S 9·2 per cent. $RuNO \cdot NO_3 \cdot SO_4, 3H_2O$ requires Ru 29·5, N 8·15, S 9·3 per cent).

Hydrogen Tetrachlorohydroxonitrosylruthenate(II), $H_2[RuNOCl_4OH], 2H_2O$

The evaporation of nitrosylruthenium nitrato complexes with hydrochloric acid usually leads to the formation of nitrosylruthenium trichloride. However, rapid evaporation with an excess of concentrated hydrochloric acid gave the purple, deliquescent, dibasic acid. (Found after drying at room temperature under reduced pressure: Ru 31·5, N 4·5, Cl 43·4 per cent. $H_2[RuNOCl_4 \cdot OH]2H_2O$ requires Ru 30·9, N 4·3, Cl 43·4 per cent.)

Nitrosylruthenium Fluoride

In view of the rarity of fluoro complexes of the platinum metals, the reaction between nitrosylruthenium hydroxide and hydrofluoric acid was examined.

Nitrosylruthenium hydroxide was heated in a platinum crucible with an excess of 20 M HF, and the resulting solution evaporated twice with further additions of acid, and finally dried under reduced pressure at room temperature in a desiccator over phosphorus pentoxide and sodium hydroxide. The product was a dark brown non-hygroscopic powder. (Found: Ru 41·5, N 5·35, F 20·7 per cent. $RuNO \cdot F_{2\cdot6}(OH)_{0\cdot4}, 3H_2O$ requires Ru 42·0, N 5·8, F 20·5 per cent.) The material gave with water a cloudy solution; when this was brought to pH 9, the solution was clear but colloidal.

3. PROPERTIES

Properties of Nitrato Complexes

(a) *In water*

Aqueous solutions of the trinitrato complex undergo fairly rapid reactions at room temperature (Table 2) which result in (i) changes in the visible colour and spectrophotometric absorption of the solution, (ii) the liberation of hydrogen and nitrate ions, (iii) a decrease in the total ruthenium extracted by organic solvents, (iv) the formation of cationic species. These properties are interpreted in terms of (a) relatively slow substitution of nitrato by aquo groups and (b) relatively fast proton transfer, e.g., from the trinitrato complex,

$$[RuNO(NO_3)_3(H_2O)_2] \xrightarrow{\text{slow}} [RuNO(NO_3)_2(H_2O)_3]^+ + NO_3^-$$
$$\downarrow \text{fast}$$
$$[RuNO(NO_3)_2OH(H_2O)_2] + H^+$$
$$\downarrow$$
$$\text{etc.}$$

From kinetic studies[7] it has been found that the time for 25 per cent of the trinitrato complex to be hydrolysed to the dinitrato complex (for dilute solution in water) is ~90 sec at 25°C. The increase in the specific conductivity of a solution of the trinitrato complex in water (Fig. 2) must be very largely due to the formation of hydrogen and nitrate ions. The curve indicates that the first of what may be several successive reactions is largely over within 10 min at 20°C.

[7] JENKINS, I.L., and WAIN, A. G. (1955). Results to be issued.

Properties which illustrate the occurrence of a fast proton transfer reaction and of anionic ruthenium species are:—

(i) Freshly prepared solutions of the trinitrato complex are acidic apart from the acid liberated by hydrolysis (Table 2); extrapolation of pH measurements to zero time gives a value of $\sim 10^{-3}$ for the dissociation constant of the aquo complex $[RuNO(NO_3)_3(H_2O)_2] \rightarrow H^+ + [RuNO(NO_3)_3OH \cdot H_2O]^-$.

(ii) Anion exchange resins in their hydroxyl form remove ruthenium from aqueous solutions ($\sim 10^{-3}$ M Ru) of the nitrato complexes. With prolonged contact at room temperature there is simultaneous adsorption of ruthenium-containing anions by the resin and of hydrolysis to lower nitrato complexes and

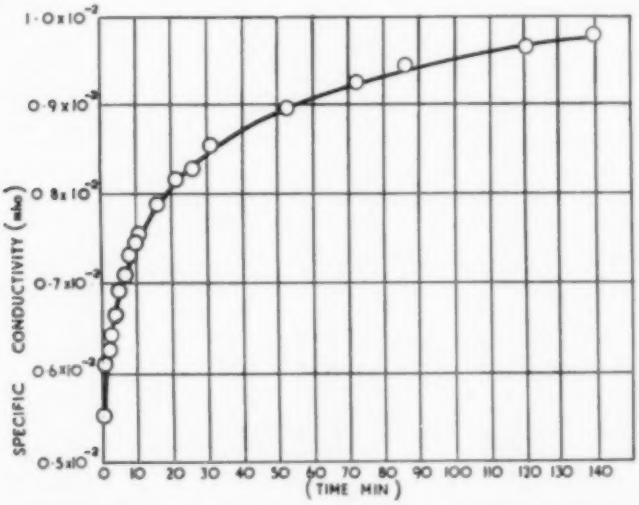

Fig. 2.—Change in conductance K with time of $2{\cdot}66 \times 10^{-3}$ M $RuNO(NO_3)_{3\text{-aq.}}$ at 20°C.

to nitrosylruthenium hydroxide. (Found after 12 hours contact with Deacidite E: Ru, 40 per cent on resin, 16 per cent in solution, and 44 per cent as insoluble hydroxide.) At lower temperatures and with shorter times of contact, hydrolysis is less prominent and adsorption of ruthenium is more nearly complete. (Found at 5°C and after 3 min contact: Ru, 98 per cent on resin; at 0°C and after 5-hr contact: 68 per cent on resin, 32 per cent in solution).

Hydrolysis in dilute aqueous solutions (10^{-4} to 10^{-3} M) of the mononuclear nitrato complexes proceeds to polynuclear species which are no longer extractable by ethers or ketones. With solutions which have aged for >24 hours or been boiled, minimum conductivity in a conductimetric titration (Fig. 3) corresponds to the presence of $(z - \frac{1}{2})$ equivalents of strong acid per gram-atom of ruthenium (Found: for preparations I ($z = 2{\cdot}7$), II ($z = 2{\cdot}3$), III ($z = 1{\cdot}7$); $[H^+]$: [Ru] after boiling, 2·2, 1·8, 1·24 respectively). Apparently after boiling these solutions the ratio [complexed NO_3] : [RuNO] is approximately 0·5.

The denitration reactions which occur in water are reversible in the presence of nitric acid or nitrate ions; hence the isolation, by evaporation of their aqueous solutions, of substances in which the value of z and the apparent M.Wt. are only slightly changed

TABLE 2.—PROPERTIES OF SOLUTIONS OF TRINITRATONITROSYLRUTHENIUM IN WATER

Property	[Ru]	Freshly Prepared Solution	Solution aged at Room temperature
1. Colour	10^{-2} M	Rose-red	Brown (1 hour)
2. Spectrophotometric absorption: broad maximum between 4500 and 4800 Å	10^{-3} M	Present (as observed in 8 M HNO_3, see Fig. 5)	Absent (>1 hour)
3. pH (at 20°C)	$1{\cdot}9 \times 10^{-2}$ M	2·72	2·70 5 min 2·68 8 „ 2·66 18 „ 2·64 31 „ 2·63 51 „ 2·44 3 days
4. Distribution coefficient of Ru (as org/Aq) with an equal vol. of dibutyl carbitol equilibrated for 30 sec.	10^{-3} M	0·6	3×10^{-3} (1 hour) $<10^{-4}$ (24 hours)
5. Ru uptake by Zeokarb 225 or Dowex 50 in their hydrogen forms	10^{-3} to 10^{-4}	29 per cent on resin in 1 min at 5°C 95 per cent on resin in 5 min at 25°C	91 per cent on resin in 1 min at 5°C (aged 24 hr). $[NO_3]$: [RuNO] = 0·6 for species on the resin after 12 hr contact at 20°C. 100 per cent on resin

from their original values (Section 2). (Found for a complex with $z = 2{\cdot}1$; apparent M.Wt. for a freshly prepared solution by depression of the F.P. of water, 155; for a solution after boiling, 79; after evaporation to dryness at 100°C, followed by making a freshly prepared solution, 160. $[RuNO(NO_3)_{1\cdot1}(OH)_{0\cdot9}(H_2O)_3]NO_3$ requires apparent M.Wt. = 165; $(RuNO)_2NO_3(OH)_5 + 1{\cdot}6\ H^+ + 1{\cdot}6\ NO_3^-$ after boiling, requires apparent M.Wt. = 78·5). With solutions in which there has been extensive polynuclear formation, it is necessary to boil with ~8 M HNO_3 to reform the trinitrato complex.

During potentiometric titrations with alkali, there is a drift of pH towards increasing acidity after each addition of alkali; the titration curve (Fig. 4) for a freshly prepared solution of the trinitrato complex, shows feeble points of inflection corresponding to the consumption of three to four equivalents of alkali per gram-atom of ruthenium. It is concluded that the mononitrato complex, $[RuNO \cdot NO_3(OH)_2(H_2O)_2]$,

reacts as a pseudo-acid by proton transfer from the aquo groups within the complex, i.e.,
$[RuNO \cdot NO_3(OH)_2(H_2O)_2] \rightarrow H[RuNO \cdot NO_3(OH)_3H_2O] \rightarrow H_2[RuNO \cdot NO_3(OH)_4]$,
in competition with the slow denitration which leads to the hydroxide.

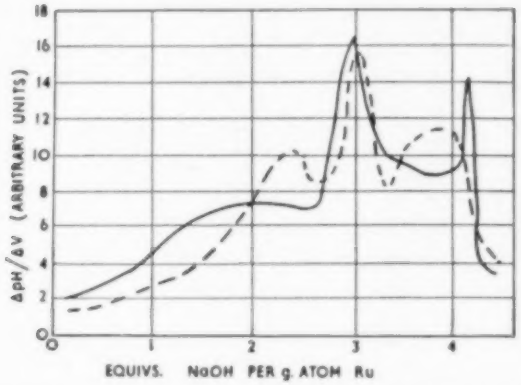

Fig. 4.—Potentiometric titration of 20 ml 0·0116 M $RuNO(NO_3)_3 \cdot 4H_2O$ with 0·0403 N NaOH. Continuous line—fresh solution. Broken line—solution aged for 24 hrs.

(b) *In Nitric Acid Solution*

The proportion of the trinitrato complexes present in a mixture of the nitrato complexes at equilibrium at 20 ± 1°C in 3–12·4 M (Table 3) has been obtained by taking advantage of the considerable differences in the extraction of the tri-, di-, and mononitrato complexes from aqueous solution by organic solvents (Section 5).

Table 3.—Percentage of trinitratonitrosylruthenium at equilibrium in 3–12·4 M HNO_3
[Ru], $\sim 10^{-1}$ M; Temp. 20 ± 1°C

HNO_3	3·0	4·6	6·3	7·5	8·7	12·4 M
Fraction of Ru as trinitrato complex	0·10	0·24	0·39	0·50	0·57	0·76
dinitrato complex	0·26			0·22		
mononitrato complex	0·64			0·28		

The relatively small proportion of the dinitrato complex found in 7·5 M HNO_3 deserves comment. Other observations on these complexes have indicated the formation of the tri- and mononitrato complexes under appropriate conditions, but rarely the dinitrato complex. Thus the conductimetric titrations referred to in (a) above indicate rapid conversion in freshly prepared solutions to the mononitrato complex, with no marked step corresponding to the dinitrato complex. Spatial considerations, using an octahedral model for the arrangement of the ligands around a ruthenium atom, suggest an explanation, *viz.*, that there is a nitrato group in position 5 (*trans* to NO) in all three complexes, and in the trinitrato complex the additional two

groups occupy *cis* positions (*e.g.*, positions 1 and 2). As such they are likely to be almost equally reactive (*cf.* properties of the tetranitro complex, see below), so that when one is removed, the other will also tend to be removed.

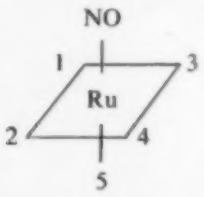

Nitrato complexing probably goes beyond the trinitrato complex in >12 M HNO_3, but no species has been isolated; a tetranitrato complex, with [N] : [Ru] = 5, would be comparable to the tetranitro and tetrachloro complexes. A solution prepared from nitrosylruthenium hydroxide and nitric acid, was aged for a month in 12·5 M HNO_3: slow evaporation at room temperature gave a dark (almost black) product with [N] : [Ru] = 4·25; Ru 25·4 per cent.

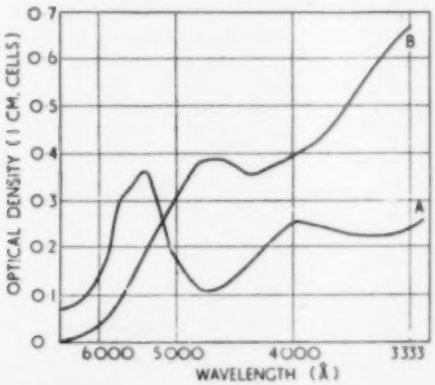

FIG. 5.—Spectrophotometric curves of nitrosylruthenium complexes in nitric acid.
A. Purple complex ([Ru] = $1·5 \times 10^{-4}$ M) in 16 M HNO_3.
B. Trinitratonitrosylruthenium ([Ru] = $5·7 \times 10^{-3}$ M) in 8 M HNO_3, aged for 3·3 hrs at 20°C.

When left in 15 M HNO_3, a solution of the nitrato complexes acquires a very strong purple colour if exposed to the air (the colour does not develop in a nitrogen atmosphere). The spectrophotometric absorption curve of this solution (Fig. 5) is quite distinct from that of the nitrato complexes and of ruthenium tetroxide; it is concluded that these solutions contain ruthenium in an oxidation state intermediate between that in RuNO complexes and that in RuO_4 (which is formed by boiling these solutions).

(c) *In Organic Solvents*

Solutions of the mononuclear nitrato complexes in dry organic solvents are stable over a period of time. However, in the presence of small amounts of water, hydrolysis occurs, nitric acid is liberated, and, in the case of diethyl ether, all the ruthenium present is adsorbed on an anion exchange resin. (Found with preparation II ($z = 2·3$)

dissolved in diethyl ether containing 1·4 M H_2O (water : ether = 2·5 per cent by volume): 100 per cent removal of Ru by Deacidite E in one hour). Solutions of those polynuclear complexes which are soluble in water-saturated methyl ethyl ketone neither give a positive test for hydrogen ions nor is there any removal of ruthenium from them by anion exchange resins. From such solutions, insoluble nitrosylruthenium hydroxide (with a small proportion of complexed NO_3 present) is deposited on prolonged ageing. (Found in the acetone-washed and air-dried deposit from methyl ethyl ketone solution: [N] : [Ru] = 1·3; Ru 27 per cent).

(d) *Displacement of the Nitrosyl Group*

When the solutions of the nitrato complexes are heated in strongly alkaline solution with Devarda's alloy the nitrosyl group is completely reduced to ammonia. In <0·2 M nitric acid, boiling with ferrous salts or a metal such as nickel results in partial displacement of the nitrosyl group. A solution of a mixture of nitrato complexes (with $y = 2{\cdot}7$) was heated on a water bath with ferrous sulphate for 5 hr. In the hydrosulphide from the resulting solution, the ratio [N] : [Ru] was found to be 0·6; in a similar experiment using ferrous sulphamate and boiling for 15 min, this ratio became 0·38.

The variable ratios of [N] : [Ru] in the solutions formed and in the sulphides precipitated from them, give no evidence for a separate class of heminitrosylruthenium compounds, e.g., derived for 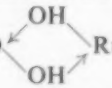 , such as might be assumed to exist from the work of Brizard[8], who treated nitrosylruthenium chloride with reducing agents.

Properties of Tetranitro Complex

Solutions of $Na_2[RuNO(NO_2)_4OH]$ in water and in 1 M acids are stable at room temperature. When they are warmed in 1 M acid, oxides of nitrogen are evolved. In the presence of oxidizing agents, the nitrous acid liberated in 1-M sulphuric acid solution at temperatures up to 65°C corresponds to only two of the four NO_2 groups present per molecule. With $Na_3[Co(NO_2)_6]$ under similar conditions, displacement of three to four (NO_2) groups per molecule occurs at room temperature, and the remaining ones are readily liberated on warming to 50°C. It has been pointed out (Chatt, J., private communication) that the greater tenacity with which two of the four NO_2 groups are held is consistent with a planar arrangement of the four NO_2 groups round each ruthenium atom; and that the high *trans*-effect of NO_2 causes two of the NO_2 groups to be more labile than the other two,[9, 10] i.e., for the case of replacement by aquo groups as shown in diagram on the opposite page.

A 0·0139 M solution of the salt was added to an excess of ceric sulphate or potassium permanganate in 1 M sulphuric acid, and the excess of oxidizing agent estimated by back titration with ferrous ions. (Found at room temperature or after a few minutes at 65°C: NO_2 liberated as nitrous acid, 22·4 per cent of the weight of the dried salt. With more prolonged heating at 65°; up to 27 per cent: cf. 48·3 per cent under alkaline conditions.) With a freshly prepared solution from dried sodium hexanitrocobaltate(III) under similar conditions, there was found at room temperature: NO_2 rapidly liberated and titrated as nitrous acid, *ca.* 35·5 per cent; on raising the temperature to 50°,

[8] Brizard, L. (1900) *Ann. Chim. Phys.*, **21**, 311.
[9] Burkin, A. R. (1951) *Quart. Reviews*, **5**, 1.
[10] Quagliano, J. V., and Schubert, L. (1952) *Chem. Reviews*, **50**, 201.

58·9 per cent. If it is assumed nitrous acid liberated also reduces Co(III) to Co(II) once the nitro complex is destroyed, the total NO_2 liberated as nitrous acid at 50° becomes 65·1 per cent, i.e., the same as under alkaline conditions.

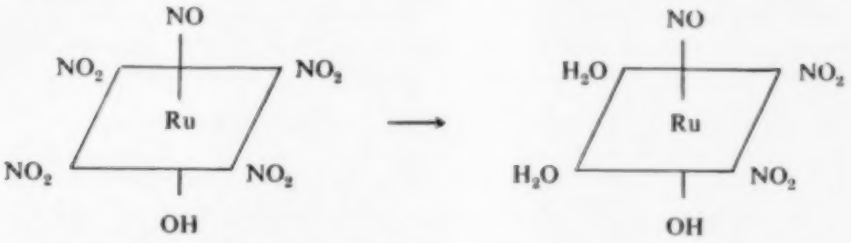

Other properties of the sodium salt are:—

(i) The spectrophotometric absorption curve of its aqueous solution shows no peaks down to 3500 Å.

(ii) The complex anion, with all the NO_2 groups present, is readily absorbed from aqueous solutions by Deacidite FF (in its hydroxyl form).

(iii) A yellow salt, insoluble in water, is formed with silver nitrate.

VOL. 1 1955

4. COMPLEXING OF NITROSYLRUTHENIUM

Differences in the conditions necessary to precipitate nitrosylruthenium hydroxide from solutions obtained by boiling it with various acids, are related to the absence or presence of complexes with the anion of the acid; the shapes of the respective potentiometric titration curves (Fig. 6) provide a qualitative indication of the strength of complexes with various ligands as increasing in the order $ClO_4^- < F^- < NO_3^- < Cl^- < NO_2^-$. The conditions under which hydroxo, sulphato, and oxalato mononitrato complexes are formed from the trinitrato complex, lead one to include the ligands OH^-, SO_4^{2-}, and $C_2O_4^{2-}$ as comparable with Cl^- in series above.

This order is typical of the stability of ligands in certain co-ordination complexes, e.g., of Co(III), Pt(IV), which involve d^2sp^3 hydridization: the familiar stability of the nitro group in this class of compounds has been explained[11] by strengthening of the "covalent" metal-ligand σ-bond, M—N$\begin{matrix}\diagup\!\!\!=\!\!\!\diagdown\,O\\ \diagdown\quad\diagup\,O\end{matrix}$, with a π-type bond ($d_\pi - p_\pi$) by which the metal donates two d_π-electrons which are utilized by a p_π-orbital of the nitrogen of the NO_2 group. Similar double bond formation accounts for the strong bonding of CO, CN and NO in d^2sp^3 complexes of these metals[12]: the experimental evidence is that in nitrosylruthenium complexes the nitrosyl group is bound considerably more firmly that the nitro group. It is now usual[13] to interpret this influence as arising from the co-ordination of the nitrosyl group, NO^+, to Ru(II), i.e., Ru ← N ⇇ O, the low valency state of ruthenium being stabilized, just as for Fe(II) in the ferrocyanides and nitroprussides. The similarity between the complexes of Ru(II), as RuNO, and those of Co(III) and Pt(IV), may be related to the similarity of the outer electron configuration of the central atom; they all possess, in contrast to cases such as

[11] Nyholm, R. S. (1954) *Reviews of Pure and Applied Chem.* **4**, 15.
[12] Craig, D. P., MacColl, A., Nyholm, R. S., Orgel, L., and Sutton, L. E. (1954) *J. Chem. Soc.* 332.
[13] Sidgwick, N. V., and Bailey, R. W. (1934) *Proc. Roy. Soc.* A, **144**, 521.

Fe(III), Ni(II), Ru(IV), the maximum number of pairs of outermost *d*-electrons suitable for d_π-bonding.

The comparison of NO_3^- and F^- as ligands for complex formation with Ru(IV) and RuNO(III) is of interest. With Ru(IV), whereas there is no nitrato complexing[14] fluoro complexing is relatively strong in spite of the small ionic radius of Ru^{4+}[15]. Fluoro complexing in such cases, e.g. for Fe(III), was formerly explained (by PAULING)

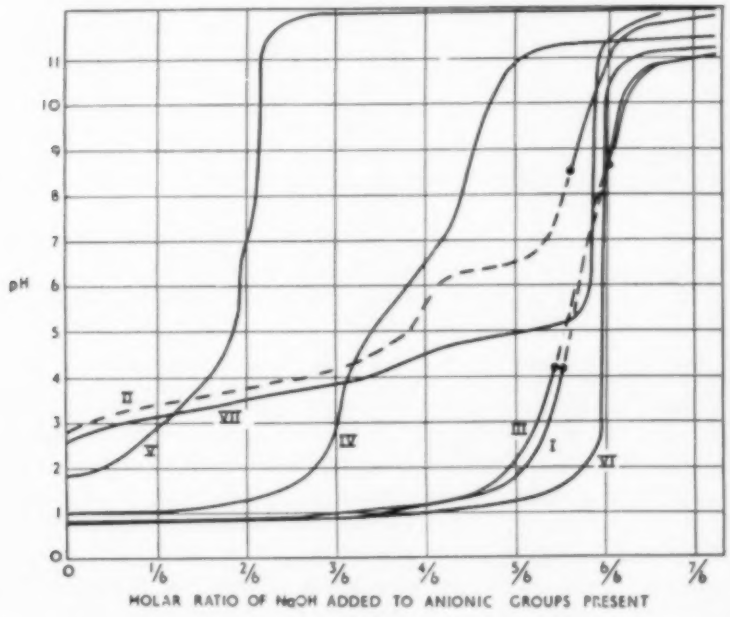

FIG. 6.—2 millimoles of various nitrosylruthenium compounds in 0·055 M solution, titrated potentiometrically with 0·5 N NaOH.

———— No precipitate present

– – – – – – Precipitate present

I Perchlorate
II Fluoride
III Nitrate
IV Chloride
V Nitro complex
VI $HClO_4$ } for comparison
VII HF

by the ionic nature of the bonds between the metal atom and the highly electronegative fluorine atom. But according to recent studies of the bonding in co-ordination compounds, the bonds in typical fluoro complexes are normal co-ordinate covalences, although they involve outer *d* orbitals, e.g. $4s4p^34d^2$ hybrids in $[FeF_6]^{3-}$, as compared with the inner *d* orbital $3d^24s4p^3$ bonds in $[Fe(CN)_6]^{3-}$.[11, 12] Outer *d* level covalences are characteristically formed by the most electronegative ligands, except, as in $[Ni^{IV}F_6]^{2-}$, where the central ion is itself of very high electronegativity. The fluoro complexes of the Ru^{4+} ion, which is of larger radius that the Ni^{4+} ion, are

[14] ANDERSON, J. S., and MCCONNELL, J. D. M. (1955) *J. Inorg. Nucl. Chem.*, **1**, 371.
[15] HEPWORTH, M. A., PEACOCK, R. D., and ROBINSON, P. L. (1954) *J. Chem. Soc.* 1197.

therefore likely to involve outer, i.e. $5s5p^35d^2$, rather than inner, $4d^25s5p^3$, *d* levels, although measurements of the magnetic moment of Cs_2RuF_6[16] leave this matter in doubt. On the other hand, in nitrosylruthenium compounds, one of the set of $4d^25s^5p^3$ bonds is already being used by the nitrosyl group: relatively weak complexing (with $4d^25s^5p^3$ hydridisation) through an oxygen atom occurs with NO_3^- as a ligand, but with the highly electronegative ligand F^-, complexing is weak ; a preparation of nitrosylruthenium fluoride has behaved largely as a mixture of hydroxoaquonitrosylruthenium complexes and of fluoride ions.

Acid solutions (approx. 0·05 M Ru) of nitrosylruthenium derivatives were made (i) for ClO_4^- Cl^- and NO_3^-, by refluxing the hydroxide with the appropriate acid (1 M) added in the ratio $[H^+] : [RuNO] = 6$; (ii) for F^-, by dissolving the fluoride in water and adding sufficient hydrofluoric acid to bring $[F^-] : [RuNO] = 6$; (iii) for the yellow tetranitro acid $H_2[RuNO(NO_3)_4OH]$, by passing the sodium salt through Zeokarb 225 in its hydrogen form. The solutions of the fluoride, perchlorate and nitrate were brown and colloidal: the other two were non-colloidal. That there was negligible complexing of nitrosylruthenium by ClO_4^- and NO_3^- and weak complexing by F^-, is indicated by a comparison of the potentiometric curves for these solutions with the curves for HF and $HClO_4$ solutions (Fig. 1); 1 M nitric acid is not sufficiently concentrated to produce the nitrato complexes. The solutions at pH > 8·4, at which point re-solution of the precipitate was complete, were colloidal. The curve for the chloride, on the other hand, indicates that chloro complexing of all the nitrosylruthenium has occurred; the first end-point, which corresponds to the titration of hydrochloric acid present in excess, is followed by partial hydrolysis of $[RuNOCl_3(H_2O)_2]$. The curve for the nitro complex is characteristic of a moderately strong dibasic acid with no subsequent hydrolysis of $[RuNO(NO_2)_4OH]^{2-}$. The shape of the curves for the fluoride and for HF are affected, in their displacement to the left, by some attack on the glass electrode used for the titrations.

For the tetra-ammino derivatives of nitrosylruthenium, JOLY[17] and WERNER[18] were able to prepare a series of complexes in which the sixth co-ordination position was occupied by a variety of ligands including NO_3 but not including NO_2. It is suggested that this position, in which the ligand is readily interchangeable, is *trans* to the strongly directing nitrosyl group in an octahedral configuration. The same freedom for substitution in this position can be expected to occur in aquo or aquohydroxo complexes of RuNO, and it is therefore likely that one of the three nitrato groups in the trinitrato complex, prepared in nitric acid solution, will occupy this position; on the other hand, the powerful *trans* directing acting of the nitro group itself prevents it occupying this position, thereby limiting the ratio $[NO_2] : [RuNO]$ to a maximum of four; but weaker *trans* directing groups can form complexes of the type $[RuNOX_5]^{2-}$, e.g. where X is Cl. The tendency for the sixth position in the tetranitro and tetrachloro complexes to be occupied by OH resembles that observed in other nitrosylruthenium complexes, e.g. $[RuNOen_2OH]^{2+}$.

It is exceptional to find as many as three nitrato groups attached to the metal atom of Group VIII co-ordination complexes. However, complexes with 3, 4 and 6 NO_3 groups per metal atom occur with the lanthanides, actinides and Group IV metals of relatively high ionic radius, examples being $[Pu(NO_3)_4]$, $[Ce(NO_3)_6]^{2-}$, $[Th(NO_3)_4]$. The uranyl radical, like the nitrosylruthenium radical, forms a series of nitrato complexes—$[UO_2 \cdot NO_3]^+$, $[UO_2(NO_3)_2]$, $[UO_2(NO_3)_3]^-$ and probably

[16] HEPWORTH, M. A., ROBINSON, P. L., and WESTLAND, G. L. (1954) *J. Chem. Soc.*, 4268.
[17] JOLY, A. (1890) *Compt. rend.*, **111**, 971.
[18] WERNER, A. (1907) *Ber.*, **40**, 2616.

VOL. 1 1955

$[UO_2(NO_3)_4]^{2-}$.[19, 20] For both series, the higher complexes are more soluble in oxygen-containing organic solvents than in water or aqueous solutions. A difference between the two series, which has repercussions on solvent extraction processes involving fission product ruthenium, as nitratonitrosylruthenium complexes, and uranium, as uranyl nitrate, lies in the rapidity with which equilibrium between the uranyl complexes is established, and the relative slowness of the reactions between the nitrosylruthenium complexes.

5. PARTICULAR ANALYTICAL METHODS

The Determination of Trinitratonitrosylruthenium in Nitric Acid Solutions of the Nitrato Complexes (with P. G. M. BROWN, D. F. SANGSTER, and A. G. WAIN)

The methods used are based on the observation that equilibrium for the distribution of the nitrato complexes between an aqueous and an (immiscible) organic phase is achieved in a few seconds if the two phases are vigorously stirred. This period of time is too small, particularly for experiments at 0°C, for there to be any significant change in the proportions of nitrato complexes in the aqueous phase as a result of the preferential removal by the organic phase of the trinitrato complex. Tri-*n*-butyl phosphate (TBP) diluted with kerosene was chosen as the organic solvent, since the partition coefficient (organic/aqueous) K_T for the trinitrato complex with this solvent exceeds by >20 the partition coefficient K_D for the dinitrato complex; the partition coefficients for the mononitrato K_M and other lower nitrato complexes are even smaller and effectively zero.

(a) *Extraction with Various Ratios of the Organic and Aqueous Volumes*

Solvent extraction can be used to obtain the proportion of a highly extractable species (T) in a mixture with a less extractable species (D), by using varying volumes of the organic solvent with a constant volume of the aqueous phase. If K_D, the partition coefficient of the less extractable species, can be neglected in comparison with K_T (in this case the partition coefficient of the trinitrato complex), the concentrations in the organic and aqueous phases after a short time of equilibration are related by the expression

$$C_{T,\text{org}} = K_T(C_{(T+D)\text{aq}} - C_{D,\text{aq}}) \qquad (1)$$

A plot of $C_{T,\text{org}}$ against $C_{(T+D)\text{aq}}$, in this case $[\text{Ru}]_{\text{org}} : [\text{Ru}]_{\text{aq}}$, would therefore give a straight line of slope K_T and intercept equal to $C_{D,\text{aq}}$.

A 10^{-1} M Ru solution (labelled with ^{106}Ru of the nitrato complexes aged in 7·5 M HNO_3 was diluted to 10^{-2} M Ru in 3·6 M HNO_3 and equilibrated at 20°C for 60 secs with various volumes of 20 per cent TBP such that $\text{Vol}_{\text{org}} : \text{Vol}_{\text{aq}}$ varied from 0·6 to 5·3. The 20 per cent TBP was previously equilibrated with a large volume of 0·75 M HNO_3 so that it could be used for subsequent experiments with 0·75 M HNO_3 solutions without any transfer of nitric acid occurring between the two phases. The concentrations of ruthenium, expressed as counts/min/ml, found in the organic and aqueous phases are plotted in Fig. 7. The value of K_T applying to 3·6 M HNO_3, 20 per cent TBP, and 20°C, is found to be 0·37; the percentage of ruthenium as nitrato complexes lower than the trinitrato (in the solution aged in 7·5 M HNO_3) is 22,000/45,000, i.e., 49 per cent. Hence $C_T/C_{\text{Ru}} = 51$ per cent, where C_{Ru} is the total concentration of ruthenium as nitrato complexes. The fact that the points lie in a straight line justifies the assumption that the partition coefficients for the lower nitrato complexes are small compared to K_T. Making an allowance for them to have an average value of 0·01 only changes the value of K_T from 0·37 to 0·36, and of C_T/C_{Ru} from 51 to 50 per cent.

A similar experiment was performed with 20 per cent TBP at 20°C after rapidly diluting the same 10^{-1} M Ru solution in 7·5 M HNO_3 to 10^{-2} M Ru in 0·75 HNO_3. At this acidity, the partition coefficients are considerably greater than from 3M HNO_3. A plot of $[\text{Ru}]_{\text{org}} : [\text{Ru}]_{\text{aq}}$ for various ratios of $\text{Vol}_{\text{org}} : \text{Vol}_{\text{aq}}$, indicated that a second species, present only to the extent of about 20 per cent, was being extracted by the solvent. Assuming

(i) that the 7·5 M HNO_3 stock solution contained concentrations of trinitrato (C_T), dinitrato (C_D) and mononitrato (C_M) complexes in the ratio 0·50 : 0·22 : 0·28.

[19] KAPLAN, L., HILDEBRANDT, R. A., and ADER, M. (1950) ANL 4520 and 4521.
[20] ADDISON, C. C., and HODGE, H. (1953) *Nature*, **171**, 569.

(ii) that in 0·75 M HNO_3, at 20°C and with 20 per cent TBP, $K_T = 24$, $K_D = 0{\cdot}5$, $K_M = 0$, observed and calculated values of $[Ru]_{org}/[Ru]_{aq}$, defined as D_{Ru}, are as follows:—

$Vol_{org} : Vol_{aq}$

	0·25	0·5	1·0	2·0	5·0	8·0
D_{Ru} observed						
Stirring time 5 secs	3·3		1·22		0·37	
Stirring time 30 secs	3·28	2·16	1·26	0·73	0·38	0·26
D_{Ru} calculated	3·3	2·05	1·24	0·75	0·376	0·257

VOL. 1 1955

Calculated values of D_{Ru} were obtained by using the expressions

$$[Ru]_{org} = \frac{1}{V}\left(C_T \frac{VK_T}{1 + VK_T} + C_D \frac{VK_D}{1 + VK_D} + C_M \frac{VK_M}{1 + VK_M}\right) \quad (2)$$

$$\text{and } [Ru]_{aq} = \frac{C_T}{1 + VK_T} + \frac{C_D}{1 + VK_D} + \frac{C_M}{1 + VK_M} \quad (3)$$

where $V = Vol_{org}/Vol_{aq}$. Values in agreement with the above observed values of D_{Ru} can also be calculated using somewhat different ratios of $C_T : C_D : C_M$ and correspondingly modified values of K_T and K_D.

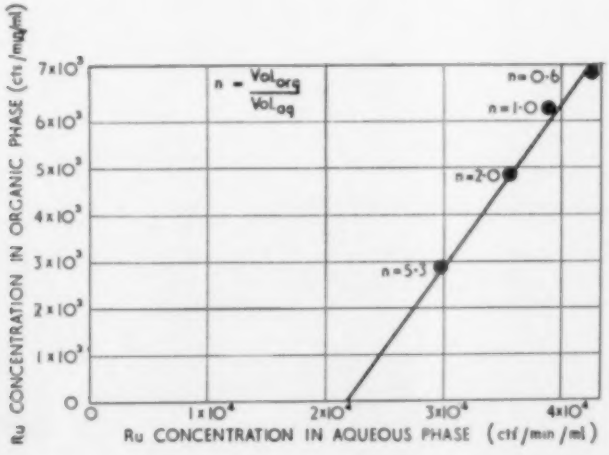

FIG. 7.—Extraction of trinitratonitrosylruthenium from 3·6 N nitric acid (containing $4{\cdot}5 \times 10^4$ cts/ml/Ru) into 20 per cent tri-*n*-butyl phosphate in kerosene.

However, the ratios of $C_T : C_D : C_M$ used above are necessary to account for the values of D_{Ru} observed in similar extractions when, instead of 20 per cent TBP at 20°C, 30 per cent TBP at 0°C is used. Under the latter conditions, K_D as well as K_T is greater than unity. Experiments (Table 4) were devised from the results of which the mole fractions and partition coefficients for the three

complexes could be closely assessed. The observed concentrations of ruthenium require for agreement (Table 4) between the observed and calculated values:

Complex	Mole Fraction at Equilibrium in 7·5 M HNO_3	Partition Coefficient at 0°C between 0·75 M HNO_3 and 30 per cent TBP
Trinitrato	0·50	120
Dinitrato	0·22	2·4
Mononitrato	0·28	0·10

(b) *Extraction from 3 M HNO_3 Solutions of Nitrato Complexes Equilibrium in 3–14·8 M HNO_3*

Stock solutions of the nitrato complexes, labelled with ^{106}Ru were prepared in 3 to 12·4 M nitric acid by dilution with water of a solution of nitratonitrosylruthenium (0·264 M Ru) in 14·8 M nitric acid. They were aged for >30 hours at room temperature for equilibrium to be established. To estimate the fraction of the trinitrato complex in these stock solutions, measurements of D_{Ru} were carried out from 3 M HNO_3 solutions at 0°C with 30 per cent TBP (suitably equilibrated with 3 M HNO_3 nitric acid to prevent transfer of acid). 3 M HNO_3 was chosen as a convenient acidity for extraction at 0°C with 30 per cent TBP since K_T and K_D are on different sides of (and widely different

Table 4.—Distribution of ruthenium at 0°C for 30 seconds equilibration between 30 per cent TBP and 0·75 M HNO_3. Ruthenium initially as Nitrato Complexes at equilibrium in 7·5 M HNO_3.

			Per cent Ru extracted by organic phase	
			Obs.	*Calc.*
A.	Extraction with an equal volume of TBP from 0·75 M HNO_3		67·7, 67·4, 67·8	67·7
B.	Successive Extractions		*[Ru] as cts/min/ml*	
			Obs.	*Calc.*
	Stock solution in 7·5 M HNO_3 diluted instantaneously to 0·75 M HNO_3		14,038	—
	(i) Extracted with an equal vol of TBP	org	9,456	9,508
		aq	4,582	4,530
	(ii) Organic phase from (i) extracted with an equal vol of 0·75 M HNO_3	org	8,444	8,476
		aq	1,030	1,032
	(iii) 1 vol of organic phase from (i) extracted first with 5 vols of 0·75 M HNO_3 and then with a single vol of 0·75 M HNO_3	org	7,17[illegible]	7,128
		aq	260	270
	(iv) 1 vol of organic phase from (ii) extracted with 20 vols of 0·75 M HNO_3	org	6,001	6,082
		aq	—	
	(v) Organic phase from (iv) extracted with an equal vol of 0·75 M HNO_3	org	5,925	5,985
		aq	—	

Note: The equilibrations followed one another within a total time of an hour. The stability of the species in the organic phase for this order of time was confirmed by performing operation (ii) at 3, 7, and 25 mins after operation (i).

from) unity, and K_M is negligible. With equal volumes of the organic and aqueous phases, the observed distribution of ruthenium D_{Ru} is related to C_T by the expression

$$\frac{D_{Ru}}{1 + D_{Ru}} = \frac{C_T}{C_{Ru}}\left(\frac{K_T}{1 + K_T}\right) + \frac{C_D}{C_{Ru}}\left(\frac{K_D}{1 + K_D}\right). \quad (4)$$

The appropriate values of K_T (5·2) and K_D (0·10) were determined as follows:—

(i) *For K_T*: A portion of the stock solution of the nitrato complexes in 7·5 M HNO_3 was cooled to 0°, diluted to 3 M HNO_3 by being pipetted into the appropriate volume of water which was already in contact at 0°C with 30 per cent TBP. After 30 secs stirring and separation of the TBP phase, the dinitrato complex in it was removed by washing with 8 volumes of 3 M HNO_3 (D_{Ru} = 5·0). From a further extraction of the TBP phase with 3 M HNO_3, D_{Ru} (=K_T in this case) was found to be 5·2.

(ii) *For K_D*: The value of D_{Ru} found by rapidly extracting at 0°C, as in (i), the stock solution in 7·5 M HNO_3, after dilution to 3 M HNO_3, with an equal volume of 30 per cent TBP was found to be 0·79. For this stock solution, C_T/C_{Ru} and C_D/C_{Ru} are known from (a) above to be 0·50 and 0·22 respectively. On substitution in equation 4, K_D is found to be 0·10.

The other stock solutions in 4·6–14·8 M HNO_3 were diluted to 3 M HNO_3 and immediately extracted with an equal volume of 30 per cent TBP at 0° (stirring being for 30 secs) in a similar manner to that used for the solution in 7·5 M HNO_3. Values found for D_{Ru}, including that for the stock solution in 3 M HNO_3, were

Stock Solution in	3·0	4·6	6·3	7·5	8·7	12·4	14·8 M HNO_3
D_{Ru}	0·122	0·29	0·54	0·79	0·99	1·92	3·0
C_T/C_{Ru}	0·10	0·24	0·39	0·50	0·57	0·76	~0·88

Included above is the mole fraction of the trinitrato complex calculated by Equation 4, using K_T = 5·2, K_D = 0·10. It is also assumed that C_D/C_{Ru} equals 0·22 for the solutions in 7·5, 8·7 and 12·4 M HNO_3, and equals 0·25 for the solutions in 3·0, 4·6, 6·3 M HNO_3; these are approximations, but the relative values of K_T and K_D are such that a considerable change in C_D/C_{Ru} does not unduly affect C_T/C_{Ru}; they are based on the value of 0·22, found in (a), for the solution in 7·5 M HNO_3, and on the value of C_M/C_{Ru} = 0·64 deduced from successive extractions with the stock solution in 3 M HNO_3. In solution in 14·8 M HNO_3 the presence of a small fraction of a nitrato complex higher than the trinitrato complex must be suspected.

Other Determinations

Total nitrogen was determined as ammonia by reduction in strongly alkaline solution with Devarda's alloy: nitrosyl nitrogen, as ammonia after quantitative precipitation of the hydrosulphide, dissolving it in a bromine-hydrochloric acid mixture, or in sodium hypobromite or hypochlorite, followed by reaction with Devarda's alloy: nitrogen present as nitrate, as nitron nitrate which was precipitated from the filtrate after removing RuNO as hydrosulphide. Sulphur in the hydrosulphide was determined as barium sulphate after dissolving the precipitate in a bromine-hydrochloric acid mixture.

Ruthenium was determined (i) by quantitative precipitation of the hydrosulphide, roasting this to the oxide, followed by reduction in hydrogen to the metal; or (ii) by absorptiometric determination of potassium ruthenate solutions.

Fluorine was determined gravimetrically as PbClF after distillation as SiF_4 at 140°C.

ACKNOWLEDGEMENTS

We are grateful to Prof. J. S. ANDERSON for his contribution to Section 4, to Mr. P. G. M. BROWN and Mr. G. M. GILLIES for experimental assistance, to Dr J. GAUNT and Mr. G. M. MEABURN for the examination and interpretation of infra-red spectra, to Dr. R. W. M. D'EYE for the X-ray examination, and to Mr. K. ALCOCK for the thermogravimetric analysis of the hydroxide. Four of the authors (A.R.P., F.M.L., R.T., and N.R.W.B.) are grateful to the Directors of JOHNSON, MATTHEY & Co. Ltd., for permission to publish their contributions to this paper.

VOL. 1 1955

J. Inorganic and Nuclear Chemistry, 1955, Vol. 1, pp. 402–410. Pergamon Press Ltd., London

THE CATALYTIC HALIDES—XIII

THE INTERACTION OF GALLIUM TRICHLORIDE WITH ETHYL, ISOPROPYL, *n*-PROPYL, AND *t*-BUTYL CHLORIDES

ROBERT WONG[1, 2] and HERBERT C. BROWN
Department of Chemistry of Purdue University, Lafayette, Indiana, U.S.A.

(*Received* 5 *May* 1955)

Abstract—The phase diagrams for the ethyl chloride—gallium chloride system were determined at four temperatures, −78.5, −64, −50, and −36°. A 1 : 1 addition compound exists in the solution phase as shown by molecular weight determinations. A solid phase corresponding to the 1 : 2 compound, $C_2H_5Cl : Ga_2Cl_6$, was identified, and the heat of dissociation, $C_2H_5Cl : Ga_2Cl_6(s) \rightleftarrows C_2H_5Cl(g) + Ga_2Cl_6(s)$ is 9.74 kcal/mole. The heat of solution of the 1 : 2 compound in ethyl chloride is 5.0 kcal/mole and the calculated m.p. is −29°. The phase diagram for the isopropyl chloride—gallium chloride system was determined at −64°. Solid phases corresponding to both the 1 : 2 and 1 : 1 compounds, $(CH_3)_2CHCl : Ga_2Cl_6$ and $(CH_3)_2CHCl : GaCl_3$, were identified. At higher temperatures, solutions of gallium chloride in isopropyl chloride evolved hydrogen chloride at an appreciable rate. Similar observations were obtained for solutions of gallium chloride in *n*-propyl and *t*-butyl chloride. Isomerization of *n*-propyl to isopropyl chloride was also observed. Under the same conditions the rate of hydrogen chloride evolution is *t*-butyl > isopropyl > *n*-propyl > ethyl chloride, which is also the order of stability of the carbonium ions of the respective alkyl groups.

INTRODUCTION

As part of our program of investigating the function of metal halides in the Friedel-Crafts reaction, we undertook an examination of the action of typical Friedel-Crafts catalysts on alkyl halides. Since aluminum chloride was found to be essentially insoluble in the alkyl chlorides, our efforts were concentrated on gallium chloride. In a previous paper,[3] we reported the results of the interaction of the methyl halides with gallium trichloride. It was found that both 1 : 1 ($CH_3Cl : GaCl_3$) and 1 : 2 ($CH_3Cl : Ga_2Cl_6$) compounds exist in the solid phase, and that only the 1 : 1 compound was present in solution. In this paper, the results of the investigation of the interaction of gallium trichloride with the chlorides higher in the homologous series are reported.

RESULTS

The System: Ethyl Chloride—Gallium Chloride

Gallium chloride is readily soluble in ethyl chloride at −50°, forming a clear, colorless solution which appears to be stable indefinitely. As the mole ratio $C_2H_5Cl/GaCl_3$ is decreased, the pressure drops smoothly until, at a mole ratio of 1.5, a white solid appears and the pressure remains sensibly constant at a value of approximately 14.7 mm. At a mole ratio of 0.5 there is a sudden drop in the pressure to a new plateau at approximately 3.3 mm. The data are summarized in Table 1.

[1] Abstracted in part from a thesis presented by ROBERT WONG in partial fulfilment of the requirements for the Ph.D. degree.

[2] Research assistant, 1952–1954 on a grant from the Atomic Energy Commission for the study of "The Chemistry of Polyvalent Metal Halides."

[3] H. C. BROWN, L. P. EDDY, and R. WONG, *J. Amer. Chem. Soc.*, **75**, 6275 (1953).

TABLE 1.—THE ETHYL CHLORIDE—GALLIUM CHLORIDE SYSTEM AT −50°

Mole ratio $C_2H_5Cl/GaCl_3$	Pressure,[a] mm	Molecular weight assuming: no compound formation	Molecular weight assuming: compound formation	Mole ratio, $C_2H_5Cl/GaCl_3$	Pressure,[a] mm
	30.20				
22.02	28.80	172	180	3.40	23.48
21.45	28.70	165	174	3.16	23.56
20.95	28.65	164	171	2.90	22.18
14.65	28.00	165	177	2.68	21.41
14.20	27.95	165	178	2.45	20.77
13.31	27.80	163	176	2.25	19.48
12.49	27.60	161	174	1.99	18.52
11.50	27.30	159	174	1.78	17.49
10.55	27.10	163	177	1.59	16.30
9.18	26.45	154	173	1.49[b]	15.83
8.11	25.90	152	174	1.44[b]	15.03
7.25	26.52			1.37[b]	14.59
6.72	26.27			1.13[b]	14.54
6.24	26.18			0.91[b]	14.18
5.74	25.74			0.83[b]	14.62
5.27	25.47			0.71[b]	14.68
4.95	25.07			0.63[b]	6.69
4.39	24.41			0.49[b]	2.93
4.14	24.11			0.39[b]	3.00
3.91	23.72			0.36[b]	3.46
3.68	23.37			0.23[b]	3.19
				0.14[b]	3.19

[a] The pressure decrease was observed directly by a differential method.
[b] Solid present.

The lower plateau evidently corresponds to the formation of a relatively stable 1 : 2 addition compound with a dissociation pressure of approximately 3.3 mm.

$$C_2H_5Cl : Ga_2Cl_6(s) \rightleftarrows C_2H_5Cl(g) + Ga_2Cl_6(s)$$

The first plateau then corresponds to an ethyl chloride solution saturated with respect to the 1 : 2 addition compound.

Molecular weights were calculated from the observed drop in the vapor pressure of the solvent at low concentrations, assuming that the gallium chloride is present in the unsolvated form. The molecular weights obtained evidently correspond to the existence of gallium chloride in the monomeric form in solution ($GaCl_3 = 176$). However, the calculated molecular weights show a continual drop as the solutions become more and more concentrated.

The molecular weight was then calculated, assuming that one mole of solvent is effectively removed to form the addition compound and exists as such in solution. In this case the molecular weight showed a satisfactory constancy up to a mole ratio of approximately 8. The values then deviated to increasingly higher values. The average of the values for the molecular weight between the mole ratios 22.02 to 8.11 is 175 ± 2.1, which is in excellent agreement with the 176-value calculated for monomeric gallium chloride. It is therefore concluded that the addition compound, $C_2H_5Cl : GaCl_3$, exists in solution. Consequently, it appears that when the 1 : 2 complex dissolves in ethyl chloride, it becomes more highly solvated and forms the 1 : 1 ($C_2H_5Cl : GaCl_3$) complex.

Similar phase studies were made at −36, −64, and −78.5°. In each case similar results were obtained, except that no pronounced saturated solution plateau was found at −36°. However, in each case the plateau corresponding to the dissociation of the 1 : 2 addition compound was obtained, and no evidence for the solid 1 : 1 addition compound was observed (Fig. 1).

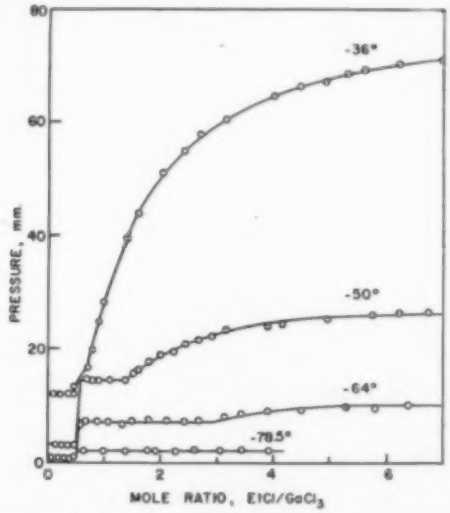

FIG. 1.—The ethyl chloride—gallium chloride system at various temperatures.

At −36° the average of thirteen observations at $C_2H_5Cl/GaCl_3$ mole ratios of 22.65 and 6.74 results in a molecular weight value of 171 ± 2, assuming one mole of ethyl chloride removed from solution to form the complex. On the basis of the alternative assumption, the calculated molecular weight decreased from 167 to 141 in the more concentrated solution. From these data it appears certain that the 1 : 1 addition compound exists as such in the ethyl chloride solutions, probably in equilibrium with minor amounts of the 1 : 2 compound.

Table 2 gives the data for the dissociation of the solid 1 : 2 addition compound at the four temperatures.

TABLE 2.—DISSOCIATION PRESSURES OF $C_2H_5Cl : Ga_2Cl_6$

Temperature, °C	Pressure, mm
−35.3	12.28
−49.8	3.20
−63.5	0.80
−78.5	0.09

From these data a heat of dissociation of 9.74 kcal/mole is calculated for the reaction:

$$C_2H_5Cl : Ga_2Cl_6(s) \rightleftarrows Ga_2Cl_6(s) + C_2H_5Cl(g)$$

The positions of the saturated solution plateaus fix the solubility at 0.182 mole fraction

at −63.5°, and 0.370 at −49.8°. Assuming ideal behavior, the heat of fusion or solution is 5.0 kcal/mole, and the calculated melting point is −29°. These data are shown in Fig. 2.

The solutions of gallium chloride in ethyl chloride are stable at low temperatures. At 0°, however, hydrogen chloride was very slowly evolved. The solution, which was initially colorless, became pale yellow. Removal of the ethyl chloride by evaporation

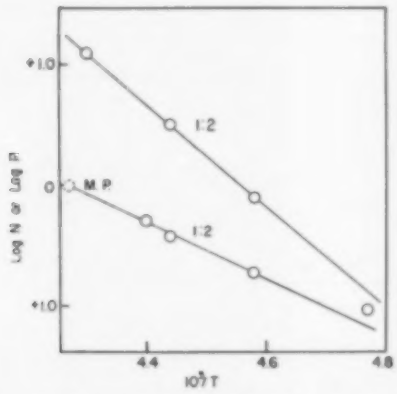

FIG. 2.—The change of pressures (dissociation) and solubility of ethyl chloride—gallium chloride with temperature.

always resulted in a small loss, and the colored material remained with the gallium chloride as a non-volatile product. This behavior was also observed in the aluminum bromide—ethyl bromide system.[4] It is probable that ethyl chloride had decomposed, yielding hydrogen chloride and a polymeric material derived from the hydrocarbon fragment.

The System: Isopropyl Chloride—Gallium Chloride

Gallium chloride dissolves in isopropyl chloride at −46° to give clear colorless solutions. On standing, hydrogen chloride was slowly evolved and the solution became yellow. This precluded any molecular weight or vapor pressure-composition studies at this temperature. However, at −64° the solution did not evolve a detectable amount of hydrogen chloride upon standing for eight hours. Consequently, the vapor pressure-composition phase diagram was determined for this system at −64° Results similar to those in the methyl chloride—gallium chloride system[2] were obtained. These data are given in Table 3 and Fig. 3.

Gallium chloride was readily soluble in isopropyl chloride, forming a clear, colorless solution. After two solvent fractions were removed, a white solid appeared and the pressure remained constant at 1.46 mm, corresponding to the solution saturated with respect to the 1 : 1 compound, $(CH_3)_2CHCl : GaCl_3$. As more solvent was withdrawn, the second plateau appeared at a mole ratio, $(CH_3)_2CHCl/GaCl_3$ of 1.02 and a pressure of 1.23 mm. This plateau represents the equilibrium:

$$2(CH_3)_2CHCl : GaCl_3(s) \rightleftarrows (CH_3)_2CHCl : Ga_2Cl_6(s) + (CH_3)_2CHCl(g)$$

[4] H. C. BROWN and W. J. WALLACE, *J. Amer. Chem. Soc.* 75, 6279 (1953).

The last plateau, which appeared at a mole ratio of 0.50 and 0.124 mm, then represents the equilibrium:

$$(CH_3)_2CHCl : Ga_2Cl_6(s) \rightleftarrows (CH_3)_2CHCl(g) + Ga_2Cl_6(s).$$

Thus this is good evidence that both the 1 : 1 and the 1 : 2 complexes of isopropyl

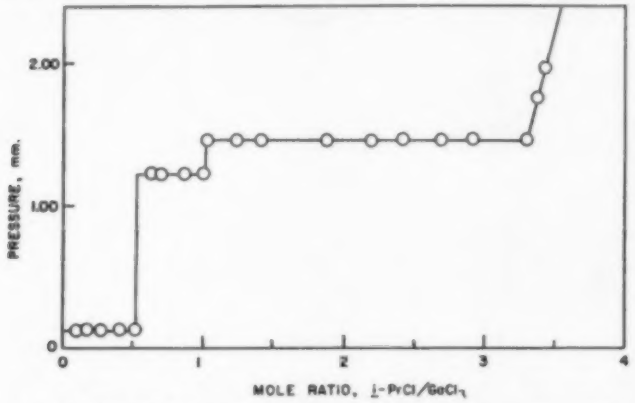

FIG. 3.—The isopropyl chloride—gallium chloride system at −64°.

chloride with gallium chloride exist in the solid phase. Although no molecular weight determinations were made for this system, it would be expected that the monomer compound, $(CH_3)_2CHCl : GaCl_3$, would be the predominant species in solution.

TABLE 3.—THE ISOPROPYL CHLORIDE—GALLIUM CHLORIDE SYSTEM AT −64°

Mole ratio, $(CH_3)_2CHCl/GaCl_3$	Pressure,[a] mm	Mole ratio, $(CH_3)_2CHCl/GaCl_3$	Pressure,[a] mm
	3.17		
3.43	1.96	1.24[b]	1.46
3.39[b]	1.74	1.14[b]	1.46
3.31[b]	1.46	1.02[b]	1.23
3.15[b]	1.46	0.87[b]	1.23
2.92[b]	1.46	0.80[b]	1.23
2.69[b]	1.46	0.72[b]	1.23
2.42[b]	1.46	0.50[b]	0.12
2.20[b]	1.46	0.42[b]	0.12
1.88[b]	1.46	0.28[b]	0.12
1.61[b]	1.46	0.18[b]	0.12
1.41[b]	1.46	0.11[b]	0.12

[a] The pressure decrease was observed directly by a differential method.
[b] Solid present.

The System: n-Propyl Chloride—Gallium Chloride

A solution of gallium chloride in *n*-propyl chloride at −46° evolved hydrogen chloride at a rate slower than that of a similar solution in isopropyl chloride under the same conditions. When the mixtures from the reaction of *n*-propyl chloride with gallium chloride were analyzed, it was found that the products consisted of hydrogen chloride,

and a mixture of gallium chloride with a red non-volatile polymeric material, *n*-propyl chloride, and a larger amount of isopropyl chloride. This indicated that most of the *n*-propyl chloride had isomerized to isopropyl chloride. In another experiment, a solution of 1.43 mmoles of $GaCl_3$ in 12.21 mmoles *n*-propyl chloride was maintained for five hours at −80°. No decomposition was observed under these conditions. The solution was then analyzed. It contained 80 per cent isopropyl chloride and 20 per cent *n*-propyl chloride, showing that extensive isomerization of the *n*-propyl chloride to isopropyl chloride had occurred even at this low temperature. Because of the complications resulting from the rapid isomerization of the *n*-propyl chloride, no attempt was made to study the phase diagram in detail.

The System: t-Butyl Chloride—Gallium Chloride

When gallium chloride was dissolved in *t*-butyl chloride at −23°, hydrogen chloride was evolved extremely rapidly. The solution was initially colorless. However, as the reaction proceeded, a heavier, yellow layer separated from solution, and the reaction ceased before the *t*-butyl chloride present had completely decomposed. The rate of the evolution of hydrogen chloride from the *t*-butyl chloride solutions was considerably faster than that from the solutions of isopropyl and *n*-propyl chlorides under similar conditions. The rapid decomposition made it impossible to study the phase relationships.

VOL. 1 1955

DISCUSSION

For convenience, the experimental observations on the gallium chloride—alkyl chloride addition compounds are summarized in Table 4.

Both the methyl chloride and the isopropyl chloride form solid 1 : 1 and 1 : 2 addition compounds with gallium chloride.

$$RCl + Ga_2Cl_6 \rightleftarrows RCl : Ga_2Cl_6$$
$$2RCl + Ga_2Cl_6 \rightleftarrows 2RCl : GaCl_3$$

On the other hand, ethyl chloride was observed to form only the solid 1 : 2 compound, although the molecular weight study of the solution indicated that the 1 : 1 compound was present as such in the solution. There is no apparent reason for the failure of the ethyl chloride to form the analogous solid 1 : 1 derivative. We can only conclude that the non-existence of the solid 1 : 1 compound must be the result of crystal lattice forces.

In view of the increasing inductive effect, the stability of the addition compounds would be expected to increase in the order: $CH_3Cl < C_2H_5Cl < (CH_3)_2CHCl < (CH_3)_3CCl$. However, data are available only for the solid phase, and crystal lattice forces undoubtedly play a major role in controlling the relative stability of the solid addition compounds. Consequently, the present study does not permit a comparison of the relative basic properties of the various halides.

It was observed that the stability of the addition compounds sharply decreased with increasing branching of the alkyl group: $CH_3Cl > C_2H_5Cl > (CH_3)_2CHCl > (CH_3)_3CCl$. Since this is the order of ease of formation of the corresponding carbonium ions, the decomposition may have the ionization of the halides into the respective carbonium ions as one of the rate-controlling steps in the formation of hydrogen chloride.

The isomerization of *n*-propyl chloride into isopropyl chloride may involve ionization. However, it is possible that the isomerization is a synchronous process not involving ionization. Certainly the physical properties of the addition compounds and the excellent agreement between the observed and theoretical molecular weights argue against the existence of any significant fraction of the addition compounds in ionized form.

TABLE 4.—ADDITION COMPOUNDS OF GALLIUM CHLORIDE WITH ALKYL CHLORIDES[a,b]

	Methyl chloride	Ethyl chloride	Isopropyl chloride
Comp'd. in soln. in alkyl chloride	$CH_3Cl : GaCl_3$	$C_2H_5Cl : GaCl_3$	
Solid phases	$CH_3Cl : GaCl_3$ $CH_3Cl : Ga_2Cl_6$	$C_2H_5Cl : Ga_2Cl_6$	$(CH_3)_2CHCl : GaCl_3$ $(CH_3)_2CHCl : Ga_2Cl_6$
Stability	No evolution of HCl observed at 0°	Slow evolution of HCl at 0°	Very rapid evolution of HCl at 0°
Dissociation pressures (1 : 1)			
Temp., −50°	84.5	—	—
−64°	25.7	—	1.2
−78.5°	8.0	—	—
Dissociation pressures (2 : 1)			
Temp., −36°	—	12.3	—
−50°	34.7	3.2	—
−64°	10.0	0.8	0.12
−78.5°	2.3	0.1	—
Melting point (calc'd)	4.8°	−29.0	—
Heat of solution (kcal/mole)	2.15	5.0	—
Heats of formation ΔH, (kcal/mole):			
$RCl(g) + \frac{1}{2}Ga_2Cl_6(s) = RCl : GaCl_3(s)$	−7.61[c]	—	—
$RCl(g) + Ga_2Cl_6(s) = RCl : Ga_2Cl_6(s)$	−8.11[c]	−9.74	—

[a] In the presence of gallium chloride, *t*-butyl chloride undergoes very rapid evolution of hydrogen chloride at −23°.

[b] In the presence of gallium chloride, *n*-propyl chloride is isomerized to isopropyl chloride at −80°.

[c] Recalculated values. The values previously reported (Ref. 3) are in error due to a mistake in the calculation.

The observation that the alkyl chlorides are capable of forming both 1 : 1 and 1 : 2 derivatives with gallium chloride emphasizes the fact that these dimeric metal halides serve to coordinate with either one or two moles of a donor molecule. Thus in the reaction of aluminum bromide with aromatic hydrocarbons two series of complexes

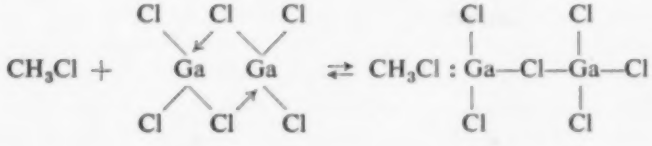

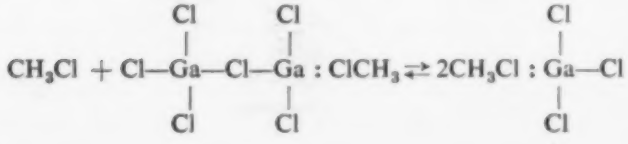

have been identified, $ArH \cdot Al_2Br_6$ and $ArH \cdot AlBr_3$.[5] Similarly, in the reaction of hydrogen bromide and aluminum bromide with aromatic hydrocarbons, two series of salts were isolated, $ArH_2^+Al_2Br_7^-$ and $ArH_2^+AlBr_4^-$.[6] Recently, in this laboratory, it has been observed that boron halides such as boron trifluoride can also form two series of addition compounds, such as $(C_2H_5)_3N : BF_3$ and $(C_2H_5)_3N : B_2F_6$.[7]

It appears that a weak base, or a stronger base in low concentrations, serves to open only one bridge of the gallium chloride dimer, whereas a strong base, or one present in relatively high concentration, is capable of opening both bridges.

EXPERIMENTAL PART

Apparatus

All experiments were carried out with high vacuum apparatus and techniques in which the materials came into contact only with glass and mercury. The general techniques are described by SANDERSON.[8] The technique and procedure utilized for the determination of the phase diagrams are as described in the previous paper on this subject.[3]

VOL. 1 1955

The apparatus used for the precise study is shown in Fig. 4. In a typical determination, 1.572 mmoles of gallium chloride was sublimed into the reaction chamber *A*, and 16.571 mmoles ethyl

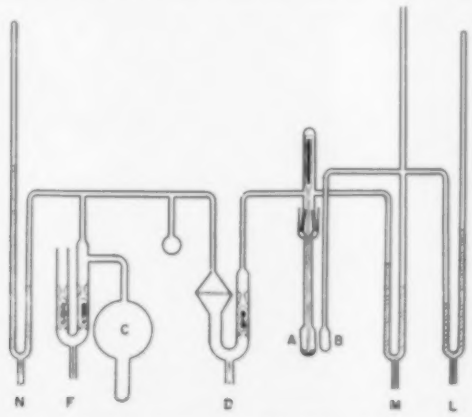

FIG. 4.—Apparatus used in phase studies.

chloride from the reservoir *C* was condensed in the tube to form the solution. The amount of ethyl chloride introduced was followed by the pressure change in the reservoir as read on the manometer *N*. Reaction vessel *A* contained a stirrer with a glass-enclosed iron core which was activated by a solenoid and timer. Several glass beads in the vessel greatly improved the efficiency of the agitation. A sample of the pure solvent was placed in *B*. The tubes *A* and *B* were maintained at the desired temperature in a single bath until equilibrium had been reached, and the decrease in the vapor pressure of the solution was measured directly on the manometer *M* with a cathetometer to the nearest 0.05 mm. The storage bulb *C* was immersed in a water-bath to minimize the effects of minor variations in the room temperature.

To obtain the vapor pressure of a new composition, the valve *D* was carefully opened, and a small quantity of the ethyl chloride in the solution was allowed to volatilize from the reaction vessel *A* into the reservoir *C*. The float-valve *F* leads to the main manifold of the high vacuum system.

The temperatures were maintained at −78.5° by the use of solid carbon dioxide at 760 mm, and −64, −50, and −36° by the use of solid-liquid slushes of chloroform, ethyl malonate, and ethylene

[5] W. J. WALLACE, C. W. FRITH, and S. U. CHOI, unpublished work.
[6] H. C. BROWN and W. J. WALLACE, *J. Amer. Chem. Soc.* **75**, 6268 (1953).
[7] P. F. STEHLE, unpublished work.
[8] R. T. SANDERSON, Vacuum Manipulation of Volatile Compounds, John Wiley and Sons, Inc., New York, 1948.

dichloride, respectively. The constancy of the baths was checked by the constancy of the vapor pressure of pure ethyl chloride on manometer *L*.

Materials

Ethyl chloride (Eastman Kodak) was introduced into the vacuum apparatus and there fractionated. A sample of liquid ethyl chloride was then maintained at −80° in contact with freshly sublimed aluminum chloride for twenty-four hours with frequent agitation. The product, distilled from a −80° bath, was tensiometrically homogeneous (475.30 mm at 0°), and was used for the phase studies.

Isopropyl chloride and *n*-propyl chloride (Columbia Chemical Co.) were distilled and rectified through 50-plate Todd columns. The accepted portions were stored over calcium hydride for twenty-four hours, after which they were introduced into the vacuum system. The samples were then fractionated in the vacuum apparatus to obtain tensiometrically pure samples. The distillates accepted for use had the following properties;

	Isopropyl chloride	*n*-propyl chloride
Boiling point, °C	35.5 (751 mm)	46.4 (750 mm)
Refractive index, n_D^{20}	1.3773	1.3884
Vapor pressure at 0°	189 mm	114 mm

t-Butyl chloride (Columbia Chemical Co.) was purified by fractionation in the high vacuum apparatus. The tensiometrically pure sample was then stored for use (108 mm at 0°).

Gallium chloride was prepared by the reaction of weighed samples of the metal with excess hydrogen chloride.[3]

ACKNOWLEDGEMENT

The authors are grateful for the support of the Atomic Energy Commission, under whose grant this work was performed.

VOL.
1
1955

LETTERS TO THE EDITORS

The Structure of Silyl *iso*-Thiocyanate

(*Received* 27 *July* 1955)

A COMPOUND has recently been prepared by the action of silyl iodide on silver thiocyanate which must be silyl *iso*-thiocyanate, or less likely, silyl thiocyanate. The preparation, analysis and physical characterization of the compound will be described elsewhere.[1] The infra-red spectrum of the compound has been examined with a Perkin-Elmer Model 21 double-beam instrument with sodium chloride optics. The perpendicular SiH_3 deformation band with its centre at 947 cm^{-1} shows well defined strong, weak and weak rotational detail. It is concluded that the molecule is a symmetric top with the Si, N, C and S atoms linear. Neither methyl thiocyanate nor methyl *iso*-thiocyanate is a symmetric top.[2]

Previously the only compound in which back co-ordination to the silicon by an attached atom had been found to change the symmetry of the molecule from that displayed by the analogous carbon compound was trisilylamine,[3] which is believed to be planar. Other silicon compounds with possibly anomalous structures have been discussed in a recent publication.[4] The linearity of the heavy atoms suggests considerable double bonding to the silicon, which is more likely by the more electronegative nitrogen than sulphur,[5] since disilyl sulphide does not appear to be linear.[4] So the infra-red spectrum provides further evidence that the compound is indeed the *iso*-thiocyanate.

The Chemical Laboratories,
Pembroke Street, Cambridge

A. G. MACDIARMID
A. G. MADDOCK

[1] A. G. MACDIARMID, *J. Inorg. Nucl. Chem.* (in press).
[2] C. I. BEARD and B. P. DAILEY, *J. Amer. Chem. Soc.*, **71**, 929 (1949).
[3] K. HEDBERG and A. J. STOSICK, XII International Congress of Pure and Applied Chemistry, New York, September (1951).
[4] H. J. EMELÉUS, A. G. MACDIARMID, and A. G. MADDOCK, *J. Inorg. Nucl. Chem.*, **1**, 195 (1955).
[5] D. P. CRAIG, A. MACCALL, R. S. NYHOLM, L. E. ORGEL, and L. E. SUTTON, *J. Chem. Soc.*, 344 (1954).

Geiger Counting of Carbon Dioxide

(*Received* 8 *September* 1955)

A SPECIAL Geiger counter for radiocarbon has been described recently.[1] The carbon is introduced into the counter as carbon dioxide gas. The discharge is quenched by addition of ethyl alcohol and use of a resistance.

Attention may be drawn to the fact that in this laboratory Geiger counting of carbon dioxide gas has been accomplished without addition of a quenching gas.[2, 3, 4] Only an external quenching circuit (Neher-Pickering) has been employed. This simplifies greatly the filling of the counters, and eliminates a possible source of errors.

The plateau obtained with pure carbon dioxide is at least 400 volts long, and the slope is usually undetectable. The vacuum of a mercury diffusion pump with liquid air trap is sufficient for filling. Though the gas is customarily dried with magnesium perchlorate, traces of water hardly affect the quality of the plateau. The filling does not take more than a few minutes, and we have often measured thirty and more samples in a day.

The volume of our counter is 25 cm^3 with a dead space of the order of 10 per cent only. Gas

[1] G. DELIBRIAS, *J. Inorg. Nucl. Chem.* **1**, 238 (1955).
[2] G. ROHRINGER and E. BRODA, *Z. Naturforsch.* **8b**, 159 (1953).
[3] E. BRODA and G. ROHRINGER, *Z. Elektrochem.* **58**, 634 (1954).
[4] E. BRODA and L. SVERAK, *Nature*, **173**, 676 (1954).

pressure usually is 0·5 atmospheres, and the voltage in this condition about 4·5 kV. More recently, 1 atmosphere has been reached with an improved power pack and quenching circuit. The background of the unprotected counting tube is of the order of 50 per min, but this can be reduced by a factor 10 through anti-coincidence.[5]

With this equipment we have carried out a number of investigations, mainly in biochemistry.[6] Hardly any of this work would have been possible with window counters, as the sensitivity of the latter is about 100 times less than that of the gas counter.

Even before the anti-coincidence circuit was built, activities as low as $2 \cdot 10^{-12}$ curies (specific activities $3 \cdot 10^{-10}$ curies/gram) were determined in routine work.[7] In one case, for the purpose of measuring the capture cross-section of the carbon isotope 13 for thermal neutrons, an activity of about 10^{-12} curies was determined with a standard error of 6% only.[8]

A table has been drawn up which shows the ranges of various methods now in use for the measurement of radiocarbon.[9] It appears that gas Geiger counting, essentially a simple method, compares favourably in sensitivity with other methods in the routine assay of samples of low mass and low specific activity.

E. Broda

I. Chemisches Laboratorium,
Universität Wien, Osterreich

[5] G. Rohringer, L. Sverak, E. Broda, and K. Liebscher, *Monatsh.* 86, 117 (1955).
[6] For references to work published up to 1953, see Broda and Sverak[4].
[7] See, e.g., W. Zischka, K. Karrer, O. Hromatka, and E. Broda, *Monatsh.* **85**, 856 (1954).
[8] E. Broda and G. Rohringer, *Naturwissenschaften* **40**, 337 (1953).
[9] M. Reinharz, G. Rohringer, and E. Broda, *Acta phys. Austr.* **8**, 285 (1954).

VOL.
1
1955